SPHINGOLIPIDS IN INFECTION CONTROL

EDITED BY: Sibylle Schneider-Schaulies, Burkhard Kleuser and Juergen Seibel
PUBLISHED IN: Frontiers in Cell and Developmental Biology and
Frontiers in Immunology

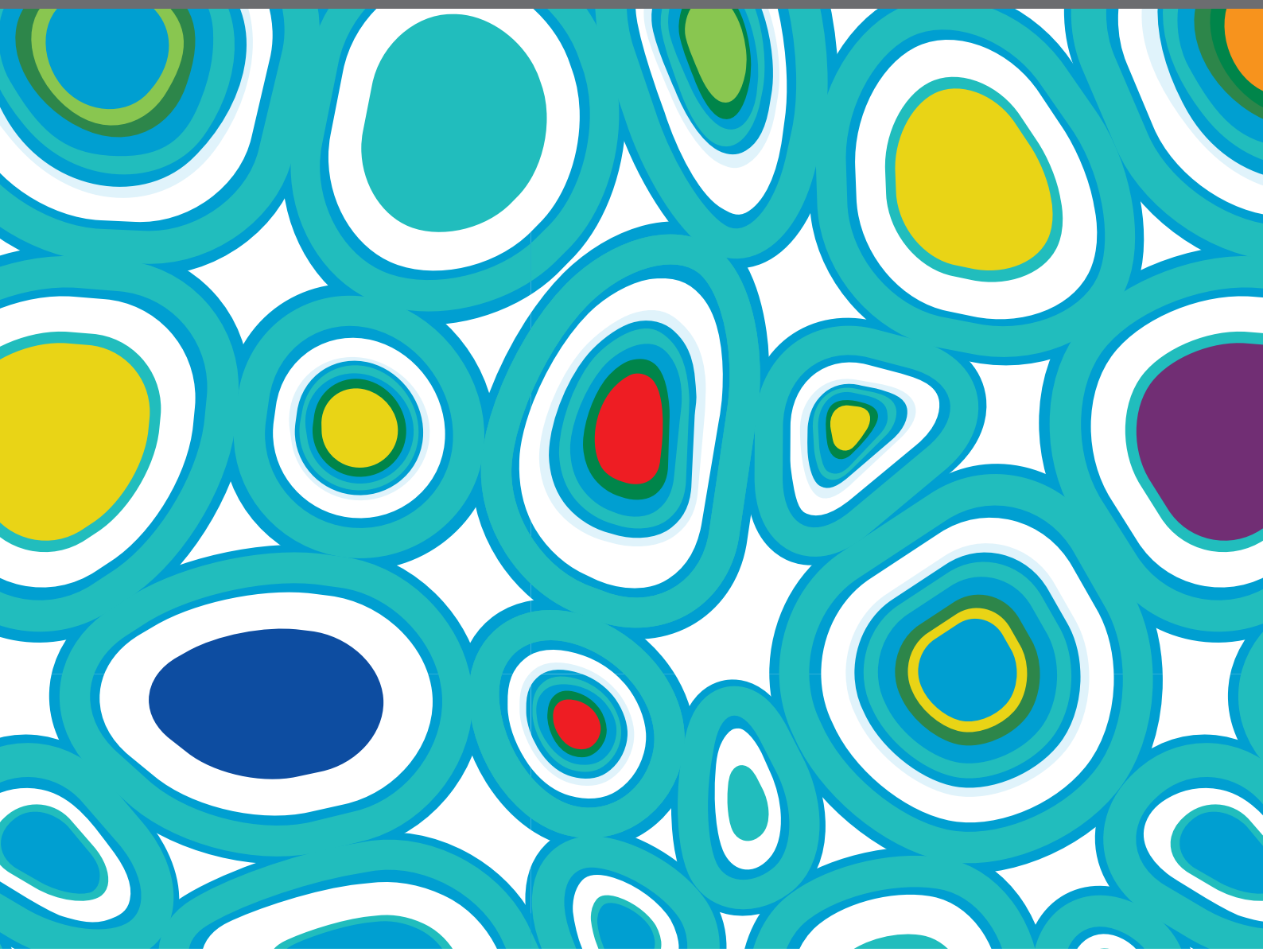

frontiers Research Topics

ISSN 1664-8714
ISBN 978-2-88971-194-9
DOI 10.3389/978-2-88971-194-9

About Frontiers

Frontiers is more than just an open-access publisher of scholarly articles: it is a pioneering approach to the world of academia, radically improving the way scholarly research is managed. The grand vision of Frontiers is a world where all people have an equal opportunity to seek, share and generate knowledge. Frontiers provides immediate and permanent online open access to all its publications, but this alone is not enough to realize our grand goals.

Frontiers Journal Series

The Frontiers Journal Series is a multi-tier and interdisciplinary set of open-access, online journals, promising a paradigm shift from the current review, selection and dissemination processes in academic publishing. All Frontiers journals are driven by researchers for researchers; therefore, they constitute a service to the scholarly community. At the same time, the Frontiers Journal Series operates on a revolutionary invention, the tiered publishing system, initially addressing specific communities of scholars, and gradually climbing up to broader public understanding, thus serving the interests of the lay society, too.

Dedication to Quality

Each Frontiers article is a landmark of the highest quality, thanks to genuinely collaborative interactions between authors and review editors, who include some of the world's best academicians. Research must be certified by peers before entering a stream of knowledge that may eventually reach the public - and shape society; therefore, Frontiers only applies the most rigorous and unbiased reviews.
Frontiers revolutionizes research publishing by freely delivering the most outstanding research, evaluated with no bias from both the academic and social point of view. By applying the most advanced information technologies, Frontiers is catapulting scholarly publishing into a new generation.

What are Frontiers Research Topics?

Frontiers Research Topics are very popular trademarks of the Frontiers Journals Series: they are collections of at least ten articles, all centered on a particular subject. With their unique mix of varied contributions from Original Research to Review Articles, Frontiers Research Topics unify the most influential researchers, the latest key findings and historical advances in a hot research area! Find out more on how to host your own Frontiers Research Topic or contribute to one as an author by contacting the Frontiers Editorial Office: frontiersin.org/about/contact

SPHINGOLIPIDS IN INFECTION CONTROL

Topic Editors:
Sibylle Schneider-Schaulies, Julius Maximilian University of Würzburg, Germany
Burkhard Kleuser, University of Potsdam, Germany
Juergen Seibel, Julius Maximilian University of Würzburg, Germany

Citation: Schneider-Schaulies, S., Kleuser, B., Seibel, J., eds. (2021). Sphingolipids in Infection Control. Lausanne: Frontiers Media SA. doi: 10.3389/978-2-88971-194-9

Table of Contents

frontiers in Cell and Developmental Biology

EDITORIAL
published: 21 June 2021
doi: 10.3389/fcell.2021.697290

Editorial: Sphingolipids in Infection Control

Jürgen Seibel[1], *Sibylle Schneider-Schaulies*[1] *and Burkhard Kleuser*[2]*

[1] Department for Organic Chemistry and Insitute for Virology and Immunobiology, Julius Maximilian University of Würzburg, Würzburg, Germany, [2] Institute of Pharmacy, Free University of Berlin, Berlin, Germany

Keywords: sphingolipid, infection, regulation, membrane, microdomain

Editorial on the Research Topic

Sphingolipids in Infection Control

INTRODUCTION

In spite of the availability of preemptive strategies, infectious diseases continue to be a major threat worldwide. Therefore, there is an urgent demand for continuous development of anti-infective and immune-therapeutic strategies in particular for conditions where conventional interventive means are not available, prohibited, or fail. It was particularly in the more recent past, sphingolipids (SLs) have been explored as crucial molecules in infection processes and targeting sphingolipid (SL) metabolism seems to be a novel strategy for intervention in infectious diseases.

As they are major components of cellular membranes, accumulation levels and turnover of SL species effectively take part in cellular processes involving membrane integrity and dynamics (Hannun and Obeid, 2008; Airola and Hannun, 2013). Biosynthesis and metabolism of SLs are highly complex and—except for initiation of their biosynthesis and irreversible degradation via hydrolysis by sphingosine-1-phosphate lyase—accumulation of any SL species is highly dynamic because they rapidly interconvert due to the activity of a plethora of metabolizing enzymes. Adding further complexity to this system, SL species substantially vary with regard to acyl chain length, saturation, hydroxylation or complexity of their head groups, and compartmentalization of their complex metabolism as exerted by a multitude of enzyme isoforms involved in these processes (excellently reviewed in Hannun and Obeid, 2008; Gault et al., 2010; Feng et al., 2018; Harayama and Riezman, 2018).

Because of their high abundance, the composition of SLs within membranes strongly impacts on their biophysical properties by regulating deformability and fluidity (as important in inward/outward vesiculation), compartmentalization of membrane proteins and associated membrane proximal signaling molecules and hence, signal initiation and cytoskeletal dynamics (Bollinger et al., 2005; Grassme et al., 2007; Hannun and Obeid, 2008). In addition, bioactive SL species such as ceramides, ceramide-1-phosphate, sphingosine and sphingosine-1-phosphate actively take part in signaling processes regulating key cellular processes including cell survival, activation and apoptosis (Schenck et al., 2007; Dimanche-Boitrel et al., 2011; Takabe and Spiegel, 2014; Spiegel et al., 2019). Seminal studies on the role of SL dynamics in various disease pathologies established therapeutic concepts and development of drugs targeting their turnover which has been particularly successful in treatment of sphingolipidoses, atherosclerosis, cystic fibrosis and cancer (Kolter, 2011; Ryland et al., 2011; Schulze and Sandhoff, 2011). In view of progress made in SL regulation at a cellular basis, development of experimental tools also including highly specific inhibitors and genetic ablation strategies as well as experimental test systems, modulation of SL metabolism as therapeutic approach will predictably increase (Loewith et al., 2019).

OPEN ACCESS

Edited by:
Brian Storrie, University of Arkansas for Medical Sciences, United States

Reviewed by:
Motohiro Tani, Kyushu University, Japan

***Correspondence:**
Burkhard Kleuser
kleuser@zedat.fu-berlin.de

Specialty section:
This article was submitted to Membrane Traffic, a section of the journal Frontiers in Cell and Developmental Biology

Received: *19 April 2021*
Accepted: *19 May 2021*
Published: *21 June 2021*

Citation:
Seibel J, Schneider-Schaulies S and Kleuser B (2021) Editorial: Sphingolipids in Infection Control. Front. Cell Dev. Biol. 9:697290. doi: 10.3389/fcell.2021.697290

Membrane dynamics, receptor sorting, cytoskeletal rearrangements and vesicular trafficking are also centrally involved in infection processes by controlling both the interaction of a pathogen with its host cell or trafficking and activity of immune (effector) cells. This Research Topic aimed at providing insight into progress made in this still emerging field in SL research.

RESEARCH CONTRIBUTION OF THE COLLECTION TO THE FIELD

Advances in Technology and Their Implementation

Mechanistical studies there have long been hampered by the lack of suitable tools and test systems which are being continuously developed. The highly cited study of Wigger et al. describes a novel methodology that for the first time allows to monitor the entire ER-associated SL *de novo* biosynthesis involving stable-isotope labeling and liquid chromatography-mass spectrometry.

The microsome based assay does allow for both modulations of this pathway *in vitro*, but also to monitor its alterations in cells or tissues also including immune cells. In addition to isotope labeled, functionalized precursors have been successfully used more recently for this purpose (Fink et al., 2021). Implementation of bio-orthogonal chemistry to generate functionalized compounds has also greatly advanced and enabled detection and trafficking of SLs in fixed and living cells (Haberkant and Holthuis, 2014; Kuerschner and Thiele, 2014). In a primary astrocyte model system, cross-linkable functionalized ceramide analogs and proximity ligation assays were combined to visualize proteins associated with ceramide-enriched platforms (Jiang et al.). Applied in this paper to ceramide tubulin and VDAC1 ceramide complexes, this technique will substantially advance studies on co-detection of proteins in ceramide-enriched microdomains and regulation of this particular interactions. SLs have also been successfully resolved by super-resolution microscopy before (Burgert et al., 2017) and this technique, combined with structured illumination microscopy (SIM) has now been used to unravel accumulation and coating of meningococci with GM1 ganglioside upon uptake into HBMEC (Schlegel et al.).

This study allowed to reveal the importance of cell cycle dependent GM1 increase at the plasma membrane for the efficiency of uptake rather than binding of the pathogen. It thereby unifies substantial advances in a technical approach to visualize SL dynamics and support for their essential role in pathogen host interactions during bacterial infection.

The Role of SL Dynamics in Infection at the Level of Pathogens

Three comprehensive reviews focus on the modulatory capacity of SLs within the life cycle of several pathogenic bacteria ranging from attachment and uptake, formation of intracellular compartments, and interaction with cell autonomous defense mechanisms. Most interestingly, Rolando and Buchrieser report on bacterial strategies, especially bacterially encoded enzymes mimicking SL metabolizing enzymes. These enable them to actively regulate the catabolic SL pathway in eukaryotic cells for their individual demands to counteract host responses and facilitate intracellular growth, and are therefore promising targets for intervention. Kunz and Kozjak-Pavlovic also elaborate on the role of SLs in attachment and uptake of bacteria, however, in common to Banhart et al., focus on sphingolipid mediated regulation of cellular signaling pathways promoting intracellular trafficking and survival. Amongst those, special emphasis is given to formation of a cellular inclusion compartment. This is essential for survival and reproduction of *Chlamydia trachomatis*, and relies for *C. trachomatis* and other chlamydia and chlamydia-like micro-organisms, on acquisition of sphingomyelin and ceramide from the host cell by as yet ill-defined transport mechanism. As referred to in all three reviews, particular SL species proved to be important for the successful interaction of bacteria with their hosts and therefore, host enzymes or bacterial gene products promoting their production might be targets for therapeutic intervention. Less well-investigated to date, targeting of SL metabolizing enzymes can also act antivirally. An example for this is provided by Grafen et al. who report sensitivity of measles virus (MV) replication in lymphocytes to inhibition of the acid ceramidase and sphingosine kinase, most reflecting the inhibitor-induced reduction of cellular metabolic activity (Grafen et al.).

Noteworthy, certain SL species including sphinganine, sphingosine and ceramides, can also directly act as antimicrobials and thereby possibly represent a novel class of antibiotics, as detailed by Kunz and Kozjak-Pavlovic.

As most recently revealed, this may also apply to viral infections (Lang et al., 2020).

The therapeutic potential of another SL subclass, glycosphingolipids (GSL), is discussed by Aerts et al. who review the dual role of those in pathogen binding and uptake, and in regulating immune cell functions important in infection control. Given that they therefore might regulate both processes, therapeutics targeting GSL biosynthesis as already approved for treatment of lysosomal glycolipid storage diseases, might, as discussed by the authors, represent new avenues for infection control.

SL Dynamics Involved in Immune Control of Pathogens

Six contributions elaborate on the impact of SL dynamics in immune cells thereby controlling infections at a cellular rather than the pathogen level. As established, sphingosine-1-phosphate (S1P) gradients effectively promote recruitment of immune cells, also including macrophages. This particular SL emerged, however, as potent regulator of macrophage function and thereby, as of crucial pathogenic importance in infectious and non-infectious diseases as comprehensively reviewed by Weigert et al.. In fact, S1P has proven to be relevant in protection against *Mycobacterium tuberculosis* via its impact on macrophage differentiation (Nadella et al.).

Several contributions to this Research Topic focus on the role of sphingolipid homeostasis in T cells and regulation thereof in response to pathogen challenge.

Hollmann and colleagues highlight current knowledge on the impact of ceramide generation on activation, differentiation and effector functions in distinct T cell populations (Hollmann et al.).

Reporting on studies involving newly generated tools such as mouse strains deficient for or overexpressing sphingolipid-metabolizing enzymes, they discuss recent progress made with regard to translational approaches aiming on T cell modulation in suitable animal (infection) models as a basis for further development in clinical use in humans. Notably, drugs already in clinical use for treatment of non-infectious diseases are amongst the potential candidates for differential modulation of T cell subpopulations. Direct experimental proof for a beneficial effect of regulating the SL pool at the level of sphingomyelin breakdown in T cells is provided by Hose et al. There, T cell specific overexpression of the acid sphingomyelinase (ASM) was protective in *Plasmodium yoelii* infected mice by enhancement of T cell mediated immunity. In line with ASM activity being supportive to T cell immunity, ASM ablation was found to augment susceptibility to *C. rodentium* infection in mice used as a model of mucosal immunity (Meiners et al.).

Strikingly, in this model ASM deficiency was associated with uncontrolled inflammatory T_h1 and T_h17 responses and thereby, progressive colonic pathology. Supporting that ablation of ASM might indeed differentially affect T cell subpopulations, the proportion of regulatory T cells among $CD4^+$ T cells was found elevated in ASM deficient mice, and this was associated with progressive CNS infection in a mouse model earlier (Hollmann et al., 2016).

Finally, two contributions focus on the specific role of sphingomyelin breakdown in T cells and its role in regulating T cell activation at a cellular level. Using Jurkat T cells deficient for the neutral sphingomyelinase 2 (NSM2), Börtlein et al. clearly revealed that this enzyme is of importance for the plasma membrane (PM) composition under homeostatic conditions. Its absence most prominently affected transport of PM cholesterol to the endoplasmic reticulum and production of cholesteryl esters (CE) there. Importantly, prevention of CE production (upon NSM2 ablation or inhibition of cholesterol acetyltransferases) significantly impaired T cell receptor (TCR) driven expansion of both, CD4+ and CD8+ T cells, indicating that the NSM2 activity is of importance for T cell expansion. Within their comprehensive review, Avota et al. provide insight into the role of ASM and NSM2 (and other SL metabolizing enzymes) in various aspects of T cell activation mainly including T cell viability, relay of signals given by TCR or upon co-stimulation or T cell motility and tissue homing. Not surprisingly, the activity of SL metabolizing enzymes needs stringent spatiotemporal control also in T cells where their deregulation by MV results in impaired T cell activation.

CONCLUDING REMARKS

In summary, understanding the role of SL dynamics in infection control can still be regarded as emerging field of research that bears substantial promise for highly fascinating insights into pathogen-host interactions and modulation of immunity, and thereby, development of therapeutics. With the substantial progress made in techniques and tools to study, quantify, visualize and specifically target and modulate SL metabolism as well as the availability of (multi) functionalized SL species in the recent past, achievement of this ambitious goal and transfer into clinical application is very likely to become possible.

AUTHOR CONTRIBUTIONS

JS, SS-S, and BK wrote and corrected the manuscript. All authors contributed to the article and approved the submitted version.

FUNDING

The laboratory work of JS, BK, and SS-S was funded by the DFG in the framework of the RU2123 (Se1410/6-1 and 6/2, Kl 988/8-2; SCHN405-10/1 and 10/2) and the RTG2581.

REFERENCES

Airola, M. V., and Hannun, Y. A. (2013). Sphingolipid metabolism and neutral sphingomyelinases. *Handb. Exp. Pharmacol.* 215, 57–76. doi: 10.1007/978-3-7091-1368-4_3

Bollinger, C. R., Teichgraber, V., and Gulbins, E. (2005). Ceramide-enriched membrane domains. *Biochim. Biophys. Acta* 1746, 284–294. doi: 10.1016/j.bbamcr.2005.09.001

Burgert, A., Schlegel, J., Becam, J., Doose, S., Bieberich, E., Schubert-Unkmeir, A., et al. (2017). Characterization of plasma membrane ceramides by super-resolution microscopy. *Angew. Chem. Int. Ed. Engl.* 56, 6131–6135. doi: 10.1002/anie.201700570

Dimanche-Boitrel, M. T., Rebillard, A., and Gulbins, E. (2011). Ceramide in chemotherapy of tumors. *Recent. Pat. Anticancer. Drug. Discov.* 6, 284–293. doi: 10.2174/157489211796957838

Feng, S., Harayama, T., Montessuit, S., David, F. P., Winssinger, N., Martinou, J. C., et al. (2018). Mitochondria-specific photoactivation to monitor local sphingosine metabolism and function. *eLife* 7:31. doi: 10.7554/eLife.34555.031

Fink, J., Schumacher, F., Schlegel, J., Stenzel, P., Wigger, D., Sauer, M., et al. (2021). Azidosphinganine enables metabolic labeling and detection of sphingolipid de novo synthesis. *Org. Biomol. Chem.* 19, 2203–2212. doi: 10.1039/d0ob02592e

Gault, C. R., Obeid, L. M., and Hannun, Y. A. (2010). An overview of sphingolipid metabolism: from synthesis to breakdown. *Adv. Exp. Med. Biol.* 688, 1–23. doi: 10.1007/978-1-4419-6741-1_1

Grassme, H., Riethmuller, J., and Gulbins, E. (2007). Biological aspects of ceramide-enriched membrane domains. *Progress Lipid Res.* 46, 161–170. doi: 10.1016/j.plipres.2007.03.002

Haberkant, P., and Holthuis, J. C. (2014). Fat & fabulous: bifunctional lipids in the spotlight. *Biochim. Biophys. Acta* 1841, 1022–1030. doi: 10.1016/j.bbalip.2014.01.003

Hannun, Y. A., and Obeid, L. M. (2008). Principles of bioactive lipid signalling: lessons from sphingolipids. *Nat. Rev. Mol. Cell Biol* 9, 139–150. doi: 10.1038/nrm2329

Harayama, T., and Riezman, H. (2018). Understanding the diversity of membrane lipid composition. *Nat. Rev. Mol. Cell Biol.* 19, 281–296. doi: 10.1038/nrm.2017.138

Hollmann, C., Werner, S., Avota, E., Reuter, D., Japtok, L., Kleuser, B., et al. (2016). Inhibition of acid sphingomyelinase allows for selective targeting of CD4(+) conventional versus Foxp3(+) regulatory

T cells. *J. Immunol.* 197, 3130–3141. doi: 10.4049/jimmunol.1600691

Kolter, T. (2011). A view on sphingolipids and disease. *Chem. Phys. Lipids* 164, 590–606. doi: 10.1016/j.chemphyslip.2011.04.013

Kuerschner, L., and Thiele, C. (2014). Multiple bonds for the lipid interest. *Biochim. Biophys. Acta* 1841, 1031–1037. doi: 10.1016/j.bbalip.2013.12.018

Lang, J., Bohn, P., Bhat, H., Jastrow, H., Walkenfort, B., Cansiz, F., et al. (2020). Acid ceramidase of macrophages traps herpes simplex virus in multivesicular bodies and protects from severe disease. *Nat. Commun.* 11:1338. doi: 10.1038/s41467-020-15072-8

Loewith, R., Riezman, H., and Winssinger, N. (2019). Sphingolipids and membrane targets for therapeutics. *Curr. Opin. Chem. Biol.* 50, 19–28. doi: 10.1016/j.cbpa.2019.02.015

Ryland, L. K., Fox, T. E., Liu, X., Loughran, T. P., and Kester, M. (2011). Dysregulation of sphingolipid metabolism in cancer. *Cancer Biol. Ther.* 11, 138–149. doi: 10.4161/cbt.11.2.14624

Schenck, M., Carpinteiro, A., Grassme, H., Lang, F., and Gulbins, E. (2007). Ceramide: physiological and pathophysiological aspects. *Arch. Biochem. Biophys.* 462, 171–175. doi: 10.1016/j.abb.2007.03.031

Schulze, H., and Sandhoff, K. (2011). Lysosomal lipid storage diseases. *Cold Spring Harb. Perspect Biol.* 3:4804. doi: 10.1101/cshperspect.a004804

Spiegel, S., Maczis, M. A., Maceyka, M., and Milstien, S. (2019). New insights into functions of the sphingosine-1-phosphate transporter SPNS2. *J. Lipid Res.* 60, 484–489. doi: 10.1194/jlr.S091959

Takabe, K., and Spiegel, S. (2014). Export of sphingosine-1-phosphate and cancer progression. *J. Lipid Res.* 55, 1839–1846. doi: 10.1194/jlr.R046656

Conflict of Interest: The authors declare that the research was conducted in the absence of any commercial or financial relationships that could be construed as a potential conflict of interest.

frontiers in Immunology

ORIGINAL RESEARCH
published: 31 May 2019
doi: 10.3389/fimmu.2019.01225

T Cell-Specific Overexpression of Acid Sphingomyelinase Results in Elevated T Cell Activation and Reduced Parasitemia During *Plasmodium yoelii* Infection

Matthias Hose[1], *Anne Günther*[1], *Hanna Abberger*[1], *Salina Begum*[2], *Marek Korencak*[3], *Katrin A. Becker*[2], *Jan Buer*[1], *Astrid M. Westendorf*[1] *and Wiebke Hansen*[1]*

[1] *Institute of Medical Microbiology, University Hospital Essen, University Duisburg-Essen, Essen, Germany,* [2] *Institute of Molecular Biology, University Hospital Essen, University Duisburg-Essen, Essen, Germany,* [3] *Institute for HIV Research, University Hospital Essen, University Duisburg-Essen, Essen, Germany*

OPEN ACCESS

Edited by:
Sibylle Schneider-Schaulies, University of Wuerzburg, Germany

Reviewed by:
Thomas Jacobs, Bernhard-Nocht-Institut für Tropenmedizin (BMITM), Germany
Marcus Altfeld, Heinrich Pette Institut, Leibniz-Institut für Experimentelle Virologie, Germany

***Correspondence:**
Wiebke Hansen
wiebke.hansen@uk-essen.de

Specialty section:
This article was submitted to Microbial Immunology, a section of the journal Frontiers in Immunology

Received: *14 February 2019*
Accepted: *14 May 2019*
Published: *31 May 2019*

Citation:
Hose M, Günther A, Abberger H, Begum S, Korencak M, Becker KA, Buer J, Westendorf AM and Hansen W (2019) T Cell-Specific Overexpression of Acid Sphingomyelinase Results in Elevated T Cell Activation and Reduced Parasitemia During Plasmodium yoelii Infection. Front. Immunol. 10:1225. doi: 10.3389/fimmu.2019.01225

The enzyme acid sphingomyelinase (ASM) hydrolyzes sphingomyelin to ceramide and is thereby involved in several cellular processes such as differentiation, proliferation, and apoptosis in different cell types. However, the function of ASM in T cells is still not well characterized. Here, we used T cell-specific ASM overexpressing mice (t-ASM/CD4cre) to clarify the impact of cell-intrinsic ASM activity on T cell function *in vitro* and *in vivo*. We showed that t-ASM/CD4cre mice exhibit decreased frequencies of Foxp3$^+$ T regulatory cells (Tregs) within the spleen. Enforced T cell-specific ASM expression resulted in less efficient induction of Tregs and promoted differentiation of CD4$^+$CD25$^-$ naïve T cells into IFN-γ producing Th1 cells *in vitro*. Further analysis revealed that ASM-overexpressing T cells from t-ASM/CD4cre mice show elevated T cell receptor (TCR) signaling activity accompanied with increased proliferation upon stimulation *in vitro*. *Plasmodium yoelii* infection of t-ASM/CD4cre mice resulted in enhanced T cell activation and was associated with reduced parasitemia in comparison to infected control mice. Hence, our results provide evidence that ASM activity modulates T cell function *in vitro* and *in vivo*.

Keywords: sphingolipids, acid sphingomyelinase, T cells, T cell activation, malaria

INTRODUCTION

The sphingolipid metabolism involves several enzymes including acid sphingomyelinase (ASM), a lipid hydrolase enzyme constitutively expressed in lysosomes and released to the outer leaflet of the cell membrane upon triggering of e.g., CD95, TNF receptors, or CD28 (1–4). ASM cleaves sphingomyelin into ceramide and phosphocholine (5), resulting in the formation of ceramide-rich signaling platforms at the outer leaflet of the plasma membrane (6), which play an important role in regulating differentiation, proliferation, and apoptosis in different cell types (7, 8). Studies performed with ASM-deficient mice or treatment of cells with ASM-inhibitors such as amitriptyline suggests that ASM activity is involved in T cell development and function (9–14). For CD8$^+$ T cells, it was shown that ASM-deficiency results in impaired secretion of IFN-γ and cytotoxic granula in lymphocytic choriomeningitis (LCMV)-infected mice (11). Recently, two independent studies

provided evidence that ASM activity is also involved in $CD4^+$ regulatory T cell (Treg) development, survival, and function (12, 13). ASM-deficient or amitriptyline-treated mice had enhanced numbers of Tregs in comparison to wildtype (WT) or non-treated mice. In addition, ASM-deficient Tregs showed enhanced turnover of CTLA-4 and exhibited increased suppressive activity *in vitro* (13). Blocking of ASM activity in human $CD4^+$ T cells by pharmacological inhibitors or by siRNAs has been shown to interfere with T cell receptor (TCR) signaling, proliferation, and T helper (Th) cell differentiation upon stimulation *in vitro* (14). However, most of these studies investigated the impact of ASM in the whole $CD4^+$ T cell population or focused on Tregs, but did not investigate the impact of ASM on $CD4^+$ non-Tregs. In addition, results from ASM-deficient mice do not exclude an indirect influence of other cells on T cell function, and treatment with ASM inhibitors might also act on other enzymes involved in the sphingolipid metabolism, such as acid ceramidase (15). Hence, the impact of cell-intrinsic ASM activity in $CD4^+$ non-Tregs still remains unclear.

Malaria, caused by the parasite *Plasmodium*, is still one of the most deadly human infectious diseases worldwide. The parasite has a complex life cycle resulting in different innate and adaptive immune mechanisms involved in parasite control and clearance (16). During the blood-stage of infection, $CD4^+$ T cells play a crucial role in regulating the immune response. While IFN-γ production by T cells and $CD4^+$ T cell help for B cell responses are required for control and elimination of infected red blood cells (iRBCs) (17), $CD4^+Foxp3^+$ Tregs counteract excessive inflammatory immune responses that might result in exacerbated tissue damage. Expansion of $Foxp3^+$ Tregs was observed in *Plasmodium*-infected patients (18, 19) as well as in different malaria mouse models (20–22) and their depletion resulted in enhanced T cell responses accompanied by reduced parasitemia (20). Besides $Foxp3^+$ Tregs, IL-10 expressing $CD4^+$ T cells with immunosuppressive function were described to be induced during *Plasmodium yoelii* (*P. yoelii*) infection (20, 23), at least in part due to stimulation of naïve T cells by IL-10 producing $CD11c^+$ dendritic cells (DCs) (24). Hence, $CD4^+$ T cells are important for the tight regulation of immune responses during *Plasmodium* infection.

In the present study, we provide evidence that T cell-intrinsic ASM activity is induced by anti-CD3/anti-CD28 stimulation. T cell-specific overexpression of ASM resulted in elevated phosphorylation of TCR signaling molecules and proliferative activity upon stimulation *in vitro*. Strikingly, *P. yoelii*-infected t-ASM/CD4cre mice exhibited a more activated T cell phenotype accompanied by improved pathogen clearance in comparison to infected control littermates. Thus, the sphingomyelin/ceramide pathway might represent a promising target for the modulation of T cell activity during ongoing immune responses *in vivo*.

MATERIALS AND METHODS

Mice and Parasites

T-ASM mice (25) and CD4cre mice (26) both on C57BL/6 background were crossed and maintained under specific pathogen-free conditions at the Animal Facility of University Hospital Essen. Cryopreserved *P. yoelii* 17NXL (non-lethal) infected red blood cells (iRBCs) were passaged once through C57BL/6 wildtype mice before being used in experimental animals. For infection 1×10^5 iRBCs were injected i.v. at day 0. The frequency of iRBCs (parasitemia) was determined by microscopic examination of Giemsa-stained blood films. All animal experiments were performed in accordance to the guidelines of the German Animal Protection Law and approved by the state authority for nature, environment, and customer protection, North Rhine-Westphalia, Germany.

Cell Isolation and Activation

Single cell suspensions of splenocytes were generated by rinsing spleens with erythrocyte lysis buffer and washing with PBS supplemented with 2% FCS and 2 mM EDTA. T cells were isolated from splenocytes either by using the $CD4^+$ or $CD8^+$ T cell isolation kit (Miltenyi Biotec, Bergisch Gladbach, Germany) alone or followed by anti-CD4, anti-CD25, anti-CD8 staining, and cell sorting using an Aria II Cell Sorter (BD Biosciences, Heidelberg, Germany). T cells were stimulated with 5 μg/ml anti-CD3 plate-bound and 1 μg/ml anti-CD28 soluble (both BD Biosciences, Heidelberg, Germany) in IMDM culture medium supplemented with 10 % heat-inactivated FCS, 25 mM β-Mercapthoethanol and antibiotics (100 U/ml penicillin, 0.1 mg/ml streptomycin).

T Cell Differentiation

For iTreg differentiation $CD4^+CD25^-$ T cells were stimulated with anti-CD3/anti-CD28 as described above in the presence of 20 ng/ml IL-2 (eBioscience, ThermoFisher Scientific, Langenselbold, Germany) and 5 ng/ml TGF-β1 (R&D Systems, Bio-Techne, Wiesbaden, Germany) for 72 h. Th1 cells were differentiated by stimulating sorted $CD4^+CD25^-$ T cells with anti-CD3/anti-CD28 in the presence of 200 ng/ml anti-IL-4 (eBioscience, ThermoFisher Scientific, Langenselbold, Germany) and 20 ng/ml IL-12 (R&D Systems, Bio-Techne, Wiesbaden, Germany) for 6 days. At day 3 cells were split and fresh IMDM medium supplemented with 1 μg/ml anti-CD28 and 200 ng/ml anti-IL-4 was added.

Proliferation

T cells were labeled with the cell proliferation dye eFluor 670 (eBioscience, ThermoFisher Scientific, Langenselbold, Germany) according to the manufacturers protocol and stimulated for 3 days with anti-CD3 and anti-CD28 antibodies in the presence of irradiated splenocytes. Proliferation was assessed as loss of the proliferation dye by flow cytometry.

Antibodies and Flow Cytometry

Anti-CD4, anti-CD8, anti-CD25, anti-IFN-γ (all BD Biosciences, Heidelberg Germany), anti-Foxp3, anti-Ki67 (eBioscience, ThermoFisher Scientific, Langenselbold, Germany), anti-Akt, anti-phosho-Akt(Ser473), anti-phospho-PLCγ1(Tyr783), anti-p38MAPK, and anti-phospho-p38MAPK(Thr180/Tyr182) (Cell Signaling, Frankfurt, Germany) were used as fluorescein isothiocyanate (FITC), pacific blue (PB), phycoerythrin (PE), BD Horizon V450, allophycocyanin (APC), AlexaFlour647 (AF647),

PE-cyanin 7 (PE-Cy7), or peridinin-chlorophyll protein (PerCp) conjugates. Dead cells were identified by staining with the fixable viability dye eFluor 780 (eBioscience, ThermoFisher Scientific, Langenselbold, Germany). Intracellular staining for Foxp3 and Ki67 was performed with the Foxp3 staining kit (eBiocience, ThermoFisher Scientific, Langenselbold, Germany) according to the manufacturer's protocol. IFN-γ expression was measured by stimulating splenocytes with 10 ng/ml phorbol 12-myristate 13-acetate (PMA) and 100 μg/ml ionomycin (both Sigma-Aldrich, München, Germany) for 4 h in the presence of 5 μg/ml Brefeldin A, followed by treatment with 2% paraformaldehyd and 0.1% IGEPAL®CA-630 (Sigma- Aldrich, München, Germany), and staining with the respective antibody for 30 min at 4°C. For analyzing phosphorylation of TCR signaling molecules, cells were stimulated with 5 μg/ml anti-CD3 and 1 μg/ml anti-CD28 for 5 or 10 min, treated with 2% paraformaldehyd and 0.1% IGEPAL®CA-630, and stained with the respective antibody for 30 min at 4°C. Flow cytometric analyses were performed with a LSR II instrument using DIVA software (BD Biosciences, Heidelberg Germany).

Serum Cytokines

Blood samples were collected, incubated at room temperature and centrifuged for 10 min at 6,797 × *g*. Cytokines were quantified by using a polystyrene bead-based Luminex Assay (R&D Systems, Abingdon, UK) and a Luminex 200 system with IS software according to the manufacturers recommendations.

ASM Activity

$CD4^+$ and $CD8^+$ T cells were isolated from spleen by using the $CD4^+$ or $CD8^+$ T cell isolation kit (Miltenyi Biotec, Bergisch Gladbach, Germany). $CD19^+$ B cells were isolated from splenocytes by cell sorting using an Aria II Cell Sorter (BD Biosciences, Heidelberg, Germany). T cells and B cells were either left untreated or stimulated with anti-CD3/anti-CD28 or 1 μg/ml LPS (Invivogen, Toulouse, France) overnight and lysed in 250 mM sodium acetate, 1% IGEPAL®CA-630 and 100 μM $ZnCl_2$ for 5 min on ice, followed by bath sonication for 10 min. BODIPY FL 12C-SM (ThermoFisher Scientific, Langenselbold, Germany) in assay buffer was added to the cells to obtain 100 pmol SM and 0.1% NP40 within the reaction mix and incubated at 37°C with shaking. Lipids were extracted by adding chloroform/ methanol (2:1) and centrifugation, followed by isolation and drying of the lower phase. Cell pellets were resuspended in chloroform/ methanol (2:1) and spotted on a thin-layer chromatography plate. After running in chloroform/ methanol (80:20), plates were air-dried, scanned with a Typhoon FLA 9,500 laser scanner and analyzed with ImageQuant software (both GE Healthcare Life Sciences, US). Specific Asm activity was calculated as conversion of product per protein and time.

Statistical Analysis

Statistical analyses were performed with Mann-Whitney *U*-test or two-way ANOVA with Bonferroni's multiple comparisons test. Statistical significance was set at the levels of $^*p < 0.05$, $^{**}p < 0.01$, and $^{***}p < 0.001$. All analyses were calculated with Graph Pad Prism Software (Graph Pad Software, La Jolla, CA).

RESULTS

Decreased Relative Numbers of $Foxp3^+$ Regulatory T Cells in T Cell-Specific ASM Overexpressing t-ASM/CD4cre Mice

To study the cell intrinsic effect of ASM on the T cell phenotype, we made use of t-ASM mice crossed with CD4cre mice. In t-ASM mice, the *hprt* gene locus was replaced by a construct consisting of the ubiquitous CMV immediate early enhancer/chicken β-actin fusion promotor, and a loxP-STOP-loxp cassette followed by the ASM encoding cDNA (Smpd1) (25). Breeding of these mice with CD4cre mice results in T cell-specific excision of the STOP cassette and enforced ASM expression. To confirm elevated ASM expression in T cells from t-ASM/CD4cre double-transgenic mice, we analyzed the ASM activity of unstimulated and anti-CD3/anti-CD28 stimulated T cells isolated from spleen of t-ASM/CD4cre (TG) and t-ASM controls (WT). $CD4^+$ and $CD8^+$ naïve T cells from t-ASM/CD4cre mice exhibited elevated ASM activity compared to T cells isolated from WT littermates. Stimulation of T cells with anti-CD3/anti-CD28 resulted in an increase of ASM activity in $CD4^+$ and $CD8^+$ T cells from WT controls. This induction in ASM activity upon stimulation was strongly enhanced in T cells isolated from t-ASM/CD4cre mice, which showed approximately 10 fold higher ASM activity than stimulated T cells from littermate controls (**Figure 1A**). Stimulation of $CD19^+$ B cells with LPS also resulted in elevated ASM activity. However, we did not observe differences in ASM activity between unstimulated or LPS-stimulated $CD19^+$ B cells isolated from t-ASM/CD4cre mice compared to control mice (**Figure 1A**). Hence, t-ASM/CD4cre mice are a suitable model to analyze the impact of ASM activity on T cell phenotype and function.

First, we asked whether enhanced T cell-specific ASM activity has an impact on the development of T cells. Therefore, we determined the frequencies of $CD4^+$ T cells, $CD8^+$ T cells, and $Foxp3^+$ Tregs of $CD4^+$ T cells in thymus and spleen isolated from t-ASM/CD4cre mice and WT controls. Whereas, we did not observe any differences in the percentage of $CD4^+$ T cells and $CD8^+$ T cells (**Figure 1B**), T cell-specific overexpression of ASM resulted in a significant reduction of Foxp3-expressing Tregs in the spleen of t-ASM/CD4cre mice compared to controls (**Figure 1C**).

ASM Overexpression Impairs Treg Differentiation and Improves Th1 Differentiation *in vitro*

Since we observed decreased frequencies of Tregs in the spleen, but not in the thymus of t-ASM/CD4cre mice (**Figure 1C**), we next analyzed the efficacy of ASM-overexpressing T cells to differentiate into induced Tregs (iTregs) *in vitro*. For this purpose, we isolated $CD4^+CD25^-$ T cells from t-ASM/CD4cre mice as well as WT littermates and stimulated them with anti-CD3/anti-CD28 in the presence (iTreg) or

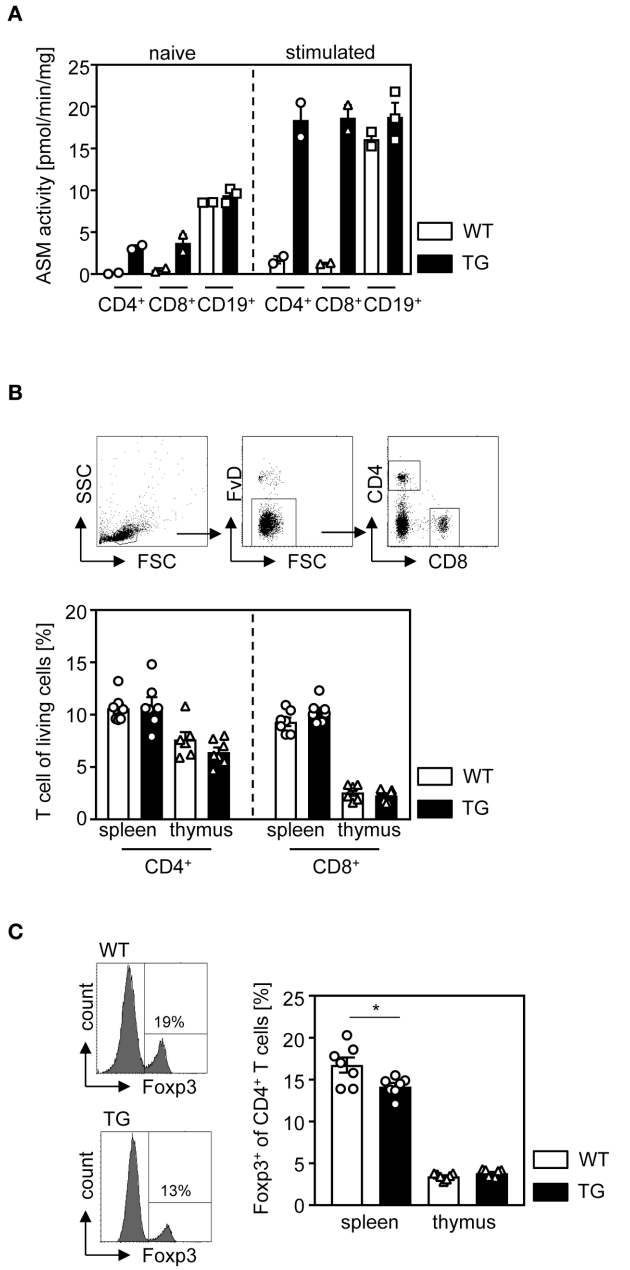

FIGURE 1 | T cell-specific overexpression of ASM results in decreased relative numbers of regulatory T cells in the spleen. **(A)** $CD4^+$ and $CD8^+$ T cells as well as $CD19^+$ B cells were isolated from t-ASM/CD4cre mice (TG) or t-ASM littermates (WT), left untreated or stimulated overnight with anti-CD3/anti-CD28 or LPS, respectively, and analyzed for ASM activity. **(B)** The percentages of $CD4^+$, $CD8^+$ T cells, and **(C)** $Foxp3^+$ Tregs of $CD4^+$ T cells within the spleen and thymus of t-ASM/CD4cre mice (TG) and t-ASM littermates (WT) were determined by flow cytometry. The gating strategy is shown in the upper panel of **(B)**. Data from **(A)** $n = 2$–3 mice and **(B,C)** two independent experiments with $n = 6$–7 mice in total are shown as mean ± SEM. $^*p < 0.05$.

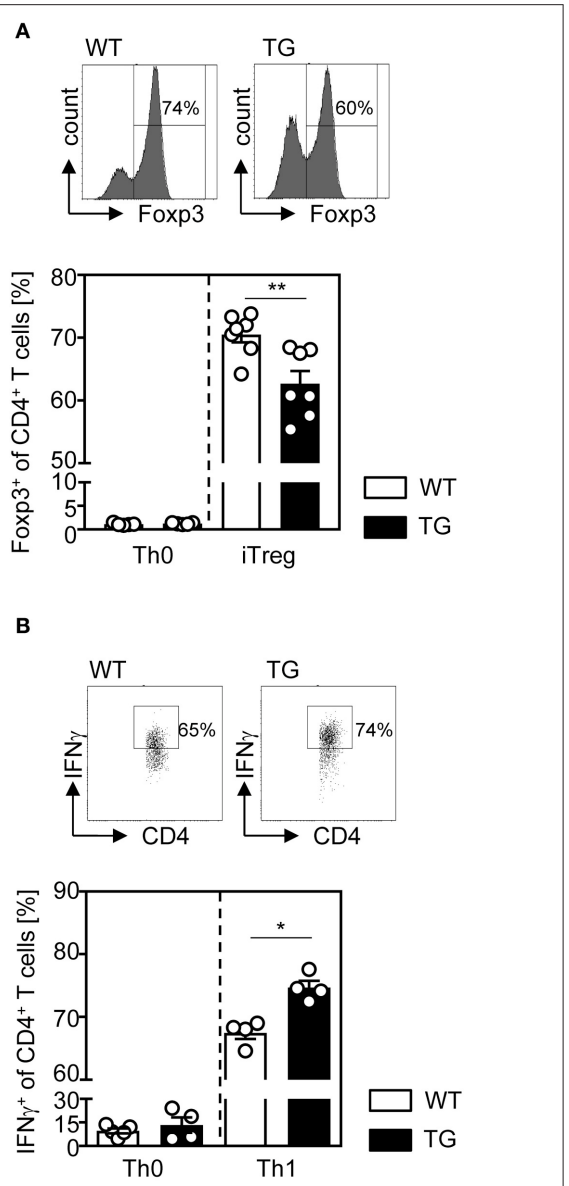

FIGURE 2 | Impaired regulatory T cell differentiation and elevated induction of Th1 cells from ASM-overexpressing $CD4^+$ T cells under respective polarizing conditions *in vitro*. **(A)** Sorted $CD4^+CD25^-$ T cells from t-ASM/CD4cre mice (TG) and t-ASM littermates (WT) were stimulated with anti-CD3 and anti-CD28 and differentiated into $Foxp3^+$ Tregs in the presence of TGF-β and IL-2 for 3 days or **(B)** into IFN-γ producing Th1 cells, by adding IL-12, and anti-IL-4 to the cells for 6 days. Respective controls (Th0) were only stimulated with anti-CD3 and anti-CD28. Data from two to three independent experiments with $n = 6$–7 mice in total are shown as mean ± SEM. $^*p < 0.05$, $^{**}p < 0.01$.

absence (Th0) of IL-2 and TGF-β. As depicted in **Figure 2A**, T cell-specific overexpression of ASM resulted in significantly reduced induction of $Foxp3^+$ iTregs compared to WT controls (**Figure 2A**). In addition, we investigated the capacity of $CD4^+CD25^-$ T cells to differentiate into IFN-γ producing Th1 cells *in vitro*. $CD4^+CD25^-$ T cells were isolated from T cell-specific ASM-overexpressing mice and WT littermates, stimulated with anti-CD3/anti-CD28 and treated with IL-12 and anti-IL-4 (Th1). As control, T cells were stimulated without adding IL-12 and anti-IL-4 (Th0). Enforced ASM expression resulted in a significantly increased induction of

IFN-γ producing T cells upon stimulation under Th1 polarizing conditions (**Figure 2B**).

ASM Overexpressing T Cells Exhibit Increased Proliferative Activity and T Cell Receptor Signaling *in vitro*

For analyzing whether ASM expression has also an impact on the proliferative response of T cells, we isolated $CD4^+CD25^-$ T cells from naïve t-ASM/CD4cre mice and control littermates, labeled them with the cell proliferation dye eFluor 670 and left them untreated or stimulated them with anti-CD3 and anti-CD28 for 3 days *in vitro*. As expected, unstimulated T cells showed only very low proliferative activity with no differences between ASM-overexpressing cells and controls. However, $CD4^+CD25^-$ T cells from t-ASM/CD4cre mice exhibited significant elevated proliferation compared to T cells from WT littermates upon stimulation *in vitro* (**Figure 3A**). To gain further insights into the underlying processes, we investigated the activation of the TCR signaling pathway in more detail. Upon TCR activation a cascade of several signaling molecules, including PLCγ, Akt and p38 is phosphorylated (27). To analyze the impact of T cell-intrinsic ASM expression on TCR signaling, we isolated splenocytes from t-ASM/CD4cre mice and respective littermates, stimulated them with anti-CD3/anti-CD28 and analyzed the phosphorylation of Akt, PLCγ, and p38 MAPK on gated $CD4^+Akt^+$, $CD4^+$, or $CD4^+p38^+$ T cells, respectively at different time points by flow cytometry. As expected, we detected an increased phosphorylation of all three molecules in WT and ASM-overexpressing T cells upon activation. Strikingly, enforced expression of ASM in T cells resulted in elevated phosphorylation of Akt, PLCγ, and p38 upon TCR stimulation *in vitro* (**Figure 3B**). These results indicate that anti-CD3/anti-CD28 stimulation induces ASM activity which in turn influences the TCR signaling pathway and thereby the proliferation and differentiation of $CD4^+$ T cells *in vitro*.

T-ASM/CD4cre Mice Show Enhanced T Cell Proliferation and IFN-γ Production in Response to *P. yoelii* Infection

Our data show that T cell-specific overexpression of ASM enhances T cell activation upon stimulation *in vitro*. Therefore, we next asked whether enforced ASM activity in T cells also results in elevated immunity in the more complex *in vivo* situation. For this purpose, we infected t-ASM/CD4cre mice and WT control littermates with *P. yoelii*. At day 14 post infection (p.i.), we analyzed the phenotype of T cells from spleen of infected mice by flow cytometry. As depicted in **Figures 4A,B**, the frequencies of $CD4^+$ T cells, $CD8^+$ T cells, as well as $Foxp3^+$ Tregs of $CD4^+$ T cells did not differ between *P. yoelii*-infected T cell-specific ASM-overexpressing mice and control littermates (**Figures 4A,B**). Well in line with our *in vitro* data, we detected significantly elevated frequencies of proliferated $CD4^+$ T cells as well as $CD8^+$ T cells in t-ASM/CD4cre mice compared to WT controls as measured by Ki67 expression (**Figure 4C**). Moreover, the percentage of IFN-γ expressing $CD4^+$ T cells and $CD8^+$ T cells was significantly increased in T cell-specific ASM overexpressing mice upon *P. yoelii* infection in comparison to WT littermates (**Figure 4D**). To gain further insights into the impact of ASM expression on *Plasmodium*-specific T cell responses, we analyzed the frequencies of $CD11a^+CD49d^+$ $CD4^+$ T cells as well as the percentage of CD11a-expressing $CD8^+$ T cells. This approach was already described for the detection of antigen-specific T cells during *Plasmodium* infection (28). We did not observe differences in the percentages of $CD11a^+CD49d^+$ $CD4^+$ T cells between T cell-specific ASM overexpressing mice and control littermates at least at day 14 p.i. (**Figure 4E**). However, *P. yoelii* infection of t-ASM/CD4cre mice resulted in significantly increased frequencies of antigen-experienced $CD8^+$ T cells in comparison to WT littermates. Together, these data suggest that T cell-intrinsic ASM activity modulates T cell activation during an ongoing immune response *in vivo*.

Enhanced Systemic Pro-Inflammatory Cytokine Production and Reduced Parasitemia in *P. yoelii*-Infected t-ASM/CD4cre Mice

To further investigate the impact of ASM-dependent increased T cell activation on the course of *P. yoelii* infection, we determined the amount of pro-inflammatory cytokines in serum of t-ASM/CD4cre mice and WT littermates at day 14 post infection (p.i.). *P. yoelii*-infected T cell-specific ASM-overexpressing mice exhibited a significant increase in systemic production of IL-6, as well as IFN-γ and TNF-α, although statistically not significant, in comparison to control mice (**Figure 5A**). Finally, we asked whether the elevated T cell response in t-ASM/CD4cre mice influences the parasitemia upon *P. yoelii* infection. For this purpose we determined the percentage of infected RBCs at day 4, 7, 9, 14, 16, 18, and 21 p.i. by Giemsa-stained blood smears and detected significantly less parasitized RBCs in t-ASM/CD4cre mice than in WT littermates at day 14 p.i. (**Figure 5B**). In summary, these results indicate that enforced ASM expression in T cells results in elevated T cell activation in *P. yoelii*-infected mice accompanied by improved parasite clearance.

DISCUSSION

The enzyme ASM hydrolyzes sphingomyelin to ceramide upon activation by several cellular stress signals (29). This results in the formation of ceramide-rich platforms within the cell membrane which have an impact on different cellular processes. It was already proposed that ASM also influences activation, differentiation, and stability of $CD4^+$ T cell subsets. However, these studies either addressed the impact of ASM on whole $CD4^+$ T cells (9, 10, 14) or focused on Tregs (12, 13) isolated from ubiquitous ASM-deficient mice or upon treatment with pharmacological inhibitors of ASM. Here, we made use of T cell-specific ASM overexpressing mice to clarify the T cell-intrinsic effect of ASM activity on T cells in more detail. By this approach we can exclude an indirect effect of ASM expressed by other cells or side effects of pharmacological ASM inhibitor treatment such as inhibition of other enzymes involved in the sphingolipid metabolism.

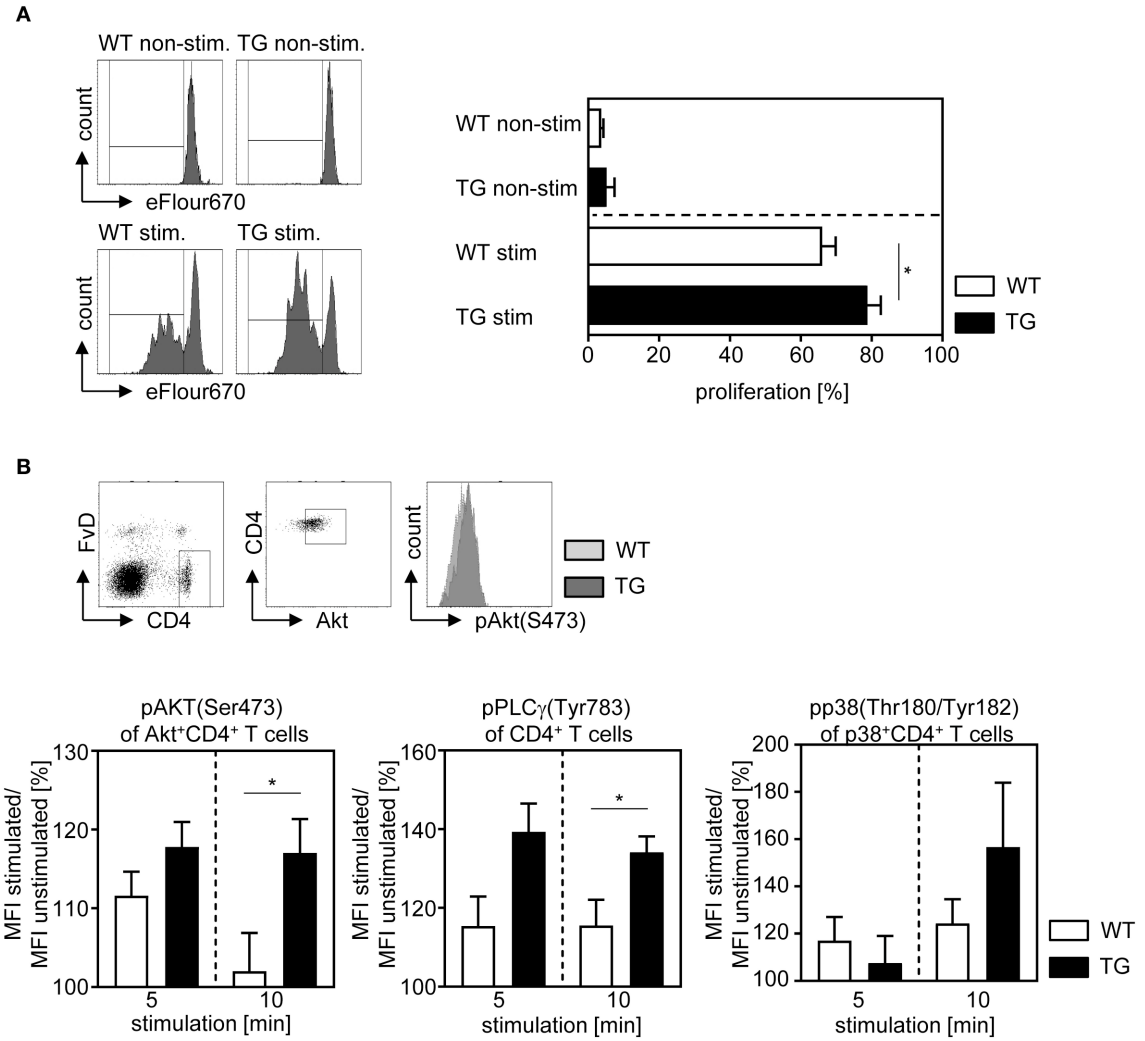

FIGURE 3 | Overexpression of ASM in T cells enhances the proliferative activity and T cell receptor signaling. **(A)** $CD4^+CD25^-$ T cells were isolated from t-ASM/CD4cre mice (TG) or t-ASM controls (WT), labeled with cell proliferation dye eFluor 670 and stimulated for 72 h with anti-CD3 and anti-CD28. Proliferation was assessed as loss of cell proliferation dye eFluor 670 by flow cytometry. **(B)** Splenocytes were isolated from t-ASM/CD4cre mice (TG) or t-ASM controls (WT), left unstimulated or stimulated with anti-CD3 and anti-CD28 for 5 or 10 min and analyzed for phospho-Akt of gated Akt^+CD4^+ T cells, phospho-PLCγ1 of gated $CD4^+$ T cells and phospho-p38 of gated $p38^+CD4^+$ T cells by flow cytometry. The gating strategy and a representative histogram-overlay of Akt phosphorylation of stimulated $CD4^+$ T cells from t-ASM/CD4cre mice (TG) and t-ASM controls (WT) are shown in the upper panel. The increase in phosphorylation was calculated as percentage MFI stimulated/ MFI unstimulated. Results from two to three independent experiments with $n = 5$–9 mice in total are summarized as mean ± SEM. $^*p < 0.05$.

Our data indicate that T cell-specific overexpression of ASM results in significantly reduced relative number of $Foxp3^+$ Tregs within the spleen (**Figure 1C**). Well in line, ASM-deficient mice showed an increase in Treg numbers (12, 13). Interestingly, we detected no differences in the percentage of Tregs within the thymus, which suggests that T cell-intrinsic ASM activity does not influence the development of thymus-derived Tregs *per se*, but rather their induction and/ or stability in the periphery. Hollmann and colleagues claimed that Tregs are more resistant to ASM-deficiency than $CD4^+Foxp3^-$ T cells, since they observed a reduction in absolute cell numbers of $CD4^+Foxp3^-$ non-Tregs, but no differences in $CD4^+CD25^+Foxp3^+$ Treg numbers in Asm-deficient mice and after treatment of mice with amitriptyline (13). In contrast, Zhou et al., detected increased relative as well as absolute numbers of $CD4^+CD25^+Foxp3^+$ Tregs in spleen of ASM-deficient mice (12). We demonstrate that sorted ASM-overexpressing $CD4^+CD25^-$ T cells differentiate less efficiently into $Foxp3^+$ Tregs upon stimulation in the presence of IL-2 and TGF-β *in vitro* than WT controls (**Figure 2A**). Similar results were also obtained from ASM-deficient T cells, which expressed more Foxp3 than WT cells under Treg polarizing conditions *in vitro* (12). Together these results provide evidence that T cell-intrinsic ASM activity is involved in the *de novo* induction of iTregs rather than in the intrathymic development.

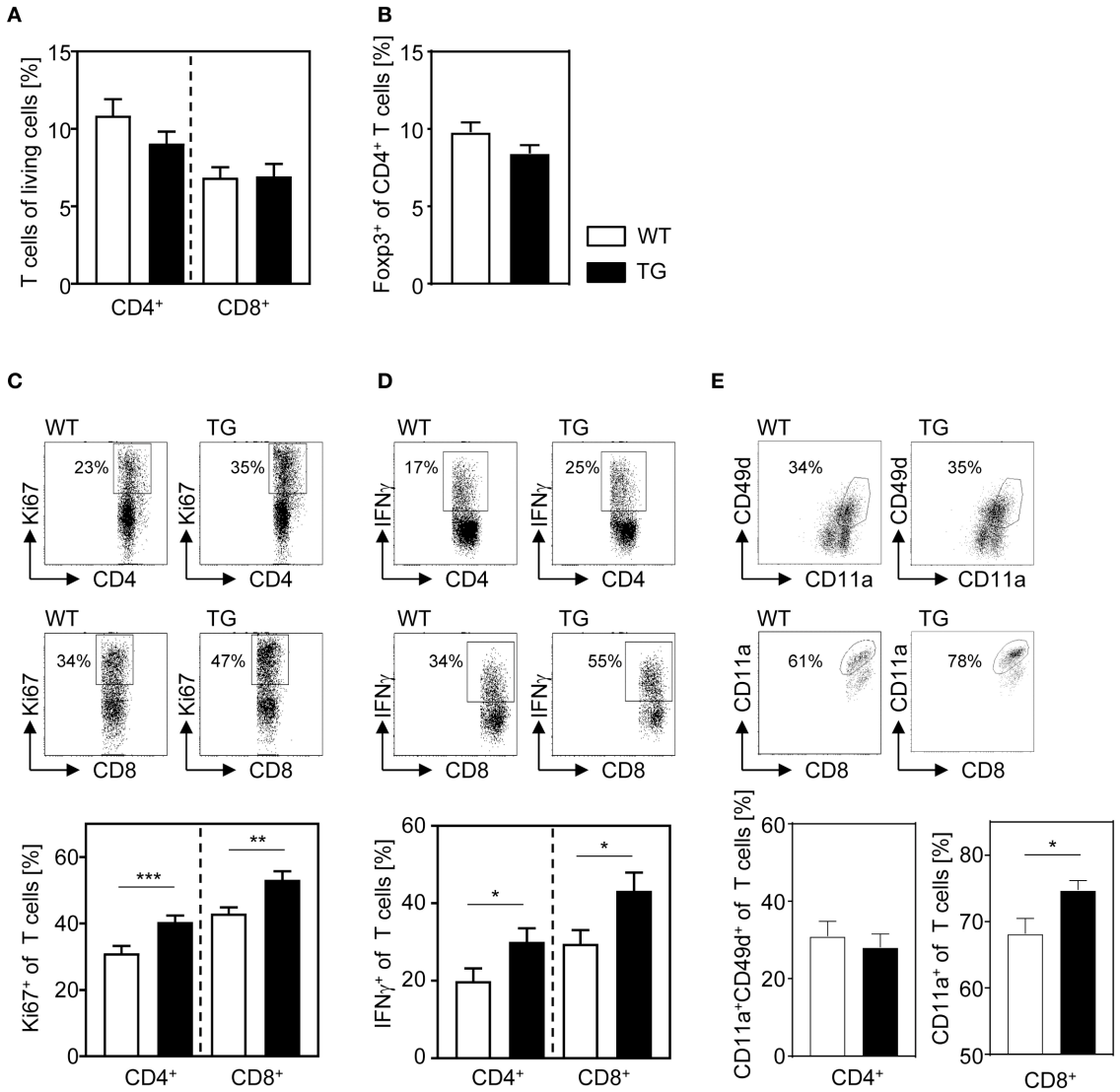

FIGURE 4 | T cell-specific overexpression of ASM results in enhanced T cell activation after *P. yoelii* infection. T-ASM/CD4cre mice (TG) and t-ASM littermates (WT) were infected with *P. yoelii* and analyzed at day 14 post infection. **(A)** The frequency of $CD4^+$ T cells and $CD8^+$ T cells, **(B)** $Foxp3^+$ regulatory T cells of $CD4^+$ T cells, **(C)** Ki67- expressing, and **(D)** IFN-γ producing $CD4^+$ T cells and $CD8^+$ T cells as well as the percentage of **(E)** $CD11a^+CD49d^+$ $CD4^+$ T cells and CD11a-expressing $CD8^+$ T cells from spleen of *P. yoelii*-infected t-ASM/CD4cre mice (TG) and t-ASM littermates (WT) were determined by flow cytometry. Representative dot blots are shown in the upper panel of **(C–E)**. Results from at least three independent experiments with $n = 14–19$ mice in total are summarized as mean ± SEM. $^*p < 0.05$, $^{**}p < 0.01$, $^{***}p < 0.001$.

To gain further insights into this process, we analyzed the phosphorylation of different TCR signaling molecules. As expected, we observed an increase in p-Akt(Ser473), p-p38 and pPLCγ-1 upon anti-CD3/anti-CD28 stimulation of WT and ASM-overexpressing cells (**Figure 3B**). However, stimulated $CD4^+$ T cells from t-ASM/CD4cre mice exhibited elevated phosphorylation of these molecules in comparison to stimulated WT cells. Similar results were also described for human $CD4^+$ T cells. Pharmacological inhibition of ASM by imipramine resulted in decreased phosphorylation of PLCγ and Akt upon anti-CD3/anti-CD28 stimulation (14), linking ASM activity to mediators of $CD4^+$ T cell signals and activation. Ser473-phosphorylated Akt has been described to preferentially phosphorylate Foxo1 and Foxo3 (30), which results in their retention within the cytoplasm (31). Nuclear exclusion of Foxo proteins prevents direct binding to the Foxp3 promotor (32, 33) and thereby interferes with Foxp3 expression. Along with elevated Akt activation, we also detected increased phosphorylation of p38. This signaling pathway also seems to negative regulate the induction of iTregs. P38-deficient T cells showed attenuated MAPK-activated proteinkinase-dependent mTOR signaling after TCR stimulation accompanied by enhanced differentiation into iTregs under appropriate polarizing conditions (34). On the other hand,

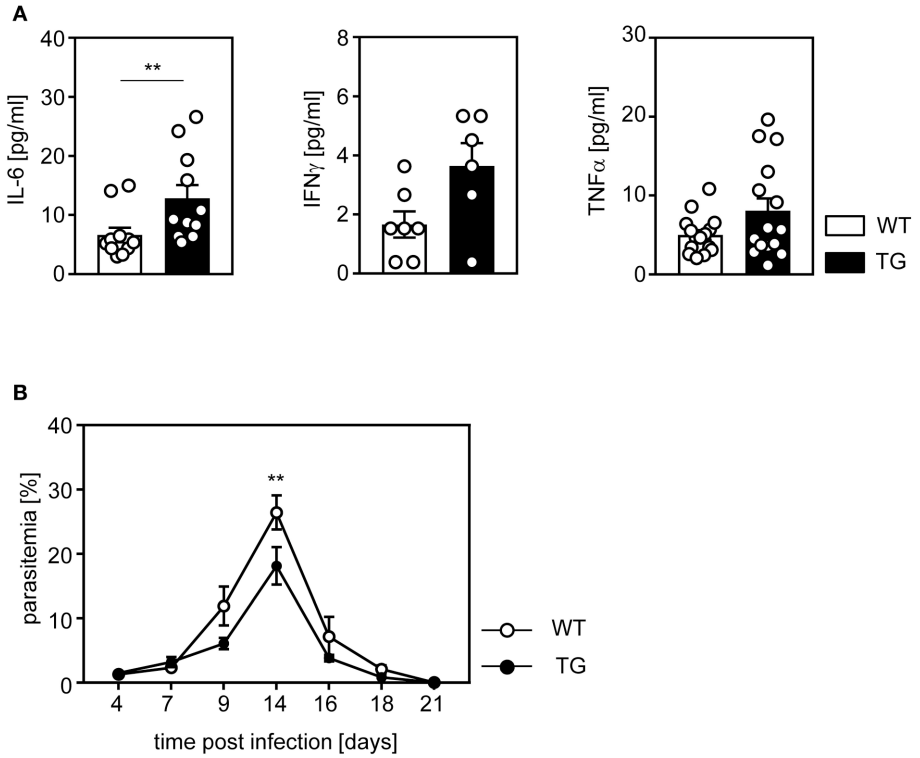

FIGURE 5 | Elevated IL-6 serum levels and improved parasite clearance in *P. yoelii*-infected t-ASM/CD4cre mice. T-ASM/CD4cre mice (TG) and t-ASM littermates (WT) were infected with *P. yoelii*. **(A)** IL-6, IFN-γ, and TNF-α serum levels were determined by Luminex technology at day 14 p.i. **(B)** Parasitemia was determined at indicated time points post infection by Giemsa staining. Results from two to four independent experiments with $n = 6$–15 mice in total are summarized as mean ± SEM. $^{**}p < 0.01$.

p38 is also involved in the regulation of IFN-γ expression. By using both, pharmacological inhibitors and genetically modified mice, it has been shown that the p38 MAPK pathway is required for the production of IFN-γ and Th1 differentiation (35). Well in line, we demonstrated that $CD4^+CD25^-$ T cells from t-ASM/CD4cre mice differentiate more efficiently into IFN-γ producing Th1 cells than WT cells upon TCR engagement in the presence of IL-12 and anti-IL-4 (**Figure 2B**). These results correlate with decreased Th1 differentiation of human $CD4^+$ T cells upon treatment with the ASM-inhibitor imipramine (14). Hence, the ASM-dependent increase in Akt and p38 phosphorylation upon TCR engagement might be responsible for the observed less effective induction of $Foxp3^+$ iTregs and elevated differentiation of stimulated $CD4^+$ T cells into Th1 cells under respective polarizing conditions. Activation of TCR signaling pathways upon anti-CD3/anti-CD28 stimulation have also an impact on T cell proliferation (36). Splenocytes from ASM-deficient mice and human $CD4^+$ T cells treated with pharmacological ASM-inhibitors showed reduced proliferation upon activation (10, 14). Well in line, we detected significant elevated proliferation of stimulated ASM-overexpressing $CD4^+CD25^-$ T cells compared to WT controls (**Figure 3A**), providing evidence that T cell-intrinsic ASM activity directly influences the proliferative activity of T cells.

To clarify whether enforced T cell-intrinsic ASM activity has also an impact on T cell function during an ongoing immune response *in vivo*, we infected t-ASM/CD4cre mice and control littermates with *P. yoelii*. It is well established that in addition to B cells, $CD4^+$ and $CD8^+$ T cells as well as IFN-γ play an important role in this mouse model for blood stage malaria (17). According to our *in vitro* analysis, we detected elevated relative numbers of proliferating and IFN-γ producing T cells (**Figure 4**). Strikingly, T cell-specific ASM overexpressing mice exhibited significantly less parasitemia than WT mice (**Figure 5B**), indicating that enforced ASM activity in T cells contributes to elevated T cell activation *in vivo*. Interestingly, infection of ASM-deficient or amitriptyline-treated mice with *P. berghei*, which causes experimental cerebral malaria, also resulted in decreased parasitemia (37). In that study the authors did not analyze the phenotype of T cells, but speculated about an impact of ASM on release or invasion of parasites from or into erythrocytes, respectively (37), which are not affected in T cell-specific ASM-overexpressing mice used in this study. We have shown that $Foxp3^+$ Tregs dampen an effective immune response resulting in impaired pathogen clearance in *P. yoelii*-infected mice (20). Interestingly, we did not detect significant differences in the relative number of $Foxp3^+$ Tregs in *P. yoelii*-infected T cell-specific ASM-overexpressing mice compared to WT controls. We could not exclude that t-ASM/CD4cre mice

have decreased Treg numbers at early time points of infection, which might impact the course of infection. However, our *in vitro* analysis indicate that ASM-overexpressing $CD4^+$ T cells exhibit enhanced proliferative activity and differentiate more effectively into IFN-γ producing Th1 cells than WT cells, even in the absence of Tregs.

Overall, our results indicate that T cell-intrinsic ASM activity plays an important role during T cell proliferation and differentiation into iTreg and Th1 $CD4^+$ T cell subsets. Hence, the ASM/sphingolipid pathway might be a novel target for the therapy of T cell-dependent diseases.

DATA AVAILABILITY

The raw data supporting the conclusions of this manuscript will be made available by the authors, without undue reservation, to any qualified researcher.

ETHICS STATEMENT

This study was carried out in accordance with the recommendations of the Society for Laboratory Animal Science (GV-SOLAS) and the European Health Law of the Federation of Laboratory Animal Science Associations (FELASA). The protocol was approved by the state authority for nature, environment and customer protection (LANUV), North Rhine-Westphalia, Germany.

AUTHOR CONTRIBUTIONS

MH, AG, HA, SB, MK, and KB designed and performed the experiments and analyzed data. JB and AW were involved in data discussion and in drafting the manuscript. WH initiated, organized and designed the study. MH and WH wrote the manuscript.

ACKNOWLEDGMENTS

We kindly thank Sina Luppus for excellent technical assistance and Witold Bartosik and Christian Fehring for cell sorting. We are grateful to Erich Gulbins for providing us with t-ASM mice. This work was supported by the Deutsche Forschungsgemeinschaft (DFG—GRK2098 to AW, KB, JB, and WH, and GRK1949 to AW, JB, and WH).

REFERENCES

1. Brenner B, Ferlinz K, Grassmé H, Weller M, Koppenhoefer U, Dichgans J, et al. Fas/CD95/Apo-I activates the acidic sphingomyelinase via caspases. *Cell Death. Differ.* (1998) 5:29–37. doi: 10.1038/sj.cdd.4400307
2. Kirschnek S, Paris F, Weller M, Grassme H, Ferlinz K, Riehle A, et al. CD95-mediated apoptosis *in vivo* involves acid sphingomyelinase. *J Biol Chem.* (2000) 275:27316–23. doi: 10.1074/jbc.M002957200
3. Schütze S, Potthoff K, Machleidt T, Berkovic D, Wiegmann K, Krönke M. TNF activates NF-kappa B by phosphatidylcholine-specific phospholipase C-induced "acidic" sphingomyelin breakdown. *Cell.* (1992) 71:765–76. doi: 10.1016/0092-8674(92)90553-O
4. Boucher LM, Wiegmann K, Fütterer A, Pfeffer K, Machleidt T, Schütze S, et al. CD28 signals through acidic sphingomyelinase. *J Exp Med.* (1995) 181:2059–68. doi: 10.1084/jem.181.6.2059
5. Kanfer JN, Young OM, Shapiro D, Brady RO. The metabolism of sphingomyelin. I. Purification and properties of a sphingomyelin-cleaving enzyme from rat liver tissue. *J Biol Chem.* (1966) 241:1081–4.
6. Gulbins E, Grassmé H. Ceramide and cell death receptor clustering. *Biochim Biophys Acta.* (2002) 1585:139–45. doi: 10.1016/S1388-1981(02)00334-7
7. Smith EL, Schuchman EH. The unexpected role of acid sphingomyelinase in cell death and the pathophysiology of common diseases. *FASEB J.* (2008) 22:3419–31. doi: 10.1096/fj.08-108043
8. Claus RA, Dorer MJ, Bunck AC, Deigner HP. Inhibition of sphingomyelin hydrolysis: targeting the lipid mediator ceramide as a key regulator of cellular fate. *Curr Med Chem.* (2009) 16:1978–2000. doi: 10.2174/092986709788682182
9. Nix M, Stoffel W. Perturbation of membrane microdomains reduces mitogenic signaling and increases susceptibility to apoptosis after T cell receptor stimulation. *Cell Death Differ.* (2000) 7:413–24. doi: 10.1038/sj.cdd.4400666
10. Stoffel B, Bauer P, Nix M, Deres K, Stoffel W. Ceramide-independent CD28 and TCR signaling but reduced IL-2 secretion in T cells of acid sphingomyelinase-deficient mice. *Eur J Immunol.* (1998) 28:874–80. doi: 10.1002/(SICI)1521-4141(199803)28:03<874::AID-IMMU874>3.0.CO;2-T
11. Herz J, Pardo J, Kashkar H, Schramm M, Kuzmenkina E, Bos E, et al. Acid sphingomyelinase is a key regulator of cytotoxic granule secretion by primary T lymphocytes. *Nat Immunol.* (2009) 10:761–8. doi: 10.1038/ni.1757
12. Zhou Y, Salker MS, Walker B, Münzer P, Borst O, Gawaz M, et al. Acid Sphingomyelinase (ASM) is a negative regulator of regulatory T cell (Treg) development. *Cell Physiol Biochem.* (2016) 39:985–95. doi: 10.1159/000447806
13. Hollmann C, Werner S, Avota E, Reuter D, Japtok L, Kleuser B, et al. Inhibition of acid sphingomyelinase allows for selective targeting of CD4+ conventional versus Foxp3+ regulatory T cells. *J Immunol.* (2016) 197:3130–41. doi: 10.4049/jimmunol.1600691
14. Bai A, Kokkotou E, Zheng Y, Robson SC. Role of acid sphingomyelinase bioactivity in human CD4+ T-cell activation and immune responses. *Cell Death Dis.* (2015) 6:e1828. doi: 10.1038/cddis.2015.178
15. Riethmüller J, Anthonysamy J, Serra E, Schwab M, Döring G, Gulbins E. Therapeutic efficacy and safety of amitriptyline in patients with cystic fibrosis. *Cell Physiol Biochem.* (2009) 24:65–72. doi: 10.1159/000227814
16. Rénia L, Goh YS. Malaria parasites: the great escape. *Front Immunol.* (2016) 7:463. doi: 10.3389/fimmu.2016.00463
17. Perez-Mazliah D, Langhorne J. CD4 T-cell subsets in malaria: TH1/TH2 revisited. *Front Immunol.* (2014) 5:671. doi: 10.3389/fimmu.2014.00671
18. Walther M, Tongren JE, Andrews L, Korbel D, King E, Fletcher H, et al. Upregulation of TGF-beta, FOXP3, and CD4+CD25+ regulatory T cells correlates with more rapid parasite growth in human malaria infection. *Immunity.* (2005) 23:287–96. doi: 10.1016/j.immuni.2005.08.006
19. Minigo G, Woodberry T, Piera KA, Salwati E, Tjitra E, Kenangalem E, et al. Parasite-dependent expansion of TNF receptor II-positive regulatory T cells with enhanced suppressive activity in adults with severe malaria. *PLoS. Pathog.* (2009) 5:e1000402. doi: 10.1371/journal.ppat.1000402
20. Abel S, Lückheide N, Westendorf AM, Geffers R, Roers A, Müller W, et al. Strong impact of CD4+ Foxp3+ regulatory T cells and limited effect of T cell-derived IL-10 on pathogen clearance during Plasmodium yoelii infection. *J Immunol.* (2012) 188:5467–77. doi: 10.4049/jimmunol.1102223
21. Abel S, Ueffing K, Tatura R, Hutzler M, Hose M, Matuschewski K, et al. Plasmodium yoelii infection of BALB/c mice results in expansion rather than induction of CD4(+) Foxp3(+) regulatory T cells. *Immunology.* (2016) 148:197–205. doi: 10.1111/imm.12602
22. Cambos M, Belanger B, Jacques A, Roulet A, Scorza T. Natural regulatory (CD4+CD25+FOXP+) T cells control the production of pro-inflammatory cytokines during Plasmodium chabaudi adami

infection and do not contribute to immune evasion. *Int J Parasitol.* (2008) 38:229–38. doi: 10.1016/j.ijpara.2007.07.006
23. Couper KN, Blount DG, Wilson MS, Hafalla JC, Belkaid Y, Kamanaka M, et al. IL-10 from CD4CD25Foxp3CD127 adaptive regulatory T cells modulates parasite clearance and pathology during malaria infection. *PLoS. Pathog.* (2008) 4:e1000004. doi: 10.1371/journal.ppat.1000004
24. Loevenich K, Ueffing K, Abel S, Hose M, Matuschewski K, Westendorf AM, et al. DC-derived IL-10 modulates pro-inflammatory cytokine production and promotes induction of CD4(+)IL-10(+) regulatory T cells during plasmodium yoelii infection. *Front Immunol.* (2017) 8:152. doi: 10.3389/fimmu.2017.00152
25. Gulbins E, Palmada M, Reichel M, Lüth A, Böhmer C, Amato D, et al. Acid sphingomyelinase-ceramide system mediates effects of antidepressant drugs. *Nat Med.* (2013) 19:934–8. doi: 10.1038/nm.3214
26. Lee PP, Fitzpatrick DR, Beard C, Jessup HK, Lehar S, Makar KW, et al. A critical role for Dnmt1 and DNA methylation in T cell development, function, and survival. *Immunity.* (2001) 15:763–74. doi: 10.1016/S1074-7613(01)00227-8
27. Mondino A, Mueller DL. mTOR at the crossroads of T cell proliferation and tolerance. *Semin Immunol.* (2007) 19:162–72. doi: 10.1016/j.smim.2007.02.008
28. Butler NS, Moebius J, Pewe LL, Traore B, Doumbo OK, Tygrett LT, et al. Therapeutic blockade of PD-L1 and LAG-3 rapidly clears established blood-stage Plasmodium infection. *Nat Immunol.* (2011) 13:188–95. doi: 10.1038/ni.2180
29. Hannun YA. Functions of ceramide in coordinating cellular responses to stress. *Science.* (1996) 274:1855–9. doi: 10.1126/science.274.5294.1855
30. Jacinto E, Facchinetti V, Liu D, Soto N, Wei S, Jung SY, et al. SIN1/MIP1 maintains rictor-mTOR complex integrity and regulates Akt phosphorylation and substrate specificity. *Cell.* (2006) 127:125–37. doi: 10.1016/j.cell.2006.08.033
31. Haxhinasto S, Mathis D, Benoist C. The AKT-mTOR axis regulates *de novo* differentiation of CD4+Foxp3+ cells. *J Exp Med.* (2008) 205:565–74. doi: 10.1084/jem.20071477
32. Harada Y, Harada Y, Elly C, Ying G, Paik JH, DePinho RA, et al. Transcription factors Foxo3a and Foxo1 couple the E3 ligase Cbl-b to the induction of Foxp3 expression in induced regulatory T cells. *J Exp Med.* (2010) 207:1381–91. doi: 10.1084/jem.20100004
33. Ouyang W, Beckett O, Ma Q, Paik JH, DePinho RA, Li MO. Foxo proteins cooperatively control the differentiation of Foxp3+ regulatory T cells. *Nat Immunol.* (2010) 11:618–27. doi: 10.1038/ni.1884
34. Hayakawa M, Hayakawa H, Petrova T, Ritprajak P, Sutavani RV, Jiménez-Andrade GY, et al. Loss of functionally redundant p38 isoforms in T cells enhances regulatory T cell induction. *J Biol Chem.* (2017) 292:1762–72. doi: 10.1074/jbc.M116.764548
35. Rincón M, Davis RJ. Regulation of the immune response by stress-activated protein kinases. *Immunol Rev.* (2009) 228:212–24. doi: 10.1111/j.1600-065X.2008.00744.x
36. Wilkinson B, Downey JS, Rudd CE. T-cell signalling and immune system disorders. *Expert Rev Mol Med.* (2005) 7:1–29. doi: 10.1017/S1462399405010264
37. Brand V, Koka S, Lang C, Jendrossek V, Huber SM, Gulbins E, et al. Influence of amitriptyline on eryptosis, parasitemia and survival of Plasmodium berghei-infected mice. *Cell Physiol Biochem.* (2008) 22:405–12. doi: 10.1159/000185482

Conflict of Interest Statement: The authors declare that the research was conducted in the absence of any commercial or financial relationships that could be construed as a potential conflict of interest.

frontiers in Immunology

ORIGINAL RESEARCH
published: 19 June 2019
doi: 10.3389/fimmu.2019.01386

Intestinal Acid Sphingomyelinase Protects From Severe Pathogen-Driven Colitis

*Jana Meiners[1], Vittoria Palmieri[1], Robert Klopfleisch[2], Jana-Fabienne Ebel[1], Lukasz Japtok[3], Fabian Schumacher[3,4], Ayan Mohamud Yusuf[5], Katrin A. Becker[4], Julia Zöller[1], Matthias Hose[1], Burkhard Kleuser[3], Dirk M. Hermann[5], Richard N. Kolesnick[6], Jan Buer[1], Wiebke Hansen[1] and Astrid M. Westendorf[1]**

[1] Institute of Medical Microbiology, University Hospital Essen, University of Duisburg-Essen, Essen, Germany, [2] Institute of Veterinary Pathology, Free University of Berlin, Berlin, Germany, [3] Department of Toxicology, Institute of Nutritional Science, University of Potsdam, Potsdam, Germany, [4] Department of Molecular Biology, University of Duisburg-Essen, Essen, Germany, [5] Department of Neurology, University Hospital Essen, University of Duisburg-Essen, Essen, Germany, [6] Laboratory of Signal Transduction, Memorial Sloan-Kettering Cancer Center, New York, NY, United States

OPEN ACCESS

Edited by:
Sibylle Schneider-Schaulies, University of Wuerzburg, Germany

Reviewed by:
Sabine Grösch, Goethe-Universität Frankfurt am Main, Germany
Markus M. Heimesaat, Charité Medical University of Berlin, Germany

***Correspondence:**
Astrid M. Westendorf
astrid.westendorf@uk-essen.de

Specialty section:
This article was submitted to Microbial Immunology, a section of the journal Frontiers in Immunology

Received: 05 March 2019
Accepted: 03 June 2019
Published: 19 June 2019

Citation:
Meiners J, Palmieri V, Klopfleisch R, Ebel J-F, Japtok L, Schumacher F, Yusuf AM, Becker KA, Zöller J, Hose M, Kleuser B, Hermann DM, Kolesnick RN, Buer J, Hansen W and Westendorf AM (2019) Intestinal Acid Sphingomyelinase Protects From Severe Pathogen-Driven Colitis. Front. Immunol. 10:1386. doi: 10.3389/fimmu.2019.01386

Inflammatory diseases of the gastrointestinal tract are emerging as a global problem with increased evidence and prevalence in numerous countries. A dysregulated sphingolipid metabolism occurs in patients with ulcerative colitis and is discussed to contribute to its pathogenesis. In the present study, we determined the impact of acid sphingomyelinase (Asm), which catalyzes the hydrolysis of sphingomyelin to ceramide, on the course of *Citrobacter (C.) rodentium*-driven colitis. *C. rodentium* is an enteric pathogen and induces colonic inflammation very similar to the pathology in patients with ulcerative colitis. We found that mice with Asm deficiency or Asm inhibition were strongly susceptible to *C. rodentium* infection. These mice showed increased levels of *C. rodentium* in the feces and were prone to bacterial spreading to the systemic organs. In addition, mice lacking Asm activity showed an uncontrolled inflammatory T_h1 and T_h17 response, which was accompanied by a stronger colonic pathology compared to infected wild type mice. These findings identified Asm as an essential regulator of mucosal immunity to the enteric pathogen *C. rodentium*.

Keywords: *Citrobacter rodentium*, colitis, acid sphingomyelinase, amitriptyline, T_h1, T_h17

INTRODUCTION

Inflammatory bowel diseases (IBD), such as ulcerative colitis and Crohn's disease, are characterized by chronic, relapsing inflammatory conditions, resulting from a dysregulation of the mucosal immune system in the gastrointestinal tract (1). The exact mechanism underlying the pathogenesis of IBD is unknown; however, it is widely accepted that immunological abnormalities, genetic and environmental factors, as well as infections are important determinants of IBD (2).

Sphingolipids are a family of metabolic lipids that are ubiquitous in cellular membranes and include a bioactive subset that regulates various cellular mechanisms and biologic processes such as cell survival, growth, differentiation, and apoptosis (3). Interestingly, sphingolipids are also essential structural components of intestinal membranes, providing protection and integrity to the intestinal mucosa and regulating intestinal absorption processes (4, 5). Studies using common acute and chronic epithelial injury colitis models have shown that bioactive sphingolipids, particularly

ceramide and sphingosine-1-phosphate, are important regulators of inflammation in IBD (6–8). The acid sphingomyelinase (Asm) is a relevant enzyme in this context, as it catalyzes the hydrolysis of sphingomyelin to ceramide. Asm is ubiquitously expressed and activated by a range of cellular stresses, including inflammatory cytokines and pathogens (9). The importance of Asm for cell functions was first recognized in Niemann-Pick disease type A and B, a genetic disorder with a severe accumulation of sphingomyelin in many organs (10). Recent studies implicated that Asm activity is also strongly involved in inflammatory processes (11). For example, Asm inhibition was shown to suppress the lipopolysaccharide (LPS) mediated release of inflammatory cytokines and to protect against disease pathology in chemical induced colitis in mice (12, 13). Furthermore, blockade of Asm bioactivity limited the *in vitro* differentiation of T helper cells derived from healthy volunteers and patients with Crohn's disease (14). These results implicate Asm inhibition as an innovative and effective immunoregulatory strategy for the treatment of IBD (12, 13, 15).

Nevertheless, the etiology of IBD is diverse and influenced by numerous factors (2). In this context, several enteropathogens have been implicated in the development of IBD (16), although to date, a causative bacterial agent for IBD has not been identified. Thus, further studies are needed to clarify the function of Asm under infectious and non-infectious conditions, as broad immunosuppression can increase the risk of infectious complications (17).

In the present study, we determined the impact of Asm activity on the course of *Citrobacter (C.) rodentium* induced colitis. In contrast to the protective effect of Asm inhibition in common acute and chronic epithelial injury colitis models, Asm inhibition or Asm deficiency strongly enhanced the susceptibility to enteric *C. rodentium* infection. Mice lacking Asm activity showed higher colon pathology, were prone to bacterial dissemination to the systemic organs, and showed an uncontrolled inflammatory T_h1 and T_h17 response compared to infected wild type mice. These findings identified Asm as a critical regulator of mucosal immunity to the enteric pathogen *C. rodentium*.

MATERIALS AND METHODS

Mice

C57BL/6 mice were purchased from ENVIGO, Netherlands. To inhibit acid sphingomyelinase activity, amitriptyline or imipramine was administered to C57BL/6 mice at 180 mg/l via drinking water for 14 days prior to bacterial challenge, and for further 10 days of infection. Acid sphingomyelinase-deficient (*Smpd1*$^{-/-}$) mice (18) were bred at the animal facility of the University Hospital Essen. All animals used in this study were 8–12 week old male or female mice kept in the animal experimental unit of the University Hospital Essen in individually ventilated cages and pathogen free conditions.

Asm Activity

The activity of Asm in colonic tissue was quantified using BODIPY-labeled sphingomyelin as a substrate. After colonic tissue was pulverized and lysed in 250 mM sodium acetate (pH 5) and 1% NP-40, 2 μg protein was incubated with 100 pmol BODIPY-labeled sphingomyelin (Thermo Fisher Scientific, Germany) for 1 h at 37°C in 250 mM sodium actetate (pH 5) and 0.1% NP-40. The reaction was terminated by the addition of chloroform:methanol (2:1, v:v) to extract the lipids. Subsequently, the lower phase containing lipids was collected, dried in a SpeedVac at 37°C, dissolved in 20 μl chloroform:methanol (2:1, v:v) and transferred onto a thin layer chromatography (TLC) plate. Product and uncleaved substrate were separated using chloroform:methanol (80:20, v/v). After separation, spots were imaged using a Typhoon FLA 9500 and quantified with ImageQuant software.

Ceramide and Sphingomyelin Quantification

Ceramide and sphingomyelin concentrations were quantified by rapid resolution liquid chromatography/mass spectrometry. Short lipids were extracted from colon biopsies with C17-ceramide and C16-d31sphingomyelin as internal standards, after homogenization of colonic tissue. Subsequently, samples were analyzed by rapid-resolution liquid chromatography-MS/MS using a Q-TOF 6530 mass spectrometer (Agilent Technologies, Waldbronn, Germany) operating in the positive ESI mode. The subsequent quantification was performed using Mass Hunter Software, and the resulting sphingolipid quantities were normalized to the actual protein content of the homogenate.

C. rodentium Infection Model

C. rodentium ICC169 strain was cultured overnight in Luria-Bertani (LB) medium at 37°C, centrifuged and washed with PBS. Mice were infected by oral gavage with $\sim 2 \times 10^9$ colony forming units (CFUs) of *C. rodentium*. After gavage, an aliquot of the bacteria was plated in serial dilutions on MacConkey agar. Bacterial numbers in the feces were determined at indicated time points after infection. Mice were analyzed at various time points after infection (d.p. infection).

Intestinal Permeability-Assay

For *in vivo* analysis of the intestinal permeability fluorescein isothiocyanate-conjugated (FITC)-dextran beads have been used. Briefly, food and water were withdrawn for 2 h and mice were orally administrated with permeability tracer (60 mg/100 g body weight of FITC-labeled dextran, MW 4000; FD4, Sigma-Aldrich, St. Louis, USA). Serum was collected 4 h later and fluorescence intensity was determined (excitation, 492 nm; emission, 525 nm; BioTek). FITC-dextran concentrations were determined using a standard curve generated by serial dilution of FITC-dextran.

Isolation of Splenocytes and Mesenteric Lymph Node Cells

Spleens were rinsed with an erythrocyte lysis buffer [containing 0.15 M NH_4Cl, 10 mM $KHCO_3$, and 0.5 M ethylenediaminetetraacetic acid (EDTA)], meshed through a 100-μm cell strainer, and washed with PBS containing 2 mM EDTA and 2% fetal calf serum (FCS). Mesenteric lymph nodes

(mLN) were meshed through a 100-μm cell strainer and washed with PBS containing 2 mM EDTA and 2% FCS.

Isolation of Lamina Propria Lymphocytes From the Colon

Lamina propria (LP) lymphocytes were isolated as described previously (19). In brief, colons were flushed with PBS, opened longitudinally, and cut into 1-cm pieces. Tissue pieces were washed twice in PBS containing 3 mM EDTA for 10 min at 37°C and twice in Roswell Park Memorial Institute (RPMI) medium containing 1% FCS, 1 mM EGTA, and 1.5 mM $MgCl_2$ for 15 min at 37°C. Colon pieces were intensively vortexed, washed with phosphate-buffered saline (PBS), and digested in RPMI containing 20% FCS and 100 U/mL collagenase (*Clostridium histolyticum*; Sigma-Aldrich, St. Louis, MO) for 60 min at 37°C. Cell suspension was passed through a 40-μm cell strainer and washed with culture medium.

Macroscopic and Histopathologic Assessment of Colitis

Colonic damage was assessed based on two main characteristics: colon length and colon weight. Colons were embedded in paraffin, and tissue sections (4 μm) were prepared for histological scoring in a blinded manner. The colon was divided into three equal portions (oral, middle, and rectal) and assessed for inflammatory cell infiltrates, epithelial damage, neutrophil infiltration, crypt abscesses, and crypt hyperplasia as describe before (20). Crypt heights were measured by micrometry; 30 measurements were taken in the distal colon for each mouse.

Cytokine Detection

Cytokines in serum samples were quantified using a Procarta Cytokine assay kit, according to the manufacturer's guidelines. The assay was run on a Luminex 200 system and cytokine levels were quantified using the Luminex IS software (Luminex Corporation, Austin, TX).

Antibodies and Flow Cytometry

Cells were stained with fluorochrome-labeled anti-mouse CD4 (RM4-5), CD11b (M1/70), F4/80 (BM8), FoxP3 (FJK-16s), IFNγ (XMG1.2), IL-17 (TC11-18H10.1), and I-A/I-E (M5/114.15.2) antibodies and analyzed by flow cytometry on an LSR II instrument using DIVA software (BD Biosciences).

Statistical Analysis

Normality of data was tested using D'Agostino & Pearson normality test and Shapiro–Wilk normality test. Statistical analysis was performed using Student's *t*-test, one-way ANOVA or two-way ANOVA followed by Tukey's multiple comparisons test, Dunn's multiple comparisons test or Bonferroni's multiple comparisons test. *P*-values were set at a level of $p < 0.05$. Statistical analyzes were performed using GraphPad Prism software version 7.

Ethics Statement

This study was carried out in accordance with the recommendations of the Society for Laboratory Animal Science (GV-SOLAS) and the European Health Law of the Federation of Laboratory Animal Science Associations (FELASA). The protocol was approved by the North Rhine-Westphalia State Agency for Nature, Environment and Consumer Protection (LANUF), Germany.

RESULTS

Alterations of the Sphingolipid Profile During *C. rodentium* Infection

Sphingolipids have been identified as important players to control intestinal inflammation. There is increasing evidence that a dyregulaton of several sphingolipid molecules occurs along with IBD and contributes to the pathogenesis and maintenance of the disease (21). To analyze the impact of the sphingolipid metabolism on pathogen-driven intestinal inflammation, C57BL/6 wild type (WT) mice were infected via oral gavage with $\sim 2 \times 10^9$ CFUs *C. rodentium*, and the sphingomyelin and ceramide concentrations were determined in the colon at indicated time points post infection by mass spectrometry. Interestingly, sphingomyelin as well as ceramide concentrations in the colon decreased during the course of infection in comparison to non-infected WT mice (**Figures 1A,B**), suggesting an involvement of the sphingolipid metabolism in intestinal inflammation.

Oral Amitriptyline Pre-treatment Inhibits the Colonic Asm Activity During *C. rodentium* Infection

Acid sphingomyelinase (Asm) metabolizes sphingomyelin into ceramide, and this enzyme can be pharmacologically inhibited by amitriptyline (Ami) (22, 23). Amitriptyline accumulates in the acid compartments of the lysosomes, interferes with the translocation of Asm to the outer leaflet of the membrane and inhibits the activation of Asm (9). As sphingomyelin and ceramide were downregulated during the course of *C. rodentium* infection, we tested if the inhibition of Asm protects from pathogen-driven intestinal inflammation. For the specific *in vivo* inhibition of Asm in the gastrointestinal tract, WT mice were provided with amitriptyline in the drinking water for 14 days before and during a 10 day course of infection (WT/Ami). To check for the inhibition of the Asm activity, colonic tissues of WT/Ami mice, infected and non-infected, were analyzed for their sphingolipid profile by mass spectroscopy during the course of infection. Although no differences in the sphingomyelin and ceramide concentration were discovered under homeostasis, we detected an accumulation of sphingomyelin and ceramide in the colon of infected WT/Ami mice with constant increase during the course of infection (**Figures 1C,D**). This data clearly demonstrated a modulation of the sphingolipid pathway in the colonic tissue by amitriptyline treatment via the drinking water.

Asm Inhibition Increases the Susceptibility to *C. rodentium* Infection

To further elucidate the physiological effect of Asm inhibition on the course of infection, we characterized the *C. rodentium*

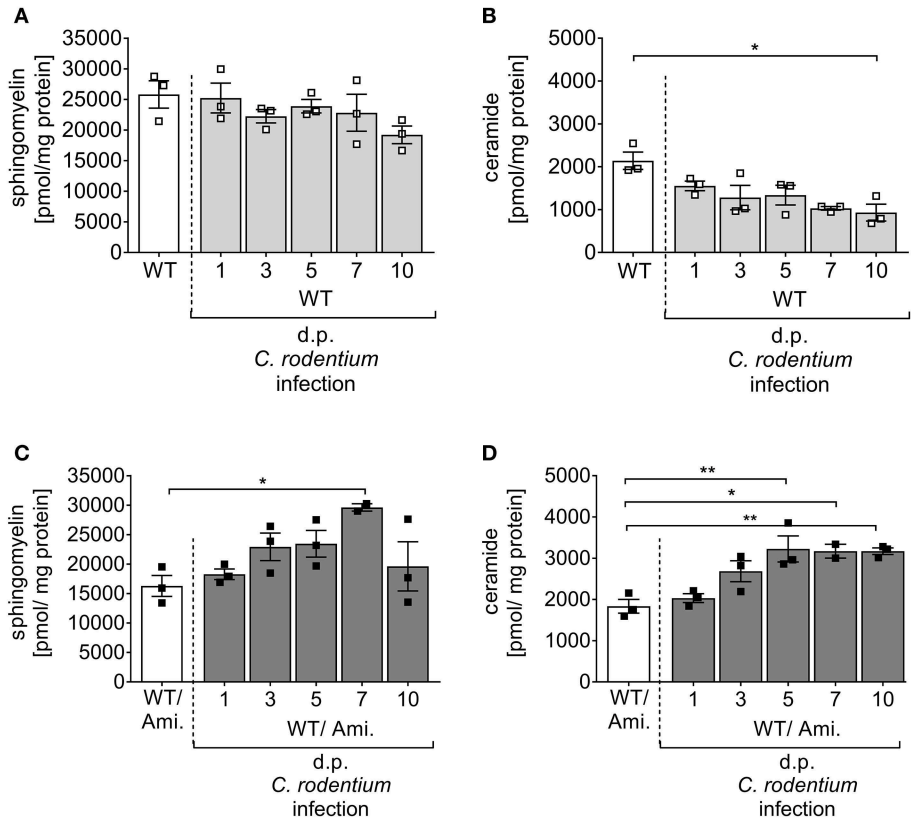

FIGURE 1 | Alterations of sphingolipid concentrations during *C. rodentium* infection. C57BL/6 mice were either left untreated (WT) or pre-treated with 180 mg/l amitriptyline in drinking water 2 weeks prior to infection (WT/Ami) and during the course of infection. Mice were orally gavaged with PBS or with ~2 × 10^9 colony forming units (CFUs) of *C. rodentium*. At indicated days post (dp) infection colons were excised. In rectal colonic tissue, the **(A,C)** sphingomyelin and **(B,D)** ceramide contents were analyzed using rapid resolution liquid chromatography/mass spectrometry. Data are presented as the concentration of ceramide and sphingomyelin in pmol/mg protein. All data are presented as mean ± SEM. Statistics were performed using the parametric one-way ANOVA test with Tukey's multiple comparison test (*$p < 0.05$; **$p < 0.01$).

induced inflammatory response in WT and WT/Ami mice in detail. First, we determined the body weight loss of the mice as indicator for diarrhea. Surprisingly, *C. rodentium* infected WT/Ami mice lost significantly more body weight within 5 and 10 days post infection compared to infected wild type mice (**Figure 2A**). Determination of the bacterial burden in the feces showed that bacterial loads were similar in WT and WT/Ami infected mice on day 3 post infection with 10^7 CFUs/g of feces. However, *C. rodentium* infected WT/Ami mice exhibited significantly higher bacterial numbers at day 5 and 7 post infection than did infected WT mice (**Figure 2B**), suggesting an impairment in the clearance of the pathogen. Interestingly, reduced bacterial eradication in WT/Ami mice was associated with exaggerated inflammation, characterized phenotypically by higher spleen weights (**Figure 2C**) and significantly higher colon weight-to-length ratios (**Figure 2D**) than in infected WT mice 10 days post infection. Well in line, histological analysis of the colon showed that *C. rodentium*-infected WT/Ami mice exhibited more severe crypt elongation and crypt hyperplasia (**Figures 2E,F**) and a higher inflammatory score compared to infected WT mice (**Figure 2G**). Of note, the same phenotype was obtained when infected mice were treated daily with amitriptyline via intraperitoneal injection (data not shown). These findings indicate that Asm activity is not only important for the eradication of *C. rodentium* but also for the control of infection-associated inflammation. Therefore, inhibition of Asm is not protective in pathogen-driven intestinal inflammation.

Asm Provides Host Resistance to Bacterial Dissemination

A consequence of certain enteric bacterial infections is a breakdown of the intestinal barrier, allowing pathogen spreading from the intestine to the systemic organs of a host. Therefore, we tested whether Asm inhibition affects the intestinal permeability *in vivo*. Non-infected and infected WT and WT/Ami mice were orally gavaged with FITC-labeled dextran beads and 4 h later the intestinal permeability was assessed as relative concentration of serum FITC-dextran. Interestingly, the FITC concentrations in the serum of WT/Ami mice were significantly increased when compared to non-infected WT/Ami controls (**Figure 3B**). In contrast, only a slight but not significant increase in serum

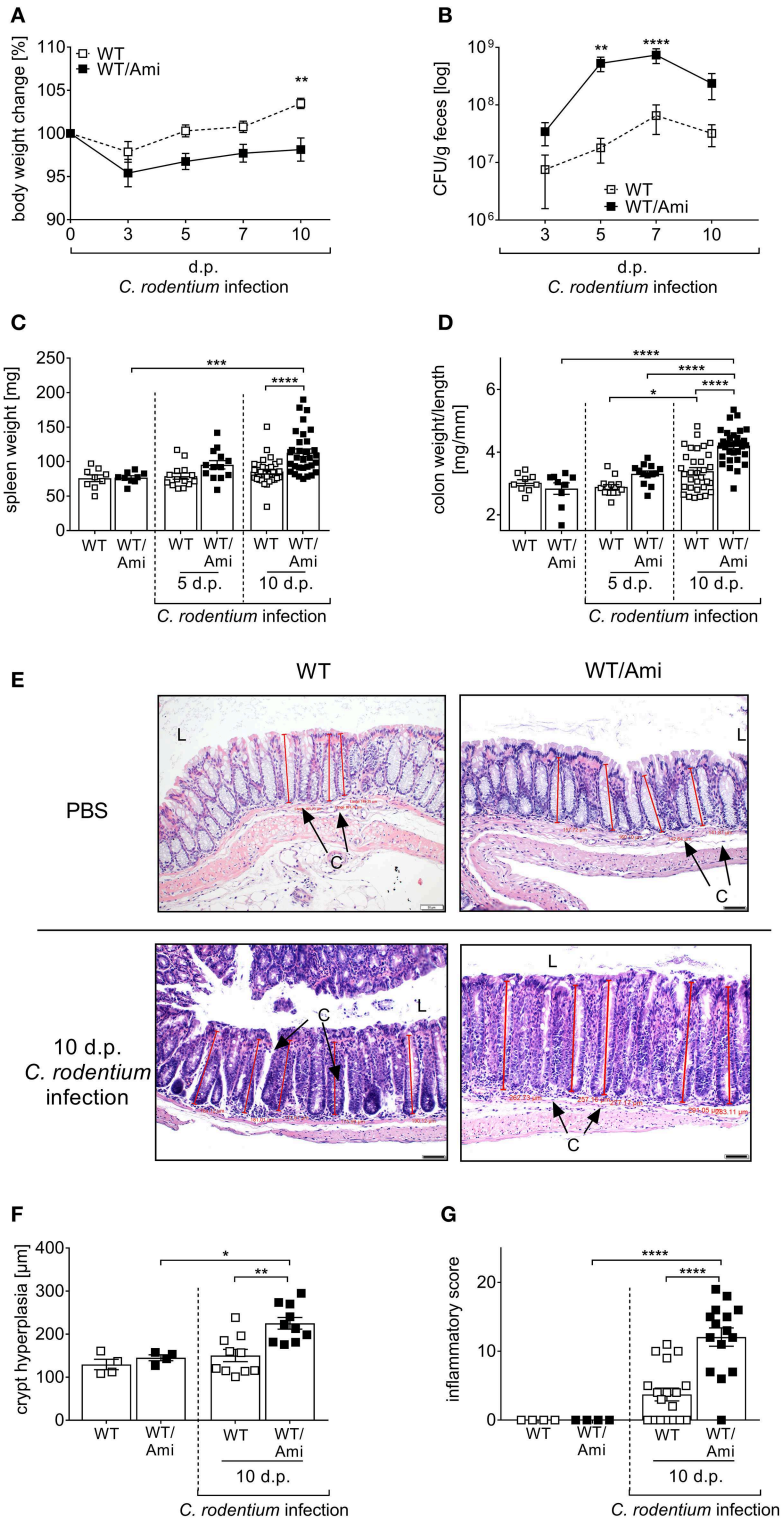

FIGURE 2 | Amitriptyline pre-treatment increases the susceptibility to *C. rodentium* challenge. C57BL/6 mice were treated as described in **Figure 1**. **(A,B)** At indicated time points body weight and CFUs in feces in WT mice (white squares; $n = 32–33$) and WT/Ami mice (black squares; $n = 32–35$) were assessed. Statistics were performed using the Mann–Whitney test. **(C)** Spleen weight ($n = 9–32$) and **(D)** colon weight-to-length ratio were determined in uninfected, untreated and uninfected amitriptyline treated mice 5 and 10 dp *C. rodentium* infection ($n = 9–32$). **(E)** Representative H&E staining of colon sections from PBS or *C. rodentium* infected WT or WT/Ami mice 10 dp challenge. [Red lines indicate the crypt length. (L) lumen, (C) crypt. Length of scale bar is 50 µm]. **(F)** Measured crypt length in

(Continued)

FIGURE 2 | colons of uninfected WT or WT/Ami mice, and infected WT and WT/Ami 10 dp *C. rodentium* infection ($n = 4$–18). **(G)** Histopathology score of uninfected WT and WT/Ami mice, and WT and WT/Ami mice 10 dp *C. rodentium* infection ($n = 4$–18). All data are presented as mean ± SEM. Statistics were performed using the two-way ANOVA test followed by Tukey's multiple comparison test (*$p < 0.05$; **$p < 0.01$; ***$p < 0.001$; ****$p < 0.0001$).

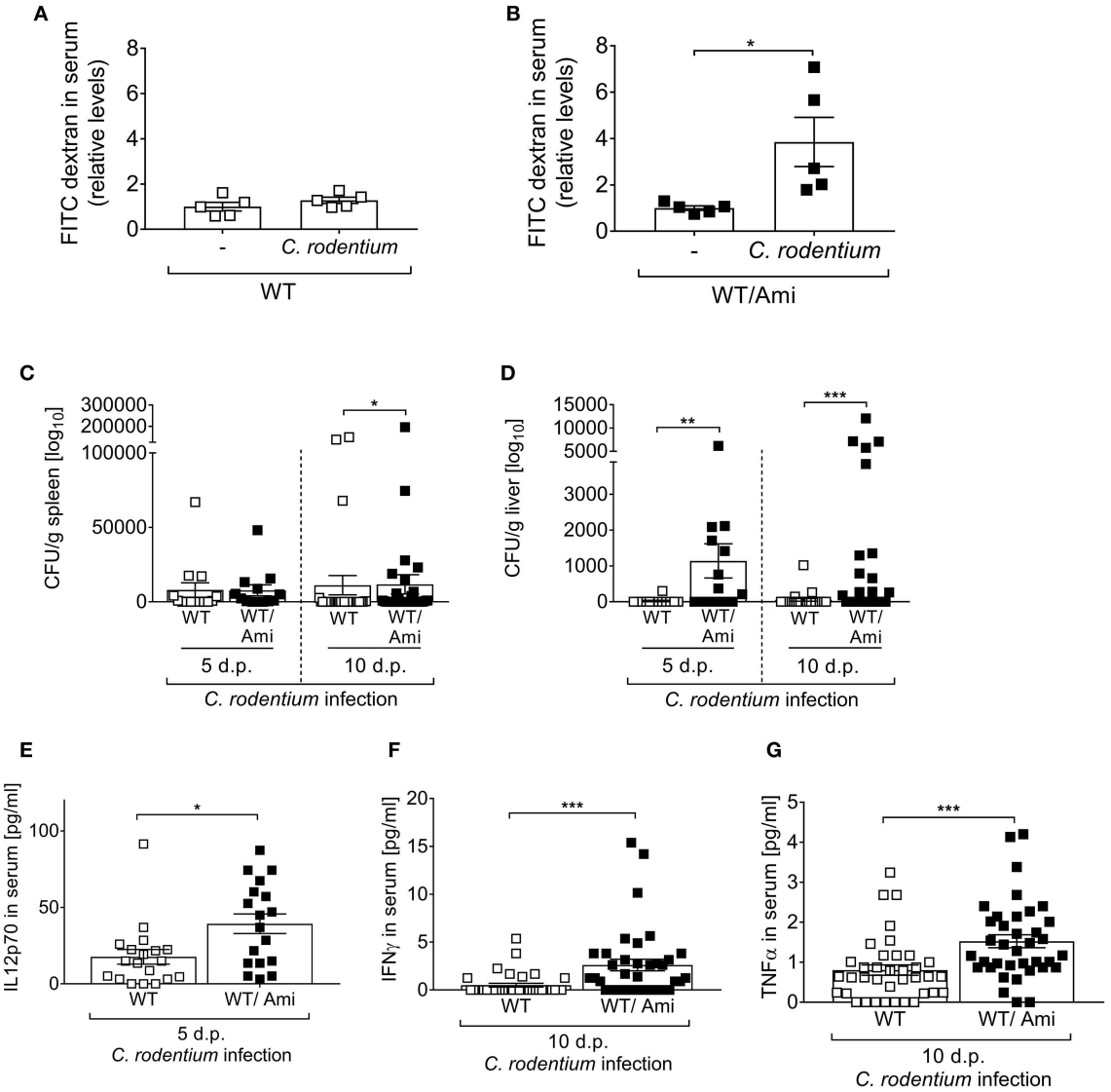

FIGURE 3 | Enhanced systemic distribution of *C. rodentium* in mice pre-treated with amitriptyline. C57BL/6 mice were treated and infected as described in **Figure 1**. **(A,B)** Mice were orally administrated with FITC-labeled dextran beads. Serum was collected 4 h later, and fluorescence intensity was determined ($n = 5$). Serum FITC concentration in infected mice was normalized to serum FITC concentration of the respective control. **(C,D)** 5 and 10 dp *C. rodentium* infection spleen and liver were isolated and CFUs of *C. rodentium* were assessed ($n = 13$–27). **(E–G)** Concentration of the cytokines IL12p70, IFNγ, and TNFα in serum of WT and WT/Ami mice 10 dp *C. rodentium* infection were measured using Luminex technologies ($n = 18$–37). All data are presented as mean ± SEM. Statistics were performed using the Mann–Whitney test or Student's *t*-test (*$p < 0.05$; **$p < 0.01$; ***$p < 0.001$).

FITC levels was detected in infected WT mice compared to non-infected WT mice (**Figure 3A**).

These results led us to hypothesize that bacteria, once invaded into the gastrointestinal tract, are spread to the systemic organs of infected WT/Ami mice. Thus, we infected WT and WT/Ami mice via oral gavage with $\sim 2 \times 10^9$ CFUs *C. rodentium* per mouse, harvested the spleen and liver 5 and 10 days post-infection and analyzed the presence of viable bacteria. Well in line with the permeability assay, a higher bacterial burden was observed in the livers and spleens of infected WT/Ami mice compared to infected WT mice (**Figures 3C,D**).

The production of protective cytokines is a hallmark of immune responses being mounted toward the infection. To assess if the systemic distribution of *C. rodentium* in WT/Ami

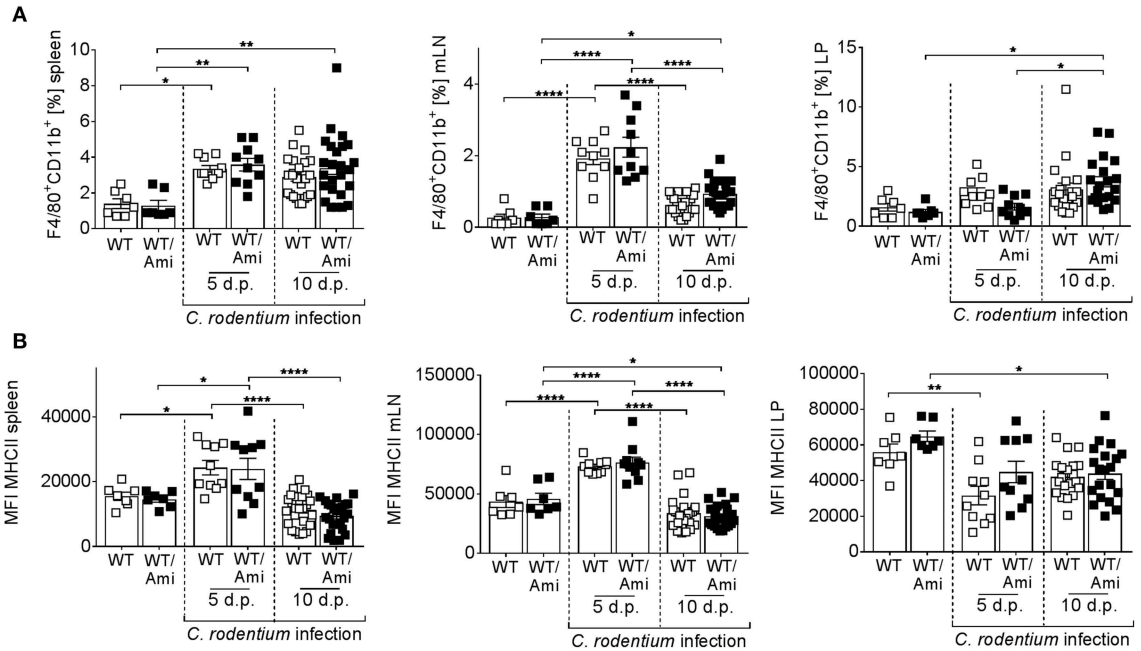

FIGURE 4 | Infiltration of macrophages into colonic tissue is not altered in amitriptyline pre-treated mice after *C. rodentium* challenge. C57BL/6 mice were treated as described in **Figure 2**. Cells from the spleen, mesenteric lymph nodes (mLNs), and the lamina propria (LP) were isolated from uninfected WT and WT/Ami mice, 5 and 10 days post *C. rodentium* infection and analyzed for the frequency for macrophages by flow cytometry. **(A)** Percentages of macrophages from living cells are displayed ($n = 7–25$). **(B)** MFI of MHCII from macrophages is displayed ($n = 7–25$). All data are presented as mean ± SEM. Statistics were performed using the two-way ANOVA test with Tukey's multiple comparison test (*$p < 0.05$; **$p < 0.01$; ****$p < 0.0001$).

mice altered the level of cytokines that have been shown to orchestrate the immune response against *C. rodentium* infection (24), we infected WT and WT/Ami mice and measured the cytokine levels of IL-12p70, IFNγ, and TNFα in the sera. Of note, we found significantly elevated levels of IL12p70, INFγ, and TNFα in the sera of infected WT/Ami mice on day 10 post infection compared to infected WT mice (**Figures 3E–G**). Hence, Asm inhibition did not impair the production of protective pro-inflammatory cytokines. The high levels of certain pro-inflammatory cytokines in infected WT/Ami mice could be a consequence of the increased number of bacteria in their colon and liver tissues.

Colonic Infiltration of Macrophages Is Not Impaired by Asm Inhibition

Intestinal macrophages and macrophage-derived IL-12 are required for the initiation of adaptive immunity in response to *C. rodentium* (25). To investigate the role of Asm in mucosal immunity against *C. rodentium* infection, we measured the frequency of macrophages in the spleen, mesenteric lymph nodes, and the colonic lamina propria of WT and WT/Ami mice infected with *C. rodentium*. At day 5 and day 10 post infection the frequencies of macrophages were enhanced in the spleen and the LP, but no differences were found between infected WT and infected WT/Ami mice (**Figure 4A**). Furthermore, the expression of MHC II, which is essential for the activation of $CD4^+$ T cells, was not impaired in infected WT/Ami mice compared to infected WT mice (**Figure 4B**). These data suggest that the function of macrophages to initiate adaptive immunity is independent of Asm during *C. rodentium* infection.

Asm Inhibition Leads to an Uncontrolled Expansion of T_h1 and T_h17 Cells

Infection with *C. rodentium* is associated with the induction of T_h1 and T_h17 adaptive immune responses (26–31). To measure the $CD4^+$ T cell response during infection of WT and WT/Ami mice, splenocytes, mLN cells, and LP cells were restimulated *ex vivo* and analyzed for IFNγ and IL-17 production via flow cytometry. Comparable frequencies of T_h1 and T_h17 cells were detected in uninfected mice treated with or without amitriptyline. In contrast, *C. rodentium* infected mice exhibited enhanced frequencies of IFNγ- and IL-17-producing cells at day 10 post infection. Compared with infected WT controls, WT/Ami mice displayed an overall increase in activated T cells, with highest frequencies of T_h1 and T_h17 cells at day 10 post infection (**Figures 5A,B**).

Regulatory T cells (T_{regs}) are important to counterbalance effector T cell responses and to protect from severe pathology (32). Recently, it was shown that deficiency of T_{regs} enhances the susceptibility to *C. rodentium* infection (32). Therefore, we assessed the frequencies of T_{regs} in the spleen, mLN, and LP of *C. rodentium* infected WT and WT/Ami mice. No differences were observed in the spleens and mLN of non-infected and infected WT mice compared to infected WT/Ami mice. Nonetheless, the

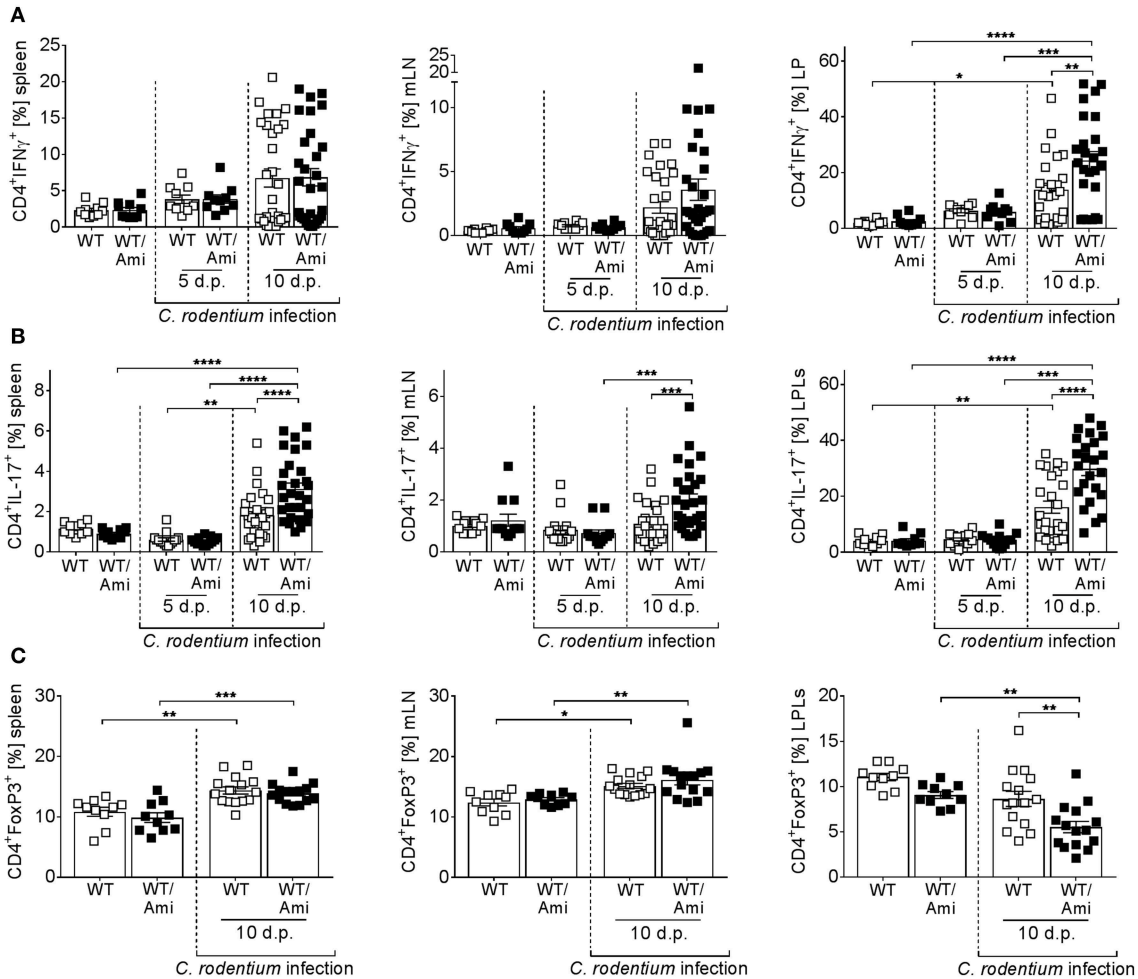

FIGURE 5 | Enhanced proportions of T_h1 and T_h17 cells in colonic tissue of amitriptyline treated mice. C57BL/6 mice were treated as described in **Figure 2**. Single cells from spleen, mesenteric lymph nodes (mLNs), and lamina propria (LP) were prepared from uninfected WT or WT/Ami mice, 5 and 10 days post *C. rodentium* infection, and analyzed for **(A)** $CD4^+IFN\gamma^+$ cells (T_h1), **(B)** $CD4^+IL\text{-}17^+$ cells (T_h17), or **(C)** $CD4^+FoxP3^+$ cells (T_{regs}) by flow cytometry. Percentages of T_h1, T_h17, and T_{regs} from $CD4^+$ T cells are displayed. All data are presented as mean ± SEM. Statistics were performed using the two-way ANOVA test with Tukey's multiple comparison test (*$p < 0.05$; **$p < 0.01$; ***$p < 0.001$; ****$p < 0.0001$).

percentage of $CD4^+Foxp3^+$ T_{regs} was significantly decreased in the LP of infected WT/Ami mice compared to infected WT mice (**Figure 5C**). In summary, Asm inhibition enhances the colonic frequencies of T_h1 and T_h17 cells in *C. rodentium* infected mice, which seems to be a consequence of increased numbers of bacteria in the colon and a disturbed counterbalanced induction of T_{regs}.

Asm Knock-Out Mice Are Strongly Susceptible to *C. rodentium* Infection

Amitriptyline was initially introduced in order to treat major depressive disorders (33). However, nowadays the use of amitriptyline has expanded to numerous types of pain and other symptoms (34–38). In addition, anti-inflammatory and anti-microbial properties of the drug have been reported as well (39, 40). To exclude eventual drug unspecific effects, we used a second pharmacological Asm inhibitor, imipramine (Imi) within the same experimental set up. Well in line with the results from amitriptyline treated mice, imipramine treated mice are more susceptible to *C. rodentium* induced colitis, as shown by increased bacterial burden in the feces, enhanced colon-weight-to-length ratios and more severe pathology compared to infected WT mice (**Figures 6A–E**).

To prove that the effect in amitriptyline and imipramine treated animals on *C. rodentium* induced inflammation is specifically due to the inhibition of Asm, we repeated the infection experiments in Asm wild type (Asm WT) and Asm knock-out (Asm KO) mice. First, we confirmed the specific depletion of Asm in Asm KO mice under homeostasis and in infected animals. Therefore, the Asm activity as well as sphingomyelin and ceramide concentrations were determined in the colon. As expected, we observed no Asm activity accompanied with a strong accumulation of sphingomyelin in non-infected and infected Asm KO mice and only slight

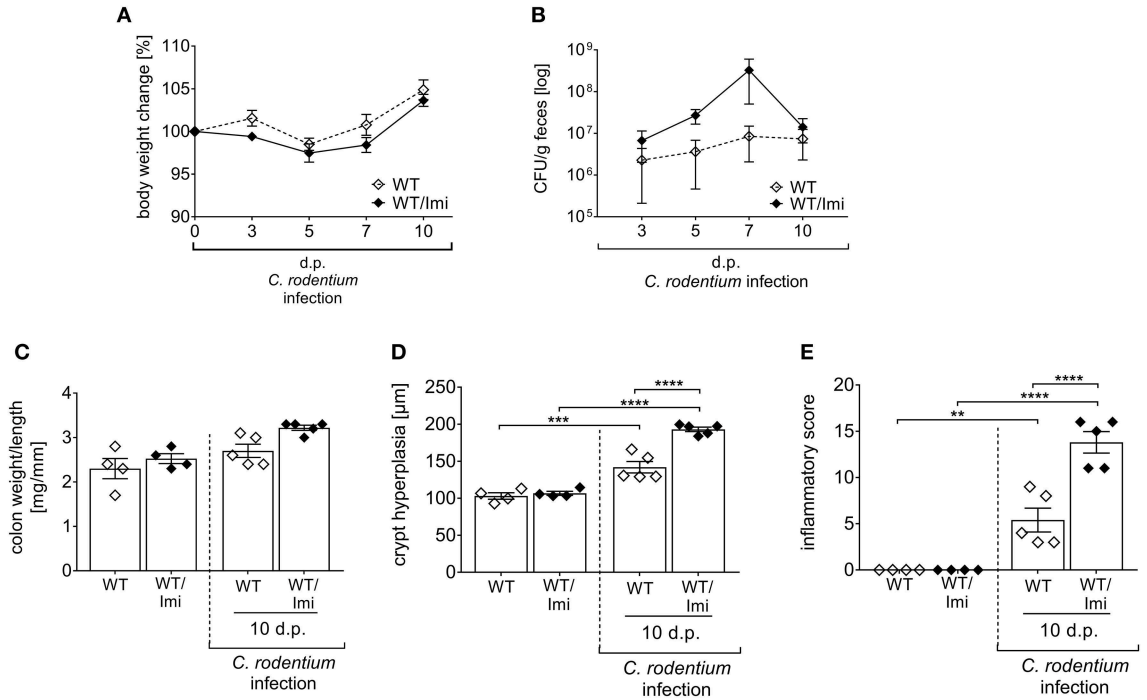

FIGURE 6 | Imipramine pre-treatment increases the susceptibility to *C. rodentium* challenge. C57BL/6 mice were either left untreated (WT) or pre-treated with 180 mg/l imipramine in drinking water 2 weeks prior to infection (WT/Imi) and during the course of infection. Mice were orally gavaged with PBS or with $\sim 2 \times 10^9$ colony forming units (CFUs) of *C. rodentium*. **(A,B)** At indicated time points body weight and CFUs in feces in WT mice (white diamonds; $n = 4$–5) and WT/Imi mice (black diamonds; $n = 4$–5) were assessed. Statistics were performed using the Mann–Whitney test. **(C)** Colon weight-to-length ratio were determined in uninfected, untreated, and uninfected imipramine treated mice 10 dp *C. rodentium* infection ($n = 4$–5). Crypt hyperplasia **(D)** and inflammation score **(E)** of uninfected WT and WT/Imi mice, and WT and WT/Imi mice 10 dp *C. rodentium* infection ($n = 4$–5). All data are presented as mean ± SEM. Statistics were performed using the one-way ANOVA test followed by Tukey's multiple comparison test (**$p < 0.01$; ***$p < 0.001$; ****$p < 0.0001$).

changes in the ceramide concentrations (**Figures 7A–C**). To approve the physiological effect of Asm deficiency in comparison to amitriptyline mediated inhibition of Asm, we infected Asm WT and Asm KO mice via oral gavage with $\sim 2 \times 10^9$ CFUs *C. rodentium* per mouse and assessed the body weight, bacterial burden, spleen weight, colon weight-to-length ratio, and the histopathological score. Importantly, non-infected Asm WT mice and Asm KO mice exhibited no difference regarding the analyzed parameters (**Figures 7D–F**). In contrast, we observed an enhanced loss of body weight at day 10 post infection in Asm KO mice compared to Asm WT mice (**Figure 7D**). Determination of the bacterial burden in the feces showed that bacterial loads were higher in infected Asm KO mice on day 5 and 10 post infection compared to infected Asm WT mice (**Figure 7G**). In addition, a tendency of systemic dissemination in the liver and the spleen was observed in infected Asm KO mice but not in infected WT mice (**Figures 7H,I**). Well in line, also spleen weights and colon weight-to-length ratios were higher in infected Asm KO mice than in Asm WT mice (**Figures 7E,F**). Finally, the histopathological analysis of colon tissues revealed significantly elevated crypt hyperplasia and inflammatory scores in infected Asm KO mice compared to infected Asm WT mice (**Figures 7J–L**). In summary, Asm KO mice are strongly susceptible to *C. rodentium* infection and show the same histopathological phenotype as infected amitriptyline treated animals.

DISCUSSION

The gastrointestinal tract is the largest mucosal surface in the human body, fulfilling the pivotal role of nutrition and water absorption. Pathogens preferentially invade the host through the gastrointestinal tract forcing it to distinguish between harmless and beneficial bacteria. Thus, the gastrointestinal tract adapted to these unique circumstances by limiting direct bacterial contact to the epithelial cell surface, rapid detection and killing of invading bacteria, and minimizing the exposure of commensal bacteria to the immune system (41). Dysregulation of this uniquely balanced system can lead to chronic inflammation, resulting in IBD (42). Although the exact etiology of IBD remains unclear, the role of sphingolipids in contributing to the inflammatory process is evident (4, 5, 43–47). Asm is of particular interest, as it catalyzes the hydrolysis of sphingomyelin to ceramide, which is the central molecule in the sphingolipid metabolism. Thus, research on therapeutic agents able to modulate Asm and tissue-specific delivery systems or application routes is mandatory (47).

The importance of Asm was first recognized in Niemann-Pick disease type A and B, also called Acid Sphingomyelinase

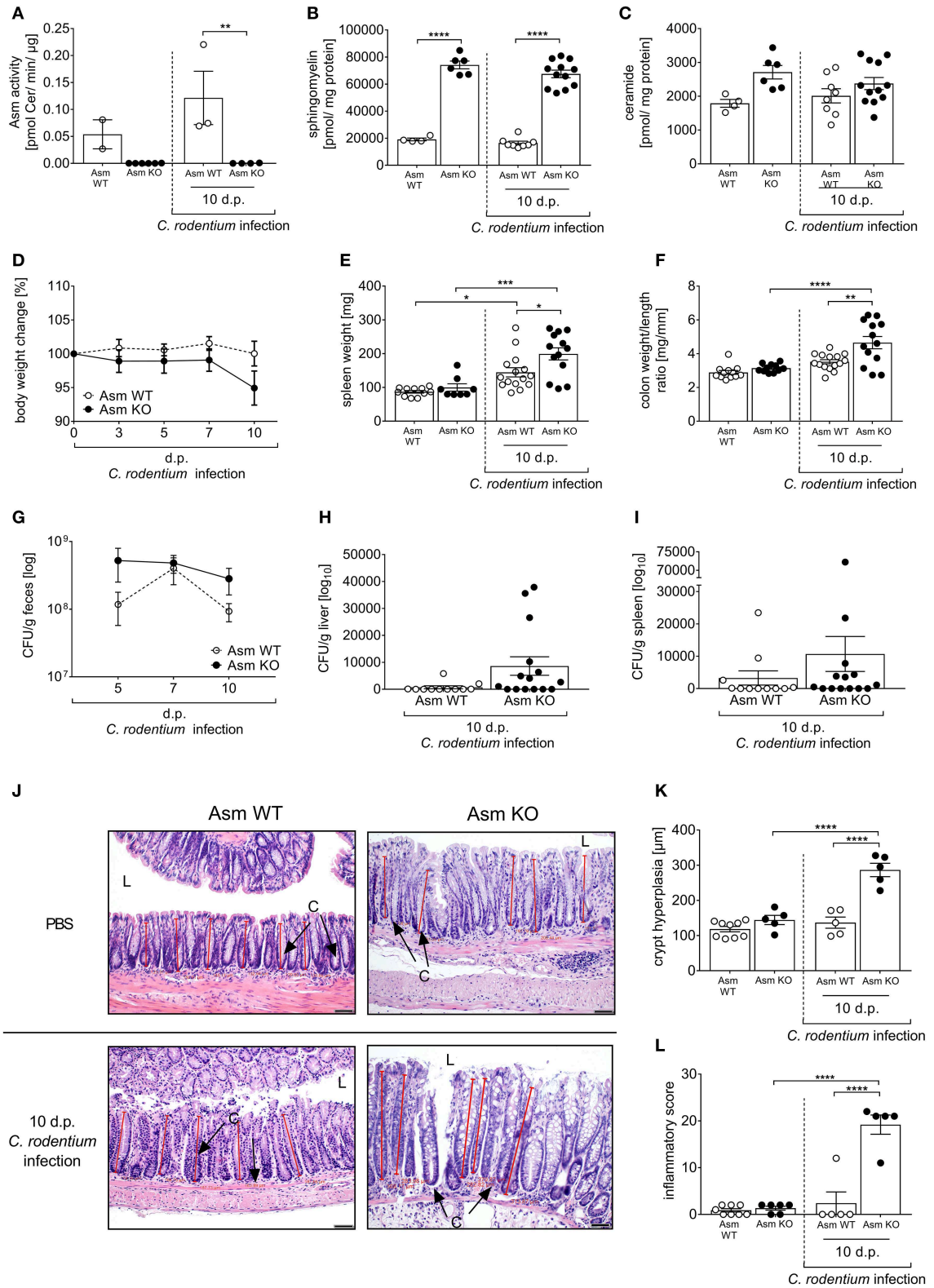

FIGURE 7 | Deficiency of acid sphingomyelinase (Asm) increases susceptibility to *C. rodentium* infection. Asm wildtype (Asm WT) and Asm knock-out (Asm KO) mice were orally gavaged with PBS or ~2 × 10^9 colony forming units (CFUs) of *C. rodentium*. Colons were excised from uninfected Asm WT and Asm KO mice and 10 dp

(Continued)

FIGURE 7 | infection. **(A)** Asm activity was analyzed in rectal colonic tissue ($n = 2$–6) by rapid resolution liquid chromatography/mass spectrometry. **(B)** Sphingomyelin ($n = 4$–12) **(C)** and ceramide ($n = 4$–12) concentrations are displayed. **(D)** At indicated time points body weight was assessed in Asm WT mice ($n = 16$–17) and Asm KO mice ($n = 14$–20). Statistics were performed using the Mann–Whitney test or the Student's *t*-test. **(E)** Spleen weight ($n = 8$–15) and **(F)** colon weight-to-length ratio were determined in uninfected, untreated, and uninfected amitriptyline treated mice 5 and 10 dp *C. rodentium* infection ($n = 11$–15). **(G–I)** At indicated time points CFUs in feces, liver, and spleen of Asm WT mice ($n = 11$–12) and Asm KO mice ($n = 14$–15) were assessed. Statistics were performed using the Mann–Whitney test or the Student's *t*-test. **(J)** Representative H&E staining of colon sections from PBS or *C. rodentium* infected Asm WT or Asm KO mice 10 dp infection. [Red lines indicate the crypt length. (*L*) lumen, (*C*) crypt. Length of scale bar−50 μm]. **(K)** Crypt length in colons of uninfected Asm WT or Asm KO mice, and infected Asm WT and Asm KO 10 dp *C. rodentium* infection ($n = 5$–9). **(L)** Histopathology score of the colon of uninfected Asm WT and Asm KO mice, and Asm WT and Asm KO mice 10 dp *C. rodentium* infection ($n = 5$–8). All data are presented as mean ± SEM. Statistics were performed using the two-way ANOVA test followed by Tukey's multiple comparison test (*$p < 0.05$; **$p < 0.01$; ***$p < 0.001$; ****$p < 0.0001$).

Deficiency. Thus, sphingomyelin cannot be metabolized properly and is accumulated within cells, eventually causing cell death and the malfunction of major organ systems (10). Of note, recent studies point out that patients with Niemann-Pick disease are susceptible to pathogen infections (14, 48), indicating the association between deficiency and aberrant immune responses. Well in line, in the present study we identified Asm as a critical regulator of mucosal immunity to the *C. rodentium*. Asm inhibition or Asm deficiency strongly enhanced the susceptibility to enteric *C. rodentium* infection.

Interestingly, the impact of Asm and ceramide on IBD is intensively discussed. Evidence that Asm may be a therapeutic target in colitis has been demonstrated by a study using the Asm inhibitor SMA-7. SMA-7 inhibited LPS-induced activation of NFκB and release of pro-inflammatory cytokines TNFα, IL-1β, and IL-6 in macrophages (12). This was correlated with decreased ceramide production. In a chemically induced mouse model of colitis, oral administration of SMA-7 resulted in decreased cytokine levels in the colon and lower severity of colonic injury. Meanwhile, also desipramine and amitriptyline treatment was shown to inhibit Asm and to decrease pathology in common acute and chronic epithelial injury colitis models (13, 49). In all three studies, Asm inhibition resulted in a decreased pro-inflammatory cytokine production and impaired lymphocyte infiltration. Importantly, broad immunosuppression increases the risk of infectious complications (17) and several enteropathogens have been implicated in the development of gastrointestinal diseases (50, 51). Infection with *Salmonella (S.) typhimurium* results in severe gastroenteritis (52, 53). The pathogen infects the host by invading macrophages in Peyer's patches. Intracellular *S. typhimurium* survives within the lysosomal compartment by preventing lysosomal maturation of the phagosomes (54). Asm activity is required for the release of the reactive oxygen species that are necessary for the killing of intracellular *S. typhimurium* (55). Therefore, Asm deficiency strongly enhance the susceptible to *S. typhimurium* infection (56). Although we also observed a strong susceptibility of Asm inhibited and Asm deficient mice to *C. rodentium* infection, we could not observe any changes in the frequency and phenotype of macrophages in infected amitriptyline treated mice compared to infected wild type mice. However, *C. rodentium* is a noninvasive, attaching-effacing enteric bacterial pathogen, which does not infect macrophages but directly interacts with the intestinal epithelial layer (57). Therefore, it is more likely that the intestinal barrier is impaired in amitriptyline treated animals, which is well in line with the enhanced systemic bacterial distribution of *C. rodentium* in amitriptyline treated mice. Indeed, intestinal sphingolipids provide a non-specific barrier. In a porcine model, inhibition of *de novo* ceramide synthesis impaired the proliferation and barrier function of intestinal epithelial cells, which in turn led to the induction of inflammation (45). Furthermore, intestinal deletion of serine palmitoyltransferase (SPT), which is the rate-limiting enzyme for sphingolipid biosynthesis, significantly decreased the ceramide and sphingomyelin levels in the plasma membrane of gut cells and promoted intestinal cell apoptosis with the impairment of gut barrier function (58). However, further investigation is required to fully understand the impact of Asm on the barrier function in infectious and non-infectious colitis.

T_h1 and T_h17 cells, as part of the adaptive immunity, mediate the host defense against *C. rodentium* via the production of their signature cytokines IFNγ and IL-17 (26, 59), and mice depleted of either cell type have an impaired ability to clear the infection (29, 60). However, an uncontrolled $CD4^+$ T cell response leads to severe immunopathology (20). Interestingly, we observed a significant increase of T_h1 and T_h17 cells accompanied with severe immunopathology in infected mice with Asm inhibition compared to infected wild type mice. Well in line, the regulation of murine T_h1 differentiation by ceramide has been reported. A ceramide analog was shown to enhance IL-12 induced T_h1 differentiation with increased T-bet expression and IFNγ production (61). In contrast, Asm inhibition in human $CD4^+$ T cells abrogates T_h1 cell differentiation (62). In addition, inhibition of Asm bioactivity by imipramine, which blocks the generation of ceramide, was shown to impair T_h17 generation by blocking both mTor and Stat3 (63). Interestingly, we showed an enhanced frequency of T_h17 cells in amitriptyline treated infected mice. Of note, amitriptyline also inhibits in part acid ceramidase, which metabolizes ceramide to sphingosine. Consequently, infected Asm inhibited mice displayed increased ceramide concentrations in the colon compared to infected wild type mice, which seems to further boost the T_h17 response. During *C. rodentium* infection, T_h1 and T_h17 immunity is counterbalanced by regulatory T cells to inhibit severe immunopathology. Asm was recently described as negative regulator of T_{reg} development (64). In comparison to wild type mice, Asm deficient mice have a higher number of systemic T_{reg} cells under homeostasis. Furthermore, inhibition of Asm and supplementation of IL-2 result in augmentation of Foxp3 expression as well as induction of T_{reg} differentiation *in vitro* (64, 65). Surprisingly, we identified lower frequencies of T_{regs} in the colon of infected Asm inhibited mice compared to infected wild type mice suggesting differences

in the polarization process under homeostasis and during infection. Finally, in most of the *in vivo* studies the Asm inhibitor was applied intraperitoneally (66–68), whereas we chose the oral route via the drinking water to specifically target the gastrointestinal tract. Hence, we cannot exclude that the specific immunosuppressive micro-milieu in the intestine interferes with the effects induced by Asm inhibition.

In summary, in contrast to the protective effect of Asm inhibition in common acute and chronic epithelial injury colitis models, Asm inhibition or Asm deficiency strongly enhanced the susceptibility to enteric *C. rodentium* infection. Therefore, understanding the sphingolipid enzymes and metabolic pathways involved in regulating intestinal inflammation under infectious and non-infectious conditions is the prerequisite for the development of new therapeutic strategies, which target the sphingolipid metabolism.

DATA AVAILABILITY

All datasets generated for this study are included in the manuscript and/or the supplementary files.

ETHICS STATEMENT

This study was carried out in accordance with the recommendations of the Society for Laboratory Animal Science (GV-SOLAS) and the European Health Law of the Federation of Laboratory Animal Science Associations (FELASA). The protocol was approved by the North Rhine-Westphalia State Agency for Nature, Environment and Consumer Protection (LANUF), Germany.

AUTHOR CONTRIBUTIONS

JM and AW: conceived and designed the experiments and wrote the paper. JM, VP, RK, J-FE, FS, LJ, AY, KB, and JZ: performed the experiments. JM, VP, RK, J-FE, LJ, WH, and AW: analyzed the data and reviewed and edited the manuscript. MH, DH, BK, RNK, JB, and WH: contributed reagents, materials, analysis tools.

FUNDING

This work was supported by the Deutsche Forschungsgemeinschaft (DFG—GRK2098 to AW, KB, JB, and WH and GRK1949 to AW, JB, and WH).

ACKNOWLEDGMENTS

We kindly thank Mechthild Hemmler-Roloff and Christina Liebig for excellent technical assistance. We are grateful to Erich Gulbins for providing us with Asm KO mice.

REFERENCES

1. Baumgart DC, Sandborn WJ. Inflammatory bowel disease: clinical aspects and established and evolving therapies. *Lancet.* (2007) 369:1641–57. doi: 10.1016/S0140-6736(07)60751-X
2. Fiocchi C. Inflammatory bowel disease: etiology and pathogenesis. *Gastroenterology.* (1998) 115:182–205. doi: 10.1016/S0016-5085(98)70381-6
3. Hannun YA, Obeid LM. Principles of bioactive lipid signalling: lessons from sphingolipids. *Nat Rev Mol Cell Biol.* (2008) 9:139–50. doi: 10.1038/nrm2329
4. Oertel S, Scholich K, Weigert A, Thomas D, Schmetzer J, Trautmann S, et al. Ceramide synthase 2 deficiency aggravates AOM-DSS-induced colitis in mice: role of colon barrier integrity. *Cell Mol Life Sci.* (2017) 74:3039–55. doi: 10.1007/s00018-017-2518-9
5. Bock J, Liebisch G, Schweimer J, Schmitz G, Rogler G. Exogenous sphingomyelinase causes impaired intestinal epithelial barrier function. *World J Gastroenterol.* (2007) 13:5217–25. doi: 10.3748/wjg.v13.i39.5217
6. Snider AJ, Kawamori T, Bradshaw SG, Orr KA, Gilkeson GS, Hannun YA, et al. A role for sphingosine kinase 1 in dextran sulfate sodium-induced colitis. *FASEB J.* (2009) 23:143–52. doi: 10.1096/fj.08-118109
7. Liang J, Nagahashi M, Kim EY, Harikumar KB, Yamada A, Huang WC, et al. Sphingosine-1-phosphate links persistent STAT3 activation, chronic intestinal inflammation, and development of colitis-associated cancer. *Cancer Cell.* (2013) 23:107–20. doi: 10.1016/j.ccr.2012.11.013
8. Huang WC, Liang J, Nagahashi M, Avni D, Yamada A, Maceyka M, et al. Sphingosine-1-phosphate phosphatase 2 promotes disruption of mucosal integrity, and contributes to ulcerative colitis in mice and humans. *FASEB J.* (2016) 30:2945–58. doi: 10.1096/fj.201600394R
9. Beckmann N, Sharma D, Gulbins E, Becker KA, Edelmann B. Inhibition of acid sphingomyelinase by tricyclic antidepressants and analogons. *Front Physiol.* (2014) 5:331. doi: 10.3389/fphys.2014.00331
10. Lloyd-Evans E, Morgan AJ, He X, Smith DA, Elliot-Smith E, Sillence DJ, et al. Niemann-Pick disease type C1 is a sphingosine storage disease that causes deregulation of lysosomal calcium. *Nat Med.* (2008) 14:1247–55. doi: 10.1038/nm.1876
11. Maceyka M, Spiegel S. Sphingolipid metabolites in inflammatory disease. *Nature.* (2014) 510:58–67. doi: 10.1038/nature13475
12. Sakata A, Ochiai T, Shimeno H, Hikishima S, Yokomatsu T, Shibuya S, et al. Acid sphingomyelinase inhibition suppresses lipopolysaccharide-mediated release of inflammatory cytokines from macrophages and protects against disease pathology in dextran sulphate sodium-induced colitis in mice. *Immunology.* (2007) 122:54–64. doi: 10.1111/j.1365-2567.2007.02612.x
13. Xiong Y, Zhu XD, Wan P, Ren YP, Wang C, Yan RW, et al. Inhibition of ASM activity ameliorates DSS-induced colitis in mice. *Prostaglandins Other Lipid Mediat.* (2018) 140:26–30. doi: 10.1016/j.prostaglandins.2018.12.002
14. Bai A, Guo Y. Acid sphingomyelinase mediates human CD4(+) T-cell signaling: potential roles in T-cell responses and diseases. *Cell Death Dis.* (2017) 8:e2963. doi: 10.1038/cddis.2017.360
15. Rahimi HR, Shiri M, Razmi A. Antidepressants can treat inflammatory bowel disease through regulation of the nuclear factor-kappaB/nitric oxide pathway and inhibition of cytokine production: a hypothesis. *World J Gastrointest Pharmacol Ther.* (2012) 3:83–5. doi: 10.4292/wjgpt.v3.i6.83
16. Campieri M, Gionchetti P. Bacteria as the cause of ulcerative colitis. *Gut.* (2001) 48:132–5. doi: 10.1136/gut.48.1.132
17. Orlicka K, Barnes E, Culver EL. Prevention of infection caused by immunosuppressive drugs in gastroenterology. *Ther Adv Chronic Dis.* (2013) 4:167–85. doi: 10.1177/2040622313485275
18. Horinouchi K, Erlich S, Perl DP, Ferlinz K, Bisgaier CL, Sandhoff K, et al. Acid sphingomyelinase deficient mice: a model of types A and B Niemann-Pick disease. *Nat Genet.* (1995) 10:288–93. doi: 10.1038/ng0795-288
19. Pastille E, Bardini K, Fleissner D, Adamczyk A, Frede A, Wadwa M, et al. Transient ablation of regulatory T cells improves antitumor immunity in colitis-associated colon cancer. *Cancer Res.* (2014) 74:4258–69. doi: 10.1158/0008-5472.CAN-13-3065
20. Seiffart V, Zoeller J, Klopfleisch R, Wadwa M, Hansen W, Buer J, et al. IL10-Deficiency in CD4(+) T cells exacerbates the IFNγ and IL17 response

during bacteria induced colitis. *Cell Physiol Biochem.* (2015) 36:1259–73. doi: 10.1159/000430295
21. Duan RD, Nilsson A. Metabolism of sphingolipids in the gut and its relation to inflammation and cancer development. *Prog Lipid Res.* (2009) 48:62–72. doi: 10.1016/j.plipres.2008.04.003
22. Kornhuber J, Tripal P, Reichel M, Muhle C, Rhein C, Muehlbacher M, et al. Functional Inhibitors of Acid Sphingomyelinase (FIASMAs): a novel pharmacological group of drugs with broad clinical applications. *Cell Physiol Biochem.* (2010) 26:9–20. doi: 10.1159/000315101
23. Kornhuber J, Tripal P, Gulbins E, Muehlbacher M. Functional inhibitors of acid sphingomyelinase (FIASMAs). *Handb Exp Pharmacol.* (2013) 169–86. doi: 10.1007/978-3-7091-1368-4_9
24. Collins JW, Keeney KM, Crepin VF, Rathinam VA, Fitzgerald KA, Finlay BB, et al. *Citrobacter rodentium*: infection, inflammation and the microbiota. *Nat Rev Microbiol.* (2014) 12:612–23. doi: 10.1038/nrmicro3315
25. Schreiber HA, Loschko J, Karssemeijer RA, Escolano A, Meredith MM, Mucida D, et al. Intestinal monocytes and macrophages are required for T cell polarization in response to *Citrobacter rodentium*. *J Exp Med.* (2013) 210:2025–39. doi: 10.1084/jem.20130903
26. Higgins LM, Frankel G, Douce G, Dougan G, Macdonald TT. *Citrobacter rodentium* infection in mice elicits a mucosal Th1 cytokine response and lesions similar to those in murine inflammatory bowel disease. *Infect Immun.* (1999) 67:3031–9.
27. Bry L, Brenner MB. Critical role of T cell-dependent serum antibody, but not the gut-associated lymphoid tissue, for surviving acute mucosal infection with *Citrobacter rodentium*, an attaching and effacing pathogen. *J Immunol.* (2004) 172:433–41. doi: 10.4049/jimmunol.172.1.433
28. Bry L, Brigl M, Brenner MB. CD4+-T-cell effector functions and costimulatory requirements essential for surviving mucosal infection with *Citrobacter rodentium*. *Infect Immun.* (2006) 74:673–81. doi: 10.1128/IAI.74.1.673-681.2006
29. Simmons CP, Goncalves NS, Ghaem-Maghami M, Bajaj-Elliott M, Clare S, Neves B, et al. Impaired resistance and enhanced pathology during infection with a noninvasive, attaching-effacing enteric bacterial pathogen, *Citrobacter rodentium*, in mice lacking IL-12 or IFN-gamma. *J Immunol.* (2002) 168:1804–12. doi: 10.4049/jimmunol.168.4.1804
30. Mundy R, Macdonald TT, Dougan G, Frankel G, Wiles S. *Citrobacter rodentium* of mice and man. *Cell Microbiol.* (2005) 7:1697–706. doi: 10.1111/j.1462-5822.2005.00625.x
31. Mangan PR, Harrington LE, O'quinn DB, Helms WS, Bullard DC, Elson CO, et al. Transforming growth factor-beta induces development of the T(H)17 lineage. *Nature.* (2006) 441:231–4. doi: 10.1038/nature04754
32. Wang Z, Friedrich C, Hagemann SC, Korte WH, Goharani N, Cording S, et al. Regulatory T cells promote a protective Th17-associated immune response to intestinal bacterial infection with *C. rodentium*. *Mucosal Immunol.* (2014) 7:1290–301. doi: 10.1038/mi.2014.17
33. Merck Sharp AD. *Amitriptyline Hydrochloride: An Antidepressive Agent: Résumé of Essential Information*. Rahway, NJ: Merck & CO (1961).
34. Carette S, McCain GA, Bell DA, Fam AG. Evaluation of amitriptyline in primary fibrositis. *A double-blind, placebo-controlled study. Arthritis Rheum.* (1986) 29:655–9. doi: 10.1002/art.1780290510
35. Couch JR, Ziegler DK, Hassanein R. Amitriptyline in the prophylaxis of migraine. *Effectiveness and relationship of antimigraine and antidepressant effects. Neurology.* (1976) 26:121–7. doi: 10.1212/WNL.26.2.121
36. Egbunike IG, Chaffee BJ. Antidepressants in the management of chronic pain syndromes. *Pharmacotherapy.* (1990) 10:262–70.
37. Mishra PC, Agarwal VK, Rahman H. Therapeutic trial of amitryptiline in the treatment of nocturnal enuresis–a controlled study. *Indian Pediatr.* (1980) 17:279–85.
38. Friedman G. Treatment of the irritable bowel syndrome. *Gastroenterol Clin North Am.* (1991) 20:325–33.
39. Mandal A, Sinha C, Kumar Jena A, Ghosh S, Samanta A. An investigation on *in vitro* and *in vivo* antimicrobial properties of the antidepressant: amitriptyline hydrochloride. *Braz J Microbiol.* (2010) 41:635–45. doi: 10.1590/S1517-83822010000300014
40. Roumestan C, Michel A, Bichon F, Portet K, Detoc M, Henriquet C, et al. Anti-inflammatory properties of desipramine and fluoxetine. *Respir Res.* (2007) 8:35. doi: 10.1186/1465-9921-8-35
41. Shale M, Schiering C, Powrie F. CD4(+) T-cell subsets in intestinal inflammation. *Immunol Rev.* (2013) 252:164–82. doi: 10.1111/imr.12039
42. Matricon J, Barnich N, Ardid D. Immunopathogenesis of inflammatory bowel disease. *Self Nonself.* (2010) 1:299–309. doi: 10.4161/self.1.4.13560
43. Zhang YZ, Li YY. Inflammatory bowel disease: pathogenesis. *World J Gastroenterol.* (2014) 20:91–9. doi: 10.3748/wjg.v20.i1.91
44. Sandborn WJ, Feagan BG, Wolf DC, D'haens G, Vermeire S, Hanauer SB, et al. Ozanimod induction and maintenance treatment for ulcerative colitis. *N Engl J Med.* (2016) 374:1754–62. doi: 10.1056/NEJMoa1513248
45. Bouhet S, Hourcade E, Loiseau N, Fikry A, Martinez S, Roselli M, et al. The mycotoxin fumonisin B1 alters the proliferation and the barrier function of porcine intestinal epithelial cells. *Toxicol Sci.* (2004) 77:165–71. doi: 10.1093/toxsci/kfh006
46. Tafazoli F, Magnusson KE, Zheng L. Disruption of epithelial barrier integrity by *Salmonella enterica* serovar typhimurium requires geranylgeranylated proteins. *Infect Immun.* (2003) 71:872–81. doi: 10.1128/IAI.71.2.872-881.2003
47. Bryan P-F, Karla C, Edgar Alejandro M-T, Sara Elva E-P, Gemma F, Luz C. Sphingolipids as mediators in the crosstalk between microbiota and intestinal cells: implications for inflammatory bowel disease. *Mediat Inflamm.* (2016) 2016:9890141. doi: 10.1155/2016/9890141
48. Gulhan B, Ozcelik U, Gurakan F, Gucer S, Orhan D, Cinel G, et al. Different features of lung involvement in Niemann-Pick disease and Gaucher disease. *Respir Med.* (2012) 106:1278–85. doi: 10.1016/j.rmed.2012.06.014
49. Fattahian E, Hajhashemi V, Rabbani M, Minaiyan M, Mahzouni P. Anti-inflammatory effect of amitriptyline on ulcerative colitis in normal and reserpine-induced depressed rats. *Iran J Pharm Res.* (2016) 15(Suppl.):125–37. doi: 10.22037/ijpr.2016.1813
50. Garcia Rodriguez LA, Ruigomez A, Panes J. Acute gastroenteritis is followed by an increased risk of inflammatory bowel disease. *Gastroenterology.* (2006) 130:1588–94. doi: 10.1053/j.gastro.2006.02.004
51. Sartor RB, Rath HC, Sellon RK. Microbial factors in chronic intestinal inflammation. *Curr Opin Gastroenterol.* (1996) 12:327–33. doi: 10.1097/00001574-199607000-00003
52. Feasey NA, Dougan G, Kingsley RA, Heyderman RS, Gordon MA. Invasive non-typhoidal salmonella disease: an emerging and neglected tropical disease in Africa. *Lancet.* (2012) 379:2489–99. doi: 10.1016/S0140-6736(11)61752-2
53. Ramachandran G, Panda A, Higginson EE, Ateh E, Lipsky MM, Sen S, et al. Virulence of invasive Salmonella Typhimurium ST313 in animal models of infection. *PLoS Negl Trop Dis.* (2017) 11:e0005697. doi: 10.1371/journal.pntd.0005697
54. McCollister BD, Bourret TJ, Gill R, Jones-Carson J, Vazquez-Torres A. Repression of SPI2 transcription by nitric oxide-producing, IFNgamma-activated macrophages promotes maturation of Salmonella phagosomes. *J Exp Med.* (2005) 202:625–35. doi: 10.1084/jem.20050246
55. McCollister BD, Myers JT, Jones-Carson J, Voelker DR, Vazquez-Torres A. Constitutive acid sphingomyelinase enhances early and late macrophage killing of *Salmonella enterica* serovar Typhimurium. *Infect Immun.* (2007) 75:5346–52. doi: 10.1128/IAI.00689-07
56. Utermohlen O, Karow U, Lohler J, Kronke M. Severe impairment in early host defense against Listeria monocytogenes in mice deficient in acid sphingomyelinase. *J Immunol.* (2003) 170:2621–8. doi: 10.4049/jimmunol.170.5.2621
57. Bergstrom KSB, Guttman JA, Rumi M, Ma C, Bouzari S, Khan MA, et al. Modulation of intestinal goblet cell function during infection by an attaching and effacing bacterial pathogen. *Infect Immun.* (2008) 76:796–811. doi: 10.1128/IAI.00093-07
58. Li Z, Kabir I, Tietelman G, Huan C, Fan J, Worgall T, et al. Sphingolipid *de novo* biosynthesis is essential for intestine cell survival and barrier function. *Cell Death Dis.* (2018) 9:173. doi: 10.1038/s41419-017-0214-1
59. Symonds EL, Riedel CU, O'mahony D, Lapthorne S, O'mahony L, Shanahan F. Involvement of T helper type 17 and regulatory T cell activity in *Citrobacter rodentium* invasion and inflammatory damage. *Clin Exp Immunol.* (2009) 157:148–54. doi: 10.1111/j.1365-2249.2009.03934.x
60. Ishigame H, Kakuta S, Nagai T, Kadoki M, Nambu A, Komiyama Y, et al. Differential roles of interleukin-17A and−17F in host defense against mucoepithelial bacterial infection and allergic responses. *Immunity.* (2009) 30:108–19. doi: 10.1016/j.immuni.2008.11.009

61. Kue CS, Jung MY, Cho D, Kim TS. C6-ceramide enhances Interleukin-12-mediated T helper type 1 cell responses through a cyclooxygenase-2-dependent pathway. *Immunobiology.* (2012) 217:601–9. doi: 10.1016/j.imbio.2011.10.021
62. Bai A, Kokkotou E, Zheng Y, Robson SC. Role of acid sphingomyelinase bioactivity in human CD4+ T-cell activation and immune responses. *Cell Death Dis.* (2015) 6:e1828. doi: 10.1038/cddis.2015.178
63. Bai A, Moss A, Kokkotou E, Usheva A, Sun X, Cheifetz A, et al. CD39 and CD161 modulate Th17 responses in Crohn's disease. *J Immunol.* (2014) 193:3366–77. doi: 10.4049/jimmunol.1400346
64. Zhou Y, Salker MS, Walker B, Munzer P, Borst O, Gawaz M, et al. Acid Sphingomyelinase (ASM) is a negative regulator of regulatory T Cell (Treg) development. *Cell Physiol Biochem.* (2016) 39:985–95. doi: 10.1159/000447806
65. Schneider-Schaulies J, Beyersdorf N. CD4+ Foxp3+ regulatory T cell-mediated immunomodulation by anti-depressants inhibiting acid sphingomyelinase. *Biol Chem.* (2018) 399:1175–82. doi: 10.1515/hsz-2018-0159
66. Peng H, Li C, Kadow S, Henry BD, Steinmann J, Becker KA, et al. Acid sphingomyelinase inhibition protects mice from lung edema and lethal *Staphylococcus aureus* sepsis. *J Mol Med.* (2015) 93:675–89. doi: 10.1007/s00109-014-1246-y
67. Johnson BL III, Rice TC, Xia BT, Boone KI, Green EA, Gulbins E, et al. Amitriptyline usage exacerbates the immune suppression following burn injury. *Shock (Augusta Ga.).* (2016) 46:541–8. doi: 10.1097/SHK.0000000000000648
68. Hollmann C, Werner S, Avota E, Reuter D, Japtok L, Kleuser B, et al. Inhibition of acid sphingomyelinase allows for selective targeting of CD4+ conventional versus Foxp3+ regulatory T cells. *J Immunol.* (2016) 197:3130–41. doi: 10.4049/jimmunol.1600691

Conflict of Interest Statement: The authors declare that the research was conducted in the absence of any commercial or financial relationships that could be construed as a potential conflict of interest.

frontiers in Immunology

REVIEW
published: 19 July 2019
doi: 10.3389/fimmu.2019.01706

Sphingosine-1-Phosphate and Macrophage Biology—How the Sphinx Tames the Big Eater

Andreas Weigert[1], *Catherine Olesch*[1] *and Bernhard Brüne*[1,2,3,4]*

[1] Faculty of Medicine, Institute of Biochemistry I, Goethe-University Frankfurt, Frankfurt, Germany, [2] German Cancer Consortium (DKTK), Partner Site Frankfurt, Frankfurt, Germany, [3] Project Group Translational Medicine and Pharmacology TMP, Fraunhofer Institute for Molecular Biology and Applied Ecology, Frankfurt, Germany, [4] Frankfurt Cancer Institute, Goethe-University Frankfurt, Frankfurt, Germany

The sphingolipid sphingosine-1-phosphate (S1P) is produced by sphingosine kinases to either signal through intracellular targets or to activate a family of specific G-protein-coupled receptors (S1PR). S1P levels are usually low in peripheral tissues compared to the vasculature, forming a gradient that mediates lymphocyte trafficking. However, S1P levels rise during inflammation in peripheral tissues, thereby affecting resident or recruited immune cells, including macrophages. As macrophages orchestrate initiation and resolution of inflammation, the sphingosine kinase/S1P/S1P-receptor axis emerges as an important determinant of macrophage function in the pathogenesis of inflammatory diseases such as cancer, atherosclerosis, and infection. In this review, we therefore summarize the current knowledge how S1P affects macrophage biology.

Keywords: sphingosine-1-phosphate, macrophages, macrophage polarization, cancer, atherosclerosis, infection, inflammation

OPEN ACCESS

Edited by:
Burkhard Kleuser,
University of Potsdam, Germany

Reviewed by:
Hridayesh Prakash,
Amity University, India
Elsa Anes,
University of Lisbon, Portugal

***Correspondence:**
Bernhard Brüne
b.bruene@biochem.uni-frankfurt.de

Specialty section:
This article was submitted to Microbial Immunology, a section of the journal Frontiers in Immunology

Received: *30 April 2019*
Accepted: *08 July 2019*
Published: *19 July 2019*

Citation:
Weigert A, Olesch C and Brüne B (2019) Sphingosine-1-Phosphate and Macrophage Biology—How the Sphinx Tames the Big Eater. Front. Immunol. 10:1706. doi: 10.3389/fimmu.2019.01706

INTRODUCTION

In 1887, Metchnikoff published work on the nature host cells combating bacterial infection. He suggested the large cells he and other before him had observed taking up whole cells or cell fragments, to be named macrophages, as opposed to microphages (polymorphonuclear leukocytes) who specialized in combating bacteria (1). The term macrophage consequently is a composite of the Greek words *makros*, meaning large, and *phagein*, to eat, and denotes big eating cells. Today we are aware that macrophages are more than just big eaters, playing a multitude of crucial roles in development and maintaining adult tissue homeostasis. To be able to fulfill these roles, they command an enormous sensory repertoire to recognize cues suggesting endangered or disturbed homeostasis. One of these cues is the sphingolipid S1P that is produced during inflammation and upon tissue damage. Sphingolipids were named after the Sphinx by J. L. W. Thudichum in 1884 due to the enigmatic biochemical properties of their common backbone, the alcohol sphingosine. The Sphinx in Greek mythology poses riddles to travelers and kills them if they fail to answer correctly, whereas in Egyptian mythology the Sphinx is a rather benevolent guardian of sacred sites. Like the enigmatic Sphinx, S1P affects macrophage biology in different, sometimes antithetical ways. Here, we review the interaction of the sphinx and the big eater. We start with an introduction of the protagonists and their role in inflammation and tissue homeostasis. Next, we summarize the current knowledge on molecular mechanisms how S1P attracts macrophages and determines their survival, followed by reviewing how S1P affects the signature functions of macrophages,

i.e., phagocytosis and the regulation of inflammation. Finally, we discuss how these S1P-dependent mechanisms affect macrophage function in pathological settings.

MORE THAN BIG EATERS—MACROPHAGE FUNCTION IN HOMEOSTASIS AND DISEASE

Macrophages are ubiquitous, yet diverse tissue-resident immune cells, involved in maintaining tissue integrity and function. They sense and actively respond to disturbances in tissue homeostasis by initiating, but also resolving inflammation (2, 3). The diverse functions of macrophages are tissues-specific and range from basic tasks, such as rearranging the extracellular matrix and taking up and recycling cellular and molecular debris, to highly specialized functions such as controlling tissue innervation or promoting conductance in the heart by modulating electrical properties of cardiomyocytes (3–6). Upon tissue injury, macrophages recognize new molecular patterns from dead cells or invading microorganisms. In turn, this mounts an immune response, e.g., by recruiting new inflammatory cells to the site of tissue disturbance. Once a noxa is cleared with the help of resident and recruited macrophages, macrophages participate in removing (dead) inflammatory cells by phagocytosis. At the same time they contribute to restore the tissue by promoting angiogenesis and reparative signaling in stroma and parenchyma (7–10). Their ability to cope with the changing demands during an acute inflammatory reaction suggests a remarkable plasticity.

Macrophage function is, to a large extent, dictated by the dominating microenvironment, rather than genetic imprinting. In tissues, macrophages have different developmental origins (11–13). They can be derived from early hematopoiesis in the yolk sac (11–17) or the fetal liver, without transitioning through a monocytic intermediate stage (16, 17). Post-natally, macrophages may derive from hematopoietic stem cell-derived monocytes from the bone marrow (18, 19). Tissue-resident macrophages of embryonic origin often self-renew by *in-situ* proliferation, whereas monocyte-derived macrophages are frequently, but not always, short-lived and continuously replaced (11–14, 20). During depletion of the resident macrophage pool upon e.g., inflammation or experimental means, monocytes or other macrophage progenitors readily integrate into the tissue macrophage pool and become self-renewing cells (11, 12, 14, 20, 21). Moreover, transplantation of mature macrophages between tissues alters their transcriptional program to fit the recipient tissue macrophage pool (20). Finally, distinct macrophage subsets, partly of similar developmental origin, are found in specialized niches within one tissue (22–25).

The notion that the microenvironment determines macrophage function is further supported by identifying tissue-specific transcription factors that are required to establish tissue macrophage identity. All macrophages depend on the lineage-determining transcription factor PU.1, whose expression is triggered by colony stimulating factor-1 (CSF1) or interleukin (IL-)34 (IL-34), which signal through colony stimulating factor-1 receptor (26, 27). Moreover, the transcription factor ZEB2 is required for macrophage identity across a number of tissues (28). On top of this basic transcriptional program, tissue-specific transcriptional regulators were identified that are activated downstream of tissue-enriched molecular cues. These include SPI-C in progenitors of red pulp and bone marrow macrophages (29), GATA6 in peritoneal macrophages (30, 31), peroxisome proliferator-activated receptor (PPAR) in alveolar macrophages (32), SMAD transcription factors and myocyte-specific enhancer factor 2c (MEF2c) in microglia (33, 34), liver x receptor (LXRα) in Kupffer cells, as well as Runt-related transcription factor 3 (RUNX3) in intestinal macrophages and Langerhans cells (20, 35).

Despite these lineage- and tissue-imprinted molecular programs, macrophages retain a remarkable degree of plasticity to respond to the appearance of new molecular cues indicative of a disturbed homeostasis. These cues are sensed by a repertoire of receptors on macrophages and activate transcriptional enhancers or repressors, generating a large number of possible activation states (36–39). A considerable body of research aimed at defining discrete macrophage polarization states *in vitro* by using sets of specific molecular or functional markers, which are thought to serve as predictors of macrophage function in living organisms (36, 40–42). Frequently used is the M1/M2 nomenclature, where M1 macrophages are stimulated with interferon-γ (IFN-γ) and lipopolysaccharide (LPS) to mimic a condition arising during type 1 inflammation (defense against microbial infection), whereas M2 macrophages are stimulated with the TH2 cytokines IL-4 or IL-13 to mimic conditions of type 2 inflammation (helminth infection). Specific marker signatures have been assigned to these cells. M1 macrophage activation creates an anti-microbial, pro-inflammatory cell with a transcriptional signature defined by activation of nuclear factor kappa-light-chain-enhancer of activated B cells (NF-κB), signal transducer and activator of transcription 1 (STAT1) and interferon regulatory factor 5 (IRF 5) (43, 44). M1 or classically activated macrophages produce pro-inflammatory mediators such as tumor necrosis factor-α (TNF-α), IL-1β, IL-6, and IL-12, generate reactive oxygen and nitrogen species (ROS/RNS), and activate T cells to produce type 1 cytokines. M2 or alternatively activated macrophages display activation of the transcription factors STAT6 and IRF4 to express specific chemokines including CCL17 and CCL18, phagocytic receptors such as the mannose receptor CD206, arginases (ARG1/2) to limit NO production, and mediators that modulate the extracellular matrix. All of them are originally induced to combat extracellular parasites (36, 39, 44–46). The M1/M2 nomenclature is useful, although naturally limited since macrophages in a tissue never face M1 or M2-specific stimuli. In fact, IL-4 and IFN-γ are often produced simultaneously during inflammation (47). In analogy to T cells, IL-4, and IFN-γ, besides inducing discreet transcriptional outputs, mutually suppress the impact of the corresponding signaling pathway to affect the macrophage phenotype. IL-4 suppresses enhancer regions in a large set of inflammatory genes directly via STAT6 (48), while IFN-γ induces a loss of enhancer binding by the transcription factor MAF in M2 genes to reduce chromatin accessibility (49). Even

when supplied together in cell culture, IFN-γ and IL-4 mutually inhibited epigenomic and transcriptional changes induced by each cytokine alone, while allowing the expression of core functional parameters such as IFN-γ-triggered antiviral genes (47). Moreover, macrophage polarization by IFN-γ or IL-4 appears to be a transient rather than a stable process (47, 50, 51), which makes sense when different functional needs arise during the course of an inflammatory reaction. Therefore, "pure" M1 or M2 macrophages will not be found in a complex environment, and claiming distinct functions from a small set of markers expressed by macrophages in a tissue needs to be approached carefully. Nevertheless, understanding mechanisms that regulate macrophage plasticity is of importance, since dysregulation of macrophage activity is connected to human pathologies including major causes of premature death such as infection, atherosclerosis, fibrotic diseases, and cancer (3, 37).

ENTER: THE SPHINX—S1P AND ITS RECEPTORS IN IMMUNITY

Sphingosine-1-phosphate (S1P) is a biologically active lipid mediator being produced in and affecting macrophages. With central roles of macrophages during inflammation and cancer the sphere of S1P actions touches ground under a number of physiological as well as pathological settings. Production, degradation, and biological actions of S1P in the mammalian system have been reviewed in depth (52–58) and are only briefly recapitulated. Central to sphingolipid metabolism is ceramide, which is a hub for sphingolipid synthesis and degradation (59). *De novo* synthesis of ceramide starts by condensation of serine and palmitoyl-CoA to form 3-keto-dihydrosphingosine, which is subsequently reduced to dihydrosphingosine and N-acylated to form a large group of dihydroceramides (60). A desaturase then produces corresponding ceramides. Ceramides can either be phosphorylated, or glycosylated to form glucosylceramides, which are processed and exposed at the plasma membrane as glycosphingolipids. Alternatively, ceramides can be converted to sphingomyelin, also being incorporated into the outer cell membrane. There, sphingomyelin can be attacked by neutral or acidic sphingomyelinase and converted back to ceramide. In turn, ceramides are cleaved by ceramidases to generate sphingosine, which gets phosphorylated by sphingosine kinase-1 (SPHK1) or−2 (SPHK2) to form S1P (55, 61). S1P can be transformed in the salvage pathway via sphingosine back to ceramide or irreversibly degraded by S1P lyase (SGPL1) to hexadecenal and phosphoethanolamine. S1P, produced at the plasma membrane, can be exported from cells by ATP-binding cassette (ABC) transporters or spinster 2 (Spns2) (62, 63). Once outside cells, S1P is recognized by a family of five distinct G-protein coupled receptors (S1PR1-5) that initiate autocrine, "inside-out," or paracrine signaling (64). Cell type-selective expression of distinct S1P receptors and their coupling to different G-alpha subunits allows S1P to exert a multitude of signaling qualities (53). S1P can also signal intracellularly via several less generalized and commonly accepted targets (65–67), which also plays a role during macrophage activation.

Macrophages express all five S1P receptors, albeit receptor expression varies among different macrophage subtypes and seems related to distinct functional properties (67). S1P receptors belong to a family of seven helix transmembrane G-protein coupled receptors (GPCR), linked to either G_i, G_q, and/or $G_{12/13}$. Concomitantly, directly tied signaling pathways including small GTPases, phospholipases, PI3K, or adenylyl cyclase are affected, which in turn initiate a myriad of diverse signals. Specific G-protein-coupled receptors (S1PR) signaling is commonly connected to cell migration, proliferation, and differentiation, with individual S1P receptors partly mediating convergent and partly mediating antithetic responses (68). For instance, S1PR1, coupling to G_i promotes the migration of lymphocytes, while S1PR2, which couples to G_i, G_q, and $G_{12/13}$, restricts migration (69). This reciprocal interaction regulates among others B cell localization in lymphatic organs. On the other hand, S1PR1/2 and 3, the latter also coupling to G_i, G_q, and $G_{12/13}$, appear to jointly coordinate vascular development during embryogenesis in mice and zebrafish (70, 71).

S1P is a prototypical molecular signal that is induced upon disturbance of tissue homeostasis. Normally, its levels in tissues are too low to activate specific receptors, with the exception of the circulation, where S1P levels reach nano- to micromolar concentrations (72). However, during inflammation S1P levels rise and are sensed, among others cells by macrophages. As macrophages are exposed to multiple signals from their environment, which allows them to adjust their output repertoire under homeostatic, inflamed, or regenerative conditions, S1P production, S1P receptor expression and/or signaling might add to the complexity of their functional properties. On the following pages we therefore summarize the impact of the S1P signaling system on macrophage responses (summarized in **Figure 1**), and discuss if modulation of this system might be therapeutically attractive.

ATTRACTING THE EATER—S1P AND MACROPHAGE HOMEOSTASIS

In the last years it became evident that S1P plays an important role in tissue surveillance by recruiting immune cells and modulating their life-span (65). Consequently, S1P affects macrophage-driven tissue homeostasis by, among others, mediating macrophage differentiation, migration and survival. S1P, as shown for various other cell types, also serves in macrophages as an anti-apoptotic signal. It is suggested that S1P prevents caspase-induced apoptosis of macrophages by inducing the expression of anti-apoptotic proteins such as B-cell lymphoma 2 (Bcl-2) and B-cell lymphoma extra-large (Bcl-XL) through the activation of phosphoinositide-3-kinase (PI3K), extracellular-signal regulated kinase (ERK)1/2 and Ca^{2+} signaling pathways or changing the cellular balance of ceramide to sphingosine or S1P (58, 73, 74). A more recent study showed that S1P acted as an anti-apoptotic component of high-density lipoprotein (HDL) by inducing inhibitor of apoptosis (IAP) family member survivin via STAT3 in THP-1 and RAW264.7 macrophages (75). This was blocked by

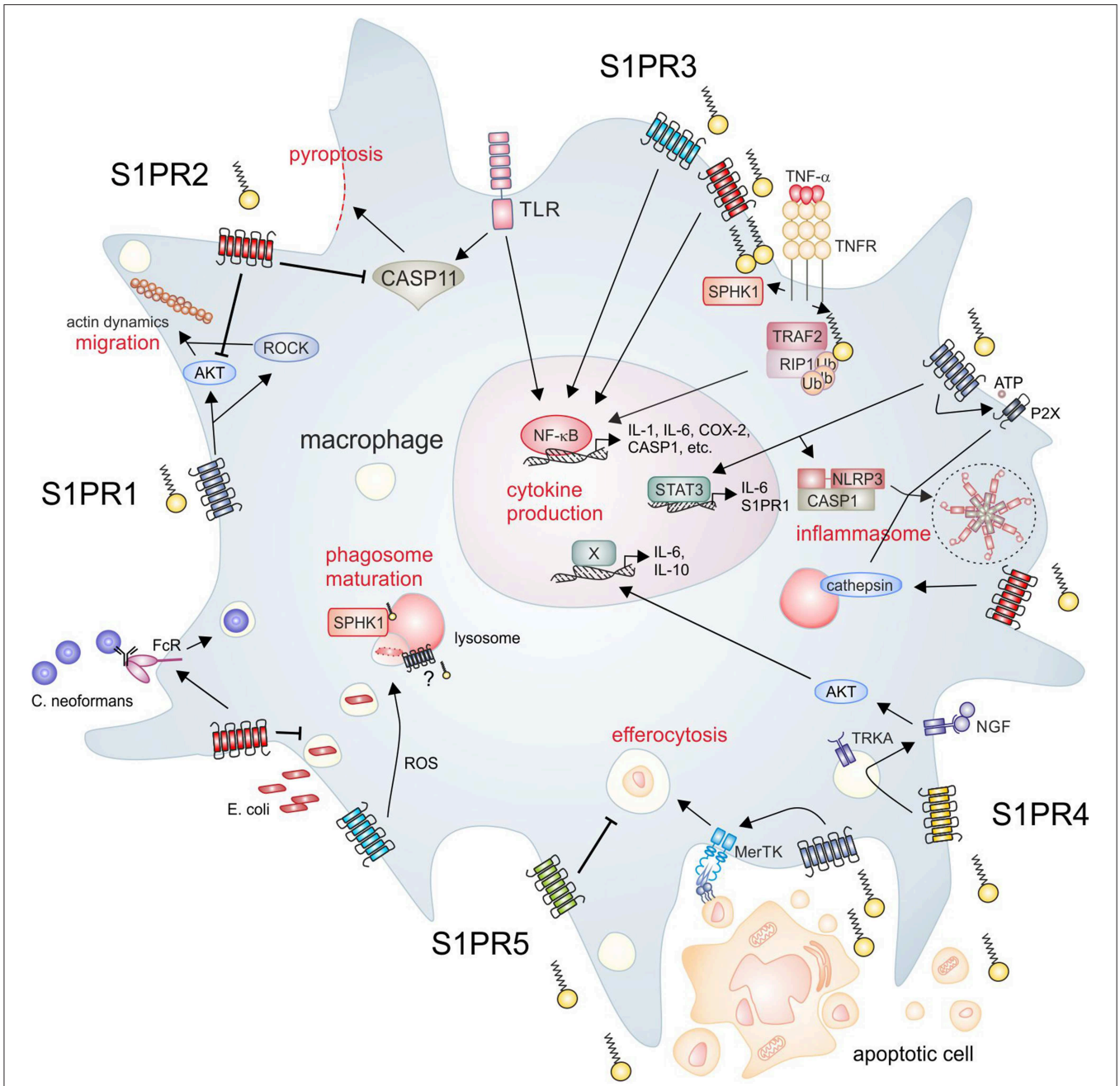

FIGURE 1 | S1P signaling and macrophage function. The SPHK/S1P/S1PR axis regulates essential macrophage functions. Clockwise from upper left, S1PR1 signaling promotes macrophage migration, which is inhibited by S1PR2. Moreover, S1PR2 inhibits endotoxin-induced pyroptosis. Intracellular S1P produced by SPHK1 activates inflammatory pathways in macrophages, which are also activated downstream of S1PR2/3. S1PR1 mainly signals through STAT3 to induce cytokine production, but also induces expression of NLRP3. S1PR1 and S1PR2 are furthermore involved in the activation of the NLRP3 inflammasome trough divergent mechanisms. S1PR2 signaling promotes the opsonin-dependent uptake of the pathogenic fungus C. neoformans, but blocks uptake of bacteria such as E. coli. S1PR3 promotes bacterial killing via promoting ROS generation. SPHK1 is required for phagosome maturation, although it is unclear if S1PR signaling is involved in this process. Apoptotic cells release S1P to activate signaling through S1PR1, which promotes efferocytosis. In turn, S1PR5 blocks efferocytosis. S1PR4 is activated by apoptotic cell derived S1P to promote cytokine expression dependent on TRKA shuttling. AKT, protein kinase B; CASP, caspase; COX-2, cyclooxygenase-2; FcR, Fc receptor; IL, interleukin; MerTK, proto-oncogene tyrosine-protein kinase MER; NF-κB, nuclear factor "kappa-light-chain-enhancer" of activated B-cells; NGF, nerve growth factor; NLRP3, NACHT, LRR, and PYD domains-containing protein 3; P2X, P2X purinoceptor; RIP, receptor interacting protein; ROCK, rho-associated, coiled-coil-containing protein kinase; ROS, reactive oxygen species; S1P, sphingosine-1-phosphate; S1PR, sphingosine-1-phosphate receptor; SPHK, sphingosine kinase; STAT, signal transducer and activator of transcription; TLR, toll-like receptor; TNF, tumor necrosis factor; TNFR, TNF receptor; TRAF, TNF receptor-associated factor; TRKA, tropomyosin receptor kinase A.

antagonists against S1PR2/3, indicating cooperative signaling by S1PR2/3 under these conditions (75). Reduced caspase-induced cell death of macrophages by S1P may extend beyond apoptosis. S1PR2 signaling was demonstrated to reduce caspase-11 protein expression in peritoneal macrophages, thereby limiting macrophage pyroptosis (76). Shifting the cellular balance of ceramide to sphingosine/S1P toward the latter seems not only to be important for macrophage survival but also plays a role during the differentiation of blood monocytes to macrophages. Monick et al. showed that during macrophage differentiation levels of acid ceramidase increased, which enhanced the lifespan of macrophages, most likely due to the conversion of ceramide to sphingosine, resulting in higher intracellular S1P levels (77).

For macrophages to maintain tissue homeostasis they not only need to regulate their number by survival, but they also have to be in the right place at the right time. Accordingly, S1P can also serve as a lipid attraction signal to guide macrophages to the sites of inflammation and tissue repair (78). It has been shown that S1P-dependent macrophage migration is strictly dependent on their S1PR profile. Thereby, S1PR1 signaling seems to be pro-migratory as shown for peritoneal macrophages involving Rho kinase and PI3K-Akt1 signaling and for bone marrow-derived macrophages (BMDM), stimulated by S1P-enriched extracellular vesicles during hepatic lipotoxicity (79, 80). S1PR1 is also essential for post-inflammatory macrophage emigration as shown in a mouse model of resolving peritoneal inflammation, harboring a macrophage-specific deletion of S1PR1, which reduced emigration of macrophages from the site of inflammation (81). More recently it has been discussed that S1PR4 signaling may inhibit the pro-migratory actions of S1PR1 and that the S1PR1/S1PR4 ratio is important for the emigration of pro-inflammatory M1 macrophages from sites of inflammation. It was demonstrated that M1 macrophages exhibit a higher S1PR1/S1PR4 ratio than M2 macrophages (82). However, further studies for example inhibiting S1PR1 and−4 individually in macrophages are needed to clarify the functional role of the S1PR4 to S1PR1 counter-regulation during inflammation. In contrast to the pro-migratory actions of S1PR1, S1PR2 signaling was proposed to inhibit macrophage trafficking by stimulating cAMP production, thereby attenuating Akt phosphorylation, as demonstrated using S1PR2 knockout mice in a peritonitis model of acute inflammation (83). These findings exemplified the antithetic properties of S1PR1 and S1PR2 in immune cell migration. In support of this concept, chemotaxis of osteoclast precursors, with osteoclasts being bone macrophages, is reciprocally regulated by S1PR1/2, which serves to fine-tune their localization in bones (84). However, Yang et al. proposed S1PR2/3 on BMDM to be pro-migratory, possibly due to the fact that both receptors share activation of similar signaling pathways involving PI3K and Ras-related C3 botulinum toxin substrate 1 (Rac1) (85). In the same study they excluded an involvement of S1PR1 in macrophage migration by stimulating BMDM with the selective S1PR1 inhibitor W146, which did not alter S1P-induced BMDM migration. This observation is rather contradictory to a number of studies discussed above, which clearly indicate a role for S1PR1 signaling in inducing macrophage migration. Macrophages may even switch their S1PR profile toward S1PR1 to allow migration to the lymphatics, similarly to dendritic cells (81, 86). Since macrophages are the most plastic cells of the immune system, contradictory studies on macrophage-specific S1P receptor functions are most likely due to different S1PR expression profiles, sources and distinct *in vitro* macrophage differentiation protocols. Further studies are required to delineate under which circumstances signaling through S1PR1 and S1PR2 cooperate or oppose each other during macrophage migration. In summary, in order to maintain tissue homeostasis, macrophages need to survive under stress conditions and need to migrate to specific tissue sites. For these actions the S1P/S1PR signaling axis appears to be critical as the above mentioned studies suggest.

PREPARING THE MEAL AND AIDING IN DIGESTION—IMPACT OF S1P ON PHAGOCYTOSIS

Phagocytosis of pathogens or cellular debris is a key function of macrophages, as their name suggests. S1P has been shown to be involved in both, uptake of pathogens and cellular debris, i.e., dying cells. While these two processes occur via different molecular mechanisms, they both can be broken down into similar steps, i.e., recognition of the phagocytic material, phagosome formation, and phagosome content removal e.g., phagosome-lysosome fusion (87). S1P signaling participates in each of these three steps in macrophages.

S1P is produced by cells upon induction of apoptosis (88). It acts on macrophages to alter their functional phenotype, as outlined in the next paragraph. Moreover, S1P serves as a find-me signal to attract phagocytes to the dying cell for removal (78). This system can be hijacked by *Yersinia pestis*, which triggers cell death in macrophages. The resulting S1P release serves to recruit further macrophages, which are then infected to promote spread of bacteria (89). Besides altering macrophage activation and promoting recruitment, recent data suggest an involvement of S1P in priming macrophages for uptake of cell debris (90). Apoptotic cell-derived S1P triggered erythropoietin (EPO) signaling in murine macrophages, which induced upregulation of phagocytic receptors, including CD36 and Mer tyrosine kinase (MerTK) (90). Accordingly, mice lacking the EPO receptor in myeloid cells showed delayed clearance of apoptotic cells and lupus-like autoimmune symptoms. Interestingly, not only S1P produced by dying cells appears to be involved in apoptotic cell phagocytosis (efferocytosis). Inhibition of SPHKs in macrophages by pharmacological inhibitors or cigarette smoke reduced efferocytosis in human THP-1 macrophages. Addition of exogenous S1P or the S1PR agonist FTY720 reversed cigarette smoke-induced inhibition of efferocytosis and promoted macrophage SPHK functionality (91). Accordingly, the S1P transporter SPNS2 was decreased in smoke-exposed bronchial epithelial mice, correlating with reduced efferocytosis (92). Unexpectedly, smoke exposure increased SPNS2 expression in alveolar macrophages and upregulation of the S1PR5 in alveolar macrophages was associated with impaired efferocytosis (92–95). Thus, S1P receptors may differ in their capacity to

promote or inhibit efferocytosis and the S1P system in both, macrophages and dying cells appears to be involved in chronic obstructive pulmonary disease (COPD), which is induced by smoking and linked to impaired efferocytosis.

It remains unclear if S1P only promotes efferocytosis by increasing phagocytic receptor expression, or whether S1P signaling may also participate in the actual engulfment machinery. So far, the picture is clearer when looking at pathogen uptake as S1P facilitates the expression of uptake receptors. The phagocytic receptor FcγRII (CD32) is induced in human macrophages (96). This may require signaling through S1PR2, since S1PR2-deficient macrophages expressed significantly lower levels of FcγRI, II, and III (97). Thereby, S1P triggered S1PR2-dependent phagocytosis of the pathogenic fungus *Cryptococcus neoformans* (*C. neoformans*) (97). Apparently, S1P promotes opsonin-dependent phagocytosis of pathogens. In contrast, S1PR2-deficient murine macrophages phagocytosed *Escherichia coli* (*E. coli*) more efficiently, which was attributed to reduced RhoA-dependent cell contraction, but increased formation of lamellipodial protrusions when S1PR2 was absent (98). Importantly, phagocytosis of *E. coli* occurred opsonin-independent, adding to the notion that S1P modulating effects on phagocytosis depend on the S1PR being triggered and the mechanism of uptake. *E. coli* phagocytosis relied on RhoA and therefore actin dynamics. Two earlier studies suggested that S1P modulates actin assembly to promote phagosome formation. S1P promoted an ADP to ATP conversion and subsequent purinergic ligand-gated ion channel P2X7 signaling in the phagosome lumen or extracellularly, both promoting actin assembly at the plasma membrane in murine macrophages (99, 100). Moreover, S1P triggered ATP release from RAW264.7 macrophages by activating volume-regulated anion channels downstream of S1PR1. This required the actin cytoskeleton, suggesting that S1PR1 signaling may affect the actin cytoskeleton to induce a feed-forward mechanism involving purinergic signaling to promote phagosome formation and maturation. A critical function for S1P in phagosome maturation is supported by the observation that exogenous S1P promotes the interaction of phagosomes with the actin cytoskeleton to allow trafficking of the phagosome toward lysosomes for lysosomal fusion (101). Phagolysosome generation in *Mycobacterium tuberculosis* (*M. tuberculosis*) infected human macrophages required exogenous S1P-dependent phospholipase D activity, thereby promoting killing of *M. tuberculosis* (102). Besides *M. tuberculosis*, exogenous S1P was also shown to enhance killing of other mycobacteria by macrophages (103). However, S1PR3 was implicated in promoting phagosome maturation in mouse macrophages, since S1PR3-deficient peritoneal macrophages treated with heat-killed *E. coli* showed reduced phagolysosome fusion (104). Besides exogenous S1P, intracellular S1P formation was required for killing of mycobacteria by macrophages. Targeting SPHK1 genetically or pharmacologically rendered murine RAW 264.7 macrophages sensitive to infection with *M. smegmatis*, whereas overexpression of SPHK1 promoted killing. This was accompanied by SPHK1-dependent expression of the late phagosome marker LAMP2, but also SPHK1-dependent NO formation (105). Strikingly, it was further shown that intracellular *M. tuberculosis* blocked phagosome maturation by impairing SPHK activity (106). *M. tuberculosis* is known to block its killing in fused acidic phagolysosomes. Ingestion of dead, but not living *M. tuberculosis* induced SPHK1 sphingosine kinase activity and translocation to nascent phagosomes in human macrophages, followed by an increase in intracellular Ca^{2+} (106, 107). SPHK1 translocation in itself was Ca^{2+} dependent as suggested by the use of an intracellular Ca^{2+} chelator. Besides mycobacteria, a role for SPHK1 in controlling *C. neoformans* infection was suggested (108). In particularly, SPHK1 restricted intracellular *C. neoformans* growth in alveolar macrophages and also restricted macrophage infection with *Leishmania donovani* (109), although it is unclear if this was dependent on phagolysosome formation.

Collectively these data indicate that intracellular as well as extracellular S1P, presumably via S1PR signaling, has microbicidal potential by modulating pathogen uptake, phagosome formation, maturation, and phagolysosome fusion. Moreover, S1PR3 activation on mouse macrophages promoted ROS formation and therefore killing of ingested bacteria (104). The notion of a crucial role of the S1P system in pathogen control is underscored by observations that microbial SGPL1 promotes their survival in macrophages. SPGL1 from *Burkholderia pseudomallei* was required for phagosome evasion, presumably by lowering S1P levels, as indicated by observations that S1P and S1PR1 agonists increased bacterial content in lysosomes and reduced their intracellular survival (110). Moreover, SGPL1 from *Legionella pneumophila* promoted intracellular pathogen survival by blocking autophagy through disrupting sphingolipid metabolism, thereby again preventing lysosomal killing of pathogens (111). Therefore, a number of different pathogens have developed strategies to target the S1P system and to evade intracellular degradation in lysosomes (106, 110, 111).

ADDING FLAVOR—S1P AND MACROPHAGE POLARIZATION

During recent years it became apparent that the impact of S1P on the macrophage phenotype is not restricted to the M1/M2 paradigm. Rather, S1P modulates macrophage responses according to the local environment, the compartmentalization of S1P, i.e., intra vs. extracellular S1P, and the S1P receptors activated on cells. Consequently, S1P not only promotes the production of M2 but also of M1-associated macrophage markers.

Intracellular S1P produced by SPHK1, likely at the plasma membrane, was suggested as a cofactor involved in inflammatory macrophage activation. Inflammatory macrophage activation is triggered by microbial components such as LPS, with or without type 1 lymphocyte-derived IFN-γ. As a consequence, TNF-α is rapidly produced by mechanisms including proteolytic shedding from the plasma membrane (112), and increasing mRNA stability (113). TNF-α then binds to its cognate receptors to feed-forward promote canonical NF-κB activation, which requires TNF receptor-associated factor 2 (TRAF2) to polyubiquitinate receptor interacting protein 1 (RIP1). SPHK1 was shown to be activated downstream of TNF receptor activation and to

physically interact with TRAF2. SPHK1-derived S1P then acted as cofactor for TRAF2, allowing polyubiquitination of RIP1 (114, 115). Also IL-1 signaling, another feed-forward NF-κB activator following microbial encounter, required SPHK1-dependent S1P as an intracellular cofactor (116). Besides TNF and IL-1β, SPHK1 is also rapidly activated downstream of other inducers of inflammatory macrophage activation, including LPS (117–119), and LPS in combination with palmitate (120), although it is unclear if SPHK1-derived S1P acts as a cofactor for intracellular LPS signaling. Stimulation of human THP-1 macrophages or mouse microglia with LPS required SPHK1 activity to produce IL-6, IL-1β, TNF-α, and/or NO (117, 118), whereas SPHK1 was dispensable for LPS, but not LPS/palmitate-induced IL-6 production, and TNF-α induced cyclooxygenase (COX)-2 expression in mouse RAW264.7 macrophages (119, 120). Accordingly, SPHK1-deficient mice showed decreased joint inflammation in a model of murine TNF-α-induced arthritis (121). In contrast, SPHK1-deficient mice were not protected from collagen-induced arthritis and thioglycollate-triggered peritonitis, indicating that SPHK1 activation may be restricted to specific inflammatory stimuli (122). It is important to note that mouse macrophages lacking both SPHK isoforms did not show any alterations in cytokine production *in vitro* and induction of LPS or thioglycollate-induced inflammation *in vivo* (123). This may be explained by divergent functions of SPHK isoforms in inflammation, as has been noted in a model of inflammation-induced colon cancer, where SPHK2 ablation triggered SPHK1-dependent cytokine production in myeloid cells and thus promoted M1 macrophage activation (124). The exact role of SPHK2 in macrophage activation is, however unclear. Besides promoting M1-like cytokine production, an increase in anti-inflammatory macrophages was reported in SPHK2-deficient obstructed kidneys. Treating SPHK2-deficient murine BMDM with IL-4 or IL-13 induced a more pronounced M2 profile compared to wild type macrophages (125). Thus, macrophage SPHK2 may restrict M1 as well as M2 activation. Further mechanistic investigations will be required to support this claim.

Despite its role in providing S1P as an intracellular cofactor, SPHK1 activation by inflammatory triggers may increase extracellular S1P, thereby provoking S1P receptor activation. The accompanying cell response appears to be highly context and receptor-dependent. Initial studies in human alveolar macrophages suggested that S1P alone induced NADPH-oxidase (NOX)2-dependent production of ROS (126) to promote IL-1β and TNF-α production by murine peritoneal macrophages (127). These findings were recently supported by a study suggesting that S1P stimulation of murine BMDM triggered the expression of inflammatory markers including TNF-α, CCL2, and inducible NO-synthase (iNOS), which were suppressed by targeting S1PR2/3 and downstream c-Jun N-terminal kinase (JNK) activation, again exemplifying the cooperate potential of S1PR2/3 signaling in macrophages (128). Increased iNOS expression was also observed when murine BMDM were subjected to LPS/IFN-γ treatment with the addition of exogenous S1P (82). The impact of S1PR3 on promoting inflammatory macrophage activation was substantiated in studies using murine microglia *in vitro* and a model of brain ischemia. A S1PR3 specific antagonist and siRNA-mediated depletion of S1PR3 reduced LPS-triggered expression of TNF-α, IL-6, and IL-1β (129). Moreover, LPS-induced expression of inflammatory genes such as iNOS, COX-2, IL-1β, IL-6, and TNF-α in primary peritoneal macrophages was reduced by an S1PR3 antagonist (130). S1PR3 may therefore be viewed as an inflammatory receptor in macrophages. While the majority of inflammatory macrophage markers depend on transcriptional induction, IL-1β maturation and release in response to microbial stimulation requires expression and activation of inflammasomes in macrophages, including the NLRP3 inflammasome, a protein complex consisting among others of the eponymous NLRP3 and inflammatory caspase-1 (131). S1P was shown to selectively promote the expression of NLRP3 among inflammasome components downstream of S1PR1 in tumor-associated macrophages (TAM), as well as LPS-stimulated mouse BMDM and human primary monocyte-derived macrophages (132). Besides NLRP3 expression, S1PR1 was also involved in promoting ATP release at least in a murine macrophage cell line, which is one of the triggers of NLRP3 inflammasome activation (133). Another activating mechanism of the NLRP3 inflammasome, the release of cathepsin B from lysosomes, was associated with S1PR2 signaling (134). Accordingly, levels of IL-1β and IL-18, which are inflammasome dependent, were reduced in the serum of S1PR2-deficient mice challenged with endotoxin (135). Thus, S1P via S1PR1/2, although not through converging signaling pathways, may cooperate toward NLRP3 inflammasome assembly and activation, promoting IL-1β maturation (136). Interestingly, the effect of S1PR1 on NLRP3 expression suggests that S1PR1 operates independently of canonical NF-κB or classical mitogen-activated protein kinase (MAPK) cascades triggered downstream of toll-like receptor (TLR), TNF receptor, or IL-1 receptor activation. Along these lines, antagonism of S1PR3, which generally reduced LPS-triggered inflammation in peritoneal macrophages, restricted caspase-1 but not NLRP3 expression (130). Indeed, S1P blocked LPS-dependent stimulation of NF-κB activation and downstream production of inflammatory cytokines such as TNF-α in murine and human macrophages (137–139), and to attenuate TLR2-dependent NF-κB activation in human monocytes (140). Also, S1PR1 triggered STAT3 signaling to promote induction of heme oxygenase-1 (73), as well as IL-6. Particularly, S1PR1 signaling promoted IL-6 production in a STAT3-dependent feedback loop, where IL-6 induced S1PR1 expression in mouse macrophages *in vitro*, in a model of sickle cell disease, and in dextran sodium sulfate (DSS)-induced colitis (124, 141). In RAW264.7 macrophages S1PR1 but also S1PR2 were involved in LPS and palmitate-induced IL-6 production (120). Moreover, S1PR1 signaling increased ARG1 activity in mouse macrophages to block the production of NO, which was induced by microbial stimuli in concert with IFN-γ, although the impact of STAT3 signaling in this context was not tested (137). S1P alone or in the supernatant of apoptotic tumor cells also elevated prostaglandin E_2 (PGE_2) production, which required stabilization of COX-2 mRNA, likely via S1PR1 (119, 142, 143). These data suggest that S1PR1 may limit microbial-induced inflammatory pathways such as canonical NF-κB activation, but

induces inflammatory mediators such as IL-1, IL-6, and PGE_2 under conditions characterized by low-grade inflammation, as found e.g., in tumors (124, 132).

The role of S1PR2 in macrophage activation appears less clear. While it was associated with inflammasome activation as outlined above, it was required for induction of ARG2 in RAW 264.7 macrophages stimulated with apoptotic cells (144), which required the transcription factor cAMP response element-binding (CREB). S1P also augmented cAMP levels in PGE_2 or isoproterenol-stimulated RAW 264.7 macrophages through S1PR2 (145). Therefore, S1PR2 signaling is coupled to increasing cAMP levels in macrophages, which was connected to resolution of inflammation (146). Pro-resolving macrophages are also generated by the interaction with apoptotic cells, which might provide a connection between apoptotic cell-derived S1P and resolution of inflammation by establishing resolution type macrophages downstream of S1PR2. However, this hypothesis remains to be tested. The impact of S1PR4 and S1PR5, whose expression is low in most macrophages, toward macrophage polarization is largely unclear. Activation of S1PR4 primed apoptotic tumor cell-stimulated macrophages for signaling via the nerve growth factor receptor TrKA, which induced among others IL-6 and IL-10 expression (147). It is unclear if S1PR4 activation has a similar effect under other conditions. S1PR5 was so far only connected to impaired phagocytosis as outlined above.

In conclusion, SPHK activity and S1PR signaling emerge as important regulators of macrophage polarization, although the impact of some components of this machinery such as SPHK2, S1PR4, and S1PR5 needs to be tested in the future. Since macrophages are implicated in the development of inflammatory diseases, altered functional macrophage responses by the S1P system are expected to affect such conditions. This will be outline in the next chapter.

THE EATER GONE ROGUE—S1P AND MACROPHAGE FUNCTION IN DISEASE

Cancer

Already in 1863, Rudolf Virchow observed that tumors are heavily infiltrated by leukocytes and proposed that a chronic inflammatory milieu promotes cancer initiation and progression (148). In the last decades it became clear that the immune system and its effector cells exhibit a multifaceted role in carcinogenesis. The immune system is capable of tumor rejection but paradoxically also able to promote cancer progression, which is mediated by the tumor microenvironment triggering immune tolerance (149, 150). One group of effector cells that contribute to the multifaceted role of the immune system in carcinogenesis are tumor-associated macrophages (TAM), which depending on their phenotype contribute to a pro- or anti-tumor immune response. Whereas, TAM expressing M1 markers produce pro-inflammatory cytokines and ROS that are crucial for tumor cell killing, TAM expressing M2 markers suppress an anti-tumor immune response by producing anti-inflammatory cytokines, which causes immune suppression and in the long term tumor outgrowth (151–153).

Tumor cells themselves can produce factors that activate and shape a pro-tumor M2-like TAM phenotype during tumor escape, provoking tumor progression including metastasis. One of the factors produced by tumor cells is S1P. S1P, already discussed as a pro-survival factor, exhibits pro-tumor functions by adding to tumor cell transformation, survival, migration, and neovascularization in different cancer types such as breast, colon and prostate cancer (154). We previously showed that S1P is released by apoptotic breast cancer cells and polarizes macrophages toward a M2-like phenotype, characterized by reduced TNF-α, IL-12 but increased IL-8 and IL-10 secretion (138). Tumor cell specific secretion of S1P, concomitant macrophage M2-like polarization, and subsequent tumor growth was recapitulated in a more recent study. Mrad et al. reported that inhibition of SPHK1-dependent production of S1P by B16 melanoma cells increased the number of M1-polarized macrophages and tumor growth. The latter was, however, mediated by a macrophage-independent mechanism, since tumor growth was accelerated by SPHK1/S1P-dependent production of transforming growth factor (TGF)-β by melanoma cells themselves (155). Apparently, not only the phenotype transition from inflammatory M1-like to immune-suppressive M2-like macrophages contributes to cancer progression, but also an overshooting inflammatory response mediated by macrophages may provoke cell transformation and tumor growth as shown for colitis-associated colon cancer (CAC). Thereby, SPHK/S1P/S1PR-dependent activation of macrophages and the subsequent production of pro-inflammatory cytokines were established as important factors in contributing to chronic intestinal inflammation resulting in CAC development. This has been proposed to be in part macrophage dependent, when SPHK1 expression was upregulated as a result of SPHK2 deletion, thereby enhancing S1P levels. In this setting, intracellular S1P activated NF-κB signaling, which culminated in pro-inflammatory gene transcription of IL-6 and TNF-α. Both cytokines triggered a feed-forward amplification loop with TNF-α amplifying NF-κB signaling and IL-6 maintaining persistent S1PR1-dependent STAT3 activation, supporting chronic inflammation and CAC development (124). Another study showed that blocking the SPHK/S1P axis and thus, macrophage activation, attenuates colon cancer. Mechanistically, inhibition of SPHK1 in peritoneal macrophages reduced COX-2 and TNF-α expression, which lowered the formation of aberrant crypt foci in the colons of mice injected with the carcinogen Azoxymethane (156). In terms of S1P-dependent production of pro-inflammatory cytokines by macrophages it apparently needs to be discriminated between the extra- and intracellular actions of S1P during carcinogenesis. As mentioned, extracellular S1P formation produced by apoptotic tumor cells induces the secretion of anti-inflammatory cytokines, while intracellular S1P induces a pro-inflammatory cytokine signature of macrophages in the context of cancer.

Besides affecting cytokine production, the S1P/S1PR axis can induce pro-angiogenic properties of macrophages and therefore contribute to tumor angiogenesis and, consequently, metastasis. Macrophage-specific deletion of S1PR1 in a mammary carcinoma model enhanced lung metastasis by

inducing tumor lymphangiogenesis. Mechanistically, S1PR1 signaling in lymph vessel-associated macrophages induced NLRP3 expression and IL-1β production, which showed direct pro-lymphangiogenic activity, thereby accelerating tumor progression by promoting metastasis (132). Beside the lymphatics, metastasis also occurs via the bloodstream, which requires tumor angiogenesis. One major driver of tumor angiogenesis is hypoxia, which at the same time affects macrophage biology in inflammation, cancer, or infection. The oxygen-sensitive transcription factors hypoxia inducible factors 1α and 2α (HIF-1α, HIF-2α) are the master regulators toward decreased oxygen tension, coordinating many of the multiple hypoxic responses. In tumor cells there is evidence that hypoxia causes a rapid activation of SPHK1, preceding HIF-1α accumulation (157). Although details remain unknown, ROS appeared to activate SPHK1, while the accumulating S1P, via the Akt/GSK3ß pathway, attenuated HIF-1α proteasomal degradation. In renal cell carcinoma, SPHK1 activity controlled HIF-2α expression (158) and the S1PR antagonist FTY720 attenuated both HIF-1α and HIF-2α accumulation in several human cancer cell lines (159). S1P released by dying cancer cells also triggered HIF-1α accumulation in macrophages downstream of S1PR1, even under normoxic conditions (160). In contrast to hypoxic tumor cells, where S1P may be self-sufficient to accumulate HIF-1α the situation in macrophages seems different. Macrophages sensing S1P from dying cancer cells required a second stimulus, most likely transforming growth factor (TGF)-β to stabilize HIF-1α under normoxia. HIF-1α expression under these conditions established a pro-angiogenic macrophage phenotype (160), indicating that S1P/S1PR1 signaling may promote tumor angiogenesis in general.

To sum up, studies so far may indicate a critical role of the SPHK/S1P/S1PR axis in macrophage activation and polarization, contributing to cancer development and metastasis. However, more studies are needed to clarify the exact role of the S1P-induced functional consequences for macrophage biology in different tumor entities, especially in respect of utilizing the SPHK/S1P/S1PR axis for cancer therapy. As outlined above, inhibiting one SPHK will provoke over-activation of the remaining SPHK and this may cause severe side effects. Therefore, a cell-type specific or S1PR-specific inhibition of the S1P/S1PR axis appears a more rational approach for intervention. Interestingly, in contrast to S1PR1, S1PR2 was reported to limit tumor development and angiogenesis in one study, which involved S1PR2 on myeloid cells (161). Thus, S1PR1 and S1PR2 may show opposing effects on tumor angiogenesis, making S1PR1 a potentially more interesting target when focusing on TAM.

Atherosclerosis

Macrophages are key cellular mediators of atherosclerosis, as they accumulate in atherosclerotic plaques and the macrophage content and activation state are linked to the progression and the regression of atherosclerosis (162). Macrophages in atherosclerotic plaques are exposed to mediators in the circulation, including S1P. In the circulation S1P is mainly derived from erythrocytes, platelets, or the endothelium. About two-thirds of the circulatory S1P is associated with HDL, followed by its association with albumin and other lipoproteins (163). HDL is known to limit inflammatory responses during atherogenesis. Besides, HDL is also recognized for its general host defense activity, which is linked to its ability to scavenge and limit endotoxin toxicity as well as immune cell modulatory responses, affecting the cholesterol content in plasma membrane lipid rafts (164). HDL functions as a reservoir for several proteins and lipids with immunomodulatory activities, among them S1P. ApoM, a genetic variant of ApoA-1, is mainly associated with HDL and the carrier of S1P in HDL (165). A lipophilic pocket of ApoM not only ligates S1P but also molecules such as oxidized phospholipids or retinol, suggesting some kind of competition (166). ApoM levels are subjected to variations, with drastically reduced amounts during diseases such as atherosclerosis, coronary artery disease, or myocardial infarction as well as acute phase responses. Several studies attributed individual HDL functions as partially or entirely dependent on HDL-bound S1P (167). The mechanism for ApoM-mediated modulation of S1P function may reside in retarding S1P degradation (168) and/or strengthening its agonistic properties by binding HDL via scavenger receptors and thereby bringing S1P in close proximity with S1PRs (169).

The nature of S1P in the pathogenesis of atherosclerosis is ambivalent, although concepts on a defensive role prevail. Toward a protective function, S1P is supposed to promote survival and prevent apoptosis of endothelial cells and macrophages, to induce phosphorylation of endothelial-type NO-synthase (eNOS), which provokes vessel relaxation, to preserve endothelial barrier function by stabilizing cell-cell junctions, and to attenuate attachment of blood cells to the endothelium by inhibiting expression of endothelial cell adhesion molecules (170, 171). Harmful properties of S1P are discussed concerning its ability to recruit lymphocytes to sites of inflammation, to act chemotactic and stimulatory for other immune cells, i.e., monocytes/macrophages, to indirectly shape the atheroprotective B1-cell population, or to augment thrombin-induced expression of tissue factor in endothelial cells to foster the coagulation cascade (170, 171). Concerning macrophages, S1PR2 retains them in atherosclerotic plaques and regulates their inflammatory cytokine secretion to promote atherosclerosis (135). Also S1PR3 on monocytes/macrophages contributes to their accumulation in atherosclerotic lesions, thereby adding to a pro-inflammatory, pro-atherogenic environment (172). Hereby S1PR2 and S1PR3 signaling both promote macrophage accumulation in plaques, although by exerting opposing effects on monocyte/macrophage migration. However, other studies see the macrophage-S1P-axis in an atheroprotective context. S1P and its analog FTY720 reduced atherosclerotic lesions, both in the aortic root and brachiocephalic artery, and almost completely blunted necrotic core formation (173). Although a direct connection to macrophages in atherosclerotic plaques was not made, this observation may refer to the modulating role of S1PR signaling in macrophage recruitment, since FTY20 targets S1PR3 but not S1PR2. Alternatively, it may be connected to polarization of macrophages toward an anti-inflammatory, regenerative, healing

phenotype as discussed above. In line, providing KRP-203, an S1PR1 agonist, to low-density lipoprotein receptor-deficient mice on a cholesterol-rich diet reduced atherosclerotic lesion formation and reduced macrophage pro-inflammatory activation (174). These experiments would argue for S1PR1 in mediating the anti-atherogenic effects of S1P. Besides the ability of S1P to induce alternative macrophage polarization and thereby to attenuate oxidized LDL-induced lipid accumulation, the atheroprotective effect of S1P was also related to its ability to enhance cell survival and to attenuate macrophage pro-apoptotic signaling (175). Mechanistically, HDL-associated S1P attenuated macrophage apoptosis by activating STAT3 and causing survivin expression, presumably via cooperate signaling through S1PR2/3, as recapitulated by pharmacological interventions (75). As many HDL effects are attributed to its S1P load, it is of interest that the physiologically crucial and most relevant role of HDL in reverse cholesterol transport is now also proven to be affected by S1P (176). The transcriptional and functional ABCA1 regulatory pathway, facilitating cholesterol efflux, demanded S1PR3. The authors established LXR to be involved in S1P facilitated cholesterol efflux and identified the critical role of S1PR3.

It is interesting to note that approaches are undertaken to make use of the beneficial HDL-S1P signaling axis for the treatment of diseases. Only HDL, manufactured to incorporate S1P, was cardioprotective in a model of ischemia reperfusion injury (177) and S1P-loaded HDL enhanced eNOS activation in endothelial cells (178). In general, the anti-inflammatory HDL function can be boosted by S1P-loading and exploited by S1P receptor-targeting to prevent and even turn off ongoing inflammation (179). Another strategy follows the observation that ApoM levels are correlative to biological S1P-signaling. Resveratrol, a proposed supplement to prevent atherosclerosis, is reported to modulate S1P levels by affecting ApoM levels (180). It can be speculated that some of the reported anti-atherosclerotic effects of resveratrol can be explained by increasing plasma levels of ApoM in conjunction with its S1P-association.

Although many details on the role of S1P and macrophages during atherosclerosis still need to be discovered, a gross simplification would favor anti-atherosclerotic actions of S1PR1 and S1PR3, while pro-atherosclerotic functions of S1PR2 may dominate. Mechanistically, the anti-inflammatory impact of S1P toward macrophages, likely transmitted via S1PR1, may add to convey atheroprotective signals. Uncertainties remain, as we are not aware how S1P concentrations, either HDL-bound or associated with other carriers, develop over time with plague progression and how the S1P receptor profile may change in early vs. late stages of the disease. As macrophages are prone to many environmental incoming signals, GPCR activation by S1P may dominate, be modulated, or be overruled. This makes predictions on the macrophage S1P-S1PR signaling axis difficult. However, controlled *in vivo* experimentation, using genetically modified animals in combination with pharmacological tools that are progressing toward higher selectivity, will help to answer some of the demanding questions in the future.

Fibrosis

Macrophages are one of the key players during resolution of inflammation as the wound healing response has to be tightly regulated (181, 182). Disturbances within any stage of the wound healing process may cause chronicity, while an overshooting healing response can induce fibrosis within different organs such as lung, liver, heart, or kidney. Tissue fibrosis is characterized by increased proliferation and activation of fibroblasts that trigger excessive accumulation of extracellular matrix components eventually initiating organ failure and death (182, 183). Macrophages may serve as critical mediator during fibroblast activation and proliferation by releasing pro-fibrotic mediators such as TGF-ß, IL-13, or platelet-derived growth factor (PDGF) (184). There is evidence that the infiltration of anti-inflammatory M2 macrophages into fibrotic areas of the lung is a key regulator for the development and progression of idiopathic pulmonary fibrosis (IPF) (185, 186).

A role for S1P in IPF progression was already assumed by showing that serum and bronchoalveolar lavage of diseased mice or patients exhibit increased S1P levels and show enhanced SPHK1 protein expression, both correlated with impaired lung function (187, 188). Mechanistically, S1P is implicated in secreting pro-fibrotic factors that cause the excessive activation and proliferation of fibroblasts, thereby advancing tissue fibrosis. Specifically, studies pointed to a role of the SPHK/S1P/S1PR axis in TGF-ß-driven fibrosis induction. This was demonstrated by blocking SPHK1, which in turn reduced TGF-ß secretion and lung fibrosis in murine models of IPF (187, 189). It has also been shown that the S1P/S1PR axis in macrophages contributes to the production of pro-fibrotic factors and thereby adds to IPF development (190). Along those lines, Zhao et al. used S1PR2$^{-/-}$ mice and noticed attenuated IPF in animals subjected to bleomycin. In this model S1PR2-expressing alveolar macrophages most likely promote IPF as shown by bone marrow transfer experiments and the enhanced S1PR2-dependent production of pro-fibrotic IL-13 that initiates a STAT6-dependent response in macrophages. More mechanistic studies using macrophage-specific S1PR$^{-/-}$ mice will be needed to decipher the exact role of the S1P/S1PR axis in the development and progression of IPF. The SPHK/S1P/S1PR signaling axis also accelerates liver fibrosis by directly activating fibroblast motility and fibrosis-induced angiogenesis (191, 192). In a more recent study it became apparent that SPHK1-induced CCL2 secretion from Kupffer cells activated fibroblasts and thereby fostered progression of liver fibrosis (193). The finding that S1P signaling adds to the pathogenesis of tissue fibrosis was already shown in the kidney, when partial nephrectomized rats were treated with FTY720. Blocking the S1P/S1PR axis by FTY720 diminished renal fibrosis, characterized by reduced expression of TNF-α, TGF-β, and the production of extracellular matrix proteins (194). For renal macrophages protection toward fibrosis was linked to SPHK2-dependent S1P signaling. SPHK2-deficient kidney-resident macrophages shifted toward the M2 phenotype due to changes in the glycolytic pathway, which reduced renal fibrosis by lowering the production of pro-inflammatory cytokines such as IL-1β and TNF-α (125).

Evidently, S1P contributes to macrophage-dependent fibrotic responses by shaping their activation, particularly the release of pro-fibrotic cytokines/chemokines such as TGF-ß, IL-13, or CCL2. Addressing the distinct role of S1P in macrophage-driven fibrosis in detail may open the potential to foster mechanisms toward resolution of fibrosis.

I/R Injury

Ischemia-reperfusion-induced injury (I/R injury) plays a major role during stroke and myocardial infarction, and is accompanied by inflammation that promotes injury. Macrophages play a crucial role in resolving inflammation and promoting repair following ischemic injury (195–197). Targeting S1P receptors has shown promising results in I/R injury models. However, while macrophages are used as read-out parameters, their functional involvement largely remains unclear. S1P levels during resolution of focal cerebral ischemia in mice increased (198), when macrophages promote repair. Treating mice in a model of experimental stroke with FTY720 reduced lesion size and improved neurological function, which was accompanied by decreased numbers of activated microglia/macrophages in the ischemic lesion (199). Reduced inflammatory microglia/macrophage infiltration was confirmed in models of focal cerebral ischemia and observed under long-term protective effects of FTY720 (200). Whether reduced infiltration of inflammatory microglia/macrophage were a result of reduced recruitment into the affected area or due to changes in cell activation remains an open question. Intraocular injection of a humanized monoclonal S1P antibody (sonepcizumab) into ischemic retina significantly reduced the macrophage influx in oxygen-induced ischemic retinopathy (201). Attenuated macrophage infiltrates and their proinflammatory cytokine expression were furthermore observed when applying the S1PR1 agonist SEW2871 in mice subjected to hepatic (202) or renal I/R injury (203). Based on the observed lymphopenia in these models, SEW2871 acted as a functional S1PR1 antagonist as expected. However, lymphopenia was not the reason for protection as mice, harboring a selective S1PR1 knockout in proximal tubule cells, were protected as well (204). In some analogy, in a model of cisplatin-induced nephropathy performed in mice with a deletion of S1PR1 in tubule cells reduced kidney damage and a lower level of proinflammatory cytokines and infiltrated macrophage were noticed (205). To conclude, the protective effect of S1PR agonism in the kidney was largely macrophage independent, whereas tissue regeneration following I/R injury required S1PR1/3 signaling and was linked to the release of neutrophil gelatinase-associated lipocalin (LCN2) from macrophages, again underscoring the role of macrophages in tissue regeneration after I/R injury (206). S1PR1/3 activation also protected against cardiac ischemia-reperfusion injury as the accompanying tissue injury in mice was reduced by myonectin, which triggered S1P and protected cardiomyocytes from apoptosis and macrophages from their inflammatory activation. Administration of the S1PR1/3 antagonist VPC23019 reduced the protective potential of myonectin and increased myocardial injury (207). Understanding the role of macrophages in S1P-dependent protection from I/R injury will require further studies by e.g., employing macrophage-specific $S1PR^{-/-}$ mice.

Infection

Sphingolipids are involved in immunity to infection, with prominent roles being assigned to ceramide and sphingosine (208–210). However, an impact of the SPHK/S1P/S1PR axis under infectious conditions requires further studying. Data from cell culture suggest a role of S1P in pathogen uptake and killing, while information from *in vivo* models is scarce. SPHK1 was required to form lung granuloma and prevented brain infection with a particular *C. neoformans* strain that is restricted to intracellular replication in macrophages (108). Logically, SPHK1-deficient showed a higher susceptibility to *C. neoformans* infection (108). SPHK1 was also required for the protective principle of glucocorticoids in a model of acute lung injury, triggered by LPS and oleic acid. Downstream of the glucocorticoid receptor SPHK1 was upregulated in macrophages, provoking a systemic S1P increases and reducing inflammatory cell infiltrates (211). Enhanced SPHK1 expression was also observed in macrophages in inflamed murine and human lungs in pneumonia, while genetic SPHK1 deletion protected mice from pneumonia-induced hyperpermeability. Unfortunately, the role of macrophage-specific SPHK1 in this process remained unclear (212). SPHK2-deficient mice showed a higher susceptibility to *Streptococcus pneumonia* induced lung inflammation, although there was no change in neutrophil function, leaving room for a role of macrophages (213).

With regard to S1P receptors, deletion of S1PR2 was protective in models of bacterial sepsis. S1PR2 promoted macrophage pyroptosis, which is linked to a cytokine storm, upon *E. coli* infection, while a S1PR2 knockout improved survival (76). Survival of S1PR2 knockout mice was also seen during cecal ligation and puncture or intratracheal administration *E. coli*, which was linked to an enhanced phagocytic function of S1PR2-deficient macrophages (98). S1PR3 supports ROS generation in macrophages, thereby aiding in killing bacteria and promoting phagosome maturation upon cecal ligation and puncture, where S1PR3 knockout showed increased lethality (104). Septic patients with monocytes showing enhanced S1PR3 expression cleared bacteria more efficiently, which was linked to a preferable outcome (104). Accordingly, the S1PR agonist FTY720 prevented clearance of bacteria albeit increasing colonic inflammation and neutrophil infiltration in a model of gastrointestinal infection with the mouse enteric pathogen *Citrobacter rodentium*. FTY720 targets all S1P receptors, with the exception of S1PR2, showing short term agonistic activity, followed by receptor desensitization due to their degradation. Thereby FTY720 traps lymphocytes in secondary lymphatic organs by disabling them to follow the S1P gradient toward the circulation. FTY720 treated animals therefore exhibit peripheral blood lymphopenia with significantly lower numbers of colonic dendritic cells, macrophages, and T cells. Infected mice treated with FTY720 revealed an impaired innate immune response and reduced type 1 adaptive immunity (214). Therefore, targeting S1PRs with rather non-specific tools will likely not be beneficial during infection. However, it might be worth considering to selectively targeting S1PR2 as it likely

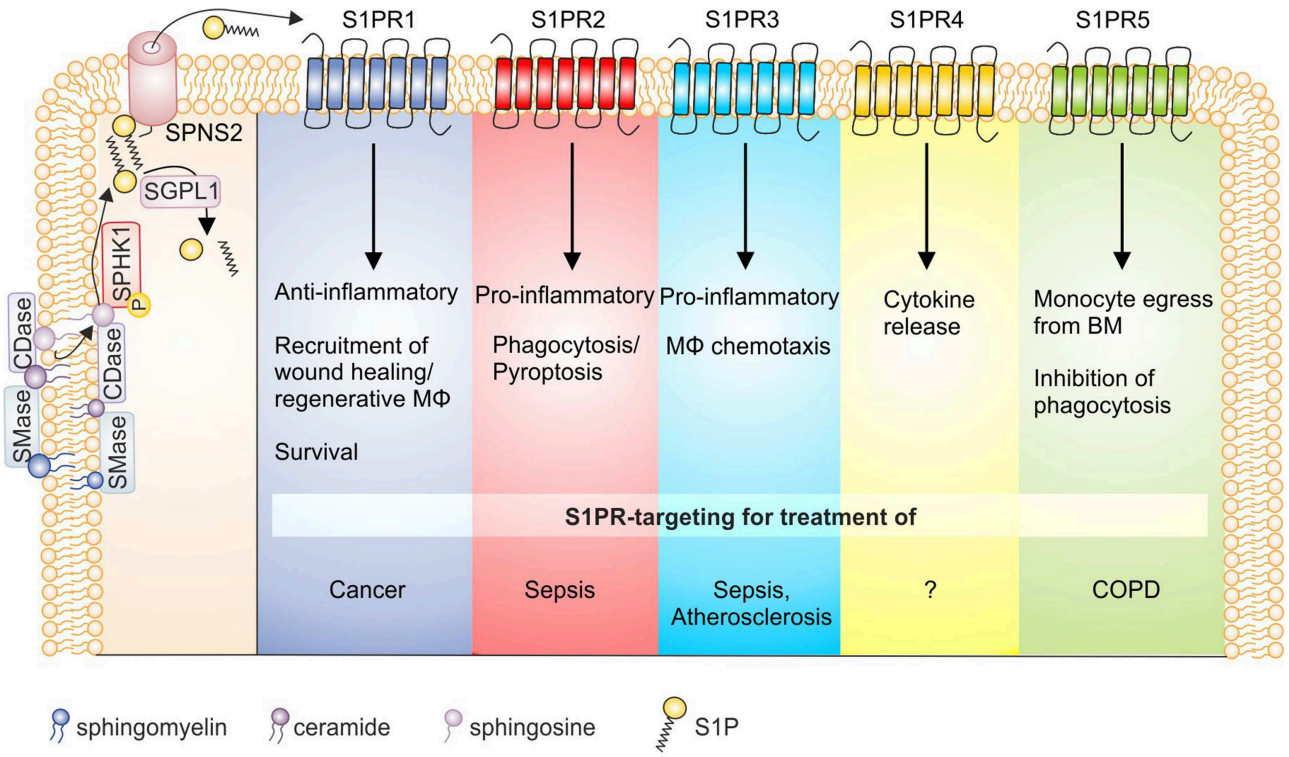

FIGURE 2 | S1P receptor signaling and macrophage function in disease. S1P is generated by the sequential breakdown of sphingomyelin and ceramide to sphingosine by sphingomyelinases and ceramidases, respectively, and the subsequent phosphorylation of sphingosine by sphingosine kinases. S1P is then degraded by S1P lyase or secreted from cells via the transporter SPNS2. Activation of S1P receptors on macrophages then triggers functional responses as indicated, whose targeting might be of interest in disease settings. Details can be found in the main text. BM, bone marrow; CDase, ceramidase; COPD, chronic obstructive pulmonary disease; MΦ, macrophage; S1P, sphingosine-1-phosphate; S1PR, sphingosine-1-phosphate receptor; SGPL1, S1P lyase; SMase, sphingomyelinase; SPHK, sphingosine kinase; SPNS2, Spinster homolog 2.

increases the anti-microbial macrophage function and enhances macrophage survival. Moreover, S1PR2 antagonism will probably not induce immune paralysis, since S1PR1 is the important receptor promoting lymphocyte recruitment to the circulation.

CONCLUSIONS

Macrophages are key players in maintaining tissue homeostasis, which requires a remarkable repertoire to sense microenvironmental cues that signal disturbed homeostasis. S1P is a good example of a sensing/signaling molecule, since its tissue levels, except for blood and lymph, are constitutively low. Rising S1P levels therefore imply an altered microenvironment, which is sensed by macrophages and their progenitors. This provokes monocyte/macrophage trafficking, survival, and altered effector functions. These changes are involved in a number of diseases as highlighted in this review (**Figure 2**). The source of S1P and the receptor profile are critical determinants of the S1P impact on macrophages. Intracellular S1P produced by **SPHK1** mostly promotes inflammatory macrophage activation and increases anti-microbial properties including phagosome maturation.

S1P signaling through individual S1PRs has pleiotropic and sometimes even divergent effects. In monocytes/macrophages **S1PR1** recruits wound healing and/or regenerative macrophages (215), acts as a survival signal (88) and predominantly causes anti-inflammatory macrophage polarization (137). In IL-4 stimulated macrophages S1PR1 expression is enhanced (81), while in pro-inflammatory activated phagocytes S1PR1 and S1PR4 appeared downregulated, at least at mRNA level (82). Moreover, S1PR1 stimulated EPO-signaling in macrophages to enhance apoptotic cell clearance through PPARγ, which adds to the anti-inflammatory/regenerative macrophage phenotype (90). However, when S1PR1 is activated in the context of endogenous SPHK1 activation in macrophages, pro-inflammatory effects may prevail (124). Therefore, targeting S1PR1 affects inflammatory macrophage activation needs to be approached in a context-dependent manner, although it emerges as a promising target in cancer. **S1PR2** generally seems to oppose S1PR1 signals. The receptor regulates macrophage retention in atherosclerotic plaques and provokes cytokine secretion to promote inflammation (135). However, more recent data proposed a S1PR2-$G_{12/13}$ signaling axis in macrophages that augmented protective B-cell populations to ameliorate atherosclerosis (216). This receptor also enhanced Fcγ receptor-facilitated phagocytosis in response to antibody opsonized particles, but not complement-mediated phagocytosis (97).

It was also proposed that S1PR2 impaired phagocytosis and antimicrobial defense in the pathogenesis of sepsis (98). Furthermore, S1PR2 deficiency/S1PR2 inhibition decreased macrophage pyroptosis and improved survival in *E. coli* sepsis, posing this receptor as a promising therapeutic approach during sepsis (76). These observations support the notion of S1PR2 in contributing toward proinflammatory macrophage polarization (128), although it may play a role in inflammation resolution by increasing cAMP levels as well (144). **S1PR3** mediates chemotaxis of macrophages, *in vitro,* and provokes migration of cells to plaques in atherosclerotic mice (172) and recruits macrophages in bile duct-ligated mice to promote hepatic inflammation and fibrosis (85). In general, S1PR3 appears to mediate pro-inflammatory responses. This is coupled to antimicrobial function as S1PR3 expression was elevated in septic patients, linked to bacterial clearance and a better outcome (104). Mechanistically, bacterial killing in macrophages was fostered by enhanced ROS formation and phagosome maturation. Activating S1PR3 on macrophages therefore might be beneficial to promote antimicrobial immunity. **S1PR4** is less well studied than S1PR1 to S1PR3, but is abundant on immune cells, among them macrophages (217). S1PR4 was required to produce the Th17 polarizing cytokine IL-6 by dendritic cells (218). This may also be true for macrophages since activation of this receptor on TAM by S1P, released from apoptotic cells, caused formation of tumor promoting cytokines, including IL-6 and IL-10 (147). Under pro-inflammatory conditions macrophages downregulate S1PR4 (82), which has also been shown for plasmacytoid dendritic cells (219). Whether S1PR4 downregulation is required for pro-inflammatory signaling to take place will require further studying. There is evidence that **S1PR5** is involved in the egress of patrolling monocytes from the bone marrow (220), thereby potentially contributing to the tissue macrophage pool during inflammation. As S1P did not function as a chemoattractant for these cells nor did it affect their viability *in vitro*, detailed mechanisms remained unexplored. Alveolar macrophages from patients with COPD are defective in their ability to phagocytose apoptotic cells. As a significant association was noted between S1PR5 expression and both lung function as well as defective phagocytosis it is concluded that this receptor might be a potential therapeutic target in COPD (93).

Besides evidence suggesting a role of S1P/S1PR signaling in shaping macrophage-specific tissue homeostasis, a number of questions still need to be addressed. The role of S1P in emerging areas such as macrophage immune metabolism and innate memory formation may require our attention. This is supported by findings that **SPHK2** deficiency reduces glycolysis in macrophages (125), and produces intracellular S1P as a cofactor for HDACs to modulate epigenetics (221), both of which are hallmarks of trained macrophage immunity (222). Moreover, experiments using specific deletion of individual components of this signaling axis, particularly individual S1PRs in macrophages will allow identifying potential pharmaceutical targets to be exploited for disease conditions mentioned above. This is of special importance given the sometimes antithetic properties of signaling through individual S1PRs. Targeting the SphK/S1P/S1PR axis is already the object of a number of clinical trials. Most notably S1PR1 modulators (Fingolimod, MT-1303, Ozanimod) are tested or already in clinical use for treating inflammation-driven diseases such as multiple sclerosis, inflammatory bowel disease and psoriasis (223). These drugs are thought to act mainly through the induction of sustained lymphopenia by trapping T cells in lymphatic organs. Thereby, S1PR1 modulators dampen the inflammatory response and thus reduce disease severity. It is unclear how these drugs affect macrophage biology in patients. Targeting macrophage S1PR1 in cancer may be of interest, as outlined above. However, in the case of cancer therapy, as well as during infection, sustained lymphopenia triggered by S1PR1 antagonism may rather be disadvantageous, since T cells are needed at the tumor site for a proper anti-tumor response (224). Targeting S1P levels globally using the anti-S1P monoclonal antibody Sonepcizumab failed in a phase II study of metastatic renal cell carcinoma (225). A phase I clinical trial with Safingol, which inhibits SphK besides other kinases, published in 2011 showed potential in treating solid tumors when combined with chemotherapy (226). Administration of Safingol alone was ineffective and further clinical were so far not conducted. The SPHK2 inhibitor ABC294640 showed promise in a phase I trial in patients with advanced solid tumors (227). However, given the opposing effects of signaling through individual S1PRs, targeting individual S1PRs may be more rational to unleash the full potential of S1P modulators. In the context of cancer and with a focus on immunity, S1PR4 may represent an interesting drug target since it is mainly expressed on immune cells including macrophages and T cells, and does not affect T cell trafficking similar to S1PR1.

AUTHOR CONTRIBUTIONS

All authors listed have made a substantial, direct and intellectual contribution to the work, and approved it for publication.

ACKNOWLEDGMENTS

We apologize to researchers whose primary observations were cited indirectly by referring to current reviews. Our work was supported by Deutsche Krebshilfe (70112451), Deutsche Forschungsgemeinschaft (SFB 1039, TP B04 and TP B06, FOR 2438 P8, GRK 2336, TP1 and TP6), and Sander Foundation.

REFERENCES

1. Kaufmann SH. Immunology's foundation: the 100-year anniversary of the Nobel Prize to Paul Ehrlich and Elie Metchnikoff. *Nat Immunol*. (2008) 9:705–12. doi: 10.1038/ni0708-705
2. Lavin Y, Merad M. Macrophages: gatekeepers of tissue integrity. *Cancer Immunol Res*. (2013) 1:201–9. doi: 10.1158/2326-6066.CIR-13-0117
3. Wynn TA, Chawla A, Pollard JW. Macrophage biology in development, homeostasis and disease. *Nature*. (2013) 496:445–55. doi: 10.1038/nature12034

4. Hulsmans M, Clauss S, Xiao L, Aguirre AD, King KR, Hanley A, et al. Macrophages facilitate electrical conduction in the heart. *Cell*. (2017) 169:510–22.e20. doi: 10.1016/j.cell.2017.03.050
5. Wolf Y, Boura-Halfon S, Cortese N, Haimon Z, Sar Shalom H, Kuperman Y, et al. Brown-adipose-tissue macrophages control tissue innervation and homeostatic energy expenditure. *Nat Immunol*. (2017) 18:665–74. doi: 10.1038/ni.3746
6. Pollard JW. Trophic macrophages in development and disease. *Nat Rev Immunol*. (2009) 9:259–70. doi: 10.1038/nri2528
7. Corliss BA, Azimi MS, Munson JM, Peirce SM, Murfee WL. Macrophages: an inflammatory link between angiogenesis and lymphangiogenesis. *Microcirculation*. (2016) 23:95–121. doi: 10.1111/micc.12259
8. Minutti CM, Modak RV, Macdonald F, Li F, Smyth DJ, Dorward DA, et al. A macrophage-pericyte axis directs tissue restoration via amphiregulin-induced transforming growth factor beta activation. *Immunity*. (2019) 50:645–54 e6. doi: 10.1016/j.immuni.2019.01.008
9. Hu MS, Walmsley GG, Barnes LA, Weiskopf K, Rennert RC, Duscher D, et al. Delivery of monocyte lineage cells in a biomimetic scaffold enhances tissue repair. *JCI Insight*. (2017) 2:96260. doi: 10.1172/jci.insight.96260
10. Minutti CM, Knipper JA, Allen JE, Zaiss DM. Tissue-specific contribution of macrophages to wound healing. *Semin Cell Dev Biol*. (2017) 61:3–11. doi: 10.1016/j.semcdb.2016.08.006
11. Guilliams M, Scott CL. Does niche competition determine the origin of tissue-resident macrophages? *Nat Rev Immunol*. (2017) 17:451–60. doi: 10.1038/nri.2017.42
12. Bain CC, Hawley CA, Garner H, Scott CL, Schridde A, Steers NJ, et al. Long-lived self-renewing bone marrow-derived macrophages displace embryo-derived cells to inhabit adult serous cavities. *Nat Commun*. (2016) 7:ncomms11852. doi: 10.1038/ncomms11852
13. Mass E, Ballesteros I, Farlik M, Halbritter F, Gunther P, Crozet L, et al. Specification of tissue-resident macrophages during organogenesis. *Science*. (2016) 353:aaf4238. doi: 10.1126/science.aaf4238
14. Ginhoux F, Jung S. Monocytes and macrophages: developmental pathways and tissue homeostasis. *Nat Rev Immunol*. (2014) 14:392–404. doi: 10.1038/nri3671
15. Brune B, Courtial N, Dehne N, Syed SN, Weigert A. Macrophage NOS2 in Tumor Leukocytes. *Antioxid Redox Signal*. (2017) 26:1023–43. doi: 10.1089/ars.2016.6811
16. Hoeffel G, Chen J, Lavin Y, Low D, Almeida FF, See P, et al. C-Myb(+) erythro-myeloid progenitor-derived fetal monocytes give rise to adult tissue-resident macrophages. *Immunity*. (2015) 42:665–78. doi: 10.1016/j.immuni.2015.03.011
17. Perdiguero EG, Klapproth K, Schulz C, Busch K, Azzoni E, Crozet L, et al. Tissue-resident macrophages originate from yolk-sac-derived erythro-myeloid progenitors. *Nature*. (2014) 518:547–51. doi: 10.1038/nature13989
18. McGovern N, Schlitzer A, Gunawan M, Jardine L, Shin A, Poyner E, et al. Human dermal $CD14^+$ cells are a transient population of monocyte-derived macrophages. *Immunity*. (2014) 41:465–77. doi: 10.1016/j.immuni.2014.08.006
19. Bain CC, Mowat AM. Macrophages in intestinal homeostasis and inflammation. *Immunol Rev*. (2014) 260:102–17. doi: 10.1111/imr.12192
20. Epelman S, Lavine KJ, Randolph GJ. Origin and functions of tissue macrophages. *Immunity*. (2014) 41:21–35. doi: 10.1016/j.immuni.2014.06.013
21. van de Laar L, Saelens W, De Prijck S, Martens L, Scott CL, Van Isterdael G, et al. Yolk sac macrophages, fetal liver, and adult monocytes can colonize an empty niche and develop into functional tissue-resident macrophages. *Immunity*. (2016) 44:755–68. doi: 10.1016/j.immuni.2016.02.017
22. Roberts AW, Lee BL, Deguine J, John S, Shlomchik MJ, Barton GM. Tissue-resident macrophages are locally programmed for silent clearance of apoptotic cells. *Immunity*. (2017) 47:913–27 e6. doi: 10.1016/j.immuni.2017.10.006
23. Sierro F, Evrard M, Rizzetto S, Melino M, Mitchell AJ, Florido M, et al. A liver capsular network of monocyte-derived macrophages restricts hepatic dissemination of intraperitoneal bacteria by neutrophil recruitment. *Immunity*. (2017) 47:374–88 e6. doi: 10.1016/j.immuni.2017.07.018
24. Bajpai G, Schneider C, Wong N, Bredemeyer A, Hulsmans M, Nahrendorf M, et al. The human heart contains distinct macrophage subsets with divergent origins and functions. *Nat Med*. (2018) 24:1234–45. doi: 10.1038/s41591-018-0059-x
25. Chakarov S, Lim HY, Tan L, Lim SY, See P, Lum J, et al. Two distinct interstitial macrophage populations coexist across tissues in specific subtissular niches. *Science*. (2019) 363:eaau0964. doi: 10.1126/science.aau0964
26. Heinz S, Benner C, Spann N, Bertolino E, Lin YC, Laslo P, et al. Simple combinations of lineage-determining transcription factors prime cis-regulatory elements required for macrophage and B cell identities. *Mol Cell*. (2010) 38:576–89. doi: 10.1016/j.molcel.2010.05.004
27. Jenkins SJ, Hume DA. Homeostasis in the mononuclear phagocyte system. *Trends Immunol*. (2014) 35:358–67. doi: 10.1016/j.it.2014.06.006
28. Scott CL, T'Jonck W, Martens L, Todorov H, Sichien D, Soen B, et al. The transcription factor ZEB2 is required to maintain the tissue-specific identities of macrophages. *Immunity*. (2018) 49:312–25. doi: 10.1016/j.immuni.2018.07.004
29. Haldar M, Kohyama M, So AY, Kc W, Wu X, Briseno CG, et al. Heme-mediated SPI-C induction promotes monocyte differentiation into iron-recycling macrophages. *Cell*. (2014) 156:1223–34. doi: 10.1016/j.cell.2014.01.069
30. Okabe Y, Medzhitov R. Tissue-specific signals control reversible program of localization and functional polarization of macrophages. *Cell*. (2014) 157:832–44. doi: 10.1016/j.cell.2014.04.016
31. Rosas M, Davies LC, Giles PJ, Liao CT, Kharfan B, Stone TC, et al. The transcription factor Gata6 links tissue macrophage phenotype and proliferative renewal. *Science*. (2014) 344:645–8. doi: 10.1126/science.1251414
32. Schneider C, Nobs SP, Kurrer M, Rehrauer H, Thiele C, Kopf M. Induction of the nuclear receptor PPAR-gamma by the cytokine GM-CSF is critical for the differentiation of fetal monocytes into alveolar macrophages. *Nat Immunol*. (2014) 15:1026–37. doi: 10.1038/ni.3005
33. Butovsky O, Jedrychowski MP, Moore CS, Cialic R, Lanser AJ, Gabriely G, et al. Identification of a unique TGF-beta-dependent molecular and functional signature in microglia. *Nat Neurosci*. (2014) 17:131–43. doi: 10.1038/nn.3599
34. Gosselin D, Link VM, Romanoski CE, Fonseca GJ, Eichenfield DZ, Spann NJ, et al. Environment drives selection and function of enhancers controlling tissue-specific macrophage identities. *Cell*. (2014) 159:1327–40. doi: 10.1016/j.cell.2014.11.023
35. Kurotaki D, Sasaki H, Tamura T. Transcriptional control of monocyte and macrophage development. *Int Immunol*. (2017) 29:97–107. doi: 10.1093/intimm/dxx016
36. Murray PJ, Allen JE, Biswas SK, Fisher EA, Gilroy DW, Goerdt S, et al. Macrophage activation and polarization: nomenclature and experimental guidelines. *Immunity*. (2014) 41:14–20. doi: 10.1016/j.immuni.2014.07.009
37. Murray PJ, Wynn TA. Protective and pathogenic functions of macrophage subsets. *Nat Rev Immunol*. (2011) 11:723–37. doi: 10.1038/nri3073
38. Stefater JA III, Ren S, Lang RA, Duffield JS. Metchnikoff's policemen: macrophages in development, homeostasis and regeneration. *Trends Mol Med*. (2011) 17:743–52. doi: 10.1016/j.molmed.2011.07.009
39. Brune B, Dehne N, Grossmann N, Jung M, Namgaladze D, Schmid T, et al. Redox control of inflammation in macrophages. *Antioxid Redox Signal*. (2013) 19:595–637. doi: 10.1089/ars.2012.4785
40. Mosser DM, Edwards JP. Exploring the full spectrum of macrophage activation. *Nat Rev Immunol*. (2008) 8:958–69. doi: 10.1038/nri2448
41. Nahrendorf M, Swirski FK. Abandoning M1/M2 for a network model of macrophage function. *Circ Res*. (2016) 119:414–7. doi: 10.1161/CIRCRESAHA.116.309194
42. Mantovani A, Sica A, Sozzani S, Allavena P, Vecchi A, Locati M. The chemokine system in diverse forms of macrophage activation and polarization. *Trends Immunol*. (2004) 25:677–86. doi: 10.1016/j.it.2004.09.015
43. Krausgruber T, Blazek K, Smallie T, Alzabin S, Lockstone H, Sahgal N, et al. IRF5 promotes inflammatory macrophage polarization and TH1-TH17 responses. *Nat Immunol*. (2011) 12:231–8. doi: 10.1038/ni.1990
44. Hu S, Liu H, Ha Y, Luo X, Motamedi M, Gupta MP, et al. Posttranslational modification of Sirt6 activity by peroxynitrite. *Free Radic Biol Med*. (2015) 79:176–85. doi: 10.1016/j.freeradbiomed.2014.11.011

45. Lawrence T, Natoli G. Transcriptional regulation of macrophage polarization: enabling diversity with identity. *Nat Rev Immunol*. (2011) 11:750–61. doi: 10.1038/nri3088
46. Martinez FO, Helming L, Milde R, Varin A, Melgert BN, Draijer C, et al. Genetic programs expressed in resting and IL-4 alternatively activated mouse and human macrophages: similarities and differences. *Blood*. (2013) 121:e57–69. doi: 10.1182/blood-2012-06-436212
47. Piccolo V, Curina A, Genua M, Ghisletti S, Simonatto M, Sabo A, et al. Opposing macrophage polarization programs show extensive epigenomic and transcriptional cross-talk. *Nat Immunol*. (2017) 18:530–40. doi: 10.1038/ni.3710
48. Czimmerer Z, Daniel B, Horvath A, Ruckerl D, Nagy G, Kiss M, et al. The transcription factor STAT6 mediates direct repression of inflammatory enhancers and limits activation of alternatively polarized macrophages. *Immunity*. (2018) 48:75–90 e6. doi: 10.1016/j.immuni.2017.12.010
49. Kang K, Park SH, Chen J, Qiao Y, Giannopoulou E, Berg K, et al. Interferon-gamma represses M2 gene expression in human macrophages by disassembling enhancers bound by the transcription factor MAF. *Immunity*. (2017) 47:235–50 e4. doi: 10.1016/j.immuni.2017.07.017
50. Cassetta L, Cassol E, Poli G. Macrophage polarization in health and disease. *Sci World J*. (2011) 11:2391–402. doi: 10.1100/2011/213962
51. Stout RD, Jiang C, Matta B, Tietzel I, Watkins SK, Suttles J. Macrophages sequentially change their functional phenotype in response to changes in microenvironmental influences. *J Immunol*. (2005) 175:342–9. doi: 10.4049/jimmunol.175.1.342
52. Strub GM, Maceyka M, Hait NC, Milstien S, Spiegel S. Extracellular and intracellular actions of sphingosine-1-phosphate. *Adv Exp Med Biol*. (2010) 688:141–55. doi: 10.1007/978-1-4419-6741-1_10
53. Mendelson K, Evans T, Hla T. Sphingosine 1-phosphate signalling. *Development*. (2014) 141:5–9. doi: 10.1242/dev.094805
54. Pyne S, Adams DR, Pyne NJ. Sphingosine 1-phosphate and sphingosine kinases in health and disease: recent advances. *Prog Lipid Res*. (2016) 62:93–106. doi: 10.1016/j.plipres.2016.03.001
55. Pitman MR, Costabile M, Pitson SM. Recent advances in the development of sphingosine kinase inhibitors. *Cell Signal*. (2016) 28:1349–63. doi: 10.1016/j.cellsig.2016.06.007
56. Maceyka M, Harikumar KB, Milstien S, Spiegel S. Sphingosine-1-phosphate signaling and its role in disease. *Trends Cell Biol*. (2012) 22:50–60. doi: 10.1016/j.tcb.2011.09.003
57. Weigert A, Weichand B, Brune B. S1P regulation of macrophage functions in the context of cancer. *Anticancer Agents Med Chem*. (2011) 11:818–29. doi: 10.2174/187152011797655096
58. Weigert A, Weis N, Brune B. Regulation of macrophage function by sphingosine-1-phosphate. *Immunobiology*. (2009) 214:748–60. doi: 10.1016/j.imbio.2009.06.003
59. Hannun YA, Obeid LM. Principles of bioactive lipid signalling: lessons from sphingolipids. *Nat Rev Mol Cell Biol*. (2008) 9:139–50. doi: 10.1038/nrm2329
60. Merrill AH Jr, Stokes TH, Momin A, Park H, Portz BJ, Kelly S, et al. Sphingolipidomics: a valuable tool for understanding the roles of sphingolipids in biology and disease. *J Lipid Res*. (2009) 50(Suppl):S97–102. doi: 10.1194/jlr.R800073-JLR200
61. Adams DR, Pyne S, Pyne NJ. Sphingosine kinases: emerging structure-function insights. *Trends Biochem Sci*. (2016) 41:395–409. doi: 10.1016/j.tibs.2016.02.007
62. Takabe K, Kim RH, Allegood JC, Mitra P, Ramachandran S, Nagahashi M, et al. Estradiol induces export of sphingosine 1-phosphate from breast cancer cells via ABCC1 and ABCG2. *J Biol Chem*. (2010) 285:10477–86. doi: 10.1074/jbc.M109.064162
63. Kawahara A, Nishi T, Hisano Y, Fukui H, Yamaguchi A, Mochizuki N. The sphingolipid transporter spns2 functions in migration of zebrafish myocardial precursors. *Science*. (2009) 323:524–7. doi: 10.1126/science.1167449
64. Rivera J, Proia RL, Olivera A. The alliance of sphingosine-1-phosphate and its receptors in immunity. *Nat Rev Immunol*. (2008) 8:753–63. doi: 10.1038/nri2400
65. Kunkel GT, Maceyka M, Milstien S, Spiegel S. Targeting the sphingosine-1-phosphate axis in cancer, inflammation and beyond. *Nat Rev Drug Discov*. (2013) 12:688–702. doi: 10.1038/nrd4099
66. Hla T, Dannenberg AJ. Sphingolipid signaling in metabolic disorders. *Cell Metab*. (2012) 16:420–34. doi: 10.1016/j.cmet.2012.06.017
67. Bryan AM, Del Poeta M. Sphingosine-1-phosphate receptors and innate immunity. *Cell. Microbiol*. (2018) 20:e12836. doi: 10.1111/cmi.12836
68. Blaho VA, Hla T. An update on the biology of sphingosine 1-phosphate receptors. *J Lipid Res*. (2014) 55:1596–608. doi: 10.1194/jlr.R046300
69. Aoki M, Aoki H, Ramanathan R, Hait NC, Takabe K. Sphingosine-1-phosphate signaling in immune cells and inflammation: roles and therapeutic potential. *Mediat Inflamm*. (2016) 2016:8606878. doi: 10.1155/2016/8606878
70. Kono M, Mi Y, Liu Y, Sasaki T, Allende ML, Wu YP, et al. The sphingosine-1-phosphate receptors S1P1, S1P2, and S1P3 function coordinately during embryonic angiogenesis. *J Biol Chem*. (2004) 279:29367–73. doi: 10.1074/jbc.M403937200
71. Mendelson K, Zygmunt T, Torres-Vazquez J, Evans T, Hla T. Sphingosine 1-phosphate receptor signaling regulates proper embryonic vascular patterning. *J Biol Chem*. (2013) 288:2143–56. doi: 10.1074/jbc.M112.427344
72. Hla T, Venkataraman K, Michaud J. The vascular S1P gradient-cellular sources and biological significance. *Biochim Biophys Acta*. (2008) 1781:477–82. doi: 10.1016/j.bbalip.2008.07.003
73. Weis N, Weigert A, von Knethen A, Brune B. Heme oxygenase-1 contributes to an alternative macrophage activation profile induced by apoptotic cell supernatants. *Mol Biol Cell*. (2009) 20:1280–8. doi: 10.1091/mbc.e08-10-1005
74. Gomez-Munoz A, Kong J, Salh B, Steinbrecher UP. Sphingosine-1-phosphate inhibits acid sphingomyelinase and blocks apoptosis in macrophages. *FEBS Lett*. (2003) 539:56–60. doi: 10.1016/S0014-5793(03)00197-2
75. Feuerborn R, Becker S, Poti F, Nagel P, Brodde M, Schmidt H, et al. High density lipoprotein (HDL)-associated sphingosine 1-phosphate (S1P) inhibits macrophage apoptosis by stimulating STAT3 activity and survivin expression. *Atherosclerosis*. (2017) 257:29–37. doi: 10.1016/j.atherosclerosis.2016.12.009
76. Song F, Hou J, Chen Z, Cheng B, Lei R, Cui P, et al. Sphingosine-1-phosphate Receptor 2 signaling promotes caspase-11-dependent macrophage pyroptosis and worsens *Escherichia coli* sepsis outcome. *Anesthesiology*. (2018) 129:311–20. doi: 10.1097/ALN.0000000000002196
77. Monick MM, Mallampalli RK, Bradford M, McCoy D, Gross TJ, Flaherty DM, et al. Cooperative prosurvival activity by ERK and Akt in human alveolar macrophages is dependent on high levels of acid ceramidase activity. *J Immunol*. (2004) 173:123–35. doi: 10.4049/jimmunol.173.1.123
78. Gude DR, Alvarez SE, Paugh SW, Mitra P, Yu J, Griffiths R, et al. Apoptosis induces expression of sphingosine kinase 1 to release sphingosine-1-phosphate as a "come-and-get-me" signal. *FASEB J*. (2008) 22:2629–38. doi: 10.1096/fj.08-107169
79. Al-Jarallah A, Chen X, Gonzalez L, Trigatti BL. High density lipoprotein stimulated migration of macrophages depends on the scavenger receptor class B, type I, PDZK1 and Akt1 and is blocked by sphingosine 1 phosphate receptor antagonists. *PLoS ONE*. (2014) 9:e106487. doi: 10.1371/journal.pone.0106487
80. Liao CY, Song MJ, Gao Y, Mauer AS, Revzin A, Malhi H. Hepatocyte-derived lipotoxic extracellular vesicle sphingosine 1-phosphate induces macrophage chemotaxis. *Front Immunol*. (2018) 9:2980. doi: 10.3389/fimmu.2018.02980
81. Weichand B, Weis N, Weigert A, Grossmann N, Levkau B, Bruene B. Apoptotic cells enhance sphingosine-1-phosphate receptor 1 dependent macrophage migration. *Eur J Immunol*. (2013) 43:3306–13. doi: 10.1002/eji.201343441
82. Muller J, von Bernstorff W, Heidecke CD, Schulze T. Differential S1P receptor profiles on M1- and M2-polarized macrophages affect macrophage cytokine production and migration. *Biomed Res Int*. (2017) 2017:7584621. doi: 10.1155/2017/7584621
83. Michaud J, Im DS, Hla T. Inhibitory role of sphingosine 1-phosphate receptor 2 in macrophage recruitment during inflammation. *J Immunol*. (2010) 184:1475–83. doi: 10.4049/jimmunol.0901586
84. Ishii M, Kikuta J, Shimazu Y, Meier-Schellersheim M, Germain RN. Chemorepulsion by blood S1P regulates osteoclast precursor mobilization and bone remodeling *in vivo*. *J Exp Med*. 207:2793–8. doi: 10.1084/jem.20101474

85. Yang L, Han Z, Tian L, Mai P, Zhang Y, Wang L, et al. Sphingosine 1-phosphate receptor 2 and 3 mediate bone marrow-derived monocyte/macrophage motility in cholestatic liver injury in mice. *Sci Rep*. (2015) 5:13423. doi: 10.1038/srep13423
86. Rathinasamy A, Czeloth N, Pabst O, Forster R, Bernhardt G. The origin and maturity of dendritic cells determine the pattern of sphingosine 1-phosphate receptors expressed and required for efficient migration. *J Immunol*. (2010) 185:4072–81. doi: 10.4049/jimmunol.1000568
87. Gordon S. Phagocytosis: an immunobiologic process. *Immunity*. (2016) 44:463–75. doi: 10.1016/j.immuni.2016.02.026
88. Weigert A, Johann AM, von Knethen A, Schmidt H, Geisslinger G, Brune B. Apoptotic cells promote macrophage survival by releasing the antiapoptotic mediator sphingosine-1-phosphate. *Blood*. (2006) 108:1635–42. doi: 10.1182/blood-2006-04-014852
89. Arifuzzaman M, Ang WXG, Choi HW, Nilles ML, St. John AL, Abraham SN. Necroptosis of infiltrated macrophages drives Yersinia pestis dispersal within buboes. *JCI Insight*. (2018) 3:122188. doi: 10.1172/jci.insight.122188
90. Luo B, Gan W, Liu Z, Shen Z, Wang J, Shi R, et al. Erythropoeitin signaling in macrophages promotes dying cell clearance and immune tolerance. *Immunity*. (2016) 44:287–302. doi: 10.1016/j.immuni.2016.01.002
91. Tran HB, Barnawi J, Ween M, Hamon R, Roscioli E, Hodge G, et al. Cigarette smoke inhibits efferocytosis via deregulation of sphingosine kinase signaling: reversal with exogenous S1P and the S1P analogue FTY720. *J Leukoc Biol*. (2016) 100:195–202. doi: 10.1189/jlb.3A1015-471R
92. Tran HB, Jersmann H, Truong TT, Hamon R, Roscioli E, Ween M, et al. Disrupted epithelial/macrophage crosstalk via Spinster homologue 2-mediated S1P signaling may drive defective macrophage phagocytic function in COPD. *PLoS ONE*. (2017) 12:e0179577. doi: 10.1371/journal.pone.0179577
93. Barnawi J, Tran H, Jersmann H, Pitson S, Roscioli E, Hodge G, et al. Potential Link between the Sphingosine-1-Phosphate (S1P) system and defective alveolar macrophage phagocytic function in Chronic Obstructive Pulmonary Disease (COPD). *PLoS ONE*. (2015) 10:e0122771. doi: 10.1371/journal.pone.0122771
94. Barnawi J, Jersmann H, Haberberger R, Hodge S, Meech R. Reduced DNA methylation of sphingosine-1 phosphate receptor 5 in alveolar macrophages in COPD: a potential link to failed efferocytosis. *Respirology*. (2017) 22:315–21. doi: 10.1111/resp.12949
95. Barnawi J, Tran HB, Roscioli E, Hodge G, Jersmann H, Haberberger R, et al. Pro-phagocytic effects of thymoquinone on cigarette smoke-exposed macrophages occur by modulation of the sphingosine-1-phosphate signalling system. *COPD*. (2016) 13:653–61. doi: 10.3109/15412555.2016.1153614
96. Duong CQ, Bared SM, Abu-Khader A, Buechler C, Schmitz A, Schmitz G. Expression of the lysophospholipid receptor family and investigation of lysophospholipid-mediated responses in human macrophages. *Biochim Biophys Acta*. (2004) 1682:112–9. doi: 10.1016/j.bbalip.2004.03.002
97. McQuiston T, Luberto C, Del Poeta M. Role of sphingosine-1-phosphate (S1P) and S1P receptor 2 in the phagocytosis of *Cryptococcus neoformans* by alveolar macrophages. *Microbiology*. (2011) 157:1416–27. doi: 10.1099/mic.0.045989-0
98. Hou J, Chen Q, Zhang K, Cheng B, Xie G, Wu X, et al. Sphingosine 1-phosphate receptor 2 signaling suppresses macrophage phagocytosis and impairs host defense against sepsis. *Anesthesiology*. (2015) 123:409–22. doi: 10.1097/ALN.0000000000000725
99. Kuehnel MP, Rybin V, Anand PK, Anes E, Griffiths G. Lipids regulate P2X7-receptor-dependent actin assembly by phagosomes via ADP translocation and ATP synthesis in the phagosome lumen. *J Cell Sci*. (2009) 122:499–504. doi: 10.1242/jcs.034199
100. Kuehnel MP, Reiss M, Anand PK, Treede I, Holzer D, Hoffmann E, et al. Sphingosine-1-phosphate receptors stimulate macrophage plasma-membrane actin assembly via ADP release, ATP synthesis and P2X7R activation. *J Cell Sci*. (2009) 122:505–12. doi: 10.1242/jcs.034207
101. Anes E, Kuhnel MP, Bos E, Moniz-Pereira J, Habermann A, Griffiths G. Selected lipids activate phagosome actin assembly and maturation resulting in killing of pathogenic mycobacteria. *Nat Cell Biol*. (2003) 5:793–802. doi: 10.1038/ncb1036
102. Garg SK, Volpe E, Palmieri G, Mattei M, Galati D, Martino A, et al. Sphingosine 1-phosphate induces antimicrobial activity both *in vitro* and *in vivo*. *J Infect Dis*. (2004) 189:2129–38. doi: 10.1086/386286
103. Gutierrez MG, Gonzalez AP, Anes E, Griffiths G. Role of lipids in killing mycobacteria by macrophages: evidence for NF-kappaB-dependent and -independent killing induced by different lipids. *Cell Microbiol*. (2009) 11:406–20. doi: 10.1111/j.1462-5822.2008.01263.x
104. Hou J, Chen Q, Wu X, Zhao D, Reuveni H, Licht T, et al. S1PR3 signaling drives bacterial killing and is required for survival in bacterial sepsis. *Am J Respir Crit Care Med*. (2017) 196:1559–70. doi: 10.1164/rccm.201701-0241OC
105. Prakash H, Luth A, Grinkina N, Holzer D, Wadgaonkar R, Gonzalez AP, et al. Sphingosine kinase-1 (SphK-1) regulates *Mycobacterium smegmatis* infection in macrophages. *PLoS ONE*. (2010) 5:e10657. doi: 10.1371/journal.pone.0010657
106. Malik ZA, Thompson CR, Hashimi S, Porter B, Iyer SS, Kusner DJ. Cutting edge: *Mycobacterium tuberculosis* blocks Ca2+ signaling and phagosome maturation in human macrophages via specific inhibition of sphingosine kinase. *J Immunol*. (2003) 170:2811–5. doi: 10.4049/jimmunol.170.6.2811
107. Thompson CR, Iyer SS, Melrose N, VanOosten R, Johnson K, Pitson SM, et al. Sphingosine kinase 1 (SK1) is recruited to nascent phagosomes in human macrophages: inhibition of SK1 translocation by *Mycobacterium tuberculosis*. *J Immunol*. (2005) 174:3551–61. doi: 10.4049/jimmunol.174.6.3551
108. McQuiston T, Luberto C, Del Poeta M. Role of host sphingosine kinase 1 in the lung response against *Cryptococcosis*. *Infect Immun*. (2010) 78:2342–52. doi: 10.1128/IAI.01140-09
109. Arish M, Husein A, Ali R, Tabrez S, Naz F, Ahmad MZ, et al. Sphingosine-1-phosphate signaling in Leishmania donovani infection in macrophages. *PLoS Negl Trop Dis*. (2018) 12:e0006647. doi: 10.1371/journal.pntd.0006647
110. Custodio R, McLean CJ, Scott AE, Lowther J, Kennedy A, Clarke DJ, et al. Characterization of secreted sphingosine-1-phosphate lyases required for virulence and intracellular survival of Burkholderia pseudomallei. *Mol Microbiol*. (2016) 102:1004–19. doi: 10.1111/mmi.13531
111. Rolando M, Escoll P, Nora T, Botti J, Boitez V, Bedia C, et al. Legionella pneumophila S1P-lyase targets host sphingolipid metabolism and restrains autophagy. *Proc Natl Acad Sci USA*. (2016) 113:1901–6. doi: 10.1073/pnas.1522067113
112. Black RA, Rauch CT, Kozlosky CJ, Peschon JJ, Slack JL, Wolfson MF, et al. A metalloproteinase disintegrin that releases tumour-necrosis factor-alpha from cells. *Nature*. (1997) 385:729–33. doi: 10.1038/385729a0
113. Schott J, Reitter S, Philipp J, Haneke K, Schafer H, Stoecklin G. Translational regulation of specific mRNAs controls feedback inhibition and survival during macrophage activation. *PLoS Genet*. (2014) 10:e1004368. doi: 10.1371/journal.pgen.1004368
114. Alvarez SE, Harikumar KB, Hait NC, Allegood J, Strub GM, Kim EY, et al. Sphingosine-1-phosphate is a missing cofactor for the E3 ubiquitin ligase TRAF2. *Nature*. (2010) 465:1084–8. doi: 10.1038/nature09128
115. Xia P, Wang L, Moretti PA, Albanese N, Chai F, Pitson SM, et al. Sphingosine kinase interacts with TRAF2 and dissects tumor necrosis factor-alpha signaling. *J Biol Chem*. (2002) 277:7996–8003. doi: 10.1074/jbc.M111423200
116. Harikumar KB, Yester JW, Surace MJ, Oyeniran C, Price MM, Huang WC, et al. K63-linked polyubiquitination of transcription factor IRF1 is essential for IL-1-induced production of chemokines CXCL10 and CCL5. *Nat Immunol*. (2014) 15:231–8. doi: 10.1038/ni.2810
117. Pchejetski D, Nunes J, Coughlan K, Lall H, Pitson SM, Waxman J, et al. The involvement of sphingosine kinase 1 in LPS-induced Toll-like receptor 4-mediated accumulation of HIF-1alpha protein, activation of ASK1 and production of the pro-inflammatory cytokine IL-6. *Immunol Cell Biol*. (2011) 89:268–74. doi: 10.1038/icb.2010.91
118. Nayak D, Huo Y, Kwang WX, Pushparaj PN, Kumar SD, Ling EA, et al. Sphingosine kinase 1 regulates the expression of proinflammatory cytokines and nitric oxide in activated microglia. *Neuroscience*. (2010) 166:132–44. doi: 10.1016/j.neuroscience.2009.12.020
119. Hammad SM, Crellin HG, Wu BX, Melton J, Anelli V, Obeid LM. Dual and distinct roles for sphingosine kinase 1 and sphingosine 1 phosphate in the response to inflammatory stimuli in RAW

macrophages. *Prostaglandins Other Lipid Mediat*. (2008) 85:107–14. doi: 10.1016/j.prostaglandins.2007.11.002
120. Jin J, Lu Z, Li Y, Ru JH, Lopes-Virella MF, Huang Y. LPS and palmitate synergistically stimulate sphingosine kinase 1 and increase sphingosine 1 phosphate in RAW264.7 macrophages. *J Leukoc Biol*. (2018) 104:843–53. doi: 10.1002/JLB.3A0517-188RRR
121. Baker DA, Barth J, Chang R, Obeid LM, Gilkeson GS. Genetic sphingosine kinase 1 deficiency significantly decreases synovial inflammation and joint erosions in murine TNF-alpha-induced arthritis. *J Immunol*. (2010) 185:2570–9. doi: 10.4049/jimmunol.1000644
122. Michaud J, Kohno M, Proia RL, Hla T. Normal acute and chronic inflammatory responses in sphingosine kinase 1 knockout mice. *FEBS Lett*. (2006) 580:4607–12. doi: 10.1016/j.febslet.2006.07.035
123. Xiong Y, Lee HJ, Mariko B, Lu YC, Dannenberg AJ, Haka AS, et al. Sphingosine kinases are not required for inflammatory responses in macrophages. *J Biol Chem*. (2013) 288:32563–73. doi: 10.1074/jbc.M113.483750
124. Liang J, Nagahashi M, Kim EY, Harikumar KB, Yamada A, Huang WC, et al. Sphingosine-1-phosphate links persistent STAT3 activation, chronic intestinal inflammation, and development of colitis-associated cancer. *Cancer Cell*. (2013) 23:107–20. doi: 10.1016/j.ccr.2012.11.013
125. Ghosh M, Thangada S, Dasgupta O, Khanna KM, Yamase HT, Kashgarian M, et al. Cell-intrinsic sphingosine kinase 2 promotes macrophage polarization and renal inflammation in response to unilateral ureteral obstruction. *PLoS ONE*. (2018) 13:e0194053. doi: 10.1371/journal.pone.0194053
126. Hornuss C, Hammermann R, Fuhrmann M, Juergens UR, Racke K. Human and rat alveolar macrophages express multiple EDG receptors. *Eur J Pharmacol*. (2001) 429:303–8. doi: 10.1016/S0014-2999(01)01329-2
127. Lee H, Liao JJ, Graeler M, Huang MC, Goetzl EJ. Lysophospholipid regulation of mononuclear phagocytes. *Biochim Biophys Acta*. (2002) 1582:175–7. doi: 10.1016/S1388-1981(02)00153-1
128. Yang J, Yang L, Tian L, Ji X, Yang L, Li L. Sphingosine 1-Phosphate (S1P)/S1P receptor2/3 axis promotes inflammatory M1 polarization of bone marrow-derived monocyte/macrophage via G(alpha)i/o/PI3K/JNK pathway. *Cell Physiol Biochem*. (2018) 49:1677–93. doi: 10.1159/000493611
129. Gaire BP, Song MR, Choi JW. Sphingosine 1-phosphate receptor subtype 3 (S1P3) contributes to brain injury after transient focal cerebral ischemia via modulating microglial activation and their M1 polarization. *J Neuroinflamm*. (2018) 15:284. doi: 10.1186/s12974-018-1323-1
130. Heo JY, Im DS. Pro-inflammatory role of S1P3 in macrophages. *Biomol Ther*. (2019) 27:373–80. doi: 10.4062/biomolther.2018.215
131. Netea MG, van de Veerdonk FL, van der Meer JW, Dinarello CA, Joosten LA. Inflammasome-independent regulation of IL-1-family cytokines. *Annu Rev Immunol*. (2015) 33:49–77. doi: 10.1146/annurev-immunol-032414-112306
132. Weichand B, Popp R, Dziumbla S, Mora J, Strack E, Elwakeel E, et al. S1PR1 on tumor-associated macrophages promotes lymphangiogenesis and metastasis via NLRP3/IL-1beta. *J Exp Med*. (2017) 214:2695–713. doi: 10.1084/jem.20160392
133. Burow P, Klapperstuck M, Markwardt F. Activation of ATP secretion via volume-regulated anion channels by sphingosine-1-phosphate in RAW macrophages. *Pflugers Arch*. (2015) 467:1215–26. doi: 10.1007/s00424-014-1561-8
134. Zhao S, Gong Z, Zhou J, Tian C, Gao Y, Xu C, et al. Deoxycholic acid triggers NLRP3 inflammasome activation and aggravates DSS-induced colitis in mice. *Front Immunol*. (2016) 7:536. doi: 10.3389/fimmu.2016.00536
135. Skoura A, Michaud J, Im DS, Thangada S, Xiong Y, Smith JD, et al. Sphingosine-1-phosphate receptor-2 function in myeloid cells regulates vascular inflammation and atherosclerosis. *Arterioscler Thromb Vasc Biol*. (2011) 31:81–5. doi: 10.1161/ATVBAHA.110.213496
136. Syed SN, Jung M, Weigert A, Brune B. S1P Provokes tumor lymphangiogenesis via macrophage-derived mediators such as IL-1beta or Lipocalin-2. *Mediators Inflamm*. (2017) 2017:7510496. doi: 10.1155/2017/7510496
137. Hughes JE, Srinivasan S, Lynch KR, Proia RL, Ferdek P, Hedrick CC. Sphingosine-1-phosphate induces an antiinflammatory phenotype in macrophages. *Circ Res*. (2008) 102:950–8. doi: 10.1161/CIRCRESAHA.107.170779
138. Weigert A, Tzieply N, von Knethen A, Johann AM, Schmidt H, Geisslinger G, et al. Tumor cell apoptosis polarizes macrophages role of sphingosine-1-phosphate. *Mol Biol Cell*. (2007) 18:3810–9. doi: 10.1091/mbc.e06-12-1096
139. Cao C, Gao Y, Li Y, Antalis TM, Castellino FJ, Zhang L. The efficacy of activated protein C in murine endotoxemia is dependent on integrin CD11b. *J Clin Invest*. (2010) 120:1971–80. doi: 10.1172/JCI40380
140. Duenas AI, Aceves M, Fernandez-Pisonero I, Gomez C, Orduna A, Crespo MS, et al. Selective attenuation of Toll-like receptor 2 signalling may explain the atheroprotective effect of sphingosine 1-phosphate. *Cardiovasc Res*. (2008) 79:537–44. doi: 10.1093/cvr/cvn087
141. Zhao S, Adebiyi MG, Zhang Y, Couturier JP, Fan X, Zhang H, et al. Sphingosine-1-phosphate receptor 1 mediates elevated IL-6 signaling to promote chronic inflammation and multitissue damage in sickle cell disease. *FASEB J*. (2018) 32:2855–65. doi: 10.1096/fj.201600788RR
142. Johann AM, Weigert A, Eberhardt W, Kuhn AM, Barra V, von Knethen A, et al. Apoptotic cell-derived sphingosine-1-phosphate promotes HuR-dependent cyclooxygenase-2 mRNA stabilization and protein expression. *J Immunol*. (2008) 180:1239–48. doi: 10.4049/jimmunol.180.2.1239
143. Brecht K, Weigert A, Hu J, Popp R, Fisslthaler B, Korff T, et al. Macrophages programmed by apoptotic cells promote angiogenesis via prostaglandin E2. *FASEB J*. (2011) 25:2408–17. doi: 10.1096/fj.10-179473
144. Barra V, Kuhn A-M, von Knethen A, Weigert A, Bruene B. Apoptotic cell-derived factors induce arginase II expression in murine macrophages by activating ERK5/CREB. *Cell Mol Life Sci*. (2011) 68:1815–27. doi: 10.1007/s00018-010-0537-x
145. Jiang LI, Collins J, Davis R, Lin KM, DeCamp D, Roach T, et al. Use of a cAMP BRET sensor to characterize a novel regulation of cAMP by the sphingosine 1-phosphate/G13 pathway. *J Biol Chem*. (2007) 282:10576–84. doi: 10.1074/jbc.M609695200
146. Bystrom J, Evans I, Newson J, Stables M, Toor I, van Rooijen N, et al. Resolution-phase macrophages possess a unique inflammatory phenotype that is controlled by cAMP. *Blood*. (2008) 112:4117–27. doi: 10.1182/blood-2007-12-129767
147. Ley S, Weigert A, Weichand B, Henke N, Mille-Baker B, Janssen RAJ, et al. The role of TRKA signaling in IL-10 production by apoptotic tumor cell-activated macrophages. *Oncogene*. (2013) 32:631–40. doi: 10.1038/onc.2012.77
148. Balkwill F, Mantovani A. Inflammation and cancer: back to Virchow? *Lancet*. (2001) 357:539–45. doi: 10.1016/S0140-6736(00)04046-0
149. Swann JB, Smyth MJ. Immune surveillance of tumors. *J Clin Invest*. (2007) 117:1137–46. doi: 10.1172/JCI31405
150. Schreiber RD, Old LJ, Smyth MJ, Cancer immunoediting: integrating immunity's roles in cancer suppression and promotion. *Science*. (2011) 331:1565–70. doi: 10.1126/science.1203486
151. Aras S, Zaidi MR. TAMeless traitors: macrophages in cancer progression and metastasis. *Br J Cancer*. (2017) 117:1583–91. doi: 10.1038/bjc.2017.356
152. Zheng X, Turkowski K, Mora J, Brune B, Seeger W, Weigert A, et al. Redirecting tumor-associated macrophages to become tumoricidal effectors as a novel strategy for cancer therapy. *Oncotarget*. (2017) 8:48436–52. doi: 10.18632/oncotarget.17061
153. Fridman WH, Zitvogel L, Sautes-Fridman C, Kroemer G. The immune contexture in cancer prognosis and treatment. *Nat Rev Clin Oncol*. (2017) 14:717–34. doi: 10.1038/nrclinonc.2017.101
154. Pyne NJ, Tonelli F, Lim KG, Long JS, Edwards J, Pyne S. Sphingosine 1-phosphate signalling in cancer. *Biochem Soc Trans*. (2012) 40:94–100. doi: 10.1042/BST20110602
155. Mrad M, Imbert C, Garcia V, Rambow F, Therville N, Carpentier S, et al. Downregulation of sphingosine kinase-1 induces protective tumor immunity by promoting M1 macrophage response in melanoma. *Oncotarget*. (2016) 7:71873–86. doi: 10.18632/oncotarget.12380
156. Furuya H, Tamashiro PM, Shimizu Y, Iino K, Peres R, Chen R, et al. Sphingosine Kinase 1 expression in peritoneal macrophages is required for colon carcinogenesis. *Carcinogenesis*. (2017) 38:1218–27. doi: 10.1093/carcin/bgx104
157. Ader I, Malavaud B, Cuvillier O. When the sphingosine kinase 1/sphingosine 1-phosphate pathway meets hypoxia signaling: new targets for cancer therapy. *Cancer Res*. (2009) 69:3723–6. doi: 10.1158/0008-5472.CAN-09-0389

158. Bouquerel P, Gstalder C, Muller D, Laurent J, Brizuela L, Sabbadini RA, et al. Essential role for SphK1/S1P signaling to regulate hypoxia-inducible factor 2alpha expression and activity in cancer. *Oncogenesis*. (2016) 5:e209. doi: 10.1038/oncsis.2016.13
159. Gstalder C, Ader I, Cuvillier O. FTY720 (Fingolimod) inhibits HIF1 and HIF2 signaling, promotes vascular remodeling, and chemosensitizes in renal cell carcinoma animal model. *Mol Cancer Ther*. (2016) 15:2465–74. doi: 10.1158/1535-7163.MCT-16-0167
160. Herr B, Zhou J, Werno C, Menrad H, Namgaladze D, Weigert A, et al. The supernatant of apoptotic cells causes transcriptional activation of hypoxia-inducible factor-1alpha in macrophages via sphingosine-1-phosphate and transforming growth factor-beta. *Blood*. (2009) 114:2140–8. doi: 10.1182/blood-2009-01-201889
161. Du W, Takuwa N, Yoshioka K, Okamoto Y, Gonda K, Sugihara K, et al. S1P(2), the G protein-coupled receptor for sphingosine-1-phosphate, negatively regulates tumor angiogenesis and tumor growth *in vivo* in mice. *Cancer Res*. (2010) 70:772–81. doi: 10.1158/0008-5472.CAN-09-2722
162. Moore KJ, Sheedy FJ, Fisher EA. Macrophages in atherosclerosis: a dynamic balance. *Nat Rev Immunol*. (2013) 13:709–21. doi: 10.1038/nri3520
163. Okajima F. Plasma lipoproteins behave as carriers of extracellular sphingosine 1-phosphate: is this an atherogenic mediator or an anti-atherogenic mediator? *Biochim Biophys Acta*. (2002) 1582:132–7. doi: 10.1016/S1388-1981(02)00147-6
164. Catapano AL, Pirillo A, Bonacina F, Norata GD. HDL in innate and adaptive immunity. *Cardiovasc Res*. (2014) 103:372–83. doi: 10.1093/cvr/cvu150
165. Christoffersen C, Obinata H, Kumaraswamy SB, Galvani S, Ahnstrom J, Sevvana M, et al. Endothelium-protective sphingosine-1-phosphate provided by HDL-associated apolipoprotein M. *Proc Natl Acad Sci USA*. (2011) 108:9613–8. doi: 10.1073/pnas.1103187108
166. Arkensteijn BW, Berbee JF, Rensen PC, Nielsen LB, Christoffersen C. The apolipoprotein m-sphingosine-1-phosphate axis: biological relevance in lipoprotein metabolism, lipid disorders and atherosclerosis. *Int J Mol Sci*. (2013) 14:4419–31. doi: 10.3390/ijms14034419
167. Sattler K, Levkau B. Sphingosine-1-phosphate as a mediator of high-density lipoprotein effects in cardiovascular protection. *Cardiovasc Res*. (2009) 82:201–11. doi: 10.1093/cvr/cvp070
168. Kurano M, Tsukamoto K, Ohkawa R, Hara M, Iino J, Kageyama Y, et al. Liver involvement in sphingosine 1-phosphate dynamism revealed by adenoviral hepatic overexpression of apolipoprotein M. *Atherosclerosis*. (2013) 229:102–9. doi: 10.1016/j.atherosclerosis.2013.04.024
169. Kimura T, Tomura H, Mogi C, Kuwabara A, Damirin A, Ishizuka T, et al. Role of scavenger receptor class B type I and sphingosine 1-phosphate receptors in high density lipoprotein-induced inhibition of adhesion molecule expression in endothelial cells. *J Biol Chem*. (2006) 281:37457–67. doi: 10.1074/jbc.M605823200
170. Levkau B. HDL-S1P: cardiovascular functions, disease-associated alterations, and therapeutic applications. *Front Pharmacol*. (2015) 6:243. doi: 10.3389/fphar.2015.00243
171. Kurano M, Yatomi Y. Sphingosine 1-phosphate and atherosclerosis. *J Atheroscler Thromb*. (2018) 25:16–26. doi: 10.5551/jat.RV17010
172. Keul P, Lucke S, von Wnuck Lipinski K, Bode C, Graler M, Heusch G, et al. Sphingosine-1-phosphate receptor 3 promotes recruitment of monocyte/macrophages in inflammation and atherosclerosis. *Circ Res*. (2011) 108:314–23. doi: 10.1161/CIRCRESAHA.110.235028
173. Nofer JR, Bot M, Brodde M, Taylor PJ, Salm P, Brinkmann V, et al. FTY720, a synthetic sphingosine 1 phosphate analogue, inhibits development of atherosclerosis in low-density lipoprotein receptor-deficient mice. *Circulation*. (2007) 115:501–8. doi: 10.1161/CIRCULATIONAHA.106.641407
174. Poti F, Gualtieri F, Sacchi S, Weissen-Plenz G, Varga G, Brodde M, et al. KRP-203, sphingosine 1-phosphate receptor type 1 agonist, ameliorates atherosclerosis in LDL-R-/- mice. *Arterioscler Thromb Vasc Biol*. (2013) 33:1505–12. doi: 10.1161/ATVBAHA.113.301347
175. Park SJ, Lee KP, Kang S, Lee J, Sato K, Chung HY, et al. Sphingosine 1-phosphate induced anti-atherogenic and atheroprotective M2 macrophage polarization through IL-4. *Cell Signal*. (2014) 26:2249–58. doi: 10.1016/j.cellsig.2014.07.009
176. Vaidya M, Jentsch JA, Peters S, Keul P, Weske S, Graler MH, et al. Regulation of ABCA1-mediated cholesterol efflux by sphingosine-1-phosphate signaling in macrophages. *J Lipid Res*. (2019) 60:506–515. doi: 10.1194/jlr.M088443
177. Brulhart-Meynet MC, Braunersreuther V, Brinck J, Montecucco F, Prost JC, Thomas A, et al. Improving reconstituted HDL composition for efficient post-ischemic reduction of ischemia reperfusion injury. *PLoS ONE*. (2015) 10:e0119664. doi: 10.1371/journal.pone.0119664
178. Sattler K, Graler M, Keul P, Weske S, Reimann CM, Jindrova H, et al. Defects of high-density lipoproteins in coronary artery disease caused by low sphingosine-1-phosphate content: correction by sphingosine-1-phosphate-loading. *J Am Coll Cardiol*. (2015) 66:1470–85. doi: 10.1016/j.jacc.2015.07.057
179. Keul P, Polzin A, Kaiser K, Graler M, Dannenberg L, Daum G, et al. Potent anti-inflammatory properties of HDL in vascular smooth muscle cells mediated by HDL-S1P and their impairment in coronary artery disease due to lower HDL-S1P: a new aspect of HDL dysfunction and its therapy. *FASEB J*. (2019) 33:1482–95. doi: 10.1096/fj.201801245R
180. Kurano M, Hara M, Nojiri T, Ikeda H, Tsukamoto K, Yatomi Y. Resveratrol exerts a biphasic effect on apolipoprotein M. *Br J Pharmacol*. (2016) 173:222–33. doi: 10.1111/bph.13360
181. Wynn TA, Vannella KM. Macrophages in tissue repair, regeneration, and fibrosis. *Immunity*. (2016) 44:450–62. doi: 10.1016/j.immuni.2016.02.015
182. Wick G, Grundtman C, Mayerl C, Wimpissinger TF, Feichtinger J, Zelger B, et al. The immunology of fibrosis. *Annu Rev Immunol*. (2013) 31:107–35. doi: 10.1146/annurev-immunol-032712-095937
183. Murray LA. Editorial: the cell types of fibrosis. *Front Pharmacol*. (2015) 6:311. doi: 10.3389/fphar.2015.00311
184. Lech M, Anders HJ. Macrophages and fibrosis: How resident and infiltrating mononuclear phagocytes orchestrate all phases of tissue injury and repair. *Biochim Biophys Acta*. (2013) 1832:989–97. doi: 10.1016/j.bbadis.2012.12.001
185. Zhang L, Wang Y, Wu G, Xiong W, Gu W, Wang CY. Macrophages: friend or foe in idiopathic pulmonary fibrosis? *Respir Res*. (2018) 19:170. doi: 10.1186/s12931-018-0864-2
186. Yao Y, Wang Y, Zhang Z, He L, Zhu J, Zhang M, et al. Chop deficiency protects mice against bleomycin-induced pulmonary fibrosis by attenuating M2 macrophage production. *Mol Ther*. (2016) 24:915–25. doi: 10.1038/mt.2016.36
187. Huang LS, Natarajan V. Sphingolipids in pulmonary fibrosis. *Adv Biol Regul*. (2015) 57:55–63. doi: 10.1016/j.jbior.2014.09.008
188. Milara J, Navarro R, Juan G, Peiro T, Serrano A, Ramon M, et al. Sphingosine-1-phosphate is increased in patients with idiopathic pulmonary fibrosis and mediates epithelial to mesenchymal transition. *Thorax*. (2012) 67:147–56. doi: 10.1136/thoraxjnl-2011-200026
189. Kono Y, Nishiuma T, Nishimura Y, Kotani Y, Okada T, Nakamura S, et al. Sphingosine kinase 1 regulates differentiation of human and mouse lung fibroblasts mediated by TGF-beta1. *Am J Respir Cell Mol Biol*. (2007) 37:395–404. doi: 10.1165/rcmb.2007-0065OC
190. Zhao J, Okamoto Y, Asano Y, Ishimaru K, Aki S, Yoshioka K, et al. Sphingosine-1-phosphate receptor-2 facilitates pulmonary fibrosis through potentiating IL-13 pathway in macrophages. *PLoS ONE*. (2018) 13:e0197604. doi: 10.1371/journal.pone.0197604
191. Li C, Jiang X, Yang L, Liu X, Yue S, Li L. Involvement of sphingosine 1-phosphate (SIP)/S1P3 signaling in cholestasis-induced liver fibrosis. *Am J Pathol*. (2009) 175:1464–72. doi: 10.2353/ajpath.2009.090037
192. Yang L, Yue S, Yang L, Liu X, Han Z, Zhang Y, et al. Sphingosine kinase/sphingosine 1-phosphate (S1P)/S1P receptor axis is involved in liver fibrosis-associated angiogenesis. *J Hepatol*. (2013) 59:114–23. doi: 10.1016/j.jhep.2013.02.021
193. Lan T, Li C, Yang G, Sun Y, Zhuang L, Ou Y, et al. Sphingosine kinase 1 promotes liver fibrosis by preventing miR-19b-3p-mediated inhibition of CCR2. *Hepatology*. (2018) 68:1070–86. doi: 10.1002/hep.29885
194. Ni HF, Chen JF, Zhang MH, Pan MM, Zhang JD, Liu H, et al. FTY720 attenuates tubulointerstitial inflammation and fibrosis in subtotally nephrectomized rats. *Ren Fail*. (2013) 35:996–1004. doi: 10.3109/0886022X.2013.809006
195. Weinberger T, Schulz C. Myocardial infarction: a critical role of macrophages in cardiac remodeling. *Front Physiol*. (2015) 6:107. doi: 10.3389/fphys.2015.00107

196. Mouton AJ, DeLeon-Pennell KY, Rivera Gonzalez OJ, Flynn ER, Freeman TC, Saucerman JJ, et al. Mapping macrophage polarization over the myocardial infarction time continuum. *Basic Res Cardiol*. (2018) 113:26. doi: 10.1007/s00395-018-0686-x
197. Kanazawa M, Ninomiya I, Hatakeyama M, Takahashi T, Shimohata T. Microglia and monocytes/macrophages polarization reveal novel therapeutic mechanism against stroke. *Int J Mol Sci*. (2017) 18:E2135. doi: 10.3390/ijms18102135
198. Nielsen MM, Lambertsen KL, Clausen BH, Meyer M, Bhandari DR, Larsen ST, et al. Mass spectrometry imaging of biomarker lipids for phagocytosis and signalling during focal cerebral ischaemia. *Sci Rep*. (2016) 6:39571. doi: 10.1038/srep39571
199. Czech B, Pfeilschifter W, Mazaheri-Omrani N, Strobel MA, Kahles T, Neumann-Haefelin T, et al. The immunomodulatory sphingosine 1-phosphate analog FTY720 reduces lesion size and improves neurological outcome in a mouse model of cerebral ischemia. *Biochem Biophys Res Commun*. (2009) 389:251–6. doi: 10.1016/j.bbrc.2009.08.142
200. Wei Y, Yemisci M, Kim HH, Yung LM, Shin HK, Hwang SK, et al. Fingolimod provides long-term protection in rodent models of cerebral ischemia. *Ann Neurol*. (2011) 69:119–29. doi: 10.1002/ana.22186
201. Xie B, Shen J, Dong A, Rashid A, Stoller G, Campochiaro PA. Blockade of sphingosine-1-phosphate reduces macrophage influx and retinal and choroidal neovascularization. *J Cell Physiol*. (2009) 218:192–8. doi: 10.1002/jcp.21588
202. Ito T, Kuriyama N, Kato H, Matsuda A, Mizuno S, Usui M, et al. Sinusoidal protection by sphingosine-1-phosphate receptor 1 agonist in liver ischemia-reperfusion injury. *J Surg Res*. (2018) 222:139–52. doi: 10.1016/j.jss.2017.09.048
203. Lien YH, Yong KC, Cho C, Igarashi S, Lai LW. S1P(1)-selective agonist, SEW2871, ameliorates ischemic acute renal failure. *Kidney Int*. (2006) 69:1601–8. doi: 10.1038/sj.ki.5000360
204. Bajwa A, Jo SK, Ye H, Huang L, Dondeti KR, Rosin DL, et al. Activation of sphingosine-1-phosphate 1 receptor in the proximal tubule protects against ischemia-reperfusion injury. *J Am Soc Nephrol*. (2010) 21:955–65. doi: 10.1681/ASN.2009060662
205. Bajwa A, Rosin DL, Chroscicki P, Lee S, Dondeti K, Ye H, et al. Sphingosine 1-phosphate receptor-1 enhances mitochondrial function and reduces cisplatin-induced tubule injury. *J Am Soc Nephrol*. (2015) 26:908–25. doi: 10.1681/ASN.2013121351
206. Sola A, Weigert A, Jung M, Vinuesa E, Brecht K, Weis N, et al. Sphingosine-1-phosphate signalling induces the production of Lcn-2 by macrophages to promote kidney regeneration. *J Pathol*. (2011) 225:597–608. doi: 10.1002/path.2982
207. Otaka N, Shibata R, Ohashi K, Uemura Y, Kambara T, Enomoto T, et al. Myonectin is an exercise-induced myokine that protects the heart from ischemia-reperfusion injury. *Circ Res*. (2018) 123:1326–38. doi: 10.1161/CIRCRESAHA.118.313777
208. Schneider-Schaulies J, Schneider-Schaulies S. Sphingolipids in viral infection. *Biol Chem*. (2015) 396:585–95. doi: 10.1515/hsz-2014-0273
209. Baker JE, Boudreau RM, Seitz AP, Caldwell CC, Gulbins E, Edwards MJ. Sphingolipids and innate immunity: a new approach to infection in the post-antibiotic era? *Surg Infect*. (2018) 19:792–803. doi: 10.1089/sur.2018.187
210. Sharma L, Prakash H. Sphingolipids are dual specific drug targets for the management of pulmonary infections: perspective. *Front Immunol*. (2017) 8:378. doi: 10.3389/fimmu.2017.00378
211. Vettorazzi S, Bode C, Dejager L, Frappart L, Shelest E, Klassen C, et al. Glucocorticoids limit acute lung inflammation in concert with inflammatory stimuli by induction of SphK1. *Nat Commun*. (2015) 6:7796. doi: 10.1038/ncomms8796
212. Gutbier B, Schonrock SM, Ehrler C, Haberberger R, Dietert K, Gruber AD, et al. Sphingosine kinase 1 regulates inflammation and contributes to acute lung injury in pneumococcal pneumonia via the sphingosine-1-phosphate receptor 2. *Crit Care Med*. (2018) 46:e258–67. doi: 10.1097/CCM.0000000000002916
213. Zemann B, Urtz N, Reuschel R, Mechtcheriakova D, Bornancin F, Badegruber R, et al. Normal neutrophil functions in sphingosinekinase type 1 and 2 knockout mice. *Immunol Lett*. (2007) 109:56–63. doi: 10.1016/j.imlet.2007.01.001
214. Murphy CT, Hall LJ, Hurley G, Quinlan A, MacSharry J, Shanahan F, et al. The sphingosine-1-phosphate analogue FTY720 impairs mucosal immunity and clearance of the enteric pathogen *Citrobacter rodentium*. *Infect Immun*. (2012) 80:2712–23. doi: 10.1128/IAI.06319-11
215. Das A, Segar CE, Hughley BB, Bowers DT, Botchwey EA. The promotion of mandibular defect healing by the targeting of S1P receptors and the recruitment of alternatively activated macrophages. *Biomaterials*. (2013) 34:9853–62. doi: 10.1016/j.biomaterials.2013.08.015
216. Grimm M, Tischner D, Troidl K, Albarran Juarez J, Sivaraj KK, Ferreiros Bouzas N, et al. S1P2/G12/13 signaling negatively regulates macrophage activation and indirectly shapes the atheroprotective B1-cell population. *Arterioscler Thromb Vasc Biol*. (2016) 36:37–48. doi: 10.1161/ATVBAHA.115.306066
217. Olesch C, Ringel C, Brune B, Weigert A. Beyond immune cell migration: the emerging role of the sphingosine-1-phosphate receptor S1PR4 as a modulator of innate immune cell activation. *Mediators Inflamm*. (2017) 2017:6059203. doi: 10.1155/2017/6059203
218. Schulze T, Golfier S, Tabeling C, Rabel K, Graler MH, Witzenrath M, et al. Sphingosine-1-phospate receptor 4 (S1P) deficiency profoundly affects dendritic cell function and TH17-cell differentiation in a murine model. *FASEB J*. (2011) 25:4024–36. doi: 10.1096/fj.10-179028
219. Dillmann C, Ringel C, Ringleb J, Mora J, Olesch C, Fink AF, et al. S1PR4 signaling attenuates ILT 7 internalization to limit IFN-alpha production by human plasmacytoid dendritic cells. *J Immunol*. (2016) 196:1579–90. doi: 10.4049/jimmunol.1403168
220. Debien E, Mayol K, Biajoux V, Daussy C, De Aguero MG, Taillardet M, et al. S1PR5 is pivotal for the homeostasis of patrolling monocytes. *Eur J Immunol*. (2013) 43:1667–75. doi: 10.1002/eji.201343312
221. Hait NC, Allegood J, Maceyka M, Strub GM, Harikumar KB, Singh SK, et al. Regulation of histone acetylation in the nucleus by sphingosine-1-phosphate. *Science*. (2009) 325:1254–7. doi: 10.1126/science.1176709
222. Arts RJ, Joosten LA, Netea MG. Immunometabolic circuits in trained immunity. *Semin Immunol*. (2016) 28:425–30. doi: 10.1016/j.smim.2016.09.002
223. Park SJ, Im DS. Sphingosine 1-phosphate receptor modulators and drug discovery. *Biomol Ther*. (2017) 25:80–90. doi: 10.4062/biomolther.2016.160
224. Binnewies M, Roberts EW, Kersten K, Chan V, Fearon DF, Merad M, et al. Understanding the tumor immune microenvironment (TIME) for effective therapy. *Nat Med*. (2018) 24:541–50. doi: 10.1038/s41591-018-0014-x
225. Pal SK, Drabkin HA, Reeves JA, Hainsworth JD, Hazel SE, Paggiarino DA, et al. A phase 2 study of the sphingosine-1-phosphate antibody sonepcizumab in patients with metastatic renal cell carcinoma. *Cancer*. (2017) 123:576–82. doi: 10.1002/cncr.30393
226. Dickson MA, Carvajal RD, Merrill AH Jr, Gonen M, Cane LM, Schwartz GK. A phase I clinical trial of safingol in combination with cisplatin in advanced solid tumors. *Clin Cancer Res*. (2011) 17:2484–92. doi: 10.1158/1078-0432.CCR-10-2323
227. Britten CD, Garrett-Mayer E, Chin SH, Shirai K, Ogretmen B, Bentz TA, et al. A Phase I study of ABC294640, a first-in-class sphingosine kinase-2 inhibitor, in patients with advanced solid tumors. *Clin Cancer Res*. (2017) 23:4642–50. doi: 10.1158/1078-0432.CCR-16-2363

Conflict of Interest Statement: The authors declare that the research was conducted in the absence of any commercial or financial relationships that could be construed as a potential conflict of interest.

frontiers in Cell and Developmental Biology

REVIEW
published: 13 August 2019
doi: 10.3389/fcell.2019.00152

Sphingomyelin Breakdown in T Cells: Role of Membrane Compartmentalization in T Cell Signaling and Interference by a Pathogen

*Elita Avota, Maria Nathalia de Lira and Sibylle Schneider-Schaulies**

Institute for Virology and Immunobiology, Julius Maximilian University of Würzburg, Würzburg, Germany

Sphingolipids are major components of cellular membranes, and at steady-state level, their metabolic fluxes are tightly controlled. On challenge by external signals, they undergo rapid turnover, which substantially affects the biophysical properties of membrane lipid and protein compartments and, consequently, signaling and morphodynamics. In T cells, external cues translate into formation of membrane microdomains where proximal signaling platforms essential for metabolic reprograming and cytoskeletal reorganization are organized. This review will focus on sphingomyelinases, which mediate sphingomyelin breakdown and ensuing ceramide release that have been implicated in T-cell viability and function. Acting at the sphingomyelin pool at the extrafacial or cytosolic leaflet of cellular membranes, acid and neutral sphingomyelinases organize ceramide-enriched membrane microdomains that regulate T-cell homeostatic activity and, upon stimulation, compartmentalize receptors, membrane proximal signaling complexes, and cytoskeletal dynamics as essential for initiating T-cell motility and interaction with endothelia and antigen-presenting cells. Prominent examples to be discussed in this review include death receptor family members, integrins, CD3, and CD28 and their associated signalosomes. Progress made with regard to experimental tools has greatly aided our understanding of the role of bioactive sphingolipids in T-cell biology at a molecular level and of targets explored by a model pathogen (measles virus) to specifically interfere with their physiological activity.

Keywords: T cell, sphingomyelinase, activation, motility, measles virus

OPEN ACCESS

Edited by:
Alessandro Prinetti, University of Milan, Italy

Reviewed by:
Toshiro Okazaki, Kanazawa Medical University, Japan
Erhard Bieberich, University of Kentucky, United States

****Correspondence:***
Sibylle Schneider-Schaulies
s-s-s@vim.uni-wuerzburg.de

Specialty section:
This article was submitted to Membrane Physiology and Membrane Biophysics, a section of the journal Frontiers in Cell and Developmental Biology

Received: *11 June 2019*
Accepted: *22 July 2019*
Published: *13 August 2019*

Citation:
Avota E, de Lira MN and Schneider-Schaulies S (2019) Sphingomyelin Breakdown in T Cells: Role of Membrane Compartmentalization in T Cell Signaling and Interference by a Pathogen. Front. Cell Dev. Biol. 7:152. doi: 10.3389/fcell.2019.00152

INTRODUCTION

Sphingolipids are abundant components of cellular membranes, and therefore, they effectively take part in cellular processes requiring membrane integrity and dynamics under rheostat and stimulated conditions (Airola and Hannun, 2013; Harayama and Riezman, 2018). Biosynthesis and metabolism of this particular class of membrane lipids are highly complex and subject to regulation by a variety of enzymes, and, except for initiation of synthesis and final hydrolysis of sphingosine-1-phosphate (S1P) into hexadecenal and phosphoethanolamine, reactions in this pathway are reversible. Thereby, many species of sphingolipids are generated that, in addition,

vary in chain length, saturation, hydroxylation, and more or less complex head groups, altogether defining sphingolipid diversity (Hannun and Obeid, 2008; Gault et al., 2010; Feng et al., 2018) (**Figure 1**). Further expanding the complexity of the system, enzymes involved in sphingolipid metabolism may come in several isoforms differing in subcellular topology and cell type-specific expression levels (Clarke et al., 2006; Gault et al., 2010; Airola and Hannun, 2013). Therefore, biological outcomes of sphingolipid dynamics expectedly substantially differ.

Because of the high abundance of sphingolipid species, their composition within the plasma and organelle membranes and the dynamic alterations substantially impact on membrane biophysics. In context with other membrane lipids such as cholesterol, sphingolipids (also dependent on their acyl chain lengths) regulate membrane fluidity, which is important for membrane deformability during inward/outward vesiculation and also endo/exocytosis (Hannun and Obeid, 2008; Feng et al., 2018). In addition, membrane proteins and associated membrane proximal signaling components compartmentalize within membrane domains formed at steady-state conditions or in response to stimulation or metabolic signals. Classically, these were termed "lipid rafts" and/or—experimentally defined—detergent-resistant membrane (DRM) domains with sphingomyelin, glycosphingolipids, and cholesterol as major components (Simons and Gerl, 2010; Nakayama et al., 2018). Their composition can be dynamically altered upon signals, for instance, provided by sensing of intracellular stress or receptor ligation. Although as for most microdomains their exact lipid composition is still not clear (Harayama and Riezman, 2018), formation of ceramide-enriched membrane domains in the anticytosolic (extrafacial) membrane leaflet has been intensively studied. These are generated as a result of sphingomyelin breakdown by acid sphingomyelinase (ASM), which results in local release of ceramide (thereby eventually displacing cholesterol) that subsequently condense into ceramide-enriched domains that serve as platforms for signal relay and initiation, which often directly involves regulation of membrane proximal cytoskeletal dynamics (Gulbins et al., 2004; Bollinger et al., 2005; Gombos et al., 2006; Adada et al., 2013; Schneider-Schaulies and Schneider-Schaulies, 2013; Avota and Schneider-Schaulies, 2014). Ceramide-enriched membrane microdomains can be visualized using specific antibodies and, more recently, by redistribution of functionalized ceramide analogs also in T cells (Collenburg et al., 2016; Walter et al., 2016). On these, sizes and distribution of ceramide clusters under steady-state conditions and after application of exogenous bacterial sphingomyelinase were determined by *d*STORM technology (Burgert et al., 2017). Bioactive sphingolipids, i.e., mainly ceramide, ceramide-1-phosphate (C1P), sphingosine, and S1P act as signaling molecules themselves, and therefore, dynamic alterations of this pool directly regulate many cellular responses ranging from development and expansion to autophagy and apoptosis (Hannun and Obeid, 2008).

In common to that of other cell types, metabolism of membrane lipids also plays a key role in T cells as excellently reviewed (Wu et al., 2015, 2016; Howie et al., 2017). This review will focus on the role of sphingomyelin breakdown and subsequent ceramide release in various aspects of T-cell biology. Given the impact of this pathway on membrane and cytoskeletal dynamics and signaling in these highly motile cells, the activity of which relies on efficient propagation of external cues, this is particularly important. Rather than discussing the role of the bioactive sphingolipids themselves, this review aims at integrating the two most prominent, best-studied enzymes catalyzing sphingomyelin breakdown at the anticytosolic or cytosolic leaflet of the T-cell plasma membrane, the ASM and neutral (NSM2) sphingomyelinase.[1]

ACID AND NEUTRAL SPHINGOMYELINASES

Isoforms of the ASM (encoded by the gene *SMPD1*) are secreted (sASM) or endolysosomal ASM, where its association to the anticytosolic membrane leaflet is required to protect the enzyme from degradation (Goni and Alonso, 2002). ASM activation is triggered by a variety of stimuli including cytokines, engagement of death receptors, or, as particularly relevant for this review, CD28. Receptor signaling-induced ASM activation can occur intracellularly after receptor signalosome fusion with endolysosomes (TNFR) or extracellularly after the enzyme is translocated from the internal storage compartment to the extrafacial leaflet of the plasma membrane (CD95) (Gulbins and Kolesnick, 2003; Henry et al., 2013) (**Figure 2**). There, ceramide release as a consequence of sphingomyelin hydrolysis promotes formation of ceramide-enriched membrane microdomains promoting formation and stabilization of receptor and signalosome complexes (Gulbins et al., 2004; Bollinger et al., 2005). At a biochemical level, ASM activation involves phosphorylation and proteolytic processing (**Figure 2**) (Henry et al., 2013). In addition to its role in cell activation, differentiation, and apoptosis, ASM has great importance for sphingolipid homeostasis as reflected by the development of severe, often fatal sphingolipidoses upon genetic ASM deficiency in mice and humans, where it is called Niemann–Pick disease (Horinouchi et al., 1995; Smith and Schuchman, 2008; Schuchman and Desnick, 2017). Though healthy at birth, ASM-deficient mice come down due to a progressive lysosomal sphingolipid storage as indicated by an increasing amount of foam cells in the bone marrow with age, extending to all visceral organs (Kuemmel et al., 1997). Activity of the ASM in the T-cell compartment has been clearly revealed where, and not surprisingly, ASM deficiency correlated with elevated levels of sphingomyelin (Boucher et al., 1995; Horinouchi et al., 1995; Herz et al., 2009; Tischner et al., 2011; Beyersdorf and Muller, 2015; Hollmann et al., 2016). ASM has been found to be particularly important in $CD4^+$ regulatory T-cell (T_{reg}) frequency and function in mice, indicating that the enzyme impacts on the composition of the T-cell compartment under homeostatic conditions (Hollmann et al., 2016; Zhou et al., 2016).

[1] ASM and NSM2 in humans, Asm and Nsm2 in mice. As some studies cited investigated both human and mouse cells, we will use the nomenclature 'ASM' and 'NSM2' to facilitate reading.

An outer membrane-resident ASM-like enzyme, SMPDL3B, was identified in macrophages, where it reduced Toll-like receptor (TLR) responsiveness (Heinz et al., 2015). Though it may also be expressed in T cells, its function there is as yet unknown. Assuming it acts as a bona fide sphingomyelinase, it appears to do so at neutral rather than acidic pH (Heinz et al., 2015; Gorelik et al., 2016a,b) and could thereby be considered as neutral rather than ASM.

The best-studied member of neutral sphingomyelinases, NSM2 (*SMPD3*-encoded), is ubiquitously expressed and most abundant in the brain (from where it was initially purified) but also in lymphatic tissues (Liu et al., 1998). It is associated with cytosolic membrane leaflets of many compartments, including the plasma, Golgi, and endolysosomal and nuclear membranes (Stoffel et al., 2005; Albi et al., 2008; Cascianelli et al., 2008; Clarke et al., 2008; Trajkovic et al., 2008; Milhas et al., 2010b; Lucki and Sewer, 2012 Airola and Hannun, 2013; Stoffel et al., 2016) (**Figure 2**). Despite that its substrate is much less abundant at the cytosolic membrane leaflets, NSM2 is important in sphingolipid homeostasis, because in the absence of its activity, ceramide levels are up to 50% reduced (Marchesini et al., 2003; Stoffel et al., 2016). NSM2 is activated in response to stress signals and ligation of receptors such as TNFR1, CD95, CD40, and, as particularly relevant here, CD3 (Tonnetti et al., 1999; Clarke et al., 2006; Wu et al., 2010; Airola and Hannun, 2013; Shamseddine et al., 2015; Bortlein et al., 2018) (**Figure 2**). Shuttling between compartments and recruitment into receptor signalosomes are important in NSM2 activation (Clarke et al., 2008; Philipp et al., 2010). Its amino-terminal (NTD) hydrophobic domain marked by two conserved hydrophobic segments (HS1 and HS2) associates with, but does not span, the membrane; is separated from the cytosolic C-terminal catalytic domain (CAT) by a juxtamembrane domain, which interacts with the CAT domain upon phosphatidylserine (PS) binding to the NTD domain; and promotes a conformational switch needed for NSM2 activation (**Figure 2**) (Airola and Hannun, 2013; Airola et al., 2017). The extended CAT domain bears phosphorylation sites and a calcineurin interaction site that possibly regulate NSM2 activity and stability *in vivo* (Filosto et al., 2010, 2012; Shamseddine et al., 2015; Airola et al., 2017) (**Figure 2**).

Mice deficient for NSM2 activity due to the fragilis ossium (fro) mutation within *Smpd3* (*Smpd3*$^{fro/fro}$) or genetic knockout (*Smpd3*-KO) reveal high embryonic lethality and, postnatally, severely impaired bone and tooth mineralization, skeletal deformation, and dwarfism, highlighting the importance of this enzyme as critical regulator of tissue development and homeostasis (Guenet et al., 1981; Aubin et al., 2005; Stoffel et al., 2005; Alebrahim et al., 2014). Limited availability of NSM2-deficient animals has as yet precluded studies on the impact of NSM2 deficiency on the lympho/monocytic compartment under homeostatic or infection conditions. Notably, mitochondrial ATP release has been shown to be regulated upon NSM2-driven ceramide generation, indicating that this enzyme takes part in metabolic homeostasis in astrocytes (Kong et al., 2018). If also applying to T cells, NSM2 activity could significantly impact on the kinetics and sustainment of T-cell activation and effector functions.

ACTIVATION OF ASM AND NSM2 IN T CELLS

Though their impact on T-cell viability, expansion, and function has been extensively studied (see below), the molecular basis of ASM/NSM activation in these cells remains anecdotal. Non-overlapping motifs were identified in the cytosolic domains of TNFR and CD95, which independently regulate activation of ASM and NSM2. For the latter, this involves plasma membrane recruitment of nuclear EED/WAIT that bridges interacting NSM2 to the receptor-associated FAN (factor associated with NSM)/RACK1 complex also in Jurkat T cells (Philipp et al., 2010). Ligation of CD3 and CD28 is known to activate NSM2 and ASM, respectively (Boucher et al., 1995; Tonnetti et al., 1999; Mueller et al., 2014; Bortlein et al., 2018), but the underlying mechanisms are as yet unknown. In addition to its extensively studied role in NFAT activation in costimulated T cells, early recruitment of calcineurin to the T-cell receptor (TCR) complex was recently reported, where it took part in Lck activation, and it is tempting to speculate that NSM2, harboring a calcineurin interaction site, would be corecruited with calcineurin upon CD3 ligation (Filosto et al., 2010; Dutta et al., 2017). Cross-regulation of sphingomyelinases has also been observed. Thus, ASM elevation at both protein and activity levels was found enhanced in NSM2-deficient fibroblasts, but not T cells (Qin and Dawson, 2012; Mueller et al., 2014). Most interestingly, NSM2 activation was retained in costimulated T cells, while that of ASM was not (Mueller et al., 2014; Bortlein et al., 2018). Cross-regulation of sphingomyelinases was also evidenced in T cells after surface interaction of measles virus (MV) with an unknown receptor on the T cells, which promoted ASM activation downstream of NSM2 (Gassert et al., 2009; Avota et al., 2010).

IMPACT OF ASM/NSM ON T-CELL ACTIVITY AND FUNCTION

Dynamic reorganization of both membrane domains with regard to receptor and signalosome segregation and the cytoskeleton is subject to regulation by sphingomyelinase activity. The very same processes are of obvious importance in essential aspects of T-cell activation and function such as (1) motility and homing, (2) activation on antigen recognition in the context of organized immunological synapses (IS) and expansion, and (3) effector functions. The following sections will therefore review the progress made in the understanding of ASM/NSM2 contribution to these processes.

IMPACT OF ASM/NSM2 ACTIVITY ON T-CELL MOTILITY AND TISSUE HOMING

T-cell migration and interaction with the endothelium during tissue homing are governed by cell and receptor polarization and signal relay provided by chemotactic gradients and adhesion molecules (Ley et al., 2007; Sadik and Luster, 2012). Filopodia formed at the leading edge of migrating T cells sense directional

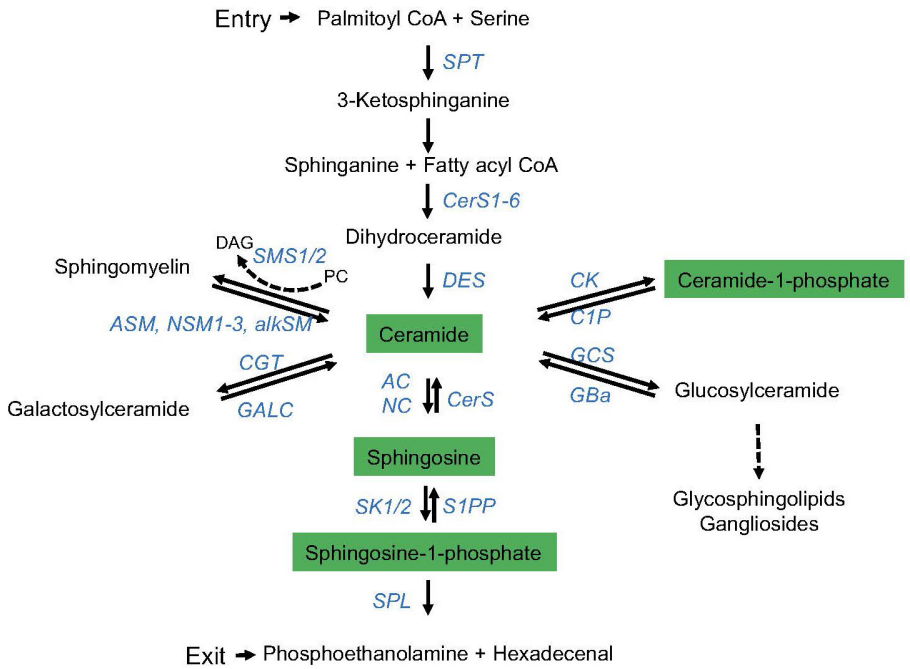

FIGURE 1 | The sphingolipid metabolic pathway. *De novo* synthesis of endoplasmatic reticulum (ER) ceramide is initiated (entry) by serine palmitoyl transferase (SPT)-driven condensation of serine and palmitoyl-CoA, and further downstream activity of ceramide synthases (CerS1-6; giving rise to ceramides of different chain lengths) and desaturase (DES). Ceramide is reversibly converted into (1) sphingomyelin by sphingomyelin synthase 1 or 2 (SMS1/2) [reversed by acid (ASM), neutral (NSM, isoforms 1–3), or alkaline sphingomyelinases (alkSM)], (2) galactosylceramide [by galactosyltransferase (CGT) (reversed by galactosylceramidase (GALC))], (3) C1P by ceramide kinase (CK) [reversed by ceramide-1-phosphatase (CP)], (4) glucosylceramide by glucosylceramide synthase (GCS) [reversed by glucocerebrosidase (GBa)], or (5) sphingosine by acid or neutral ceramidase (AC, NC) (reversed by ceramide synthase, CerS). By phosphorylation, sphingosine kinases (SK1/2) generate S1P from sphingosine (reversed by S1P phosphatase, S1PP). S1P is irreversibly degraded into hexadecenal and ethanolamine by the activity of the S1P lyase (SPL) (exit of the sphingolipid metabolic pathway). Enzymes involved are marked in blue, and bioactive sphingolipids are highlighted in green.

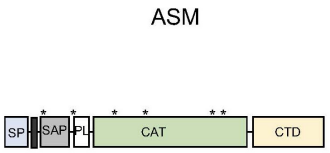

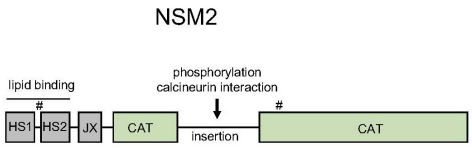

	ASM	NSM2
localisation	anti-cytosolic leaflet: endolysosomal and, on activation, plasma membrane	cytosolic leaflet: plasma membrane, Golgi membrane, endosomal and nuclear membrane, shuttling
activation	Zn^{2+}, proteolytic processing, phosphorylation? conformational switch	Mg^{2+}, anionic lipids, phosphorylation?, conformational switch peroxide
receptor effector in T cells	CD28, TNFR1, CD95	TNFR1, CD95, IL-1β, CD3, recX (MV)§

FIGURE 2 | Acid and neutral sphingomyelinase 2: domains, subcellular distribution, and activation *in vitro* and in T cells. Schematic representation of functional domains within the ASM [signal peptide (SP), transmembrane domain (black bar), saposin domain (SAP), proline rich domain (PL), CAT and C-terminal domain (CTD) with glycosylation sites indicated by asterisks] and the NSM2 [hydrophobic segments 1 and 2 (HS1, HS2), juxtamembrane region (JX), and CAT, interspersed by an insertion that bears phosphorylation and protein interaction sites (including a calcineurin binding site); palmitoylation sites are indicated by hashtags] (Goni and Alonso, 2002; Airola and Hannun, 2013; Airola et al., 2017). The table summarized basic features of localization and activation of the enzymes and indicates receptors known to promote ASM or NSM2 activation in T cells. §: The identity of recX activating NSM2 in T cells by MV contact is as yet unknown (Gassert et al., 2009; Avota and Schneider-Schaulies, 2014; Mueller et al., 2014).

information, which is translated into dynamic assembly of actin filaments pushing the leading edge forward until membrane-tension-generated forces lead to their retraction (Bornschlogl, 2013; Leijnse et al., 2015; Leithner et al., 2016). When coupled to adhesion to the extracellular matrix, the retrograde actin flow generates cell movement, which is supported by stress fiber contraction and actin disassembly in the retracting uropod (Nordenfelt et al., 2016). On endothelial cells, T-cell rolling and polarization are followed by activation of β2-integrins, most prominently lymphocyte function-associated antigen 1 (LFA-1), that switch between high- and low-affinity states (Shulman et al., 2009; Nourshargh and Alon, 2014; Katsuno et al., 2015). T-cell

transmigration through the endothelium relies on the interaction of activated LFA-1 with endothelial cell intercellular adhesion molecule 1 (ICAM-1), and integrin clusters arranged as focal adhesions, which are linked *via* talin, kindlin, and vinculin to the cytoskeleton (Moser et al., 2009; Hogg et al., 2011; Nourshargh and Alon, 2014).

Supporting important roles of sphingomyelinases activity in this process, ASM deficiency conferred protection against the development of experimental autoimmune encephalitis (EAE) in mice in which T-cell adhesion, blood–brain barrier disruption, and intracerebral infiltration of inflammatory cells were blocked (Becker et al., 2017). Similarly, NSM2 activity was found to contribute to rapid homing of $CD4^+$ T cells *in vivo*. When exposed to an NSM inhibitor prior to adoptive transfer, these accumulated to lower levels in spleen and lymph nodes than solvent-treated control cells (Collenburg et al., 2017). Impaired navigational capacity of leukocytes in zebrafish larvae in the absence of FAN further supported the potential role of NSM in cellular motility (Boecke et al., 2012).

Morphological polarization requires cytoskeletal dynamics. In the steady state, NSM2 may negatively control actin metabolism in T cells, because the average cell volume and frequencies of hairy-appearing, abundant protrusions are significantly elevated in NSM2-deficient Jurkat cells (Schoenauer et al., 2019). On stimulation, the role of NSM2 in T-cell morphology driven by actin reorganization may differ depending on receptor signaling: while NSM2 ablation in primary T cells enhanced spreading responses in response to CD3/CD28 engagement, morphological polarization of $CD4^+$ T cells on fibronectin-coated surfaces and brain endothelial cells was effectively limited (Mueller et al., 2014; Collenburg et al., 2017) (**Figure 3**). While ASM deficiency did not detectably affect T-cell morphology, its hyperactivation in response to MV caused collapse of actin-based protrusions in ASM-sufficient cells (Gassert et al., 2009; Schoenauer et al., 2019). This could be rescued by ablation of the ASM, but also of the NSM2. In this particular activation system, NSM2 acts upstream of the ASM because both genetic and pharmacologic NSM inhibition prevent ceramide release at the cell surface (Gassert et al., 2009). Whether sphingomyelinase-driven actin cytoskeletal collapse observed in this system is specific for the receptor involved, signal strength, or the cell type is currently unknown as it has not been reported to occur upon ligation of classical activators including TNFR1, CD95, CD3, or CD28.

Morphological polarization associated with that of receptors is of obvious importance for spatial perception of chemoattractants. NSM2-deficient CD4 + T cells largely failed to polarize and to redistribute CXCR4 and thus, not surprisingly, were substantially impaired in directional migration and velocity in response to SDF-1α or in collagen matrices (mimicking extracellular matrix or tissue interaction) (Collenburg et al., 2017, 2018). Though not detectably affecting morphological polarization, pharmacological NSM2 inhibition also ablated directionality of human polymorphonuclear neutrophils (PMNs) in response to formyl methionine leucyl phenylalanine (FMLP), but not their overall motility (Sitrin et al., 2011). There, exogenous ceramide restored chemotactic responses indicating that loss of ceramide production due to loss of NSM2 activity causally related to inhibition of directionality (Sitrin et al., 2011). Exogenously added ceramides most likely incorporate into the outer leaflet, and therefore, compensation of ceramide loss at the inner leaflet would rely on flipping, which, at present, cannot be directly shown in living cells. Because SDF-1α and β1-integrins do not and FMLP is not known to activate NSM2, steady-state rather than stimulated activity of the enzyme is apparently required for morphological polarization of both $CD4^+$ T cells and PMNs. There is, so far, no evidence that sphingomyelinases contribute to chemokine receptor or β1-integrin signaling directly, and therefore, impaired directional motility of NSM2-deficient T cells most likely reflects their inability to spatially perceive exogenous signals.

Failure to perceive exogenous signals may also be of crucial importance for explaining impaired adhesion of NSM2-deficient cells to interferon-γ (IFN-γ)/tumor necrosis factor-α (TNF-α)-activated endothelial cells both under static and shear stress conditions (Collenburg et al., 2017), which, as crawling and *trans*-endothelial migration (TEM), again depends on the relay of chemokine signals promoting polarization followed by integrin affinity maturation. In line with polarizing signals and associated

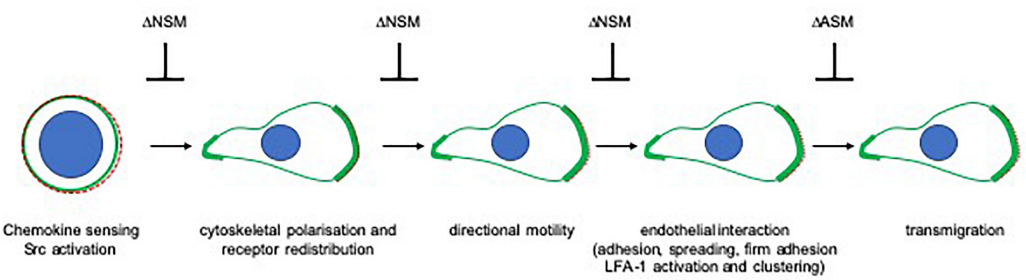

FIGURE 3 | The role of sphingomyelinases in directional sensing and translation of chemotactic and endothelial signals in T cells. Perception of chemotactic signals through specific receptors (depicted as dashed red line) has not been found to be sensitive to ablation of NSM or ASM in T cells. Relay of these signals into morphological front-rear and actin (shown in green) polarization as well as receptor segregation to the leading edge is sensitive to NSM ablation as, consequently, are subsequent steps requiring directional sensing of external cues (directional migration, loose and firm adhesion, and spreading on epithelial cells as well as LFA-1 activation and clustering). In contrast, TEM of T cells relies on ASM rather than NSM activity. Notably, endothelial cell ASM is also required in this process.

actin reorganization being a prerequisite for firm adhesion to endothelial cells, NSM2-deficient $CD4^+$ T cells seeded on brain endothelial cells failed to promote formation of activated LFA-1 clusters, which could not be stabilized by ICAM-1 clustered on endothelial cells. Possibly, sphingomyelinase activity may also directly impact on formation of activated LFA-1 clusters. Not shown to apply to T cells, LFA-1 clusters were found trapped in ceramide-enriched membrane domains on epithelial cells (Grassme et al., 2017), and exogenously provided ASM caused β1-integrin activation or modulated LFA-1-dependent adhesion to ICAM-1 (Carpinteiro et al., 2016; Eich et al., 2016).

In endothelial cells, ICAM-1 clustering and cytoskeletal anchoring as required for TEM was found to be dependent on ASM activity, which, in contrast to that of NSM2, was also required for transmigration in both endothelial and T cells (Lopes Pinheiro et al., 2016; Collenburg et al., 2017). Because NSM2 and ASM regulate cytoskeletal dynamics, their differential roles in T-cell polarization and transmigration most likely reflect differential cytoskeletal processes involved. Thus, pushing forces for scanning endothelial cells for suitable TEM spots, formation of focal adhesions and uropod contraction driven by microtubule depolymerization and increased RhoA/ROCK activity (Takesono et al., 2010) may be promoted by ASM activity (Chang et al., 2008; Stroka et al., 2013), while acquisition of a migratory, highly polarized lamellipodia/uropod-based phenotype in T cells rather relies on NSM2 activity (**Figure 3**).

SPHINGOMYELINASES IN TCR SIGNALING, COSTIMULATION, AND EXPANSION

Immunological synapses formation requires attachment of scanning T cells followed by spreading to allow for functional organization of the antigen-presenting cell (APC)/T-cell interface. As detailed above, NSM2 supported T-cell attachment to endothelia, and it is unknown as yet whether it also takes part in mediating or stabilizing APC/T-cell conjugate formation. The latter has been found to be unstable when T cells were exposed to MV prior to dendritic cell (DC) conjugation (Shishkova et al., 2007), and though not experimentally addressed in this study, NSM2/ASM-mediated paralysis of the actin cytoskeleton might contribute to IS destabilization. Surface-bound chemokines are also important in capturing and priming T cells for synapse formation (Friedman et al., 2006), which, as described above, might be less efficient for NSM2-deficient cells. Conceivably, timing and magnitude of sphingomyelinase activation might define to what extent these enzymes take part in conjugate formation.

Much more is known about their role in the efficiency of T-cell activation. As for other cell types, ceramide release in response to death receptor ligation induces apoptosis in T cells (Andrieu-Abadie and Levade, 2002; Grassme et al., 2003; Detre et al., 2006; Edelmann et al., 2011), and especially for that of CD95, this contributes to activation-induced cell death and, thereby, homeostasis of the T-cell compartment. TNFR1 and CD95 ligation also inhibited mitogen-, αCD3/CD28-, or phorbol ester/ionomycin-stimulated Ca^{2+} influx, NFAT activation, and IL-2 synthesis in lymphoblasts and Jurkat cells *via* ASM induction, indicating that ceramide release catalyzed through its activity interferes with T-cell activation (Lepple-Wienhues et al., 1999; Church et al., 2005) (**Figure 4A**). In line with this hypothesis, accumulation of ceramides as measured in $CD4^+$ T-cell IS and non-IS membrane fractions of aging mice correlated with decreased proliferative responses (Molano et al., 2012). In turn, NSM2-deficient cells proved to be hyperresponsive to αCD3/CD28 costimulation with regard to cytoskeletal reorganization, Ca^{2+} mobilization, and initiation of proliferation, and NSM2 activation at least partially accounted for the loss of T-cell proliferation induced through MV surface exposure (Mueller et al., 2014) (**Figure 4B**), altogether indicating that sphingomyelinase-mediated ceramide release might be inhibitory to T-cell activation, irrespective as to whether it is generated in the extrafacial or cytosolic leaflet of the plasma membrane. Notably, ceramide was found largely excluded from T-cell plasma membrane domains engaged in TCR signaling (Zech et al., 2009).

Strikingly, ligation of CD3 or CD28 by antibodies individually was found to cause activation of NSM2 or ASM, respectively. Interestingly, only NSM2 activation was retained upon αCD3/CD28 coligation by antibodies, and both NSM2 protein and ceramides accumulated in the lamellopodial area of the IS (though excluded from its center and the lamellum), indicating that sphingomyelin breakdown, if spatiotemporally controlled, may indeed take part in T-cell activation (Boucher et al., 1995; Tonnetti et al., 1999; Mueller et al., 2014; Bortlein et al., 2018) (**Figure 4B**).

In support of its importance in TCR signaling, NSM2-deficient cells proved to be highly dependent on costimulation and unable to mobilize Ca^{2+} at low (most likely physiologically more relevant) antigen doses (Bortlein et al., 2018). Acting at the cytosolic leaflet of the plasma membrane, NSM2 could potentially be involved in modulating the microenvironment of the TCR by possibly facilitating exposure of the CD3β chain, formation of TCR microclusters, displacement of cholesterol from the TCRβ chain, or Lck recruitment (Gagnon et al., 2012; Kapoor-Kaushik et al., 2016; Swamy et al., 2016; Pageon et al., 2016). However, neither formation of CD3 clusters nor activation of Lck was found to be affected in Jurkat cells deficient for NSM2, whose CD3-dependent activation occurred downstream of Lck, indicating that NSM2 might not be required for initiation of TCR signaling but rather its sustainment (Bortlein et al., 2018). This involves TCR microcluster trafficking, endocytosis, and directional exocytosis at the peripheral IS (Fooksman et al., 2010; Hashimoto-Tane et al., 2011). Moreover, production of TCR-containing vesicles and their release into the synaptic cleft have been found to enhance T-cell activation (Choudhuri et al., 2014). Though both NSM2 and ASM are known to regulate both cytoskeletal activity and endo/exocytosis (Draeger and Babiychuk, 2013; Schoenauer et al., 2019) (see also below), their involvement in these particular features of the mature IS has not been revealed as yet. In contrast, NSM-dependent formation and polarized release of exosomes from T cells toward the APC

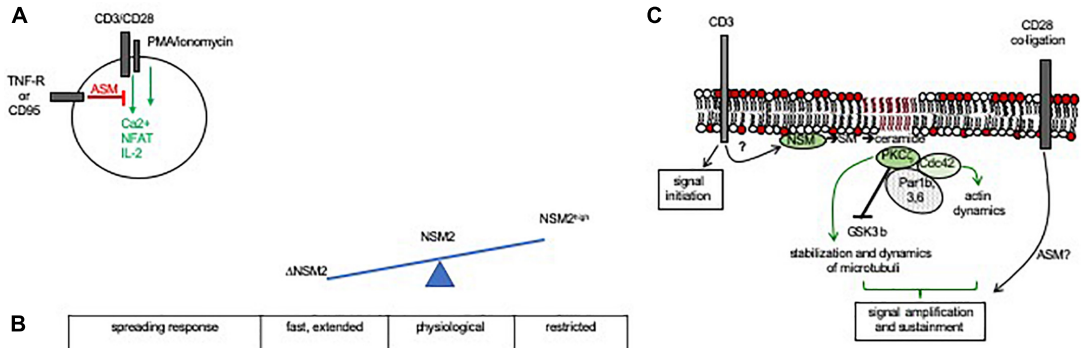

FIGURE 4 | Role of sphingomyelinase activity in IS formation and T-cell activation. **(A)** ASM activation through death receptor signaling abrogated Ca^{2+} mobilization, NFAT activation, and IL-2 synthesis in costimulated or PMA/ionomycin-activated primary or Jurkat T cells (Lepple-Wienhues et al., 1999; Church et al., 2005). **(B)** In CD3/CD28 costimulated T cells, NSM2 activity is spatiotemporally tightly controlled under physiological conditions to promote actin cytoskeletal rearrangements required for IS formation (spreading response) and activity (as indicated by kinetics and magnitude of accumulating p-tyrosine protein species and proliferation). NSM2 hyperactivation in response to MV exposure causes loss of actin remodeling, enzyme and ceramide confinement to the lamellopodium, and impairment of IS activity, while NSM2 deficiency is associated with exaggerated cytoskeletal remodeling and early T-cell activation (Mueller et al., 2014). **(C)** NSM2 activation in response to CD3 ligation takes part in early TCR signaling. Though capable of initiating a first wave of TCR signaling, NSM2-deficient cells are unable to recruit a polarity complex (in T cells confirmed for PKCζ and Cdc42, not yet for Par1b, 3, and 6) and subsequently, the actin and microtubular system required for signal amplification and sustainment. NSM2 activity in TCR signaling is particularly relevant at low antigen doses, and in its absence, T-cell activation is highly dependent on signaling provided through costimulation. Whether or not ASM is also activated in costimulation is not entirely resolved as yet (Bai et al., 2015; Bortlein et al., 2018).

were described, revealing that this enzyme indeed contributes to communication at the level of the IS (Mittelbrunn et al., 2011).

Sustainment of TCR signaling relies on cytoskeletal reorganization and rapid polarization of organelles promoting the activity of the IS such as the microtubule organizing center (MTOC), Golgi, and mitochondria (Martin-Cofreces et al., 2008; Martin-Cofreces et al., 2014). In line with the key role of NSM2 in this process, NSM2-deficient cells, though capable of signal initiation, were unable to sustain Lck tyr398 phosphorylation and largely failed to polarize CD3 molecules and relocalize the MTOC in response to TCR ligation (**Figure 4C**). As reported previously in non-T cells (Krishnamurthy et al., 2007; Bieberich, 2011), NSM2 promoted membrane recruitment and activation of the atypical PKCζ, which proved to be crucial to support MTOC IS polarization. Exogenously applied ceramide efficiently rescued PKCζ membrane recruitment and MTOC polarization, indicating that formation of ceramide-enriched domains at the inner leaflet required for PKCζ activation was ablated in NSM2-deficient T cells. In line with previously reported microtubular stabilization due to either NSM2 or ASM activity as well as physical interaction of ceramide and tubuli, NSM2 deficiency resulted in microtubular destabilization also in T cells (He et al., 2012, 2014; Bortlein et al., 2018; Kong et al., 2018) (**Figure 4C**).

Though there is a clear role for NSM2 in TCR signaling, it is dispensable at high antigen dose and strong costimulation through CD28 (Mueller et al., 2014; Bortlein et al., 2018). The role of ASM in regulation of T-cell functions is multifaceted as it is reported to modulate TCR signaling *via* engagement of inhibitory (TNFR) and costimulatory (CD28) receptors. CD28 signaling pathways in costimulated T cells have been extensively refereed and will not be reiterated herein. We rather focus on the potential role of ASM activation seen upon engagement of CD28 for T-cell activation (Boucher et al., 1995; Collenburg et al., 2016; Bortlein et al., 2018). ASM overexpression in Jurkat cells substituted for CD28 engagement with regard to NF-κB activation, suggesting that ASM activation and extrafacial ceramide release might be favorable for T-cell activation (Boucher et al., 1995). This was supported by studies revealing attenuated $CD8^+$ cell proliferation and activation in a graft-versus-host model in ASM-deficient mice and interference of pharmacological and genetic ASM activation with activation and functional differentiation of human naïve $CD4^+$ T cells stimulated with α-CD3/CD28 coated beads *in vitro* (Rotolo et al., 2009; Bai et al., 2015). In contrast, costimulation of primary T cells on a planar surface was associated with retention of NSM2 activity, but not of ASM. This suggested the ASM activity might be promoted by ligation of CD28 alone to prevent T-cell activation and that activation of the enzyme might rather be silenced upon antigen recognition (Mueller et al., 2014; Bortlein et al., 2018). Interestingly, uncontrolled inflammatory T helper 1 (Th1) and Th17 responses were observed in ASM-deficient mice in a pathogen-driven colitis model (Meiners et al., 2019). Taking into account the differential effect of genetic ASM deficiency on T-cell subsets in this and another study (Hollmann et al., 2016) (detailed below), there is an obvious need to ultimately resolve the

role of ASM in T-cell viability, activation, and expansion before this pathway can be explored for therapeutical intervention.

As referred to above, ASM activity and extrafacial ceramide release upon CD95 or TNFR ligation interfered with T-cell activation, and homeostatic ASM activity dampened their T_{reg} function, further suggesting a negative rather than supportive role of this enzyme in T cells (Lepple-Wienhues et al., 1999; Church et al., 2005). Among other potential mechanisms, cross-regulation at the level of outer and inner leaflet membrane microdomains might contribute to ASM-mediated interference with TCR signaling. Hence, integrity of extrafacial nanodomains enriched in sphingomyelin was found to play a crucial role in triggering the phosphatidylinositol-3 kinase/Akt signaling pathway at the inner membrane leaflet by facilitating Akt recruitment and activation upon phosphatidylinositol-3,4,5-triphosphate accumulation (Lasserre et al., 2008). Remarkably, exogenously added sphingomyelinase prevented formation of inner leaflet nanodomains and, thereby, Akt activation, which is a central effector in costimulation. Moreover, ASM activation may result in collapse and paralysis of the T-cell actin cytoskeleton as revealed by MV surface contact (Gassert et al., 2009). In contrast to stimulated conventional T cells, the steady-state activity of ASM appears to negatively regulate the T_{reg} compartment because this T-cell subset was represented at higher frequencies in ASM-deficient mice at the expense of conventional $CD4^+$ T-cell (T_{conv}) frequencies (Hollmann et al., 2016; Zhou et al., 2016).

IMPACT OF SPHINGOMYELINASES ON T-CELL DIFFERENTIATION AND EFFECTOR FUNCTION

The role of ASM in differentiation of the $CD4^+$ T_{conv} subset following clonal expansion is as yet unclear. While $CD4^+$ T cells of ASM-deficient mice effectively differentiated into Th1 and Th17 cells with comparable kinetics and magnitude as their wild-type kins, ASM deficiency abrogated *in vitro* differentiation of human $CD4^+$ T cells into Th17 cells (Tischner et al., 2011; Bai et al., 2015). Sphingomyelinase activity-dependent regulation of T_{conv} effector functions was clearly identified at the level of cytokine release. Mechanistically, this may relate to the documented impact of both ASM and NSM2 on the vesicular secretory pathway alluded to above (Stoffel et al., 2016), with specificities for individual cytokines/effectors being noted. Revealing the importance for ASM in IL-2 release, this cytokine was produced to lower amounts by ASM-deficient splenocytes and $CD4^+$ T cells (Stoffel et al., 1998; Tischner et al., 2011), and this should have an obvious effect on the activity of other T-cell subsets depending on this cytokine. In fact, ASM-deficient effector memory T cells reacquired resistance against glucocorticoid-induced cell death upon IL-2 addition, and reduced levels of IL-2 secretion by ASM-deficient $CD4^+$ T cells contributed to impairment of primary $CD8^+$ T-cell responses in mice infected with lymphocytic choriomeningitis virus (LCMV) (Herz et al., 2009; Tischner et al., 2011). In this model, viral clearance was less efficient in the absence of ASM with impairment of IFN-γ production and full degranulation of $CD8^+$ T cells being strongly affected. While ASM might control IFN-γ release [as that of IL-17 in human T cells (Bai et al., 2015)] in this setting *via* its impact on the secretory pathway, defective degranulation was attributed to lack of membrane tension as required for efficient expulsion in the absence of ASM (Herz et al., 2009).

A role for NSM2 in the development and differentiation of the T-cell compartment has not yet been established. NSM2 catalyzes formation of exosomes which, as efficient subcellular vectors, would be expected to take part in regulating release of effector molecules from T cells (Trajkovic et al., 2008). Thus, NSM2-dependent unidirectional exosomal transfer of micro-RNAs from T cells to APCs was reported (Mittelbrunn et al., 2011), and this mechanism may also apply to transfer of coinhibitory micro-RNAs, which are released from T_{reg}, thereby contributing to T_{reg}-mediated suppression (Okoye et al., 2014). Again not yet directly proven, NSM2 may take part in T_{reg} TCR activation upon engagement of auto-antigens and thereby contribute to survival and replenishment of the T_{reg} pool. As pointed out above, ASM activity has a significant impact on the T_{reg} compartment that is increased upon both genetic and pharmacological inhibition of the enzyme (Hollmann et al., 2016; Zhou et al., 2016). Basal ASM activity and levels of accumulated ceramides measured in T_{reg} cells exceed those of T_{conv} cells, possibly reflecting the role of ASM in T_{reg} survival, which is highly dependent on CD28 signaling (Hollmann et al., 2016). Moreover, Akt ser473 phosphorylation and Rictor levels were reduced in ASM-deficient T_{reg}, indicating that the enzyme controls metabolic activity in these cells (Zhou et al., 2016). In addition to their frequency, ASM also negatively regulates T_{reg} function because their suppressive activity and CTLA-4 turnover is enhanced in the absence of Asm. Importantly, enhancement of T_{reg} activity upon ASM depletion was reflected by reduction of MV-specific $CD8^+$ T cells in spleens, lymph nodes, and brains of experimentally infected animals and, thereby, enhancement of viral central nervous system (CNS) infection (Hollmann et al., 2016). ASM targets downregulating T_{reg} activity are undefined as is the role of ASM catalyzed ceramide release in this process. Curiously, ceramide levels were found even increased in ASM-deficient T cells, including T_{reg} (Horinouchi et al., 1995; Hollmann et al., 2016; Schuchman and Desnick, 2017), indicating that compensatory activities act to modulate this pool. A recent study provided clear evidence that ceramide accumulation is particularly important in T_{reg} metabolism, and function is driven by Foxp3 activity (Apostolidis et al., 2016; Kasper et al., 2016). The latter suppressed sphingomyelin synthase 1 (SMS1) expression and, thereby, conversion of ceramide into sphingomyelin. Accumulated ceramides promoted PP2A activation by trapping its inhibitory factor SET. Thereby, mTORC1 activity was downregulated while Foxp3 expression was stabilized in T_{reg}, and their suppressive activity was enhanced. ASM-catalyzed ceramide release obviously had the opposite effect on T_{reg} function (Hollmann et al., 2016; Zhou et al., 2016), and kinetics,

magnitude, or compartmentalization of enzyme activity and/or ceramide release may contribute.

SPHINGOMYELINASES TAKE PART IN BUT ARE NOT THE SOLE PLAYERS IN MODULATING T-CELL BIOLOGY AT THE LEVEL OF SPHINGOLIPID METABOLISM

As introduced earlier (**Figure 1**), biosynthesis and metabolization of sphingolipids is a highly dynamic process. Though this review has focused on the activity of sphingomyelinases and subsequent ceramide production, virtually all enzymes acting to define membrane sphingolipid composition are therefore important in cellular responses, also T cells and selected examples will be briefly considered here.

Thus, ceramide species generated by the activity of ER-resident ceramide synthases (CerS1–CerS6) differing in acyl chain length specificity (C_{14} to C_{26}). These are expressed in a tissue-specific manner, with CerS2 and CerS4 being most abundant in lymphatic tissues and in leukocytes, thereby defining the accumulation of intermediate (C_{18}–C_{20}) or long or very long chain (C_{20}–C_{26}) ceramides as building blocks (Levy and Futerman, 2010; Stiban et al., 2010). Studies mainly conducted in CerS2 mice revealed the importance of especially very long chain sphingolipids (VLC-SLs) in immune cell functions. This may occur at the level of membrane microdomain composition as shown in liver cells, and neutrophil receptor sorting, signaling, or stability of receptors in lipid rafts was affected in the absence of CerS2 (Park et al., 2013; Barthelmes et al., 2015). In the T-cell compartment, CerS2 has been found to facilitate thymocyte egress by its ability to regulate S1P gradients, and as key to production of VLC-SLs for development and homeostasis of invariant NKT cells, for which they serve as activating ligands (Rieck et al., 2017; Saroha et al., 2017).

As already alluded to above, glycosphingolipids are major constituents of lipid rafts, the role of which in T-cell development, activation, and signal initiation has been amply documented (for a review, see Wu et al., 2016; Nakayama et al., 2018) and will not be reiterated here. Of note, T-cell subsets substantially differ with regard to their membrane composition of membrane gangliosides. This proved to be critical for their function and has been suggested to link to organization of specific membrane microdomains by the respective gangliosides (Inokuchi et al., 2013). The importance of another ceramide derivative, C1P, generated through the activity of the ceramide kinase, for T cells is less well investigated. In contrast to what has been reported for ceramide accumulation, increased levels of C1P were found to activate Ca^{2+} mobilization *via* store-operated channeling in Jurkat cells (Church et al., 2005; Colina et al., 2005).

Ceramide accumulation due to sphingomyelin breakdown is counter-regulated by the activity of two enzyme species, ceramidases and sphingomyelin synthases, giving rise to sphingosine or sphingomyelin, respectively (**Figure 1**). In line with its ability to metabolize ceramide, genetic depletion of acid ceramidase increased overall ceramide levels, while its overexpression promoted cell growth as analyzed in non-lymphoid cancer cells (Saad et al., 2007; Brodlie et al., 2010). More recently, exogenous application of acid ceramidase was found to cause Akt kinase activation in Jurkat cells, and, however, affected their expansion. The latter was suggested to relate to the inability of the added ceramidase to promote activation of sphingosine kinase and, thereby, production of S1P in this system (Baduva et al., 2019). The ability of this particular bioactive sphingolipid to substantially regulate survival, trafficking, and activity of immune cells including T cells is well established, and with FTY720, a drug targeting S1P activity is in clinical use. Though it is therefore of critical importance to fully appreciate the relevance of the sphingolipid metabolism on T cells, it is far beyond the scope of this review to extend on this topic (for excellent reviews, see Pyne and Pyne, 2010; Stepanovska and Huwiler, 2019).

SMS1 and 2 both localize to the Golgi compartment, while SMS2 is also found at the plasma membrane. As being crucial for *de novo* sphingomyelin synthesis, they regulate availability of this sphingolipid (and thereby glycosphingolipids) for organization and integrity of lipid rafts. Therefore, their activity is also of crucial importance in the regulation of T-cell biology, and this has been highlighted in studies revealing that TCR signaling, migration, and apoptosis are highly sensitive to the absence of SMS1 (Jin et al., 2008; Lafont et al., 2010; Asano et al., 2012). Because its catalytic site locates to the extrafacial leaflet of the plasma membrane, SMS2 can directly oppose ASM activity and, thereby, ceramide accumulation by regenerating sphingomyelin (Milhas et al., 2010a). The role of SMS2 in T-cell development and activation has, however, not yet been investigated. Curiously, SMS2 rather than SMS1 was found to be involved in HIV-1 env-mediated membrane fusion with T cells, and this activity was attributed to the SMS2 protein itself rather than to its enzymatic activity (Hayashi et al., 2014).

OUTLOOK

Common to that of other cell types and compartments, the spatiotemporal resolution of the sphingolipid metabolism will crucially advance our understanding of the impact of this system on T-cell activation, trafficking, differentiation and effector functions, and, thereby, in protection or pathophysiology. At a cellular level, this, for instance, applies to the enzyme NSM2, which, in non-T cells, appears to shuttle between the plasma membrane, endo-lysosomal, Golgi, and nuclear membranes (Albi et al., 2008; Cascianelli et al., 2008; Clarke et al., 2008; Trajkovic et al., 2008; Milhas et al., 2010b; Airola and Hannun, 2013), where conceivably the sphingomyelin breakdown may differ in kinetics, efficiency, and physiological responses. The advent of bio-orthogonally mono-, bi-, or tri-functionalized sphingolipids in conjunction with targeted enzymes has enabled us and others to investigate trafficking and compartment-specific metabolization of sphingolipids (Haberkant et al., 2013, 2016; Hoglinger et al., 2014, 2017; Collenburg et al., 2016; Walter et al., 2016, 2017; Feng et al., 2018; Laguerre and Schultz, 2018), and if further advanced, this toolbox will allow to study the impact of compartment-specific enzyme activity

and lipid localization on signaling and the metabolic fate of T cells. This also applies to detailed studies on membrane topology of sphingolipid metabolites being generated and/or accumulating at cytosolic or anticytosolic membrane leaflets and organizing membrane microdomains there, which will be a challenging task. Reagents and microscopical techniques allowing to resolve lipid association with membrane leaflets ideally also allowing for codetection and copurification of proteins continue to be developed (Heilemann et al., 2009; Collenburg et al., 2016; Burgert et al., 2017). In combination with mass spectrometry performed on protein complexes crosslinking to functionalized sphingolipids after photoactivation (Hoglinger et al., 2014, 2017; Haberkant et al., 2016), detailed analyses on the organization of functionally active membrane microdomains such as, for instance, lamellopodia or immune synapses, will become possible.

Mass spectroscopy-based analytical approaches have substantially increased the sensitivity to detect and quantify sphingolipids and, when coupled to imaging, enabled spatial resolution of sphingolipid classes accumulating in tissue specimens, for the time being, at the expense of sensitivity (reviewed in Luberto et al., 2019). If further advanced, this technology will be very instrumental in relating sphingolipid patterning to the architecture of lymphoid tissue and, ideally, cellular compartments therein. At an organismic level, inbred mouse strain deficient for or overexpressing sphingolipid metabolizing enzymes have provided important insight into the importance of this system also in T-cell biology (see above). Ubiquitous disruption of enzyme activity was often associated with the development of lipid storage or other severe diseases in mice, thereby precluding long-term analyses or—except for adoptive transfer approaches—hampered assignment of immunological alterations to a specific compartment *in vivo*. In conjunction with the progress made in evaluating the sphingolipid metabolism in T cells at a subcellular, cellular and tissue level, the recent advent of novel mouse strains allowing for cell-specific inducible expression or ablation of sphingolipid-modifying enzymes will doubtlessly enable the understanding of this system for T-cell biology and delineate targets and strategies for specific intervention.

AUTHOR CONTRIBUTIONS

All authors listed have made a substantial, direct and intellectual contribution to the work, and approved it for publication.

FUNDING

This work was funded by the Deutsche Forschungsgemeinschaft for financial support of our work (SCHN405-10/1 and 10-2). This publication was funded by the German Research Foundation (DFG) and the University of Würzburg in the funding program Open Access Publishing.

ACKNOWLEDGMENTS

We apologize to all our colleagues whose studies we could not include into this review. We thank Niklas Beyersdorf and Jürgen Schneider-Schaulies for the critical reading of the manuscript.

REFERENCES

Adada, M., Canals, D., Hannun, Y. A., and Obeid, L. M. (2013). Sphingolipid regulation of ezrin, radixin, and moesin protein families: implications for cell dynamics. *Biochim. Biophys. Acta* 1841, 727–737. doi: 10.1016/j.bbalip.2013.07.002

Airola, M. V., and Hannun, Y. A. (2013). Sphingolipid metabolism and neutral sphingomyelinases. *Handb. Exp. Pharmacol.* 215, 57–76. doi: 10.1007/978-3-7091-1368-4_3

Airola, M. V., Shanbhogue, P., Shamseddine, A. A., Guja, K. E., Senkal, C. E., Maini, R., et al. (2017). Structure of human nSMase2 reveals an interdomain allosteric activation mechanism for ceramide generation. *Proc. Natl. Acad. Sci. U.S.A.* 114, E5549–E5558. doi: 10.1073/pnas.1705134114

Albi, E., Lazzarini, R., and Viola Magni, M. (2008). Phosphatidylcholine/sphingomyelin metabolism crosstalk inside the nucleus. *Biochem. J.* 410, 381–389. doi: 10.1042/bj20070758

Alebrahim, S., Khavandgar, Z., Marulanda, J., and Murshed, M. (2014). Inducible transient expression of Smpd3 prevents early lethality in fro/fro mice. *Genesis* 52, 408–416. doi: 10.1002/dvg.22765

Andrieu-Abadie, N., and Levade, T. (2002). Sphingomyelin hydrolysis during apoptosis. *Biochim. Biophys. Acta* 1585, 126–134. doi: 10.1016/s1388-1981(02)00332-3

Apostolidis, S. A., Rodriguez-Rodriguez, N., Suarez-Fueyo, A., Dioufa, N., Ozcan, E., Crispin, J. C., et al. (2016). Phosphatase PP2A is requisite for the function of regulatory T cells. *Nat. Immunol.* 17, 556–564. doi: 10.1038/ni.3390

Asano, S., Kitatani, K., Taniguchi, M., Hashimoto, M., Zama, K., Mitsutake, S., et al. (2012). Regulation of cell migration by sphingomyelin synthases: sphingomyelin in lipid rafts decreases responsiveness to signaling by the CXCL12/CXCR4 pathway. *Mol. Cell Biol.* 32, 3242–3252. doi: 10.1128/MCB.00121-12

Aubin, I., Adams, C. P., Opsahl, S., Septier, D., Bishop, C. E., Auge, N., et al. (2005). A deletion in the gene encoding sphingomyelin phosphodiesterase 3 (Smpd3) results in osteogenesis and dentinogenesis imperfecta in the mouse. *Nat. Genet.* 37, 803–805. doi: 10.1038/ng1603

Avota, E., Gassert, E., and Schneider-Schaulies, S. (2010). Measles virus-induced immunosuppression: from effectors to mechanisms. *Med. Microbiol. Immunol.* 199, 227–237. doi: 10.1007/s00430-010-0152-3

Avota, E., and Schneider-Schaulies, S. (2014). The role of sphingomyelin breakdown in measles virus immunmodulation. *Cell Physiol. Biochem.* 34, 20–26. doi: 10.1159/000362981

Baduva, K., Buchter, L., Kreyenkamp, K., Westphal, L., Wilker, B., Kohnen, M., et al. (2019). Signalling effects induced by acid ceramidase in human epithelial or leukemic cell lines. *Cell Physiol. Biochem.* 52, 1092–1102. doi: 10.33594/000000074

Bai, A., Kokkotou, E., Zheng, Y., and Robson, S. C. (2015). Role of acid sphingomyelinase bioactivity in human CD4+ T-cell activation and immune responses. *Cell Death Dis.* 6:e1828. doi: 10.1038/cddis.2015.178

Barthelmes, J., de Bazo, A. M., Pewzner-Jung, Y., Schmitz, K., Mayer, C. A., Foerch, C., et al. (2015). Lack of ceramide synthase 2 suppresses the development of experimental autoimmune encephalomyelitis by impairing the migratory capacity of neutrophils. *Brain Behav. Immun.* 46, 280–292. doi: 10.1016/j.bbi.2015.02.010

Becker, K. A., Halmer, R., Davies, L., Henry, B. D., Ziobro-Henry, R., Decker, Y., et al. (2017). Blockade of experimental multiple sclerosis by inhibition of the

acid sphingomyelinase/ceramide system. *Neurosignals* 25, 88–97. doi: 10.1159/000484621

Beyersdorf, N., and Muller, N. (2015). Sphingomyelin breakdown in T cells: role in activation, effector functions and immunoregulation. *Biol. Chem.* 396, 749–758. doi: 10.1515/hsz-2014-0282

Bieberich, E. (2011). Ceramide in stem cell differentiation and embryo development: novel functions of a topological cell-signaling lipid and the concept of ceramide compartments. *J. Lipids* 2011:610306. doi: 10.1155/2011/610306

Boecke, A., Sieger, D., Neacsu, C. D., Kashkar, H., and Kronke, M. (2012). Factor associated with neutral sphingomyelinase activity mediates navigational capacity of leukocytes responding to wounds and infection: live imaging studies in zebrafish larvae. *J. Immunol.* 189, 1559–1566. doi: 10.4049/jimmunol.1102207

Bollinger, C. R., Teichgraber, V., and Gulbins, E. (2005). Ceramide-enriched membrane domains. *Biochim. Biophys. Acta* 1746, 284–294. doi: 10.1016/j.bbamcr.2005.09.001

Bornschlogl, T. (2013). How filopodia pull: what we know about the mechanics and dynamics of filopodia. *Cytoskeleton* 70, 590–603. doi: 10.1002/cm.21130

Bortlein, C., Draeger, A., Schoenauer, R., Kuhlemann, A., Sauer, M., Schneider-Schaulies, S., et al. (2018). The neutral sphingomyelinase 2 is required to polarize and sustain T cell receptor signaling. *Front. Immunol.* 9:815. doi: 10.3389/fimmu.2018.00815

Boucher, L. M., Wiegmann, K., Futterer, A., Pfeffer, K., Machleidt, T., Schutze, S., et al. (1995). CD28 signals through acidic sphingomyelinase. *J. Exp. Med.* 181, 2059–2068. doi: 10.1084/jem.181.6.2059

Brodlie, M., McKean, M. C., Johnson, G. E., Gray, J., Fisher, A. J., Corris, P. A., et al. (2010). Ceramide is increased in the lower airway epithelium of people with advanced cystic fibrosis lung disease. *Am. J. Respir. Crit. Care Med.* 182, 369–375. doi: 10.1164/rccm.200905-0799OC

Burgert, A., Schlegel, J., Becam, J., Doose, S., Bieberich, E., Schubert-Unkmeir, A., et al. (2017). Characterization of plasma membrane ceramides by super-resolution microscopy. *Angew. Chem. Int. Ed. Engl.* 56, 6131–6135. doi: 10.1002/anie.201700570

Carpinteiro, A., Beckmann, N., Seitz, A., Hessler, G., Wilker, B., Soddemann, M., et al. (2016). Role of acid sphingomyelinase-induced signaling in melanoma cells for hematogenous tumor metastasis. *Cell Physiol. Biochem.* 38, 1–14. doi: 10.1159/000438604

Cascianelli, G., Villani, M., Tosti, M., Marini, F., Bartoccini, E., Magni, M. V., et al. (2008). Lipid microdomains in cell nucleus. *Mol. Biol. Cell* 19, 5289–5295. doi: 10.1091/mbc.E08-05-0517

Chang, Y. C., Nalbant, P., Birkenfeld, J., Chang, Z. F., and Bokoch, G. M. (2008). GEF-H1 couples nocodazole-induced microtubule disassembly to cell contractility via RhoA. *Mol. Biol. Cell* 19, 2147–2153. doi: 10.1091/mbc.E07-12-1269

Choudhuri, K., Llodra, J., Roth, E. W., Tsai, J., Gordo, S., Wucherpfennig, K. W., et al. (2014). Polarized release of T-cell-receptor-enriched microvesicles at the immunological synapse. *Nature* 507, 118–123. doi: 10.1038/nature12951

Church, L. D., Hessler, G., Goodall, J. E., Rider, D. A., Workman, C. J., Vignali, D. A., et al. (2005). TNFR1-induced sphingomyelinase activation modulates TCR signaling by impairing store-operated Ca2+ influx. *J. Leukoc. Biol.* 78, 266–278. doi: 10.1189/jlb.1003456

Clarke, C. J., Guthrie, J. M., and Hannun, Y. A. (2008). Regulation of neutral sphingomyelinase-2 (nSMase2) by tumor necrosis factor-alpha involves protein kinase C-delta in lung epithelial cells. *Mol. Pharmacol.* 74, 1022–1032. doi: 10.1124/mol.108.046250

Clarke, C. J., Snook, C. F., Tani, M., Matmati, N., Marchesini, N., and Hannun, Y. A. (2006). The extended family of neutral sphingomyelinases. *Biochemistry* 45, 11247–11256. doi: 10.1021/bi061307z

Colina, C., Flores, A., Castillo, C., Garrido Mdel, R., Israel, A., DiPolo, R., et al. (2005). Ceramide-1-P induces Ca2+ mobilization in Jurkat T-cells by elevation of Ins(1,4,5)-P3 and activation of a store-operated calcium channel. *Biochem. Biophys. Res. Commun.* 336, 54–60. doi: 10.1016/j.bbrc.2005.08.039

Collenburg, L., Beyersdorf, N., Wiese, T., Arenz, C., Saied, E. M., Becker-Flegler, K. A., et al. (2017). The activity of the neutral sphingomyelinase is important in T cell recruitment and directional migration. *Front. Immunol.* 8:1007. doi: 10.3389/fimmu.2017.01007

Collenburg, L., Schneider-Schaulies, S., and Avota, E. (2018). The neutral sphingomyelinase 2 in T cell receptor signaling and polarity. *Biol. Chem.* 399, 1147–1155. doi: 10.1515/hsz-2017-0280

Collenburg, L., Walter, T., Burgert, A., Muller, N., Seibel, J., Japtok, L., et al. (2016). A functionalized sphingolipid analogue for studying redistribution during activation in living T cells. *J. Immunol.* 196, 3951–3962. doi: 10.4049/jimmunol.1502447

Detre, C., Kiss, E., Varga, Z., Ludanyi, K., Paszty, K., Enyedi, A., et al. (2006). Death or survival: membrane ceramide controls the fate and activation of antigen-specific T-cells depending on signal strength and duration. *Cell. Signal.* 18, 294–306. doi: 10.1016/j.cellsig.2005.05.012

Draeger, A., and Babiychuk, E. B. (2013). Ceramide in plasma membrane repair. *Handb. Exp. Pharmacol.* 216, 341–353. doi: 10.1007/978-3-7091-1511-4_17

Dutta, D., Barr, V. A., Akpan, I., Mittelstadt, P. R., Singha, L. I., Samelson, L. E., et al. (2017). Recruitment of calcineurin to the TCR positively regulates T cell activation. *Nat. Immunol.* 18, 196–204. doi: 10.1038/ni.3640

Edelmann, B., Bertsch, U., Tchikov, V., Winoto-Morbach, S., Perrotta, C., Jakob, M., et al. (2011). Caspase-8 and caspase-7 sequentially mediate proteolytic activation of acid sphingomyelinase in TNF-R1 receptosomes. *EMBO J.* 30, 379–394. doi: 10.1038/emboj.2010.326

Eich, C., Manzo, C., Keijzer, S., Bakker, G. J., Reinieren-Beeren, I., Garcia-Parajo, M. F., et al. (2016). Changes in membrane sphingolipid composition modulate dynamics and adhesion of integrin nanoclusters. *Sci. Rep.* 6:20693. doi: 10.1038/srep20693

Feng, S., Harayama, T., Montessuit, S., David, F. P., Winssinger, N., Martinou, J. C., et al. (2018). Mitochondria-specific photoactivation to monitor local sphingosine metabolism and function. *eLife* 7:e34555. doi: 10.7554/eLife.34555

Filosto, S., Ashfaq, M., Chung, S., Fry, W., and Goldkorn, T. (2012). Neutral sphingomyelinase 2 activity and protein stability are modulated by phosphorylation of five conserved serines. *J. Biol. Chem.* 287, 514–522. doi: 10.1074/jbc.M111.315481

Filosto, S., Fry, W., Knowlton, A. A., and Goldkorn, T. (2010). Neutral sphingomyelinase 2 (nSMase2) is a phosphoprotein regulated by calcineurin (PP2B). *J. Biol. Chem.* 285, 10213–10222. doi: 10.1074/jbc.M109.069963

Fooksman, D. R., Vardhana, S., Vasiliver-Shamis, G., Liese, J., Blair, D. A., Waite, J., et al. (2010). Functional anatomy of T cell activation and synapse formation. *Annu. Rev. Immunol.* 28, 79–105. doi: 10.1146/annurev-immunol-030409-101308

Friedman, R. S., Jacobelli, J., and Krummel, M. F. (2006). Surface-bound chemokines capture and prime T cells for synapse formation. *Nat. Immunol.* 7, 1101–1108. doi: 10.1038/ni1384

Gagnon, E., Schubert, D. A., Gordo, S., Chu, H. H., and Wucherpfennig, K. W. (2012). Local changes in lipid environment of TCR microclusters regulate membrane binding by the CD3epsilon cytoplasmic domain. *J. Exp. Med.* 209, 2423–2439. doi: 10.1084/jem.20120790

Gassert, E., Avota, E., Harms, H., Krohne, G., Gulbins, E., and Schneider-Schaulies, S. (2009). Induction of membrane ceramides: a novel strategy to interfere with T lymphocyte cytoskeletal reorganisation in viral immunosuppression. *PLoS Pathog.* 5:e1000623. doi: 10.1371/journal.ppat.1000623

Gault, C. R., Obeid, L. M., and Hannun, Y. A. (2010). An overview of sphingolipid metabolism: from synthesis to breakdown. *Adv. Exp. Med. Biol.* 688, 1–23. doi: 10.1007/978-1-4419-6741-1_1

Gombos, I., Kiss, E., Detre, C., Laszlo, G., and Matko, J. (2006). Cholesterol and sphingolipids as lipid organizers of the immune cells' plasma membrane: their impact on the functions of MHC molecules, effector T-lymphocytes and T-cell death. *Immunol. Lett.* 104, 59–69. doi: 10.1016/j.imlet.2005.11.021

Goni, F. M., and Alonso, A. (2002). Sphingomyelinases: enzymology and membrane activity. *FEBS Lett.* 531, 38–46. doi: 10.1016/s0014-5793(02)03482-8

Gorelik, A., Heinz, L. X., Illes, K., Superti-Furga, G., and Nagar, B. (2016a). Crystal structure of the acid sphingomyelinase-like phosphodiesterase SMPDL3B provides insights into determinants of substrate specificity. *J. Biol. Chem.* 291, 24054–24064. doi: 10.1074/jbc.m116.755801

Gorelik, A., Illes, K., Heinz, L. X., Superti-Furga, G., and Nagar, B. (2016b). Crystal structure of mammalian acid sphingomyelinase. *Nat. Commun.* 7:12196. doi: 10.1038/ncomms12196

Grassme, H., Cremesti, A., Kolesnick, R., and Gulbins, E. (2003). Ceramide-mediated clustering is required for CD95–DISC formation. *Oncogene* 22, 5457–5470. doi: 10.1038/sj.onc.1206540

Grassme, H., Henry, B., Ziobro, R., Becker, K. A., Riethmuller, J., Gardner, A., et al. (2017). Beta1-integrin accumulates in cystic fibrosis luminal airway epithelial membranes and decreases sphingosine, promoting bacterial infections. *Cell Host Microbe* 21, 707–718.e8. doi: 10.1016/j.chom.2017.05.001

Guenet, J. L., Stanescu, R., Maroteaux, P., and Stanescu, V. (1981). Fragilitas ossium: a new autosomal recessive mutation in the mouse. *J. Hered.* 72, 440–441. doi: 10.1093/oxfordjournals.jhered.a109554

Gulbins, E., Dreschers, S., Wilker, B., and Grassme, H. (2004). Ceramide, membrane rafts and infections. *J. Mol. Med.* 82, 357–363. doi: 10.1007/s00109-004-0539-y

Gulbins, E., and Kolesnick, R. (2003). Raft ceramide in molecular medicine. *Oncogene* 22, 7070–7077. doi: 10.1038/sj.onc.1207146

Haberkant, P., Raijmakers, R., Wildwater, M., Sachsenheimer, T., Brugger, B., Maeda, K., et al. (2013). In vivo profiling and visualization of cellular protein–lipid interactions using bifunctional fatty acids. *Angew. Chem. Int. Ed. Engl.* 52, 4033–4038. doi: 10.1002/anie.201210178

Haberkant, P., Stein, F., Hoglinger, D., Gerl, M. J., Brugger, B., Van Veldhoven, P. P., et al. (2016). Bifunctional sphingosine for cell-based analysis of protein–sphingolipid interactions. *ACS Chem. Biol.* 11, 222–230. doi: 10.1021/acschembio.5b00810

Hannun, Y. A., and Obeid, L. M. (2008). Principles of bioactive lipid signalling: lessons from sphingolipids. *Nat. Rev. Mol. Cell Biol.* 9, 139–150. doi: 10.1038/nrm2329

Harayama, T., and Riezman, H. (2018). Understanding the diversity of membrane lipid composition. *Nat. Rev. Mol. Cell Biol.* 19, 281–296. doi: 10.1038/nrm.2017.138

Hashimoto-Tane, A., Yokosuka, T., Sakata-Sogawa, K., Sakuma, M., Ishihara, C., Tokunaga, M., et al. (2011). Dynein-driven transport of T cell receptor microclusters regulates immune synapse formation and T cell activation. *Immunity* 34, 919–931. doi: 10.1016/j.immuni.2011.05.012

Hayashi, Y., Nemoto-Sasaki, Y., Tanikawa, T., Oka, S., Tsuchiya, K., Zama, K., et al. (2014). Sphingomyelin synthase 2, but not sphingomyelin synthase 1, is involved in HIV-1 envelope-mediated membrane fusion. *J. Biol. Chem.* 289, 30842–30856. doi: 10.1074/jbc.M114.574285

He, Q., Wang, G., Dasgupta, S., Dinkins, M., Zhu, G., and Bieberich, E. (2012). Characterization of an apical ceramide-enriched compartment regulating ciliogenesis. *Mol. Biol. Cell* 23, 3156–3166. doi: 10.1091/mbc.E12-02-0079

He, Q., Wang, G., Wakade, S., Dasgupta, S., Dinkins, M., Kong, J. N., et al. (2014). Primary cilia in stem cells and neural progenitors are regulated by neutral sphingomyelinase 2 and ceramide. *Mol. Biol. Cell* 25, 1715–1729. doi: 10.1091/mbc.E13-12-0730

Heilemann, M., van de Linde, S., Mukherjee, A., and Sauer, M. (2009). Super-resolution imaging with small organic fluorophores. *Angew. Chem. Int. Ed. Engl.* 48, 6903–6908. doi: 10.1002/anie.200902073

Heinz, L. X., Baumann, C. L., Koberlin, M. S., Snijder, B., Gawish, R., Shui, G., et al. (2015). The lipid-modifying enzyme SMPDL3B negatively regulates innate immunity. *Cell Rep.* 11, 1919–1928. doi: 10.1016/j.celrep.2015.05.006

Henry, B., Ziobro, R., Becker, K. A., Kolesnick, R., and Gulbins, E. (2013). Acid sphingomyelinase. *Handb. Exp. Pharmacol.* 215, 77–88.

Herz, J., Pardo, J., Kashkar, H., Schramm, M., Kuzmenkina, E., Bos, E., et al. (2009). Acid sphingomyelinase is a key regulator of cytotoxic granule secretion by primary T lymphocytes. *Nat. Immunol.* 10, 761–768. doi: 10.1038/ni.1757

Hogg, N., Patzak, I., and Willenbrock, F. (2011). The insider's guide to leukocyte integrin signalling and function. *Nat. Rev. Immunol.* 11, 416–426. doi: 10.1038/nri2986

Hoglinger, D., Nadler, A., Haberkant, P., Kirkpatrick, J., Schifferer, M., Stein, F., et al. (2017). Trifunctional lipid probes for comprehensive studies of single lipid species in living cells. *Proc. Natl. Acad. Sci. U.S.A.* 114, 1566–1571. doi: 10.1073/pnas.1611096114

Hoglinger, D., Nadler, A., and Schultz, C. (2014). Caged lipids as tools for investigating cellular signaling. *Biochim. Biophys. Acta* 1841, 1085–1096. doi: 10.1016/j.bbalip.2014.03.012

Hollmann, C., Werner, S., Avota, E., Reuter, D., Japtok, L., Kleuser, B., et al. (2016). Inhibition of acid sphingomyelinase allows for selective targeting of CD4(+) conventional versus Foxp3(+) regulatory T cells. *J. Immunol.* 197, 3130–3141. doi: 10.4049/jimmunol.1600691

Horinouchi, K., Erlich, S., Perl, D. P., Ferlinz, K., Bisgaier, C. L., Sandhoff, K., et al. (1995). Acid sphingomyelinase deficient mice: a model of types A and B Niemann–Pick disease. *Nat. Genet.* 10, 288–293. doi: 10.1038/ng0795-288

Howie, D., Ten Bokum, A., Necula, A. S., Cobbold, S. P., and Waldmann, H. (2017). The role of lipid metabolism in T lymphocyte differentiation and survival. *Front. Immunol.* 8:1949. doi: 10.3389/fimmu.2017.01949

Inokuchi, J., Nagafuku, M., Ohno, I., and Suzuki, A. (2013). Heterogeneity of gangliosides among T cell subsets. *Cell Mol. Life Sci.* 70, 3067–3075. doi: 10.1007/s00018-012-1208-x

Jin, Z. X., Huang, C. R., Dong, L., Goda, S., Kawanami, T., Sawaki, T., et al. (2008). Impaired TCR signaling through dysfunction of lipid rafts in sphingomyelin synthase 1 (SMS1)-knockdown T cells. *Int. Immunol.* 20, 1427–1437. doi: 10.1093/intimm/dxn100

Kapoor-Kaushik, N., Hinde, E., Compeer, E. B., Yamamoto, Y., Kraus, F., Yang, Z., et al. (2016). Distinct mechanisms regulate Lck spatial organization in activated T cells. *Front. Immunol.* 7:83. doi: 10.3389/fimmu.2016.00083

Kasper, I. R., Apostolidis, S. A., Sharabi, A., and Tsokos, G. C. (2016). Empowering regulatory T cells in autoimmunity. *Trends Mol. Med.* 22, 784–797. doi: 10.1016/j.molmed.2016.07.003

Katsuno, H., Toriyama, M., Hosokawa, Y., Mizuno, K., Ikeda, K., Sakumura, Y., et al. (2015). Actin migration driven by directional assembly and disassembly of membrane-anchored actin filaments. *Cell Rep.* 12, 648–660. doi: 10.1016/j.celrep.2015.06.048

Kong, J. N., Zhu, Z., Itokazu, Y., Wang, G., Dinkins, M. B., Zhong, L., et al. (2018). Novel function of ceramide for regulation of mitochondrial ATP release in astrocytes. *J. Lipid. Res.* 59, 488–506. doi: 10.1194/jlr.M081877

Krishnamurthy, K., Wang, G., Silva, J., Condie, B. G., and Bieberich, E. (2007). Ceramide regulates atypical PKCzeta/lambda-mediated cell polarity in primitive ectoderm cells. A novel function of sphingolipids in morphogenesis. *J. Biol. Chem.* 282, 3379–3390. doi: 10.1074/jbc.m607779200

Kuemmel, T. A., Thiele, J., Schroeder, R., and Stoffel, W. (1997). Pathology of visceral organs and bone marrow in an acid sphingomyelinase deficient knock-out mouse line, mimicking human Niemann–Pick disease type A. A light and electron microscopic study. *Pathol. Res. Pract.* 193, 663–671. doi: 10.1016/s0344-0338(97)80025-8

Lafont, E., Milhas, D., Carpentier, S., Garcia, V., Jin, Z. X., Umehara, H., et al. (2010). Caspase-mediated inhibition of sphingomyelin synthesis is involved in FasL-triggered cell death. *Cell Death Differ.* 17, 642–654. doi: 10.1038/cdd.2009.130

Laguerre, A., and Schultz, C. (2018). Novel lipid tools and probes for biological investigations. *Curr. Opin. Cell. Biol.* 53, 97–104. doi: 10.1016/j.ceb.2018.06.013

Lasserre, R., Guo, X. J., Conchonaud, F., Hamon, Y., Hawchar, O., Bernard, A. M., et al. (2008). Raft nanodomains contribute to Akt/PKB plasma membrane recruitment and activation. *Nat. Chem. Biol.* 4, 538–547. doi: 10.1038/nchembio.103

Leijnse, N., Oddershede, L. B., and Bendix, P. M. (2015). An updated look at actin dynamics in filopodia. *Cytoskeleton* 72, 71–79. doi: 10.1002/cm.21216

Leithner, A., Eichner, A., Muller, J., Reversat, A., Brown, M., Schwarz, J., et al. (2016). Diversified actin protrusions promote environmental exploration but are dispensable for locomotion of leukocytes. *Nat. Cell Biol.* 18, 1253–1259. doi: 10.1038/ncb3426

Lepple-Wienhues, A., Belka, C., Laun, T., Jekle, A., Walter, B., Wieland, U., et al. (1999). Stimulation of CD95 (Fas) blocks T lymphocyte calcium channels through sphingomyelinase and sphingolipids. *Proc. Natl. Acad. Sci. U.S.A.* 96, 13795–13800. doi: 10.1073/pnas.96.24.13795

Levy, M., and Futerman, A. H. (2010). Mammalian ceramide synthases. *IUBMB Life* 62, 347–356. doi: 10.1002/iub.319

Ley, K., Laudanna, C., Cybulsky, M. I., and Nourshargh, S. (2007). Getting to the site of inflammation: the leukocyte adhesion cascade updated. *Nat. Rev. Immunol.* 7, 678–689. doi: 10.1038/nri2156

Liu, B., Hassler, D. F., Smith, G. K., Weaver, K., and Hannun, Y. A. (1998). Purification and characterization of a membrane bound neutral pH optimum magnesium-dependent and phosphatidylserine-stimulated sphingomyelinase from rat brain. *J. Biol. Chem.* 273, 34472–34479. doi: 10.1074/jbc.273.51.34472

Lopes Pinheiro, M. A., Kroon, J., Hoogenboezem, M., Geerts, D., van Het Hof, B., van der Pol, S. M., et al. (2016). Acid sphingomyelinase-derived

ceramide regulates ICAM-1 function during T cell transmigration across brain endothelial cells. *J. Immunol.* 196, 72–79. doi: 10.4049/jimmunol.1500702

Luberto, C., Haley, J. D., and Del Poeta, M. (2019). Imaging with mass spectrometry, the next frontier in sphingolipid research? A discussion on where we stand and the possibilities ahead. *Chem. Phys. Lipids* 219, 1–14. doi: 10.1016/j.chemphyslip.2019.01.001

Lucki, N. C., and Sewer, M. B. (2012). Nuclear sphingolipid metabolism. *Annu. Rev. Physiol.* 74, 131–151. doi: 10.1146/annurev-physiol-020911-153321

Marchesini, N., Luberto, C., and Hannun, Y. A. (2003). Biochemical properties of mammalian neutral sphingomyelinase 2 and its role in sphingolipid metabolism. *J. Biol. Chem.* 278, 13775–13783. doi: 10.1074/jbc.m212262200

Martin-Cofreces, N. B., Baixauli, F., and Sanchez-Madrid, F. (2014). Immune synapse: conductor of orchestrated organelle movement. *Trends Cell Biol.* 24, 61–72. doi: 10.1016/j.tcb.2013.09.005

Martin-Cofreces, N. B., Robles-Valero, J., Cabrero, J. R., Mittelbrunn, M., Gordon-Alonso, M., Sung, C. H., et al. (2008). MTOC translocation modulates IS formation and controls sustained T cell signaling. *J. Cell. Biol.* 182, 951–962. doi: 10.1083/jcb.200801014

Meiners, J., Palmieri, V., Klopfleisch, R., Ebel, J. F., Japtok, L., Schumacher, F., et al. (2019). Intestinal acid sphingomyelinase protects from severe pathogen-driven colitis. *Front. Immunol.* 10:1386. doi: 10.3389/fimmu.2019.01386

Milhas, D., Clarke, C. J., and Hannun, Y. A. (2010a). Sphingomyelin metabolism at the plasma membrane: implications for bioactive sphingolipids. *FEBS Lett.* 584, 1887–1894. doi: 10.1016/j.febslet.2009.10.058

Milhas, D., Clarke, C. J., Idkowiak-Baldys, J., Canals, D., and Hannun, Y. A. (2010b). Anterograde and retrograde transport of neutral sphingomyelinase-2 between the Golgi and the plasma membrane. *Biochim. Biophys. Acta* 1801, 1361–1374. doi: 10.1016/j.bbalip.2010.08.001

Mittelbrunn, M., Gutierrez-Vazquez, C., Villarroya-Beltri, C., Gonzalez, S., Sanchez-Cabo, F., Gonzalez, M. A., et al. (2011). Unidirectional transfer of microRNA-loaded exosomes from T cells to antigen-presenting cells. *Nat. Commun.* 2:282. doi: 10.1038/ncomms1285

Molano, A., Huang, Z., Marko, M. G., Azzi, A., Wu, D., Wang, E., et al. (2012). Age-dependent changes in the sphingolipid composition of mouse CD4+ T cell membranes and immune synapses implicate glucosylceramides in age-related T cell dysfunction. *PLoS One* 7:e47650. doi: 10.1371/journal.pone.0047650

Moser, M., Bauer, M., Schmid, S., Ruppert, R., Schmidt, S., Sixt, M., et al. (2009). Kindlin-3 is required for beta2 integrin-mediated leukocyte adhesion to endothelial cells. *Nat. Med.* 15, 300–305. doi: 10.1038/nm.1921

Mueller, N., Avota, E., Collenburg, L., Grassme, H., and Schneider-Schaulies, S. (2014). Neutral sphingomyelinase in physiological and measles virus induced T cell suppression. *PLoS Pathog.* 10:e1004574. doi: 10.1371/journal.ppat.1004574

Nakayama, H., Nagafuku, M., Suzuki, A., Iwabuchi, K., and Inokuchi, J. I. (2018). The regulatory roles of glycosphingolipid-enriched lipid rafts in immune systems. *FEBS Lett.* 592, 3921–3942. doi: 10.1002/1873-3468.13275

Nordenfelt, P., Elliott, H. L., and Springer, T. A. (2016). Coordinated integrin activation by actin-dependent force during T-cell migration. *Nat. Commun.* 7:13119. doi: 10.1038/ncomms13119

Nourshargh, S., and Alon, R. (2014). Leukocyte migration into inflamed tissues. *Immunity* 41, 694–707. doi: 10.1016/j.immuni.2014.10.008

Okoye, I. S., Coomes, S. M., Pelly, V. S., Czieso, S., Papayannopoulos, V., Tolmachova, T., et al. (2014). MicroRNA-containing T-regulatory-cell-derived exosomes suppress pathogenic T helper 1 cells. *Immunity* 41, 89–103. doi: 10.1016/j.immuni.2014.05.019

Pageon, S. V., Tabarin, T., Yamamoto, Y., Ma, Y., Bridgeman, J. S., Cohnen, A., et al. (2016). Functional role of T-cell receptor nanoclusters in signal initiation and antigen discrimination. *Proc. Natl. Acad. Sci. U.S.A.* 113, E5454–E5463. doi: 10.1073/pnas.1607436113

Park, J. W., Park, W. J., Kuperman, Y., Boura-Halfon, S., Pewzner-Jung, Y., and Futerman, A. H. (2013). Ablation of very long acyl chain sphingolipids causes hepatic insulin resistance in mice due to altered detergent-resistant membranes. *Hepatology* 57, 525–532. doi: 10.1002/hep.26015

Philipp, S., Puchert, M., Adam-Klages, S., Tchikov, V., Winoto-Morbach, S., Mathieu, S., et al. (2010). The Polycomb group protein EED couples TNF receptor 1 to neutral sphingomyelinase. *Proc. Natl. Acad. Sci. U.S.A.* 107, 1112–1117. doi: 10.1073/pnas.0908486107

Pyne, N. J., and Pyne, S. (2010). Sphingosine 1-phosphate and cancer. *Nat. Rev. Cancer* 10, 489–503. doi: 10.1038/nrc2875

Qin, J., and Dawson, G. (2012). Evidence for coordination of lysosomal (ASMase) and plasma membrane (NSMase2) forms of sphingomyelinase from mutant mice. *FEBS Lett.* 586, 4002–4009. doi: 10.1016/j.febslet.2012.09.039

Rieck, M., Kremser, C., Jobin, K., Mettke, E., Kurts, C., Graler, M., et al. (2017). Ceramide synthase 2 facilitates S1P-dependent egress of thymocytes into the circulation in mice. *Eur. J. Immunol.* 47, 677–684. doi: 10.1002/eji.201646623

Rotolo, J. A., Stancevic, B., Lu, S. X., Zhang, J., Suh, D., King, C. G., et al. (2009). Cytolytic T cells induce ceramide-rich platforms in target cell membranes to initiate graft-versus-host disease. *Blood* 114, 3693–3706. doi: 10.1182/blood-2008-11-191148

Saad, A. F., Meacham, W. D., Bai, A., Anelli, V., Elojeimy, S., Mahdy, A. E., et al. (2007). The functional effects of acid ceramidase overexpression in prostate cancer progression and resistance to chemotherapy. *Cancer Biol. Ther.* 6, 1455–1460.

Sadik, C. D., and Luster, A. D. (2012). Lipid–cytokine–chemokine cascades orchestrate leukocyte recruitment in inflammation. *J. Leukoc. Biol.* 91, 207–215. doi: 10.1189/jlb.0811402

Saroha, A., Pewzner-Jung, Y., Ferreira, N. S., Sharma, P., Jouan, Y., Kelly, S. L., et al. (2017). Critical role for very-long chain sphingolipids in invariant natural killer T cell development and homeostasis. *Front. Immunol.* 8:1386. doi: 10.3389/fimmu.2017.01386

Schneider-Schaulies, J., and Schneider-Schaulies, S. (2013). Viral infections and sphingolipids. *Handb. Exp. Pharmacol.* 216, 321–340. doi: 10.1007/978-3-7091-1511-4_16

Schoenauer, R., Larpin, Y., Babiychuk, E. B., Drucker, P., Babiychuk, V. S., Avota, E., et al. (2019). Down-regulation of acid sphingomyelinase and neutral sphingomyelinase-2 inversely determines the cellular resistance to plasmalemmal injury by pore-forming toxins. *FASEB J.* 33, 275–285. doi: 10.1096/fj.201800033R

Schuchman, E. H., and Desnick, R. J. (2017). Types A and B Niemann–Pick disease. *Mol. Genet. Metab.* 120, 27–33. doi: 10.1016/j.ymgme.2016.12.008

Shamseddine, A. A., Airola, M. V., and Hannun, Y. A. (2015). Roles and regulation of neutral sphingomyelinase-2 in cellular and pathological processes. *Adv. Biol. Regul.* 57, 24–41. doi: 10.1016/j.jbior.2014.10.002

Shishkova, Y., Harms, H., Krohne, G., Avota, E., and Schneider-Schaulies, S. (2007). Immune synapses formed with measles virus-infected dendritic cells are unstable and fail to sustain T cell activation. *Cell Microbiol.* 9, 1974–1986. doi: 10.1111/j.1462-5822.2007.00928.x

Shulman, Z., Shinder, V., Klein, E., Grabovsky, V., Yeger, O., Geron, E., et al. (2009). Lymphocyte crawling and transendothelial migration require chemokine triggering of high-affinity LFA-1 integrin. *Immunity* 30, 384–396. doi: 10.1016/j.immuni.2008.12.020

Simons, K., and Gerl, M. J. (2010). Revitalizing membrane rafts: new tools and insights. *Nat. Rev. Mol. Cell Biol.* 11, 688–699. doi: 10.1038/nrm2977

Sitrin, R. G., Sassanella, T. M., and Petty, H. R. (2011). An obligate role for membrane-associated neutral sphingomyelinase activity in orienting chemotactic migration of human neutrophils. *Am. J. Respir. Cell Mol. Biol.* 44, 205–212. doi: 10.1165/rcmb.2010-0019OC

Smith, E. L., and Schuchman, E. H. (2008). The unexpected role of acid sphingomyelinase in cell death and the pathophysiology of common diseases. *FASEB J.* 22, 3419–3431. doi: 10.1096/fj.08-108043

Stepanovska, B., and Huwiler, A. (2019). Targeting the S1P receptor signaling pathways as a promising approach for treatment of autoimmune and inflammatory diseases. *Pharmacol. Res.* doi: 10.1016/j.phrs.2019.02.009 [Epub ahead of print].

Stiban, J., Tidhar, R., and Futerman, A. H. (2010). Ceramide synthases: roles in cell physiology and signaling. *Adv. Exp. Med. Biol.* 688, 60–71. doi: 10.1007/978-1-4419-6741-1_4

Stoffel, B., Bauer, P., Nix, M., Deres, K., and Stoffel, W. (1998). Ceramide-independent CD28 and TCR signaling but reduced IL-2 secretion in T cells of acid sphingomyelinase-deficient mice. *Eur. J. Immunol.* 28, 874–880. doi: 10.1002/(sici)1521-4141(199803)28:03<874::aid-immu874>3.0.co;2-t

Stoffel, W., Hammels, I., Jenke, B., Binczek, E., Schmidt-Soltau, I., Brodesser, S., et al. (2016). Neutral sphingomyelinase (SMPD3) deficiency disrupts the Golgi secretory pathway and causes growth inhibition. *Cell Death Dis.* 7:e2488. doi: 10.1038/cddis.2016.385

Stoffel, W., Jenke, B., Block, B., Zumbansen, M., and Koebke, J. (2005). Neutral sphingomyelinase 2 (smpd3) in the control of postnatal growth and development. *Proc. Natl. Acad. Sci. U.S.A.* 102, 4554–4559. doi: 10.1073/pnas.0406380102

Stroka, K. M., Hayenga, H. N., and Aranda-Espinoza, H. (2013). Human neutrophil cytoskeletal dynamics and contractility actively contribute to trans-endothelial migration. *PLoS One* 8:e61377. doi: 10.1371/journal.pone.0061377

Swamy, M., Beck-Garcia, K., Beck-Garcia, E., Hartl, F. A., Morath, A., Yousefi, O. S., et al. (2016). A Cholesterol-based allostery model of T cell receptor phosphorylation. *Immunity* 44, 1091–1101. doi: 10.1016/j.immuni.2016.04.011

Takesono, A., Heasman, S. J., Wojciak-Stothard, B., Garg, R., and Ridley, A. J. (2010). Microtubules regulate migratory polarity through Rho/ROCK signaling in T cells. *PLoS One* 5:e8774. doi: 10.1371/journal.pone.0008774

Tischner, D., Theiss, J., Karabinskaya, A., van den Brandt, J., Reichardt, S. D., Karow, U., et al. (2011). Acid sphingomyelinase is required for protection of effector memory T cells against glucocorticoid-induced cell death. *J. Immunol.* 187, 4509–4516. doi: 10.4049/jimmunol.1100911

Tonnetti, L., Veri, M. C., Bonvini, E., and D'Adamio, L. (1999). A role for neutral sphingomyelinase-mediated ceramide production in T cell receptor-induced apoptosis and mitogen-activated protein kinase-mediated signal transduction. *J. Exp. Med.* 189, 1581–1589. doi: 10.1084/jem.189.10.1581

Trajkovic, K., Hsu, C., Chiantia, S., Rajendran, L., Wenzel, D., Wieland, F., et al. (2008). Ceramide triggers budding of exosome vesicles into multivesicular endosomes. *Science* 319, 1244–1247. doi: 10.1126/science.1153124

Walter, T., Collenburg, L., Japtok, L., Kleuser, B., Schneider-Schaulies, S., Muller, N., et al. (2016). Incorporation and visualization of azido-functionalized N-oleoyl serinol in Jurkat cells, mouse brain astrocytes, 3T3 fibroblasts and human brain microvascular endothelial cells. *Chem. Commun.* 52, 8612–8614. doi: 10.1039/c6cc02879a

Walter, T., Schlegel, J., Burgert, A., Kurz, A., Seibel, J., and Sauer, M. (2017). Incorporation studies of clickable ceramides in Jurkat cell plasma membranes. *Chem. Commun.* 53, 6836–6839. doi: 10.1039/c7cc01220a

Wu, B. X., Clarke, C. J., and Hannun, Y. A. (2010). Mammalian neutral sphingomyelinases: regulation and roles in cell signaling responses. *Neuromol. Med.* 12, 320–330. doi: 10.1007/s12017-010-8120-z

Wu, W., Shi, X. S., and Xu, C. Q. (2016). Regulation of T cell signalling by membrane lipids. *Nat. Rev. Immunol.* 16, 690–701. doi: 10.1038/nri.2016.103

Wu, W., Yan, C. S., Shi, X. S., Li, L. Y., Liu, W. L., and Xu, C. Q. (2015). Lipid in T-cell receptor transmembrane signaling. *Prog. Biophys. Mol. Biol.* 118, 130–138. doi: 10.1016/j.pbiomolbio.2015.04.004

Zech, T., Ejsing, C. S., Gaus, K., de Wet, B., Shevchenko, A., Simons, K., et al. (2009). Accumulation of raft lipids in T-cell plasma membrane domains engaged in TCR signalling. *EMBO J.* 28, 466–476. doi: 10.1038/emboj.2009.6

Zhou, Y., Salker, M. S., Walker, B., Munzer, P., Borst, O., Gawaz, M., et al. (2016). Acid sphingomyelinase (ASM) is a negative regulator of regulatory T cell (Treg) development. *Cell Physiol. Biochem.* 39, 985–995. doi: 10.1159/000447806

Conflict of Interest Statement: The authors declare that the research was conducted in the absence of any commercial or financial relationships that could be construed as a potential conflict of interest.

frontiers in Cell and Developmental Biology

ORIGINAL RESEARCH
published: 16 August 2019
doi: 10.3389/fcell.2019.00166

Visualization of Ceramide-Associated Proteins in Ceramide-Rich Platforms Using a Cross-Linkable Ceramide Analog and Proximity Ligation Assays With Anti-ceramide Antibody

*Xue Jiang[1,2], Zhihui Zhu[2], Haiyan Qin[2], Priyanka Tripathi[2], Liansheng Zhong[2,3], Ahmed Elsherbini[2], Sanjib Karki[2], Simone M. Crivelli[2], Wenbo Zhi[4], Guanghu Wang[2], Stefanka D. Spassieva[2] and Erhard Bieberich[2]**

[1] Department of Rehabilitation, ShengJing Hospital of China Medical University, Shenyang, China, [2] Department of Physiology, University of Kentucky, Lexington, KY, United States, [3] College of Life Sciences, China Medical University, Shenyang, China, [4] Center for Biotechnology and Genomic Medicine, Medical College of Georgia, Augusta University, Augusta, GA, United States

Ceramide-rich platforms (CRPs) mediate association of proteins with the sphingolipid ceramide and may regulate protein interaction in membrane contact sites to the cytoskeleton, organelles, and infectious pathogens. However, visualization of ceramide association to proteins is one of the greatest challenges in understanding the cell biology of ceramide. Here we introduce a novel labeling technique for ceramide-associated proteins (CAPs) by combining photoactivated cross-linking of a bioorthogonal and bifunctional ceramide analog, pacFACer with proximity ligation assays (PLAs). pacFACer cross-linked to CAPs is covalently attached to a fluorophore using click chemistry. PLAs use antibodies to: (1) the candidate CAP and the fluorophore (PLA1); and (2) the CAP and ceramide (PLA2). PLA1 shows the subcellular localization of a particular CAP that is cross-linked to pacFACer, while PLA2 tests if the cross-linked CAP forms a complex with endogenous ceramide. Two proteins, tubulin and voltage-dependent anion channel 1 (VDAC1), were cross-linked to pacFACer and showed PLA signals for a complex with ceramide and pacFACer, which were predominantly colocalized with microtubules and mitochondria, respectively. Binding of tubulin and VDAC1 to ceramide was confirmed by coimmunoprecipitation assays using anti ceramide antibody. Cross-linking to pacFACer was confirmed using click chemistry-mediated attachment of biotin and streptavidin pull-down assays. Inhibition of ceramide synthases with fumonisin B1 (FB1) reduced the degree of pacFACer cross-linking and complex formation with ceramide, while it was enhanced by amyloid beta peptide (Aβ). Our results show that endogenous ceramide is critical for mediating cross-linking of CAPs to pacFACer and that a combination of cross-linking with PLAs (cross-link/PLA) is a novel tool to visualize CAPs and to understand the regulation of protein interaction with ceramide in CRPs.

Keywords: ceramide, proximity ligation assay, cross-link, lipid raft, microtubules, mitochondria, VDAC1, acetylated tubulin

OPEN ACCESS

Edited by:
Burkhard Kleuser, University of Potsdam, Germany

Reviewed by:
Liana C. Silva, University of Lisbon, Portugal
Dimitra Mangoura, Biomedical Research Foundation, Academy of Athens, Greece

***Correspondence:**
Erhard Bieberich
erhard.bieberich@uky.edu

Specialty section:
This article was submitted to Membrane Physiology and Membrane Biophysics, a section of the journal Frontiers in Cell and Developmental Biology

Received: *01 May 2019*
Accepted: *30 July 2019*
Published: *16 August 2019*

Citation:
Jiang X, Zhu Z, Qin H, Tripathi P, Zhong L, Elsherbini A, Karki S, Crivelli SM, Zhi W, Wang G, Spassieva SD and Bieberich E (2019) Visualization of Ceramide-Associated Proteins in Ceramide-Rich Platforms Using a Cross-Linkable Ceramide Analog and Proximity Ligation Assays With Anti-ceramide Antibody. Front. Cell Dev. Biol. 7:166. doi: 10.3389/fcell.2019.00166

INTRODUCTION

The function of ceramide as precursor and intermediate in sphingolipid metabolism is well investigated for many decades. About 30 years ago, it was shown that ceramide plays an additional role in cell signaling pathways for regulation of cell cycle arrest and apoptosis (Merrill et al., 1986; Mathias et al., 1991; Dobrowsky and Hannun, 1992). Since then, thousands of studies have extended our knowledge on the role of ceramide in many different aspects of cell biology from embryo development to aging and disease. However, to understand the molecular mechanism(s) underlying this plethora of different functions, it is critical to develop methods analyzing the interaction of ceramide with other cellular components, particularly proteins binding to ceramide (Canals et al., 2018). In recent years, novel probes were developed to identify and visualize these ceramide-associated proteins (CAPs). These probes are ceramide analogs that are termed bioorthogonal because labeling of CAPs is achieved in living cells (Walter et al., 2016; Fink and Seibel, 2018). They are also bifunctional in that these ceramide analogs are: (1) cross-linked to CAPs by photoactivation; and (2) can be covalently attached to fluorophores and other functional groups using click chemistry. However, since introduction of the first bioorthogonal, bifunctional ceramide analog, N-(9-(3-pent-4-ynyl-3-H-diazirin-3-yl)-nonanoyl)-D-erythro-sphingosine (pacFACer) (**Figure 1A**), the number of cross-linked proteins has substantially grown. To understand which of these proteins are actually CAPs mediating the biological function of ceramide, it is critical to develop methods that verify the interaction of the pacFACer cross-linked proteins with endogenous ceramide.

Previously, we showed that pacFACer was UV cross-linked to tubulin in living cells (Kong et al., 2018). Cross-linking was consistent with association of tubulin with ceramide in ceramide-enriched mitochondria-associated membranes (CEMAMs), a MAM subcompartment that was recently discovered by our group (Kong et al., 2018). Our data showed that ceramide-associated tubulin (CAT) regulates opening of the ATP/ADP channel protein VDAC1 in mitochondria. Our results also indicated that additional proteins are cross-linked to pacFACer and colocalized with ceramide, particularly at mitochondria, the cytoskeleton, and the plasma membrane. However, the identity of these proteins is not clear. To test if a particular protein is cross-linked to pacFACer and colocalized with ceramide, we developed a novel labeling technique for visualization of CAPs in cells and tissues using immunocytochemistry.

To achieve labeling of CAPs we first identified candidate proteins using cross-linking to pacFACer followed by click chemistry-mediated covalent attachment of a fluorophore and biotin, ideally as a dual-label click probe such as TAMRA-biotin azide or Cy5-biotin azide. After protein solubilization and copper-catalyzed click reaction, cross-linked protein was isolated using streptavidin pull-down followed by SDS-PAGE and proteomics analysis of fluorescent bands. Based on our previously published data, we focused on two proteins detectable in the proteomics screen: tubulin and its binding partner VDAC1. In addition to CEMAMs, we detected colocalization of ceramide with tubulin at microtubules and the plasma membrane, suggesting that CAT may also partake in the tubulin pool at microtubules and cellular membranes. In particular, membrane tubulin, a minor portion of tubulin associated with cellular membranes, is a candidate for interaction with ceramide in ceramide-rich platforms (CRPs) potentially mediating attachment of ceramide microdomains or rafts to the cytoskeleton (Burgert et al., 2017). Membrane tubulin was shown to regulate channels in cellular membranes, including VDAC1 and the Na/K channel in the plasma membrane (Rostovtseva and Bezrukov, 2008; Rostovtseva et al., 2008; Maldonado and Lemasters, 2012; Kong et al., 2018; Santander et al., 2019). In addition to interacting with CAT, VDAC1 was detected in our initial screen, suggesting that it binds to ceramide itself. However, it is not known if cross-linking to pacFACer is a sufficient indicator for ceramide association of a particular protein in cells. Further, it is also not clear how pacFACer cross-linking and location of CAPs in CRPs is regulated by ceramide.

To test cross-linking of pacFACer with a particular candidate CAP and its distribution to CRPs, cross-linking was combined with proximity ligation assays (PLAs) using antibodies to the CAP and the fluorophore attached to pacFACer (PLA1), and the CAP and ceramide (PLA2). PLAs are based on secondary antibodies covalently attached to oligonucleotide primers that initiate rolling circle PCR and incorporation of fluorescent nucleotides if the distance of primary antibodies is smaller than 40 nm (Weibrecht et al., 2010; Kong et al., 2018). PLA1 shows the subcellular localization of a particular CAP that is cross-linked to pacFACer, while PLA2 tests if the cross-linked CAP forms a complex with endogenous ceramide. We used the novel cross-link/PLA assay to visualize CRP association of (acetylated) tubulin and VDAC1 at membranes, microtubules, and mitochondria, respectively. We confirmed cross-linking of the two CAPs to pacFACer by streptavidin pull-down assays. In addition, coimmunoprecipitation assays using anti-ceramide antibody confirmed that the CAPs were associated with ceramide in cellular membranes. Ceramide depletion using the ceramide synthase inhibitor fumonisin B1 (FB1) indicated that that a microenvironment of endogenous ceramide in CRPs is critical for cross-linking of CAPs to pacFACer. Finally, incubation with amyloid beta (Aβ) peptide enhanced pacFACer cross-linking to VDAC1, suggesting that Aβ induces or facilitates interaction of CAPs with ceramide in CRPs. In summary, our results show that CRPs are critical for mediating cross-linking to pacFACer and that the cross-link/PLA assay is a novel tool to visualize CAPs and protein interaction with ceramide.

MATERIALS AND METHODS

Reagents and Antibodies

Dulbecco Modified Eagle Medium (DMEM) was from Hyclone (Logan, UT, United States), and Fetal Bovine Serum (FBS) was from Atlanta Biologicals (Flowery Branch, GA, United States). Penicillin and streptomycin (cat# 15146) were purchased from GIBCO (Grand Island, NY, United States). HEK293T cells were received from Dr. Lin Mei (Augusta University, Augusta,

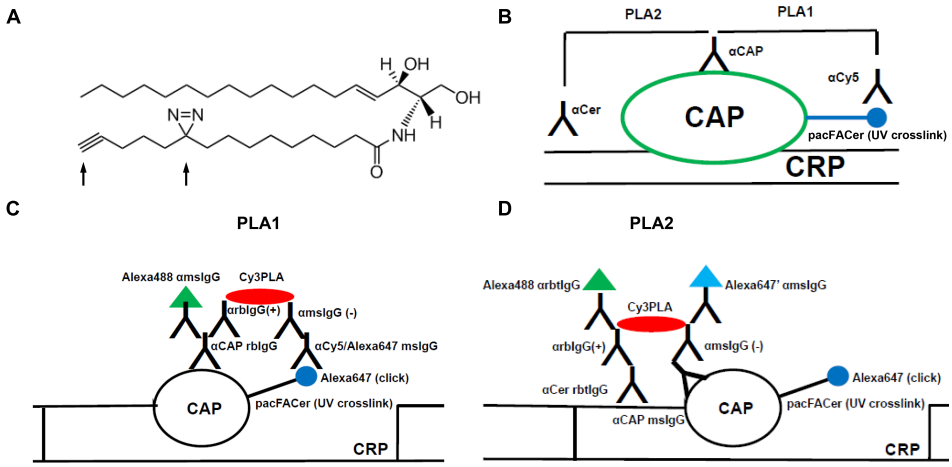

FIGURE 1 | Schematic description of the cross-link/PLA assay. **(A)** Structure of N-(9-(3-pent-4-ynyl-3-H-diazirin-3-yl)-non-anoyl)-D-erythro-sphingosine (pacFACer). Arrows point at the diazirine and alkyne groups used for UV cross-linking and click chemistry-mediated cycloaddition, respectively. **(B)** Overview on PLA1 [using antibodies (anti-cy5/Alexa647 mouse IgG)] to Alexa Fluor 647 conjugated to cross-linked pacFACer and ceramide-associated protein (CAP), and PLA2 (using antibodies to CAP and ceramide). **(C,D)** Details on antibodies used for PLA1 and PLA2. CRP, ceramide-rich platform.

GA, United States) and Neuro2a (N2a) cells (ATCC CCL-131) were obtained from ATCC (Manassas, VA, United States). Duolink PLA probe anti-rabbit plus (DUO92002), Duolink PLA probe anti-mouse minus (DUO92004), and Duolink detection reagent red (DUO92008) were purchased from Sigma Aldrich (St. Louis, MO, United States). N-(9-(3-pent-4-ynyl-3-H-diazirin-3-yl)-non-anoyl)-D-erythro-shpingosine (pacFACer, cat# 900404) was obtained from Avanti Polar Lipids (Alabaster, AL, United States). Click-iT cell reaction kits (cat# C10269), Alexa Fluor 647 azide (cat# A10277), protease and phosphatase inhibitors (cat# A32961) were from ThermoFisher Scientific (West Columbia, SC, United States); Click chemistry protein reaction buffer kits (cat# 1001) and TAMRA-biotin-azide (cat# 1048-5) were from Click Chemistry Tools (Scottsdale, AZ, United States). SDS-PAGE sample buffer (cat# S3401) was from Sigma-Aldrich (St. Louis, MO, United States).Fumonisin B1 (cat# 62580) was purchased from Cayman Che mical (Ann Arbor, MI, United States). Amyloid β_{1-42} (cat# AS-60479-01) was obtained from Anaspec (Freemont, CA, United States) was dissolved in 1% ammonia and diluted to 1 mg/ml and neutralized in PBS prior to use. Protein A/G magnetic beads (cat# 88803) was from Pierce Biotechnology (Rockford, IL, United States). Antibodies: Anti ceramide rabbit IgG (1:100 for immunocytochemistry; 1:200 for PLAs) was generated in our laboratory (Krishnamurthy et al., 2007). Anti-GAPDH antibody (cat# D16H11, 1:1000) was obtained from Cell Signaling Technology (Danvers, MA, United States). Anti-acetylated tubulin mouse IgG (cat# T6793, 1:3000 immunocytochemistry; 1:5000 for immunoblot and PLAs) was purchased from Sigma-Aldrich (St. Louis, MO, United States). Anti cy5/Alexa Fluor 647 (cat# sc-166896, 1:100 for PLAs) was from Santa Cruz Biotechnology (Dallas, TX, United States). Anti VDAC1 rabbit IgG (cat# ab15895, 1:200 for immunocytochemistry and PLAs; 1:500 for immunoblots) was purchased from abcam (Cambridge, MA, United States). Secondary antibodies conjugated to Alexa or Cy fluorophores were raised in donkey and purchased from the Jackson Laboratory (Bar Harbor, ME, United States).

Primary Cultures of Astrocytes

All experiments using primary cultures of astrocytes were carried out according to an Animal Use Protocol approved by the Institutional Animal Care and Use Committee at University of Kentucky. Primary glial cells were isolated from brains of P0-P1 C57BL/6 mice following a protocol previously published (Kong et al., 2018). In brief, brains were dissociated in PBS containing 0.1M glucose, passed through a 40 μm filter, and plated in T-25 flasks in DMEM supplemented with 10% fetal bovine serum, and 1% penicillin/streptomycin solution at 37°C in a humidified atmosphere containing 5% CO_2. After 7 days, adherent cells were passed to 24-well plates containing uncoated glass coverslips and cultured in DMEM as described above.

Cross-Linking to pacFACer and Click Chemistry-Mediated Conjugation With Fluorophores

N2a cells or primary cultured astrocytes were incubated under protection from light for 30 min in DMEM medium with 5 μM of the bifunctional ceramide analog N-(9-(3-pent-4-ynyl-3-H-diazirin-3-yl)-non-anoyl)-D-erythro-shpingosine (pacFACer, 1:1000 from a stock in ethanol/2% dodecane). Cells were UV irradiated at 365 nm for 15 min at 37°C in a humidified atmosphere containing 5% CO_2. Cells were further processed under different treatment conditions depending on final labeling requirements. For visualization of cross-linked proteins at their initial subcellular labeling site, cells were fixed with 4% *p*-formaldehyde/0.5% glutaraldehyde for 15 min at room temperature. For visualization of cross-linked proteins after intracellular transport, cells were washed with PBS and then further incubated for 16 h in medium prior to fixation. Following

fixation with *p*-formaldehyde/glutaraldehyde, cells were either directly subjected to the click reaction or first permeabilized by treatment with 0.2% Triton X-100 in PBS for 5 min at room temperature, followed by blocking of non-specific binding sites with 3% ovalbumin in PBS for 1 h at 37°C, and then incubation with anti-ceramide antibody for overnight at 4°C. In this case, cells were subjected to a second fixation reaction with *p*-formaldehyde/glutaraldehyde prior to the click reaction. Cells were washed with PBS and then twice with methanol to remove non-cross-linked pacFACer. The click reaction was performed as previously described using the Click-iT Cell Reaction buffer kit (Thermo Fisher Scientific) and Alexa Fluor 647 azide as fluorophore following the protocol provided by the manufacturer.

pacFACer Cross-Linking and Streptavidin Pull-Down

N2a cells were incubated with pacFACer (5 μM) for 30 min and then UV irradiated at 365 nm for 15 min at 37°C in a humidified atmosphere containing 5% CO_2. After washing with PBS twice, non-cross-linked pacFACer was removed by washing and fixing cells with ice-cold methanol for 30 min at −20°C. Cells were scraped off in 1 ml of PBS and collected by centrifugation at 15,000 × *g* for 10 min. Cell pellets were solubilized in 400 μl of 1% SDS in PBS containing protease and phosphatase inhibitors and heated for 10 min at 60°C. Insoluble material was removed by centrifugation at 15,000 × *g* for 10 min at room temperature. The click reaction was performed using the protein reaction kit (Click Chemistry Tools) with 50 μM TAMRA-biotin-azide (Click Chemistry Tools) following the protocol provided by the manufacturer. Non-conjugated TAMRA-biotin-azide was removed by precipitating protein with chloroform/methanol as previously described (Kong et al., 2015, 2018). The resulting protein pellets were solubilized with 100 μl of 1% SDS in PBS containing protease and phosphatase inhibitors and heating for 10 min at 60°C. Insoluble material was removed by centrifugation at 15,000 × *g* for 10 min at room temperature. SDS was neutralized by 10-fold dilution of the sample with 1% Triton X-100 in PBS and the sample centrifuged again to remove any residual insoluble material emerging after dilution. Proteins were then incubated with 50 μl of pre-equilibrated NeutrAvidin beads (ThermoFisher Scientific) for overnight at 4°C. Beads were washed twice with 0.1% SDS and 1% Triton X-100 in PBS, and then once with 50 mM Tris–HCl, pH 7.5. Beads were eluted with SDS-sample buffer (Sigma) containing 6 M urea for 10 min at 60°C and protein analyzed by SDS-PAGE and immunoblotting.

Immunoprecipitation of Ceramide-Enriched Vesicles

Immunprecipitation of ceramide-enriched vesicles was performed using a method established in our laboratory as previously published (He et al., 2012). HEK293T cell pellets were lysed using a Dounce homogenizer in lipid binding buffer [20 mM Tris–HCl, 150 mM NaCl, 1 mM EDTA, pH 7.5, supplemented with protein inhibitor cocktail (Roche)]. Any insoluble debris was removed by centrifugation at 20,800 × *g* for 30 min at 4°C. Lysates (1 ml) were then pre-cleared with Pierce protein A/G magnetic beads (Pierce Biotechnology, CAT#88802, Rockford, United States) and incubated overnight with non-specific rabbit IgG (control) or anti-ceramide rabbit IgG (5 μg/ml) at 4°C under rotational movement. Fifteen microliters of Pierce protein A/G magnetic beads were added to the samples and incubated for 2 h at room temperature under rotational movement. The beads were washed three times using lipid binding buffer. Protein bound to the beads was eluted by SDS-sample buffer and then subjected to SDS-PAGE for immunoblotting using anti-acetylated tubulin mouse IgG or anti-VDAC1 rabbit IgG.

Proximity Ligation Assays (PLAs) and Immunocytochemistry

N2a cells, HEK293T cells, and primary cultured astrocytes grown on glass cover slips were subjected to the pacFACer cross-linking and click reactions as described and then further analyzed in two distinct PLA assays. PLA1 used primary antibodies against the candidate CAP presumably cross-linked to pacFACer and the fluorophore attached via click addition. In our study, we used anti acetylated tubulin or anti VDAC1 rabbit IgGs and anti Cy5/Alexa Fluor 647 mouse IgG. PLA2 used primary antibodies raised in mouse against the candidate CAP and anti-ceramide rabbit IgG. Accordingly, PLA1 and 2 were performed using anti-rabbit PLUS affinity-purified donkey anti-rabbit IgG (H + L) and anti-mouse MINUS affinity-purified donkey anti-mouse IgG (H + L). This reaction and the consecutive ligation and amplification steps were performed following the protocol provided by the manufacturer [Duolink PLA kit red (Texas Red) from Sigma-Aldrich] as previously described (Kong et al., 2018). After completion of the PLA1 and 2 reactions, samples were post-incubated with secondary antibodies conjugated to fluorophores in unused fluorescence channels to visualize the intracellular distribution of antigens tested in the PLA assay. Epifluorescence microscopy was performed with a Nikon Ti2 Eclipse microscope equipped with NIS Elements software using Z-scanning with 60× or 100× oil immersion objectives at the step size (0.2–0.3 μm) recommended by the software. Images were processed using the NIS Elements 3D deconvolution program at settings recommended by the software (automated) and PLA signals counted using NIS Elements and NIH Image J software. Images shown in figures are 3D rendered Z-scans. For counting, Z-scan images were collapsed onto one plane and thresholds for pixel size and fluorescence intensity defined based on comparison with non-deconvolved images to represent authentic signals. All of the data were collected by laboratory personnel blinded to the origin of the samples from at least three independent cell cultures using at least five randomly selected areas/culture. Images obtained with secondary antibody only were used as negative controls.

Statistical Analysis

Statistical significance was calculated using Student's *t*-test with or one-way ANOVA and Tukey's *post hoc* with GraphPad Prism. $P < 0.05$ was considered significant.

Miscellaneous

Protein concentrations of input used for pull-down experiments were determined using the RD/DC protein assay (Bio Rad), following a protocol provided by the manufacturer. For immunoblot analysis, equal amounts of protein were loaded onto a 10% denaturing and reducing SDS gel and SDS-PAGE was performed using the Laemmli method. For the immunoblotting reaction, membranes were first blocked with 3% BSA in PBST (PBS containing 0.1% Tween-20) and incubated with primary antibodies in blocking buffer overnight at 4°C. Membranes were then washed three times with PBST and incubated with the appropriate horseradish peroxidase-conjugated secondary antibodies for 1 h at room temperature. After washing, bands were detected using the Pico or Femto ECL assay from Pierce/Thermo Fisher Scientific and Azure imager.

RESULTS

Cross-Linking/PLA Using pacFACer – Principle of Method

To test association of a cross-linked protein with CRPs, cells were incubated with pacFACer and exposed to UV radiation. Cells were either fixed with para-formaldehyde/glutaraldehyde to identify the initial cellular site of pacFACer cross-linking, or alternatively, they were further incubated to monitor intracellular transport and distribution of the cross-linked protein over time. After fixation, two sets of cells underwent copper-mediated click chemistry reactions to attach the Alexa Fluor 647 fluorophore, which were followed by two distinct PLAs (**Figure 1B**). For the first PLA reaction (PLA1), fixed cells were directly subjected to the click reaction and then incubated with antibodies to perform the PLA1 reaction (**Figure 1C**). For the second PLA reaction (PLA2), cells were first incubated with antibodies – one of which was anti-ceramide antibody – and then fixed again prior to the click reaction (**Figure 1D**). The second fixation step was critical to keep anti-ceramide antibody in place since click chemistry requires wash steps with organic solvent that would remove ceramide as antigen from cellular membranes.

The PLAs were used for *in situ* visualization of antigen complexes using fluorescence microscopy. PLA1 used a combination of antibodies to a potential CAP and the fluorophore attached by the click reaction. This PLA reaction tested if pacFACer was cross-linked to the CAP of interest. PLA1 was complemented by pull-down assays with streptavidin beads after using biotin azide for cross-linking. PLA2 used a combination of antibodies to the specific CAP and ceramide. This PLA reaction tested if the CAP cross-linked to pacFACer formed a complex with endogenous ceramide. PLA2 was complemented by coimmunoprecipitation assays using anti-ceramide antibody.

The cross-link/PLA assay was supplemented by additional colabeling experiments and PLA reactions with or without click addition of the fluorophore. For example, the PLA1 reaction was combined with antibodies against organelle markers to identify the subcellular localization of the cross-linked CAP. When omitting click addition or even crosslinking, PLA2 was followed by incubation with fluorescent secondary antibodies to the primary antibodies used for PLA. This reaction visualized the intracellular distribution of the complex between the candidate CAP and endogenous ceramide within the entire pool of ceramide and the CAP. It is important that all secondary antibodies used for PLA or immunofluorescence were raised in a species distinct from that of any of the primary antibodies. Alternatively, kits are commercially available for direct labeling of the primary antibodies with oligonucleotides for PLA or fluorophores for immunofluorescence microscopy.

pacFACer Is Cross-Linked to Tubulin and VDAC1 at Microtubules and Mitochondria, Respectively

pacFACer was UV cross-linked to proteins in intact cells and then covalently attached to a fluorescent dye that also carries a biotin group (TAMRA-biotin-azide). Streptavidin pull-down/fluorescent blot analysis showed that a variety of proteins were cross-linked to pacFACer (**Figure 2A**). Our previous studies – including proteomics analyses of ceramide-binding proteins – indicated that tubulin and VDAC1 are among these proteins, which was confirmed by immunoblot analyses (**Figure 2B** and see **Supplementary Figure 1** for original images from immunoblots) (Kong et al., 2018). The housekeeping protein GAPDH was not among the pulled-down proteins demonstrating the specificity of the pacFACer cross-linking reaction. The significance of pacFACer cross-linking for identifying binding of tubulin and VDAC1 to endogenous ceramide was tested by coimmunoprecipitation of the two proteins using anti-ceramide IgG. Previously, we introduced this method to isolate ceramide-enriched vesicles from cell lysates and identify proteins associated with these vesicles (He et al., 2012; Kong et al., 2018; Zhu et al., 2019). **Figure 2C** shows that acetylated tubulin and VDAC1 were coimmuniprecipitated with anti-ceramide IgG confirming that these two proteins are associated with endogenous ceramide (see **Supplementary Figure 1** for original images from immunoblots).

Next, we tested if acetylated tubulin and VDAC1 were cross-linked to pacFACer at microtubules and mitochondria, respectively. Acetylated tubulin was chosen because of our previously published studies showing colocalization of ceramide with acetylated tubulin (He et al., 2014; Kong et al., 2015, 2018). **Figures 3A,B** shows that the fluorescence signal for cross-linked pacFACer (visualized by attaching Alexa Fluor 647) was colocalized with the PLA1 signal (Texas Red fluorescence) for a complex of pacFACer and acetylated tubulin at microtubules (visualized by Alexa Fluor 488 for acetylated tubulin). The PLA1 reaction was also performed with the cell types used for the pull-down assays (N2a and HEK293T cells, see **Supplementary Figure 2**), confirming results obtained with primary cultured astrocytes (**Figure 3**). **Figures 4A,B** shows the results of the PLA2 reaction using antibodies to acetylated tubulin and ceramide (see also **Supplementary Figure 3**). The results of the PLA2 reaction indicated that ceramide formed a complex with acetylated tubulin cross-linked to pacFACer at microtubules (arrows in **Figure 4A**). In addition, complexes for ceramide and acetylated tubulin were

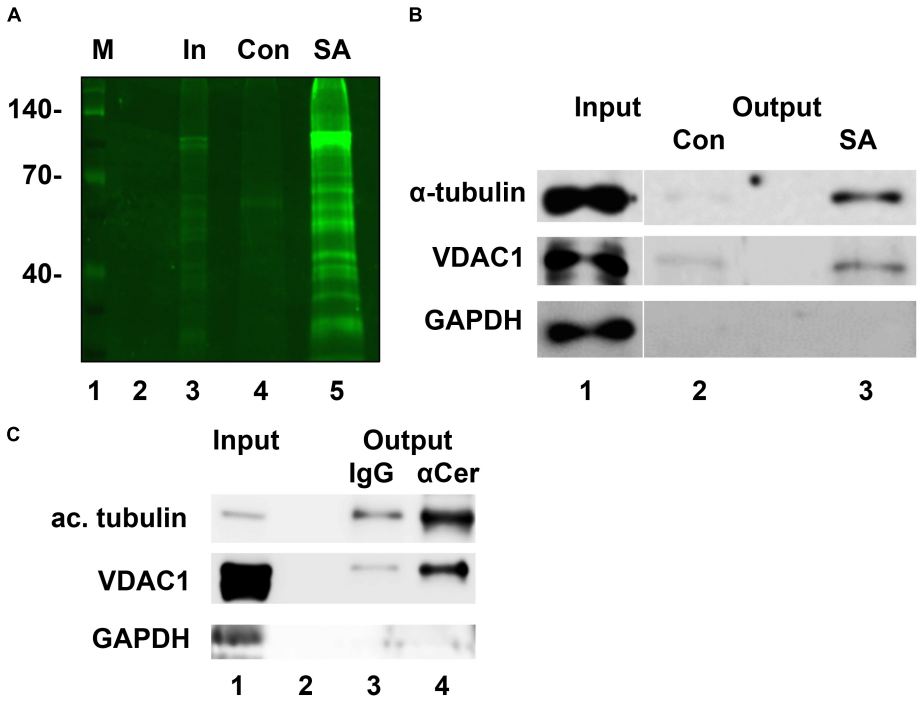

FIGURE 2 | Tubulin and VDAC1 are cross-linked to pacFACer and associated with ceramide vesicles. **(A)** N2a cells were incubated with pacFACer, UV cross-linked, and fixed with ice-cold methanol. Cells were scraped off, pelleted, and protein solubilized with 1% SDS in PBS. The copper-mediated click addition was performed using TAMRA-biotin-azide and non-incorporated reagent removed by chloroform/methanol extraction. Precipitated protein was re-solubilized and pacFACer cross-linked protein isolated by pull-down with streptavidin beads. Bound protein was eluted by heating in SDS sample buffer and separated by SDS gelectrophoresis. Lane 1, marker; lane 2, empty; lane 3, input used for streptavidin pull-down; lane 4, pull-down with streptavidin beads saturated with biotin (control); lane 5, pull-down with streptavidin beads (SA). **(B)** Assay performed as described in **(A)**, but gel immunoblotted and probed with antibodies to tubulin, VDAC1, and GAPDH. **(C)** Coimmunoprecipitation of acetylated tubulin and VDAC1 using antibody to ceramide to precipitate ceramide-enriched vesicles from lysates of HEK293T cells (lane 4). Non-specific rabbit IgG was used as the control (lane 3). Lane 1, input; lane 2, empty. GAPDH was not coimmunoprecipitated.

detected at the plasma membrane, particularly at microtubule attachment sites (arrows in **Figure 4B**). **Figures 5A,B** shows that cross-linked pacFACer was also colocalized with the PLA1 reaction for pacFACer and VDAC1 at mitochondria (see **Supplementary Figure 2** for PLA1 with N2a and HEK293T cells). The PLA2 reaction could not be reliably performed because of some degree of non-specific reactions with anti VDAC1 mouse IgG.

pacFACer Cross-Linking of Tubulin and VDAC1 Is Decreased by FB1 and Increased by Aβ

The colocalization of pacFACer cross-linked tubulin and VDAC1 with ceramide suggested that a ceramide-enriched membrane environment affects the cross-linking reaction. To test the effect of ceramide on pacFACer cross-linking we pre-incubated N2a cells and primary cultured astrocytes with fumonisin B1 (FB1), a fungus toxin specifically inhibiting ceramide synthase and reliably decreasing the ceramide concentration in a variety of cell types (Wang et al., 2009; Stiban et al., 2010; Lee et al., 2011; Kong et al., 2018). **Figures 6A–E** shows that ceramide depletion with FB1 reduced the amount of pacFACer cross-linked tubulin and VDAC1, suggesting that endogenous ceramide mediated the cross-linking reaction to pacFACer. This conclusion was confirmed by PLA1 assays after pre-incubation with FB1 [**Figure 6F** and see **Supplementary Figure 1** (original images of immunoblots), 4 (fluorescence images) for details on quantitation shown in **Figure 6**], showing that the number of PLA signals for pacFACer cross-linked tubulin and VDAC1 was reduced by 50–70%.

In addition to direct interference with ceramide generation, we incubated N2a cells and primary astrocytes with Aβ to test the effect on pacFACer cross-linking of tubulin and VDAC1. We chose Aβ because it is known to increase the ceramide level in astrocytes and to interact with tubulin and VDAC1 (Manczak and Reddy, 2012; Wang et al., 2012; Fernandez-Echevarria et al., 2014; Saha et al., 2015; Smilansky et al., 2015). Our previous studies also showed that it is an infectious protein the spreading of which is mediated by association with ceramide-enriched exosomes (Wang et al., 2012; Dinkins et al., 2016a,b). **Figures 7A,B** shows that overnight incubation with 1 μM oligomeric Aβ increased the amount of pacFACer cross-linked VDAC1, suggesting that Aβ enhanced the effect of ceramide on facilitating cross-linking to pacFACer (see **Supplementary Figure 1** for original images of immunoblots shown in **Figure 7**). Consistent with the pull-down assay, immunocytochemistry showed that Aβ induced colocalization between VDAC1 and cross-linked pacFACer as

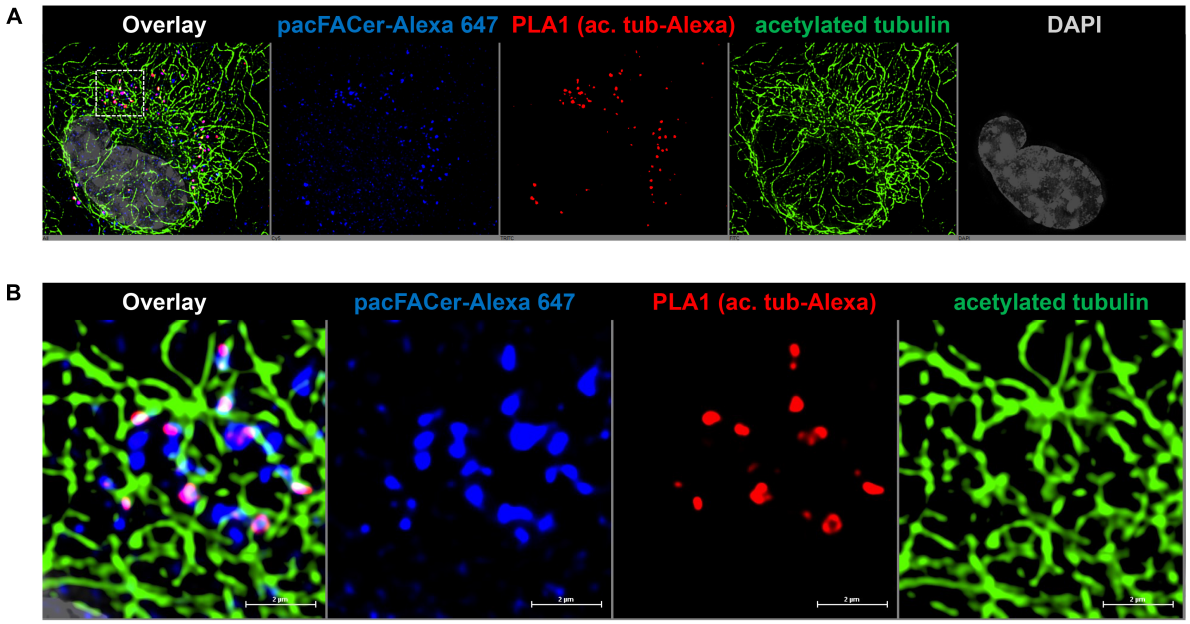

FIGURE 3 | PLA1 reaction using antibodies against acetylated tubulin and Alexa Fluor 647. **(A)** Primary cultured astrocytes were subjected to the PLA1 reaction (fluorescence signals for complexes of acetylated tubulin with Alexa Fluor 647-pacFACer are pseudo-colored in red) and then post-incubated with Alexa Fluor 488-conjugated secondary antibody to visualize microtubules (pseudo-colored in green). Cross-linked pacFACer (conjugated to Alexa Fluor 647) is pseudo-colored in blue. **(B)** Detail from **(A)** shows microtubules with acetylated tubulin cross-linked to pacFACer.

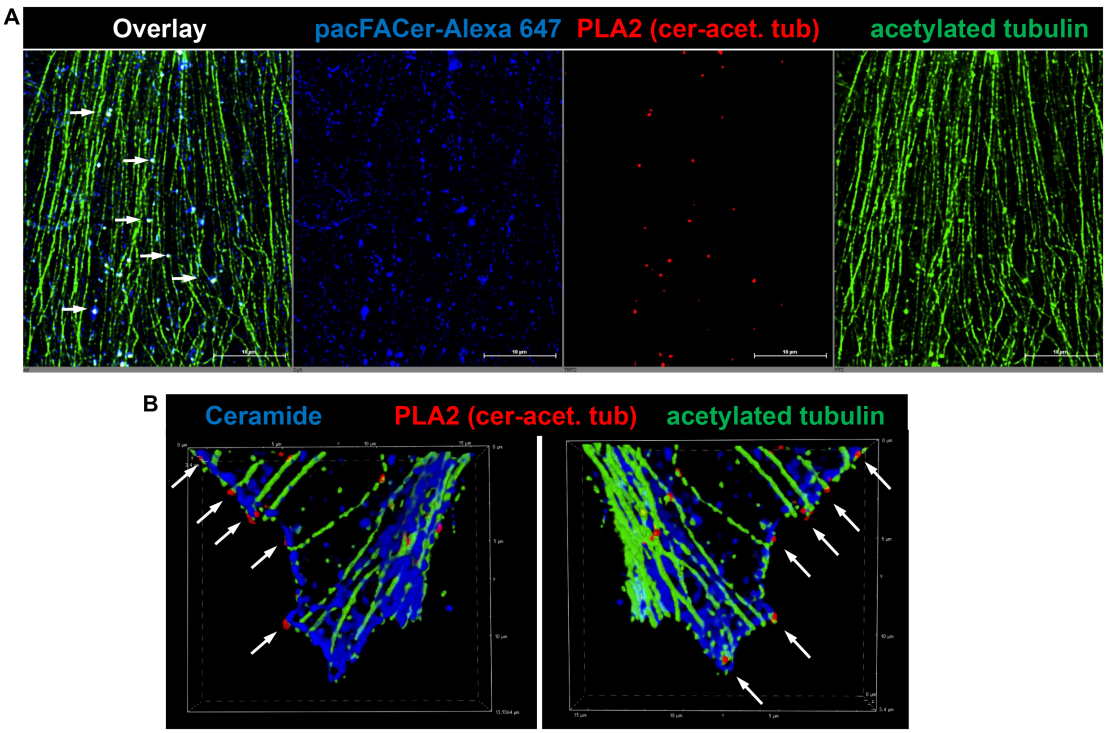

FIGURE 4 | PLA2 reaction using antibodies against acetylated tubulin and ceramide. **(A)** Primary cultured astrocytes were subjected to the PLA2 reaction (fluorescence signals for complexes of acetylated tubulin with ceramide are pseudo-colored in red) and then post-incubated with Alexa Fluor 488-conjugated secondary antibody to visualize microtubules (pseudo-colored in green). Cross-linked pacFACer (conjugated to Alexa Fluor 647) is pseudo-colored in blue. **(B)** PLA2 reaction performed as in **(A)**, but pacFACer not conjugated to Alexa Fluor 647. The PLA2 reaction was post-incubated with Alexa Fluor 488-conjugated anti mouse IgG to visualize acetylated tubulin (pseudo-colored in green) and Alexa Fluor 647-conjugated anti-rabbit IgG to visualize ceramide (pseudo-colored in blue).

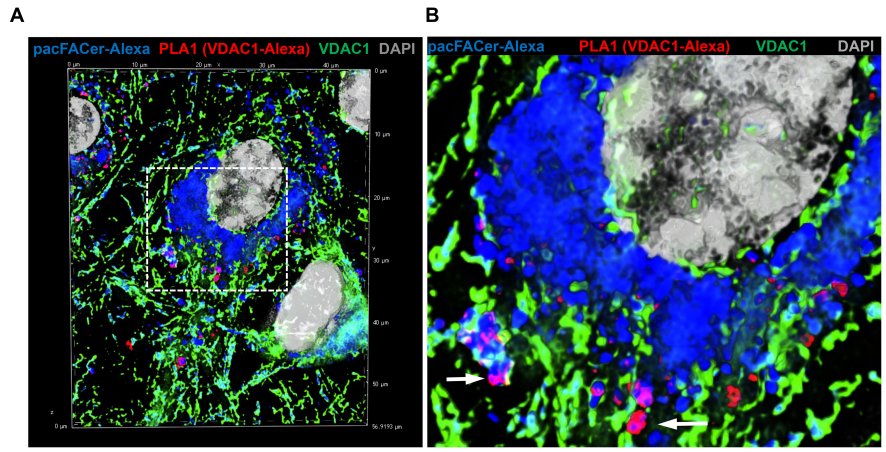

FIGURE 5 | PLA1 reaction using antibodies against VDAC1 and Alexa Fluor 647. **(A)** Primary cultured astrocytes were subjected to the PLA1 reaction (fluorescence signals for complexes of VDAC1 with Alexa Fluor 647-pacFACer are pseudo-colored in red) and then post-incubated with Alexa Fluor 488-conjugated anti-rabbit IgG to visualize mitochondria (pseudo-colored in green). Cross-linked pacFACer (conjugated to Alexa Fluor 647) is pseudo-colored in blue. **(B)** Detail from **(A)** shows mitochondria with VDAC1 cross-linked to pacFACer.

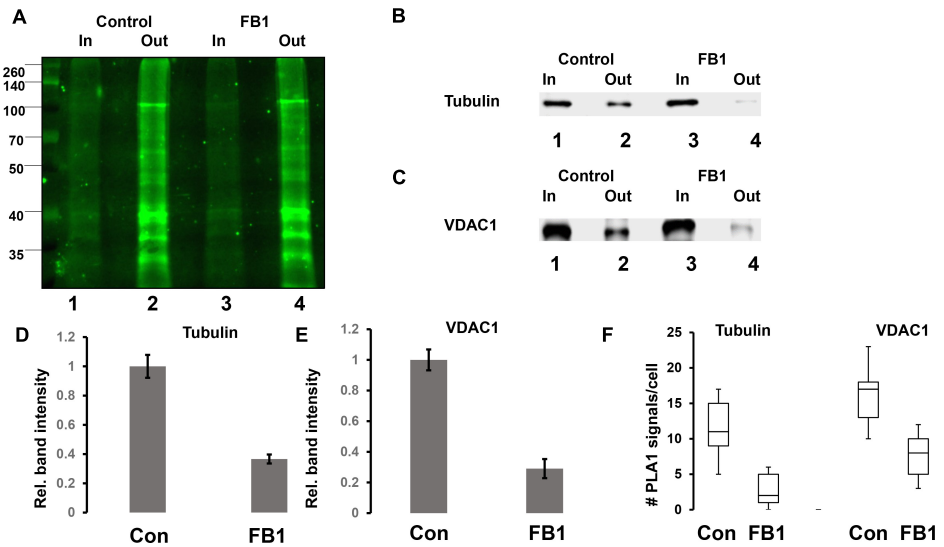

FIGURE 6 | Ceramide depletion reduces cross-linking of pacFACer to tubulin and VDAC1. **(A)** N2a cells with or without pre-incubation for 48 h with 5 μM FB1 were treated with pacFACer and cross-linked protein isolated and separated by SDS-PAGE as described in the legend for **Figure 2**. Lane 1, input for pull-down of pacFACer cross-linked protein from non-treated control cells; lane 2, output from pull-down; lane 3, input for pull-down of pacFACer cross-linked protein from FB1-treated cells; lane 4, output from pull-down. **(B,C)** Assay performed as described in **(A)**, but gel immunoblotted and probed with antibodies to tubulin **(B)** and VDAC1 **(C)**. **(D)** Quantitation of **(B)**. $n = 7$, $P < 0.05$. **(E)** Quantitation of **(C)**. $n = 5$, $P < 0.005$. **(F)** Quantitation of PLA1 signals for pacFACer cross-linked tubulin and VDAC1 in primary cultured astrocytes with or without ceramide depletion by incubation with FB1. $n = 5$, $P < 0.05$.

well as ceramide (**Figure 7C**). In summary, our results indicated that the extent of pacFACer cross-linking to VDAC1 was correlated with the extent of ceramide interaction.

DISCUSSION

Ceramide is a sphingolipid the interaction of which with proteins is implicated in a plethora of physiological and pathophysiological processes. In cellular membranes, it is enriched in microdomains or rafts, currently referred to as CRPs (Burgert et al., 2017; Bieberich, 2018). CRPs are suggested to form contact sites with the cytoskeleton, intracellular membranes and organelles, and infectious proteins, cells, and viruses. One of the greatest challenges in determining the function of CRPs is to visualize the interaction of ceramide with proteins in these contact sites. Since pacFACer is taken up by living cells, cross-linking can be used to identify and visualize proteins potentially associated with ceramide. We and others used this method to visualize pacFACer cross-linked tubulin and other CAPs (Kong

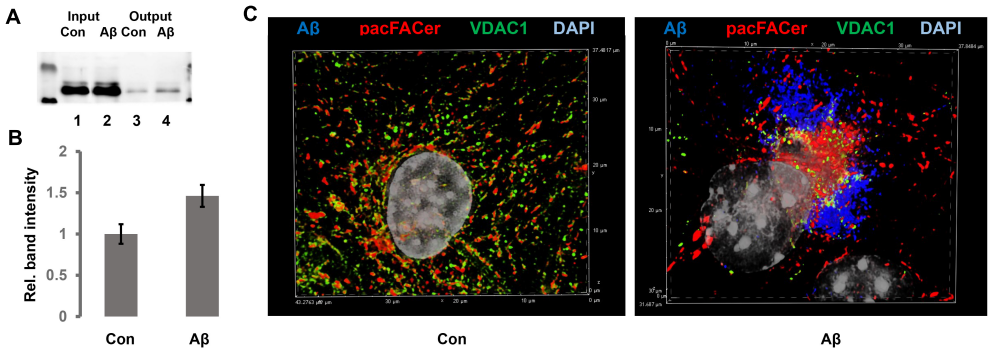

FIGURE 7 | Aβ enhances cross-linking of pacFACer to VDAC1. **(A)** N2a cells with or without pre-incubation for 24 h with 1 μM $Aβ_{42}$ were treated with pacFACer and cross-linked protein isolated and separated by SDS-PAGE, followed by immunoblotting using antibody to VDAC1. Lane 1, input for pull-down of pacFACer cross-linked protein from non-treated control cells; lane 2, input for pull-down of pacFACer cross-linked protein from $Aβ_{42}$-treated cells; lane 3, output from pull-down control; lane 4, output from pull-down Aβ. **(B)** Quantitation of **(A)**. $n = 6$, $P < 0.005$. **(C)** Immunocytochemistry of pacFACer cross-linked astrocytes (pseudo-colored in red) with or without Aβ treatment. VDAC1 was labeled with anti-VDAC1 rabbit IgG and Alexa Fluor 488 anti-rabbit IgG (pseudo-colored in green) and $Aβ_{42}$ was labeled with anti-$Aβ_{42}$ mouse IgG (clone 4G8, pseudo-colored in blue).

et al., 2015, 2018; Dinkins et al., 2016a; Bockelmann et al., 2018). However, there are two major limitations to this method. When using photoactivatable sphingolipid analogs for labeling in fluorescence microscopy, the first limitation arises from the spatial resolution of the fluorescence signal, which is 200 nm at best. The spatial resolution can be improved up to 10-fold using superresolution microscopy (Burgert et al., 2017). However, there is still the possibility that the CAP is co-localized with the cross-linked protein, but not identical to it. Therefore, visualization of cross-linked CAPs using colabeling in immunofluorescence microscopy should be complemented by another method such as cross-linking to biotin and pull-down with immobilized streptavidin, followed by immunoblotting or proteomics analysis of the CAP. Unfortunately, there is not always sufficient amount of protein to perform this type of analysis and pull-down from a cell homogenate does not mean that a colabeled protein is also cross-linked in a complex with ceramide visualized by immunocytochemistry. Recent studies addressed a similar problem in the context of visualizing palmitoylated proteins using incorporation of a clickable palmitic acid analog (Gao and Hannoush, 2014, 2016). After attaching the fluorophore to protein-linked palmitic azide using click chemistry, PLA was performed using antibodies against the fluorophore and the presumably palmitoylated protein. We modified this approach using Alexa Fluor 647 azide clicked to cross-linked pacFACer and anti-Cy5/Alexa647 mouse IgG for the PLA reaction with antibody against the presumed CAP. In our assays to detect pacFACer cross-linked tubulin and VDAC1, this reaction is referred to as PLA1.

The second limitation of cross-linking sphingolipid analogs is the lack of information on colocalization of the cross-linked protein with the actual sphingolipid in cells. It is not clear if a protein cross-linked to pacFACer colocalizes or associates with endogenous ceramide. This limitation mainly arises from the non-fixability of lipids with *p*-formaldehyde or incompatibility of membrane lipids with fixation using organic solvents such as methanol or acetone. We developed a protocol bypassing this problem by fixing the anti-ceramide antibody instead of the lipid. Using clickable (not-crosslinked) ceramide analogs we demonstrated that this method reliably labels the subcellular distribution of endogenous ceramide (Walter et al., 2016). The colocalization of the pacFACer cross-linked protein with ceramide is tested in the PLA2 reaction. We show that any PLA reaction can be complemented by post-incubation with a second set of secondary antibodies conjugated to fluorophores. This reaction visualizes the distribution of the CAP and ceramide and at the same time, localization of their complexes. Combining PLA with the click addition of a fluorophore to pacFACer visualizes distribution of the cross-linked protein within CRPs. In our study, PLA2 showed complexes of cross-linked tubulin and VDAC1 with ceramide that are localized in CRPs, suggesting that ceramide affects the cross-linking reaction or distribution of the cross-linked CAP.

Ceramide can affect the cross-linking reaction of a CAP to pacFACer in two ways: it can either compete with pacFACer for the binding site to ceramide or it can facilitate cross-linking by embedding pacFACer in CRPs. These opposite effects were tested by depleting astrocytes and N2a cells of ceramide with fumonisin B1 (FB1), a fungus toxin specifically inhibiting ceramide synthases. The pull-down assays showed that FB1 reduced the amount of cross-linked tubulin and VDAC1 suggesting that ceramide facilitates cross-linking of CAPs to pacFACer, probably by embedding pacFACer into the ceramide microenvironment of CRPs. This conclusion is consistent with the observation that other ceramide analogs are embedded into CRPs when exogenously administered to cells (Walter et al., 2016). While these results cannot demonstrate the role of ceramide binding for the function of a particular protein, they suggest that cross-linking to pacFACer and monitoring complex formation of the cross-linked protein with ceramide (cross-link/PLA assay) can be used to probe the distribution of CAPs to CRPs.

We used the cross-link/PLA assay to test the effect of Aβ on pacFACer cross-linking to VDAC1. Our results showed that Aβ

increased the amount of cross-linked VDAC1, suggesting that it is embedded into CRPs promoting the pacFACer cross-linking reaction. Most recently, we reported that ceramide-associated tubulin (CAT) forms a complex with VDAC1 that blocks ADP/ATP transport through the outer mitochondrial membrane (Kong et al., 2018). Results in this study suggest that ceramide association of VDAC1 takes part in this process. In addition to pacFACer cross-linking, ceramide association of VDAC1 is consistent with the observation that it is coimmunoprecipitated with anti ceramide antibody. We also showed that Aβ incubation of astrocytes led to clustering of mitochondria, which was confirmed in the studies presented here. It is currently not known if Aβ first binds to VDAC1 and enhances cross-linking to pacFACer or if Aβ initially associates with CRPs and then enhances pacFACer cross-linking of VDAC1 (Gulbins et al., 2004; Bollinger et al., 2005; Grassme et al., 2008). It is also not known if other VDAC isoforms associate with CRPs. Most recently, VDAC2 was found to bind to ceramide and cross-link to pacFACer (Dadsena et al., 2019), suggesting that several CAPs are cross-linked to pacFACer after embedding into CRPs. In summary, our data show that the novel labeling technique (cross-link/PLA) is a valuable tool to visualize CAPs in CRPs, which will also help determine the function of ceramide in contact sites to infectious proteins and other pathogens.

DATA AVAILABILITY

All datasets generated for this study are included in the manuscript and/or the **Supplementary Files**.

ETHICS STATEMENT

All experiments using primary cultures of astrocytes were carried out according to an Animal Use Protocol approved by the Institutional Animal Care and Use Committee at the University of Kentucky.

AUTHOR CONTRIBUTIONS

XJ performed the key experiments (cross-linking and click chemistry) and wrote the critical parts of the manuscript. ZZ also performed the click chemistry experiments. PT performed the pull-down with anti-ceramide antibody. LZ and HQ performed the FB1 incubation. AE, SK, and SC performed the *in vitro* experiments with amyloid. WZ performed the proteomics analysis. GW and SS wrote parts of the manuscript. EB performed parts of the microscopy experiments and PLAs, and wrote parts of the manuscript.

FUNDING

This work was supported by the National Institutes of Health grants (R01AG034389 and R01NS095215), and the National Science Foundation grant (NSF 1615874).

ACKNOWLEDGMENTS

The authors thank Chair Dr. Alan Daugherty, the Department of Physiology, College of Medicine, University of Kentucky, for institutional support.

SUPPLEMENTARY MATERIAL

The Supplementary Material for this article can be found online at: https://www.frontiersin.org/articles/10.3389/fcell.2019.00166/full#supplementary-material

REFERENCES

Bieberich, E. (2018). Sphingolipids and lipid rafts: novel concepts and methods of analysis. *Chem. Phys. Lipids* 216, 114–131. doi: 10.1016/j.chemphyslip.2018.08.003

Bockelmann, S., Mina, J. G. M., Korneev, S., Hassan, D. G., Muller, D., Hilderink, A., et al. (2018). A search for ceramide binding proteins using bifunctional lipid analogs yields CERT-related protein Stard7. *J. Lipid Res.* 59, 515–530. doi: 10.1194/jlr.M082354

Bollinger, C. R., Teichgraber, V., and Gulbins, E. (2005). Ceramide-enriched membrane domains. *Biochim. Biophys. Acta* 1746, 284–294. doi: 10.1016/j.bbamcr.2005.09.001

Burgert, A., Schlegel, J., Becam, J., Doose, S., Bieberich, E., Schubert-Unkmeir, A., et al. (2017). Characterization of Plasma Membrane Ceramides by Super-Resolution Microscopy. *Angew. Chem. Int. Ed Engl.* 56, 6131–6135. doi: 10.1002/anie.201700570

Canals, D., Salamone, S., and Hannun, Y. A. (2018). Visualizing bioactive ceramides. *Chem. Phys. Lipids* 216, 142–151. doi: 10.1016/j.chemphyslip.2018.09.013

Dadsena, S., Bockelmann, S., Mina, J. G. M., Hassan, D. G., Korneev, S., Razzera, G., et al. (2019). Ceramides bind VDAC2 to trigger mitochondrial apoptosis. *Nat. Commun.* 10:1832. doi: 10.1038/s41467-019-09654-4

Dinkins, M. B., Enasko, J., Hernandez, C., Wang, G., Kong, J., Helwa, I., et al. (2016a). Neutral Sphingomyelinase-2 Deficiency Ameliorates Alzheimer's Disease Pathology and Improves Cognition in the 5XFAD Mouse. *J. Neurosci.* 36, 8653–8667. doi: 10.1523/JNEUROSCI.1429-16.2016

Dinkins, M. B., Wang, G., and Bieberich, E. (2016b). Sphingolipid-enriched extracellular vesicles and Alzheimer's disease: a decade of research. *J Alzheimers Dis.* 60, 757–768. doi: 10.3233/JAD-160567

Dobrowsky, R. T., and Hannun, Y. A. (1992). Ceramide stimulates a cytosolic protein phosphatase. *J. Biol. Chem.* 267, 5048–5051.

Fernandez-Echevarria, C., Diaz, M., Ferrer, I., Canerina-Amaro, A., and Marin, R. (2014). Abeta promotes VDAC1 channel dephosphorylation in neuronal lipid rafts. Relevance to the mechanisms of neurotoxicity in Alzheimer's disease. *Neuroscience* 278, 354–366. doi: 10.1016/j.neuroscience.2014.07.079

Fink, J., and Seibel, J. (2018). Click reactions with functional sphingolipids. *Biol. Chem.* 399, 1157–1168. doi: 10.1515/hsz-2018-0169

Gao, X., and Hannoush, R. N. (2014). Method for cellular imaging of palmitoylated proteins with clickable probes and proximity ligation applied to hedgehog, tubulin, and Ras. *J. Am. Chem. Soc.* 136, 4544–4550. doi: 10.1021/ja410068g

Gao, X., and Hannoush, R. N. (2016). Visualizing Wnt Palmitoylation in single cells. *Methods Mol. Biol.* 1481, 1–9. doi: 10.1007/978-1-4939-6393-5_1

Grassme, H., Becker, K. A., Zhang, Y., and Gulbins, E. (2008). Ceramide in bacterial infections and cystic fibrosis. *Biol. Chem.* 389, 1371–1379. doi: 10.1515/BC.2008.162

Gulbins, E., Dreschers, S., Wilker, B., and Grassme, H. (2004). Ceramide, membrane rafts and infections. *J. Mol. Med.* 82, 357–363. doi: 10.1007/s00109-004-0539-y

He, Q., Wang, G., Dasgupta, S., Dinkins, M., Zhu, G., and Bieberich, E. (2012). Characterization of an apical ceramide-enriched compartment regulating ciliogenesis. *Mol. Biol. Cell* 23, 3156–3166. doi: 10.1091/mbc.E12-02-0079

He, Q., Wang, G., Wakade, S., Dasgupta, S., Dinkins, M., Kong, J. N., et al. (2014). Primary cilia in stem cells and neural progenitors are regulated by neutral sphingomyelinase 2 and ceramide. *Mol. Biol. Cell* 25, 1715–1729. doi: 10.1091/mbc.E13-12-0730

Kong, J. N., Hardin, K., Dinkins, M., Wang, G., He, Q., Mujadzic, T., et al. (2015). Regulation of *Chlamydomonas flagella* and ependymal cell motile cilia by ceramide-mediated translocation of GSK3. *Mol. Biol. Cell* 26, 4451–4465. doi: 10.1091/mbc.E15-06-0371

Kong, J. N., Zhu, Z., Itokazu, Y., Wang, G., Dinkins, M. B., Zhong, L., et al. (2018). Novel function of ceramide for regulation of mitochondrial ATP release in astrocytes. *J Lipid Res.* 59, 488–506. doi: 10.1194/jlr.M081877

Krishnamurthy, K., Dasgupta, S., and Bieberich, E. (2007). Development and characterization of a novel anti-ceramide antibody. *J Lipid Res* 48, 968–975. doi: 10.1194/jlr.d600043-jlr200

Lee, H., Rotolo, J. A., Mesicek, J., Penate-Medina, T., Rimner, A., Liao, W. C., et al. (2011). Mitochondrial ceramide-rich macrodomains functionalize bax upon irradiation. *PLoS One* 6:e19783. doi: 10.1371/journal.pone.0019783

Maldonado, E. N., and Lemasters, J. J. (2012). Warburg revisited: regulation of mitochondrial metabolism by voltage-dependent anion channels in cancer cells. *J. Pharmacol. Exp. Ther.* 342, 637–641. doi: 10.1124/jpet.112.192153

Manczak, M., and Reddy, P. H. (2012). Abnormal interaction of VDAC1 with amyloid beta and phosphorylated tau causes mitochondrial dysfunction in Alzheimer's disease. *Hum. Mol. Genet.* 21, 5131–5146. doi: 10.1093/hmg/dds360

Mathias, S., Dressler, K. A., and Kolesnick, R. N. (1991). Characterization of a ceramide-activated protein kinase: stimulation by tumor necrosis factor alpha. *Proc. Natl. Acad. Sci. U.S.A.* 88, 10009–10013. doi: 10.1073/pnas.88.22.10009

Merrill, A. H. Jr., Sereni, A. M., Stevens, V. L., Hannun, Y. A., Bell, R. M., and Kinkade, J. M. Jr. (1986). Inhibition of phorbol ester-dependent differentiation of human promyelocytic leukemic (HL-60) cells by sphinganine and other long-chain bases. *J. Biol. Chem.* 261, 12610–12615.

Rostovtseva, T. K., and Bezrukov, S. M. (2008). VDAC regulation: role of cytosolic proteins and mitochondrial lipids. *J. Bioenerg. Biomembr.* 40, 163–170. doi: 10.1007/s10863-008-9145-y

Rostovtseva, T. K., Sheldon, K. L., Hassanzadeh, E., Monge, C., Saks, V., Bezrukov, S. M., et al. (2008). Tubulin binding blocks mitochondrial voltage-dependent anion channel and regulates respiration. *Proc. Natl. Acad. Sci. U.S.A.* 105, 18746–18751. doi: 10.1073/pnas.0806303105

Saha, A., Mohapatra, S., Kurkute, P., Jana, B., Mondal, P., Bhunia, D., et al. (2015). Interaction of abeta peptide with tubulin causes an inhibition of tubulin polymerization and the apoptotic death of cancer cells. *Chem. Commun.* 51, 2249–2252. doi: 10.1039/c4cc09390a

Santander, V. S., Campetelli, A. N., Monesterolo, N. E., Rivelli, J. F., Nigra, A. D., Arce, C. A., et al. (2019). Tubulin-Na(+), K (+) -ATPase interaction: involvement in enzymatic regulation and cellular function. *J. Cell Physiol.* 234, 7752–7763. doi: 10.1002/jcp.27610

Smilansky, A., Dangoor, L., Nakdimon, I., Ben-Hail, D., Mizrachi, D., and Shoshan-Barmatz, V. (2015). The Voltage-dependent anion channel 1 mediates amyloid beta toxicity and represents a potential target for Alzheimer disease therapy. *J. Biol. Chem.* 290, 30670–30683. doi: 10.1074/jbc.M115.691493

Stiban, J., Tidhar, R., and Futerman, A. H. (2010). Ceramide synthases: roles in cell physiology and signaling. *Adv. Exp. Med. Biol.* 688, 60–71. doi: 10.1007/978-1-4419-6741-1_4

Walter, T., Collenburg, L., Japtok, L., Kleuser, B., Schneider-Schaulies, S., Muller, N., et al. (2016). Incorporation and visualization of azido-functionalized N-oleoyl serinol in Jurkat cells, mouse brain astrocytes, 3T3 fibroblasts and human brain microvascular endothelial cells. *Chem. Commun.* 52, 8612–8614. doi: 10.1039/c6cc02879a

Wang, G., Dinkins, M., He, Q., Zhu, G., Poirier, C., Campbell, A., et al. (2012). Astrocytes secrete exosomes enriched with proapoptotic ceramide and prostate apoptosis response 4 (PAR-4): potential mechanism of apoptosis induction in Alzheimer disease (AD). *J. Biol. Chem.* 287, 21384–21395. doi: 10.1074/jbc.M112.340513

Wang, G., Krishnamurthy, K., and Bieberich, E. (2009). Regulation of primary cilia formation by ceramide. *J. Lipid Res.* 50, 2103–2110. doi: 10.1194/jlr.M900097-JLR200

Weibrecht, I., Leuchowius, K. J., Clausson, C. M., Conze, T., Jarvius, M., Howell, W. M., et al. (2010). Proximity ligation assays: a recent addition to the proteomics toolbox. *Expert Rev. Proteomics* 7, 401–409. doi: 10.1586/epr.10.10

Zhu, Z., Chen, J., Wang, G., Elsherbini, A., Zhong, L., Jiang, X., et al. (2019). Ceramide regulates interaction of Hsd17b4 with Pex5 and function of peroxisomes. *Biochim. Biophys. Acta Mol. Cell. Biol. Lipids* 1864, 1514–1524. doi: 10.1016/j.bbalip.2019.05.017

Conflict of Interest Statement: The authors declare that the research was conducted in the absence of any commercial or financial relationships that could be construed as a potential conflict of interest.

frontiers in Cell and Developmental Biology

REVIEW
published: 21 August 2019
doi: 10.3389/fcell.2019.00168

A Comprehensive Review on the Manipulation of the Sphingolipid Pathway by Pathogenic Bacteria

Monica Rolando and Carmen Buchrieser**

Biologie des Bactéries Intracellulaires, CNRS UMR 3525, Institut Pasteur, Paris, France

Bacterial pathogens have developed many different strategies to hijack host cell responses to promote their own survival. The manipulation of lipid biogenesis and cell membrane stability is emerging as a key player in bacterial host cell control. Indeed, many bacterial pathogens such as *Legionella, Pseudomonas, Neisseria, Staphylococci, Mycobacteria, Helicobacter,* or *Clostridia* are able to manipulate and use host sphingolipids during multiple steps of the infectious process. Sphingolipids have long been considered only as structural components of cell membranes, however, it is now well known that they are also intracellular and intercellular signaling molecules that play important roles in many eukaryotic cell functions as well as in orchestrating immune responses. Furthermore, they are important to eliminate invading pathogens and play a crucial role in infectious diseases. In this review, we focus on the different strategies employed by pathogenic bacteria to hijack the sphingolipid balance in the host cell to promote cellular colonization.

Keywords: sphingolipids, host-pathogen interactions, *Legionella*, *Pseudomonas*, *Mycobacteria*

OPEN ACCESS

Edited by:
Sibylle Schneider-Schaulies, Julius Maximilian University of Würzburg, Germany

Reviewed by:
Astrid M. Westendorf, University of Duisburg-Essen, Germany
Martin Fraunholz, Julius Maximilian University of Würzburg, Germany

****Correspondence:***
Monica Rolando
mrolando@pasteur.fr
Carmen Buchrieser
cbuch@pasteur.fr

Specialty section:
This article was submitted to Membrane Physiology and Membrane Biophysics, a section of the journal Frontiers in Cell and Developmental Biology

Received: *08 July 2019*
Accepted: *06 August 2019*
Published: *21 August 2019*

Citation:
Rolando M and Buchrieser C (2019) A Comprehensive Review on the Manipulation of the Sphingolipid Pathway by Pathogenic Bacteria. Front. Cell Dev. Biol. 7:168. doi: 10.3389/fcell.2019.00168

INTRODUCTION

Sphingolipids constitute an important class of lipids that are structural modules in eukaryotic membranes. However, they have also been shown to act as signaling molecules that play critical roles in regulating diverse physiological processes including signal transduction, regulation of cell growth and death, adhesion, migration, and inflammation. Indeed, sphingolipids are also bioactive molecules and their highly interconnected and spatially regulated pathways are very complex (Hannun and Obeid, 2008).

Briefly, the main hub in the sphingolipid pathway is ceramide that can be synthesized *de novo* from serine and palmitate, present in the endoplasmic reticulum (ER) and in ER-associated membranes, or from the breakdown of sphingomyelin (SM) into ceramide and phosphatidylcholine catalyzed by sphingomyelinase enzymes (SMases) (**Figure 1**). Sphingomyelinases are classified as acidic, neutral or alkaline, based on their optimal pH and they are located in distinct cellular sub-compartments, where their products eventually mediate specific functions (Goni and Alonso, 2002). The ceramide generated by acidic SMase (ASM), for example, resides either in the lysosome or at the plasma membrane, where ceramide aggregates into microdomains. Later, aggregation of those microdomains into ceramide-enriched membrane platforms induces local changes in the membrane environment thereby affecting the permeability and the fluidity of the membrane and causing conformational changes in membrane-associated enzymes or receptors (Cremesti et al., 2002).

Ceramides themselves function also as bioactive molecules and provide a basis for the synthesis of other signaling molecules such as ceramide-1-phosphate or glucosylceramide, or they can eventually, through the catabolic pathway, be hydrolyzed by ceramidases to form sphingosine (**Figure 1**). Sphingosine can then be recycled into the sphingolipid pathway, the "salvage" pathway, where ceramide synthase hydrolyzes ceramide directly from sphingosine, or is phosphorylated by the sphingosines kinases (SKs). The product sphingosine-1-phosphate (S1P) can be dephosphorylated to regenerate sphingosine (through the action of specific S1P-phosphatases) or can be irreversibly cleaved by a sphingosine phosphate lyase (SPL) to generate ethanolamine phosphate and hexadecenal (which, in turn, can be reduced to palmitate and subsequently reincorporated into lipid metabolic pathways) (**Figure 1**). S1P is one of the most soluble sphingolipids, it is able to move between membranes, as well as act extracellularly. It interacts with sphingosine-1-phosphate receptors, S1PRs, which are high-affinity G-protein coupled receptors (Lee et al., 1998). S1PRs display selective tissue expression and activate specific intracellular signaling pathway, providing to S1P crucial roles in cell survival, cell migration and inflammation (Hla, 2004).

The sphingolipid mediators described above, play a role in many different cellular processes. For example, they modulate the reorganization of cellular membrane receptors and thus regulate the internalization of bacteria in the host cell, as well as the subsequent fusion of phagosomes and lysosomes. They are also implicated in intracellular signaling following bacterial internalization such as cytokine release, inflammatory responses and initiation of apoptosis of the infected cell (Maceyka and Spiegel, 2014). However, many bacterial pathogens have acquired the ability to counteract the cellular response and to change the sphingolipid balance of the cell they infect. The majority of these bacterial pathogens hijack different host cell factors to interfere with the sphingolipid signaling to their advantage. In contrast, a small number of them acquired the ability to produce enzymes that directly change the sphingolipid composition of host membranes in order to promote their colonization (**Figure 1**).

BACTERIAL PATHOGENS EXPLOIT AND HIJACK THE HOST CELL SPHINGOLIPID PATHWAY

Adhesion and Bacterial Uptake

The first critical step of hot-pathogen interaction is the bacteria-cell contact and eventually the entry of the pathogen into the host cell. Thus, bacterial pathogens may modulate membrane properties and signaling pathways to invade eukaryotic cells, therefore exploiting the sphingolipid pathway. In this context, one of the frequent targets of bacteria is the ASM that is known to participate in membrane reorganization and formation of ceramide-enriched platforms. Several bacterial pathogens have been shown to activate the ASM, a mechanism that promotes bacterial colonization. Furthermore, sphingosine has been shown to have antimicrobial properties as it inhibits growth and kills many Gram-positive and Gram-negative bacteria (Fischer et al., 2013). Thus decreasing sphingosine levels indirectly by activating ASM is beneficial for survival and replication of intracellular pathogens.

Pseudomonas aeruginosa, the primary cause of morbidity and mortality in patients with cystic fibrosis, is the bacterium for which the interaction with sphingolipids upon infection is the best studied (Teichgraber et al., 2008). In particular, *P. aeruginosa* infection triggers the activation of the ASM at the plasma membrane, with the subsequent production and release of ceramide that clusters at ceramide-enriched platforms required for bacterial internalization (Grassme et al., 2003). The increase of ceramide-enriched platforms induces a local accumulation of ß1-integrins that downregulate acid ceramidase expression, resulting in further accumulation of ceramide and consequently a reduction of surface sphingosine, a lipid that kills bacteria (Grassme et al., 2017).

Pathogenic *Neisseria* are Gram-negative pathogens that are able to bind mucosal surfaces by employing multiple strategies to interact with various cell receptors. *Neisseria gonorrhoeae*, the etiological agent of gonorrhea, and *Neisseria meningitis*, the major cause of meningitis and septicemia worldwide, are able to transiently activate the ASM to mediate the formation of ceramide-enriched platforms that favor bacterial infection. The internalization is mediated by outer membrane proteins, Opa and Opc, expressed by *N. gonorrhoeae* and *N. meningitis*, respectively. Opa is responsible for ASM activation by binding to the CEACAM receptor family (CD66) (Hauck et al., 2000), whereas Opc-expressing *N. meningitidis* induces ceramide-enriched platforms that serve to cluster the ErbB2 receptor underneath adherent bacteria (Simonis et al., 2014).

Staphylococcus aureus, a common commensal bacterium, but also an opportunistic pathogen that frequently causes different diseases, such as pneumonia, endocarditis, or toxic shock syndrome (Tong et al., 2015), also activates ASM. Recent studies have demonstrated that staphylococcal α-toxin is one of the factors mediating the activation of ASM and the release of ceramide via ADAM10, which is linked to the degradation of tight junctions (Becker et al., 2018). This mechanism reveals a central role for α-toxin and ASM in *S. aureus* infection, in particular in cystic fibrosis patients (Keitsch et al., 2018).

Clostridium botulinum C2 toxin, the binding component of the binary C2I/C2II toxin, induces a release of sphingomyelinase from lysosomes which leads to an increased level of ceramide that is responsible for the endocytosis of the toxin (Nagahama et al., 2017). Similar to *C. botulinum*, *Clostridium difficile* exploits the sphingolipid machinery to colonize the host cells as clostridium difficile toxin (CDT) causes actin ADP-ribosylation and a subsequent formation of microtubule-based membrane protrusions depending on sphingolipid-rich microdomains (Schwan et al., 2011).

The ASM is not the only sphingomyelinase playing a role in bacterial invasion as it has been shown that the neutral sphingomyelinase 2 (Nsm2) plays a role in the formation of granuloma induced by *Mycobacterium tuberculosis* in mice (Wu et al., 2018). Nsm2 is located in the inner leaflet of the plasma and Golgi membranes and has been shown to induce ceramide release

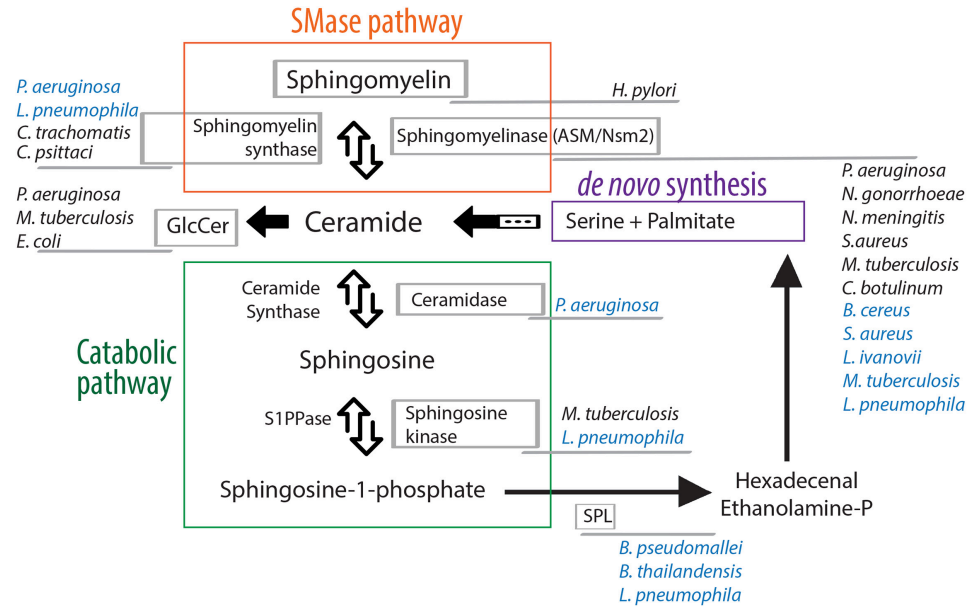

FIGURE 1 | Manipulation of the sphingolipid pathway by bacterial pathogens. Ceramide, the hub of the sphingolipid pathway, can be formed by two different routes: *de novo* synthesis, that starts by the condensation of the amino acid serine and the saturated fatty acid palmitate (purple), or the sphingomyelinase pathway that allows the degradation of sphingomyelin in ceramide (orange). The catabolic pathway (green) leads to the formation of bioactive lipids via the action of different enzymes. All steps are reversible, except the sphingosine lyase activity that irreversibly cleaves sphingosine-1-phosphate to generate ethanolamine phosphate and hexadecenal, which can be subsequently reincorporated into the *de novo* synthesis. Bacterial pathogens that target host cell sphingolipid enzymes are indicated. Their names are written next to the host enzyme they target/manipulate either directly (written in blue color) or indirectly (written in black color). For a comprehensive review describing the subcellular localization of sphingolipid enzymes refer to Yamaji and Hanada (2015). SMase, sphingomyelinase; GlcCer, glucosylceramide; S1PPase, sphingosine-1-phosphate phosphatase; SPL, sphingosine-1-phosphate lyase.

upon several cellular and pathological processes (Shamseddine et al., 2015). Nsm2 is also a key factor for *N. gonorrhoeae* invasion, in particular strains expressing the major outer membrane protein PorB that binds the SREC-I receptor and triggers Nsm2 activation (Faulstich et al., 2015).

Several bacterial pathogens can directly use glycosphingolipids of the plasma membrane as receptors, in order to internalize into the target cell. In particular, lactosylceramide (LacCer) acts as a pattern recognition receptor (Nakayama et al., 2013). One example is *M. tuberculosis*, that can bind LacCer- enriched lipid rafts of human neutrophils via its membrane lipoarabinomannans (LAMs) to stimulate phagocytosis (Nakayama et al., 2016).

Glycosphingolipids are also exploited by bacterial toxins to translocate into target cells. It has been shown that globotriaosylceramide (Gb3), also known as CD77 or Pk blood group antigen, is the ligand of *Escherichia coli* shiga toxins (Lingwood et al., 2010) and lectin 1 (LecA), an outer membrane virulence factor of *P. aeruginosa*. In the case of shiga toxins, the receptor binding allows the toxin internalization and, once into the cell cytosol, the triggering of cell toxicity (Melton-Celsa, 2014), whereas LecA once it binds Gb3 triggers a signaling cascade through CrkII phosphorylation (Zheng et al., 2017). This interaction also promotes a cell membrane engulfment, that prompts *P. aeruginosa* uptake by host cells (Eierhoff et al., 2014).

Sphingomyelin is also required for entry of *Helicobacter pylori*, a gastric pathogen causing chronic infections that are a significant risk factor for the development of ulcer disease or gastric adenocarcinoma in epithelial cells. The secreted vacuolating cytotoxin (VacA) plays an important role in bacterial colonization and multiple putative VacA receptors have been reported (Foegeding et al., 2016). Between them sphingomyelin is essential for targeting VacA to membrane rafts and subsequent Cdc42-dependent pinocytic cellular entry (Gupta et al., 2010).

Phagolysosome Fusion and Formation of Intracellular Compartments for Bacterial Replication

An efficient host response to bacterial invasion consists in an appropriate fusion between phagosomes and lysosomes carrying the pathogens to elimination. Interestingly sphingolipids, and in particular ASM, play a role in mediating phagolysosome fusion and degradation of bacteria. In fact, a high susceptibility to bacterial infection of *Listeria monocytogenes* and *S. aureus* has been shown in ASM deficient models. The role of ASM in *L. monocytogenes* uptake and invasion has been shown both in cellular (macrophages) (Schramm et al., 2008), and in animal models (mice) (Utermöhlen et al., 2003).

Staphylococcus aureus infection causes the activation of CD44 receptor, which is stimulating ASM via the generation of reactive oxygen species (ROS), resulting in ceramide release and increased formation of ceramide-enriched domains after infection. These domains cluster and thereby amplify CD44 signaling resulting

in further activation of the ASM providing a positive forward feedback loop between CD44 and the ASM. CD44 activation by *S. aureus* stimulates small G proteins, a reorganization of the cytoskeleton, internalization of the pathogen, and fusion of phagosomes with lysosomes, a process that requires again ASM (Li et al., 2017).

Mycobacterium tuberculosis is able to actively inhibit phagosome maturation by acting on sphingosine kinase 1. This pathogen inhibits both, the activation and the translocation of SK1 to block the cytosolic Ca^{2+} signaling, required for normal maturation of phagosomes (Thompson et al., 2005). In contrast to *M. tuberculosis, Chlamydia trachomatis,* a Gram-negative obligate intracellular pathogen responsible for trachoma and sexually transmitted diseases, develops, after binding and entry into target cells, a membrane-bound vacuole, termed inclusion that minimizes the interaction with immune defenses and other host-derived molecules. It has been shown that the inclusion membrane contains sphingomyelin (Hackstadt et al., 1996) and that *C. trochomatis* and *Chlamydia psittaci* actively redirect sphingomyelin biosynthesis at the inclusion membrane by recruitment of sphingomyelin synthases, a step strictly necessary for inclusion growth and stability (Elwell et al., 2011; Koch-Edelmann et al., 2017).

Signal Transduction, Apoptosis, and Autophagy

Sphingolipid turnover affects the intracellular trafficking of important membrane microdomains, impacting their associated receptors, transporters and the production of a cascade of products, each of which can interact with multiple intracellular targets (Ohanian and Ohanian, 2001). Several pathogens are able to modulate the cellular transduction during infection upon a direct targeting of sphingolipid enzymes. One example is the signaling pathway activated by sphingosine kinase 1 upon *Mycobacterium smegmatis* infection. Prakash et al. (2010) showed that sphingosine kinase 1 inhibition in infected macrophages leads to a decrease in anti-mycobacterial proteins-pp38 and iNOS, via dampened NF-kB and p38-MAPK activities. In a similar manner, specific activation of mitochondrial ASM by *P. aeruginosa* triggers the release of mitochondrial ceramide and the release of cytochrome-c from mitochondria, leading to cell death (Manago et al., 2015). Possibly this apoptotic process is mediated by the formation of ceramide channels in the mitochondrial outer membrane through which cytochrome c can exit mitochondria and activate apoptotic pathway (Ganesan et al., 2010).

Sphingolipids are well known in mediating key cellular processes, including autophagy (Bedia et al., 2011; Jiang and Ogretmen, 2014). *Salmonella* spp. is a food-borne Gram-negative entero-pathogen that remains a major public health problem word wide. After internalization, a type-III secretion system (T3SS) is necessary to remodel the phagosome into a *Salmonella* containing vacuole (SCV) where the bacterium replicates. *Salmonella*, depending on the stage of replication, can induce a suppression of autophagy, in order to enhance bacterial survival (Owen et al., 2014). This induction seems to be orchestrated by sphingolipid biomolecules, as inhibition of *de novo* sphingolipid synthesis leads to decreased *Salmonella*-induced autophagy (Huang, 2016).

BACTERIAL PATHOGENS MIMIC HOST SPHINGOLIPID ENZYMES

While most bacteria do not contain sphingolipids, some of them have evolved mechanisms by which they can utilize sphingolipids of the eukaryotic cells. Interestingly, certain bacterial pathogens encode enzymes implicated in the catabolic pathway of sphingolipids in the eukaryotic cells (**Figure 1** and **Table 1**).

Examples are *Bacillus cereus*, a facultative anaerobic Gram-positive bacterium associated with food poisoning and nosocomial infections, *S. aureus* a Gram-positive facultative pathogen and *Listeria Ivanovii*, a ruminant pathogen. All three encode enzymes with a high degree of amino acid sequence

TABLE 1 | Bacterial enzymes that mimic host sphingolipids.

Bacterium	Enzyme	Gene	Protein	References
B. cereus	Sphingomyelinase	*sph*	*Bc*-SMase	Oda et al., 2012
S. aureus	Sphingomyelinase	*hlb*	ß-toxin	Herrera et al., 2017
L. ivanovii	Sphingomyelinase	*smcL*	SmcL	Gonzalez-Zorn et al., 1999
M. tuberculosis	Sphingomyelinase	*rv0888*	SpmT	Speer et al., 2015
L. pneumophila strain Paris	Sphingomyelinase*	*lpp2641*	–	Cazalet et al., 2004
L. pneumophila strain Longbeachae	Sphingomyelinase*	*llo2622 llo1999 llo1141*	–	Cazalet et al., 2004
P. aeuroginosa	Sphingomyelin synthase	*PlcH*	PlcH	Luberto et al., 2003
P. aeuroginosa strain AN17	Ceramidase	*PA0845*	PaCD	Okino et al., 1998
L. pneumophila strain Paris	Sphingosine kinase*	*lpp2295*	–	Cazalet et al., 2004
B. pseudomallei strain K96243	Sphingosine phosphate lyase	*BPSS2021 BPSS2025*	BPSS2021 BPSS2025	Custodio et al., 2016
B. thailandensis strain E264	Sphingosine phosphate lyase	*BTH_II0309 BTH_II0311*	BTH_II0309 BTH_II0311	Custodio et al., 2016
L. pneumophila strain Paris	Sphingosine phosphate lyase*	*lpp2128*	LpSPL	Cazalet et al., 2004; Rolando et al., 2016a

**The functional annotation is based on sequence similarity.*

homology that encode sphingomyelinase (Smase) activities. *S. aureus* ß-toxin confers to the bacterium its hemolytic and lympholytic activities (Herrera et al., 2017), whereas *Bc*-Smase, produced in large amounts by clinical isolates of *B. cereus*, enhances bacterial colonization by inducing clustering of ceramide and attenuation of membrane fluidity (Oda et al., 2012). *L. ivanovii* Smase, encoded by the *smcL* gene induces hemolysis and facilitates the disruption of the phagocytic vacuole thereby promoting intracellular survival and propagation (Gonzalez-Zorn et al., 1999).

Pseudomonas species are also known to express and secrete sphingolipid-metabolizing enzymes. *P. aeruginosa* encodes a sphingomyelin synthase, PlcH, which specifically recognizes the choline head-group of sphingomyelin as well as the primary hydroxyl group of ceramide (Luberto et al., 2003) and its gene expression is strictly regulated by cellular amounts of sphingolipids (Okino and Ito, 2016). Furthermore, *P. aeruginosa* seems also to be able to hydrolyze ceramide as an alkaline ceramidase (Cdase) has been characterized from the *P. aeruginosa* strain AN17 isolated from the skin of a patient with atopic dermatitis (Okino et al., 1998). Enzymatic characterization of the *P. aeruginosa* Cdase showed that it can be inhibited by sphingosine and by sphingosine analogs, but not by typical mammalian Cdase inhibitors. This suggests that the bacterial Cdase has a novel active site and/or substrate-binding region (Nieuwenhuizen et al., 2002).

Mycobacterium tuberculosis encodes a sphingomyelinase, SpmT, that is a cell-surface exposed protein, anchored in the outer membrane, that possesses a strong sphingomyelinase activity which is required for bacterial growth and nutrient acquisition (Speer et al., 2015). The hydrolyzed products, ceramide and phosphocholine, are utilized by *M. tuberculosis* as source of carbon, nitrogen and phosphorous, respectively, explaining the stimulating activity of sphingomyelin on bacterial growth described in the past (Dubos, 1948).

Burkholderia pseudomallei and *Burkholderia thailandensis*, two closely related intracellular Gram-negative pathogens found in soils and water, encode SPL like proteins (Custodio et al., 2016). *B. pseudomallei*, the causative agent of melioidosis, is able to invade, survive and replicate in both phagocytic and non-phagocytic cells, whilst *B. thailandensis*, although it displays a similar intracellular phenotype, exhibits an attenuated form of the disease (Lennings et al., 2018). Custodio et al. (2016) showed that orthologs *Burkholderia* SPL proteins possess SPL activity and that they play a critical role in virulence. In addition, treatment of *Burkholderia*-infected macrophages with exogenous SPL-receptor agonists enhances their bactericidal activity (Custodio et al., 2016).

A striking example of a bacterial pathogen encoding sphingolipid enzymes is *Legionella pneumophila*, a Gram-negative intracellular bacterium responsible for Legionnaire' disease, a severe pneumonia that is often fatal when not treated rapidly (Steinert et al., 2007). Shortly after its discovery in 1977, it has been shown that *L. pneumophila* is pathogenic for freshwater and soil amoebae (Rowbotham, 1980), leading to the new perception in microbiology, whereby bacteria that parasitize protozoa can utilize similar processes to infect human cells (Escoll et al., 2013). Genome analyses uncovered that the ability of *Legionella* to infect eukaryotic cell is partly due to the acquisition of eukaryotic gene functions from their protozoan hosts due to the *Legionella*-protozoa coevolution (Nora et al., 2009; Gomez-Valero and Buchrieser, 2013). Interestingly, *L. pneumophila* has been shown to encode for at least three proteins mimicking the host sphingolipid pathway (Cazalet et al., 2004): a sphingomyelinase, a sphingosine kinase and a sphingosine-1-phosphate lyase (Rolando et al., 2016a).

Till now only the sphingosine-1-phosphate lyase has been characterized functionally (Khweek et al., 2013; Rolando et al., 2016b). Indeed, *Legionella* SPL is encoded by all *L. pneumophila* strains analyzed, but *Legionella Longbeachae*, and is highly homologous to the eukaryotic SPL (Gomez-Valero and Buchrieser, 2019). The secreted protein effector (named *Lp*Spl and LegS2 in *L. pneumophila* strains Paris and Philadelphia, respectively) possesses SPL activity and triggers the reduction of several sphingolipids in infected host cells. Thus, *Lp*SPL alone is sufficient to prevent an increase in sphingosine levels in infected cells in order to inhibit autophagy during infection (Rolando et al., 2016b). This strategy allows the bacterium to counteract the host cell response and to facilitate intracellular growth.

CONCLUSION AND OUTLOOK

Several bacterial pathogens have been shown to actively modulate the sphingolipid pathway of their host cells to promote cellular colonization. Among the different strategies employed one of the commonly targeted activity is that of the acid sphingomyelinase (ASM), which can be regulated by bacterial virulence factors. ASM activation leads to an increase of the membrane levels of ceramide resulting in the formation of ceramide-enriched membrane platforms. These structures form a unique microenvironment with biophysical properties that allow them to trap and cluster receptor molecules and intracellular signaling molecules, thereby permitting and amplifying signal transduction. Thus, ceramide acts by re-organizing molecules in cells and in that way bacteria can regulate their internalization in the host cell, the subsequent cytokine release and inflammatory response or the regulation of cell death (Gulbins et al., 2004). This specific ASM activation is driven not only by secreted virulence factors and toxins, but also by the bacterial lippopolysaccaride (LPS) itself. Indeed, the exposure of diverse cell types to LPS induces an activation of ASM and a release of ceramide.

Sphingolipids play also an important role in respiratory tract infections, as they are one of the active constituents of the mucus secreted by the alveolar epithelium, which protects the lung tissue from invading pathogens. A large number of intermediate metabolites in the mucus are secreted by the alveolar epithelium where they act as surfactants and maintain the barrier integrity. Thus, the sphingolipid balance plays an additional role in lung infection diseases. Sphingolipids, in particular ceramide and sphingosine, are in particular important in lung antibacterial defense (Seitz et al., 2015). It is thought, that in healthy individuals the constitutive presence of sphingosine in upper airway cells helps to eliminate pathogens that become

highly infective in diseased lungs, e.g., cystic fibrosis, where the concentrations of both sphingosine and ceramide are altered (downregulated and upregulated, respectively). Indeed, the normalization of the lipid levels in a mouse model of cystic fibrosis was shown to be sufficient to prevent infections (Pewzner-Jung et al., 2014).

These observations point to a possible antibacterial effect of sphingolipids which could perhaps be exploited in times where antibiotic resistance has become a severe threat to global public health and it has become highly important to identify novel therapeutic targets to fight bacterial infections. Antibacterial activity of diverse sphingolipids has been shown in several types of bacterial infections and thus they are a potential new tool to fight them (Baker et al., 2018).

Actually, sphingosine has been shown to prevent *P. aeuroginosa* and *S. aureus* infections in mice (Pewzner-Jung et al., 2014; Tavakoli Tabazavareh et al., 2016). At present it is unknown how it is able to kill pathogens, however, recent findings suggest that it can cause ultrastructural damages, both extracellularly and intracellularly (Fischer et al., 2013). Resistant *S. aureus* strains, in particular methicillin-resistant *S. aureus* strains, have become an important clinical problem and are recognized as serious threats in communities and hospitals worldwide (Grundmann et al., 2006). It is thus crucial to find new therapeutic strategies and to provide alternatives to existing approaches. One possibility could be the combination of antibiotics with new target drugs as, for example, a specific inhibitor of the sphingolipid catabolic pathway. Peng et al. (2015) showed that ASM inhibition successfully rescues mice from the lethality of *S. aureus* infection.

It has also been suggested that sphingosine possesses an anti-biofilm activity by inhibiting bacterial adherence of *Streptococcus mutans*, a highly cariogenic bacterium (Cukkemane et al., 2015). An antibacterial activity has been shown also for ceramide, that has been proven to actively kill pathogenic *Neisseriae,* likely by causing dissipation of the membrane potential (Becam et al., 2017). In addition to ceramide and sphingosine, other sphingolipid metabolites, in particular S1P may offer therapeutic benefits when managing bacterial diseases. S1P has been shown to increase intracellular killing of *M. tuberculosis* by macrophages (Garg et al., 2004), as well as to reduce neonatal death associated with pertussis infections (Scanlon et al., 2015). As sphingolipids play important roles in controlling infection, future research to get a deeper insight in their functioning and the different signaling roles might allow to develop new strategies to fight bacterial pathogens. However, it would also be very interesting to study in depth how bacterial pathogens may exploit sphingolipids to their own advantage. Indeed, as discussed in this review, several intracellular pathogens that live in close contact with eukaryotic hosts have evolved strategies allowing them to mimic their functions and thereby to promote their intracellular replication. One example is *L. pneumophila,* a bacterium that has acquired several eukaryotic-like proteins in its effector arsenal among which are three enzymes that share activities of eukaryotic enzymes that act in the sphingolipid degradation pathway. However, many other intracellular pathogens, such as *Coxiella*, *Brucella,* or *Chlamydia* may encode among the many effectors for which the functions are not known yet, effectors mimicking or targeting the sphingolipid pathway. Their identification and characterization would help to not only better understand the bacterial strategy, but probably also new cellular pathways regulated by the sphingolipid bioactive molecules.

AUTHOR CONTRIBUTIONS

Both authors listed have made a substantial, direct and intellectual contribution to the work, and approved it for publication.

FUNDING

Work in the CB Laboratory was financed by the Institut Pasteur and has received funding from the French Government (Grant ANR-10-LABX-62-IBEID to CB and Grant ANR-18-CE15-0005-01 to MR).

REFERENCES

Baker, J. E., Boudreau, R. M., Seitz, A. P., Caldwell, C. C., Gulbins, E., and Edwards, M. J. (2018). Sphingolipids and innate immunity: a new approach to infection in the post-antibiotic era? *Surg. Infect.* 19, 792–803. doi: 10.1089/sur.2018.187

Becam, J., Walter, T., Burgert, A., Schlegel, J., Sauer, M., Seibel, J., et al. (2017). Antibacterial activity of ceramide and ceramide analogs against pathogenic *Neisseria*. *Sci. Rep.* 7:17627. doi: 10.1038/s41598-017-18071-w

Becker, K. A., Fahsel, B., Kemper, H., Mayeres, J., Li, C., Wilker, B., et al. (2018). Staphylococcus aureus alpha-toxin disrupts endothelial-cell tight junctions via acid sphingomyelinase and ceramide. *Infect. Immun.* 86:e00606-17. doi: 10.1128/IAI.00606-17

Bedia, C., Levade, T., and Codogno, P. (2011). Regulation of autophagy by sphingolipids. *Anticancer Agents Med. Chem.* 11, 844–853. doi: 10.2174/187152011797655131

Cazalet, C., Rusniok, C., Bruggemann, H., Zidane, N., Magnier, A., Ma, L., et al. (2004). Evidence in the *Legionella pneumophila* genome for exploitation of host cell functions and high genome plasticity. *Nat. Genet.* 36, 1165–1173. doi: 10.1038/ng1447

Cremesti, A. E., Goni, F. M., and Kolesnick, R. (2002). Role of sphingomyelinase and ceramide in modulating rafts: do biophysical properties determine biologic outcome? *FEBS Lett.* 531, 47–53. doi: 10.1016/s0014-5793(02)03489-0

Cukkemane, N., Bikker, F. J., Nazmi, K., Brand, H. S., Sotres, J., Lindh, L., et al. (2015). Anti-adherence and bactericidal activity of sphingolipids against *Streptococcus mutans*. *Eur. J. Oral Sci.* 123, 221–227. doi: 10.1111/eos.12200

Custodio, R., McLean, C. J., Scott, A. E., Lowther, J., Kennedy, A., Clarke, D. J., et al. (2016). Characterization of secreted sphingosine-1-phosphate lyases required for virulence and intracellular survival of *Burkholderia pseudomallei*. *Mol. Microbiol.* 102, 1004–1019. doi: 10.1111/mmi.13531

Dubos, R. J. (1948). The effect of sphingomyelin on the growth of tubercle bacilli. *J. Exp. Med.* 88, 73–79. doi: 10.1084/jem.88.1.73

Eierhoff, T., Bastian, B., Thuenauer, R., Madl, J., Audfray, A., Aigal, S., et al. (2014). A lipid zipper triggers bacterial invasion. *Proc. Natl. Acad. Sci. U.S.A.* 111, 12895–12900. doi: 10.1073/pnas.1402637111

Elwell, C. A., Jiang, S., Kim, J. H., Lee, A., Wittmann, T., Hanada, K., et al. (2011). Chlamydia trachomatis co-opts GBF1 and CERT to acquire host sphingomyelin for distinct roles during intracellular development. *PLoS Pathog* 7:e1002198. doi: 10.1371/journal.ppat.1002198

Escoll, P., Rolando, M., Gomez-Valero, L., and Buchrieser, C. (2013). From amoeba to macrophages: exploring the molecular mechanisms of *Legionella pneumophila* infection in both hosts. *Curr. Top. Microbiol. Immunol.* 376, 1–34. doi: 10.1007/82_2013_351

Faulstich, M., Hagen, F., Avota, E., Kozjak-Pavlovic, V., Winkler, A. C., Xian, Y., et al. (2015). Neutral sphingomyelinase 2 is a key factor for PorB-dependent invasion of *Neisseria gonorrhoeae*. *Cell. Microbiol.* 17, 241–253. doi: 10.1111/cmi.12361

Fischer, C. L., Walters, K. S., Drake, D. R., Blanchette, D. R., Dawson, D. V., Brogden, K. A., et al. (2013). Sphingoid bases are taken up by *Escherichia coli* and Staphylococcus aureus and induce ultrastructural damage. *Skin Pharmacol. Physiol.* 26, 36–44. doi: 10.1159/000343175

Foegeding, N. J., Caston, R. R., McClain, M. S., Ohi, M. D., and Cover, T. L. (2016). An overview of *Helicobacter* pylori VacA toxin biology. *Toxins* 8:E173. doi: 10.3390/toxins8060173

Ganesan, V., Perera, M. N., Colombini, D., Datskovskiy, D., Chadha, K., and Colombini, M. (2010). Ceramide and activated Bax act synergistically to permeabilize the mitochondrial outer membrane. *Apoptosis* 15, 553–562. doi: 10.1007/s10495-009-0449-0

Garg, S. K., Volpe, E., Palmieri, G., Mattei, M., Galati, D., Martino, A., et al. (2004). Sphingosine 1-phosphate induces antimicrobial activity both in vitro and in vivo. *J. Infect. Dis.* 189, 2129–2138. doi: 10.1086/386286

Gomez-Valero, L., and Buchrieser, C. (2013). Genome dynamics in *Legionella*: the basis of versatility and adaptation to intracellular replication. *Cold Spring Harb. Perspect. Med.* 3:a009993. doi: 10.1101/cshperspect.a009993

Gomez-Valero, L., and Buchrieser, C. (2019). Intracellular parasitism, the driving force of evolution of *Legionella pneumophila* and the genus *Legionella*. *Genes Immun.* 20, 394–402. doi: 10.1038/s41435-019-0074-z

Goni, F. M., and Alonso, A. (2002). Sphingomyelinases: enzymology and membrane activity. *FEBS Lett.* 531, 38–46. doi: 10.1016/s0014-5793(02)03482-8

Gonzalez-Zorn, B., Dominguez-Bernal, G., Suarez, M., Ripio, M. T., Vega, Y., Novella, S., et al. (1999). The smcL gene of *Listeria ivanovii* encodes a sphingomyelinase C that mediates bacterial escape from the phagocytic vacuole. *Mol. Microbiol.* 33, 510–523. doi: 10.1046/j.1365-2958.1999.01486.x

Grassme, H., Henry, B., Ziobro, R., Becker, K. A., Riethmuller, J., Gardner, A., et al. (2017). beta1-integrin accumulates in cystic fibrosis luminal airway epithelial membranes and decreases sphingosine, promoting bacterial infections. *Cell Host Microbe* 21, 707.e8–718.e8. doi: 10.1016/j.chom.2017.05.001

Grassme, H., Jendrossek, V., Riehle, A., von Kurthy, G., Berger, J., Schwarz, H., et al. (2003). Host defense against *Pseudomonas aeruginosa* requires ceramide-rich membrane rafts. *Nat. Med.* 9, 322–330. doi: 10.1038/nm823

Grundmann, H., Aires-de-Sousa, M., Boyce, J., and Tiemersma, E. (2006). Emergence and resurgence of meticillin-resistant *Staphylococcus aureus* as a public-health threat. *Lancet* 368, 874–885. doi: 10.1016/S0140-6736(06)68853-3

Gulbins, E., Dreschers, S., Wilker, B., and Grassme, H. (2004). Ceramide, membrane rafts and infections. *J. Mol. Med.* 82, 357–363. doi: 10.1007/s00109-004-0539-y

Gupta, V. R., Wilson, B. A., and Blanke, S. R. (2010). Sphingomyelin is important for the cellular entry and intracellular localization of *Helicobacter* pylori VacA. *Cell. Microbiol.* 12, 1517–1533. doi: 10.1111/j.1462-5822.2010.01487.x

Hackstadt, T., Rockey, D. D., Heinzen, R. A., and Scidmore, M. A. (1996). Chlamydia trachomatis interrupts an exocytic pathway to acquire endogenously synthesized sphingomyelin in transit from the Golgi apparatus to the plasma membrane. *EMBO J.* 15, 964–977. doi: 10.1002/j.1460-2075.1996.tb00433.x

Hannun, Y. A., and Obeid, L. M. (2008). Principles of bioactive lipid signalling: lessons from sphingolipids. *Nat. Rev. Mol. Cell Biol.* 9, 139–150. doi: 10.1038/nrm2329

Hauck, C. R., Grassme, H., Bock, J., Jendrossek, V., Ferlinz, K., Meyer, T. F., et al. (2000). Acid sphingomyelinase is involved in CEACAM receptor-mediated phagocytosis of *Neisseria gonorrhoeae*. *FEBS Lett.* 478, 260–266. doi: 10.1016/s0014-5793(00)01851-2

Herrera, A., Kulhankova, K., Sonkar, V. K., Dayal, S., Klingelhutz, A. J., Salgado-Pabon, W., et al. (2017). Staphylococcal beta-toxin modulates human aortic endothelial cell and platelet function through sphingomyelinase and biofilm ligase activities. *mBio* 8:e00273-17. doi: 10.1128/mBio.00273-17

Hla, T. (2004). Physiological and pathological actions of sphingosine 1-phosphate. *Semin. Cell Dev. Biol.* 15, 513–520. doi: 10.1016/j.semcdb.2004.05.002

Huang, F. C. (2016). De Novo sphingolipid synthesis is essential for *Salmonella*-induced autophagy and human beta-defensin 2 expression in intestinal epithelial cells. *Gut Pathog.* 8:5. doi: 10.1186/s13099-016-0088-2

Jiang, W., and Ogretmen, B. (2014). Autophagy paradox and ceramide. *Biochim. Biophys. Acta* 1841, 783–792. doi: 10.1016/j.bbalip.2013.09.005

Keitsch, S., Riethmuller, J., Soddemann, M., Sehl, C., Wilker, B., Edwards, M. J., et al. (2018). Pulmonary infection of cystic fibrosis mice with *Staphylococcus aureus* requires expression of alpha-toxin. *Biol. Chem.* 399, 1203–1213. doi: 10.1515/hsz-2018-0161

Khweek, A. A., Caution, K., Akhter, A., Abdulrahman, B. A., Tazi, M., Hassan, H., et al. (2013). A bacterial protein promotes the recognition of the *Legionella pneumophila* vacuole by autophagy. *Eur. J. Immunol.* 43, 1333–1344. doi: 10.1002/eji.201242835

Koch-Edelmann, S., Banhart, S., Saied, E. M., Rose, L., Aeberhard, L., Laue, M., et al. (2017). The cellular ceramide transport protein CERT promotes *Chlamydia psittaci* infection and controls bacterial sphingolipid uptake. *Cell. Microbiol.* 19:e12752. doi: 10.1111/cmi.12752

Lee, M. J., Van Brocklyn, J. R., Thangada, S., Liu, C. H., Hand, A. R., Menzeleev, R., et al. (1998). Sphingosine-1-phosphate as a ligand for the G protein-coupled receptor EDG-1. *Science* 279, 1552–1555. doi: 10.1126/science.279.5356.1552

Lennings, J., West, T. E., and Schwarz, S. (2018). The burkholderia type VI secretion system 5: composition, regulation and role in virulence. *Front. Microbiol.* 9:3339. doi: 10.3389/fmicb.2018.03339

Li, C., Wu, Y., Riehle, A., Orian-Rousseau, V., Zhang, Y., Gulbins, E., et al. (2017). Regulation of *Staphylococcus aureus* infection of macrophages by CD44, reactive oxygen species, and acid sphingomyelinase. *Antioxid. Redox Signal.* doi: 10.1089/ars.2017.6994 [Epub ahead of print].

Lingwood, C. A., Binnington, B., Manis, A., and Branch, D. R. (2010). Globotriaosyl ceramide receptor function - where membrane structure and pathology intersect. *FEBS Lett.* 584, 1879–1886. doi: 10.1016/j.febslet.2009.11.089

Luberto, C., Stonehouse, M. J., Collins, E. A., Marchesini, N., El-Bawab, S., Vasil, A. I., et al. (2003). Purification, characterization, and identification of a sphingomyelin synthase from *Pseudomonas aeruginosa*. PlcH is a multifunctional enzyme. *J. Biol. Chem.* 278, 32733–32743. doi: 10.1074/jbc.M300932200

Maceyka, M., and Spiegel, S. (2014). Sphingolipid metabolites in inflammatory disease. *Nature* 510, 58–67. doi: 10.1038/nature13475

Manago, A., Becker, K. A., Carpinteiro, A., Wilker, B., Soddemann, M., Seitz, A. P., et al. (2015). *Pseudomonas aeruginosa* pyocyanin induces neutrophil death via mitochondrial reactive oxygen species and mitochondrial acid sphingomyelinase. *Antioxid. Redox Signal.* 22, 1097–1110. doi: 10.1089/ars.2014.5979

Melton-Celsa, A. R. (2014). Shiga Toxin (Stx) classification, structure, and function. *Microbiol. Spectr.* 2:EHEC–0024–2013. doi: 10.1128/microbiolspec.EHEC-0024-2013

Nagahama, M., Takehara, M., Takagishi, T., Seike, S., Miyamoto, K., and Kobayashi, K. (2017). cellular uptake of clostridium botulinum C2 toxin requires acid sphingomyelinase activity. *Infect. Immun.* 85:e00966-16. doi: 10.1128/IAI.00966-16

Nakayama, H., Kurihara, H., Morita, Y. S., Kinoshita, T., Mauri, L., Prinetti, A., et al. (2016). Lipoarabinomannan binding to lactosylceramide in lipid rafts is essential for the phagocytosis of mycobacteria by human neutrophils. *Sci. Signal.* 9:ra101. doi: 10.1126/scisignal.aaf1585

Nakayama, H., Ogawa, H., Takamori, K., and Iwabuchi, K. (2013). GSL-enriched membrane microdomains in innate immune responses. *Arch. Immunol. Ther. Exp.* 61, 217–228. doi: 10.1007/s00005-013-0221-6

Nieuwenhuizen, W. F., van Leeuwen, S., Gotz, F., and Egmond, M. R. (2002). Synthesis of a novel fluorescent ceramide analogue and its use in the characterization of recombinant ceramidase from *Pseudomonas aeruginosa* PA01. *Chem. Phys. Lipids* 114, 181–191. doi: 10.1016/s0009-3084(01)00206-7

Nora, T., Lomma, M., Gomez-Valero, L., and Buchrieser, C. (2009). Molecular mimicry: an important virulence strategy employed by *Legionella pneumophila* to subvert host functions. *Future Microbiol.* 4, 691–701. doi: 10.2217/fmb.09.47

Oda, M., Hashimoto, M., Takahashi, M., Ohmae, Y., Seike, S., Kato, R., et al. (2012). Role of sphingomyelinase in infectious diseases caused by Bacillus cereus. *PLoS One* 7:e38054. doi: 10.1371/journal.pone.0038054

Ohanian, J., and Ohanian, V. (2001). Sphingolipids in mammalian cell signalling. *Cell. Mol. Life. Sci.* 58, 2053–2068. doi: 10.1007/PL00000836

Okino, N., and Ito, M. (2016). Molecular mechanism for sphingosine-induced *Pseudomonas* ceramidase expression through the transcriptional regulator SphR. *Sci. Rep.* 6:38797. doi: 10.1038/srep38797

Okino, N., Tani, M., Imayama, S., and Ito, M. (1998). Purification and characterization of a novel ceramidase from *Pseudomonas aeruginosa*. *J. Biol. Chem.* 273, 14368–14373. doi: 10.1074/jbc.273.23.14368

Owen, K. A., Meyer, C. B., Bouton, A. H., and Casanova, J. E. (2014). Activation of focal adhesion kinase by *Salmonella* suppresses autophagy via an Akt/mTOR signaling pathway and promotes bacterial survival in macrophages. *PLoS Pathog* 10:e1004159. doi: 10.1371/journal.ppat.1004159

Peng, H., Li, C., Kadow, S., Henry, B. D., Steinmann, J., Becker, K. A., et al. (2015). Acid sphingomyelinase inhibition protects mice from lung edema and lethal Staphylococcus aureus sepsis. *J. Mol. Med.* 93, 675–689. doi: 10.1007/s00109-014-1246-y

Pewzner-Jung, Y., Tavakoli Tabazavareh, S., Grassme, H., Becker, K. A., Japtok, L., Steinmann, J., et al. (2014). Sphingoid long chain bases prevent lung infection by *Pseudomonas aeruginosa*. *EMBO Mol. Med.* 6, 1205–1214. doi: 10.15252/emmm.201404075

Prakash, H., Luth, A., Grinkina, N., Holzer, D., Wadgaonkar, R., Gonzalez, A. P., et al. (2010). Sphingosine kinase-1 (SphK-1) regulates *Mycobacterium smegmatis* infection in macrophages. *PLoS One* 5:e10657. doi: 10.1371/journal.pone.0010657

Rolando, M., Escoll, P., and Buchrieser, C. (2016a). *Legionella pneumophila* restrains autophagy by modulating the host's sphingolipid metabolism. *Autophagy* 12, 1053–1054. doi: 10.1080/15548627.2016.1166325

Rolando, M., Escoll, P., Nora, T., Botti, J., Boitez, V., Bedia, C., et al. (2016b). *Legionella pneumophila* S1P-lyase targets host sphingolipid metabolism and restrains autophagy. *Proc. Natl. Acad. Sci. U.S.A.* 113, 1901–1906. doi: 10.1073/pnas.1522067113

Rowbotham, T. J. (1980). Preliminary report on the pathogenicity of *Legionella pneumophila* for freshwater and soil amoebae. *J. Clin. Pathol.* 33, 1179–1183. doi: 10.1136/jcp.33.12.1179

Scanlon, K. M., Skerry, C., and Carbonetti, N. H. (2015). Novel therapies for the treatment of pertussis disease. *Pathog. Dis.* 73:ftv074. doi: 10.1093/femspd/ftv074

Schramm, M., Herz, J., Haas, A., Krönke, M., and Utermöhlen, O. (2008). Acid sphingomyelinase is required for efficient phago-lysosomal fusion. *Cell Microbiol.* 10, 1839–1853. doi: 10.1111/j.1462-5822.2008.01169.x

Schwan, C., Nolke, T., Kruppke, A. S., Schubert, D. M., Lang, A. E., and Aktories, K. (2011). Cholesterol- and sphingolipid-rich microdomains are essential for microtubule-based membrane protrusions induced by clostridium difficile transferase (CDT). *J. Biol. Chem.* 286, 29356–29365. doi: 10.1074/jbc.M111.261925

Seitz, A. P., Grassme, H., Edwards, M. J., Pewzner-Jung, Y., and Gulbins, E. (2015). Ceramide and sphingosine in pulmonary infections. *Biol. Chem.* 396, 611–620. doi: 10.1515/hsz-2014-0285

Shamseddine, A. A., Airola, M. V., and Hannun, Y. A. (2015). Roles and regulation of neutral sphingomyelinase-2 in cellular and pathological processes. *Adv. Biol. Regul.* 57, 24–41. doi: 10.1016/j.jbior.2014.10.002

Simonis, A., Hebling, S., Gulbins, E., Schneider-Schaulies, S., and Schubert-Unkmeir, A. (2014). Differential activation of acid sphingomyelinase and ceramide release determines invasiveness of *Neisseria meningitidis* into brain endothelial cells. *PLoS Pathog* 10:e1004160. doi: 10.1371/journal.ppat.1004160

Speer, A., Sun, J., Danilchanka, O., Meikle, V., Rowland, J. L., Walter, K., et al. (2015). Surface hydrolysis of sphingomyelin by the outer membrane protein Rv0888 supports replication of *Mycobacterium tuberculosis* in macrophages. *Mol. Microbiol.* 97, 881–897. doi: 10.1111/mmi.13073

Steinert, M., Heuner, K., Buchrieser, C., Albert-Weissenberger, C., and Glockner, G. (2007). *Legionella* pathogenicity: genome structure, regulatory networks and the host cell response. *Int. J. Med. Microbiol.* 297, 577–587. doi: 10.1016/j.ijmm.2007.03.009

Tavakoli Tabazavareh, S., Seitz, A., Jernigan, P., Sehl, C., Keitsch, S., Lang, S., et al. (2016). Lack of sphingosine causes susceptibility to pulmonary staphylococcus aureus infections in cystic fibrosis. *Cell. Physiol. Biochem.* 38, 2094–2102. doi: 10.1159/000445567

Teichgraber, V., Ulrich, M., Endlich, N., Riethmuller, J., Wilker, B., De Oliveira-Munding, C. C., et al. (2008). Ceramide accumulation mediates inflammation, cell death and infection susceptibility in cystic fibrosis. *Nat. Med.* 14, 382–391. doi: 10.1038/nm1748

Thompson, C. R., Iyer, S. S., Melrose, N., VanOosten, R., Johnson, K., Pitson, S. M., et al. (2005). Sphingosine kinase 1 (SK1) is recruited to nascent phagosomes in human macrophages: inhibition of SK1 translocation by *Mycobacterium tuberculosis*. *J. Immunol.* 174, 3551–3561. doi: 10.4049/jimmunol.174.6.3551

Tong, S. Y., Davis, J. S., Eichenberger, E., Holland, T. L., and Fowler, V. G. Jr. (2015). Staphylococcus aureus infections: epidemiology, pathophysiology, clinical manifestations, and management. *Clin. Microbiol. Rev* 28, 603–661. doi: 10.1128/CMR.00134-14

Utermöhlen, O., Karow, U., Löhler, J., and Krönke, M. (2003). Severe impairment in early host defense against *Listeria monocytogenes* in mice deficient in acid sphingomyelinase. *J. Immunol.* 170, 2621–2628. doi: 10.4049/jimmunol.170.5.2621

Wu, Y., Li, C., Riehle, A., Pollmeier, B., Gulbins, E., and Grassme, H. (2018). Mycobacterial infection is promoted by neutral sphingomyelinase 2 regulating a signaling cascade leading to activation of beta1-integrin. *Cell. Physiol. Biochem.* 51, 1815–1829. doi: 10.1159/000495683

Yamaji, T., and Hanada, K. (2015). Sphingolipid metabolism and interorganellar transport: localization of sphingolipid enzymes and lipid transfer proteins. *Traffic* 16, 101–122. doi: 10.1111/tra.12239

Zheng, S., Eierhoff, T., Aigal, S., Brandel, A., Thuenauer, R., de Bentzmann, S., et al. (2017). The *Pseudomonas aeruginosa* lectin LecA triggers host cell signalling by glycosphingolipid-dependent phosphorylation of the adaptor protein CrkII. *Biochim. Biophys. Acta Mol. Cell. Res.* 1864, 1236–1245. doi: 10.1016/j.bbamcr.2017.04.005

Conflict of Interest Statement: The authors declare that the research was conducted in the absence of any commercial or financial relationships that could be construed as a potential conflict of interest.

frontiers in Cell and Developmental Biology

CORRECTION
published: 03 February 2021
doi: 10.3389/fcell.2021.647045

Corrigendum: A Comprehensive Review on the Manipulation of the Sphingolipid Pathway by Pathogenic Bacteria

Monica Rolando and Carmen Buchrieser**

Biologie des Bactéries Intracellulaires, CNRS UMR 3525, Institut Pasteur, Paris, France

Keywords: sphingolipids, host-pathogen interactions, *Legionella*, *Pseudomonas*, *Mycobacteria*

OPEN ACCESS

Approved by:
Frontiers Editorial Office, Frontiers Media SA, Switzerland

****Correspondence:***
Monica Rolando
mrolando@pasteur.fr
Carmen Buchrieser
cbuch@pasteur.fr

Specialty section:
This article was submitted to Membrane Traffic, a section of the journal Frontiers in Cell and Developmental Biology

Received: *28 December 2020*
Accepted: *20 January 2021*
Published: *03 February 2021*

Citation:
Rolando M and Buchrieser C (2021) Corrigendum: A Comprehensive Review on the Manipulation of the Sphingolipid Pathway by Pathogenic Bacteria. Front. Cell Dev. Biol. 9:647045. doi: 10.3389/fcell.2021.647045

A Corrigendum on

A Comprehensive Review on the Manipulation of the Sphingolipid Pathway by Pathogenic Bacteria
by Rolando, M., and Buchrieser, C. (2019). Front. Cell Dev. Biol. 7:168. doi: 10.3389/fcell.2019.00168

There is an error in the Funding statement. The correct number for **ANR-18-CE18-0005-01** is **ANR-18-CE15-0005-01**.

The authors apologize for this error and state that this does not change the scientific conclusions of the article in any way. The original article has been updated.

frontiers in Cell and Developmental Biology

ORIGINAL RESEARCH
published: 13 September 2019
doi: 10.3389/fcell.2019.00194

Super-Resolution Microscopy Reveals Local Accumulation of Plasma Membrane Gangliosides at *Neisseria meningitidis* Invasion Sites

*Jan Schlegel[1], Simon Peters[2], Sören Doose[1], Alexandra Schubert-Unkmeir[2] and Markus Sauer[1]**

[1] Department of Biotechnology and Biophysics, Biocenter, Julius Maximilian University Würzburg, Würzburg, Germany,
[2] Institute of Hygiene and Microbiology, Julius Maximilian University Würzburg, Würzburg, Germany

Neisseria meningitidis (meningococcus) is a Gram-negative bacterium responsible for epidemic meningitis and sepsis worldwide. A critical step in the development of meningitis is the interaction of bacteria with cells forming the blood-cerebrospinal fluid barrier, which requires tight adhesion of the pathogen to highly specialized brain endothelial cells. Two endothelial receptors, CD147 and the β2-adrenergic receptor, have been found to be sequentially recruited by meningococci involving the interaction with type IV pilus. Despite the identification of cellular key players in bacterial adhesion the detailed mechanism of invasion is still poorly understood. Here, we investigated cellular dynamics and mobility of the type IV pilus receptor CD147 upon treatment with pili enriched fractions and specific antibodies directed against two extracellular Ig-like domains in living human brain microvascular endothelial cells. Modulation of CD147 mobility after ligand binding revealed by single-molecule tracking experiments demonstrates receptor activation and indicates plasma membrane rearrangements. Exploiting the binding of Shiga (STxB) and Cholera toxin B (CTxB) subunits to the two native plasma membrane sphingolipids globotriaosylceramide (Gb3) and raft-associated monosialotetrahexosylganglioside GM1, respectively, we investigated their involvement in bacterial invasion by super-resolution microscopy. Structured illumination microscopy (SIM) and *direct* stochastic optical reconstruction microscopy (*d*STORM) unraveled accumulation and coating of meningococci with GM1 upon cellular uptake. Blocking of CTxB binding sites did not impair bacterial adhesion but dramatically reduced bacterial invasion efficiency. In addition, cell cycle arrest in G1 phase induced by serum starvation led to an overall increase of GM1 molecules in the plasma membrane and consequently also in bacterial invasion efficiency. Our results will help to understand downstream signaling events after initial type IV pilus-host cell interactions and thus have general impact on the development of new therapeutics targeting key molecules involved in infection.

Keywords: *Neisseria meningitidis*, sphingolipids, gangliosides and lipid rafts, super-resolution microscopy, single-molecule tracking

OPEN ACCESS

Edited by:
Burkhard Kleuser,
University of Potsdam, Germany

Reviewed by:
Jörg Enderlein,
University of Göttingen, Germany
Erdinc Sezgin,
University of Oxford, United Kingdom

***Correspondence:**
Markus Sauer
m.sauer@uni-wuerzburg.de

Specialty section:
This article was submitted to Membrane Physiology and Membrane Biophysics, a section of the journal Frontiers in Cell and Developmental Biology

Received: *02 July 2019*
Accepted: *29 August 2019*
Published: *13 September 2019*

Citation:
Schlegel J, Peters S, Doose S, Schubert-Unkmeir A and Sauer M (2019) Super-Resolution Microscopy Reveals Local Accumulation of Plasma Membrane Gangliosides at Neisseria meningitidis Invasion Sites. Front. Cell Dev. Biol. 7:194. doi: 10.3389/fcell.2019.00194

INTRODUCTION

The obligate human pathogenic Gram-negative bacterium *Neisseria meningitidis* can cause epidemic meningitis and in severe cases sepsis and progressing fatal shock (Stephens et al., 2007). In healthy individuals the meningococci may reside as commensal organisms in the nasopharynx without affecting the host (Yazdankhah and Caugant, 2004). Under certain circumstances, the bacteria can enter the bloodstream and adhere to endothelial cells of blood microvessels, also known as vascular colonization (Melican and Dumenil, 2012) leading to inflammatory processes and disruption of the blood-cerebrospinal fluid barrier, a crucial step in disease progression into meningitis (reviewed in Lemichez et al., 2010). The initial process of bacterial adhesion to brain endothelial cells is mediated by type IV pili and its adhesion receptor CD147 on the host cell (Bernard et al., 2014).

Recently, super-resolution microscopy by *direct* stochastic optical reconstruction microscopy (*d*STORM) (Heilemann et al., 2008) demonstrated that *N. meningitidis* binding to endothelial cells requires CD147/β2-adrenergic receptor clustering at bacterial adhesion sites (Maïssa et al., 2017). Here, the assembly of plasma membrane receptors might serve as platform to support host-pathogen interactions. However, the molecular process of subsequent barrier-crossing is still under debate. Besides the investigated loosening of endothelial tight junctions (Coureuil et al., 2009; Schubert-Unkmeir et al., 2010) there is evidence that meningococci may use transcytotic pathways to enter perivascular tissues (Nikulin et al., 2006; Sutherland et al., 2010). Since signaling and interactions of CD147 is dependent on plasma membrane cholesterol (Wu et al., 2017) and ganglioside-enriched lipid rafts (Li et al., 2013) downstream rearrangement of the plasma membrane might facilitate bacterial invasion of cells.

Indeed, recent data suggests meningococcal type IV pili dependent binding to gangliosides (Mubaiwa et al., 2017), which has already been known for several pathogens colonizing the respiratory tract (Krivan et al., 1988). Glycosphingolipids in general are important host cell targets for a plenitude of pathogens such as fungi, bacteria, and viruses (Nakayama et al., 2018). They are composed of complex, highly variable glycan moieties linked to a lipophilic ceramide backbone with extensive molecular heterogeneity (Lingwood, 2011). Two well studied glycosphingolipids with receptor functions are the monosialotetrahexosylganglioside GM1, a prototype ganglioside, and the globotriaosylceramide Gb3, which both interact with protein receptors within lipid rafts to generate signaling platforms (Mutoh et al., 1995; Ichikawa et al., 2009; Lingwood et al., 2010; Prasanna et al., 2016).

Besides its importance in neuronal plasticity, GM1 can be targeted by Simian virus 40 (Tsai et al., 2003), *Brucella suis* (Naroeni and Porte, 2002), Cholera toxin B subunit (Cuatrecasas, 1973), *Escherichia coli* enterotoxin (Hyun and Kimmich, 1984), and *Vibrio cholerae* enterotoxin (Otnaess et al., 1983). Gb3, also known as CD77, is a marker for B cells entering apoptosis, but is also exploited by the Human Immunodeficiency Virus (HIV), or Shiga Toxin from *Shigella dysenteriae* (Lindberg et al., 1987; Mangeney et al., 1991; Hammache et al., 1999). Interestingly, the two glycosphingolipids are differentially expressed depending on the cell-cycle with an upregulation of GM1 in G0/G1 phase and increased expression of Gb3 in G2/M phase (Majoul et al., 2002).

Here, we first set out to investigate the mobility of CD147 upon *N. meningitidis* infection by single-molecule tracking experiments. Next, we investigated the role of the two sphingolipids GM1 and Gb3 during infection with *N. meningitidis* using fluorescently labeled CTxB and STxB subunits, respectively. Super-resolution microscopy by structured illumination microscopy (SIM) (Gustafsson, 2000) and *direct* stochastic optical reconstruction microscopy (*d*STORM) (Heilemann et al., 2008; van de Linde et al., 2011) shows GM1 accumulation around meningococci highlighting their significant importance for bacterial invasion.

MATERIALS AND METHODS

Bacterial Strains

Neisseria meningitidis strain MC58 was used in this study as a representative strain. Strain MC58 is a serogroup (Sg) B strain of the sequence type (ST)-74 (ST-32 clonal complex [cc]), which was isolated in 1983 in the United Kingdom and was kindly provided by E. R. Moxon (McGuinness et al., 1991). *N. meningitidis* strain 8013 (clone 12, also designated 2C43) was used for the preparation of the pili enriched fraction (PeF). This strain is a piliated capsulated Opa-, Opc- variant of the serogroup C meningococcal clinical isolate 8013 (ST-77/ST-8 clonal complex (cc), Institut Pasteur, 1989) and was kindly provided by M. Taha (Nassif et al., 1993). *N. meningitidis* strains were grown overnight on Columbia blood agar plates (bioMérieux) at 37°C and 5% CO_2 in a humidity incubator and cultured on the next day in PPM + medium (proteose-peptone medium supplemented with 1× Kellogg's supplement, 0.01 M $MgCl_2$ and 0.005 M $NaHCO_3$).

Cell Culture

Immortalized human brain microvascular endothelial cells (HBMEC) were kindly provided by K. S. Kim (Stins et al., 1997) and were cultured as described previously (Unkmeir et al., 2002). Briefly, cells were cultured in RPMI-1640 medium supplemented with 1% sodium pyruvate (1 mM), 1% L-glutamine (2 mM), 1% non-essential amino acids (all purchased from GE Healthcare, Little Chalfont, United Kingdom), 5 U/ml heparin (Biochrom, Berlin, Germany) and 30 μg/ml endothelial cell growth supplement (ECGS, CellSystems, Troisdorf, Germany). Cells were incubated at 37°C and 5% CO_2 in a humidified atmosphere.

Infection Assays

Adhesion and invasion was determined by using the gentamicin protection assays as described elsewhere (Simonis et al., 2014). Briefly, cells between the 10th and 25th passages were used for infection assays at a density of 4×10^5 cells/well. Cell medium was changed to infection medium [RPMI + 10% human serum (HS)] and cells were infected with MC58 at a multiplicity of infection (MOI) of 100 for 4 h. If indicated, cells were pre-incubated with 6.6 μg/ml CTxB in RPMI for 30 min prior to the

medium change. To determine the number of adherent bacteria, cells were washed three times with phosphate buffered saline (PBS), to remove unbound bacteria, and afterward incubated with 1% saponin in RPMI to lyse the cells. Then, the cell-lysates were collected, diluted and plated on blood agar plates. To determine invasive bacteria, cells were handled similar to the adherent set with the exception of an additional incubation of the cells with gentamicin (200 μg/ml) for 2 h prior to the saponin treatment to kill all extracellular bacteria.

Immunofluorescence and Fluorescence Microscopy

HBMEC were seeded onto 0.2% gelatine coated 8-well chamber slides (Sarstedt) at a density of 2×10^4 cells/well and incubated for at least 24 h. To avoid possible interference of labeled CD147 receptors with the coating during single-molecule tracking, HBMEC were seeded onto KOH cleaned 8-well glass instead. Following infection with the indicated bacterial strain, cells were fixed with 2% formaldehyde and 0.2% glutaraldehyde for 15 min and washed. Labeling was performed with CTxB and/or STxB (Sigma-Aldrich, custom conjugated to Alexa Fluor 647 or Alexa Fluor 555) at a concentration of 5 μg/ml for 1 h. Alternatively, cells were incubated over night with Alexa Fluor 488 phalloidin as recommended by standard protocols (Thermo Fisher Scientific). To immobilize the toxin subunits, cells were again fixed by 2% formaldehyde and washed with PBS before *d*STORM imaging. Samples were embedded in prolong glass antifade mountant for SIM (Zeiss Elyra S.1) or covered with switching buffer (100 mM Cysteamine in PBS, pH 7.7) for *d*STORM. Imaging conditions and microscope setups were used as previously described (Burgert et al., 2017). Reconstruction from the raw data was performed with ThunderSTORM (Ovesný et al., 2014) or Zeiss ZEN software for *d*STORM and SIM, respectively. Spatial analysis of localization data was done with custom-made Python software. Ripley's h function was computed and analyzed as described in Burgert et al. (2017). Ripley's h function (Kiskowski et al., 2009) was computed for experimental and simulated data. Synthetic data with a localization density and region equal to the experimental data was prepared from a homogeneous point process of complete spatial randomness and from a clustered Neyman-Scott point process in which parent localizations are homogeneously distributed and accompanied by normal-distributed child localizations. The number of child localizations is Poisson distributed with a mean equal to the number of localizations per cluster as found for the experimental data sets. The standard deviation of the normal distribution is set to 8 nm resembling the localization precision. Ripley's h function was computed 100 times from 200 random data points in order to estimate the variance.

Single-Molecule Tracking

To perform single-molecule tracking, the non-competitive monoclonal CD147 antibody (clone: MEM-M6/1, Biorad) was directly coupled to the amine-reactive dye SeTau-647-NHS (SETA Biomedicals) to obtain a degree of labeling of 1.7. After purification by size-exclusion (Zeba spin desalting columns 40K MWCO Thermo Fisher Scientific) HBMEC were labeled with 0.17 nM antibody solution for 5 min at 37°C and washed twice before imaging in FluoroBrite DMEM media (Thermo Fisher Scientific). If stated, HBMEC were incubated for 30 min with 10 μg/ml MEM-M6/6 CD147 antibody or 2 μg PeF/well before labeling with MEM-M6/1 antibody. Imaging was performed at the setup described in the microscopy methods section with exposure time 20 ms for a total acquisition time of 100 s. Spot detection was performed by fitting with ThunderSTORM (Ovesný et al., 2014) and tracks generated and filtered for minimal track length of 20 frames with the Python implementation of the Crocker-Grier (Crocker and Grier, 1996) algorithm Trackpy (Allan et al., 2016). Mean squared displacements of each measurement were calculated and the resulting ensemble MSD was fit with a power law (Manzo and Garcia-Parajo, 2015; Shen et al., 2017), $\mathrm{MSD}(\tau) = \alpha t^n$, yielding the distribution of the generalized diffusion constant [α] and anomalous exponent [n].

G1 Synchronization of HBMEC

G1 synchronization was performed using the method of serum starvation. 24 h prior to the experiment, HBMEC growth medium was removed and cells were washed once with PBS. Afterward, RPMI was added and the cells were further incubated as mentioned bevor. The cell population shift was controlled by propodium iodid (PI) staining. For that, cells were washed once with PBS and harvested in Eppendorf tubes. Afterward cells were washed three times with PBS, fixed in 3.7% formaldehyde for 30 min on ice and permeabilized with 0.25% Triton X-100 in PBS on ice. Cells were then stained with 10 μg/ml PI + 25 μg/ml RNase and incubated for 30 min at room temperature in the dark and immediately analyzed afterward. 10,000 cells were analyzed using the FACSCalibur™ flow cytometer (BD Bioscience) and data were analyzed and graphed using FlowJo v10 (FlowJo, LLC). The gating strategy for G1, S, and G2 phase is shown in **Supplementary Figure S5B**.

Flow Cytometry

Three days prior to the experiment, 1.25×10^5 cells/ml were seeded in a 24-well plate and grown to approximately 1×10^6 cells/ml. On the day of the infection experiment, cell medium was replaced by RPMI + 10% HS. Cells were infected with bacteria for 4 h. After infection, cells were washed once with PBS, trypsinized and harvested in an Eppendorf tube. After washing with ice cold FACS buffer (5% FCS in PBS), cells were incubated with Alexa Fluor 647 labeled CTxB for 30 min at room temperature in the dark. After incubation, cells were washed three times with FACS buffer and fixed in 3.7% paraformaldehyde in PBS for 30 min at 4°C. Afterward, cells were washed three times with FACS buffer and 500 μl were transferred into a FACS-tube for the measurement. 10,000 cells were analyzed using the FACSCalibur™ flow cytometer (BD Bioscience) and data were analyzed and graphed using FlowJo v10 (FlowJo, LLC).

Preparation of Pilus Enriched Fractions (PeF)

Pilus enriched fractions (PeF) were prepared as described previously (Peters et al., 2019). The bacterial content of 50 blood agar plates was harvested in 40 ml of 0.15 M ethanolamine (in PBS) with a pH of 10.5. Pili were sheared of by intensive vortexing for 2 min followed by centrifugation at 12.000 × *g* for 10 min at room temperature to remove cellular debris. The supernatant was used for an additional centrifugation step at 21.000 × *g* for 90 min to remove smaller debris. Then, the supernatant was transferred to an Erlenmeyer flask and ammonium sulfate saturated 0.15 M ethanolamine was added to a concentration of 10% and was incubated under continuous shacking for 30 min at room temperature. The protein-ammonium sulfate precipitate was then harvested by centrifugation at 21.000 × *g* for 15 min. The supernatant was discarded and the pellet was re-suspended in 0.05 M Tris buffer saline (TBS) pH 7.5. Protein solutions were then applied to a 6 ml Viva Spin column with a 7 kDa molecular weight cut of (MWCO) and were centrifuged at 4000 × *g* at room temperature until the volume reaches 1 ml. To clean the sample, TBS was added again to 6 ml followed by centrifugation as mentioned above.

Statistical Analysis and Data Visualization

Statistical analysis was performed by either unpaired two-tailed Student's *t*-test or analysis of variance (ANOVA) test followed by a *post hoc* test. Significance values are indicated by asterisks: $^{*}P < 0.05$; $^{**}P < 0.01$; $^{***}P < 0.001$; $^{****}P < 0.0001$. Normality was tested using the Kolmogorov–Smirnov test. Data was visualized as box plots showing the interquartile range (IQR) of the data with median as line and mean as square. The whiskers represent the lowest and highest value within 1.5 IQR of the lower and upper quartile, respectively. Outliers are shown as filled squares outside the IQR box.

RESULTS

Single-Molecule Tracking Reveals Modulation of CD147 Receptor Mobility Upon Interaction

It has been shown that CD147 and β2-adrenergic receptor (ß2AR) are organized in pre-existing complexes at the plasma membrane of endothelial cells, which accumulate at sites of meningococcal adhesion (Maïssa et al., 2017). This local enrichment of CD147-ß2AR complexes in the plasma membrane possibly allows bacteria to adhere to vascular walls *in vivo* and resist hemodynamic forces of blood flow. Since accumulation of receptors at bacterial adhesion sites requires a high mobility in the plasma membrane we performed live-cell single-molecule tracking experiments of CD147 under various experimental conditions using an N-terminal binding monoclonal antibody (MEM-6/1) directly conjugated to the photostable fluorescent dye SeTau-647 (Tsunoyama et al., 2018). In contrast to the membrane-proximal binding monoclonal antibody MEM-6/6 (**Figure 1A**) MEM-6/1 does not compete with the binding site of type IV pili as demonstrated by single-molecule tracking experiments of human brain microvascular endothelial cells (HBMEC) pretreated with saturating concentrations of pilus enriched fraction (PeF) (**Figure 1A** and **Supplementary Figure S1**; Bernard et al., 2014). Pretreatment with saturating PeF concentration did significantly reduce the number of accessible MEM-M6/1 epitopes during individual single-molecule tracking experiments (**Supplementary Figure S1**).

Using SeTau-647 labeled MEM-6/1 antibodies we followed CD147 on the basal plasma membrane of human brain microvascular endothelial cells (HBMEC) for a duration of 100 s with a time resolution of 20 ms using total internal reflection fluorescence (TIRF) microscopy (**Figure 1B** and **Supplementary Video S1**). For quantification of diffusion dynamics, we analyzed the mean square displacement (MSD) and fitted it with a power law (Manzo and Garcia-Parajo, 2015; Shen et al., 2017):

$$\mathrm{MSD}(\tau) = \alpha \tau^{n}$$

Treatment of HBMEC with the competitive MEM 6/6 antibody reduced the generalized diffusion constant α (**Figure 1C**) as well as the number of localized CD147 molecules (**Supplementary Figure S1**) whereas the anomalous diffusion exponent *n* remained unaltered (**Figure 1D**). Addition of meningococcal PeF before (pre-treated) and after labeling (post-treated) increased α and *n* only slightly (**Figures 1C,D**) demonstrating that PeF does not significantly change the mobility of the neisserial type IV pili receptor CD147. Still, the slight changes in mobility observed may indicate cytoskeletal rearrangements of the plasma membrane sphingolipid organization. Indeed a recent study revealed an increase in ceramide-rich platforms upon treatment of HBMEC with type IV pili (Peters et al., 2019). Therefore, we investigated the distribution and localization of the native glycosphingolipids GM1 and Gb3 by super-resolution microscopy.

Rearrangement of Plasma Membrane Sphingolipids During Meningococcal Infection

To investigate possible changes in lipid organization upon meningococcal adhesion we visualized the distribution of the two sphingolipids GM1 and Gb3 in the plasma membrane of brain endothelial cells using the cholera toxin B (CTxB) and shiga toxin B (STxB) subunit, respectively. Two-color confocal laser scanning images of HBMEC show that GM1 and Gb3 exhibit cell-cycle dependent expression rates (**Figure 2A**), only in S phase both sphingolipids are expressed and simultaneously detectable in the plasma membrane (Majoul et al., 2002). Corresponding *d*STORM images show that GM1 and Gb3 are homogeneously distributed throughout the plasma membrane of HBMEC (**Figures 2B–D**) without clear indication of clustering (**Supplementary Figure S2**). Analysis of the spatial distribution of localization data by Ripley's h function indicates merely clusters on length scales similar to the *d*STORM localization precision (∼8 nm). These clusters originate from repeated detection of fluorophores on each toxin subunit. The number

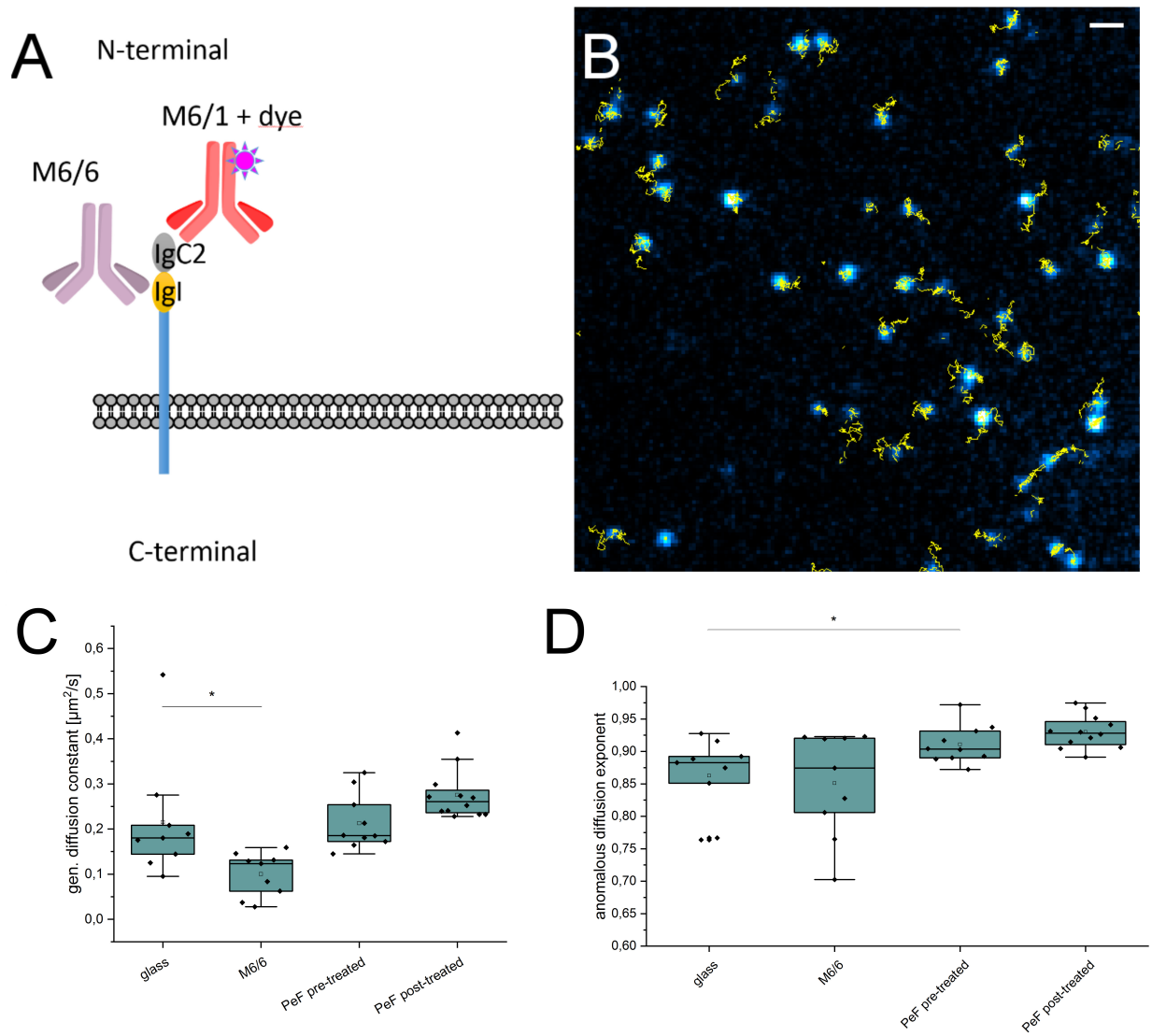

FIGURE 1 | Single-molecule tracking of CD147 on HBMEC using monoclonal antibodies. **(A)** CD147 is a single pass membrane protein with two extracellular Ig-like domains. The N-terminal IgC2 domain is recognized by the MEM-M6/1 antibody which was conjugated to the photostable dye SeTau-647 (Tsunoyama et al., 2018) and used for single-molecule tracking. The membrane proximal IgI domain is the binding site for MEM-M6/6 and type IV pili of *N. meningitidis*. **(B)** Example of CD147 single-molecule tracks. SeTau-647 coupled MEM-M6/1 is depicted in cyan with corresponding local tracks in yellow. Overlay was created with the Fiji (Schindelin et al., 2012) plugin TrackMate (Tinevez et al., 2017). Scale bar, 1 µm. **(C)** The diffusion coefficient of CD147 is reduced upon pretreatment with 10 µg/ml MEM-M6/6 and hardly affected by PeF treatment. Values represent individual single-molecule tracking experiments. **(D)** The anomalous diffusion exponent is not affected by MEM-M6/6 treatment but increases slightly upon PeF treatment. Significance values are indicated by asterisks: *$P < 0.05$; **$P < 0.01$; ***$P < 0.001$; ****$P < 0.0001$.

of localizations per cluster (as quantified by the DBSCAN clustering algorithm) follows the degree of labeling of pentameric CTxB (0.9) and STxB (0.5). The same observations were made on toxin subunits unspecifically bound to the glass surface (**Supplementary Figure S3**).

Upon infection of cells with *N. meningitidis* the plasma membrane distribution of Gb3 remained unchanged (**Figures 3A,B**). In contrast GM1 showed a remarkable increase in fluorescence intensity around adhesive meningococci on the plasma membrane of HBMEC (**Figure 4A**). *d*STORM images of CTxB labeled HBMEC in the presence of meningococci were recorded from an axial plane slightly above the equatorial plane under epi-illumination to ensure imaging of a large part of the cellular plasma membrane with adhesive bacteria (**Figure 4B**). Our data clearly demonstrate strong accumulation of the ganglioside GM1 around adhesive bacteria (**Figure 4B**) whereas uninfected HBMEC show a homogeneous distribution of GM1 in the plasma membrane (**Figure 2**). To exclude non-specific binding of CTxB and STxB to meningococci, bacteria were seeded onto glass without HBMEC, labeled and imaged by *d*STORM. The corresponding images show that the two

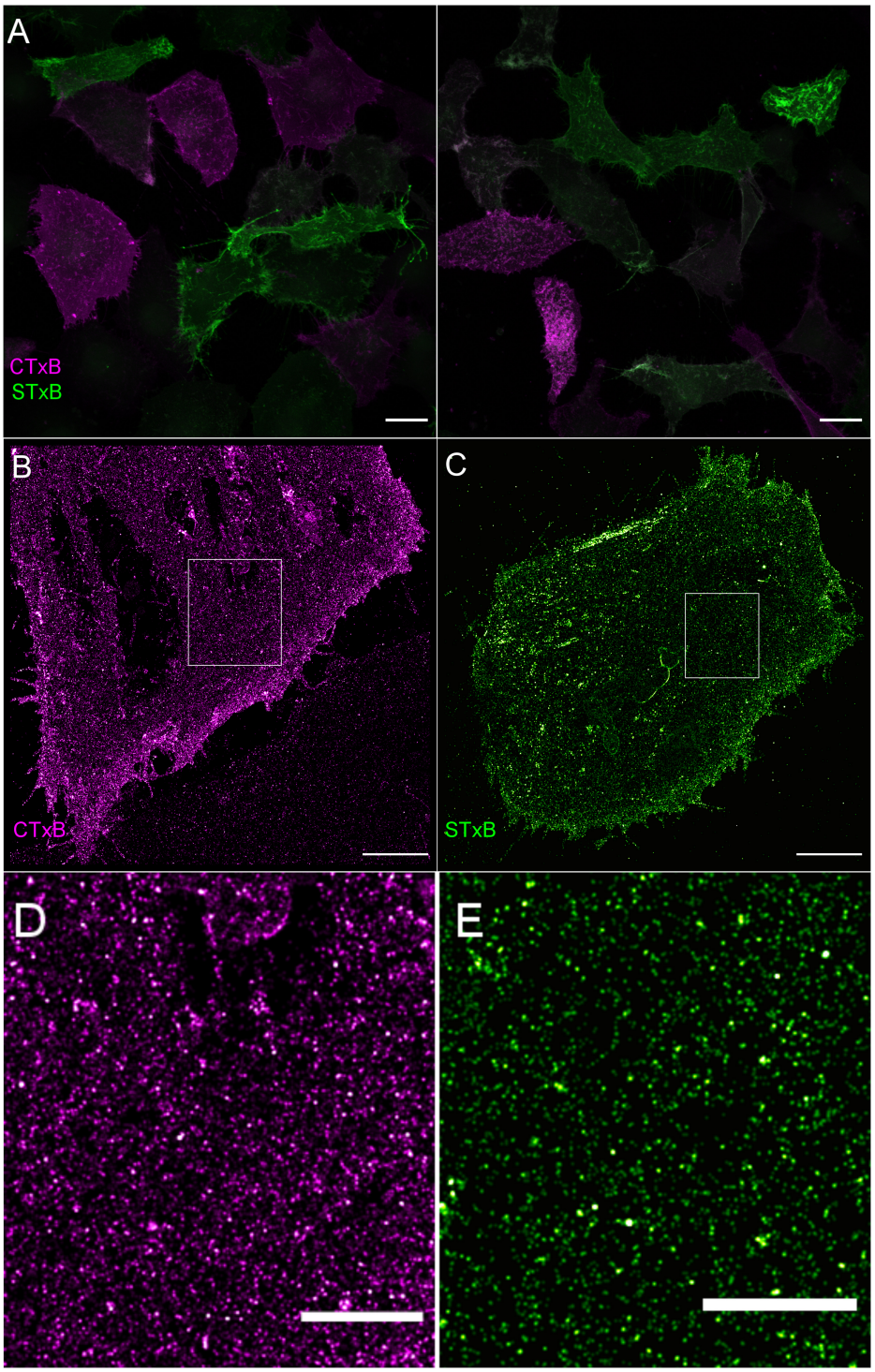

FIGURE 2 | Visualization of sphingolipids GM1 and Gb3 in the plasma membrane of brain endothelial cells. **(A)** Confocal laser scanning microscopy images of GM1 (magenta) and Gb3 (green) labeled with CTxB-Alexa Fluor 647 (magenta) and STxB-Alexa Fluor 555 (green), respectively. Scale bar, 20 μm. **(B)** 2D dSTORM images of GM1 labeled with CTxB-Alexa Fluor 647, and **(C)** Gb3 labeled with STxB-Alexa Fluor 647 showing a homogeneous distribution of the two sphingolipids in the plasma membrane of HBMEC. Scale bar, 5 μm. **(D)** Expanded views of the white boxed regions showing homogeneous distributions of CTxB **(D)** and STxB **(E)**. Both regions are representative areas which were used for cluster analysis by Ripley's h function **(Supplementary Figure S2)**. Scale bar 2 μm.

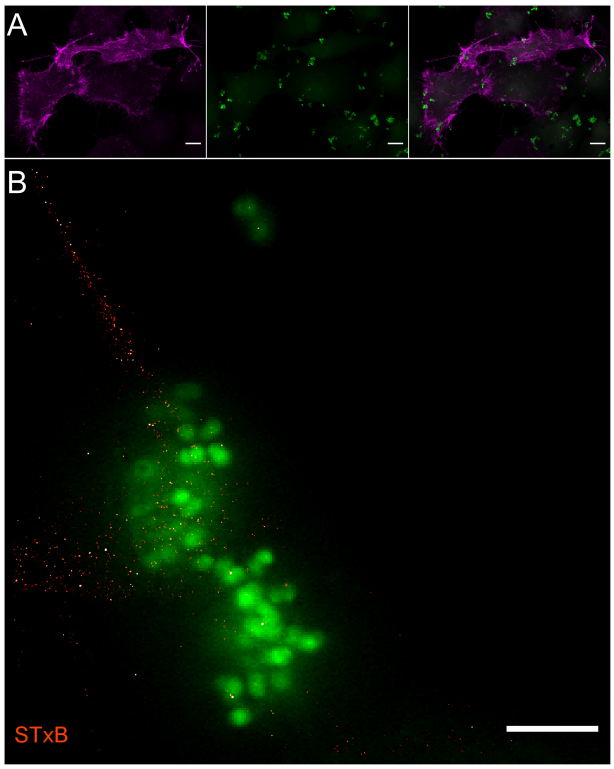

FIGURE 3 | Fluorescence microscopy of Gb3 in the plasma membrane of brain endothelial cells during *N. meningitidis* infection. **(A)** Confocal laser scanning microscopy of HBMEC labeled with STxB-Alexa Fluor 555 (magenta) and infected with GFP expressing *N. meningitidis* (green). No accumulation of Gb3 was observed at invasion sites. Scale bar, 5 μm. **(B)** Super-resolution *d*STORM image showing that the distribution of Gb3 in the plasma membrane of HBMEC does not change upon infection with meningococci (green). Gb3 was labeled with Alexa Fluor 647 conjugated STxB (red). The diffraction limited GFP signal was upscaled for the overlay. Same imaging and analysis parameters were used for the *d*STORM image as in **Figure 2**. Scale bar, 5 μm.

sphingolipids do not bind non-specifically to meningococci (**Supplementary Figure S3**).

Next, we tested if CD147 and actin as highly conserved key cytoskeletal protein involved in organization of the plasma membrane, colocalize with GM1 and accumulate around meningococci adhesion sites on the plasma membrane of HBMEC (Coureuil et al., 2010; Maïssa et al., 2017). However, SIM images show strong colocalization of the adhesion receptor CD147 and actin but no enrichment or morphological change at invasion sites of bacteria (**Supplementary Figure S4**).

Increased Bacterial Invasion Upon G1 Phase Arrest and GM1 Upregulation

Since the expression of GM1 and Gb3 is highest in G1 and G2 phase of the cell cycle, respectively (Majoul et al., 2002) we next investigated cell cycle dependent effects on the adhesion and invasion efficiency of *N. meningitidis*. Serum starvation 24 h before the experiment caused a significant increase of HBMEC residing in G1 phase as demonstrated by PI staining of the DNA and flow cytometry analysis (**Supplementary Figures S5A,B**). Simultaneously the concentration of ganglioside GM1 present in the plasma membrane in G1 phase increased substantially (**Supplementary Figure S5C**).

Interestingly, infection of G1 phase arrested cells caused an even more pronounced increase of GM1 levels present in the plasma membrane of HBMEC (**Supplementary Figure S5C**). To analyze effects of increased GM1 levels during G1 phase on bacterial adhesion and invasion we performed gentamicin protection assays to estimate the number of adherent or invasive bacteria by counting of residual bacterial colonies. Here, bacterial adhesion was neither influenced by serum starvation of host cells nor blocking of GM1 by unlabeled CTxB (**Figure 5B**). In contrast, invasion of HBMEC by meningococci was significantly increased in synchronized cells and this effect could be abolished by blocking of GM1 (**Figure 5A**).

DISCUSSION

Single-molecule tracking enables the observation of highly dynamic processes from viral cell entry mechanisms (Ruthardt et al., 2011) to ligand-binding (Yanagawa et al., 2018) at high spatiotemporal resolution. Upon ligand-binding and subsequent activation, receptors typically undergo conformational changes and/or changes in oligomerization states, which is often accompanied by reduced mobility resulting in decreased diffusion coefficients (Chung et al., 2010; Yanagawa et al., 2018). In this study, we could show that the presence of a PeF alone did not significantly change the diffusion coefficient of neisserial type IV pilus receptor CD147. Rather, our data indicate a slightly altered type of mobility toward normal diffusion which might indicate cytoskeletal rearrangements or modulation of the plasma membrane lipid environment. Interestingly, addition of the monoclonal M6/6 antibody before single-molecule tracking experiments resulted in a strong decrease in the number of M6/1 antibodies bound on the plasma membrane.

Since both antibodies are capable to bind to monomeric and dimeric CD147 molecules (Koch et al., 1999) M6/6 antibody-induced clustering resulting in a reduced M6/1 antibody epitope accessibility can be excluded as explanation. Instead, the following hypotheses seem to be more plausible. Binding of M6/6 to the membrane proximal Ig-like domain might activate the receptor and induce the local production of matrix metalloproteinases leading to subsequent receptor shedding. Indeed, CD147-induced expression of matrix metalloproteinases results in proteolytic cleavage of membrane-associated CD147 and an increase of its soluble form (Tang et al., 2004). Additionally, the diffusion coefficient of CD147 was significantly reduced upon M6/6 antibody binding indicating that activation of CD147 reduces its mobility in the plasma membrane (**Figure 1C**). Notably, the M6/6 antibody has unique properties and can inhibit OKT3-induced T cell proliferation (Koch et al., 1999) or modulate multidrug resistance (Somno et al., 2016). This implies that CD147 signaling might influence plasma membrane organization and promote immobilization of the receptor. For

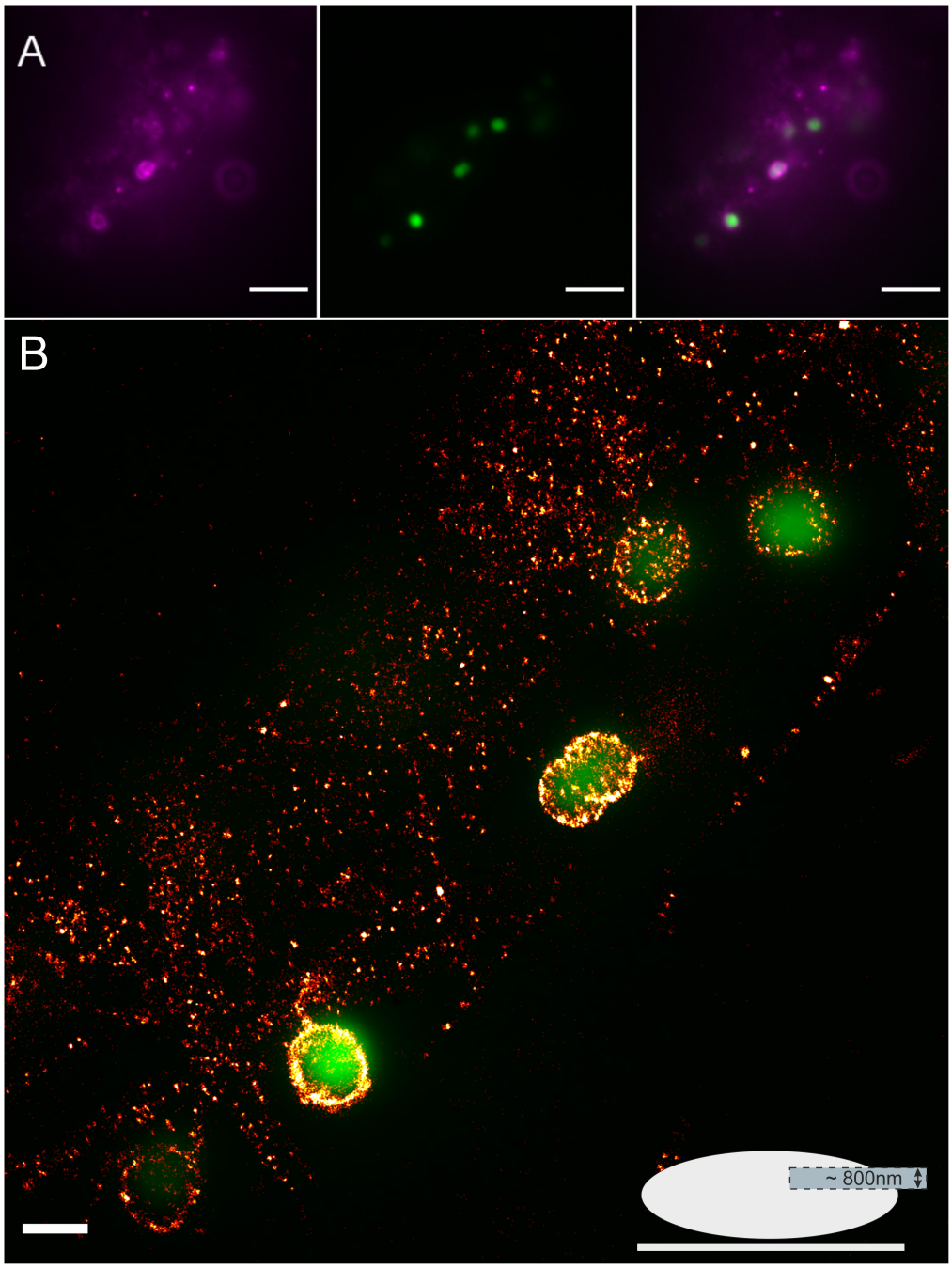

FIGURE 4 | Fluorescence imaging of GM1 in HBMEC upon infection with GFP expressing *N. meningitidis*. **(A)** Widefield fluorescence images of meningococci (green) and GM1 labeled with Alexa Fluor 647 CTxB (magenta). Scale bar, 5 μm. **(B)** *d*STORM image showing strong accumulation of GM1 around infection sites. The lower right corner shows a schematic model illustrating the mode of imaging. Adherent HBMEC were irradiated by epi-illumination. Detection was performed in an axial plane ensuring the imaging of a substantial part of the plasma membrane (light blue area). The axial area captured by the 2D *d*STORM image is determined to approximately 800 nm by the blurring of the point spread function above and below the imaging plane and data analysis parameter. Scale bar 1 μm.

this reason, following studies should dissect effects introduced by specific binding characteristics of the antibodies by using monovalent Fab fragments.

In contrast, addition of PeF did slightly increase the mobility of CD147 receptors (**Figure 1D**) although neisserial type IV pili and the M6/6 antibody compete for the same binding site (Bernard et al., 2014). In general, the affinity of the PilE and PilV monomers to CD147 is low and the need for multimeric organization as type IV pili seems to play an important role in mediating adherence (Bernard et al., 2014).

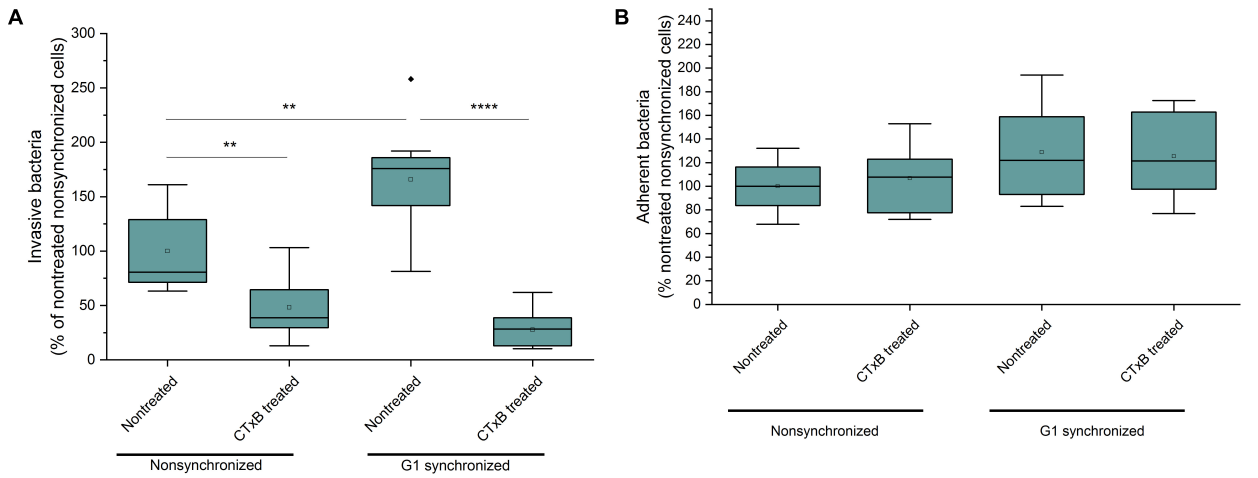

FIGURE 5 | Adhesion and invasion efficacy of *N. meningitidis* upon cell cycle arrest of HBMEC in G1 phase and CTxB pre-treatment. **(A)** The number of invasive meningococci was determined by gentamicin protection assays. Here, all extracellular bacteria were killed by incubation for 2 h in gentamicin solution and intracellular bacteria counted. Non-synchronized or G1 synchronized cells were preincubated with 6.6 μg/ml CtxB for 30 min at 37°C (if indicated) and afterward infected with MC58 for 4 h with a MOI of 100. **(B)** The number of adhesive bacteria was determined by counting of residual meningococci colonies after thorough washing and lysis of HBMEC.

Since our pili preparation contains mainly monomeric pilin subunits, as shown by Peters et al. (2019), incubation with our PeF preparation might not resemble the native condition where in addition to the multimeric assembly as pilus fibers whole micrometer-sized bacteria are attached to CD147. It seems thus more likely, that binding of the competitive M6/6 antibody reflects the native interaction of type IV pili with CD147 although this has to be verified in future experiments.

Glycosphingolipids represent important pathogen receptors (Nakayama et al., 2018) with thousands of possible structures. Notably, bacterial lipopolysaccharides are able to mimic host cell glycosphingolipids causing evasion of the immune system or leading to autoimmune diseases (Harvey et al., 2001).

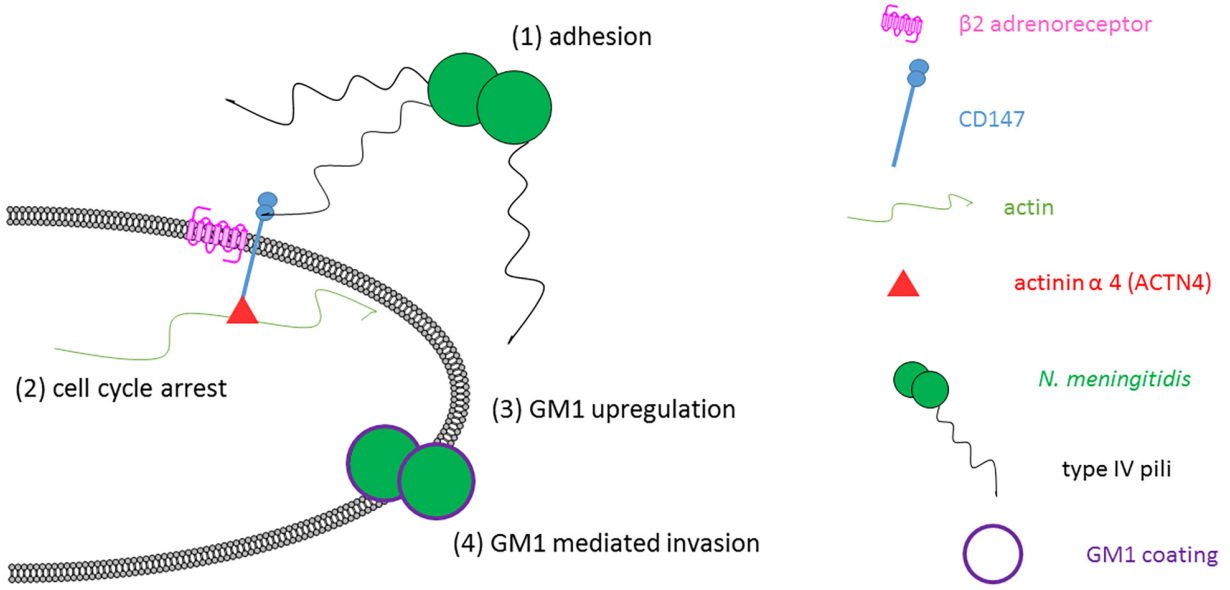

FIGURE 6 | Hypothetic model of meningococcal host cell invasion. *N. meningitidis* adhere with type IV pili to the membrane proximal Ig-like domain of CD147. After enrichment of β2-adrenergic receptor and actin downstream signaling cascades are triggered causing cell cycle arrest in G1 to S phase. Cell cycle dependent upregulation of GM1 at the plasma membrane increases the invasion efficacy of *N. meningitidis*. Bacteria interact with plasma membrane GM1 gangliosides facilitating entry into the cell or evasion from the human immune system. Drawing not to scale.

Although several possible host glycosphingolipids binding partners have been identified for *N. meningitidis* (Hugosson et al., 1998; Mubaiwa et al., 2017) molecular information about their involvement in pathogen interactions remained elusive. Furthermore, with a bacteria size of approximately 1 μm, the molecular details of host-bacteria interactions are difficult to image with conventional diffraction-limited fluorescence microscopy. Using single-molecule sensitive *d*STORM we could show that gangliosides are important host cell receptors mediating cellular entry of meningococcus by accumulating at bacterial adhesion sites (**Figure 4B**). Here, it has to be considered that CTxB does not exclusively bind to GM1 but possibly also to a plethora of other gangliosides (Kuziemko et al., 1996). Upon binding CTxB can be endocytosed via caveolae and clathrin-independent pathways although clathrin-mediated endocytosis seems to cover the major fraction (Torgersen et al., 2001). Which pathways are used in the context of meningococcal invasion and whether the bacteria are able to locally induce upregulation of GM1 or if this is a passive event triggered by cell cycle modulation is presently unknown and requires further experiments. Of note, pentameric STxB and CTxB possess multiple binding sites for individual glycosphingolipids and binding can be influenced by the chain length and saturation state of the attached fatty acid (Pellizzari et al., 1992; Kiarash et al., 1994). In order to reduce possible effects induced by multivalent toxin binding we fixed the cells before labeling to immobilize the binding partners.

However, our findings demonstrate that cell cycle arrest in G1 phase causes an increase of plasma membrane GM1 molecules leading to enhanced bacterial uptake. Blocking of GM1 strongly reduces infection efficiency implying the importance of plasma membrane gangliosides for bacterial invasion. *N. meningitidis* infection can cause accumulation of brain endothelial cells in S phase (Oosthuysen et al., 2016) and of human epithelial cells in G1 phase (Papen et al., 2016) and both cell cycle phases are positive for CTxB labeling (Majoul et al., 2002). Therefore, we propose a model where meningococci regulate their own uptake by initiating a positive feedback loop (**Figure 6**). The increased invasion efficacy should thus even be more pronounced in human epithelial cells whose gangliosides have already been described to interact with *Pseudomonas aeruginosa* pili (Comolli et al., 1999). We assume that this mechanism might play an important role in the initial uptake from the nasopharynx into the blood. Blocking this interaction could represent a promising method to avoid life-threatening dissemination of meningococci and help to develop therapeutic approaches for bacterial clearance.

DATA AVAILABILITY

The raw data supporting the conclusions of this manuscript will be made available by the authors, without undue reservation, to any qualified researcher.

AUTHOR CONTRIBUTIONS

JS designed and performed the experiments, applied the data analysis, and wrote the manuscript. SP performed the experiments involving living *N. meningitidis*, analyzed the data, and wrote the manuscript. SD performed the cluster analysis and data simulation, and provided the discussion. AS-U and MS guided the project, developed concepts, and wrote the manuscript.

FUNDING

This work was supported by the Deutsche Forschungsgemeinschaft (DFG SA829/16-2 and GRK2157 to MS and SCHU 2394/2-2 to AS-U) and the University of Würzburg in the funding programme Open Access Publishing.

ACKNOWLEDGMENTS

We thank Petra Gessner and Lisa Behringer-Pliess for assistance in cell culture and technical help.

SUPPLEMENTARY MATERIAL

The Supplementary Material for this article can be found online at: https://www.frontiersin.org/articles/10.3389/fcell.2019.00194/full#supplementary-material

FIGURE S1 | Number of localizations detected during individual CD147 single-molecule tracking experiments on HBMEC. CD147 was labeled with subnanomolar concentrations of monoclonal CD147 MEM-M6/1 antibody conjugated to SeTau647. Localizations were detected by fitting with ThunderSTORM (Ovesný et al., 2014). HBMEC were seeded on KOH cleaned glass and pre-treated with 10 μg/ml MEM-M6/6 CD147 antibody or 2 μg PeF/well before labeling with MEM-M6/1 antibody, if stated.

FIGURE S2 | Spatial distribution analysis of dSTORM data (red line). Ripley's h function was estimated 100 times (gray data curves with mean shown in color) for the dSTORM data representing GM1 labeled with CTxB-Alexa647 (left) and Gb3 labeled with STxB-Alexa647 (right) as shown in **Figures 2C,D**, respectively. For comparisn, Ripley's h function is shown for simulated data that represents a point process of complete spatial randomness (blue) and a clustered point process representing spatial clusters due to repeated localizations per toxin. The data indicates that experimental data is largely controlled by the photophysical clustering showing a homogeneous distribution of the two sphingolipids in the plasma membrane of HBMEC. The peak positions are found at nearly identical positions of (left) 27 nm and 22 nm and of (right) 38 nm and 21 nm for experimental and simulated data, representatively.

FIGURE S3 | *d*STORM images of GM1 and Gb3 of GFP expressing *N. meningitidis* (green) without HBMEC labeled with Alexa Fluor 647 conjugated CTxB or STxB. Both toxins non-specifically bind to the coverslip but do not show any accumulation at bacteria. The diffraction limited GFP signal was upscaled for the overlay. Scale bar, 5 μm.

FIGURE S4 | SIM images of GFP expressing meningococci infected HBMEC. CD147 labeled with monoclonal MEM-M6/1 and secondary F(ab)2-Alexa Fluor 647 (magenta). Actin labeled with phalloidin Atto565 (gray). GFP signal of meningococci (green) and overlay of the three images showing that CD147 and actin colocalize but do not accumulate at bacterial adhesion sites. Scale bar, 10 μm.

FIGURE S5 | Flow cytometry analysis of cell cycle state and average ganglioside GM1 concentration present in the plasma membrane of HMBEC. **(A)** Serum starvation was performed 24 h prior to the experiment by replacing the growth medium with RPMI. On the next day, cells were harvested, fixed, permeabilized and stained with PI (10 μg/ml PI + 25 μg/ml RNase) for 30 min in the dark at

room temperature. Afterward, PI incooperation was estimated via flow cytometry. Histogram of unsynchronized and G1 synchronized cells with the indicated gating strategy shown in **(B)**. **(C)** For the analysis of cell surface GM1, cells were stained with Alexa Fluor 647 conjugated CtxB for 30 min at room temperature in the dark. Then, cells were fixed for 30 min at 4°C, washed three times with FACS buffer and analyzed by flow cytometry.

VIDEO S1 | Examples of CD147 single-molecule tracks measured from one cell.

REFERENCES

Allan, D., Caswell, T., Keim, N., and van der Wel, C. (2016). *Trackpy: Trackpy V0.3.2*. Zenodo.

Bernard, S. C., Simpson, N., Join-Lambert, O., Federici, C., Laran-Chich, M.-P., Maïssa, N., et al. (2014). Pathogenic *Neisseria meningitidis* utilizes CD147 for vascular colonization. *Nat. Med.* 20, 725–731. doi: 10.1038/nm.3563

Burgert, A., Schlegel, J., Bécam, J., Doose, S., Bieberich, E., Schubert-Unkmeir, A., et al. (2017). Characterization of plasma membrane ceramides by super-resolution microscopy. *Angew. Chem. Int. Ed. Engl.* 56, 6131–6135. doi: 10.1002/anie.201700570

Chung, I., Akita, R., Vandlen, R., Toomre, D., Schlessinger, J., and Mellman, I. (2010). Spatial control of EGF receptor activation by reversible dimerization on living cells. *Nature* 464, 783–787. doi: 10.1038/nature08827

Comolli, J. C., Waite, L. L., Mostov, K. E., and Engel, J. N. (1999). Pili binding to asialo-GM1 on epithelial cells can mediate cytotoxicity or bacterial internalization by *Pseudomonas aeruginosa*. *Infect. Immun.* 67, 3207–3214.

Coureuil, M., Lécuyer, H., Scott, M. G. H., Boularan, C., Enslen, H., Soyer, M., et al. (2010). Meningococcus hijacks a β2-adrenoceptor/β-Arrestin pathway to cross brain microvasculature endothelium. *Cell* 143, 1149–1160. doi: 10.1016/j.cell.2010.11.035

Coureuil, M., Mikaty, G., Miller, F., Lécuyer, H., Bernard, C., Bourdoulous, S., et al. (2009). Meningococcal type IV pili recruit the polarity complex to cross the brain endothelium. *Science* 325, 83–87. doi: 10.1126/science.1173196

Crocker, J. C., and Grier, D. G. (1996). Methods of digital video microscopy for colloidal studies. *J. Colloid Interface Sci.* 179, 298–310. doi: 10.1006/jcis.1996.0217

Cuatrecasas, P. (1973). Gangliosides and membrane receptors for cholera toxin. *Biochemistry* 12, 3558–3566. doi: 10.1021/bi00742a032

Gustafsson, M. G. (2000). Surpassing the lateral resolution limit by a factor of two using structured illumination microscopy. *J. Microsc.* 198, 82–87. doi: 10.1046/j.1365-2818.2000.00710.x

Hammache, D., Yahi, N., Maresca, M., Piéroni, G., and Fantini, J. (1999). Human erythrocyte glycosphingolipids as alternative cofactors for human immunodeficiency virus type 1 (HIV-1) entry: evidence for CD4-induced interactions between HIV-1 gp120 and reconstituted membrane microdomains of glycosphingolipids (Gb3 and GM3). *J. Virol.* 73, 5244–5248.

Harvey, H. A., Swords, W. E., and Apicella, M. A. (2001). The mimicry of human glycolipids and glycosphingolipids by the lipooligosaccharides of pathogenic neisseria and haemophilus. *J. Autoimmun.* 16, 257–262. doi: 10.1006/jaut.2000.0477

Heilemann, M., van de Linde, S., Schüttpelz, M., Kasper, R., Seefeldt, B., Mukherjee, A., et al. (2008). Subdiffraction-resolution fluorescence imaging with conventional fluorescent probes. *Angew. Chem. Int. Ed. Engl.* 47, 6172–6176. doi: 10.1002/anie.200802376

Hugosson, S., Angström, J., Olsson, B. M., Bergström, J., Fredlund, H., Olcén, P., et al. (1998). Glycosphingolipid binding specificities of *Neisseria meningitidis* and *Haemophilus influenzae*: detection, isolation, and characterization of a binding-active glycosphingolipid from human oropharyngeal epithelium. *J. Biochem.* 124, 1138–1152. doi: 10.1093/oxfordjournals.jbchem.a022232

Hyun, C. S., and Kimmich, G. A. (1984). Interaction of cholera toxin and *Escherichia coli* enterotoxin with isolated intestinal epithelial cells. *Am. J. Physiol.* 247, G623–G631. doi: 10.1152/ajpgi.1984.247.6.G623

Ichikawa, N., Iwabuchi, K., Kurihara, H., Ishii, K., Kobayashi, T., Sasaki, T., et al. (2009). Binding of laminin-1 to monosialoganglioside GM1 in lipid rafts is crucial for neurite outgrowth. *J. Cell Sci.* 122, 289–299.doi: 10.1242/jcs.030338

Kiarash, A., Boyd, B., and Lingwood, C. A. (1994).). Glycosphingolipid receptor function is modified by fatty acid content. *Verotoxin* 1 and verotoxin 2c preferentially recognize different globotriaosyl ceramide fatty acid homologues. *J. Biol. Chem.* 269, 11138–11146.

Kiskowski, M. A., Hancock, J. F., and Kenworthy, A. K. (2009). On the use of Ripley's K-function and its derivatives to analyze domain size. *Biophys. J.* 97, 1095–1103. doi: 10.1016/j.bpj.2009.05.039

Koch, C., Staffler, G., Hüttinger, R., Hilgert, I., Prager, E., Cerný, J., et al. (1999). T cell activation-associated epitopes of CD147 in regulation of the T cell response, and their definition by antibody affinity and antigen density. *Int. Immunol.* 11, 777–786. doi: 10.1093/intimm/11.5.777

Krivan, H. C., Roberts, D. D., and Ginsburg, V. (1988). Many pulmonary pathogenic bacteria bind specifically to the carbohydrate sequence GalNAc beta 1-4Gal found in some glycolipids. *Proc. Natl. Acad. Sci. U.S.A.* 85, 6157–6161. doi: 10.1073/pnas.85.16.6157

Kuziemko, G. M., Stroh, M., and Stevens, R. C. (1996). Cholera toxin binding affinity and specificity for gangliosides determined by surface plasmon resonance. *Biochemistry* 35, 6375–6384. doi: 10.1021/bi952314i

Lemichez, E., Lecuit, M., Nassif, X., and Bourdoulous, S. (2010). Breaking the wall: targeting of the endothelium by pathogenic bacteria. *Nat. Rev. Microbiol.* 8, 93–104. doi: 10.1038/nrmicro2269

Li, L., Tang, W., Wu, X., Karnak, D., Meng, X., Thompson, R., et al. (2013). HAb18G/CD147 promotes pSTAT3-mediated pancreatic cancer development via CD44s. *Clin. Cancer Res.* 19, 6703–6715. doi: 10.1158/1078-0432.CCR-13-0621

Lindberg, A. A., Brown, J. E., Strömberg, N., Westling-Ryd, M., Schultz, J. E., and Karlsson, K. A. (1987). Identification of the carbohydrate receptor for Shiga toxin produced by *Shigella* dysenteriae type 1. *J. Biol. Chem.* 262, 1779–1785.

Lingwood, C. A. (2011). Glycosphingolipid functions. *Cold Spring Harb. Perspect. Biol.* 3, a004788. doi: 10.1101/cshperspect.a004788

Lingwood, C. A., Binnington, B., Manis, A., and Branch, D. R. (2010). Globotriaosyl ceramide receptor function - where membrane structure and pathology intersect. *FEBS Lett.* 584, 1879–1886. doi: 10.1016/j.febslet.2009.11.089

Maïssa, N., Covarelli, V., Janel, S., Durel, B., Simpson, N., Bernard, S. C., et al. (2017). Strength of *Neisseria meningitidis* binding to endothelial cells requires highly-ordered CD147/β2-adrenoceptor clusters assembled by alpha-actinin-4. *Nat. Commun.* 8:15764. doi: 10.1038/ncomms15764

Majoul, I., Schmidt, T., Pomasanova, M., Boutkevich, E., Kozlov, Y., and Söling, H.-D. (2002). Differential expression of receptors for shiga and cholera toxin is regulated by the cell cycle. *J. Cell Sci.* 115, 817–826.

Mangeney, M., Richard, Y., Coulaud, D., Tursz, T., and Wiels, J. (1991). CD77: an antigen of germinal center B cells entering apoptosis. *Eur. J. Immunol.* 21, 1131–1140. doi: 10.1002/eji.1830210507

Manzo, C., and Garcia-Parajo, M. F. (2015). A review of progress in single particle tracking: from methods to biophysical insights. *Rep. Prog. Phys.* 78:124601. doi: 10.1088/0034-4885/78/12/124601

McGuinness, B. T., Clarke, I. N., Lambden, P. R., Barlow, A. K., Poolman, J. T., Jones, D. M., et al. (1991). Point mutation in meningococcal por a gene associated with increased endemic disease. *Lancet* 337, 514–517. doi: 10.1016/0140-6736(91)91297-8

Melican, K., and Dumenil, G. (2012). Vascular colonization by *Neisseria meningitidis*. *Curr. Opin. Microbiol.* 15, 50–56. doi: 10.1016/j.mib.2011.10.008

Mubaiwa, T. D., Hartley-Tassell, L. E., Semchenko, E. A., Jen, F. E.-C., Srikhanta, Y. N., Day, C. J., et al. (2017). The glycointeractome of serogroup B *Neisseria meningitidis* strain MC58. *Sci. Rep.* 7:5693. doi: 10.1038/s41598-017-05894-w

Mutoh, T., Tokuda, A., Miyadai, T., Hamaguchi, M., and Fujiki, N. (1995). Ganglioside GM1 binds to the Trk protein and regulates receptor function. *Proc. Natl. Acad. Sci. U.S.A.* 92, 5087–5091. doi: 10.1073/pnas.92.11.5087

Nakayama, H., Nagafuku, M., Suzuki, A., Iwabuchi, K., and Inokuchi, J.-I. (2018). The regulatory roles of glycosphingolipid-enriched lipid rafts in immune systems. *FEBS Lett.* 592, 3921–3942. doi: 10.1002/1873-3468.13275

Naroeni, A., and Porte, F. (2002). Role of cholesterol and the ganglioside GM(1) in entry and short-term survival of *Brucella suis* in murine macrophages. *Infect. Immun.* 70, 1640–1644. doi: 10.1128/IAI.70.3.1640-1644.2002

Nassif, X., Lowy, J., Stenberg, P., O'Gaora, P., Ganji, A., and So, M. (1993). Antigenic variation of pilin regulates adhesion of *Neisseria meningitidis* to

human epithelial cells. *Mol. Microbiol.* 8, 719–725. doi: 10.1111/j.1365-2958.1993.tb01615.x

Nikulin, J., Panzner, U., Frosch, M., and Schubert-Unkmeir, A. (2006). Intracellular survival and replication of *Neisseria meningitidis* in human brain microvascular endothelial cells. *Int. J. Med. Microbiol.* 296, 553–558. doi: 10.1016/j.ijmm.2006.06.006

Oosthuysen, W. F., Mueller, T., Dittrich, M. T., and Schubert-Unkmeir, A. (2016). *Neisseria meningitidis* causes cell cycle arrest of human brain microvascular endothelial cells at S phase via p21 and cyclin G2. *Cell Microbiol.* 18, 46–65. doi: 10.1111/cmi.12482

Otnaess, A. B., Laegreid, A., and Ertresvåg, K. (1983). Inhibition of enterotoxin from *Escherichia coli* and *Vibrio cholerae* by gangliosides from human milk. *Infect. Immun.* 40, 563–569.

Ovesný, M., Křížek, P., Borkovec, J., Svindrych, Z., and Hagen, G. M. (2014). ThunderSTORM: a comprehensive imagej plug-in for PALM and STORM data analysis and super-resolution imaging. *Bioinformatics* 30, 2389–2390. doi: 10.1093/bioinformatics/btu202

Papen, M., von Oosthuysen, W. F., Becam, J., Claus, H., and Schubert-Unkmeir, A. (2016). Disease and carrier isolates of *Neisseria meningitidis* Cause G1 Cell Cycle Arrest in Human Epithelial Cells. *Infect. Immun.* 84, 2758–2770. doi: 10.1128/IAI.00296-16

Pellizzari, A., Pang, H., and Lingwood, C. A. (1992). Binding of verocytotoxin 1 to its receptor is influenced by differences in receptor fatty acid content. *Biochemistry* 31, 1363–1370. doi: 10.1021/bi00120a011

Peters, S., Schlegel, J., Becam, J., Avota, E., Sauer, M., and Schubert-Unkmeir, A. (2019). *Neisseria meningitidis* type IV pili trigger Ca2+-dependent lysosomal trafficking of the acid sphingomyelinase to enhance surface ceramide levels. *Infect. Immun.* 87:e00410-19. doi: 10.1128/IAI.00410-19

Prasanna, X., Jafurulla, M., Sengupta, D., and Chattopadhyay, A. (2016). The ganglioside GM1 interacts with the serotonin1A receptor via the sphingolipid binding domain. *Biochim. Biophys. Acta* 1858, 2818–2826. doi: 10.1016/j.bbamem.2016.08.009

Ruthardt, N., Lamb, D. C., and Bräuchle, C. (2011). Single-particle tracking as a quantitative microscopy-based approach to unravel cell entry mechanisms of viruses and pharmaceutical nanoparticles. *Mol. Ther.* 19, 1199–1211. doi: 10.1038/mt.2011.102

Schindelin, J., Arganda-Carreras, I., Frise, E., Kaynig, V., Longair, M., Pietzsch, T., et al. (2012). Fiji: an open-source platform for biological-image analysis. *Nat. Methods* 9, 676–682. doi: 10.1038/nmeth.2019

Schubert-Unkmeir, A., Konrad, C., Slanina, H., Czapek, F., Hebling, S., and Frosch, M. (2010). *Neisseria meningitidis* induces brain microvascular endothelial cell detachment from the matrix and cleavage of occludin: a role for MMP-8. *PLoS Pathog.* 6:e1000874. doi: 10.1371/journal.ppat.1000874

Shen, H., Tauzin, L. J., Baiyasi, R., Wang, W., Moringo, N., Shuang, B., et al. (2017). Single particle tracking: from theory to biophysical applications. *Chem Rev.* 117, 7331–7376. doi: 10.1021/acs.chemrev.6b00815

Simonis, A., Hebling, S., Gulbins, E., Schneider-Schaulies, S., and Schubert-Unkmeir, A. (2014). Differential activation of acid sphingomyelinase and ceramide release determines invasiveness of *Neisseria meningitidis* into brain endothelial cells. *PLoS Pathog.* 10:e1004160. doi: 10.1371/journal.ppat.1004160

Somno, A., Anuchapreeda, S., Chruewkamlow, N., Pata, S., Kasinrerk, W., and Chiampanichayakul, S. (2016). Involvement of CD147 on multidrug resistance through the regulation of P-glycoprotein expression in K562/ADR leukemic cell line. *Leuk. Res. Rep.* 6, 33–38. doi: 10.1016/j.lrr.2016.08.001

Stephens, D. S., Greenwood, B., and Brandtzaeg, P. (2007). Epidemic meningitis, meningococcaemia, and *Neisseria meningitidis*. *Lancet* 369, 2196–2210. doi: 10.1016/S0140-6736(07)61016-61012

Stins, M. F., Gilles, F., and Kim, K. S. (1997). Selective expression of adhesion molecules on human brain microvascular endothelial cells. *J. Neuroimmunol.* 76, 81–90. doi: 10.1016/s0165-5728(97)00036-2

Sutherland, T. C., Quattroni, P., Exley, R. M., and Tang, C. M. (2010). Transcellular passage of *Neisseria meningitidis* across a polarized respiratory epithelium. *Infect. Immun.* 78, 3832–3847. doi: 10.1128/IAI.01377-1379

Tang, Y., Kesavan, P., Nakada, M. T., and Yan, L. (2004). Tumor-stroma interaction: positive feedback regulation of extracellular matrix metalloproteinase inducer (EMMPRIN) expression and matrix metalloproteinase-dependent generation of soluble EMMPRIN. *Mol. Cancer Res.* 2, 73–80.

Tinevez, J.-Y., Perry, N., Schindelin, J., Hoopes, G. M., Reynolds, G. D., Laplantine, E., et al. (2017). TrackMate: an open and extensible platform for single-particle tracking. *Methods* 115, 80–90. doi: 10.1016/j.ymeth.2016.09.016

Torgersen, M. L., Skretting, G., van Deurs, B., and Sandvig, K. (2001). Internalization of cholera toxin by different endocytic mechanisms. *J. Cell Sci.* 114, 3737–3747.

Tsai, B., Gilbert, J. M., Stehle, T., Lencer, W., Benjamin, T. L., and Rapoport, T. A. (2003). Gangliosides are receptors for murine polyoma virus and SV40. *EMBO J.* 22, 4346–4355. doi: 10.1093/emboj/cdg439

Tsunoyama, T. A., Watanabe, Y., Goto, J., Naito, K., Kasai, R. S., Suzuki, K. G. N., et al. (2018). Super-long single-molecule tracking reveals dynamic-anchorage-induced integrin function. *Nat. Chem. Biol.* 14, 497–506. doi: 10.1038/s41589-018-0032-35

Unkmeir, A., Latsch, K., Dietrich, G., Wintermeyer, E., Schinke, B., Schwender, S., et al. (2002). Fibronectin mediates Opc-dependent internalization of *Neisseria meningitidis* in human brain microvascular endothelial cells. *Mol. Microbiol.* 46, 933–946. doi: 10.1046/j.1365-2958.2002.03222.x

van de Linde, S., Löschberger, A., Klein, T., Heidbreder, M., Wolter, S., Heilemann, M., et al. (2011). Direct stochastic optical reconstruction microscopy with standard fluorescent probes. *Nat. Protoc.* 6, 991–1009. doi: 10.1038/nprot.2011.336

Wu, B., Cui, J., Yang, X.-M., Liu, Z.-Y., Song, F., Li, L., et al. (2017). Cytoplasmic fragment of CD147 generated by regulated intramembrane proteolysis contributes to HCC by promoting autophagy. *Cell Death Dis.* 8:e2925. doi: 10.1038/cddis.2017.251

Yanagawa, M., Hiroshima, M., Togashi, Y., Abe, M., Yamashita, T., Shichida, Y., et al. (2018). Single-molecule diffusion-based estimation of ligand effects on G protein-coupled receptors. *Sci. Signal.* 11:eaao1917. doi: 10.1126/scisignal.aao1917

Yazdankhah, S. P., and Caugant, D. A. (2004). *Neisseria meningitidis*: an overview of the carriage state. *J. Med. Microbiol.* 53, 821–832. doi: 10.1099/jmm.0.45529-45520

Conflict of Interest Statement: The authors declare that the research was conducted in the absence of any commercial or financial relationships that could be construed as a potential conflict of interest.

The handling Editor declared a past co-authorship with one of the authors MS.

frontiers in Cell and Developmental Biology

REVIEW
published: 19 September 2019
doi: 10.3389/fcell.2019.00203

Diverse Facets of Sphingolipid Involvement in Bacterial Infections

*Tobias C. Kunz and Vera Kozjak-Pavlovic**

Department of Microbiology, Biocenter, University of Würzburg, Würzburg, Germany

Sphingolipids are constituents of the cell membrane that perform various tasks as structural elements and signaling molecules, in addition to regulating many important cellular processes, such as apoptosis and autophagy. In recent years, it has become increasingly clear that sphingolipids and sphingolipid signaling play a vital role in infection processes. In many cases the attachment and uptake of pathogenic bacteria, as well as bacterial development and survival within the host cell depend on sphingolipids. In addition, sphingolipids can serve as antimicrobials, inhibiting bacterial growth and formation of biofilms. This review will give an overview of our current information about these various aspects of sphingolipid involvement in bacterial infections.

Keywords: infection, pathogenic bacteria, sphingolipids, ceramide, autophagy

OPEN ACCESS

Edited by:
Burkhard Kleuser,
University of Potsdam, Germany

Reviewed by:
Rodrigo F. M. De Almeida,
University of Lisbon, Portugal
Luis M. S. Loura,
University of Coimbra, Portugal
Pedro Escoll,
Institut Pasteur, France

****Correspondence:***
Vera Kozjak-Pavlovic
vera.kozjak@uni-wuerzburg.de

Specialty section:
This article was submitted to Membrane Physiology and Membrane Biophysics, a section of the journal Frontiers in Cell and Developmental Biology

Received: *28 June 2019*
Accepted: *05 September 2019*
Published: *19 September 2019*

Citation:
Kunz TC and Kozjak-Pavlovic V (2019) Diverse Facets of Sphingolipid Involvement in Bacterial Infections. Front. Cell Dev. Biol. 7:203. doi: 10.3389/fcell.2019.00203

INTRODUCTION

Sphingolipids belong to a class of lipids defined by their amino-alcohol backbone. They were considered merely to be ubiquitous components of the eukaryotic cell membrane, shown to play a critical role in the formation of membrane microdomains called lipid rafts that are important for cell signaling (Simons and Ikonen, 1997). However, in the past decades, it has been revealed that many sphingolipids are bioactive lipids that regulate a large subset of cellular functions, such as apoptosis or autophagy (Cuvillier et al., 1996; Harvald et al., 2015). Although sphingolipids vary greatly in their structure and function, their synthesis and degradation are mediated by common synthetic and catabolic pathways. Sphingolipids can be synthesized *de novo*, by the hydrolysis of sphingomyelin, or through the salvage pathway, by recovery of sphingosine from complex sphingolipids (**Figure 1**). In all cases the result is the synthesis of ceramide, which represents the starting point for the creation of complex sphingolipids and thus is involved in many regulating processes within the cell. The metabolism of sphingolipids has been extensively reviewed by Gault et al. (2010). Ceramide itself regulates growth and development and promotes cell survival and division (Mencarelli and Martinez-Martinez, 2013).

The *de novo* biosynthesis of ceramide starts at the endoplasmic reticulum (ER) with an enzyme called serine palmitoyltransferase. This enzyme catalyzes the condensation of serine and fatty acid-CoA to 3-ketosphinganine. Afterward, 3-ketosphinganine gets reduced by 3-ketosphinganine reductase and then is processed by dihydroceramide synthase to dihydroceramide. In the final step of the *de novo* ceramide biosynthesis, a dihydroceramide desaturase introduces a double bond to create ceramide (Perry, 2002; Menaldino et al., 2003; **Figure 1**).

Constitutive degradation of sphingolipids and glycosphingolipids takes place in the late endosomes and lysosomes at acidic pH to form sphingosine (Riboni et al., 1997; Kolter and Sandhoff, 2005). The oligosaccharide chains of glycosphingolipids are stepwise removed by the release of monosaccharide units through exohydrolases. In the salvage pathway, long-chain sphingoid bases are broken down to sphingosine, which is reacylated to form ceramide by an

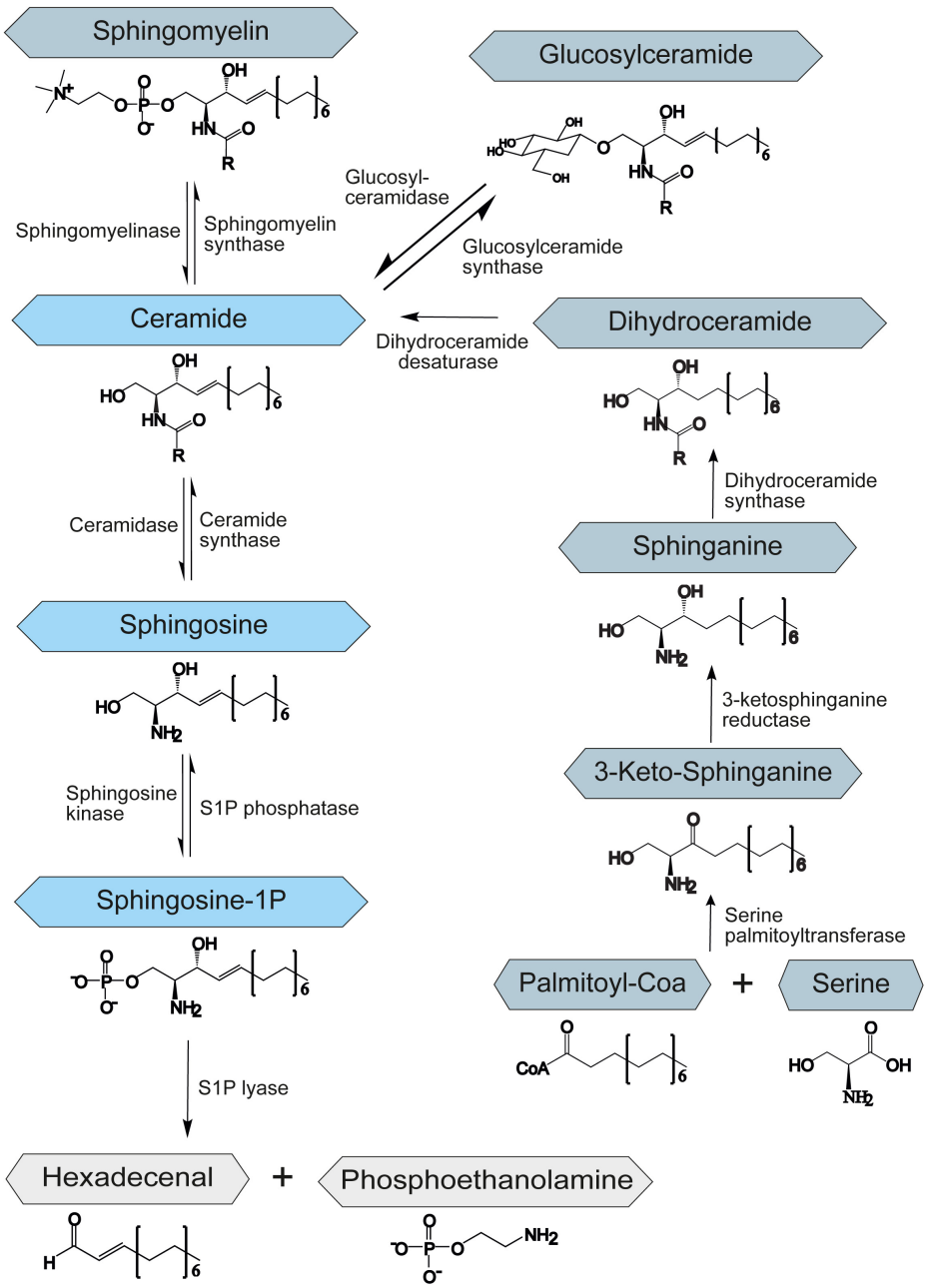

FIGURE 1 | Schematic representation of the sphingolipid metabolism. S1P – sphingosine-1-phosphate. The central role of the sphingolipid metabolism plays ceramide. It is synthesized *de novo* from serine and palmitoyl-CoA, by hydrolysis of sphingomyelin or through the salvage pathway by recovery of sphingosine from complex sphingolipids. Degradation of sphingolipids occurs through the degradation of S1P to hexadecenal and phosphoethanolamine by an enzyme called S1P-lyase.

enzyme called ceramide synthase. Thus, ceramide synthase family members probably trap free sphingosine released from the lysosome at the surface of the ER or in ER-associated membranes. The salvage pathway is estimated to contribute to 50–90% of sphingolipid biosynthesis (Gillard et al., 1998; Tettamanti et al., 2003).

During the generation of ceramide from sphingosine, ceramide synthases add different fatty acyl chains at the C2-amino group of the sphingosine backbone, resulting in numerous and diverse sphingolipids. Variations in the chain length of ceramide acyl chains are linked to potentially altered membrane bilayer dynamics or differential signaling properties by recruitment of different binding partners. This topic has previously been reviewed by Grösch et al. (2012). However, the effect of different length of acyl chains on ceramide properties and function is poorly understood and needs further investigation.

Ceramide exerts a specific function in mitochondria, where the increase in ceramide has been linked to the induction of apoptosis. Ceramide pool in mitochondria seems to be regulated by the localized activity of ceramide synthase, sphingomyelinases, and neutral ceramidase. However, another source of mitochondrial ceramide could be the ER, due to the proximity and close interaction of these two organelles (Hernández-Corbacho et al., 2017).

Apart from ceramide, sphingosine-1-phosphate (S1P) has been shown to be a potent signaling molecule. It is linked to the regulation of mitochondrial function (Bajwa et al., 2015), gene expression (Davaille et al., 2000), and ER stress (Lépine et al., 2011). Moreover, it was implicated in the regulation of important processes such as apoptosis, autophagy, and cell proliferation (Harvald et al., 2015). S1P is synthesized by the sphingosine kinase-1 and -2 (SPHK1/2) by phosphorylation of sphingosine and degraded by the S1P phosphatase (SGPP) or lyase (SGPL1) to sphingosine or hexadecenal and phosphoethanolamine, respectively (**Figure 1**). While SPHK1 is mainly associated with cell survival (Sarkar et al., 2005), SPHK2 has been shown to influence mitochondrial function and homeostasis. It has also been involved in regulation of histone deacetylases and thereby in suppression of cell growth and promotion of apoptosis (Liu et al., 2003). SGPP and SGPL1 ensure balanced levels of S1P and other sphingolipid intermediates that may control cell growth and death. The upregulation of SGPL1 results in an accumulation of hexadecenal, which was shown to be cytotoxic (James and Zoeller, 1997).

In the last years, sphingolipids have been revealed as key players in infection processes. Even though most pathogenic bacteria do not produce their own sphingolipids, they are capable of utilizing or degrading host sphingolipids to promote their virulence. This review will summarize some of our current knowledge about involvement of sphingolipids in bacterial infection, starting from the interaction with pathogenic bacteria on the surface of the cell, including the uptake of bacteria, immune response, survival and propagation of intracellular bacteria, and ending with several remarks on the bactericidal effects of sphingolipids.

BACTERIAL ENTRY - ROLE OF SPHINGOLIPIDS IN BACTERIAL ADHESION AND UPTAKE

Glycosphingolipids frequently serve as receptors for *Escherichia coli* and other bacteria such as *Pseudomonas aeruginosa*, *Bordetella pertussis*, *Mycoplasma pneumoniae,* and *Helicobacter pylori* [reviewed in Hanada (2005)]. A prominent example is GM1 ganglioside, which serves as a receptor for cholera toxin (Holmgren et al., 1975). Also, ceramide-enriched lipid rafts acting as binding platforms, as well as sphingolipid signaling, such as through the activation of acid sphingomyelinase (ASM) (Simonis and Schubert-Unkmeir, 2018), often mediate the entry of bacterial pathogens into host cells, which is a step important for infection and establishment of bacteria in an intracellular niche (**Figure 2**).

For pathogenic *Neisseria*, sphingolipids play an important role in the adhesion and invasion into the host cell. *Neisseria meningitidis*, a causative agent of meningitis and meningococcal sepsis, similar to *Haemophilus influenzae* binds to specific glycosphingolipids on the host cell surface, which can be found on human granulocytes and oropharyngeal epithelium, the preferential habitat for these two pathogens (Hugosson et al., 1998). *Neisseria* express highly variable lipooligosaccharides (LOS) on their surface, molecular mimics of glycosphingolipids found on human cells. LOS undergo phase variation, which is important for immune evasion, as well as adherence and invasion (Harvey et al., 2001).

Several reports emphasize the role of sphingomyelinases in the invasion of pathogenic *Neisseria*. The activation of ASM by *N. gonorrhoeae*, a bacterium causing sexually transmitted disease gonorrhea, is important for the entry of these bacteria into non-phagocytic cells (Grassmé et al., 1997), which occurs through the Opa-mediated interaction of bacteria with carcinoembryonic antigen-related cell adhesion molecule (CEACAM) receptors (Hauck et al., 2000). Neutral sphingomyelinase (NSM) also plays a role in the uptake of *N. gonorrhoeae* (Faulstich et al., 2015), but by a different mechanism, the so-called $PorB_{IA}$-mediated low phosphate-dependent invasion (Kühlewein et al., 2006). *N. meningitidis* likewise causes the activation of ASM and ceramide release that are essential for the internalization of meningococci into brain endothelial cells, which is connected to the expression of the outer membrane protein OpcA and binding to cell surface heparan sulfate proteoglycans (HSPGs) (Simonis et al., 2014). Recently, a role of meningococcal pilus in the translocation of ASM to the surface of infected cells has been described (Peters et al., 2019). In all cases, invasion of the host cell contributes to immune evasion and spreading of these pathogenic bacteria from the site of the initial contact to other tissues.

Uptake of bacteria through activation of sphingomyelinases as seen for *Neisseria* is not always beneficial for the pathogen but represents a host defense mechanism, as well. For example, *P. aeruginosa*, associated with serious hospital-acquired and opportunistic infections, activates host ASM, leading to generation of plasma membrane ceramide-enriched platforms that mediate the internalization of bacteria, apoptosis induction and cytokine response (Grassme et al., 2003). In macrophages, as well as in neutrophils, infection with *P. aeruginosa* leads to cell death, which is important for the clearing of infection. In both cases the role of sphingomyelinases in this process has been proposed. For alveolar macrophages, after the activation of the ASM upon infection, the formation of ceramide-enriched platforms serves to amplify ASM-mediated redox signaling, which eventually leads to macrophage apoptosis (Zhang et al., 2008). In the case of neutrophils, the apoptosis is mediated through pyocyanin, a pigment and toxin released by *P. aeruginosa*, and through mitochondrial ASM (Managò et al., 2015). However, *P. aeruginosa* can possibly counteract the increase in ceramide through secretion of hemolytic phospholipase C that can synthesize sphingomyelin from ceramide, and alkaline ceramidase, which can break down

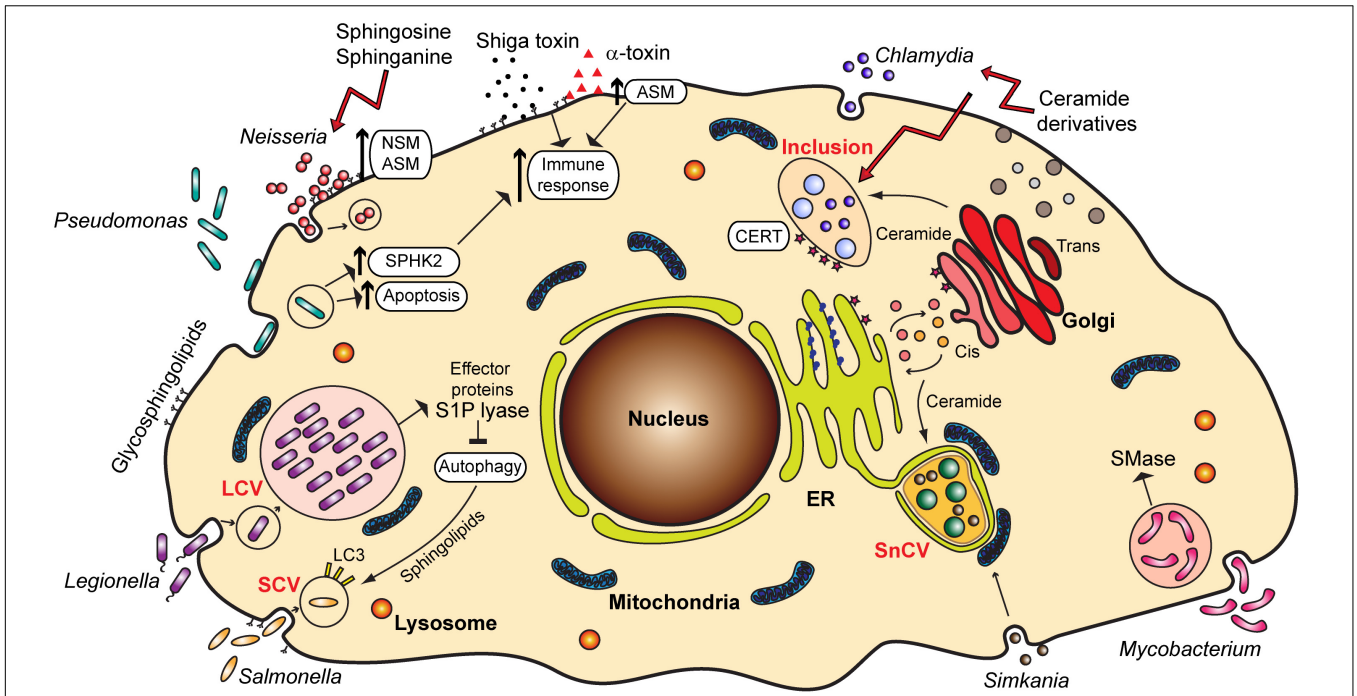

FIGURE 2 | Overview of the various bacterial pathogens and their interaction with sphingolipids and sphingolipid signaling pathways. ER, endoplasmic reticulum; LCV, *Legionella*-containing vacuole; SCV, *Salmonella*-containing vacuole; SnCV, *Simkania negevensis*-containing vacuole; ASM, acid sphingomyelinase; NSM, neutral sphingomyelinase; SPHK2, sphingosine kinase 2; S1P, sphingosine-1-phosphate; SMase, sphingomyelinase; CERT, ceramide transfer protein; LC3, Microtubule-associated protein 1A/1B-light chain 3.

ceramide to avoid generation of ceramide-enriched platforms and uptake, and increase hemolysis (Okino et al., 1998; Okino and Ito, 2007).

Not only ceramide, but sphingosine and S1P play a part in lung inflammatory injury caused by *P. aeruginosa*. SPHK2 is phosphorylated upon *P. aeruginosa* infection, which increases its nuclear localization, leading to higher levels of S1P and increased histone acetylation. This as a consequence has an enhanced expression of pro-inflammatory genes and secretion of pro-inflammatory cytokines, interleukin-6, and tumor necrosis factor-α (Ebenezer et al., 2019). Lastly, surface sphingolipids are also involved in infection with *P. aeruginosa*. The bacterial pilin binds to asialo GM1, but not to sialylated gangliosides. Considering that the surface of epithelial cells from cystic fibrosis patients shows differences in sialylation of glycolipids, this might enhance susceptibility of cystic fibrosis patients to infections with *P. aeruginosa* (Saiman and Prince, 1993).

Sphingolipids seem also to play a specific role in the internalization of *Mycobacteria*, among which are the causative agents of tuberculosis and leprosy, by macrophages, as shown for *Mycobacterium smegmatis*. For this bacterium, the metabolic depletion of sphingolipids in J774a.1 macrophages led to a decrease in entry of bacteria into the host cells (Viswanathan et al., 2018).

Finally, the pathogenicity of bacteria is often mediated by the binding of bacterial toxins to gangliosides and glycosphingolipids, but this aspect of the role of sphingolipids in bacterial infections will not be reviewed here in detail. Prominent examples are Shiga toxin from *Shigella dysenteriae* [reviewed in Kavaliauskiene et al. (2017)] and *Staphylococcus aureus* and its α-toxin. α-toxin has been reported to activate ASM, which leads to changes in permeability and lung edema (Becker et al., 2017). Ceramide increase upon *S. aureus* infection also stimulates pro-inflammatory signaling through a release of cathepsin B and D from lysosomes (Ma et al., 2017; **Figure 2**). Therefore, the inflammation, edema and lung tissue damage upon *S. aureus* infection seem to be induced by the binding of α-toxin and activation of ASM.

Inhibition of sphingomyelinases as a means of controlling inflammation and spread of infection might be consequently beneficial for *S. aureus* infection (Peng et al., 2015), or infection with pathogenic *Neisseria*, but is detrimental in case of infection with *P. aeruginosa* (Grassme et al., 2003). It is therefore of great importance to understand the mechanisms underlying infections with different pathogenic bacteria, so that this knowledge could be translated to appropriate treatments.

ONCE INSIDE - ROLE OF SPHINGOLIPIDS IN BACTERIAL REPRODUCTION AND SURVIVAL

Uptake of bacteria into cells can be a mechanism for bacterial killing, through formation of phagolysosomes or induction of autophagy. However, bacteria can avoid death by escaping into the cytosol, preventing fusion of phagosomes and lysosomes,

blocking autophagy, or, in some cases, surviving within the lysosomal environment. Certain bacteria also reside in non-lysosomal compartments inside the cell where they multiply, avoiding recognition and immune response. Sphingolipids have important function in many of these strategies for the survival of pathogenic bacteria within the host cell.

Sphingolipids in Bacterial Development and Reproduction

Obligate intracellular bacteria heavily depend on the host cell for the procurement of the metabolites required for their development. Sphingolipids represent important building blocks for the membranes of compartments in which these bacteria reside and multiply (**Figure 2**).

Chlamydia trachomatis, a causative agent of trachoma and sexually transmitted disease, is characterized by a biphasic life cycle, in which a reproductive part is spent inside the host cell, within a vesicular compartment known as an inclusion. *Chlamydia* directly obtain ceramide from the host cell Golgi and incorporate it into the inclusion membrane (Hackstadt et al., 1995; **Figure 2**). This is a process essential for the pathogen survival, in which chlamydial inclusion fuses with *trans*-Golgi network-derived secretory vesicles (van Ooij et al., 2000) in an Akt and Rab14-mediated way (Capmany and Damiani, 2010; Capmany et al., 2019). *C. trachomatis* has also been reported to cause the fragmentation of Golgi and to induce formation of mini stacks in the vicinity of the inclusion membrane, which supports lipid acquisition from the host (Heuer et al., 2009). Interestingly, it is possible that *C. trachomatis* establishes a sphingomyelin biosynthetic factory at or near the inclusion with the help of host cell proteins. Moreover, Elwell et al. (2011) showed that *C. trachomatis* co-opts Golgi-specific Brefeldin A resistance guanine nucleotide exchange factor 1 (GBF1), a protein important for the assembly and maintenance of the Golgi stack, for sphingomyelin acquisition contributing to the growth and stability of the inclusion. For the replication, however, *C. trachomatis* recruits ceramide transfer protein (CERT), vesicle-associated membrane protein-associated protein A (VAP-A), and sphingomyelin synthases, SMS1 and SMS2 to the inclusion membrane, therewith obtaining ceramide and converting it into sphingomyelin close to the inclusion (Elwell et al., 2011). Recruitment of CERT occurs with the help of chlamydial effector protein IncD present in the inclusion membrane (Agaisse and Derre, 2014). Other reports implicate additionally the Src family tyrosine kinase Fyn (Mital and Hackstadt, 2011), as well as *trans*-Golgi SNARE protein syntaxin 6 (Moore et al., 2011) in sphingolipid trafficking to chlamydial inclusion.

The described acquisition of sphingolipids from the host cells seems to be a common occurrence among chlamydia. Both *Chlamydia pneumoniae* and *Chlamydia psittaci* follow similar mechanisms, involving exocytic vesicles or CERT protein (Wolf and Hackstadt, 2001; Koch-Edelmann et al., 2017). In addition, a chlamydia-like microorganism *Simkania negevensis* has been likewise reported to obtain ceramide from the host cell, a process most likely dependent on the retrograde transport (Herweg et al., 2016).

Mycobacterium tuberculosis, although not strictly intracellular, uses host macrophages and dendritic cells for replication. During this process, the mycobacteria have been shown to depend on sphingomyelin. *M. tuberculosis* express the protein Rv0888, which exhibits a sphingomyelinase activity and cleaves host sphingomyelin into ceramide and phosphorylcholine. These compounds are used by bacteria as the sources of carbon, nitrogen and phosphorus (Speer et al., 2015). However, the purpose of *M. tuberculosis*-produced sphingomyelinases might be not only to provide a source of nutrients, but to modulate sphingolipid signaling and cell death induction, thereby controlling the immune response to this pathogen (Castro-Garza et al., 2016).

Sphingolipid Importance for the Survival of Intracellular Bacteria

Autophagy and apoptosis play a crucial role in controlling infection with various bacteria and viruses, representing an important part of innate immunity, but also being manipulated occasionally by pathogens for the purpose of survival or replication (Rudel et al., 2010; Siqueira et al., 2018). Sphingolipids were shown to be involved in the regulation of both apoptosis and autophagy, with ceramide being associated with cell death and S1P promoting cell survival (Young et al., 2013). Increase in intracellular levels of ceramide or treatment with sphingomyelinase has been reported to induce apoptosis in HL-60 or U937 cells, an effect which could be prevented by exposure of the cells to S1P (Cuvillier et al., 1996). For this, the term "sphingolipid rheostat" has been introduced to describe regulation of cell fate through the interconversion between ceramide and S1P. However, a multitude of later studies has shown a great complexity of the signaling mechanisms by which these sphingolipid metabolites influence cell death (Newton et al., 2015). As bacteria often modulate apoptosis to accommodate the host cell to their own needs (Rudel et al., 2010) it is possible that this modulation partially takes place through sphingolipid signaling, and that mitochondrial sphingolipids play a special role in this process. This direction is certainly worth exploring in the future, especially for intracellular bacteria.

In addition to apoptosis, autophagy and the associated cell death have also been subject to regulation by "sphingolipid rheostat" (Taniguchi et al., 2012; Young et al., 2013). Autophagy is a highly conserved catabolic process through which unnecessary or damaged components are degraded to maintain cellular homeostasis (Young et al., 2013; Young and Wang, 2018). In brief: a cargo is engulfed by a membrane forming the so-called autophagosome. Mature autophagosomes can then fuse with lysosomes, leading to the degradation of the cargo (Miller and Celli, 2016). It has been shown that S1P upregulates autophagy, therefore promoting cell survival, although several reports indicated that S1P can also act as an inhibitor of autophagy through activation of the mammalian target of rapamycin (mTOR) (Harvald et al., 2015). Ceramide induces autophagy and mitophagy, could be important for fusion of autophagosomes with lysosomes, and is involved in induction of autophagic cell death. In addition, the "many ceramides"

hypothesis implies that the function of ceramide depends on the chain length, adding a level of complexity to the regulation of autophagy through sphingolipids (Young et al., 2013; Harvald et al., 2015). Autophagy can be further subdivided in selective and non-selective. Non-selective autophagy describes the degradation of a random portion of a cytosol to provide nutrients during starvation or to degrade long-lived proteins. Selective autophagy targets specific cellular compartments. This includes utilizing the autophagy machinery for the removal of mitochondria (mitophagy) or the clearance of intracellular pathogens (xenophagy) (Deretic et al., 2013; Huang and Brumell, 2014). Hence, evading or regulating autophagy is important for the pathogen survival.

One well-studied pathogen regulating the autophagic machinery is *Legionella pneumophila*, a gram-negative bacterium naturally replicating in protists in aquatic environments. It is the causative agent of the Legionnaires' disease (Newton et al., 2010). As many signaling pathways are conserved in human macrophages and protists, *L. pneumophila* are capable of invading human cells, where they replicate in vacuoles, the so-called *Legionella*-containing vacuole (LCV). Inside the cell, *L. pneumophila* secretes over 300 effector proteins interfering with a broad range of cellular pathways. It has been shown that many of these effector proteins have a structure similar to eukaryotic proteins that are never or rarely found in prokaryotic genomes. It is hypothesized that *L. pneumophila* acquired these proteins through horizontal gene transfer from its host (Cazalet et al., 2004; Gomez-Valero and Buchrieser, 2013). Among those proteins, three proteins share similarities to eukaryotic proteins of the sphingolipid pathway: Lpp2641 (putative sphingomyelinase), Lpp2295 (putative sphingosine kinase) and Lpp2128 or *Lp*SPL (S1P lyase) (Rolando et al., 2016a). The latter, being a S1P lyase, leads to the degradation of S1P, which is a critical mediator for controlling the balance between sphingolipid-induced autophagy and cell death. Moreover, macrophages infected with *L. pneumophila* show an overall reduction of bioactive sphingolipids. Macrophages infected with an *Lp*SPL mutant strain show increased levels of sphingosine compared to wildtype *L. pneumophila* and indeed, *Lp*SPL was confirmed to restrain autophagy by acting on autophagosome biogenesis. Thus, *L. pneumophila* actively modulates sphingolipid metabolism to evade the cell autophagic response (Rolando et al., 2016b; **Figure 2**).

Another pathogen indicated to manipulate autophagy via sphingolipids is *Salmonella enterica*, an intestinal pathogen that represents a major public health threat due to increasing antibiotic resistance. Similar to *Legionella*, *Salmonella* forms a vacuole, called the *Salmonella*-containing vacuole (SCV). A recent publication extensively reviews the importance of sphingolipids for *Salmonella* infection from adherence to clearance, discussing the interaction of *Salmonella*, sphingolipids and the autophagic machinery (Huang, 2017).

Salmonella has been shown to activate the focal adhesion kinase and to recruit it to the SCV. This kinase promotes the activation of the Akt pathway and consequently mTOR is stimulated. This results in the suppression of autophagy and bacterial survival (Owen et al., 2014). More recent studies demonstrate that *Salmonella* does not only inhibit but actively regulates the autophagic pathway. In the early stages of infection, *Salmonella* triggers the amino acid starvation and mTOR inhibition, resulting in the induction of autophagy (Tattoli et al., 2012). However, in later stages the increase of cytosolic amino acid levels in infected cells reactivates mTOR at the surface of the SCV (Narayanan and Edelmann, 2014; **Figure 2**).

Inhibition of Akt signaling as well as the activation of extracellular signal-regulated kinase (ERK) 1/2 activity is associated with autophagy in colon adenocarcinoma cells (e.g., HT29 and HCT-15) (Ogier-Denis et al., 2000; Kanazawa et al., 2004; Ellington et al., 2006). In this regard, activated ERK was shown to upregulate beclin-1 expression, resulting in the induction of autophagy (Liu et al., 2012). Inhibition of the *de novo* biosynthesis of sphingolipids by myriocin, an inhibitor of the enzyme serine palmitoyl transferase, leads to decreased autophagy through the activation of Akt and downregulation of beclin-1 (Scarlatti et al., 2004). Moreover, myriocin downregulates ERK and represses the membrane recruitment of NOD2 and ATG16L1. The interaction of ATG16L1 and NOD2 in epithelial cells leads to autophagic degradation of *Salmonella*. In addition, myriocin decreased the *Salmonella*-induced LC3-II expression (Huang, 2016). These findings suggest that sphingolipids may play a role in *Salmonella*-induced cellular autophagy of damaged SCVs.

The cell ubiquitinates SCVs to trigger nuclear factor-κB (NF-κB) activation, which can lead to a reduction of bacterial propagation by the induction of inflammation. Furthermore, *Salmonella* escaping to the cytosol are tagged by a dense polyubiquitin coat (Narayanan and Edelmann, 2014). Both ceramide and NSM2 are connected to the regulation or modulation of protein ubiquitination and subsequent degradation (Chapman et al., 2005; Dobierzewska et al., 2011). Taking these facts into consideration, it is possible that sphingolipids play a role in the ubiquitination of the SCV.

BETTER SAFE THAN SORRY - SPHINGOLIPIDS AS ANTIMICROBIALS

Sphingolipids and sphingolipid signaling contribute to the immune response upon bacterial infection. Acid sphingomyelinase and ceramide play a decisive role in bacterial internalization and inflammatory response (Li et al., 2019). Sphingolipids, however, can also be applied as antimicrobial substances, regulating the growth and propagation of bacteria.

Around 30 years ago Bibel and colleagues pioneered the investigation of antimicrobial effects of sphingolipids. They reported that sphinganine influences the growth of *N. meningitidis* and *Acinetobacter lwoffii* and damages the cell wall of *S. aureus* (Bibel et al., 1993). Moreover, they tested sphinganine on human volunteers as a preventative antiseptic against subsequently applied *S. aureus* and observed an up to three-log reduction in the population of target micro-organisms compared to untreated controls (Bibel et al., 1995). Furthermore, it was shown that sphingosine effectively killed *S. aureus*, *Streptococcus pyogenes*, *Micrococcus luteus*,

Propionibacterium acnes, *Staphylococcus epidermidis* and moderately killed *P. aeruginosa*. However, sphingosine was demonstrated to not influence the growth of *E. coli* and *Serratia marcescens* (Bibel et al., 1992). Although more research is needed to understand these differences in the effect of sphingosine, one can speculate that it might be related to the fact that *E. coli* and *S. marcescens* are Gram-negative enterobacteria, as opposed to the others, which are Gram-positive.

The increasing lack of antibiotic treatments due to the development of resistances demands novel approaches for therapies. A better understanding of the antibacterial effect of sphingolipids may offer novel targets for treatment. Within the last decade, the number of publications reporting antimicrobial effects of different derivatives of sphingolipids has increased.

For instance, Banhart et al. (2014) demonstrated that the sphingomyelin synthase inhibitor D609, which has an effect on the uptake of fluorescently labeled ceramide by *Chlamydia muridarum* (Elwell et al., 2011), reduces the propagation of *C. trachomatis*. To better understand the impact of sphingomyelin production on the growth of *C. trachomatis*, they synthesized several ceramide derivatives, such as nitrobenzooxadiazole (NBD)-labeled 1-*O*-methyl-ceramide-C_{16}. This derivative resembles to a large extent a compound called 1-*O*-methyl-C_6-NBD-ceramide, which has been shown not to be converted to sphingomyelin. Interestingly, the treatment with this newly synthetized ceramide inhibits chlamydial growth similar to chloramphenicol and 17 times more effectively than D609 (Banhart et al., 2014).

In another study, the antibacterial activity of sphingosine, as well as short-chain C6 and long-chain C16-ceramides and azido functionalized ceramide analogs was tested. The study revealed that short-chain ceramides and a ω-azido-C6-ceramide had antibacterial effects on *N. meningitidis* and *N. gonorrhoeae*. The uptake of ceramides by *Neisseria* happened rapidly within 5 min, and the killing occurred within 2 h. In contrast to *Neisseria*, these analogs did not display any effects on *E. coli* and *S. aureus* (Becam et al., 2017). However, *E. coli* and *S. aureus* were shown to be efficiently killed by the treatment of dihydrosphingosine and sphingosine (Fischer et al., 2013). During *P. aeruginosa* infection, lower levels of sphingosine were observed due to a reduced activity of acid ceramidase, catalyzing the reaction of ceramide to sphingosine. By normalization of sphingosine levels, the susceptibility to *P. aeruginosa* could be decreased (Pewzner-Jung et al., 2014). Sphingosine, sphinganine and phytosphingosine were demonstrated to have a strong effect on biofilm formation and adherence of *Streptococcus mutans* (Cukkemane et al., 2015; **Figure 2**).

Beside host sphingolipids or chemically synthesized sphingolipids, extracted sphingolipids of plants have antibacterial activity, as well. For example, the sphingolipids ficusamide, (S)-(−) oxypeucedanin hydrate and (R)-(+) oxypeucedanin hydrate of *Ficus exasperata* showed antibacterial activity. While ficusamide had only a low activity against *E. coli*, (S)-(−) oxypeucedanin hydrate and (R)-(+) oxypeucedanin hydrate showed significant activity against *Bacillus cereus* (Dongfack et al., 2012).

CONCLUDING REMARKS

In the recent years, we have become increasingly aware of the importance of lipids, and sphingolipids in particular, for the processes of infection with and defense against pathogenic bacteria. Bacterial invasion or uptake are often mediated by bacterial attachment to glycosphingolipids or regulated by the increase in plasma membrane ceramide. Bacterial internalization can be a mechanism that increases pathogen survival, but sometimes it is also a part of the immunity, where again sphingolipids participate in the destruction of bacteria through regulating phagosome/lysosome fusion, apoptosis, or the inflammatory response. Intracellular bacteria face the challenges of survival within the cell and here also sphingolipids can be a tool to control autophagy and enable survival, or serve as building blocks for bacterial inclusions, ensuring their reproduction. However, sphingolipids can be applied as antimicrobials, as well, negatively influencing bacterial growth and biofilm formation. Understanding exact mechanisms behind these processes remains a challenge for the future and, in the wake of increasing antibiotic resistance, will be of great value in our fight against bacterial pathogens.

AUTHOR CONTRIBUTIONS

TK and VK-P wrote the manuscript and prepared the figures.

FUNDING

This publication was funded by the German Research Foundation (DFG) and the University of Würzburg in the funding program Open Access Publishing.

ACKNOWLEDGMENTS

We thank David Krones for critically reading the manuscript.

REFERENCES

Agaisse, H., and Derre, I. (2014). Expression of the effector protein IncD in *Chlamydia trachomatis* mediates recruitment of the lipid transfer protein CERT and the endoplasmic reticulum-resident protein VAPB to the inclusion membrane. *Infect. Immun.* 82, 2037–2047. doi: 10.1128/IAI.01530-14

Bajwa, A., Rosin, D. L., Chroscicki, P., Lee, S., Dondeti, K., Ye, H., et al. (2015). Sphingosine 1-phosphate receptor-1 enhances mitochondrial function and reduces cisplatin-induced tubule injury. *J. Am. Soc. Nephrol.* 26, 908–925. doi: 10.1681/ASN.2013121351

Banhart, S., Saied, E. M., Martini, A., Koch, S., Aeberhard, L., Madela, K., et al. (2014). Improved plaque assay identifies a novel anti-Chlamydia ceramide

derivative with altered intracellular localization. *Antimicrob. Agents Chemother.* 58, 5537–5546. doi: 10.1128/AAC.03457-14

Becam, J., Walter, T., Burgert, A., Schlegel, J., Sauer, M., Seibel, J., et al. (2017). Antibacterial activity of ceramide and ceramide analogs against pathogenic *Neisseria*. *Sci. Rep.* 7:17627. doi: 10.1038/s41598-017-18071-w

Becker, K. A., Fahsel, B., Kemper, H., Mayeres, J., Li, C., Wilker, B., et al. (2017). Staphylococcus aureus alpha-toxin disrupts endothelial-cell tight junctions via acid sphingomyelinase and ceramide. *Infect. Immun.* 86:e00606-17. doi: 10.1128/IAI.00606-17

Bibel, D. J., Aly, R., Shah, S., and Shinefield, H. R. (1993). Sphingosines: antimicrobial barriers of the skin. *Acta Derm. Venereol.* 73, 407–411.

Bibel, D. J., Aly, R., and Shinefield, H. R. (1992). Antimicrobial activity of sphingosines. *J. Invest. Dermatol.* 98, 269–273.

Bibel, D. J., Aly, R., and Shinefield, H. R. (1995). Topical sphingolipids in antisepsis and antifungal therapy. *Clin. Exp. Dermatol* 20, 395–400. doi: 10.1111/j.1365-2230.1995.tb01356.x

Capmany, A., and Damiani, M. T. (2010). Chlamydia trachomatis intercepts Golgi-derived sphingolipids through a Rab14-mediated transport required for bacterial development and replication. *PLoS One* 5:e14084. doi: 10.1371/journal.pone.0014084

Capmany, A., Gambarte Tudela, J., Alonso Bivou, M., and Damiani, M. T. (2019). Akt/AS160 signaling pathway inhibition impairs infection by decreasing Rab14-controlled sphingolipids delivery to chlamydial inclusions. *Front. Microbiol.* 10:666. doi: 10.3389/fmicb.2019.00666

Castro-Garza, J., González-Salazar, F., Quinn, F. D., Karls, R. K., De La Garza-Salinas, L. H., Guzmán-de la Garza, F. J., et al. (2016). An acidic sphingomyelinase Type C activity from *Mycobacterium tuberculosis*. *Rev. Argent. Microbiol.* 48, 21–26. doi: 10.1016/j.ram.2016.01.001

Cazalet, C., Rusniok, C., Bruggemann, H., Zidane, N., Magnier, A., Ma, L., et al. (2004). Evidence in the *Legionella pneumophila* genome for exploitation of host cell functions and high genome plasticity. *Nat. Genet.* 36, 1165–1173. doi: 10.1038/ng1447

Chapman, H., Ramstrom, C., Korhonen, L., Laine, M., Wann, K. T., Lindholm, D., et al. (2005). Downregulation of the HERG (KCNH2) K(+) channel by ceramide: evidence for ubiquitin-mediated lysosomal degradation. *J. Cell Sci.* 118, 5325–5334. doi: 10.1242/jcs.02635

Cukkemane, N., Bikker, F. J., Nazmi, K., Brand, H. S., Sotres, J., Lindh, L., et al. (2015). Anti-adherence and bactericidal activity of sphingolipids against *Streptococcus mutans*. *Eur. J. Oral Sci.* 123, 221–227. doi: 10.1111/eos.12200

Cuvillier, O., Pirianov, G., Kleuser, B., Vanek, P. G., Coso, O. A., Gutkind, J. S., et al. (1996). Suppression of ceramide-mediated programmed cell death by sphingosine-1-phosphate. *Nature* 381, 800–803. doi: 10.1038/381800a0

Davaille, J., Gallois, C., Habib, A., Li, L., Mallat, A., Tao, J., et al. (2000). Antiproliferative properties of sphingosine 1-phosphate in human hepatic myofibroblasts: a cyclooxygenase-2 mediated pathway. *J. Biol. Chem.* 275, 34628–34633. doi: 10.1074/jbc.m006393200

Deretic, V., Saitoh, T., and Akira, S. (2013). Autophagy in infection, inflammation and immunity. *Nat. Rev. Immunol.* 13, 722–737. doi: 10.1038/nri3532

Dobierzewska, A., Giltiay, N. V., Sabapathi, S., Karakashian, A. A., and Nikolova-Karakashian, M. N. (2011). Protein phosphatase 2A and neutral sphingomyelinase 2 regulate IRAK-1 protein ubiquitination and degradation in response to interleukin-1beta. *J. Biol. Chem.* 286, 32064–32073. doi: 10.1074/jbc.M111.238030

Dongfack, M. D., Lallemand, M. C., Kuete, V., Mbazoa, C. D., Wansi, J. D., Trinh-van-Dufat, H., et al. (2012). A new sphingolipid and furanocoumarins with antimicrobial activity from *Ficus exasperata*. *Chem. Pharm. Bull.* 60, 1072–1075. doi: 10.1248/cpb.c12-00279

Ebenezer, D. L., Berdyshev, E. V., Bronova, I. A., Liu, Y., Tiruppathi, C., Komarova, Y., et al. (2019). *Pseudomonas aeruginosa* stimulates nuclear sphingosine-1-phosphate generation and epigenetic regulation of lung inflammatory injury. *Thorax* 74, 579–591. doi: 10.1136/thoraxjnl-2018-212378

Ellington, A. A., Berhow, M. A., and Singletary, K. W. (2006). Inhibition of Akt signaling and enhanced ERK1/2 activity are involved in induction of macroautophagy by triterpenoid B-group soyasaponins in colon cancer cells. *Carcinogenesis* 27, 298–306. doi: 10.1093/carcin/bgi214

Elwell, C. A., Jiang, S., Kim, J. H., Lee, A., Wittmann, T., Hanada, K., et al. (2011). Chlamydia trachomatis co-opts GBF1 and CERT to acquire host sphingomyelin for distinct roles during intracellular development. *PLoS Pathog.* 7:e1002198. doi: 10.1371/journal.ppat.1002198

Faulstich, M., Hagen, F., Avota, E., Kozjak-Pavlovic, V., Winkler, A.-C., Xian, Y., et al. (2015). Neutral sphingomyelinase 2 is a key factor for PorB-dependent invasion of *Neisseria gonorrhoeae*. *Cell Microbiol.* 17, 241–253. doi: 10.1111/cmi.12361

Fischer, C. L., Walters, K. S., Drake, D. R., Blanchette, D. R., Dawson, D. V., Brogden, K. A., et al. (2013). Sphingoid bases are taken up by *Escherichia coli* and *Staphylococcus aureus* and induce ultrastructural damage. *Skin Pharmacol. Physiol.* 26, 36–44. doi: 10.1159/000343175

Gault, C. R., Obeid, L. M., and Hannun, Y. A. (2010). An overview of sphingolipid metabolism: from synthesis to breakdown. *Adv. Exp. Med. Biol.* 688, 1–23. doi: 10.1007/978-1-4419-6741-1_1

Gillard, B. K., Clement, R. G., and Marcus, D. M. (1998). Variations among cell lines in the synthesis of sphingolipids in de novo and recycling pathways. *Glycobiology* 8, 885–890. doi: 10.1093/glycob/8.9.885

Gomez-Valero, L., and Buchrieser, C. (2013). Genome dynamics in *Legionella*: the basis of versatility and adaptation to intracellular replication. *Cold Spring Harb. Perspect. Med.* 3:a009993. doi: 10.1101/cshperspect.a009993

Grassmé, H., Gulbins, E., Brenner, B., Ferlinz, K., Sandhoff, K., Harzer, K., et al. (1997). Acidic sphingomyelinase mediates entry of *N. gonorrhoeae* into nonphagocytic cells. *Cell* 91, 605–615. doi: 10.1016/s0092-8674(00)80448-1

Grassme, H., Jendrossek, V., Riehle, A., von Kurthy, G., Berger, J., Schwarz, H., et al. (2003). Host defense against *Pseudomonas aeruginosa* requires ceramide-rich membrane rafts. *Nat. Med.* 9, 322–330. doi: 10.1038/nm823

Grösch, S., Schiffmann, S., and Geisslinger, G. (2012). Chain length-specific properties of ceramides. *Prog. Lipid Res.* 51, 50–62. doi: 10.1016/j.plipres.2011.11.001

Hackstadt, T., Scidmore, M. A., and Rockey, D. D. (1995). Lipid metabolism in *Chlamydia trachomatis*-infected cells: directed trafficking of Golgi-derived sphingolipids to the chlamydial inclusion. *Proc. Natl. Acad. Sci. U.S.A.* 92, 4877–4881. doi: 10.1073/pnas.92.11.4877

Hanada, K. (2005). Sphingolipids in infectious diseases. *Jpn. J. Infect. Dis.* 58, 131–148.

Harvald, E. B., Olsen, A. S. B., and Faergeman, N. J. (2015). Autophagy in the light of sphingolipid metabolism. *Apoptosis* 20, 658–670. doi: 10.1007/s10495-015-1108-2

Harvey, H. A., Swords, W. E., and Apicella, M. A. (2001). The mimicry of human glycolipids and glycosphingolipids by the lipooligosaccharides of pathogenic *Neisseria* and *Haemophilus*. *J. Autoimmun.* 16, 257–262. doi: 10.1006/jaut.2000.0477

Hauck, C. R., Grassmé, H., Bock, J., Jendrossek, V., Ferlinz, K., Meyer, T. F., et al. (2000). Acid sphingomyelinase is involved in CEACAM receptor-mediated phagocytosis of *Neisseria gonorrhoeae*. *FEBS Lett.* 478, 260–266. doi: 10.1016/s0014-5793(00)01851-2

Hernández-Corbacho, M. J., Salama, M. F., Canals, D., Senkal, C. E., and Obeid, L. M. (2017). Sphingolipids in mitochondria. *Biochim. Biophys. Acta Mol. Cell Biol. Lipids* 1862, 56–68.

Herweg, J. A., Pons, V., Becher, D., Hecker, M., Krohne, G., Barbier, J., et al. (2016). Proteomic analysis of the *Simkania*-containing vacuole: the central role of retrograde transport. *Mol. Microbiol.* 99, 151–171. doi: 10.1111/mmi.13222

Heuer, D., Rejman Lipinski, A., Machuy, N., Karlas, A., Wehrens, A., Siedler, F., et al. (2009). Chlamydia causes fragmentation of the Golgi compartment to ensure reproduction. *Nature* 457, 731–735. doi: 10.1038/nature07578

Holmgren, J., Lönnroth, I., Månsson, J., and Svennerholm, L. (1975). Interaction of cholera toxin and membrane GM1 ganglioside of small intestine. *Proc. Natl. Acad. Sci. U.S.A.* 72, 2520–2524. doi: 10.1073/pnas.72.7.2520

Huang, F. C. (2016). De Novo sphingolipid synthesis is essential for *Salmonella*-induced autophagy and human beta-defensin 2 expression in intestinal epithelial cells. *Gut. Pathog.* 8:5. doi: 10.1186/s13099-016-0088-2

Huang, F. C. (2017). The role of sphingolipids on innate immunity to intestinal *Salmonella* Infection. *Int. J. Mol. Sci.* 18:1720. doi: 10.3390/ijms18081720

Huang, J., and Brumell, J. H. (2014). Bacteria-autophagy interplay: a battle for survival. *Nat. Rev. Microbiol.* 12, 101–114. doi: 10.1038/nrmicro3160

Hugosson, S., Angström, J., Olsson, B.-M., Bergströmlm, J., Fredlund, H., Olcen, P., et al. (1998). Glycosphingolipid binding specificities of *Neisseria meningitidis* and *Haemophilus influenzae*: detection, isolation, and characterization of

a binding-active glycosphingolipid from human oropharyngeal epithelium. *J. Biochem.* 124, 1138–1152. doi: 10.1093/oxfordjournals.jbchem.a022232

James, P. F., and Zoeller, R. A. (1997). Isolation of animal cell mutants defective in long-chain fatty aldehyde dehydrogenase: sensitivity to fatty aldehydes and Schiff's base modification of phospholipids: implications for Sjörgen-Larsson syndrome. *J. Biol. Chem.* 272, 23532–23539. doi: 10.1074/jbc.272.38.23532

Kanazawa, T., Taneike, I., Akaishi, R., Yoshizawa, F., Furuya, N., Fujimura, S., et al. (2004). Amino acids and insulin control autophagic proteolysis through different signaling pathways in relation to mTOR in isolated rat hepatocytes. *J. Biol. Chem.* 279, 8452–8459. doi: 10.1074/jbc.m306337200

Kavaliauskiene, S., Dyve Lingelem, A. B., Skotland, T., and Sandvig, K. (2017). Protection against shiga toxins. *Toxins* 9:e44.

Koch-Edelmann, S., Banhart, S., Saied, E. M., Rose, L., Aeberhard, L., Laue, M., et al. (2017). The cellular ceramide transport protein CERT promotes *Chlamydia psittaci* infection and controls bacterial sphingolipid uptake. *Cell Microbiol.* 19:e12752. doi: 10.1111/cmi.12752

Kolter, T., and Sandhoff, K. (2005). Principles of lysosomal membrane digestion: stimulation of sphingolipid degradation by sphingolipid activator proteins and anionic lysosomal lipids. *Annu. Rev. Cell Dev. Biol.* 21, 81–103. doi: 10.1146/annurev.cellbio.21.122303.120013

Kühlewein, C., Rechner, C., Meyer, T. F., and Rudel, T. (2006). Low-phosphate-dependent invasion resembles a general way for *Neisseria gonorrhoeae* to enter host cells. *Infect. Immun.* 74, 4266–4273. doi: 10.1128/iai.00215-06

Lépine, S., Allegood, J. C., Park, M., Dent, P., Milstien, S., and Spiegel, S. (2011). Sphingosine-1-phosphate phosphohydrolase-1 regulates ER stress-induced autophagy. *Cell Death Differ.* 18, 350–361. doi: 10.1038/cdd.2010.104

Li, C., Wang, A., Wu, Y., Gulbins, E., Grassme, H., and Zhao, Z. (2019). Acid sphingomyelinase-ceramide system in bacterial infections. *Cell Physiol. Biochem* 52, 280–301. doi: 10.33594/000000021

Liu, H., Toman, R. E., Goparaju, S. K., Maceyka, M., Nava, V. E., Sankala, H., et al. (2003). sphingosine kinase type 2 is a putative BH3-only protein that induces apoptosis. *J. Biol. Chem.* 278, 40330–40336. doi: 10.1074/jbc.m304455200

Liu, Y., Yang, Y., Ye, Y. C., Shi, Q. F., Chai, K., Tashiro, S., et al. (2012). Activation of ERK-p53 and ERK-mediated phosphorylation of Bcl-2 are involved in autophagic cell death induced by the c-Met inhibitor SU11274 in human lung cancer A549 cells. *J. Pharmacol. Sci.* 118, 423–432. doi: 10.1254/jphs.11181fp

Ma, J., Gulbins, E., Edwards, M. J., Caldwell, C. C., Fraunholz, M., and Becker, K. A. (2017). Staphylococcus aureus α-Toxin induces inflammatory cytokines via lysosomal acid sphingomyelinase and ceramides. *Cell Physiol. Biochem.* 43, 2170–2184. doi: 10.1159/000484296

Managò, A., Becker, K. A., Carpinteiro, A., Wilker, B., Soddemann, M., Seitz, A. P., et al. (2015). *Pseudomonas aeruginosa* pyocyanin induces neutrophil death via mitochondrial reactive oxygen species and mitochondrial acid sphingomyelinase. *Antioxid. Redox. Signal.* 22, 1097–1110. doi: 10.1089/ars.2014.5979

Menaldino, D. S., Bushnev, A., Sun, A., Liotta, D. C., Symolon, H., Desai, K., et al. (2003). Sphingoid bases and de novo ceramide synthesis: enzymes involved, pharmacology and mechanisms of action. *Pharmacol. Res.* 47, 373–381. doi: 10.1016/s1043-6618(03)00054-9

Mencarelli, C., and Martinez-Martinez, P. (2013). Ceramide function in the brain: when a slight tilt is enough. *Cell Mol. Life Sci.* 70, 181–203. doi: 10.1007/s00018-012-1038-x

Miller, C., and Celli, J. (2016). Avoidance and subversion of eukaryotic homeostatic autophagy mechanisms by bacterial pathogens. *J. Mol. Biol.* 428, 3387–3398. doi: 10.1016/j.jmb.2016.07.007

Mital, J., and Hackstadt, T. (2011). Role for the SRC family kinase Fyn in sphingolipid acquisition by chlamydiae. *Infect. Immun.* 79, 4559–4568. doi: 10.1128/IAI.05692-11

Moore, E. R., Mead, D. J., Dooley, C. A., Sager, J., and Hackstadt, T. (2011). The trans-Golgi SNARE syntaxin 6 is recruited to the chlamydial inclusion membrane. *Microbiology* 157, 830–838. doi: 10.1099/mic.0.045856-0

Narayanan, L. A., and Edelmann, M. J. (2014). Ubiquitination as an efficient molecular strategy employed in *Salmonella* infection. *Front Immunol* 5:558. doi: 10.3389/fimmu.2014.00558

Newton, H. J., Ang, D. K., van Driel, I. R., and Hartland, E. L. (2010). Molecular pathogenesis of infections caused by *Legionella pneumophila*. *Clin. Microbiol. Rev.* 23, 274–298. doi: 10.1128/CMR.00052-09

Newton, J., Lima, S., Maceyka, M., and Spiegel, S. (2015). Revisiting the sphingolipid rheostat: evolving concepts in cancer therapy. *Exp. Cell Res.* 333, 195–200. doi: 10.1016/j.yexcr.2015.02.025

Ogier-Denis, E., Pattingre, S., El Benna, J., and Codogno, P. (2000). Erk1/2-dependent phosphorylation of Galpha-interacting protein stimulates its GTPase accelerating activity and autophagy in human colon cancer cells. *J. Biol. Chem.* 275, 39090–39095. doi: 10.1074/jbc.m006198200

Okino, N., and Ito, M. (2007). Ceramidase enhances phospholipase C-induced hemolysis by *Pseudomonas aeruginosa*. *J. Biol. Chem.* 282, 6021–6030. doi: 10.1074/jbc.m603088200

Okino, N., Tani, M., Imayama, S., and Ito, M. (1998). Purification and characterization of a novel ceramidase from *Pseudomonas aeruginosa*. *J. Biol. Chem.* 273, 14368–14373. doi: 10.1074/jbc.273.23.14368

Owen, K. A., Meyer, C. B., Bouton, A. H., and Casanova, J. E. (2014). Activation of focal adhesion kinase by *Salmonella* suppresses autophagy via an Akt/mTOR signaling pathway and promotes bacterial survival in macrophages. *PLoS Pathog.* 10:e1004159. doi: 10.1371/journal.ppat.1004159

Peng, H., Li, C., Kadow, S., Henry, B. D., Steinmann, J., Becker, K. A., et al. (2015). Acid sphingomyelinase inhibition protects mice from lung edema and lethal *Staphylococcus aureus* sepsis. *J. Mol. Med.* 93, 675–689. doi: 10.1007/s00109-014-1246-y

Perry, D. K. (2002). Serine palmitoyltransferase: role in apoptotic de novo ceramide synthesis and other stress responses. *Biochim. Biophys. Acta* 1585, 146–152. doi: 10.1016/s1388-1981(02)00335-9

Peters, S., Schlegel, J., Becam, J., Avota, E., Sauer, M., and Schubert-Unkmeir, A. (2019). *Neisseria meningitidis* type IV pili trigger Ca2+-dependent lysosomal trafficking of the acid sphingomyelinase to enhance surface ceramide levels. *Infect. Immun.* 87:e00410-19. doi: 10.1128/IAI.00410-19

Pewzner-Jung, Y., Tavakoli Tabazavareh, S., Grassme, H., Becker, K. A., Japtok, L., Steinmann, J., et al. (2014). Sphingoid long chain bases prevent lung infection by *Pseudomonas aeruginosa*. *EMBO Mol Med* 6, 1205–1214. doi: 10.15252/emmm.201404075

Riboni, L., Viani, P., Bassi, R., Prinetti, A., and Tettamanti, G. (1997). The role of sphingolipids in the process of signal transduction. *Prog. Lipid Res.* 36, 153–195. doi: 10.1016/s0163-7827(97)00008-8

Rolando, M., Escoll, P., and Buchrieser, C. (2016a). *Legionella pneumophila* restrains autophagy by modulating the host's sphingolipid metabolism. *Autophagy* 12, 1053–1054. doi: 10.1080/15548627.2016.1166325

Rolando, M., Escoll, P., Nora, T., Botti, J., Boitez, V., Bedia, C., et al. (2016b). *Legionella pneumophila* S1P-lyase targets host sphingolipid metabolism and restrains autophagy. *Proc. Natl. Acad. Sci. U.S.A.* 113, 1901–1906. doi: 10.1073/pnas.1522067113

Rudel, T., Kepp, O., and Kozjak-Pavlovic, V. (2010). Interactions between bacterial pathogens and mitochondrial cell death pathways. *Nat. Rev. Microbiol.* 8, 693–705. doi: 10.1038/nrmicro2421

Saiman, L., and Prince, A. (1993). *Pseudomonas aeruginosa* pili bind to asialoGM1 which is increased on the surface of cystic fibrosis epithelial cells. *J. Clin. Invest.* 92, 1875–1880. doi: 10.1172/jci116779

Sarkar, S., Maceyka, M., Hait, N. C., Paugh, S. W., Sankala, H., Milstien, S., et al. (2005). Sphingosine kinase 1 is required for migration, proliferation and survival of MCF-7 human breast cancer cells. *FEBS Lett.* 579, 5313–5317. doi: 10.1016/j.febslet.2005.08.055

Scarlatti, F., Bauvy, C., Ventruti, A., Sala, G., Cluzeaud, F., Vandewalle, A., et al. (2004). Ceramide-mediated macroautophagy involves inhibition of protein kinase B and up-regulation of beclin 1. *J. Biol. Chem.* 279, 18384–18391. doi: 10.1074/jbc.m313561200

Simonis, A., Hebling, S., Gulbins, E., Schneider-Schaulies, S., and Schubert-Unkmeir, A. (2014). Differential activation of acid sphingomyelinase and ceramide release determines invasiveness of *Neisseria meningitidis* into brain endothelial cells. *PLoS Pathog.* 10:e1004160. doi: 10.1371/journal.ppat.1004160

Simonis, A., and Schubert-Unkmeir, A. (2018). The role of acid sphingomyelinase and modulation of sphingolipid metabolism in bacterial infection. *Biol. Chem.* 399, 1135–1146. doi: 10.1515/hsz-2018-0200

Simons, K., and Ikonen, E. (1997). Functional rafts in cell membranes. *Nature* 387, 569–572. doi: 10.1038/42408

Siqueira, M. D. S., Ribeiro, R. M., and Travassos, L. H. (2018). Autophagy and its interaction with intracellular bacterial pathogens. *Front. Immunol.* 9:935. doi: 10.3389/fimmu.2018.00935

Speer, A., Sun, J., Danilchanka, O., Meikle, V., Rowland, J. L., Walter, K., et al. (2015). Surface hydrolysis of sphingomyelin by the outer membrane protein Rv0888 supports replication of *Mycobacterium tuberculosis* in macrophages. *Mol. Microbiol.* 97, 881–897. doi: 10.1111/mmi.13073

Taniguchi, M., Kitatani, K., Kondo, T., Hashimoto-Nishimura, M., Asano, S., Hayashi, A., et al. (2012). Regulation of autophagy and its associated cell death by "sphingolipid rheostat": reciprocal role of ceramide and sphingosine 1-phosphate in the mammalian target of rapamycin pathway. *J. Biol. Chem.* 287, 39898–39910. doi: 10.1074/jbc.M112.416552

Tattoli, I., Sorbara, M. T., Vuckovic, D., Ling, A., Soares, F., Carneiro, L. A., et al. (2012). Amino acid starvation induced by invasive bacterial pathogens triggers an innate host defense program. *Cell Host Microbe* 11, 563–575. doi: 10.1016/j.chom.2012.04.012

Tettamanti, G., Bassi, R., Viani, P., and Riboni, L. (2003). Salvage pathways in glycosphingolipid metabolism. *Biochimie* 85, 423–437. doi: 10.1016/s0300-9084(03)00047-6

van Ooij, C., Kalman, L., van, I., Nishijima, M., Hanada, K., Mostov, K., et al. (2000). Host cell-derived sphingolipids are required for the intracellular growth of *Chlamydia trachomatis*. *Cell Microbiol.* 2, 627–637. doi: 10.1046/j.1462-5822.2000.00077.x

Viswanathan, G., Jafurulla, M., Kumar, G. A., Raghunand, T. R., and Chattopadhyay, A. (2018). Macrophage sphingolipids are essential for the entry of mycobacteria. *Chem. Phys. Lipids* 213, 25–31. doi: 10.1016/j.chemphyslip.2018.03.004

Wolf, K., and Hackstadt, T. (2001). Sphingomyelin trafficking in *Chlamydia pneumoniae*-infected cells. *Cell Microbiol.* 3, 145–152. doi: 10.1046/j.1462-5822.2001.00098.x

Young, M. M., Kester, M., and Wang, H. G. (2013). Sphingolipids: regulators of crosstalk between apoptosis and autophagy. *J. Lipid Res.* 54, 5–19. doi: 10.1194/jlr.R031278

Young, M. M., and Wang, H. G. (2018). Sphingolipids as regulators of autophagy and endocytic trafficking. *Adv. Cancer Res.* 140, 27–60. doi: 10.1016/bs.acr.2018.04.008

Zhang, Y., Li, X., Carpinteiro, A., and Gulbins, E. (2008). Acid sphingomyelinase amplifies redox signaling in *Pseudomonas aeruginosa*-induced macrophage apoptosis. *J. Immunol.* 181, 4247–4254. doi: 10.4049/jimmunol.181.6.4247

Conflict of Interest: The authors declare that the research was conducted in the absence of any commercial or financial relationships that could be construed as a potential conflict of interest.

The reviewer PE declared a past supervisory role with one of the authors TK to the handling Editor.

frontiers in Cell and Developmental Biology

ORIGINAL RESEARCH
published: 01 October 2019
doi: 10.3389/fcell.2019.00218

Use of Acid Ceramidase and Sphingosine Kinase Inhibitors as Antiviral Compounds Against Measles Virus Infection of Lymphocytes *in vitro*

*Anika Grafen[1], Fabian Schumacher[2,3], Janice Chithelen[1], Burkhard Kleuser[2], Niklas Beyersdorf[1] and Jürgen Schneider-Schaulies[1]**

[1] Institute for Virology and Immunobiology, University of Würzburg, Würzburg, Germany, [2] Institute of Nutritional Science, University of Potsdam, Nuthetal, Germany, [3] Department of Molecular Biology, University of Duisburg-Essen, Essen, Germany

OPEN ACCESS

Edited by:
Masaru Katoh, National Cancer Center Hospital, Japan

Reviewed by:
Eswaran Sreekumar, Rajiv Gandhi Centre for Biotechnology, India
Shinji Ohno, University of the Ryukyus, Japan

***Correspondence:**
Jürgen Schneider-Schaulies
jss@vim.uni-wuerzburg.de

Specialty section:
This article was submitted to Molecular Medicine, a section of the journal Frontiers in Cell and Developmental Biology

Received: *27 June 2019*
Accepted: *18 September 2019*
Published: *01 October 2019*

Citation:
Grafen A, Schumacher F, Chithelen J, Kleuser B, Beyersdorf N and Schneider-Schaulies J (2019) Use of Acid Ceramidase and Sphingosine Kinase Inhibitors as Antiviral Compounds Against Measles Virus Infection of Lymphocytes in vitro. Front. Cell Dev. Biol. 7:218. doi: 10.3389/fcell.2019.00218

As structural membrane components and signaling effector molecules sphingolipids influence a plethora of host cell functions, and by doing so also the replication of viruses. Investigating the effects of various inhibitors of sphingolipid metabolism in primary human peripheral blood lymphocytes (PBL) and the human B cell line BJAB we found that not only the sphingosine kinase (SphK) inhibitor SKI-II, but also the acid ceramidase inhibitor ceranib-2 efficiently inhibited measles virus (MV) replication. Virus uptake into the target cells was not grossly altered by the two inhibitors, while titers of newly synthesized MV were reduced by approximately 1 log (90%) in PBL and 70–80% in BJAB cells. Lipidomic analyses revealed that in PBL SKI-II led to increased ceramide levels, whereas in BJAB cells ceranib-2 increased ceramides. SKI-II treatment decreased sphingosine-1-phosphate (S1P) levels in PBL and BJAB cells. Furthermore, we found that MV infection of lymphocytes induced a transient (0.5–6 h) increase in S1P, which was prevented by SKI-II. Investigating the effect of the inhibitors on the metabolic (mTORC1) activity we found that ceranib-2 reduced the phosphorylation of p70 S6K in PBL, and that both inhibitors, ceranib-2 and SKI-II, reduced the phosphorylation of p70 S6K in BJAB cells. As mTORC1 activity is required for efficient MV replication, this effect of the inhibitors is one possible antiviral mechanism. In addition, reduced intracellular S1P levels affect a number of signaling pathways and functions including Hsp90 activity, which was reported to be required for MV replication. Accordingly, we found that pharmacological inhibition of Hsp90 with the inhibitor 17-AAG strongly impaired MV replication in primary PBL. Thus, our data suggest that treatment of lymphocytes with both, acid ceramidase and SphK inhibitors, impair MV replication by affecting a number of cellular activities including mTORC1 and Hsp90, which alter the metabolic state of the cells causing a hostile environment for the virus.

Keywords: measles virus, sphingolipids, acid ceramidase, acid ceramidase inhibitor ceranib-2, sphingosine kinase, sphingosine kinase inhibitor SKI-II

INTRODUCTION

Sphingolipids are major membrane lipid constituents and as such, their biogenesis, modifications, and turnover are tightly linked to all processes involving membrane dynamics and the cellular metabolism. Their local segregation and metabolites directly affect biophysical properties of membranes including membrane deformation, fusion, and vesicle formation, however, they also act as signal transducing molecules. Being used as signaling molecules, they govern the metabolic state and fundamental host cell responses such as apoptosis, survival, autophagy, and proliferation (Hannun and Obeid, 2008). Therefore, sphingolipids and their metabolites are potential key regulators in the life cycle of obligatory intracellular pathogens such as viruses, which rely on cellular metabolism.

Several findings revealing effects of the sphingolipid metabolism on viral infections came from animal models (Schneider-Schaulies and Schneider-Schaulies, 2015). Acid sphingomyelinase (ASM)-deficient mice are more susceptible to Sindbis virus-induced encephalomyelitis (Ng and Griffin, 2006; Ng et al., 2008), ceramides enhance the infection with Japanese encephalitis virus (Takamatsu et al., 2010), and $CD8^+$ T cells of lymphocytic choriomeningitis virus (LCMV)-infected ASM-deficient mice secrete reduced levels of IFN-γ and cytotoxic granules resulting in delayed viral clearance (Herz et al., 2009). In addition, certain viruses such as major- and minor-group human rhinoviruses are able to promote the formation of ceramide-enriched membrane platforms thereby supporting their own entry into target cells (Grassme et al., 2005). Similarly, MV induces surface expression of its receptor CD150 via DC-SIGN-mediated activation of sphingomyelinases in dendritic cells, and thereby stimulates its own uptake into these cells (Avota et al., 2011). Adenovirus stimulates calcium influx and lysosomal exocytosis, a membrane repair mechanism resulting in the release of ASM and degradation of sphingomyelin (SM) to ceramides in the plasma membrane (Luisoni et al., 2015). Furthermore, SM and ASM activity appear to be involved in early steps of Ebola virus infection. In addition, the endo/lysosomal cholesterol transporter NPC1 residing in an intracellular compartment rather than at the plasma membrane serves as an entry receptor for Ebola virus (Miller et al., 2012). We found that MV brain infection in ASM-deficient mice, or after pharmacological inhibition of the ASM in mice, is enhanced due to an increased frequency of $CD4^+$ $Foxp3^+$ regulatory T cells (Hollmann et al., 2016). These findings highlight the potential of manipulations of the sphingolipid metabolism for novel therapeutic or immunomodulatory applications against viral infections.

In order to investigate the interference of sphingolipid metabolism with a viral infection, we used measles virus (MV) infection of lymphocytes as a model system. During the infection of a person MV first interacts with the receptor CD150 on the surface of macrophages, dendritic cells, as well as activated and memory B and T cells and is predominantly taken up by pH-independent receptor-mediated membrane fusion at the plasma membrane (Tatsuo et al., 2000; Erlenhoefer et al., 2001). Later, the virus interacts with nectin-4 to infect polarized epithelial cells (Muhlebach et al., 2011; Noyce et al., 2011). Despite the availability of an effective vaccine, measles remains a leading cause of mortality and morbidity in young children causing approximately 100,000 deaths each year worldwide (World Health Organization [WHO], 2018). The infection is associated with a number of complications including immunosuppression, and may also persist and cause subacute sclerosing panencephalitis (SSPE) (Reuter and Schneider-Schaulies, 2010; Mina et al., 2015). A specific antiviral therapy is not yet available. However, several compounds manipulating sphingolipid metabolism are available, and some of them are already in clinical use mainly applied against various forms of cancer. We wondered, if such drugs could also be used to manipulate MV replication. Vijayan et al. (2014) recently described that overexpression of the SphK-1 enhanced, and inhibition of SphK-1 (and -2) by the inhibitor SKI-II reduced MV replication in epithelial and lymphoid cell lines. They found that after MV infection of these cell lines the activity of the sphingosine kinases (SphK) and the phosphorylation of NF-kB p65 was increased. Furthermore, the NF-kB inhibitor Bay-11-7082 also reduced MV protein synthesis by preventing the phosphorylation and subsequent degradation of IkB (Vijayan et al., 2014). Accordingly, S1P-metabolizing enzymes reduced influenza virus (IAV) propagation and cytopathogenicity (Seo et al., 2010).

In the present study we investigated if some well-known inhibitors of the sphingolipid metabolism, which are partially already in clinical use, may inhibit MV replication in its primary natural target cells, i.e., $CD150^+$ cells. We found that not only SKI-II (French et al., 2003; Draper et al., 2011), but also ceranib-2 (Draper et al., 2011), an inhibitor of the acid ceramidase, efficiently reduced MV replication in primary human PBL and the human B cell line BJAB. The data suggest that MV replication can be impaired by several mechanisms regulated by sphingolipid-mediated signaling pathways.

MATERIALS AND METHODS

Cells, Viruses, and Inhibitors

All experiments involving human cells were conducted according to the principles expressed in the Declaration of Helsinki and ethically approved by the Ethics Committee of the Medical Faculty of the University of Würzburg. Primary human peripheral blood mononuclear cells (PBMCs) obtained from leuko-reduction chambers of thrombocyte donations of anonymous healthy adult volunteers were diluted 1:6 in Versene (Gibco), layered on Histopaque® 1077 and purified by density gradient centrifugation. Isolated PBMCs were washed three times with (PBL) and suspended in RPMI 1640 (Gibco) medium containing 10% FBS and incubated for 2 h on plastic dishes to remove adherent monocytes. Peripheral blood lymphocytes (PBL) were collected and stimulated with phytohemagglutinin-L (PHA, 2.5 µg/ml, Roche). Stimulation was controlled by measuring CD69 expression by flow cytometry. The human B cell line BJAB was cultivated using RPMI 1640 medium containing 5% FBS. The recombinant wild-type MV

$rMV_{IC323}eGFP$ (Hashimoto et al., 2002) was propagated using Vero cells expressing CD150 (Vero-hSLAM). For the described experiments, cells were infected for 2 h, washed with PBS, and further incubated for indicated times in medium. Virus was harvested by freezing and thawing the complete cultures, thus cell-associated and supernatant virus were harvested together, and titrated using Vero-hSLAM cells. The inhibitors of SphK-1 and -2, SKI-II, of acid ceramidase, ceranib-2, of ASM, amitriptyline, of NSM, GW4869, and of Hsp90, 17-AAG, were purchased from Sigma–Aldrich. All inhibitors except amitriptyline were dissolved in dimethyl sufoxide (DMSO). The viability of cells in the presence of inhibitors was determined after 48 h incubation by flow cytometry using propidium iodide (PI; Biolegend) staining for dead cells. The percentage of dead cells in the presence of corresponding concentrations DMSO was subtracted from values obtained for various concentrations of inhibitors and the viability in the presence of 0.2% DMSO normalized to 100%.

Antibodies and Flow Cytometry

The following primary antibodies were used in immunoblotting and flow cytometry: rabbit anti-GAPDH (Santacruz), rabbit anti-phospho-p70 S6 kinase (S6K) (Thr 389) (Cell Signaling), rabbit anti-p70 S6K (Cell Signaling), and APC-conjugated anti-human CD69 (Biolegend). Anti-human CD150 antibody clone 5C6 was generated in our laboratory (Erlenhoefer et al., 2001). The following labeled secondary antibodies were used: Alexa488-conjugated anti-mouse (Life Technology), Alexa594-conjugated anti-rabbit (Life Technology), and horseradish peroxidase (HRP)-conjugated goat anti-rabbit IgG (Cell Signaling). For flow cytometry 2×10^5 cells per sample were stained with respective antibodies in FACS buffer (PBS containing 0.4% bovine serum albumin (BSA) and 0.02% sodium azide). Dead cells were stained with PI (Biolegend). Cells were acquired immediately using a LSR II flow cytometer (BD) and the data were analyzed using FlowJo (Cytek Development) software.

Virus Uptake Assay

To measure virus uptake, cells were pretreated with increasing concentrations of inhibitors as indicated for 1 h prior to infection with MV (MOI = 0.5 for primary PBL and MOI = 0.1 for BJAB cells) for 2 h at 37°C. Then the cells were washed with PBS and further incubated in medium for 22 h at 37°C to allow viral transcription and protein expression. The percentage of infected (viral eGFP-positive) cells was then determined by flow cytometry (not the mean fluorescence intensity which reflects the amount of viral protein expression).

SDS-PAGE and Immunoblotting

Cells (5×10^6) were lysed at 4°C for 1 h in 1 ml of lysis buffer [50 mM Tris–HCl, pH 8.0, 150 mM sodium chloride (NaCl), 1.0% Igepal CA-630 (NP-40), 0.5% sodium deoxycholate, 0.1% sodium dodecyl sulfate (SDS)] containing complete protease inhibitor cocktail (Sigma–Aldrich) and 1 mM DL-dithiothreitol (DTT). The protein quantification was done using the bicinchoninic acid (BCA) assay. An equal amount of proteins was heated at 95°C for 5 min in reducing sample buffer (50 mM Tris–HCl, pH 6.8, 2% SDS, 10% glycerol, 1% β-mercaptoethanol, 12.5 mM ethylenediaminetetraacetic acid (EDTA), 0.02% bromophenol blue) and applied to 12% SDS-polyacrylamide gel electrophoresis. Proteins were blotted semidry on nitrocellulose membranes (Amersham) followed by blocking with 5% dry milk (AppliChem) or 5% BSA in Tris-buffered saline with 0.05% Tween-20. The membranes were then incubated with specific primary antibodies and HRP-conjugated secondary antibodies. Signals were visualized using Chemiluminescent FemtoMax™ Super Sensitive HRP Substrate (Rockland). The densitometric quantification of protein bands of target proteins and respective housekeeping gene were done using Li-Cor Odyssey Pc imaging System Image Studio Version 4.0 (Li-Cor Biosciences). The fold changes in target proteins were normalized to band densities of respective GAPDH and fold changes in phosphorylated proteins were normalized to the band densities of total protein or GAPDH levels. All western blotting experiments were repeated at least three times and representative images are shown.

Lipid Analysis

For lipid analysis 8×10^6 PBL or 1×10^6 BJAB cells per sample were resuspended in 500 µl methanol and subsequently subjected to lipid extraction using methanol/chloroform (2:1, v:v) (Gulbins et al., 2018). The extraction solvent contained d_7-Sph, d_7-sphingosine-1-phosphate (d_7-S1P), C17-ceramide, and C16-d_{31}-SM (all Avanti Polar Lipids, Alabaster, United States) as internal standards. Sample analysis was carried out by liquid chromatography tandem–mass spectrometry (LC–MS/MS) using either a TQ 6490 mass spectrometer (for Sph and S1P) or a QTOF 6530 mass spectrometer (for ceramides and SMs) (Agilent Technologies) operating in the positive electrospray ionization mode (ESI+). The following selected reaction monitoring (SRM) transitions were used for quantification: m/z 300.3 → 282.3 for Sph, m/z 380.3 → 264.3 for S1P, m/z 307.3 → 289.3 for d_7-Sph, and m/z 387.3 → 271.3 for d_7-S1P. The precursor ions of ceramide or SM species (differing in their fatty acid chain lengths) were cleaved into the fragment ions m/z 264.270 or m/z 184.074, respectively (Kachler et al., 2017). Quantification was performed with Mass Hunter Software (Agilent Technologies).

Statistical Analysis

Statistical analysis was performed using Microsoft Excel or GraphPad Prism 6. Two groups were analyzed using unpaired two-tailed Student's t-test and more than two groups were analyzed with one-way ANOVA. P-values lower than or equal to 0.05 were considered statistically significant ($^*P \leq 0.05$, $^{**}P \leq 0.01$, $^{***}P \leq 0.001$). The data represent mean ± SD of at least three independent experiments.

RESULTS

The Sphingosine Kinase Inhibitor SKI-II Inhibits MV Replication in Primary Human PBL

Peripheral blood lymphocytes from healthy donors were stimulated with PHA for 24 h prior to treatment with inhibitors

and infection with MV. Their activation, infection, and viability in the presence of inhibitors were controlled by flow cytometry (**Figures 1A–C**). A representative control showing 24 h PHA-stimulated PBL, which were subsequently infected for 48 h with MV at a MOI of 0.1 is given in **Figure 1A**. We were using PHA-stimulated PBL since stimulation increases the titer of newly synthesized MV approximately 20-fold (**Figure 1B**). The viability of PHA-stimulated PBL was determined using PI in the presence of increasing concentrations of SKI-II (**Figure 1C**). In further experiments we used 1 and 5 μM SKI-II, concentrations at which ≥95 and ≥85%, respectively, of PBL were viable.

To determine the effect of SphK inhibition on MV replication, PBL from six healthy donors were infected with MV at a MOI of 0.1 in the absence and presence of 0, 1, and 5 μM of SKI-II, and the newly synthesized MV (cell bound plus supernatant) was prepared and titrated after 1, 2, and 3 days (**Figure 1D**). The viral titers were similar at day 1, and reduced 2 and 3 days after infection. At day 3 the reduction was approximately 1 log (90%). Results at day 3 are presented as percentage of control cells with significances (**Figure 1E**). In order to investigate if viral entry into PBL is affected by SKI-II, we first measured if expression of the MV receptor CD150 is altered by SKI-II. This was not the case after 1, 24, and 48 h of treatment with 1 and 5 μM of the inhibitor (not shown). Then we did a virus uptake assay and quantified the percentage of infected (viral eGFP-positive) cells at day 1 after infection by flow cytometry. The percentage of infected cells (and thus virus uptake) was not reduced by SKI-II, but there was rather a tendency (not significant) toward increased virus uptake

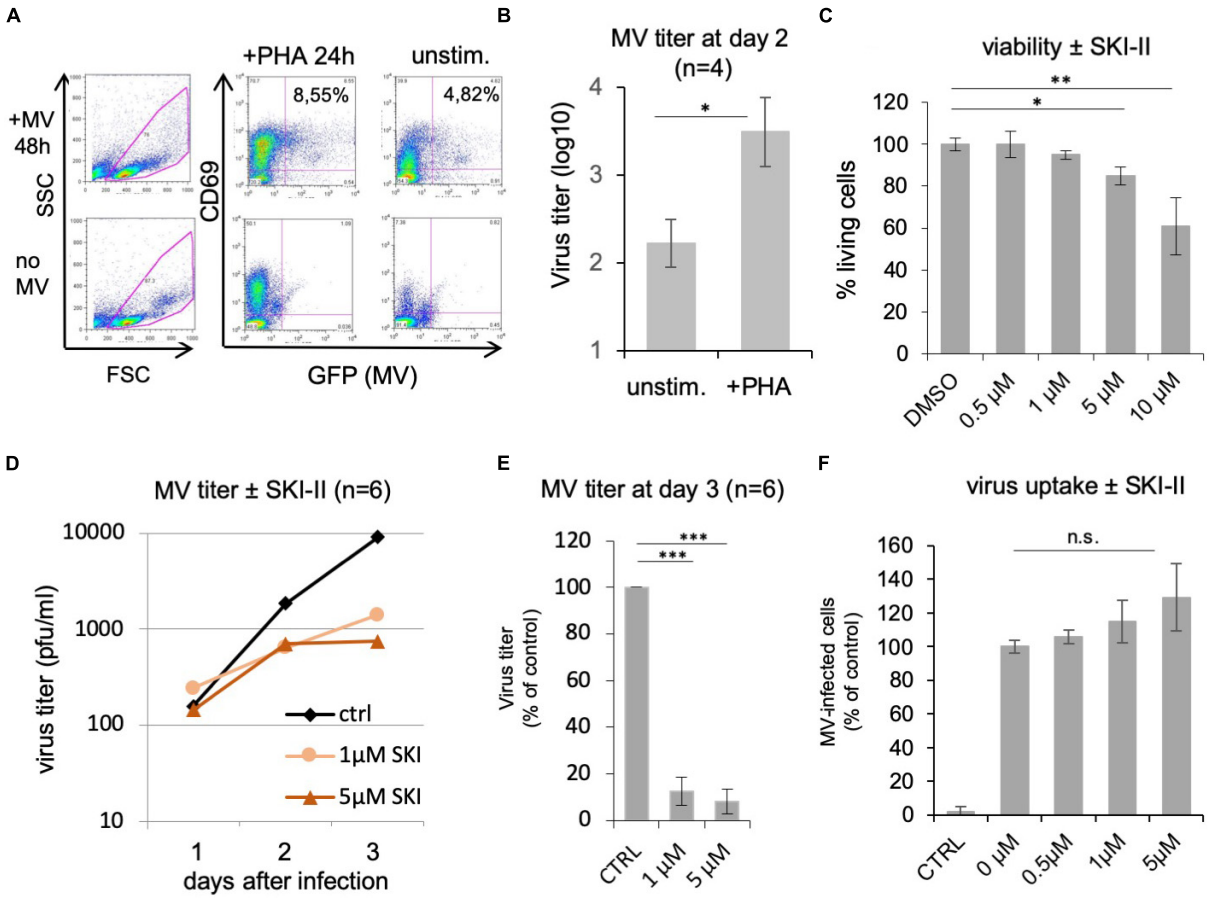

FIGURE 1 | SKI-II inhibits MV replication in primary human PBL. The stimulation, infection, and viability of the PBL without and with PHA (2.5 μg/ml) for 24 h was controlled by flow cytometry measuring the expression of CD69, viral eGFP, and propidium iodide (PI). An example of infected and uninfected PBL in the presence and absence of PHA is shown in panel **(A)**. Panel **(B)** shows a comparison of the MV titer produced by unstimulated and PHA-stimulated PBL (1×10^6 cells) as determined at day 2 after infection at a MOI of 0.1 ($n = 4$; with $^*P \leq 0.05$) using Vero-hSLAM cells for titration. **(C)** PI incorporation assay as control for the viability of the cells. PHA-stimulated PBL were treated for 48 h with SKI-II as indicated, dead cells were stained with PI, and percentages of living cells determined by flow cytometry (normalized to DMSO control: 100%). **(D)** Primary human PBL were stimulated with PHA and 1 h pretreated with 0.2% DMSO as mock-treated control (ctrl) or 1 and 5 μM SKI-II prior to infection with MV (MOI = 0.1). Newly synthesized infectious virus (cell bound plus supernatant) was titrated using Vero-hSLAM cells 1, 2, and 3 days after infection ($n = 6$ with PBL from six independent blood donors). **(E)** Virus titers at day 3 after infection in the presence of SKI-II (same data as in panel **D**) were significantly reduced (Student's t-test with $^{***}P < 0.001$) and are presented as percentage of mock-treated control. **(F)** To measure the virus uptake by PBL, cells were pretreated with 0.2% DMSO (=0 μM inhibitor) or increasing concentrations of SKI-II as indicated for 1 h prior to infection with MV (MOI = 0.5). The percentage of infected eGFP-positive cells was quantified by flow cytometry 24 h after infection and is presented as percentage of DMSO (=0 μM inhibitor) control. CTRL is the negative control without virus. $^{**}P \leq 0.01$.

(**Figure 1F**). These results show that virus uptake is not impaired by SKI-II, but that intracellular virus replication is reduced later (at days 2 and 3) after infection.

Effects of Other Inhibitors of the Sphingolipid Metabolism

Having observed this inhibition of MV replication by the inhibitor of the SphKs, we wondered if inhibition of other enzymes of the sphingolipid metabolism may also influence virus replication. While inhibition of the sphingomyelinases is supposed to reduce cellular ceramide content, inhibition of the ceramidase should increase the amount of ceramide in the cell. We therefore investigated the effects of the well-established inhibitors of acid and neutral sphingomyelinases, amitriptyline, and GW4869, respectively, and of the acid ceramidase, ceranib-2 (**Figure 2A**). The toxicity of the inhibitors was determined and the concentrations used accordingly (**Figure 2F**; not shown for amitriptyline and GW4869). Analyzing the effects on MV replication in PBL, we found that amitriptyline and GW4869 had no inhibitory effect (**Figures 2B,C**). Interestingly, GW4869 even had a replication stimulating effect within the first 24 h after infection, which at days 2 and 3 after infection was not detected any more. In contrast to the sphingomyelinase inhibitors, ceranib-2 inhibited MV replication at days 2 and 3 after infection (**Figure 2D**). At day 3 after infection, 0.5 and 1 μM ceranib-2 inhibited MV replication in PBL by approximately 90% (**Figure 2E**). The viability of the PBL was not affected at these concentrations of ceranib-2 (**Figure 2F**). CD150 expression was not altered in dependency of ceranib-2 after 1, 24, and 48 h of treatment (not shown). Determining virus uptake in the presence of ceranib-2 we found, similar as with the inhibitor SKI-II, that the percentage of MV-infected cells 24 h after infection was not reduced, but rather slightly increased with increasing concentrations of ceranib-2 (**Figure 2G**). Thus, inhibition of the acid ceramidase in primary human PBL had very similar effects on MV replication as inhibition of SphKs.

Sphingolipid Composition in PBL After Treatment With the Inhibitors Ceranib-2 and SKI-II

Based on their similar effects, the question arises of whether both inhibitors (SKI-II and ceranib-2) might act via similar or different mechanisms on MV replication, and which sphingolipids might potentially act as signaling molecules. To investigate the inhibitor effects on the sphingolipid rheostat, we treated PHA-stimulated PBL with these inhibitors and quantified SMs, ceramides, Sph, and S1P by LC–MS/MS (**Figure 3**). For the analysis we chose 1 μM ceranib-2 and 5 μM SKI-II, because these concentrations led to good inhibition of MV infection. Ceranib-2 had no significant effect on SM and ceramide levels except ceramide C20 which was slightly increased at 24 h (**Figure 3F**). Surprisingly, 5 μM SKI-II caused significant increases in total ceramide and C16, C18, C20, C22, and C24:1 ceramides. As expected, SKI-II treatment reduced S1P concentrations in PBL (**Figure 3K**). Likewise, there was a tendency that SKI-II led to increased Sph concentrations, which however was not significant due to the high variability between blood donors (**Figure 3J**).

SKI-II and Ceranib-2 Inhibit MV Replication in BJAB Cells

Because variations between primary PBL from different donors may have hampered the achievement of more significant results, we decided to use a human B cells line, BJAB, to analyze effects of the inhibitors. However, before doing so, we confirmed that both inhibitors reduce MV replication similarly in BJAB cells as in primary PBL. Treatment of BJAB cells with 1 or 2 μM SKI-II led to a dose-dependent reduction of newly synthesized virus at days 1, 2, and 3 after infection with MV (**Figure 4A**). Higher concentrations of SKI-II were not used because BJAB cells were more sensitive to SKI-II than primary PBL and approximately 80% died in the presence of 10 μM SKI-II (**Figure 4B**). In contrast to primary PBL (**Figure 1D**), the titration of newly synthesized virus from infected BJAB cells showed that SKI-II reduced viral titers already within the first 24 h after infection (**Figures 4A,G**), while this reduction was generally not as pronounced as in primary cells (**Figures 1A,E**). Investigating viral uptake, similarly as in PBL (**Figure 1F**) and in spite of the titer reduction, the percentage of infected cells 24 h after infection was not reduced with increasing concentrations of SKI-II (**Figure 4C**). Thus, virus uptake was not affected by SKI-II, but intracellular viral replication was inhibited.

Using the acid ceramidase inhibitor, there was a clear reduction of newly synthesized viral titers in the presence of 1 or 2 μM ceranib-2 (**Figure 4D**). Higher concentrations of ceranib-2 (3–10 μM) led to a reduction of the viability (**Figure 4E**). Virus uptake was not affected by 1 or 2 μM ceranib-2 (**Figure 4F**). As observed with SKI-II, MV replication was reduced by ceranib-2 in BJAB cells already at day 1. Inhibition was, however, more pronounced at day 3 (**Figure 4H**). Taken together, both inhibitors impaired MV replication in BJAB cells similarly as observed in primary PBL, although the inhibitory effects emerged faster in BJAB cells being detected already at day 1 after infection.

Sphingolipid Composition in BJAB Cells Treated With Inhibitors in the Presence and Absence of MV Infection

For the sphingolipid analysis in BJAB cells we chose 3 μM ceranib-2 in order to see clearer effect on ceramide levels than in PBL, and 3 μM SKI-II. Treatment of the cells with ceranib-2 led to reduced levels of total SMs and C16 SM at 48 h in the presence or absence of infection (dark and light blue bars) in comparison to the DMSO control (gray bar; **Figure 5A**), while total ceramide levels were increased after 6, 24, and 48 h (**Figure 5C**). Increased ceramide levels were found for total ceramide, C16, and C24:1, but not for C18, C20, C22, and C24 ceramides. Interestingly, MV infection and ceranib-2 treatment led to increased S1P levels at 6 h (**Figure 5K**). SKI-II treatment led to reduced total SM, C16 SM levels, total ceramide, C16, and C24: levels at 48 h in the absence and presence of infection (**Figures 5A–I**; dark and light orange bars). In addition, Sph was increased at 6 h after infection

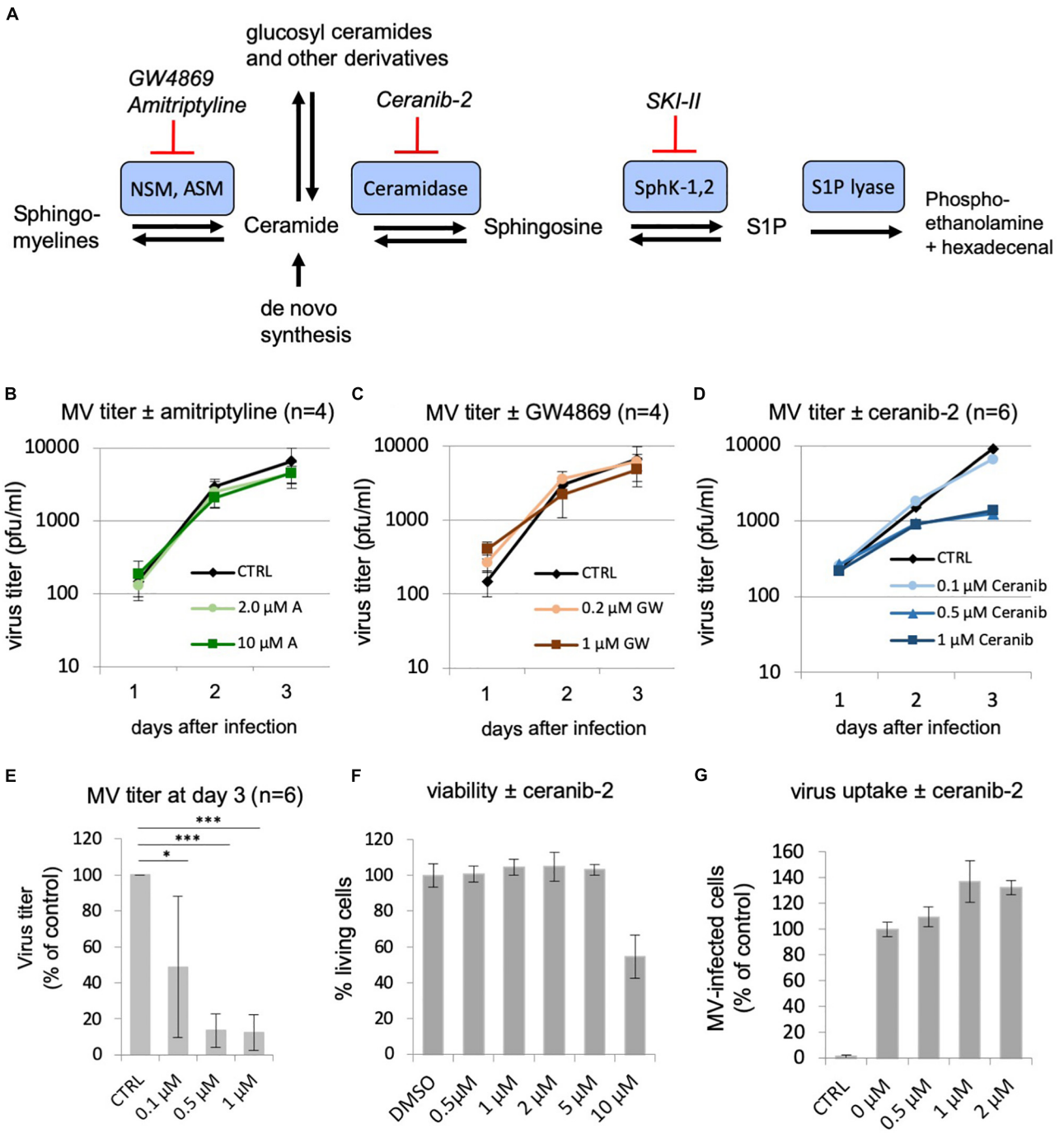

FIGURE 2 | Effects of other inhibitors of the sphingolipid metabolism: inhibition of MV replication by the acid ceramidase inhibitor ceranib-2. **(A)** Schematic representation of a part of the sphingolipid metabolism with involved enzymes (the biosynthesis pathway of ceramides from serine and palmitoyl-CoA and modification pathways to ceramide-1-phosphate and glucosyl-ceramides and complex glycosphingolipids are not shown). NSM, neutral sphingomyelinase; ASM, acid sphingomyelinase; SKI-II, sphingosine kinase inhibitor 2; S1P, sphingosine-1-phosphate. **(B–D)** Primary human PBL were stimulated with PHA (2.5 µg/ml) for 24 h and pretreated with DMSO vehicle (CTRL) or increasing concentrations of inhibitor 1 h prior to infection with MV (MOI = 0.1). Newly synthesized infectious virus (cell bound plus supernatant) was titrated using Vero-hSLAM cells 1, 2, and 3 days after infection. PBL were treated with amitriptyline (2 and 10 µM; $n = 4$; **B**), GW4869 (0.2 and 1.0 µM; $n = 4$; **C**), and ceranib-2 (0.1, 0.5, and 1 µM; $n = 6$ with PBL from independent blood donors; **D**). **(E)** Virus titers at day 3 after infection in the presence of ceranib-2 are significantly reduced. Standard deviations are shown. The statistical evaluation was done using Student's *t*-test. **(F)** The viability of the PBL was controlled using propidium iodide incorporation assay. **(G)** To measure virus uptake by PBL, cells were pretreated with increasing concentrations of ceranib-2 as indicated for 1 h prior to infection with MV (MOI = 0.5). The percentage of infected eGFP-positive cells was quantified by flow cytometry 24 h after infection and is presented as percentage of DMSO (=0 µM inhibitor) control. CTRL is the negative control without virus.

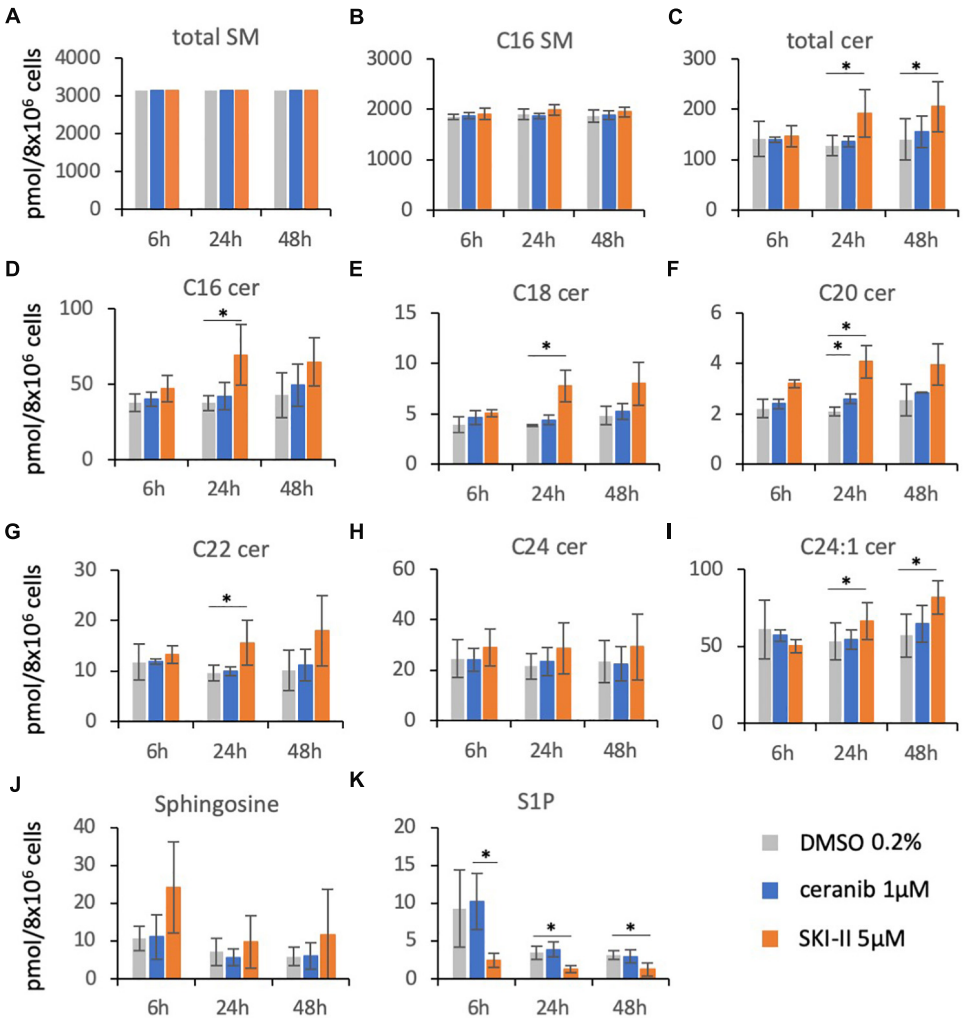

FIGURE 3 | Sphingolipid composition in primary human PBL after treatment with the inhibitors ceranib-2 and SKI-II. PBL were treated for 6, 24, and 48 h with DMSO 0.2% as vehicle control (gray), or 1 μM ceranib-2 (blue) or 5 μM SKI-II (orange). The samples (8×10^6 cells per sample) were processed for analysis of sphingomyelins (total SM and C16 SM), ceramides (total Cer, C16, C18, C20, C22, C24, C24:1), sphingosine, and S1P by mass spectrometry. Results from PBL of three independent donors ($n = 3$) were normalized to the mean amount of total SM measured **(A)** and are presented as pmol/sample, as indicated **(A–K)**.
* represents significant differences calculated by Student's *t*-test ($n = 3$).

(**Figure 5J**), while the S1P concentrations were decreased by SKI-II at 6, 24, and 48 h (**Figure 5K**).

In order to have a closer look at the MV-induced increase of S1P at early times after infection (**Figure 5K**), we did an additional experiment analyzing sphingolipids at 0.5, 1, 2, 6, and 24 h after infection in the presence and absence of inhibitors. Here we observed increased total ceramide concentrations shortly after treatment with the inhibitors (**Figure 5L**), and a strong S1P increase after 0.5–6 h after MV infection also in the presence of ceranib-2, which, however, was not observed in the presence of SKI-II (**Figure 5M**). Thus, SKI-II prevented the transient increase of S1P induced by the MV infection. In summary these data in BJAB cells showed that ceranib-2 led to clearly increased ceramide levels, while SKI-II led to decreased levels of S1P and some ceramide species. The data suggest that in these cells ceranib-2 may act antivirally via the increase in ceramide concentrations, whereas SKI-II may predominantly act antivirally via the reduction of S1P concentrations.

Reduced Metabolic Activity in Inhibitor-Treated Lymphocytes Affects MV Replication

One common effect of increased ceramide concentrations as well as decreased S1P concentrations is to impair cell metabolism and mTORC1 activity (Dobrowsky et al., 1993; Mukhopadhyay et al., 2009; Apostolidis et al., 2016), while efficient MV replication in PBL depends on mTORC1 activity (Tiwarekar et al., 2018). We therefore investigated if the inhibitors ceranib-2 and/or SKI-II may lead to reduced mTORC1 activity. We used the phosphorylation of p70 S6K as marker

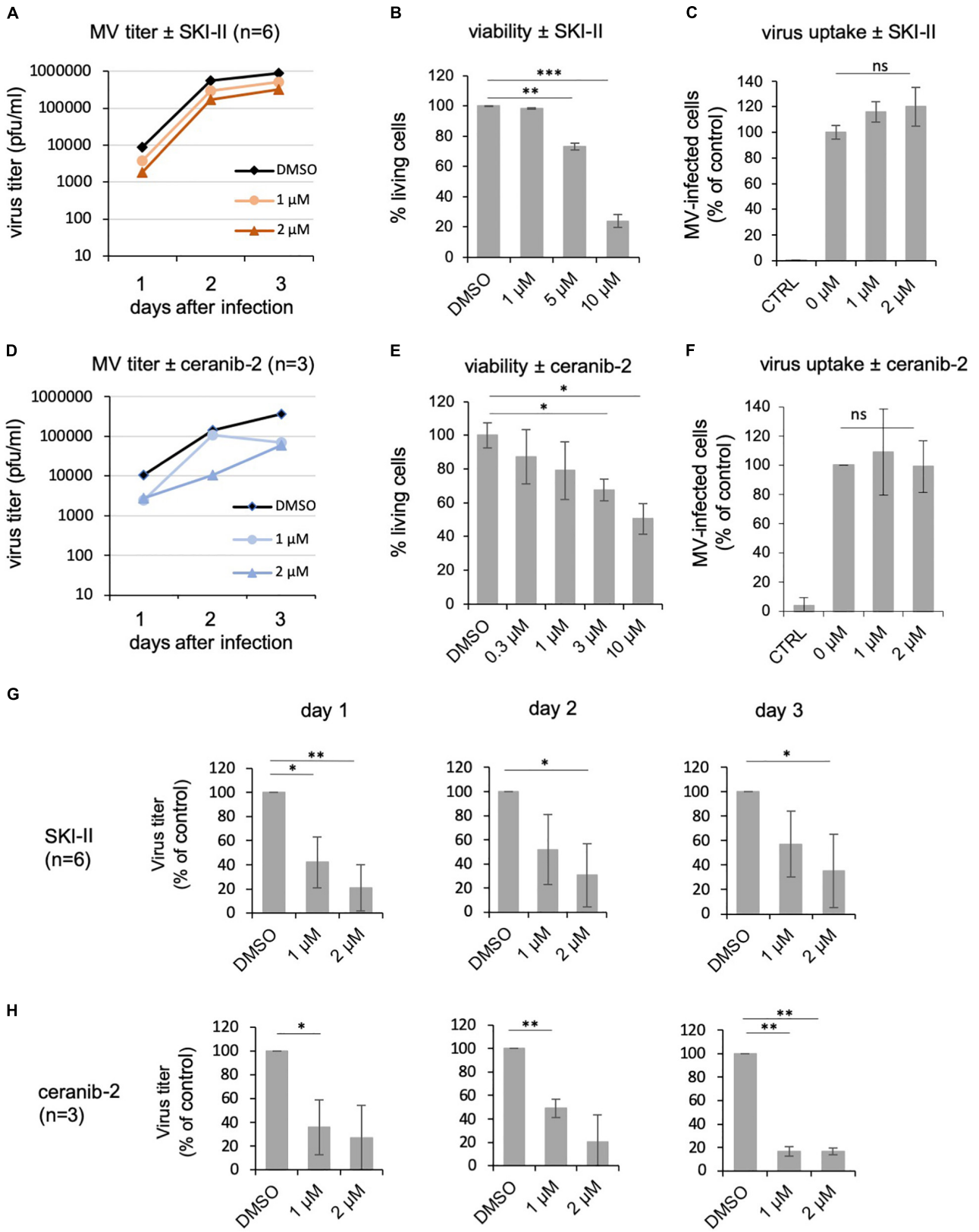

FIGURE 4 | Continued

FIGURE 4 | SKI-II and ceranib-2 inhibit MV replication in BJAB cells. BJAB cells were pretreated with DMSO 0.2% as vehicle control or 1 and 2 μM SKI-II **(A)** and ceranib-2 **(D)**, prior to infection with MV (MOI = 0.1), and newly synthesized virus was titrated using Vero-hSLAM cells. The viability of the BJAB cells was determined by propidium iodide incorporation by FACS in the presence of increasing concentrations of SKI-II **(B)** and ceranib-2 **(E)**. To determine the effect of the inhibitors on virus uptake, BJAB cells were treated with inhibitors for 1 h prior to infection with MV (MOI = 0.1). The percentage of infected eGFP-positive BJAB cells in the presence of increasing concentrations of SKI-II **(C)** and ceranib-2 **(F)** was quantified by flow cytometry 24 h after infection and is presented as percent of DMSO control (=0 μM inhibitor). The reductions in viral titers by SKI-II and ceranib-2 (same data as in panels **A,D**) are shown separately for days 1, 2, and 3 after infection and after treatment of cells with SKI-II **(G)** and ceranib-2 **(H)** to demonstrate more clearly the inhibitor effects at different days and to show variations with significances. The statistical evaluation was done using the Student's *t*-test.

for mTORC1 activity. We found that ceranib-2 reduced the phosphorylation of p70 S6K in comparison to DMSO-treated controls in PBL, and that both inhibitors, ceranib-2 and SKI-II, reduced the phosphorylation of p70 S6K in BJAB cells (**Figures 6A,B**). These results suggest that both inhibitors act at least by one common pathway reducing the metabolic activity of the cells, which reduces the capacity to replicate MV.

In addition, it is known that S1P also targets and activates chaperones such as GRP94 and Hsp90, which among other effects enable NF-kB activation (Xia et al., 2002; Alvarez et al., 2010; Park et al., 2015, 2016), and that Hsp90 activity is required for the replication of a number of viruses including MV (Connor et al., 2007; Smith et al., 2010; Bloyet et al., 2016; Katoh et al., 2017). Therefore, we tested the effect of the Hsp90 inhibitor 17-AAG in primary human PBL. Treatment of PBL with 0.5 and 1 μM 17-AAG strongly reduced viral titers 2 and 3 days after infection, but not yet at day 1 after infection (**Figure 6C**). This observed kinetic of inhibition was similar to that observed with the inhibitors SKI-II (**Figure 1D**) and ceranib-2 (**Figure 2D**) in PBL. The viability and virus uptake were not affected by 17-AAG (**Figures 6D,E**).

DISCUSSION

The two inhibitors ceranib-2 and SKI-II have been described as compounds with excellent potential for development as new anticancer drugs (French et al., 2003; Draper et al., 2011; Aurelio et al., 2016). SphKs are upregulated in many cancers and thought to play a key role in disease progression through increases in S1P and decreases in ceramide and Sph levels, promoting tumor growth and survival (Santos and Lynch, 2015). Acid ceramidase is highly upregulated in breast tumors and treatment with ceranib-2 significantly induced apoptosis in human breast cancer cell lines (Vethakanraj et al., 2018). In mice, ceranib-2 was found to delay tumor growth in a syngeneic tumor model without hematologic suppression or overt signs of toxicity (Draper et al., 2011). In contrast to cancer cells, normal primary cells are less prone to induction of apoptosis and cell death upon treatment with such inhibitors. This led us to the hypothesis that these inhibitors could eventually be applied against viral infections without damaging primary cells including antiviral lymphocytes. Indeed, we found that already relatively low concentrations of SKI-II (1 μM) and ceranib-2 (0.5 μM) reduced MV replication in primary PBL, while the expression of the MV receptor CD150 and viral uptake was not altered.

That increased ceramide can have an antiviral role has been described earlier for various viruses such as HIV (Finnegan et al., 2004), hepatitis B virus (HBV) (Tatematsu et al., 2011), Dengue virus (Perera et al., 2012), and IAV (Hidari et al., 2006; Tafesse et al., 2013; Soudani et al., 2019). In the case of HIV, this was mediated through a reduction in virus entry and perturbation of host cell membrane structure leading to the production of non-infectious viral progeny, and in the case of IAV through impaired glycoprotein transport and maturation of viral particles. However, on the other hand, sphingolipids including ceramides may also be supportive for virus replication as in the case of hepatitis C and West Nile virus (Zhang et al., 2019). Our sphingolipid analyses after treatment of cells with SKI-II and ceranib-2 led to different results for PBL and BJAB cells. In PBL, SKI-II increased the concentrations of some ceramides and ceranib-2 had no significant effect. In BJAB cells, SKI-II decreased the concentration of some ceramides, while ceranib-2 led to an increase. Furthermore, SKI-II reduced S1P concentrations in PBL and BJAB cells. Thus, because of these findings and because intracellular signaling effects of ceramides and S1P may be locally limited events (for example at lysosomes or the endoplasmic reticulum), these results unfortunately did not allow clear conclusions. Interestingly, both, increased ceramide as well as decreased S1P concentrations, reduce the mTORC activity as it is known that ceramide acts on the SET protein and decreases mTORC activity via the phosphatase PP2A (Dobrowsky et al., 1993; Li et al., 1996; Neviani et al., 2005; Trotta et al., 2007; Mukhopadhyay et al., 2009; Shi, 2009; Oaks and Ogretmen, 2014) and that S1P affects mTORC activity via Hsp90 and raptor (Delgoffe et al., 2009). As demonstrated for regulatory T cells, dephosphorylation by PP2A inactivates mTORC1 and thus reduces the cell metabolism including protein translation and lipid synthesis (Apostolidis et al., 2016). Among others, mTORC1 regulates the ribosomal S6 protein kinase-1, of which due to alternative translation two isoforms are known in mammalian cells, p85 and p70. The mTOR kinase phosphorylates and thereby activates p70 at T389 and p85 at T412 (Ruvinsky and Meyuhas, 2006). Now we found that treatment of cells with ceranib-2 reduced the phosphorylation of p70 S6K in PBL and that SKI-II reduced p70 S6K phosphorylation in PBL and BJAB cells indicating reduced mTORC1 activity. Because MV replication requires mTORC activity (Tiwarekar et al., 2018), it is likely that this is a common effect of the inhibitors affecting MV replication. We cannot exclude other (side-)effects of the inhibitors; however, the main point of the paper remains that the inhibitors affect MV replication. The finding suggests that the inhibitor-induced reduction of the MV replication is at least partially due to this reduction in mTORC1 activity.

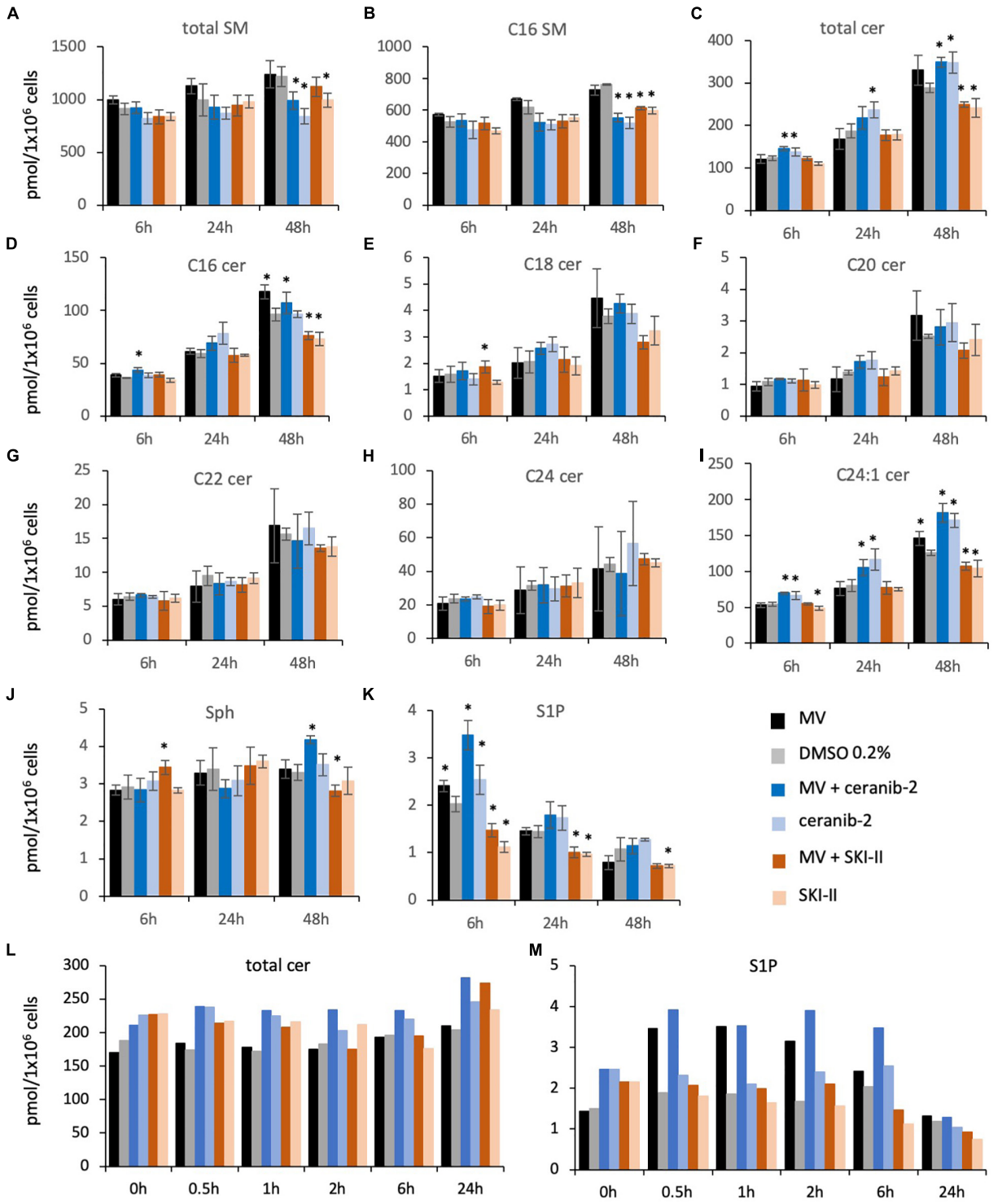

FIGURE 5 | Sphingolipid composition in BJAB cells after treatment with the inhibitors ceranib-2 and SKI-II and infection with MV. The sphingolipid composition was determined in MV-infected (black bars; MOI = 0.5) and uninfected control (0.2% DMSO)-treated (gray bars) BJAB cells (1×10^6 per sample), in 3 μM ceranib-2-treated infected (dark blue) and uninfected (light blue), and in 3 μM SKI-II-treated infected (dark orange) and uninfected (light orange) BJAB cells. Results for total sphingomyelins (SM), C16 SM, ceramides (total Cer, C16, C18, C20, C22, C24, C24:1), sphingosine (Sph), and S1P are presented as pmol/sample per 1×10^6 cells as indicated **(A–M)**. Stars in panels **A–K** designate significant ($^*P \leq 0.05$) differences in comparison to control (0.2% DMSO-treated) cells ($n = 3$; Student's *t*-test). In panels **L,M** ($n = 1$), the significances between treatment groups were calculated by paired *T*-test and one-way ANOVA. In panel **L**, the DMSO control values (0–6 h) were significantly different from MV + ceranib-2- and ceranib-2-treated cell values ($P = 0.001$ and $P = 0.002$, respectively). In panel **M**, the DMSO control values were significantly different from MV and MV + ceranib-2-treated cell values ($P = 0.04$ and $P = 0.007$, respectively).

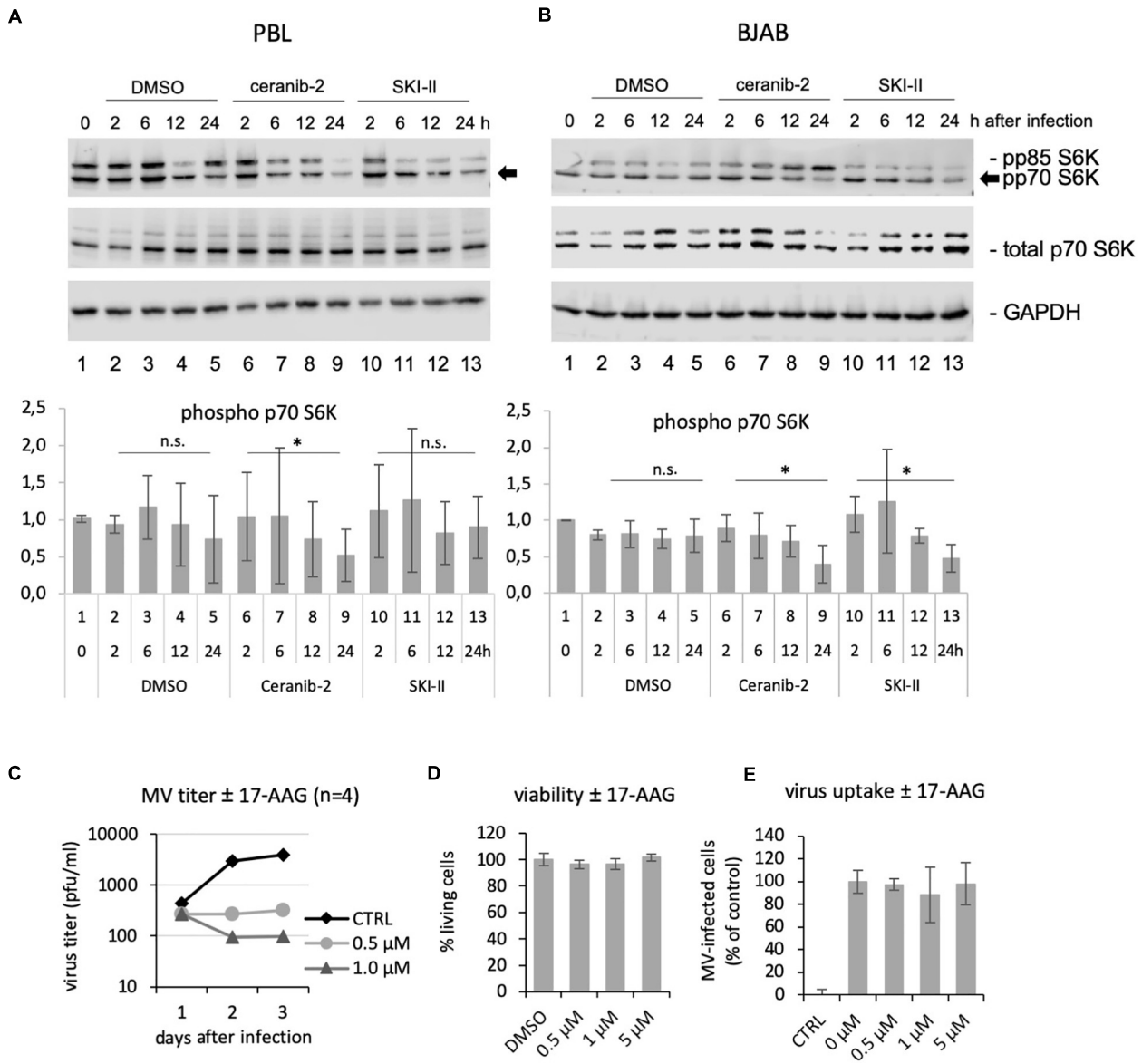

FIGURE 6 | Ceranib-2 and SKI-II-mediated reduction of p70 S6K phosphorylation, and inhibition of MV replication by the Hsp90 inhibitor 17-AAG. Western blots from cell extracts of human primary PBL **(A)** and BJAB cells **(B)** which were treated with 0.2% DMSO as control, 3 μM ceranib-2, and 5 μM SKI-II for 2, 6, 12, and 24 h as indicated were developed with antibodies against phosphorylated p70 S6K (also detecting p85), total p70 S6K, and GAPDH. Quantifications of phosphorylated p70 S6K related to GAPDH of three blots of PBL from independent blood donors and BJAB of independent experiments are shown. **(C)** PBL were treated with increasing concentrations of the Hsp90 inhibitor 17-AAG, infected with MV at a MOI of 0.1, and newly synthesized virus titrated after 1, 2, and 3 days using Vero-hSLAM cells (n = 4). **(D)** Viability and virus uptake **(E)** was assessed as described (n = 3).

We also found that MV infection led to a strong S1P increase between 0.5 and 6 h after infection, which was prevented by SKI-II and thus a potential S1P anti-apoptotic/pro-survival signal that may support MV replication is not provided. S1P and SphK1 were demonstrated to signal intracellularly via interaction with TRAF2, RIP1 to activate Hsp90 and NF-κB (Xia et al., 2002; Alvarez et al., 2010; Park et al., 2015, 2016). Thus, SKI-II prevents a signal that the virus itself induces in order to support its own replication. Interestingly, the chaperone Hsp90 is required for the function of polymerases of many viruses including MV (Connor et al., 2007; Smith et al., 2010; Bloyet et al., 2016; Katoh et al., 2017). In Vero and HeLa cells and brain slices of MV-susceptible mice it has been observed that Hsp90 inhibition impairs MV replication (Bloyet et al., 2016). Inhibition or lack of Hsp90 is preventing the proper folding of newly synthesized viral polymerases and facilitates their degradation (Bloyet et al., 2016). Because S1P regulates Hsp90 activity, it is likely that the SKI-II-mediated decrease in S1P concentrations also impairs Hsp90 in PBL, which may contribute to the observed inhibition of MV replication. We showed here that Hsp90 inhibition in PBL

strongly reduced MV replication at days 2 and 3 after infection, but did not affect MV replication at day 1. This kinetic of inhibition is typically observed when functional viral polymerases have been brought into the cell with infectious viral particles, but newly synthesized viral polymerases at later times after infection remain non-functional (Bloyet et al., 2016). In the presence of SKI-II and ceranib-2, we observed similar kinetics of the inhibition of the synthesis of new viruses in primary PBL. It is not clear if and how ceranib-2 may influence Hsp90 activity; however, it is probably part of the SKI-II-mediated inhibition of MV in PBL. This might be different in BJAB cells, which responded faster (already at day 1) to SKI-II (and ceranib-2).

A number of reports have described ceramide interacting proteins such as the anti-oncogene p53 (Fekry et al., 2018), ceramide activated protein kinase (CAPK) (Huwiler et al., 1996), protein kinase C-ζ (PKCζ) (Wang et al., 2005), cathepsins (Heinrich et al., 1999), and the ribosomal voltage dependent anion channel 2 (VDAC2) (Dadsena et al., 2019), which can induce apoptosis or other types of cell death. Predominantly C18 ceramide has been reported to interact with the SET (I2PP2A) protein and to inhibit its activity, which leads to an activation of the serine/threonine phosphatase PP2A, which dephosphorylates and inactivates the anti-apoptotic protein BCL2 (Dobrowsky et al., 1993; Li et al., 1996; Neviani et al., 2005; Trotta et al., 2007; Mukhopadhyay et al., 2009; Oaks and Ogretmen, 2014). For SKI-II it has been described mainly for cancer cells that this inhibitor can also induce cell death (Leroux et al., 2007; LeBlanc et al., 2015; Yang et al., 2015). Thus, increased ceramide concentrations, as well as decreased S1P concentrations can induce apoptosis or other forms of cell death (Hannun and Obeid, 2008; Young et al., 2013; Oaks and Ogretmen, 2014). In our study, low concentrations of the inhibitors (1 μM SKI-II and 0.5 μM ceranib-2), which induced <5% dead PBL, clearly reduced MV replication. Thus, this suggested that cell death is not responsible for the observed reduction in MV replication.

CONCLUSION

In summary, our data indicate that MV replication is reduced by inhibitors of the acid ceramidase and SphKs in primary human PBL and suggest that viral replication is impaired by several mechanisms regulated by sphingolipid-mediated signaling pathways. We can add the aspect that the inhibitors SKI-II and ceranib-2 affect the activities of mTORC1 and Hsp90, and thus reduce MV replication. Future work is required to reveal the exact mechanisms involved and to optimize the use of compounds regulating sphingolipid metabolism in order to inhibit virus replication while maintaining a functional antiviral immune response *in vivo*.

DATA AVAILABILITY STATEMENT

The datasets generated for this study are available on request to the corresponding author.

AUTHOR CONTRIBUTIONS

NB and JS-S: conceptualization. AG, FS, JC, and BK: methodology. JS-S: writing – original draft preparation.

FUNDING

This study was funded by the German Research Foundation (DFG), research group FOR2123, grant SCHN 320/24-2, and the University of Würzburg in the funding program Open Access Publishing.

ACKNOWLEDGMENTS

We thank Hannah Franke and Nora Länder for technical assistance; Katrin Kreisel, Laura Grimm, Martin Bach, Lisa Paulini, Carla Cleve, Annika Kittel, and Ann-Katrin Wolf for contributing bits and pieces; Claudia Hollmann, Teresa Wiese, and Elita Avota for practical advice; Daniel Herrmann for assistance in the mass spectrometric analyses; and Sibylle Schneider-Schaulies and the whole research group FOR2123 for helpful discussions.

REFERENCES

Alvarez, S. E., Harikumar, K. B., Hait, N. C., Allegood, J., Strub, G. M., Kim, E. Y., et al. (2010). Sphingosine-1-phosphate is a missing cofactor for the E3 ubiquitin ligase TRAF2. *Nature* 465, 1084–1088. doi: 10.1038/nature09128

Apostolidis, S. A., Rodriguez-Rodriguez, N., Suarez-Fueyo, A., Dioufa, N., Ozcan, E., Crispin, J. C., et al. (2016). Phosphatase PP2A is requisite for the function of regulatory T cells. *Nat. Immunol.* 17, 556–564. doi: 10.1038/ni.3390

Aurelio, L., Scullino, C. V., Pitman, M. R., Sexton, A., Oliver, V., Davies, L., et al. (2016). From sphingosine kinase to dihydroceramide desaturase: a structure-activity relationship (SAR) study of the enzyme inhibitory and anticancer activity of 4-((4-(4-Chlorophenyl)thiazol-2-yl)amino)phenol (SKI-II). *J. Med. Chem.* 59, 965–984. doi: 10.1021/acs.jmedchem.5b01439

Avota, E., Gulbins, E., and Schneider-Schaulies, S. (2011). DC-SIGN mediated sphingomyelinase-activation and ceramide generation is essential for enhancement of viral uptake in dendritic cells. *PLoS Pathog.* 7:e1001290. doi: 10.1371/journal.ppat.1001290

Bloyet, L. M., Welsch, J., Enchery, F., Mathieu, C., de Breyne, S., Horvat, B., et al. (2016). HSP90 chaperoning in addition to phosphoprotein required for folding but not for supporting enzymatic activities of measles and nipah virus L polymerases. *J. Virol.* 1, 6642–6656. doi: 10.1128/JVI.00602-16

Connor, J. H., McKenzie, M. O., Parks, G. D., and Lyles, D. S. (2007). Antiviral activity and RNA polymerase degradation following Hsp90 inhibition in a range of negative strand viruses. *Virology* 362, 109–119. doi: 10.1016/j.virol.2006.12.026

Dadsena, S., Bockelmann, S., Mina, J. G. M., Hassan, D. G., Korneev, S., Razzera, G., et al. (2019). Ceramides bind VDAC2 to trigger mitochondrial apoptosis. *Nat. Commun.* 23:1832. doi: 10.1038/s41467-019-09654-4

Delgoffe, G. M., Kole, T. P., Cotter, R. J., and Powell, J. D. (2009). Enhanced interaction between Hsp90 and raptor regulates mTOR signaling upon T cell activation. *Mol. Immunol.* 46, 2694–2698. doi: 10.1016/j.molimm.2009.05.185

Dobrowsky, R. T., Kamibayashi, C., Mumby, M. C., and Hannun, Y. A. (1993). Ceramide activates heterotrimeric protein phosphatase 2A. *J. Biol. Chem.* 25, 15523–15530.

Draper, J. M., Xia, Z., Smith, R. A., Zhuang, Y., Wang, W., and Smith, C. D. (2011). Discovery and evaluation of inhibitors of human ceramidase. *Mol. Cancer Ther.* 10, 2052–2061. doi: 10.1158/1535-7163.MCT-11-0365

Erlenhoefer, C., Wurzer, W. J., Loffler, S., Schneider-Schaulies, S., ter Meulen, V., and Schneider-Schaulies, J. (2001). CD150 (SLAM) is a receptor for measles virus but is not involved in viral contact-mediated proliferation inhibition. *J. Virol.* 75, 4499–4505. doi: 10.1128/jvi.75.10.4499-4505.2001

Fekry, B., Jeffries, K. A., Esmaeilniakooshkghazi, A., Szulc, Z. M., Knagge, K. J., Kirchner, D. R., et al. (2018). C16-ceramide is a natural regulatory ligand of p53 in cellular stress response. *Nat. Commun.* 9:4149. doi: 10.1038/s41467-018-06650-y

Finnegan, C. M., Rawat, S. S., Puri, A., Wang, J. M., Ruscetti, F. W., and Blumenthal, R. (2004). Ceramide, a target for antiretroviral therapy. *Proc. Natl. Acad. Sci. U.S.A.* 101, 15452–15457. doi: 10.1073/pnas.0402874101

French, K. J., Schrecengost, R. S., Lee, B. D., Zhuang, Y., Smith, S. N., Eberly, J. L., et al. (2003). Discovery and evaluation of inhibitors of human sphingosine kinase. *Cancer Res.* 63, 5962–5969.

Grassme, H., Riehle, A., Wilker, B., and Gulbins, E. (2005). Rhinoviruses infect human epithelial cells via ceramide-enriched membrane platforms. *J. Biol. Chem.* 280, 26256–26262. doi: 10.1074/jbc.m500835200

Gulbins, A., Schumacher, F., Becker, K. A., Wilker, B., Soddemann, M., Boldrin, F., et al. (2018). Antidepressants act by inducing autophagy controlled by sphingomyelin-ceramide. *Mol. Psychiatry* 23, 2324–2346. doi: 10.1038/s41380-018-0090-9

Hannun, Y. A., and Obeid, L. M. (2008). Principles of bioactive lipid signalling: lessons from sphingolipids. *Nat. Rev. Mol. Cell Biol.* 9, 139–150. doi: 10.1038/nrm2329

Hashimoto, K., Ono, N., Tatsuo, H., Minagawa, H., Takeda, M., Takeuchi, K., et al. (2002). SLAM (CD150)-independent measles virus entry as revealed by recombinant virus expressing green fluorescent protein. *J. Virol.* 76, 6743–6749. doi: 10.1128/jvi.76.13.6743-6749.2002

Heinrich, M., Wickel, M., Schneider-Brachert, W., Sandberg, C., Gahr, J., Schwandner, R., et al. (1999). Cathepsin D targeted by acid sphingomyelinase-derived ceramide. *EMBO J.* 18, 5252–5263. doi: 10.1093/emboj/18.19.5252

Herz, J., Pardo, J., Kashkar, H., Schramm, M., Kuzmenkina, E., Bos, E., et al. (2009). Acid sphingomyelinase is a key regulator of cytotoxic granule secretion by primary T lymphocytes. *Nat. Immunol.* 10, 761–768. doi: 10.1038/ni.1757

Hidari, K. I., Suzuki, Y., and Suzuki, T. (2006). Suppression of the biosynthesis of cellular sphingolipids results in the inhibition of the maturation of influenza virus particles in MDCK cells. *Biol. Pharm. Bull.* 29, 1575–1579. doi: 10.1248/bpb.29.1575

Hollmann, C., Werner, S., Avota, E., Reuter, D., Japtok, L., Kleuser, B., et al. (2016). Inhibition of acid sphingomyelinase allows for selective targeting of CD4+ conventional versus Foxp3+ regulatory T cells. *J. Immunol.* 197, 3130–3141. doi: 10.4049/jimmunol.1600691

Huwiler, A., Brunner, J., Hummel, R., Vervoordeldonk, M., Stabel, S., van den Bosch, H., et al. (1996). Ceramide-binding and activation defines protein kinase c-Raf as a ceramide-activated protein kinase. *Proc. Natl. Acad. Sci. U.S.A.* 93, 6959–6963. doi: 10.1073/pnas.93.14.6959

Kachler, K., Bailer, M., Heim, L., Schumacher, F., Reichel, M., Holzinger, C. D., et al. (2017). Enhanced acid sphingomyelinase activity drives immune evasion and tumor growth in non-small cell lung carcinoma. *Cancer Res.* 77, 5963–5976. doi: 10.1158/0008-5472.CAN-16-3313

Katoh, H., Kubota, T., Nakatsu, Y., Tahara, M., Kidokoro, M., and Takeda, M. (2017). Heat shock protein 90 ensures efficient mumps virus replication by assisting with viral polymerase complex formation. *J. Virol.* 91:e02220-16. doi: 10.1128/JVI.02220-16

LeBlanc, F. R., Liu, X., Hengst, J., Fox, T., Calvert, V., Petricoin, E. F. III, et al. (2015). Sphingosine kinase inhibitors decrease viability and induce cell death in natural killer-large granular lymphocyte leukemia. *Cancer Biol. Ther.* 16, 1830–1840. doi: 10.1080/15384047.2015.1078949

Leroux, M. E., Auzenne, E., Evans, R., Hail, N. Jr., Spohn, W., Ghosh, S. C., et al. (2007). Sphingolipids and the sphingosine kinase inhibitor, SKI II, induce BCL-2-independent apoptosis in human prostatic adenocarcinoma cells. *Prostate* 67, 1699–1717. doi: 10.1002/pros.20645

Li, M., Makkinje, A., and Damuni, Z. (1996). The myeloid leukemia-associated protein SET is a potent inhibitor of protein phosphatase 2A. *J. Biol. Chem.* 271, 11059–11062. doi: 10.1074/jbc.271.19.11059

Luisoni, S., Suomalainen, M., Boucke, K., Tanner, L. B., Wenk, M. R., Guan, X. L., et al. (2015). Co-option of membrane wounding enables virus penetration into cells. *Cell Host. Microb.* 18, 75–85. doi: 10.1016/j.chom.2015.06.006

Miller, E. H., Obernosterer, G., Raaben, M., Herbert, A. S., Deffieu, M. S., Krishnan, A., et al. (2012). Ebola virus entry requires the host-programmed recognition of an intracellular receptor. *EMBO J.* 31, 1947–1960. doi: 10.1038/emboj.2012.53

Mina, M. J., Metcalf, C. J., de Swart, R. L., Osterhaus, A. D., and Grenfell, B. T. (2015). Long-term measles-induced immunomodulation increases overall childhood infectious disease mortality. *Science* 348, 694–699. doi: 10.1126/science.aaa3662

Muhlebach, M. D., Mateo, M., Sinn, P. L., Prufer, S., Uhlig, K. M., Leonard, V. H., et al. (2011). Adherens junction protein nectin-4 is the epithelial receptor for measles virus. *Nature* 480, 530–533. doi: 10.1038/nature10639

Mukhopadhyay, A., Saddoughi, S. A., Song, P., Sultan, I., Ponnusamy, S., Senkal, C. E., et al. (2009). Direct interaction between the inhibitor 2 and ceramide via sphingolipid-protein binding is involved in the regulation of protein phosphatase 2A activity and signaling. *FASEB J.* 23, 751–763. doi: 10.1096/fj.08-120550

Neviani, P., Santhanam, R., Trotta, R., Notari, M., Blaser, B. W., Liu, S., et al. (2005). The tumor suppressor PP2A is functionally inactivated in blast crisis CML through the inhibitory activity of the BCR/ABL-regulated SET protein. *Cancer Cell* 8, 355–368. doi: 10.1016/j.ccr.2005.10.015

Ng, C. G., Coppens, I., Govindarajan, D., Pisciotta, J., Shulaev, V., and Griffin, D. E. (2008). Effect of host cell lipid metabolism on alphavirus replication, virion morphogenesis, and infectivity. *Proc. Natl. Acad. Sci. U.S.A.* 105, 16326–16331. doi: 10.1073/pnas.0808720105

Ng, C. G., and Griffin, D. E. (2006). Acid sphingomyelinase deficiency increases susceptibility to fatal alphavirus encephalomyelitis. *J. Virol.* 80, 10989–10999. doi: 10.1128/jvi.01154-06

Noyce, R. S., Bondre, D. G., Ha, M. N., Lin, L. T., Sisson, G., Tsao, M. S., et al. (2011). Tumor cell marker PVRL4 (Nectin 4) is an epithelial cell receptor for measles virus. *PLoS Pathog.* 7:e1002240. doi: 10.1371/journal.ppat.1002240

Oaks, J., and Ogretmen, B. (2014). Regulation of PP2A by sphingolipid metabolism and signaling. *Front. Oncol.* 4:388. doi: 10.3389/fonc.2014.00388

Park, E. S., Choi, S., Shin, B., Yu, J., Yu, J., Hwang, J. M., et al. (2015). Tumor necrosis factor (TNF) receptor-associated factor (TRAF)-interacting protein (TRIP) negatively regulates the TRAF2 ubiquitin-dependent pathway by suppressing the TRAF2-sphingosine 1-phosphate (S1P) interaction. *J. Biol. Chem.* 290, 9660–9673. doi: 10.1074/jbc.M114.609685

Park, K., Ikushiro, H., Seo, H. S., Shin, K. O., Kim, Y. I., Kim, J. Y., et al. (2016). ER stress stimulates production of the key antimicrobial peptide, cathelicidin, by forming a previously unidentified intracellular S1P signaling complex. *Proc. Natl. Acad. Sci. U.S.A.* 113, E1334–E1342. doi: 10.1073/pnas.1504555113

Perera, R., Riley, C., Isaac, G., Hopf-Jannasch, A. S., Moore, R. J., Weitz, K. W., et al. (2012). Dengue virus infection perturbs lipid homeostasis in infected mosquito cells. *PLoS Pathog.* 8:e1002584. doi: 10.1371/journal.ppat.1002584

Reuter, D., and Schneider-Schaulies, J. (2010). Measles virus infection of the CNS: human disease, animal models, and approaches to therapy. *Med. Microbiol. Immunol.* 199, 261–271. doi: 10.1007/s00430-010-0153-2

Ruvinsky, I., and Meyuhas, O. (2006). Ribosomal protein S6 phosphorylation: from protein synthesis to cell size. *Trends Biochem. Sci.* 31, 342–348. doi: 10.1016/j.tibs.2006.04.003

Santos, W. L., and Lynch, K. R. (2015). Drugging sphingosine kinases. *ACS Chem. Biol.* 16, 225–233. doi: 10.1021/cb5008426

Schneider-Schaulies, J., and Schneider-Schaulies, S. (2015). Sphingolipids in viral infection. *Biol. Chem.* 396, 585–595. doi: 10.1515/hsz-2014-0273

Seo, Y. J., Blake, C., Alexander, S., and Hahm, B. (2010). Sphingosine 1-phosphate-metabolizing enzymes control influenza virus propagation and viral cytopathogenicity. *J. Virol.* 84, 8124–8131. doi: 10.1128/JVI.00510-10

Shi, Y. (2009). Serine/threonine phosphatases: mechanism through structure. *Cell* 139, 468–484. doi: 10.1016/j.cell.2009.10.006

Smith, D. R., McCarthy, S., Chrovian, A., Olinger, G., Stossel, A., Geisbert, T. W., et al. (2010). Inhibition of heat-shock protein 90 reduces ebola virus replication. *Antivir. Res.* 87, 187–194. doi: 10.1016/j.antiviral.2010.04.015

Soudani, N., Hage-Sleiman, R., Karam, W., Dbaibo, G., and Zaraket, H. (2019). Ceramide suppresses influenza a virus replication in vitro. *J. Virol.* 93:e00053-19. doi: 10.1128/JVI.00053-19

Tafesse, F. G., Sanyal, S., Ashour, J., Guimaraes, C. P., Hermansson, M., Somerharju, P., et al. (2013). Intact sphingomyelin biosynthetic pathway is essential for intracellular transport of influenza virus glycoproteins. *Proc. Natl. Acad. Sci. U.S.A.* 110, 6406–6411. doi: 10.1073/pnas.1219909110

Takamatsu, H., Takegahara, N., Nakagawa, Y., Tomura, M., Taniguchi, M., Friedel, R. H., et al. (2010). Semaphorins guide the entry of dendritic cells into the lymphatics by activating myosin II. *Nat. Immunol.* 11, 594–600. doi: 10.1038/ni.1885

Tatematsu, K., Tanaka, Y., Sugiyama, M., Sudoh, M., and Mizokami, M. (2011). Host sphingolipid biosynthesis is a promising therapeutic target for the inhibition of hepatitis B virus replication. *J. Med. Virol.* 83, 587–593. doi: 10.1002/jmv.21970

Tatsuo, H., Ono, N., Tanaka, K., and Yanagi, Y. (2000). SLAM (CDw150) is a cellular receptor for measles virus. *Nature* 406, 893–897. doi: 10.1038/35022579

Tiwarekar, V., Wohlfahrt, J., Fehrholz, M., Scholz, C. J., Kneitz, S., and Schneider-Schaulies, J. (2018). APOBEC3G-regulated host factors interfere with measles virus replication: role of REDD1 and mammalian TORC1 inhibition. *J. Virol.* 92:e00835-18. doi: 10.1128/JVI.00835-18

Trotta, R., Ciarlariello, D., Dal Col, J., Allard, J. II, Neviani, P., Santhanam, R., et al. (2007). The PP2A inhibitor SET regulates natural killer cell IFN-gamma production. *J. Exp. Med.* 204, 2397–2405. doi: 10.1084/jem.20070419

Vethakanraj, H. S., Sesurajan, B. P., Padmanaban, V. P., Jayaprakasam, M., Murali, S., and Sekar, A. K. (2018). Anticancer effect of acid ceramidase inhibitor ceranib-2 in human breast cancer cell lines MCF-7, MDA MB-231 by the activation of SAPK/JNK, p38 MAPK apoptotic pathways, inhibition of the Akt pathway, downregulation of ERalpha. *Anticancer Drugs.* 29, 50–60. doi: 10.1097/CAD.0000000000000566

Vijayan, M., Seo, Y. J., Pritzl, C. J., Squires, S. A., Alexander, S., and Hahm, B. (2014). Sphingosine kinase 1 regulates measles virus replication. *Virology* 450-451, 55–63. doi: 10.1016/j.virol.2013.11.039

Wang, G., Silva, J., Krishnamurthy, K., Tran, E., Condie, B. G., and Bieberich, E. (2005). Direct binding to ceramide activates protein kinase Czeta before the formation of a pro-apoptotic complex with PAR-4 in differentiating stem cells. *J. Biol. Chem.* 280, 26415–26424. doi: 10.1074/jbc.m501492200

World Health Organization [WHO] (2018). *Fact Sheets, Detail, Measles 2018*. Available at: https://www.who.int/news-room/fact-sheets/detail/measles (accessed May 09, 2019).

Xia, P., Wang, L., Moretti, P. A., Albanese, N., Chai, F., Pitson, S. M., et al. (2002). Sphingosine kinase interacts with TRAF2 and dissects tumor necrosis factor-alpha signaling. *J. Biol. Chem.* 277, 7996–8003. doi: 10.1074/jbc.m111423200

Yang, L., Weng, W., Sun, Z. X., Fu, X. J., Ma, J., and Zhuang, W. F. (2015). SphK1 inhibitor II (SKI-II) inhibits acute myelogenous leukemia cell growth in vitro and in vivo. *Biochem. Biophys. Res. Commun.* 460, 903–908. doi: 10.1016/j.bbrc.2015.03.114

Young, M. M., Kester, M., and Wang, H. G. (2013). Sphingolipids: regulators of crosstalk between apoptosis and autophagy. *J. Lipid Res.* 54, 5–19. doi: 10.1194/jlr.R031278

Zhang, Z., He, G., Filipowicz, N. A., Randall, G., Belov, G. A., Kopek, B. G., et al. (2019). Host lipids in positive-strand RNA virus genome replication. *Front. Microbiol.* 10:286. doi: 10.3389/fmicb.2019.00286

Conflict of Interest: The authors declare that the research was conducted in the absence of any commercial or financial relationships that could be construed as a potential conflict of interest.

frontiers in Cell and Developmental Biology

ORIGINAL RESEARCH
published: 01 October 2019
doi: 10.3389/fcell.2019.00210

Monitoring the Sphingolipid *de novo* Synthesis by Stable-Isotope Labeling and Liquid Chromatography-Mass Spectrometry

*Dominik Wigger[1], Erich Gulbins[2,3], Burkhard Kleuser[1] and Fabian Schumacher[1,2]**

[1] Department of Toxicology, University of Potsdam, Nuthetal, Germany, [2] Department of Molecular Biology, University of Duisburg-Essen, Essen, Germany, [3] Department of Surgery, University of Cincinnati, Cincinnati, OH, United States

Sphingolipids are a class of lipids that share a sphingoid base backbone. They exert various effects in eukaryotes, ranging from structural roles in plasma membranes to cellular signaling. *De novo* sphingolipid synthesis takes place in the endoplasmic reticulum (ER), where the condensation of the activated C_{16} fatty acid palmitoyl-CoA and the amino acid L-serine is catalyzed by serine palmitoyltransferase (SPT). The product, 3-ketosphinganine, is then converted into more complex sphingolipids by additional ER-bound enzymes, resulting in the formation of ceramides. Since sphingolipid homeostasis is crucial to numerous cellular functions, improved assessment of sphingolipid metabolism will be key to better understanding several human diseases. To date, no assay exists capable of monitoring *de novo* synthesis sphingolipid in its entirety. Here, we have established a cell-free assay utilizing rat liver microsomes containing all the enzymes necessary for bottom-up synthesis of ceramides. Following lipid extraction, we were able to track the different intermediates of the sphingolipid metabolism pathway, namely 3-ketosphinganine, sphinganine, dihydroceramide, and ceramide. This was achieved by chromatographic separation of sphingolipid metabolites followed by detection of their accurate mass and characteristic fragmentations through high-resolution mass spectrometry and tandem-mass spectrometry. We were able to distinguish, unequivocally, between *de novo* synthesized sphingolipids and intrinsic species, inevitably present in the microsome preparations, through the addition of stable isotope-labeled palmitate-d_3 and L-serine-d_3. To the best of our knowledge, this is the first demonstration of a method monitoring the entirety of ER-associated sphingolipid biosynthesis. Proof-of-concept data was provided by modulating the levels of supplied cofactors (e.g., NADPH) or the addition of specific enzyme inhibitors (e.g., fumonisin B_1). The presented microsomal assay may serve as a useful tool for monitoring alterations in sphingolipid *de novo* synthesis in cells or tissues. Additionally, our methodology may be used for metabolism studies of atypical substrates – naturally occurring or chemically tailored – as well as novel inhibitors of enzymes involved in sphingolipid *de novo* synthesis.

Keywords: sphingolipid *de novo* synthesis, serine palmitoyltransferase, mass spectrometry, stable-isotope labeling, ceramides

OPEN ACCESS

Edited by:
Eleonora Napoli,
University of California, Davis,
United States

Reviewed by:
Pushpendra Singh,
Johns Hopkins University,
United States
Justin Snider,
Stony Brook University, United States

***Correspondence:**
Fabian Schumacher
fabian.schumacher@uni-potsdam.de

Specialty section:
This article was submitted to Cellular Biochemistry, a section of the journal Frontiers in Cell and Developmental Biology

Received: *27 June 2019*
Accepted: *11 September 2019*
Published: *01 October 2019*

Citation:
Wigger D, Gulbins E, Kleuser B and Schumacher F (2019) Monitoring the Sphingolipid de novo Synthesis by Stable-Isotope Labeling and Liquid Chromatography-Mass Spectrometry. Front. Cell Dev. Biol. 7:210. doi: 10.3389/fcell.2019.00210

INTRODUCTION

Sphingolipids are a lipid class of great physiological importance to the homeostasis of mammalian cells, eukaryotes as a whole, and some prokaryotes. Structurally, all sphingolipids share a C_{18} amino alcohol backbone, to which fatty acids of different chain lengths and head groups of varied polarity can be attached. Due to their amphipathic character, sphingolipids play significant roles in membrane biology, including the maintenance of barrier function and fluidity (Breslow and Weissman, 2010). Beyond this, sphingolipids include bioactive species that are involved in numerous cellular signaling cascades such as ceramides (Cer), sphingosine (Sph, synonymous with d18:1 Sph), and sphingosine 1-phosphate (S1P) (Hannun and Obeid, 2008). It has been shown that different bioactive sphingolipids can cause opposing biological effects. For instance, while Cer act pro-apoptotically (Obeid et al., 1993; Gulbins et al., 1995), S1P production correlates with proliferative (Olivera and Spiegel, 1993) and anti-apoptotic effects (Cuvillier et al., 1996). Concordantly, the relative levels of sphingolipid metabolites are key to cellular homeostasis and, as such, are tightly regulated, a process widely referred to as "sphingolipid rheostat" (Newton et al., 2015). Disturbances to sphingolipid metabolism are associated with numerous pathogenic states involved in, e.g., several cancers (Ogretmen, 2017), cardiovascular diseases (Borodzicz et al., 2015), metabolic diseases such as type 2 diabetes (Meikle and Summers, 2016), neuro-psychiatric disorders (Mühle et al., 2013), and bacterial and viral infections (Grassmé et al., 2003; Grassmé et al., 2005). To date, however, many mechanistic details regarding the involvement of sphingolipids in such pathologies remain poorly understood. Likewise, a complete understanding of the complex and highly interlinked metabolism of sphingolipids is still ongoing.

Cer are the base molecules from which the synthesis of more complex sphingolipids, such as sphingomyelin and glycosphingolipids, takes place. They are also the precursors for bioactive lipid mediators such as Sph and S1P. Cer can be generated by sphingomyelin hydrolysis in membranes or *via* the catabolic salvage pathway, in which complex sphingolipids undergo lysosomal breakdown resulting in Cer (Hannun and Obeid, 2008). The *de novo* synthesis of Cer takes place in the endoplasmic reticulum (ER), and involves four enzymatic steps (**Figure 1**). The initial step is the condensation of the activated C_{16} fatty acid palmitoyl-CoA and the amino acid L-serine, which is catalyzed by pyridoxal 5'-phosphate (PLP)-dependent serine palmitoyltransferase (SPT). This produces 3-ketosphinganine (3KS), which is then rapidly reduced to sphinganine (dihydrosphingosine, d18:0 Sph) by 3-ketosphinganine reductase (also known as 3-ketodihydrosphingosine reductase, KDSR) in a NADPH dependent manner. Sphinganine, a so called long-chain base (LCB), is further *N*-acylated by the action of six ceramide synthase isoforms (CerS1-6) encoded by six distinct genes. Each CerS has a different acyl-CoA preference that can overlap within their isoforms. For example, CerS5 and CerS6 preferably use palmitoyl-CoA as their substrate, thus mainly forming C16 dihydroceramide (C16 dhCer, Cer d18:0/16:0) as a product. The last step in the sphingolipid *de novo* synthesis is catalyzed by dihydroceramide Δ4-desaturase (DEGS), which occurs in two isoforms: DEGS1 and DEGS2. Firstly, DEGS introduces a hydroxyl group at the C-4 position of the d18:0 Sph backbone using molecular oxygen. Next, a dehydration reaction follows in which DEGS, by means of NADPH (or NADH), introduces a double bond between carbons C-4 and C-5 to yield the Cer core-structure (Gault et al., 2010). For all enzymes involved in sphingolipid *de novo* synthesis (SPT, KDSR, CerS, and DEGS), there is strong evidence to suggest they are located on the cytosolic leaflet of the ER membrane (Gault et al., 2010; Yamaji and Hanada, 2015).

As with all enzymes involved in cellular metabolism, those regulating the sphingolipid biosynthesis can be affected by endogenous and exogenous factors as well as genetic alterations. Mammalian SPT is a heterodimer consisting of the two subunits SPTLC1 and SPTLC2 with the latter found as two isoforms (Tidhar and Futerman, 2013). Most patients suffering from hereditary sensory and autonomic neuropathy type 1 (HSAN1) carry mutations in *SPTLC1* or *SPTLC2*. These mutations do not affect the activity of the SPT-complex, but instead shift its substrate affinity so that in addition to canonical SPT products, cytotoxic 1-deoxysphingolipids are formed through the incorporation of L-alanine instead of L-serine. The disease phenotype varies with *SPT* mutations, producing a range of severe symptoms such as muscle atrophy, growth retardation, and lung complications (Bode et al., 2016). It was recently demonstrated that *KDSR* mutations causing structural and functional defects in KDSR, the next enzyme in sequence of *de novo* sphingolipid synthesis, have been shown to associate with the inherited skin disorder progressive symmetric erythrokeratoderma (Boyden et al., 2017). Likewise, genetic defects in *CerS* have been described and discussed as the cause of several human diseases. For instance, a missense coding single-nucleotide polymorphism in *CerS2* has been associated with rhegmatogenous retinal detachment (Kirin et al., 2013), while mutations in *CerS3* leading to impaired activity and expression of CerS3 have been linked to skin ichthyosis (Eckl et al., 2013). In addition, there are numerous examples in which changes in the expression or activity of CerS isoforms correlate with human diseases, cancers in particular. Subsequently, the use of CerS as therapeutic targets is currently under intense scrutiny (Park et al., 2014). Recently, a genetic defect in *DEGS1,* in conjunction with substantial increases of dihydroceramides in fibroblasts and muscles, was identified as causative of hypomyelinating leukodystrophy (Pant et al., 2019). Of therapeutic relevance, several modulators of DEGS1 activity have been identified, as summarized by Rodriguez-Cuenca et al. (2015). These include the DEGS1 inducers palmitate and interleukin-2, and the DEGS1 repressors vitamin E and oxidative stress.

All enzymes involved in the *de novo* synthesis of sphingolipids can be modulated and can act as central "crossroads" in numerous human diseases. Techniques that assess the affinities and activities of the individual enzymes are, therefore, of great importance. Since each step of ER-centered biosynthetic pathways influences the next, it is essential to empirically capture the complete sphingolipid *de novo* synthesis. As far as we

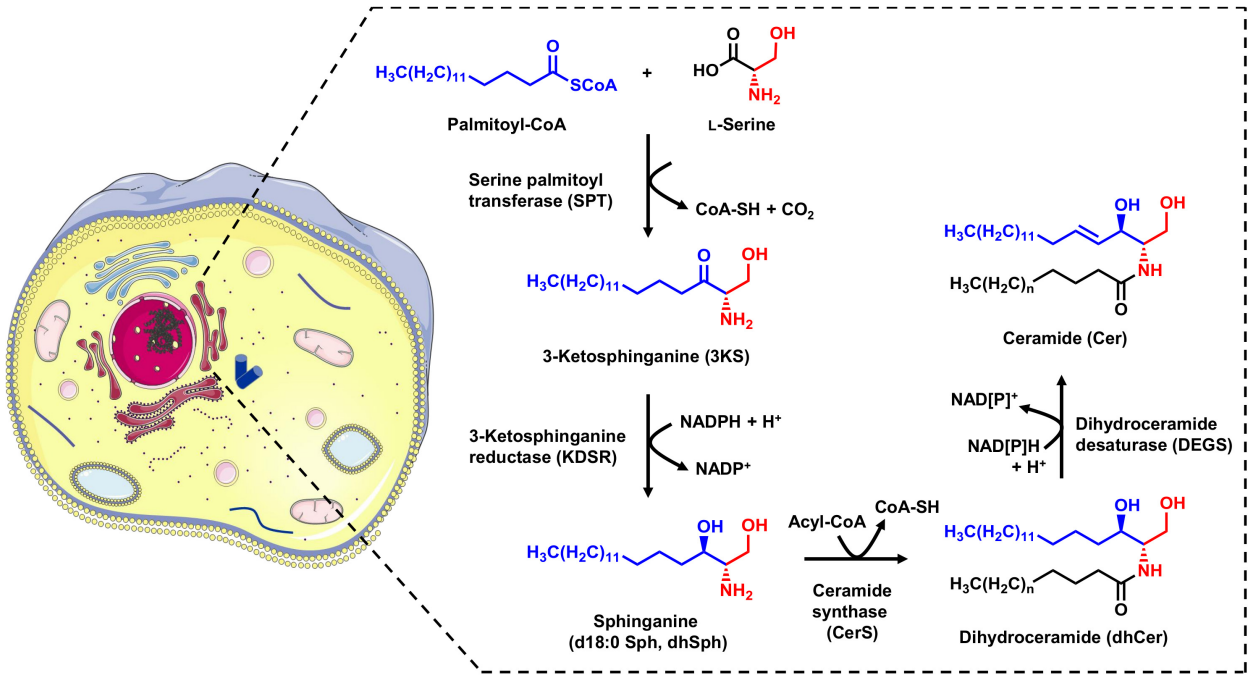

FIGURE 1 | Schematic overview of the sphingolipid *de novo* synthesis located in the ER. Serine palmitoyltransferase (SPT) catalyzes the condensation of palmitoyl-CoA and L-serine. The product of this reaction, 3-ketosphinganine (3KS), is further NADPH-dependently reduced to sphinganine (dihydrosphingosine, d18:0 Sph) by 3-ketosphinganine reductase (KDSR). Ceramide synthases (CerS) couple fatty acyl-CoAs to the amino group of the long-chain base d18:0 Sph. This leads to the formation of dihydroceramides (dhCer), differing in the chain length of the amide-bound fatty acid. The final step is the introduction of a double bond between carbons C-4 and C-5 mediated by dihydroceramide desaturase (DEGS) under NAD[P]H consumption. The formed ceramides (Cer) are subsequently shuttled to the Golgi apparatus for further metabolism. The cell image (left) was taken from https://smart.servier.com (freely accessible).

know, there is currently no cell-free assay available capable of tracking the status of the SPT substrates palmitate and L-serine from the initial condensation product up to their incorporation within the Cer scaffold. Here, we present a microsomal *in vitro* assay using stable-isotope labeled starting materials (palmitate-d_3 and L-serine-d_3) along with state-of-the-art detection techniques [high-performance liquid chromatography (HPLC) coupled to high-resolution and tandem-mass spectrometry] for unambiguous monitoring sphingolipid biosynthetics within the ER in its entirety. Doing so, we were able to track the incorporation of palmitate and serine beyond the formation of LCBs to (dh)Cer.

MATERIALS AND METHODS

Chemicals and Reagents

Palmitic acid (16,16,16-d_3) was obtained from Cortecnet (Voisins-le-Bretonneux, France) and L-serine (2,3,3-d_3) was from CDN Isotopes (Pointe-Claire, Canada). Cer d18:0/16:0 (C16 dhCer), Cer d18:1/16:0 (C16 Cer), Cer d18:1/17:0 (C17 Cer), d18:0 Sph (dhSph) and d17:0 Sph were from Avanti Polar Lipids (Alabaster, United States). 4-(2-hydroxyethyl)-1-piperazineethanesulfonic acid (HEPES), dimethyl sulfoxide (DMSO), disodium hydrogen phosphate dihydrate (Na_2HPO_4), dithiothreitol (DTT), fatty acid-free bovine serum albumin (BSA), glacial acetic acid, glycerol, magnesium chloride hexahydrate ($MgCl_2$), potassium chloride (KCl), sodium chloride (NaCl), sodium dihydrogen phosphate monohydrate (NaH_2PO_4), sodium hydroxide (NaOH) and tris(hydroxymethyl)aminomethane (Tris) were purchased from Carl Roth (Karlsruhe, Germany). Potassium hydroxide was from Merck KGaA (Darmstadt, Germany). Coenzyme A (CoA), fumonisin B_1 (FB_1) and nicotinamide adenine dinucleotide phosphate sodium salt (NADPH) were received from Cayman Chemicals (Ann Arbor, United States). Adenosine 5′-triphosphate disodium salt hydrate (ATP), β-glycerophosphate disodium salt hydrate, calcium chloride dihydrate ($CaCl_2$), cOmplete™ Protease Inhibitor Cocktail, myriocin from *Mycelia sterilia*, nicotinamide adenine dinucleotide dipotassium salt (NADH), phenylmethylsulfonyl fluoride (PMSF), pyridoxal 5′-phosphate hydrate (PLP), *sn*-glycerol 3-phosphate lithium salt and sodium orthovanadate (Na_3VO_4) were ordered from Sigma-Aldrich (Taufkirchen, Germany). All solvents and additives used were of LC-MS grade. 1-Butanol was from Merck KGaA, formic acid from VWR (Darmstadt, Germany) and acetonitrile as well as methanol from Carl Roth. Water was purified by a Millipore apparatus (Millipore GmbH, Darmstadt, Germany).

Preparation of Rat Liver Microsomes

Liver tissue of adult, male Wistar rats (2 g wet weight) was homogenized in 6 mL ice-cold homogenization buffer

(10 mM NaH_2PO_4/Na_2HPO_4, 150 mM KCl, pH 7.4) using an Ultra Turrax T25 basic (IKA, Staufen, Germany). Cell debris were removed by centrifugation at 9,000 *g* for 20 min (4°C). To pellet microsomes, the supernatant was centrifuged for 1 h at 100,000 *g* (4°C) in a Beckman Coulter Optima LE-80K ultracentrifuge (Beckman Coulter, Krefeld, Germany) equipped with a Type 90 Ti fixed-angle rotor (Beckman Coulter). Microsomes were purified under the same conditions (1 h, 100,000 *g*, 4°C) in 4 mL homogenization buffer. After removal of the supernatant, the pellet was resuspended in microsomal buffer (5% (*w/v*) glycerol in homogenization buffer) and stored at −80°C. Protein concentration of the final microsome preparation was determined by Bradford assay.

In vitro Sphingolipid *de novo* Synthesis Assay

The method was modified from a thin-layer chromatography-based protocol applied for investigations of *in vitro* S1P metabolism in membrane fractions published by Wakashima and co-workers (Wakashima et al., 2014). Rat liver microsomes (200 μg) were incubated with 0.3 mM palmitate-d_3 and 4 mM L-serine-d_3 for 1 h at 37°C under gentle shaking (120 rpm). The assay mixture with a total volume of 500 μL also contained 4 mM ATP, 5 mM β-glycerophosphate, 1 mM $CaCl_2$, 160 μM CoA, cOmplete™ Protease Inhibitor (2.7-fold), 0.8 mM DTT, 40 mM HEPES-NaOH, 2 mM $MgCl_2$, 121 mM NaCl, 1 mM NADPH, 5 mM Na_3VO_4, 250 μM PLP, 0.8 mM PMSF and 1 mM *sn*-glycerol 3-phosphate (in the following referred to as "standard condition"). In order to modulate the sphingolipid *de novo* synthesis the following modifications of the standard protocol were applied: omission of NADPH, addition of 1 mM NADH, addition of 1 mM NADH and 5 μM FB_1, addition of 1 mM NADH and 50 μM myriocin. Stock solutions of FB_1, myriocin and PMSF were prepared in DMSO. All other substances were dissolved in water. To obtain an 8 mM palmitate-d_3 stock solution, 41 mg were dissolved in 2 mL of 0.1 M NaOH at 75°C. Next, the solution was transferred at 55°C in 200 μL increments into 18 mL of a 10% BSA solution (in PBS). For the aqueous ATP solution, the pH had to be adjusted to 7.0 with Tris (1 M) to maintain stability at −20°C for 6 months. With the exception of CoA, NADPH and NADH that were freshly prepared on the day of the assay, stock solutions were stored at −20°C. Assay negative control samples were prepared under "standard conditions" with palmitate-d_3 replaced by the vehicle BSA. *In vitro* sphingolipid biosynthesis was stopped by addition of 200 μL 1 M methanolic KOH. Sphingolipid extraction was carried out by addition of 1 mL 1-butanol (containing 20 pmol Cer d18:1/17:0 and 2 pmol d17:0 Sph as internal standards) and 0.5 mL of water-saturated 1-butanol. After extraction for 10 min under shaking (1,500 rpm) and centrifugation (2,300 *g*, 10 min, 4°C) the upper organic phase was neutralized with 16 μL glacial acetic acid and subsequently evaporated to dryness under reduced pressure using a Savant SpeedVac Concentrator (Thermo Fisher Scientific, Dreieich, Germany). Dried samples were dissolved in 100 μL of HPLC eluent mixture B/A (95:5, *v/v,* see next paragraph) (1,500 rpm, 10 min) and centrifuged at 2,300 *g* for 10 min (4°C). The supernatants were split into two vials and subjected to HPLC-MS analysis.

Analysis of *de novo* Formed Labeled Sphingolipids by High-Performance Liquid Chromatography-Mass Spectrometry

All assay samples were subjected to HPLC coupled to both a quadrupole time-of-flight mass spectrometer (QTOF MS) and a triple quadrupole mass spectrometer (TQ MS). The rationale was to obtain accurate mass data (QTOF MS) as well as structural information by means of compound specific fragmentations with particularly high sensitivity (TQ MS). Chromatographic separations were performed with Agilent 1260 Infinity HPLC systems (Agilent Technologies, Waldbronn, Germany) coupled to the respective mass spectrometer, an Agilent 6530 QTOF MS or an Agilent 6490 TQ MS, *via* electrospray ion sources operating in the positive ion mode (ESI+). Samples (10 μL) were injected onto an Eclipse Plus C8 column (3.5 μm, 2.1 × 150 mm) guarded by a pre-column of the same material (both Agilent) that was tempered to 30°C. Water (eluent A) and methanol/acetonitrile (1:1, *v/v,* eluent B), both acidified with 0.1% formic acid, were used as eluents. Sphingolipid metabolites were eluted from the column by gradient elution using the settings given in **Table 1**. The total run time for one analysis was 30 min, including re-equilibration of the HPLC system. The following ion source parameters were used and, if not stated otherwise, maintained for both types of mass spectrometer used: drying gas temperature = 225°C, drying gas flow = 13 L/min of nitrogen (TQ MS: 15 L/min), sheath gas temperature = 380°C, sheath gas flow = 12 L/min of nitrogen, nebulizer pressure = 45 psi, capillary voltage = 4500 V, nozzle voltage = 2000 V. The ion funnel parameters (TQ MS only) were: high pressure RF voltage = 150 V and low pressure RF voltage = 60 V. The QTOF MS was operated in full scan mode, acquiring data in the mass-to-charge ratio (*m/z*) range of 100–750 with a scan rate of 2 spectra/s. TQ MS detection was accomplished in selected reaction monitoring (SRM) or, if applicable, in multiple reaction monitoring

TABLE 1 | HPLC gradient for separation of sphingolipids formed *de novo* in the microsomal assay[a].

Time (min)	Eluent A (%)[b]	Eluent B (%)[c]	Flow rate (mL/min)
0	40	60	0.5
3	40	60	0.5
10	5	95	0.5
12	5	95	0.5
13	5	95	0.7
14	0	100	0.8
23	0	100	0.8
24	40	60	0.8
25	40	60	0.5

[a]Analytical separation column: Eclipse Plus C8 (3.5 μm, 2.1 × 150 mm) + guard column of the same material (both Agilent Technologies). [b]Water containing 0.1% formic acid. [c]Methanol/acetonitrile (1:1, v:v) containing 0.1% formic acid.

TABLE 2 | MS/MS parameters for detection of *de novo* formed sphingolipids using the TQ MS system.

Sphingolipid species	Mass transition (*m/z*)	Collision energy (eV)	Dwell time (ms)
3KS-d_5	305.3 → 273.3	19	160
d18:0 Sph-d_5	307.3 → 289.3	15	160
Cer d18:0-d_5/16:0-d_3	548.6 → 530.6	15	160
	548.6 → 289.3	25	160
Cer d18:1-d_5/16:0-d_3	528.6 → 269.3	25	160
REFERENCE COMPOUNDS			
d17:0 Sph (IS)[a]	288.5 → 270.5	12	160
Cer d18:1/17:0 (IS)[b]	534.5 → 264.3	25	160
d18:0 Sph	302.3 → 284.3	15	160
Cer d18:0/16:0	540.5 → 522.5	15	160
	540.5 → 284.3	25	160
Cer d18:1/16:0	520.5 → 264.3	25	160

[a]*Used as internal standard (IS) for labeled 3KS and d18:0 Sph.* [b]*Used as IS for labeled C16 dhCer and C16 Cer.*

(MRM) mode. Fragmentations measured by collision-induced dissociation (CID) of investigated sphingolipids are given in **Table 2**. Most mass spectrometric results presented in this study are qualitative in nature. However, in experiments on modulation of sphingolipid biosynthesis *in vitro* (impact of enzyme inhibitors and cofactor supplementation), internal standards (d17:0 Sph and Cer d18:1/17:0) were used for semi-quantitative considerations. Furthermore, newly formed, labeled sphingolipids were quantified in technical assay replicates (using rat liver microsomes of the same batch) by means of d18:0 Sph, Cer d18:0/16:0, and Cer d18:1/16:0 as reference compounds for external calibration, as well as d17:0 Sph and Cer d18:1/17:0 as internal standards.

Statistical Analysis

Differences in quantities of *de novo* formed sphingolipid intermediates generated *via* two different assay conditions were statistically evaluated by multiple *t*-tests (***$p < 0.001$; n.s., non-significant) using the software GraphPad Prism Version 6.5 (GraphPad Software, Inc., La Jolla, United States).

RESULTS

Formation of 3KS-d_5 by the SPT-Catalyzed Reaction of d_3-Palmitoyl-CoA and Serine-d_3

The first step in sphingolipid *de novo* synthesis is the SPT-catalyzed reaction of palmitoyl-CoA with L-serine, and the subsequent formation of 3KS (**Figure 1**). For the *in vitro* assay presented herein, palmitate-d_3 and L-serine-d_3 were applied as SPT substrates. A prerequisite for this strategy was the *in situ* activation of the fatty acid palmitate-d_3. This was achieved by addition of CoA and ATP to the microsome preparations containing the fatty acyl-CoA synthetases (Normann et al., 1981) responsible for the formation of d_3-palmitoyl-CoA. First, we ran the *in vitro* assay without the addition of NADPH in order to stop sphingolipid biosynthesis after the initial SPT catalysis. Thus, we were able to maximize product concentrations, as reducing equivalents are necessary for the subsequent step in sphingolipid biosynthesis. We analyzed the corresponding lipid extract by HPLC-QTOF MS (**Figures 2A,B**) and HPLC-TQ MS (**Figure 2C**). Using high-resolution MS, we observed a compound eluting at 7.1 min with the accurate *m/z* of 305.3222 that was not present in the negative control (complete assay with palmitate-d_3 substituted by the vehicle BSA). This *m/z* matched the protonated molecular ion $[M+H]^+$ of 3KS-d_5 (chemical structure given in the topmost panel of **Figure 2**) with a mass error of only 3.60 ppm. At first glance, it seems surprising that the reaction of substrates, each of them labeled three-times, yields a product that is only quintuply labeled. However, a detailed consideration of the intensely studied SPT catalytic cycle reveals the fate of one particular deuterium atom, the α-deuterium located at C-2 position of the L-serine (2,3,3-d_3) used as substrate. As illustrated in **Figure 3**, an internal aldimine (Enz-Lys-PLP) formed between the cofactor PLP and a lysine residue of the enzyme's active site is replaced by the external aldimine composed of PLP and the incoming serine-d_3. Binding of palmitoyl-CoA – in this case (16,16,16-d_3)-palmitoyl-CoA – results in transfer of the α-deuterium from the external aldimine to an enzymatic lysine residue. This previously described deuterium loss (Ren et al., 2018) leads, after completion of SPT catalysis, to the formation of a five-times labeled 3KS, deuterated twice at the amino acid moiety and three times at the terminus of the fatty acid. To verify the formation of 3KS-d_5 from palmitate-d_3 and serine-d_3 under the chosen experimental conditions, we subjected the lipid extract to HPLC-TQ MS in order to confirm structural identity by MS/MS. Cleavage of the terminal CH_2O group has been reported as the predominant fragmentation of the natural SPT product 3KS, as reflected by the mass transition *m/z* 300.3 → 270.3 used for SRM analysis (Merrill et al., 2005). We transferred this structural information to the initial SPT product that is generated in our assay and, therefore, analyzed the CID of the terminal CD_2O group of 3KS-d_5. A clear signal for the SRM transition *m/z* 305.3 → 273.3, absent in the negative control (**Figure 2C**), further confirmed the proper function of the SPT and, thus, the first step of the presented *in vitro* sphingolipid *de novo* synthesis assay.

De novo Formation of d18:0 Sph-d_5 From 3KS-d_5

Following the formation of 3KS, sphingolipid biosynthesis proceeds with the reduction of 3KS to d18:0 Sph catalyzed by KDSR (**Figure 1**). Within this, the presence of NADPH is essential to the conversion of the C-3 keto group to a hydroxyl group. We thus performed our assay under "standard conditions" – in the presence of all cofactors necessary for full ER-based sphingolipid biosynthesis (see section Materials and Methods). Again, we performed accurate mass HPLC-QTOF MS with the extracted assay sample. Knowing that the presumable product should be five-times deuterated (chemical structure given in **Figure 4**), we extracted the $[M+H]^+$ ion with *m/z* 307.3367 from the QTOF MS full scan. As can

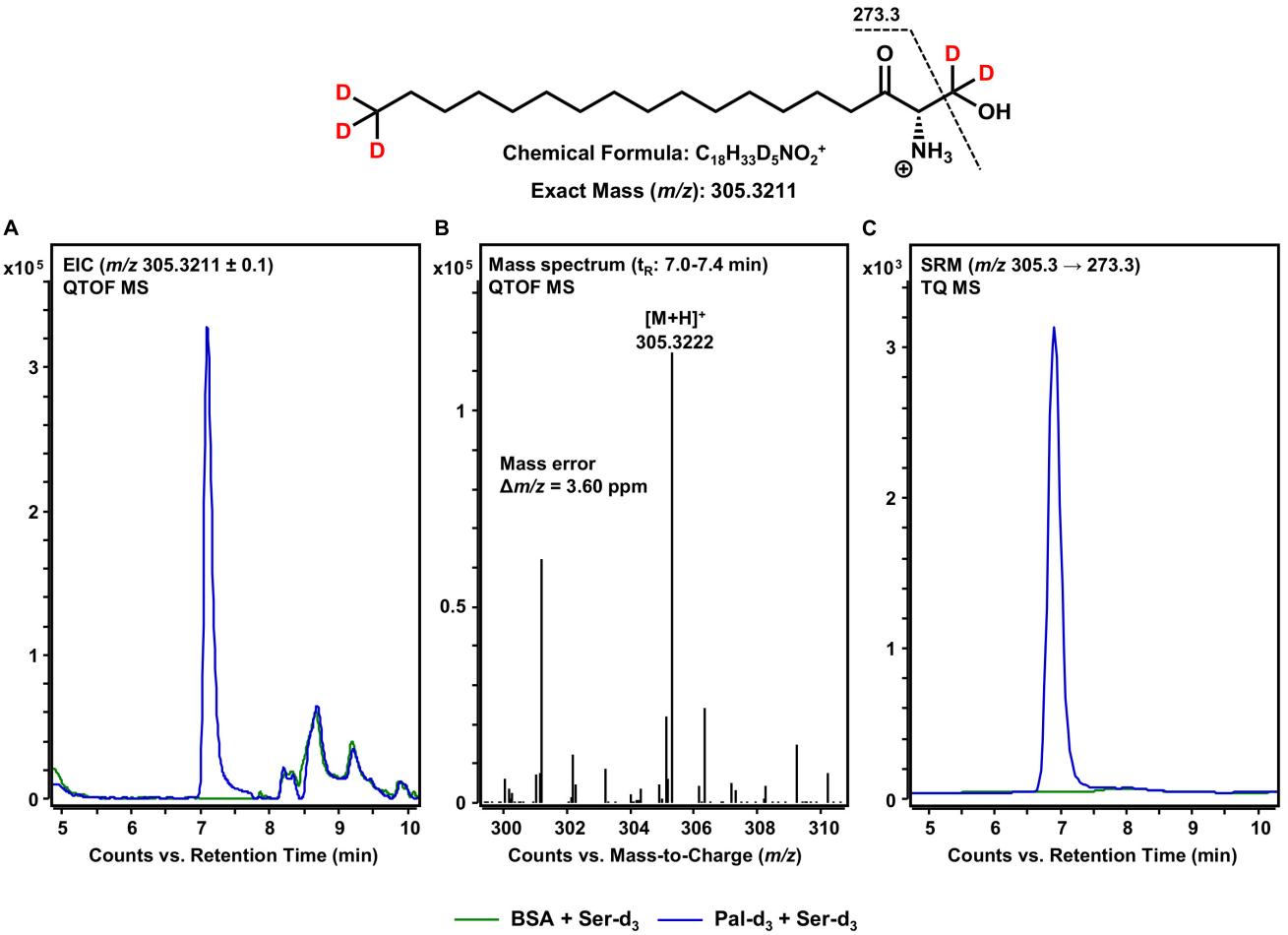

FIGURE 2 | SPT-catalyzed formation of 3KS-d_5 from the *in vitro* assay substrates palmitate-d_3 and L-serine-d_3. **(Top)** Chemical structure, formula, and exact mass of the protonated molecular ion $[M+H]^+$ of 3KS-d_5 generated during electrospray ionization. Dashed black line represents the mass transition used for selected reaction monitoring (SRM). **(A)** Overlay of extracted ion chromatograms (EIC) of the microsomal *de novo* synthesis assay using palmitate-d_3 and serine-d_3 as substrates (blue) compared to the negative control omitting palmitate-d_3 (green). **(B)** Mass spectrum extracted from the EIC in the retention time window of eluting 3KS-d_5 with annotation of the molecular ion peak and the calculated mass error. **(A,B)** Analysis was conducted on a quadrupole time-of-flight mass spectrometer (QTOF MS). **(C)** Overlay of SRM analyses of assay (blue) compared to negative control sample (green) performed with a triple quadrupole mass spectrometer (TQ MS). t_R, retention time. **(A)** In the t_R range of 8–10 min, relatively abundant unidentified matrix components (m/z: $305.2211 \leq \times \leq 305.4211$) eluted from both the assay and negative control samples. **(C)** Concordant matrix signals were diminished, with increased specificity achieved by analyzing compound-specific fragmentation.

be seen in **Figure 4A**, an intense signal not present when palmitate-d_3 was excluded from the assay reaction mixture, was detected. The corresponding mass spectrum (**Figure 4B**) confirmed the presence of d18:0 Sph-d_5 with high mass accuracy (mass error less than 4 ppm). The slightly shorter retention time (6.9 min) compared to those observed for 3KS-d_5 (7.1 min, **Figure 2**) is in agreement with the higher polarity of the hydroxyl compared to the keto group. Additionally, we performed MS/MS fragmentation of *de novo* synthesized d18:0 Sph-d_5 using the TQ MS system. We monitored the mass transition m/z 307.3 → 289.3, as water loss accompanied by a mass shift of 18 Da has been reported during CID of unlabeled sphinganine (Cho et al., 2019). Indeed, a sharp SRM signal not seen in the negative control was obtained (**Figure 4C**). The data presented so far demonstrate the functionality of our novel microsomal assay over the first two steps of sphingolipid *de novo* synthesis starting from palmitate-d_3 and serine-d_3.

Formation of Cer d18:0-d_5/16:0-d_3 From *de novo* Formed d18:0 Sph-d_5 and Assay Component Palmitate-d_3

After the formation of the sphingoid base backbone, biosynthesis of sphingolipids continues with the incorporation of a further fatty acid side chain (**Figure 1**). This central step is catalyzed by six different CerS that differ in their ability to incorporate fatty acids of varying chain lengths (Levy and Futerman, 2010). Within the here presented assay, both exogenous palmitate-d_3 and those fatty acids inevitably contained within the microsomal preparation are available. We focused on the use of palmitate-d_3

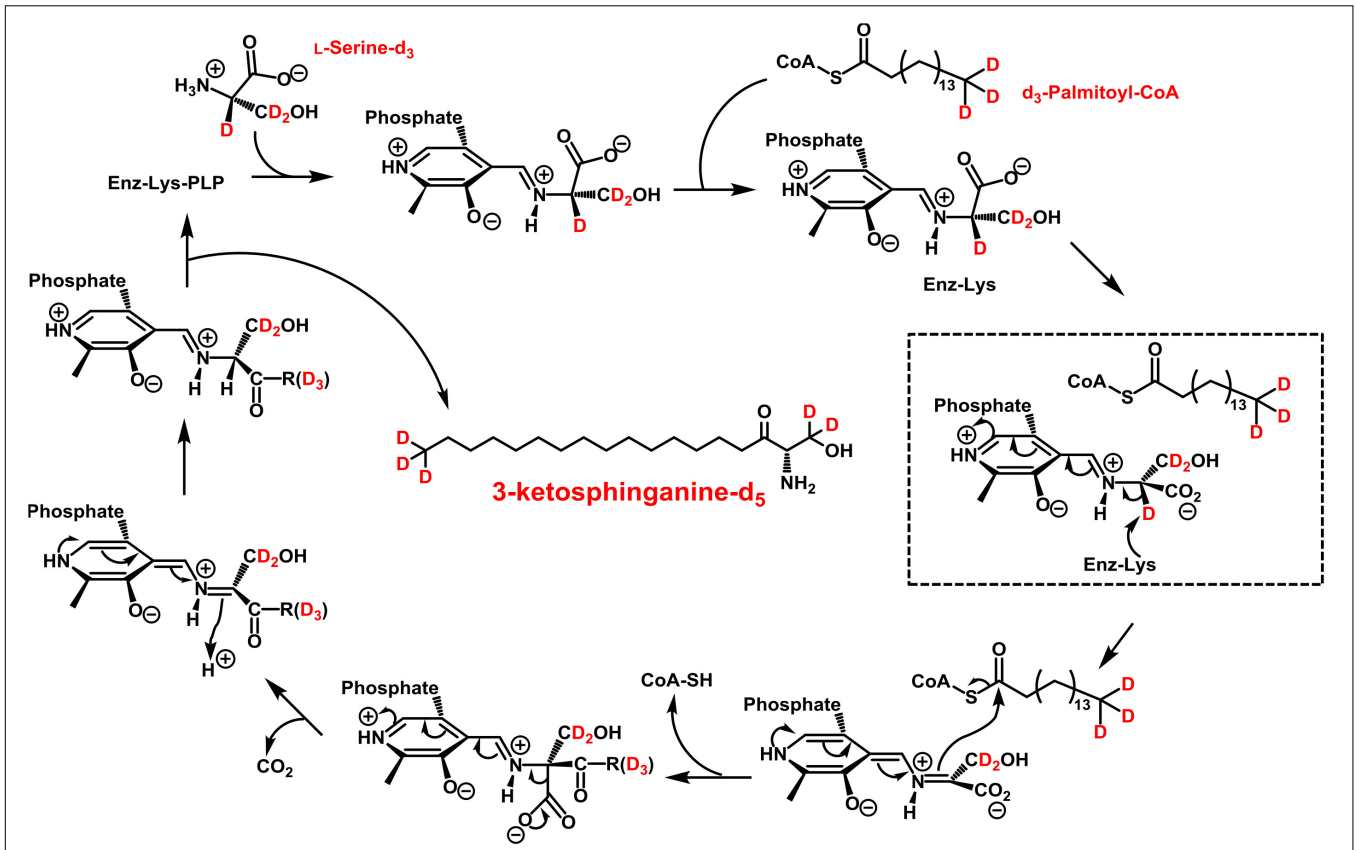

FIGURE 3 | Proposed catalytic cycle for serine palmitoyltransferase (SPT) with d_3-palmitoyl-CoA and L-serine-d_3 being the substrates. This scheme was modified from A. H. Merrill, Jr. (Merrill, 2011). An internal aldimine (Schiff base) formed between the cofactor pyridoxal 5'-phosphate (PLP) and an active site lysine residue (Enz-Lys-PLP, upper left) is replaced by the external aldimine through the incoming L-serine-d_3. Binding of d_3-palmitoyl-CoA results in transfer of serine α-deuterium to an enzymatic lysine residue (dashed box). The reaction proceeds as shown with free CoA, CO_2, and 3-ketosphinganine-d_5 (3KS-d_5) are released as products.

as a CerS substrate and, thus, on the production of Cer d18:0-d_5/16:0-d_3 as assessed by mass spectrometry. It should be noted here that the incorporation of any other fatty acid could be tracked in this same fashion. We analyzed samples of our *in vitro* assay for $[M+H]^+$ ions with *m/z* 548.5852 corresponding to eightfold deuterated Cer d18:0-d_5/16:0-d_3 (also referred to as C16 dhCer-d_8 for simplicity; chemical structure given in **Figure 5**). HPLC-QTOF MS analysis gave two adjacent signals in the retention time range between 14 and 15 min, with only one of them (14.4 min) not appearing in the negative control (**Figure 5A**). The mass spectrum of this particular signal revealed a molecular ion peak at *m/z* 548.5879 (**Figure 5B**) that corresponded to the sought product, with a mass error of not more than 4.9 ppm. To ensure that the correct biosynthetic product was detected, we performed an MRM analysis with the HPLC-TQ MS. At least two characteristic MS/MS fragmentations have been described for dihydroceramides. The first, loss of water at, presumably, the C-3 position of the sphingoid base backbone (Mi et al., 2016). The second, dehydration in conjunction with cleavage of the fatty acid bound to the amino group (Schiffmann et al., 2009). Both mass transitions – *m/z* 548.6 → 530.6 and *m/z* 548.6 → 289.3, respectively – were recorded in order to verify the presence of C16 dhCer-d_8. Unlike the negative control (omission of palmitate-d_3), clear signals were observed for both fragmentations (**Figure 5C**), co-eluting as expected and from which the loss of water gave the higher intensity. The successful detection of C16 dhCer-d_8 represents the first documented *in vitro* cell-free tracking of sphingolipid biosynthesis starting from SPT substrates to the construction of the Cer scaffold. However, one further step is required to complete the *de novo* synthesis of sphingolipids.

Detection of Cer d18:1-d_5/16:0-d_3 as the Terminal Product of the *in vitro* Sphingolipid *de novo* Synthesis Assay

The final step in the *de novo* synthesis of sphingolipids in the ER is the desaturation of dihydroceramide, leading to the formation of Cer (**Figure 1**). Here, DEGS introduces a double bond in the sphingoid base backbone between the C-4 and C-5 carbons, crucial to the biological activity of Cer (Bielawska et al., 1993; Brockman et al., 2004). As reported by us (Kachler et al., 2017) and others (Liebisch et al., 1999), Cer yield abundant $[M\text{-}H_2O+H]^+$ precursor ions during the ESI process. Hence, we conducted HPLC-QTOF MS for *m/z*

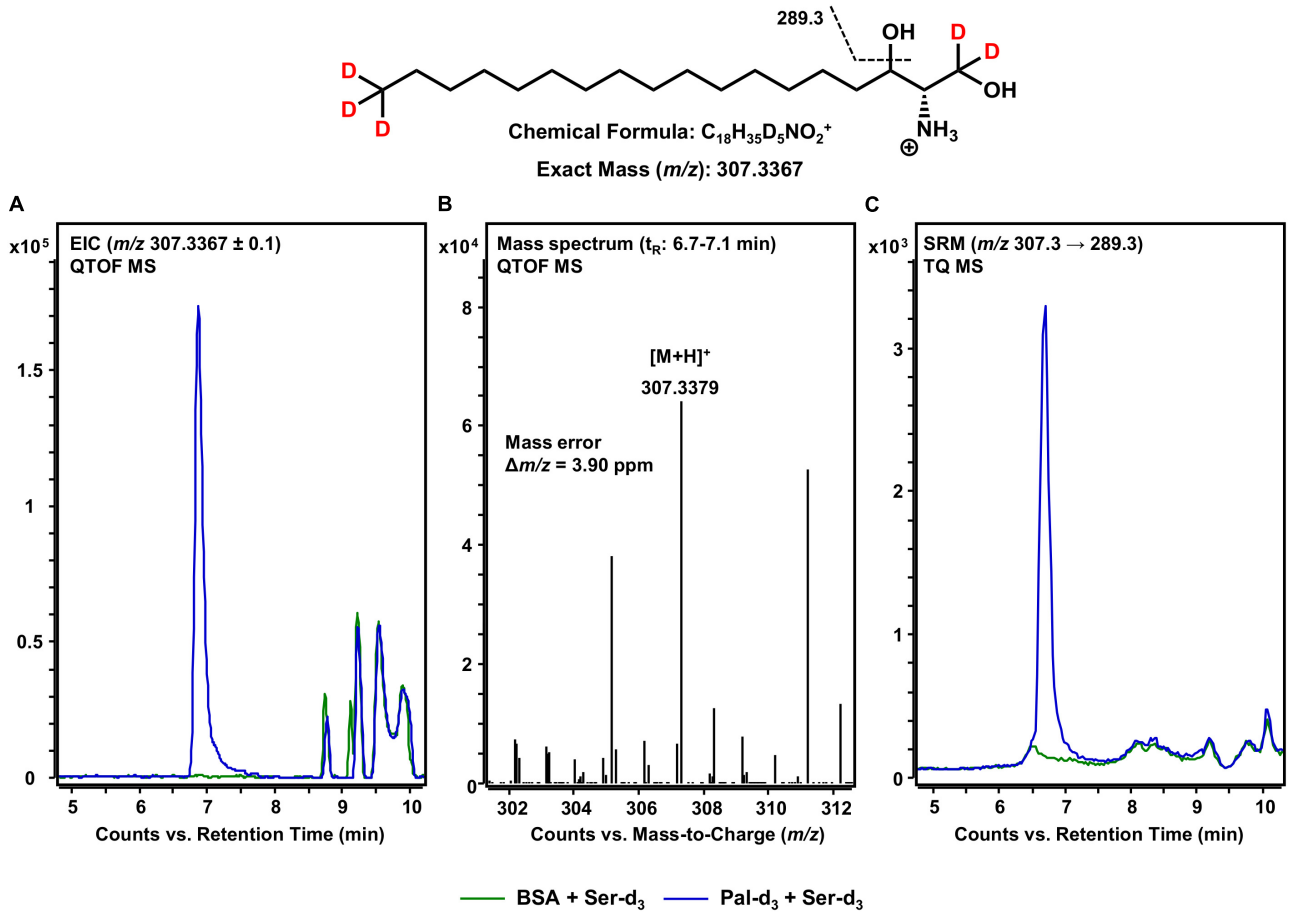

FIGURE 4 | *De novo* formation of d18:0 Sph-d_5 from 3KS-d_5 in the *in vitro* assay. **(Top)** Chemical structure, formula, and exact mass of the protonated molecular ion $[M+H]^+$ of d18:0 Sph-d_5 generated during electrospray ionization. Dashed black line represents the mass transition used for selected reaction monitoring (SRM). **(A)** Overlay of extracted ion chromatograms (EIC) of the microsomal *de novo* synthesis assay using palmitate-d_3 and serine-d_3 as substrates (blue) compared to the negative control omitting palmitate-d_3 (green). **(B)** Mass spectrum extracted from the EIC in the retention time window of eluting d18:0 Sph-d_5 with annotation of the molecular ion peak and the calculated mass error. **(A,B)** Analysis was conducted on a quadrupole time-of-flight mass spectrometer (QTOF MS). **(C)** Overlay of SRM analyses of assay (blue) compared to negative control sample (green) performed with a triple quadrupole mass spectrometer (TQ MS). t_R, retention time. **(A)** In the t_R range of 8.5–10 min, relatively abundant unidentified matrix components (*m/z*: $307.2367 \leq \times \leq 307.4367$) eluted from both the assay and negative control samples. **(C)** Concordant matrix signals were diminished, with increased specificity achieved by analyzing compound-specific fragmentation.

528.5590 ions representing Cer d18:1-d_5/16:0-d_3 (also referred to as C16 Cer-d_8 for simplicity). As we were unable to obtain a signal clearly distinguishable from that of the negative control using HPLC-QTOF MS (not shown), we applied the technique of highest detection sensitivity to the assay samples. Using the HPLC-TQ MS system we analyzed the extracted assay sample for the major MS/MS fragmentation reported for Cer; the loss of the amide-bound fatty acid plus the dehydration of carbon C-1 of the sphingoid base (Liebisch et al., 1999), expressed as *m/z* 528.6 → 269.3 for C16 Cer-d_8. Using this analytical approach, we could obtain an unambiguous signal for C16 Cer-d_8, eluting at 14.1 min from the separation column (**Figure 6**), which was absent in the negative control. As one would expect, the introduction of a double bond shortened the retention time in the reversed-phase separation column as compared to the saturated C16 dhCer-d_8 (**Figure 5**). To confirm our observation, we analyzed an unlabeled Cer d18:1/16:0 reference standard under identical instrumental conditions. This compound showed the same retention time as the C16 Cer-d_8 formed *de novo,* as well as an analogous MS/MS fragmentation (*m/z* 520.5 → 264.3) (**Figure 6**). Although the obtained signal intensity for C16 Cer-d_8 was comparatively small (the following section details a quantitative consideration in this regard), the MS-based tracking of labeled palmitate and serine through to the synthesis of Cer is, nevertheless, remarkable and has not previously been described.

Regulation of Sphingolipid *de novo* Synthesis by Cofactor Supplementation and Addition of Enzyme Inhibitors

The biosynthesis of sphingolipids in the ER requires the activity of four different enzymes should the six CerS isoforms are considered as one, which themselves require the presence of

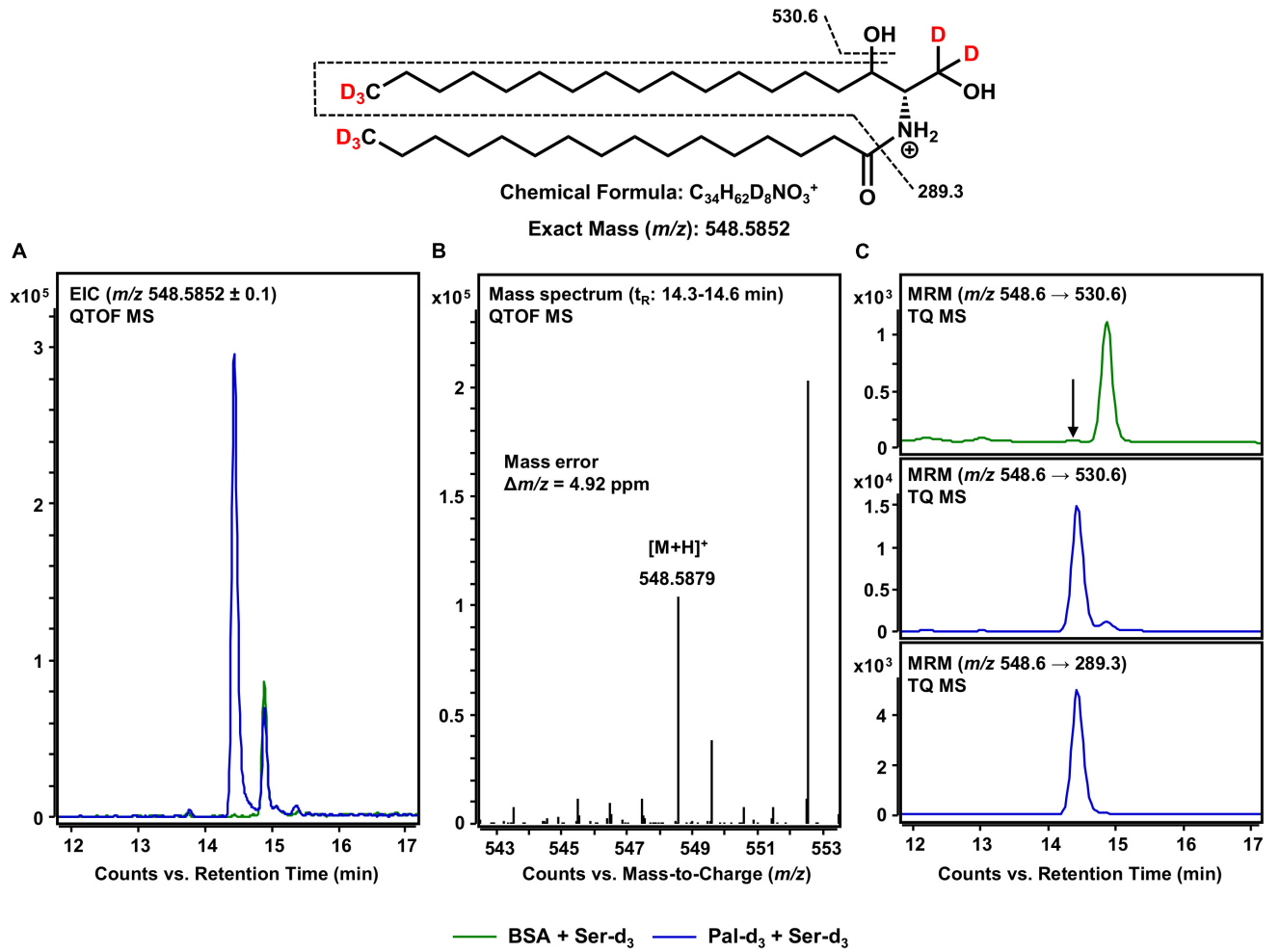

FIGURE 5 | Formation of Cer d18:0-d_5/16:0-d_3 from *de novo* formed d18:0 Sph-d_5 and assay substrate palmitate-d_3. **(Top)** Chemical structure, formula, and exact mass of the protonated molecular ion $[M+H]^+$ of Cer d18:0-d_5/16:0-d_3 generated during electrospray ionization. Dashed black lines represent the mass transitions used for multiple reaction monitoring (MRM). **(A)** Overlay of extracted ion chromatograms (EIC) from the microsomal *de novo* synthesis assay using palmitate-d_3 and serine-d_3 as substrates (blue), compared to the negative control omitting palmitate-d_3 (green). **(B)** Mass spectrum extracted from the EIC in the retention time window of eluting Cer d18:0-d_5/16:0-d_3 with annotation of the molecular ion peak and the calculated mass error. **(A,B)** Analysis was conducted on a quadrupole time-of-flight mass spectrometer (QTOF MS). **(C)** MRM analyses of assay (blue) compared to negative control sample (green) performed with a triple quadrupole mass spectrometer (TQ MS). For the negative control, only the mass transition with highest intensity (*m/z* 548.6 → 530.6) is shown. The arrow indicates the retention time (t_R) of Cer d18:0-d_5/16:0-d_3. **(A)** At t_R = 15 min, a relatively abundant unidentified compound (*m/z*: $548.4852 \leq x \leq 548.6852$) eluted that was present in both assay and negative control samples. **(C)** Analysis of two analyte-specific fragmentations allowed for unambiguous discrimination between Cer d18:0-d_5/16:0-d_3 and matrix components.

several cofactors (**Figure 1**). By modification of the latter, it is possible to influence the progression of *de novo* sphingolipid synthesis at several points, a procedure we decided to perform to acquire proof-of-concept data regarding the here presented assay's potential application. *In vitro* sphingolipid *de novo* synthesis was investigated under the conditions given in the Materials and Methods section with the following modifications: (1) omission of NADPH, (2) addition of NADPH ("standard condition"), (3) addition of NADPH and NADH, (4) as 3. with FB_1, (5) as 3. with myriocin. With the described HPLC-MS methodology, we had a valuable tool to evaluate the individual assay conditions. It was initially decided to compare different assay conditions semi-quantitatively, using d17:0 Sph and Cer d18:1/17:0 as internal standards, in order to correct for analyte losses during sample preparation and for fluctuations of the mass spectrometer's performance.

Standard conditions without NADPH are sufficient for the initial SPT-catalyzed reaction, as only CoA, ATP (for activation of palmitate-d_3) and PLP (SPT cofactor) are required. Accordingly, a clear SRM signal for 3KS-d_5 was detected. However, signals for the three downstream products of the *de novo* synthesis were missing (first row of **Figure 7**). NADPH is essential for the reduction of 3KS-d_5 to d18:0 Sph-d_5. Subsequently, *de novo* synthesis stops after the SPT reaction when NADPH is absent. By contrast, NADPH or NADPH/NADH supplementation enables the sphingolipid biosynthesis to reach its final stage, the

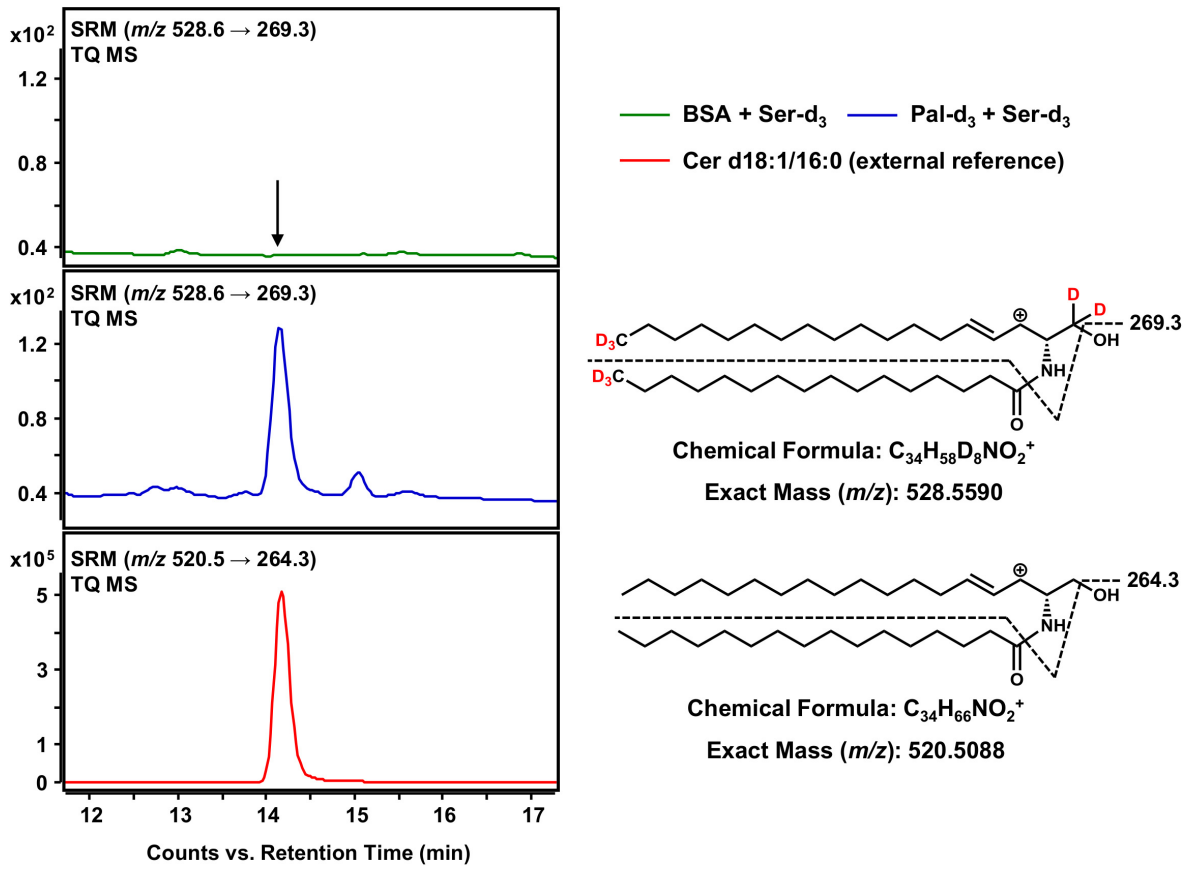

FIGURE 6 | Detection of Cer d18:1-d_5/16:0-d_3 as the terminal product of the sphingolipid *de novo* synthesis assay. **(Right)** Chemical structures, formulas and exact masses of the dehydrated, protonated molecular ions $[M\text{-}H_2O+H]^+$ of Cer d18:1-d_5/16:0-d_3 and the unlabeled analog Cer d18:1/16:0, generated during electrospray ionization. Dashed black lines represent the mass transitions used for selected reaction monitoring (SRM). **(Left)** SRM analyses of assay sample (addition of palmitate-d_3 and serine-d_3, blue), negative control sample (omission of palmitate-d_3, green) and external Cer d18:1/16:0 standard (red) were performed with a triple quadrupole mass spectrometer (TQ MS). The arrow indicates the retention time of Cer d18:1/16:0 (labeled and unlabeled).

formation of C16 Cer-d_8 (second and third row of **Figure 7**). In addition to the formation of d18:0 Sph, NADPH is also required for the desaturation of dhCer (**Figure 1**). For the latter step, NADH has also been described as a reduction agent (Michel et al., 1997), which is the rational for the integration of this component into our assay. CerS, enzymes central to sphingolipid *de novo* synthesis, can be competitively inhibited by FB_1, a mycotoxin structurally related to sphingosine (Wang et al., 1991). The presence of FB_1 drastically reduced the abundance of C16 dhCer-d_8 and subsequently C16 Cer-d_8 (**Figure 7**, fourth row). The addition of myriocin completely prevented the formation of deuterated sphingolipids (**Figure 7**, fifth row). This natural fungal product is a potent SPT inhibitor (Miyake et al., 1995) and thus suppresses the condensation of d_3-palmitoyl-CoA and L-serine-d_3.

Peak areas of detected *de novo* formed, labeled sphingolipids were related to those of internal standards (d17:0 Sph for 3KS-d_5, d18:0 Sph-d_5 and Cer d18:1/17:0 for C16 dhCer-d_8, C16 Cer-d_8) added prior to lipid extraction. Internal standard areas under the curves (AUCs) were stable throughout the assays, with standard deviations of less than 10%. The presence of both NADPH and NADH in the assay mixture increased signals of d18:0 Sph-d_5 (1.2-fold), C16 dhCer-d_8 (2.0-fold), and C16 Cer-d_8 (1.5-fold) compared to solely NADPH. Concordantly, the 3KS-d_5 signal also decreased (by 20%). Inhibition of CerS by FB_1 increased the amount of substrate d18:0 Sph-d_5 to 135% and drastically diminished the product C16 dhCer-d_8 by more than 90%. As expected, the formation of the consecutive product, C16 Cer-d_8, was reduced similarly in the presence of FB_1. The 3KS-d_5 signal was highest in samples without reducing equivalents, where *de novo* synthesis was stopped after SPT catalysis. In all other samples (except in presence of myriocin) intensity of d18:0 Sph-d_5 exceeded those of 3KS-d_5 (1.7–3.2-fold). Unexpectedly, C16 dhCer-d_8 was detected in significantly greater quantities than C16 Cer-d_8. On a semi-quantitative basis, this difference ranged between 80 and 149-fold. In assay samples containing myriocin, signals of the internal standards were detected, while those of *de novo* formed deuterated sphingolipids were not.

Intra-assay variability was assessed in a separate experiment using a new batch of rat liver microsomes. "Standard conditions" plus NADH were applied to five technical replicates. In addition

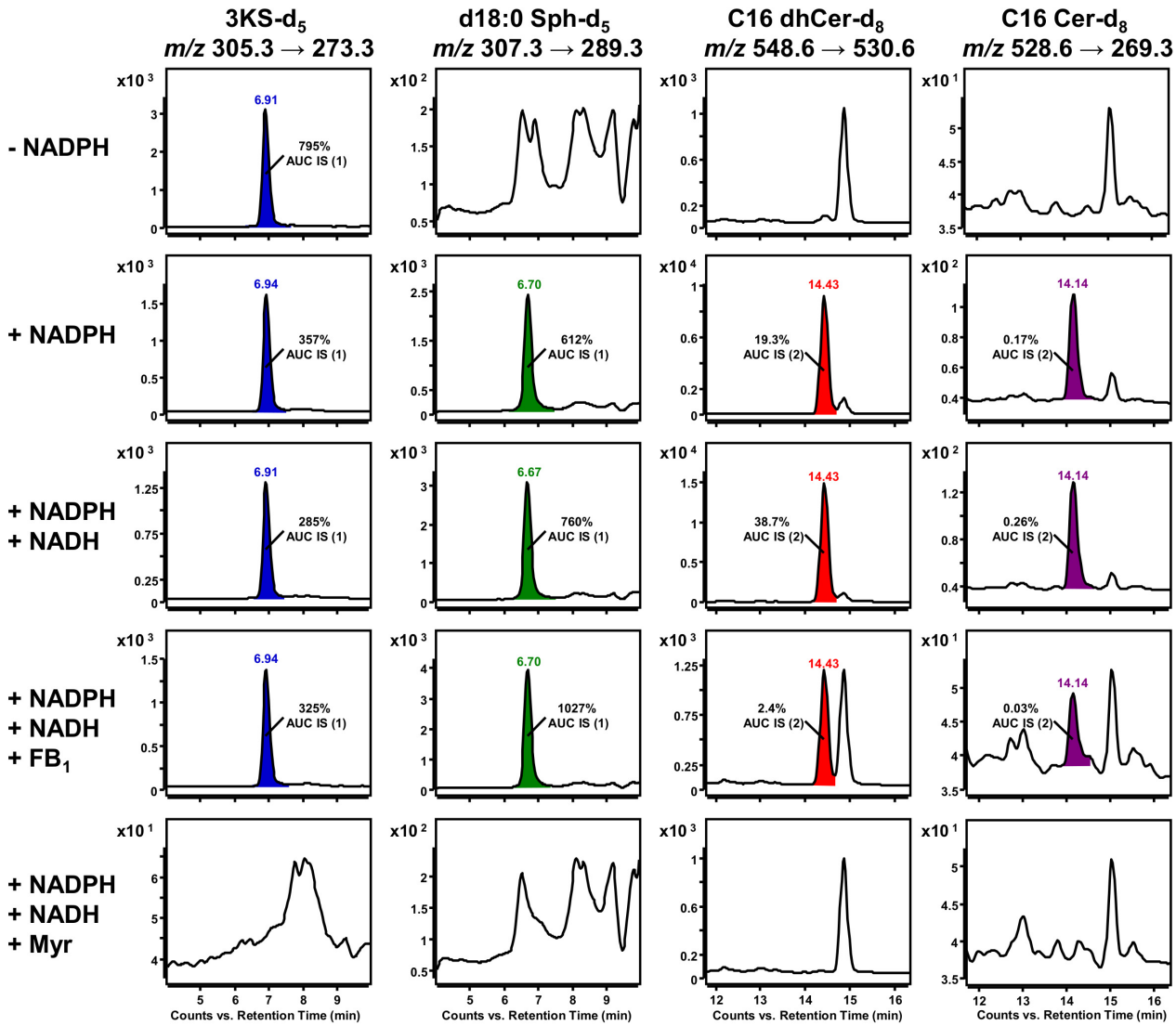

FIGURE 7 | Impact of cofactor supplementation and presence of enzyme inhibitors on *de novo* formation of deuterated sphingolipid metabolites in the microsomal assay. Selected reaction monitoring (SRM) using a triple quadrupole mass spectrometer (TQ MS) was conducted to investigate the formation of 3KS-d_5 (first column), d18:0 Sph-d_5 (second column), Cer d18:0-d_5/16:0-d_3 (C16 dhCer-d_8, third column) and Cer d18:1-d_5/16:0-d_3 (C16 Cer-d_8, fourth column) under different assay conditions. The *in vitro* assay reaction mixture was prepared as described in section Materials and Methods with the following modifications: omission of NADPH (first row), "standard conditions" (with NADPH, second row), supplemented with NADPH and NADH (third to fifth row), addition of ceramide synthase (CerS) inhibitor fumonisin B_1 (FB_1, fourth row), and addition of serine palmitoyltransferase (SPT) inhibitor myriocin (Myr, fifth row). Signals that were not present in the corresponding negative controls were integrated and colored. d17:0 Sph (0.2 pmol injected on column) and Cer d18:1/17:0 (2 pmol injected on column), referred to as internal standards (IS) 1 and 2, respectively, were used to normalize areas under the curves (AUC). Corresponding relations are indicated as insets. Y axes are scaled differently, while x axes are maintained for each sphingolipid metabolite.

to NADH, FB_1 was added to another five replicates. *De novo* formed deuterated sphingolipids were quantified by external calibration using unlabeled analogs as reference compounds (concentrated from 0 to 1000 nM), as well as d17:0 Sph and Cer d18:1/17:0 as internal standards. As can be seen from **Figure 8**, the intra-assay variability (expressed as average % CV) was low, accounting for 11% and 15% for samples with or without FB_1 addition, respectively. In the final sample volume (100 μL) the mean concentrations of 3KS-d_5, d18:0 Sph-d_5, C16 dhCer-d_8, and C16 Cer-d_8 were, respectively, 39.3, 201.3, 21.6, and 0.94 nM ("standard conditions" plus NADH). Addition of FB_1 did not affect the formation of 3KS-d_5 (30.4 nM) but did significantly increase d18:0 Sph-d_5 (447.7 nM). Consistently, C16 dhCer-d_8 and C16 Cer-d_8 were reduced to 28% (6.1 nM) and 18% (0.17 nM). Taken together, using aliquots of identical batches of microsomes and reagents, the presented assay is reproducible. Larger variations are expected when different microsomal preparations are used due to deviating enzyme activities. However, this is precisely the intended field of application for the here established assay: the

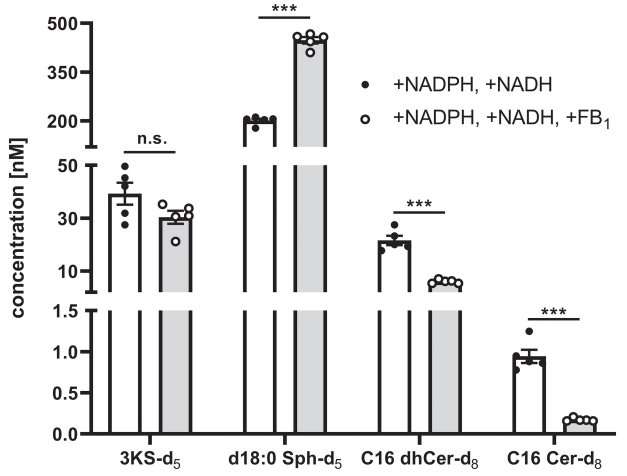

FIGURE 8 | Intra-assay variability of the sphingolipid *de novo* synthesis assay. A total of 10 technical assay replicates were prepared, five of which were supplemented with NADPH and NADH (white bars and solid circles), while the remaining five replicates were additionally with fumonisin B_1 (FB_1, gray bars and open circles). Assays were performed as described in the Materials and Methods section using identical batches of microsomes and reagents. Concentrations of *de novo* formed, deuterated sphingolipid metabolites in the final sample volume (100 μL) were quantified by HPLC-MS/MS using external calibration (concentration range: 0–1000 nM). To this end, 3KS-d_5 and d18:0 Sph-d_5 were quantified *via* d18:0 Sph, whereas calibration curves of Cer d18:0/16:0 and Cer d18:1/16:0 were used to quantify Cer d18:0-d_5/16:0-d_3 (C16 dhCer-d_8) and Cer d18:1-d_5/16:0-d_3 (C16 Cer-d_8), respectively. Cer d18:1/17:0 and d17:0 Sph were used as internal standards. Bars represent mean concentrations (detailed in the main text) ± SEM (***$p < 0.001$; n.s., non-significant; $n = 5$). Additionally, individual values of the replicates are depicted as circles.

study of altered sphingolipid *de novo* synthesis in microsomal fractions of defined origin.

DISCUSSION

Cer are sphingolipid species central to sphingolipid metabolism and play key roles in the pathogenesis of a variety of human diseases. Modification to Cer metabolism has been linked, among others, to the onset of various cancers, type 2 diabetes, Alzheimer's disease, and major depression (Kurz et al., 2019). An important metabolic pathway through which Cer are formed in the cell is *de novo* synthesis within the ER. It is, therefore, consistent that therapies targeting the modulation of enzymes involved in *de novo* synthesis have been developed for diseases associated with Cer dysregulation. For instance, it has been shown that myriocin, a potent SPT inhibitor, suppresses murine melanoma growth (Lee et al., 2012) and mediates the regression of atherosclerotic lesions in hyperlipidemic apolipoprotein E knockout mice (Park et al., 2008). Efforts have also been made to develop specific CerS inhibitors as novel therapeutic treatment options (Schiffmann et al., 2012), one of which was recently used to elucidate the role of CerS1 and its product Cer d18:1/18:0 (C18 Cer) in the storage of dietary lipids (Turner et al., 2018). Accordingly, methods have been developed to determine the activities of individual enzymes involved in the biosynthesis of sphingolipids, and various activity assays for SPT (Rütti et al., 2009), KDSR (Fornarotto et al., 2006), CerS (Couttas et al., 2015), and DEGS (Munoz-Olaya et al., 2008) are now available. Up to this point in time, however, there existed no cell-free assay capable of concurrently assessing the activities of all four enzyme families involved in sphingolipid *de novo* synthesis. A prerequisite for such an assay would be the specific tracking of SPT substrates as they are incorporated into the Cer framework. One approach for this would be the use of exogenous enzyme substrates alien to eukaryotic cells (e.g., carrying odd-numbered carbon chains or stable-isotope labels) and highly specific and sensitive detection by means of mass spectrometry.

Ren and co-workers developed an *in vitro* SPT activity test system utilizing yeast microsomes treated with palmitoyl-CoA and deuterated L-serine as SPT substrates. By means of HPLC-TQ MS, they were able to follow the incorporation of the labeled amino acid into 3KS and d18:0 Sph, which they used to determine SPT kinetics in yeast (Ren et al., 2018). More recently, Harrison et al. used differentially labeled L-serine isotopologs and either palmitoyl-CoA or pentadecanoyl-CoA as SPT substrates to study the impact of stable-isotope label number and position in L-serine on the kinetics of recombinant human and bacterial SPT. For this, they applied HPLC equipped with a fluorescence detector to quantify C17 LCBs, and direct infusion high-resolution MS for detection of 3KS products (Harrison et al., 2019). Both studies used state-of-the-art techniques but limited their scopes to the first two steps of sphingolipid *de novo* synthesis. Another recently published study presented a more complex approach that allows comprehensive monitoring of sphingolipid metabolism, not restricted to the ER. The authors tracked the flux of d17:0 Sph through the sphingolipid metabolism of MCF-7 human breast adenocarcinoma cells in an one-step *in situ* assay using HPLC-TQ MS. Data on complex sphingolipids carrying a C17 sphingoid base backbone, such as dhCer, Cer, sphingomyelin, and hexosylceramide, were presented (Snider et al., 2018). However, the choice of d17:0 Sph as a starting material inevitably excludes the first two steps of *de novo* synthesis, catalyzed by SPT and KDSR. Strategies for monitoring sphingolipid metabolism in mammalian cells have recently been reviewed (Snider et al., 2019). To the best of our knowledge, the here presented method is the first reported cell-free assay capable of assessing *de novo* sphingolipid synthesis in its entirety. This results in two major innovations applicable to this field of research. First, the complete sphingolipid *de novo* synthesis can now be monitored in tissues or cells of choice, *ex vivo*. Second, our assay is the first that allows investigation of the complete ER-based metabolism of atypical or chemically tailored sphingoid bases, molecules that are of growing interest to the field.

We have established a protocol that uses rat liver microsomes as a source of enzymes, and palmitate-d_3 and serine-d_3 as initial labeled substrates for sphingolipid synthesis. Thus, unlike other published SPT activity assays, we use a non-activated fatty acid as our substrate precursor. This strategy requires *in situ* fatty acid activation, for which we added CoA and ATP to the microsomal fraction containing acyl-CoA synthetases (Normann et al., 1981). This procedure offers several advantages.

First, we are able to test atypical SPT substrates – e.g., other fatty acids or derivatives – and so are not dependent on commercially available acyl-CoAs. Decades ago, it was described that the (rat liver) SPT affinity to fatty acyl-CoAs is rather broad and not restricted to the endogenous substrate palmitoyl-CoA (Williams et al., 1984). Likewise, it would be possible to change the amino acid precursor. For instance, if L-serine-d_3 were replaced by L-alanine or L-glycine (preferably labeled) while palmitate-d_3 is maintained, the formation of deuterated 1-deoxysphingolipids or 1-deoxymethylsphingolipids can be monitored, respectively (Duan and Merrill, 2015). Another advantage of this procedure is that all molecular requirements to monitor the *N*-acylation of d18:0 Sph catalyzed by CerS are met simultaneously. In this third step of sphingolipid biosynthesis, acyl-CoAs of different chain lengths serve as substrates for six different CerS isoforms (**Figure 1**). The addition of ATP and CoA to the assay also would permit the observation of different fatty acids as they were incorporated into the developing Cer backbone. In fact, the *de novo* formation of C16 dhCer-d_8 from the assay substrates palmitate-d_3 and serine-d_3 (**Figure 5**) confirmed the activity of CerS5 and CerS6 in our assay, since these isoforms prefer palmitate (Levy and Futerman, 2010) and, thus, palmitate-d_3 as a substrate. It would be straightforward to add the preferred fatty acids of other CerS isoforms, with or without labels, to increase the complexity of the assay and to assure even more detailed insights into sphingolipid *de novo* synthesis. In the present study, however, we focused on labeled physiological SPT substrates. In the future, follow-up studies with atypical SPT substrates, a broader spectrum of CerS substrates (all preferably stable-isotopically labeled), and combinations of these are envisaged. From an analytical point of view, the labeling of both the fatty acid and amino acid precursor molecules with stable-isotopes is advantageous. Most published MS-based SPT assays used labeled serine only (Ren et al., 2018; Harrison et al., 2019). Since serine is a small molecule (chemical formula: $C_3H_7NO_3$), the number of introducible labels is limited. Taking into account the losses of α-deuterium and ^{13}C-isotope at the carboxylic acid group (depending on the labeled serine reference substance used) during SPT catalysis (**Figure 3**), the labeling may be too low to avoid interferences with unlabeled assay components. More precisely, the use of labeled serine in combination with unlabeled palmitoyl-CoA, as done in the Ren et al. (2018) study using L-serine (2,3,3-d_3), leads to the formation of 3KS-d_2 as the initial SPT product. Following the *de novo* synthesis under these conditions, Cer d18:1-d_2/16:0 (C16 Cer-d_2) would be formed as the consistent product. Using a TQ MS for detection (as done in the above-mentioned study) will inevitably cause interferences with unlabeled Cer d18:1/16:0 (C16 Cer) present in the microsome preparation, due to the low mass accuracy of the quadrupole mass analyzer. The natural isotope pattern of the molecular ion $[M\text{-}H_2O+H]^+$ of C16 Cer is as follows (relative abundances in parentheses): (*m/z*) 520.5088 (100%), 521.5122 (36.8%), and 522.5155 (3.9%). The monoisotopic (exact) mass of C16 Cer-d_2 is *m/z* 522.5214. With a TQ MS it is not possible to resolve the mass difference between the two nominally equal masses (*m/z* 522.5155 for C16 Cer and *m/z* 522.5214 for C16 Cer-d_2). Since C16 Cer is present in microsomes in significant amounts, as confirmed by our QTOF raw data (not shown), misidentification of labeled, *de novo* formed Cer is very likely. For these reasons, we performed our assay with both labeled fatty acid and labeled amino acid to increase the deuteration level of the metabolites (products identified in the current study were five to eight-times labeled; see **Figures 2**, **4–6**). Furthermore, besides TQ MS as a very sensitive detection system, we also used QTOF MS, a technique with high mass accuracy. Thus, we can unequivocally distinguish between *de novo* formed products and intrinsic sphingolipids present in the microsome preparation. Recently, Harrison and co-workers found that the presence of a serine α-deuterium significantly decreased the reaction rate of recombinant bacterial SPT, a point also applicable to L-serine (2,3,3-d_3) used in the present study. However, recombinant human SPT was unaffected by the deuterium label at Cα position (Harrison et al., 2019). We used rat liver-derived SPT, which has a greater homology to human SPT than that of bacterial SPT. Nonetheless, testing of differently labeled serine substrates seems worthwhile and is planned for the future.

With our established sphingolipid *de novo* synthesis assay, we have identified four distinct and sequential metabolites, namely 3KS-d_5, d18:0 Sph-d_5, C16 dhCer-d_8, and C16 Cer-d_8. The latter two have, as yet, not been demonstrated using comparable test strategies. The use of enzyme inhibitors and varied cofactor quantities validated our approach. The following observations (illustrated in **Figure 7**) are in agreement with the well-studied progress of the sphingolipid biosynthesis in the ER (Gault et al., 2010): (1) *de novo* synthesis was abolished in the presence of the SPT inhibitor myriocin, (2) omission of reducing agents (NADPH/NADH) caused *de novo* synthesis to halt after SPT reaction (in conjunction with highest 3KS-d_5 signal intensity), and (3) addition of the CerS inhibitor FB_1 drastically reduced the *N*-acylation of d18:0 Sph-d_5 (in agreement with its highest signal response) and thus the abundance of labeled dhCer and Cer. Two further observations need to be addressed. Firstly, assay supplementation with NADPH and NADH increased detected amounts of d18:0 Sph-d_5, C16 dhCer-d_8, and C16 Cer-d_8 compared to addition of NADPH alone (in line with a 3KS-d_5 signal reduction). This effect was particularly pronounced for dhCer and Cer, which were almost doubled. Microsomal preparations used for metabolism studies are usually supplemented with reducing agents. Under "standard conditions," we added a threefold excess of reducing equivalents (1 mM NADPH) compared to the conversion limiting substrate palmitate-d_3 (0.3 mM). This excess was doubled when a surplus of 1 mM NADH was added. It is therefore unlikely that under "standard conditions," the amount of reducing agent was insufficient for quantitative conversions. At least for the DEGS-catalyzed step of sphingolipid biosynthesis in rat liver microsomes, it has been reported that NADPH and NADH function equally well as cofactors (Michel et al., 1997). Since the addition of NADH appears to have a positive effect on the first reductive step, the formation of d18:0 Sph-d_5, our results give rise to more detailed investigations. The second aspect of our data to be discussed, and a possible limitation of this assay, is the relatively small amount of C16 Cer-d_8 detected. As outlined before, we are the first to track the incorporation of palmitate and

serine into the Cer core-structure of complex sphingolipids in a structure-specific manner within a cell-free system. However, the obtained ratio between detected Cer and its direct precursor dhCer is in contrast to published lipidomics data (Barbarroja et al., 2015; Mielke et al., 2015; Hernández-Tiedra et al., 2016). For instance, in healthy humans, molar Cer/dhCer ratios in both serum and liver account for approximately 10:1 (Apostolopoulou et al., 2018). Although lipidomics data are subject to a certain degree of variability, depending on species, tissue, body fluid, cell line etc. studied, the Cer/dhCer ratio found in our assay was 0.044 (**Figure 8**, white bars) and is therefore substantially lower than previously reported. Reasons for this could be extraordinarily high CerS activity and/or low DEGS activity. Since *in vitro* systems are rarely more metabolically competent than living organisms, the former seems unlikely. Loss of DEGS activity in the microsomes is probably the most plausible explanation, although the reasons for this remain speculative. There may have been some mechanical phenomena in the production of microsomes that interfere with DEGS activity, but not those of SPT, KDSR and CerS. However, all four enzyme families are localized adjacent at the ER membrane with their catalytic sites facing cytosolically (Yamaji and Hanada, 2015), making the impairment of DEGS alone implausible. An inadequate provision of cofactors can also be excluded for reasons described above. Various rat liver microsome-based DEGS activity assays have been published (Michel et al., 1997; Munoz-Olaya et al., 2008; Rahmaniyan et al., 2011). Unlike these, our assay applies the substrates of an enzyme located three steps upstream in the *de novo* synthesis pathway, rather than those directly relevant to DEGS activity. Thus, inhibitory effects of upstream sphingolipid metabolites or assay components cannot be ruled out. Possibly, the lack of Cer trafficking into other cell compartments (e.g., Golgi apparatus) contributes to the lower amounts of labeled Cer d18:1/16:0 formed in the presented microsomal approach. To account for the possibility that ER-resident alkaline ceramidases (ACERs) (Coant et al., 2017) hydrolyzed the *de novo* formed Cer d18:1-d_5/16:0-d_3, we analyzed the lipid extracts for d18:1 Sph-d_5 (*m/z* 305.3 → 287.3). In addition, we searched for Cer t18:0-d_5/16:0-d_3, as the DEGS2 isoform, typically found at low levels, has been shown to catalyze C4-hydroxylation (without Δ4-desaturation) of the d18:0 backbone (Mizutani et al., 2004; Omae et al., 2004). According to Sullards et al. (2011), ceramide species containing a 4-hydroxysphinganine (t18:0) base also produce the *m/z* 264.3 fragment specific for ceramides. Hence, we analyzed our samples for the adjusted mass transition *m/z* 564.6 → 269.3 (deuterium labels on t18:0 backbone and fatty acid moeity). However, we were unable to detect either d18:1 Sph-d_5 or Cer t18:0-d_5/16:0-d_3 in our assay. Further studies should be conducted to shed light on this issue.

CONCLUSION

In conclusion, we have developed a microsomal *in vitro* assay to study the entire *de novo* synthesis of stable-isotopically labeled sphingolipids by HPLC-MS(/MS). Obtained results are in agreement with the proposed cascade of sphingolipid biosynthesis taking place in the ER. The presented methodology with low intra-assay variability may serve as a useful tool for monitoring alterations in sphingolipid *de novo* synthesis in the microsomal preparations of cells or tissues. Doing so, it is possible to track natural SPT substrates or downstream metabolites, as well as sphingolipid analogs that are of increasing importance to the field. For instance, the visualization of biomolecular processes, physiological or pathophysiological in nature, in which sphingolipids are involved, is an especially important area of discussion in current literature. In this regard, a useful tool is "click chemistry," in which functionalized, tailor-made sphingolipid derivatives can be coupled with fluorophores (or other labels) and thus made visible (Fink and Seibel, 2018). The here presented assay in combination with mass-specific detection will be of substantial importance for such studies, as it is now possible to investigate whether customized sphingolipids are metabolized in the ER and, if so, at which specific step. This will be crucial in estimating their cellular fates and physiological impacts. Likewise, our method may be applied to a variety of different natural and hypothesized LCB analogs that have been synthesized in order to study the metabolism of disease-related 1-deoxysphingolipids (Saied et al., 2018). Furthermore, the efficacy of newly designed inhibitors of enzymes involved in *de novo* sphingolipid synthesis can be tested with our protocol.

DATA AVAILABILITY STATEMENT

All datasets generated for this study are included in the manuscript/supplementary files.

ETHICS STATEMENT

The animal study was reviewed and approved by the Landesamt für Arbeitsschutz, Verbraucherschutz und Gesundheit Brandenburg.

AUTHOR CONTRIBUTIONS

DW, EG, BK, and FS conceptualized the study and interpreted the data. DW performed the *in vitro* experiments. FS was responsible for LC-MS analytics and wrote the manuscript with the help of DW and BK. All authors have read and approved the manuscript.

FUNDING

This study was funded by the German Research Foundation (DFG), research group FOR 2123 (grant JA 2651/2-2 to BK and Gu 335/34-1 to EG), and research training group GRK 2098 to BK and EG.

ACKNOWLEDGMENTS

We thank Susanne Scheu and Daniel Herrmann for the excellent technical assistance and Dr. Guy Yealland for language editing.

REFERENCES

Apostolopoulou, M., Gordillo, R., Koliaki, C., Gancheva, S., Jelenik, T., De Filippo, E., et al. (2018). Specific hepatic sphingolipids relate to insulin resistance, oxidative stress, and inflammation in nonalcoholic steatohepatitis. *Diabetes Care* 41, 1235–1243. doi: 10.2337/dc17-1318

Barbarroja, N., Rodriguez-Cuenca, S., Nygren, H., Camargo, A., Pirraco, A., Relat, J., et al. (2015). Increased dihydroceramide/ceramide ratio mediated by defective expression of degs1 impairs adipocyte differentiation and function. *Diabetes* 64, 1180–1192. doi: 10.2337/db14-0359

Bielawska, A., Crane, H. M., Liotta, D., Obeid, L. M., and Hannun, Y. A. (1993). Selectivity of ceramide-mediated biology: lack of activity of erythro-dihydroceramide. *J. Biol. Chem.* 268, 26226–26232.

Bode, H., Bourquin, F., Suriyanarayanan, S., Wei, Y., Alecu, I., Othman, A., et al. (2016). HSAN1 mutations in serine palmitoyltransferase reveal a close structure–function–phenotype relationship. *Hum. Mol. Genet.* 25, 853–865. doi: 10.1093/hmg/ddv611

Borodzicz, S., Czarzasta, K., Kuch, M., and Cudnoch-Jedrzejewska, A. (2015). Sphingolipids in cardiovascular diseases and metabolic disorders. *Lipids Health Dis.* 14:55. doi: 10.1186/s12944-015-0053-y

Boyden, L. M., Vincent, N. G., Zhou, J., Hu, R., Craiglow, B. G., Bayliss, S. J., et al. (2017). Mutations in KDSR cause recessive progressive symmetric erythrokeratoderma. *Am. J. Hum. Gene.* 100, 978–984. doi: 10.1016/j.ajhg.2017.05.003

Breslow, D. K., and Weissman, J. S. (2010). Membranes in balance: mechanisms of sphingolipid homeostasis. *Mol. Cell.* 40, 267–279. doi: 10.1016/j.molcel.2010.10.005

Brockman, H. L., Momsen, M. M., Brown, R. E., He, L., Chun, J., Byun, H.-S., et al. (2004). The 4,5-double bond of ceramide regulates its dipole potential, elastic properties, and packing behavior *Biophys. J.* 87, 1722–1731. doi: 10.1529/biophysj.104.044529

Cho, H. E., Maurer, B. J., Reynolds, C. P., and Kang, M. H. (2019). Hydrophilic interaction liquid chromatography–tandem mass spectrometric approach for simultaneous determination of safingol and D-erythro-sphinganine in human plasma. *J. Chromatogr. B* 1112, 16–23. doi: 10.1016/j.jchromb.2019.02.023

Coant, N., Sakamoto, W., Mao, C., and Hannun, Y. A. (2017). Ceramidases, roles in sphingolipid metabolism and in health and disease. *Adv. Biol. Regul.* 63, 122–131. doi: 10.1016/j.jbior.2016.10.002

Couttas, T. A., Lim, X. Y., and Don, A. S. (2015). A three-step assay for ceramide synthase activity using a fluorescent substrate and HPLC. *Lipids* 50, 101–109. doi: 10.1007/s11745-014-3969-3965

Cuvillier, O., Pirianov, G., Kleuser, B., Vanek, P. G., Coso, O. A., Gutkind, J. S., et al. (1996). Suppression of ceramide-mediated programmed cell death by sphingosine-1-phosphate. *Nature* 381, 800–803. doi: 10.1038/381800a0

Duan, J., and Merrill, A. H. (2015). 1-deoxysphingolipids encountered exogenously and made de novo: dangerous mysteries inside an enigma. *J. Biol. Chem.* 290, 15380–15389. doi: 10.1074/jbc.R115.658823

Eckl, K.-M., Tidhar, R., Thiele, H., Oji, V., Hausser, I., Brodesser, S., et al. (2013). Impaired epidermal ceramide synthesis causes autosomal recessive congenital ichthyosis and reveals the importance of ceramide acyl chain length. *J. Invest. Dermatol.* 133, 2202–2211. doi: 10.1038/jid.2013.153

Fink, J., and Seibel, J. (2018). Click reactions with functional sphingolipids. *Biol. Chem.* 399:1157. doi: 10.1515/hsz-2018-2169

Fornarotto, M., Xiao, L., Hou, Y., Koch, K. A., Chang, E., O'Malley, R. M., et al. (2006). Sphingolipid biosynthesis in pathogenic fungi: identification and characterization of the 3-ketosphinganine reductase activity of *Candida albicans* and *Aspergillus fumigatus*. *Biochim. Biophys. Acta* 1761, 52–63. doi: 10.1016/j.bbalip.2005.11.013

Gault, C. R., Obeid, L. M., and Hannun, Y. A. (2010). An overview of sphingolipid metabolism: from synthesis to breakdown. *Adv. Exp. Med. Biol.* 688, 1–23. doi: 10.1007/978-1-4419-6741-1_1

Grassmé, H., Jendrossek, V., Riehle, A., von Kürthy, G., Berger, J., Schwarz, H., et al. (2003). Host defense against *Pseudomonas aeruginosa* requires ceramide-rich membrane rafts. *Nat. Med.* 9, 322–330. doi: 10.1038/nm823

Grassmé, H., Riehle, A., Wilker, B., and Gulbins, E. (2005). Rhinoviruses infect human epithelial cells via ceramide-enriched membrane platforms. *J. Biol. Chem.* 280, 26256–26262. doi: 10.1074/jbc.M500835200

Gulbins, E., Bissonnette, R., Mahboubi, A., Martin, S., Nishloka, W., Brunner, T., et al. (1995). FAS-induced apoptosis is mediated via a ceramide-initiated RAS signaling pathway. *Immunity* 2, 341–351. doi: 10.1016/1074-7613(95)90142-90146

Hannun, Y. A., and Obeid, L. M. (2008). Principles of bioactive lipid signalling: lessons from sphingolipids. *Nat. Rev. Mol. Cell Biol.* 9, 139–150. doi: 10.1038/nrm2329

Harrison, P. J., Gable, K., Somashekarappa, N., Kelly, V., Clarke, D. J., Dunn, T. M., et al. (2019). Use of isotopically labelled substrates reveals kinetic differences between human and bacterial serine palmitoyltransferase. *J. Lipid Res.* 60, 953–962. doi: 10.1194/jlr.M089367

Hernández-Tiedra, S., Fabriàs, G., Dávila, D., Salanueva, ÍJ., Casas, J., Montes, L. R., et al. (2016). Dihydroceramide accumulation mediates cytotoxic autophagy of cancer cells via autolysosome destabilization. *Autophagy* 12, 2213–2229. doi: 10.1080/15548627.2016.1213927

Kachler, K., Bailer, M., Heim, L., Schumacher, F., Reichel, M., Holzinger, C. D., et al. (2017). Enhanced acid sphingomyelinase activity drives immune evasion and tumor growth in non–small cell lung carcinoma. *Cancer Res.* 77, 5963–5976. doi: 10.1158/0008-5472.can-16-3313

Kirin, M., Chandra, A., Charteris, D. G., Hayward, C., Campbell, S., Celap, I., et al. (2013). Genome-wide association study identifies genetic risk underlying primary rhegmatogenous retinal detachment. *Hum. Mol. Genet.* 22, 3174–3185. doi: 10.1093/hmg/ddt169

Kurz, J., Parnham, M. J., Geisslinger, G., and Schiffmann, S. (2019). Ceramides as novel disease biomarkers. *Trends Mol. Med.* 25, 20–32. doi: 10.1016/j.molmed.2018.10.009

Lee, Y.-S., Choi, K.-M., Lee, S., Sin, D.-M., Yoo, K.-S., Lim, Y., et al. (2012). Myriocin, a serine palmitoyltransferase inhibitor, suppresses tumor growth in a murine melanoma model by inhibiting de novo sphingolipid synthesis. *Cancer Biol. Ther.* 13, 92–100. doi: 10.4161/cbt.13.2.18870

Levy, M., and Futerman, A. H. (2010). Mammalian ceramide synthases. *IUBMB Life* 62, 347–356. doi: 10.1002/iub.319

Liebisch, G., Drobnik, W., Reil, M., Trümbach, B., Arnecke, R., Olgemöller, B., et al. (1999). Quantitative measurement of different ceramide species from crude cellular extracts by electrospray ionization tandem mass spectrometry (ESI-MS/MS). *J. Lipid Res.* 40, 1539–1546.

Meikle, P. J., and Summers, S. A. (2016). Sphingolipids and phospholipids in insulin resistance and related metabolic disorders. *Nat. Rev. Endocrinol.* 13, 79–91. doi: 10.1038/nrendo.2016.169

Merrill, A. H. (2011). Sphingolipid and glycosphingolipid metabolic pathways in the era of sphingolipidomics. *Chem. Rev.* 111, 6387–6422. doi: 10.1021/cr2002917

Merrill, A. H., Sullards, M. C., Allegood, J. C., Kelly, S., and Wang, E. (2005). Sphingolipidomics: high-throughput, structure-specific, and quantitative analysis of sphingolipids by liquid chromatography tandem mass spectrometry. *Methods* 36, 207–224. doi: 10.1016/j.ymeth.2005.01.009

Mi, S., Zhao, Y.-Y., Dielschneider, R. F., Gibson, S. B., and Curtis, J. M. (2016). An LC/MS/MS method for the simultaneous determination of individual sphingolipid species in B cells. *J. Chromatogr. B* 1031, 50–60. doi: 10.1016/j.jchromb.2016.07.028

Michel, C., van Echten-Deckert, G., Rother, J., Sandhoff, K., Wang, E., and Merrill, A. H. (1997). Characterization of ceramide synthesis: a dihydroceramide desaturase introduces the 4,5-trans-double bond of sphingosine at the level of dihydroceramide. *J. Biol. Chem.* 272, 22432–22437. doi: 10.1074/jbc.272.36.22432

Mielke, M. M., Bandaru, V. V. R., Han, D., An, Y., Resnick, S. M., Ferrucci, L., et al. (2015). Demographic and clinical variables affecting mid- to late-life trajectories of plasma ceramide and dihydroceramide species. *Aging Cell* 14, 1014–1023. doi: 10.1111/acel.12369

Miyake, Y., Kozutsumi, Y., Nakamura, S., Fujita, T., and Kawasaki, T. (1995). Serine palmitoyltransferase is the primary target of a sphingosine-like immunosuppressant, ISP-1/myriocin. *Biochem. Biophys. Res. Commun.* 211, 396–403. doi: 10.1006/bbrc.1995.1827

Mizutani, Y., Kihara, A., and Igarashi, Y. (2004). Identification of the human sphingolipid C4-hydroxylase, hDES2, and its up-regulation during keratinocyte differentiation. *FEBS Lett.* 563, 93–97. doi: 10.1016/s0014-5793(04)00274-271

Mühle, C., Reichel, M., Gulbins, E., and Kornhuber, J. (2013). "Sphingolipids in psychiatric disorders and pain syndromes," in *Sphingolipids in Disease*, eds E.

Gulbins, and I. Petrache, (Vienna: Springer Vienna), 431–456. doi: 10.1007/978-3-7091-1511-4_22

Munoz-Olaya, J. M., Matabosch, X., Bedia, C., Egido-Gabás, M., Casas, J., Llebaria, A., et al. (2008). Synthesis and biological activity of a novel inhibitor of dihydroceramide desaturase. *ChemMedChem* 3, 946–953. doi: 10.1002/cmdc.200700325

Newton, J., Lima, S., Maceyka, M., and Spiegel, S. (2015). Revisiting the sphingolipid rheostat: evolving concepts in cancer therapy. *Exp. Cell Res.* 333, 195–200. doi: 10.1016/j.yexcr.2015.02.025

Normann, P. T., Thomassen, M. S., Christiansen, E. N., and Flatmark, T. (1981). Acyl-CoA synthetase activity of rat liver microsomes substrate specificity with special reference to very-long-chain and isomeric fatty acids. *Biochim. Biophys. Acta* 664, 416–427. doi: 10.1016/0005-2760(81)90064-90063

Obeid, L., Linardic, C., Karolak, L., and Hannun, Y. (1993). Programmed cell death induced by ceramide. *Science* 259, 1769–1771. doi: 10.1126/science.8456305

Ogretmen, B. (2017). Sphingolipid metabolism in cancer signalling and therapy. *Nat. Rev. Cancer* 18, 33–50. doi: 10.1038/nrc.2017.96

Olivera, A., and Spiegel, S. (1993). Sphingosine-1-phosphate as second messenger in cell proliferation induced by PDGF and FCS mitogens. *Nature* 365, 557–560. doi: 10.1038/365557a0

Omae, F., Miyazaki, M., Enomoto, A., and Suzuki, A. (2004). Identification of an essential sequence for dihydroceramide C-4 hydroxylase activity of mouse DES2. *FEBS Lett.* 576, 63–67. doi: 10.1016/j.febslet.2004.08.060

Pant, D. C., Dorboz, I., Schluter, A., Fourcade, S., Launay, N., Joya, J., et al. (2019). Loss of the sphingolipid desaturase DEGS1 causes hypomyelinating leukodystrophy. *J. Clin. Invest.* 129, 1240–1256. doi: 10.1172/JCI123959

Park, J.-W., Park, W.-J., and Futerman, A. H. (2014). Ceramide synthases as potential targets for therapeutic intervention in human diseases. *Biochim. Biophys. Acta* 1841, 671–681. doi: 10.1016/j.bbalip.2013.08.019

Park, T.-S., Rosebury, W., Kindt, E. K., Kowala, M. C., and Panek, R. L. (2008). Serine palmitoyltransferase inhibitor myriocin induces the regression of atherosclerotic plaques in hyperlipidemic ApoE-deficient mice. *Pharmacol. Res.* 58, 45–51. doi: 10.1016/j.phrs.2008.06.005

Rahmaniyan, M., Curley, R. W., Obeid, L. M., Hannun, Y. A., and Kraveka, J. M. (2011). Identification of dihydroceramide desaturase as a direct in vitro target for fenretinide. *J. Biol. Chem.* 286, 24754–24764. doi: 10.1074/jbc.M111.250779

Ren, J., Snider, J., Airola, M. V., Zhong, A., Rana, N. A., Obeid, L. M., et al. (2018). Quantification of 3-ketodihydrosphingosine using HPLC-ESI-MS/MS to study SPT activity in yeast *Saccharomyces cerevisiae*. *J. Lipid Res.* 59, 162–170. doi: 10.1194/jlr.D078535

Rodriguez-Cuenca, S., Barbarroja, N., and Vidal-Puig, A. (2015). Dihydroceramide desaturase 1, the gatekeeper of ceramide induced lipotoxicity. *Biochim. Biophys. Acta* 1851, 40–50. doi: 10.1016/j.bbalip.2014.09.021

Rütti, M. F., Richard, S., Penno, A., von Eckardstein, A., and Hornemann, T. (2009). An improved method to determine serine palmitoyltransferase activity. *J. Lipid Res.* 50, 1237–1244. doi: 10.1194/jlr.D900001-JLR200

Saied, E. M., Le, T. L.-S., Hornemann, T., and Arenz, C. (2018). Synthesis and characterization of some atypical sphingoid bases. *Bioorg. Med. Chem.* 26, 4047–4057. doi: 10.1016/j.bmc.2018.06.031

Schiffmann, S., Hartmann, D., Fuchs, S., Birod, K., Ferreiròs, N., Schreiber, Y., et al. (2012). Inhibitors of specific ceramide synthases. *Biochimie* 94, 558–565. doi: 10.1016/j.biochi.2011.09.007

Schiffmann, S., Sandner, J., Birod, K., Wobst, I., Angioni, C., Ruckhäberle, E., et al. (2009). Ceramide synthases and ceramide levels are increased in breast cancer tissue. *Carcinogenesis* 30, 745–752. doi: 10.1093/carcin/bgp061

Snider, J. M., Luberto, C., and Hannun, Y. A. (2019). Approaches for probing and evaluating mammalian sphingolipid metabolism. *Anal. Biochem.* 575, 70–86. doi: 10.1016/j.ab.2019.03.014

Snider, J. M., Snider, A. J., Obeid, L. M., Luberto, C., and Hannun, Y. A. (2018). Probing de novo sphingolipid metabolism in mammalian cells utilizing mass spectrometry. *J. Lipid Res.* 59, 1046–1057. doi: 10.1194/jlr.D081646

Sullards, M. C., Liu, Y., Chen, Y., and Merrill, A. H. (2011). Analysis of mammalian sphingolipids by liquid chromatography tandem mass spectrometry (LC-MS/MS) and tissue imaging mass spectrometry (TIMS). *Biochim. Biophys. Acta* 1811, 838–853. doi: 10.1016/j.bbalip.2011.06.027

Tidhar, R., and Futerman, A. H. (2013). The complexity of sphingolipid biosynthesis in the endoplasmic reticulum. *Biochim. Biophys. Acta* 1833, 2511–2518. doi: 10.1016/j.bbamcr.2013.04.010

Turner, N., Lim, X. Y., Toop, H. D., Osborne, B., Brandon, A. E., Taylor, E. N., et al. (2018). A selective inhibitor of ceramide synthase 1 reveals a novel role in fat metabolism. *Nat. Commun.* 9:3165. doi: 10.1038/s41467-018-05613-5617

Wakashima, T., Abe, K., and Kihara, A. (2014). Dual functions of the trans-2-Enoyl-CoA reductase TER in the sphingosine 1-phosphate metabolic pathway and in fatty acid elongation. *J. Biol. Chem.* 289, 24736–24748. doi: 10.1074/jbc.M114.571869

Wang, E., Norred, W. P., Bacon, C. W., Riley, R. T., and Merrill, A. H. (1991). Inhibition of sphingolipid biosynthesis by fumonisins. implications for diseases associated with *Fusarium moniliforme*. *J. Biol. Chem.* 266, 14486–14490.

Williams, R. D., Wang, E., and Merrill, A. H. (1984). Enzymology of long-chain base synthesis by liver: characterization of serine palmitoyltransferase in rat liver microsomes. *Arch. Biochem. Biophys.* 228, 282–291. doi: 10.1016/0003-9861(84)90069-90069

Yamaji, T., and Hanada, K. (2015). Sphingolipid metabolism and interorganellar transport: localization of sphingolipid enzymes and lipid transfer proteins. *Traffic* 16, 101–122. doi: 10.1111/tra.12239

Conflict of Interest: The authors declare that the research was conducted in the absence of any commercial or financial relationships that could be construed as a potential conflict of interest.

frontiers in Cell and Developmental Biology

MINI REVIEW
published: 04 October 2019
doi: 10.3389/fcell.2019.00223

Sphingolipid Metabolism and Transport in *Chlamydia trachomatis* and *Chlamydia psittaci* Infections

*Sebastian Banhart, Elena K. Schäfer, Jean-Marc Gensch and Dagmar Heuer**

Unit 'Sexually Transmitted Bacterial Infections', Department for Infectious Diseases, Robert Koch Institute, Berlin, Germany

Chlamydia species infect a large range of vertebral hosts and have become of major economic and public health concern over the last decades. They are obligate intracellular bacteria that undergo a unique cycle of development characterized by the presence of two distinct bacterial forms. After infection of the host cell, *Chlamydia* are found inside a membrane-bound compartment, the inclusion. The surrounding membrane of the inclusion contributes to the host-*Chlamydia* interface and specific pathogen-derived Inc proteins shape this interface allowing interactions with distinct cellular proteins. In contrast to many other bacteria, *Chlamydia* species acquire sphingomyelin from the host cell. In recent years a clearer picture of how *Chlamydia trachomatis* acquires this lipid emerged showing that the bacteria interact with vesicular and non-vesicular transport pathways that involve the recruitment of specific RAB proteins and the lipid-transfer protein CERT. These interactions contribute to the development of a new sphingomyelin-producing compartment inside the host cell. Interestingly, recruitment of CERT is conserved among different *Chlamydia* species including *Chlamydia psittaci*. Here we discuss our current understanding on the molecular mechanisms used by *C. trachomatis* and *C. psittaci* to establish these interactions and to create a novel sphingomyelin-producing compartment inside the host cell important for the infection.

Keywords: *Chlamydia*, sphingolipid, sphingomyelin (SM), ceramide (CER), CERT (CERamide Transfer protein), Inc proteins, infection, RAB proteins

OPEN ACCESS

Edited by:
Sibylle Schneider-Schaulies, Julius Maximilian University of Würzburg, Germany

Reviewed by:
Vera Kozjak-Pavlovic, Julius Maximilian University of Würzburg, Germany
Maria Teresa Damiani, Instituto de Histología y Embriología Dr. Mario H. Burgos (IHEM CONICET), Argentina

***Correspondence:**
Dagmar Heuer
heuerd@rki.de

Specialty section:
This article was submitted to Membrane Physiology and Membrane Biophysics, a section of the journal Frontiers in Cell and Developmental Biology

Received: *28 June 2019*
Accepted: *20 September 2019*
Published: *04 October 2019*

Citation:
Banhart S, Schäfer EK, Gensch J-M and Heuer D (2019) Sphingolipid Metabolism and Transport in Chlamydia trachomatis and Chlamydia psittaci Infections. Front. Cell Dev. Biol. 7:223. doi: 10.3389/fcell.2019.00223

INTRODUCTION

Lipids are important factors in bacterial infections. They serve as energy source, structural components and are involved in the immune response. Like many bacteria, *Chlamydia trachomatis* is able to synthesize most phospholipids except for sphingomyelin, cholesterol and phosphatidylcholine. Sphingomyelin is mainly produced by eukaryotic cells thus; the detection of sphingomyelin inside chlamydial cells was astonishing. This review summarizes recent advances in our understanding of how *Chlamydia* spp. acquire sphingolipids from the host cell and describes their functions for *Chlamydia* biology.

CLINICS OF *Chlamydia trachomatis* AND *C. psittaci* INFECTIONS

Chlamydia trachomatis strains can be divided into biovars. The trachoma biovar (serovars A-C) can cause trachoma, the leading cause of preventable blindness that is hyperendemic in many rural

areas of Africa, Central and South America, Asia, Australia and the Middle East. Infections with the urogenital tract biovar (serovars D-K) are among the most frequently sexually transmitted bacterial infections world-wide. They affect mainly young adults and persons with multiple sex partners (Newman et al., 2015). Symptoms range from asymptomatic to urethritis and proctitis in both genders and cervicitis in females. In particular, untreated or re-occurring infections in women have been associated with severe outcomes including pelvic inflammatory diseases (PID), ectopic pregnancies and infertility. Furthermore, during pregnancy, untreated *C. trachomatis* infections are a risk factor of preterm birth, conjunctivitis and pneumonia of the newborn. *C. trachomatis* belonging to the lymphogranuloma venereum biovar (LGV, L1-L3) is also sexually transmitted and can cause urogenital or anorectal infections in humans that can be more invasive by disseminating to the lymph nodes (Elwell et al., 2016).

Chlamydia psittaci is a zoonotic pathogen that causes respiratory disease in humans and avian species, also known as psittacosis or ornithosis (Knittler et al., 2014; Knittler and Sachse, 2015). The agent was originally isolated from birds, but meanwhile it has been found in different mammalian hosts like cattle, horses and pigs (Longbottom and Coulter, 2003). *C. psittaci* can be transmitted from domestic birds to humans by inhalation of aerosolized bacteria from the feces of infected avian species (Knittler et al., 2014; Knittler and Sachse, 2015). In many cases *C. psittaci* infections remain undetected and undiagnosed due to unspecific symptoms (fever, chills, headache, malaise, myalgia) (Knittler et al., 2014; Knittler and Sachse, 2015).

BIOLOGY OF *Chlamydiaceae*

Both *C. trachomatis* and *C. psittaci* belong to the family of *Chlamydiaceae*. A hallmark of all members of this family is their obligate intracellular, biphasic cycle of development that takes place in a membrane-bound compartment inside a eukaryotic host cell (Moulder, 1991; Hybiske, 2015).

It is characterized by the switch between the extracellular, infectious elementary bodies (EBs) and the intracellular, non-infectious, metabolically active reticulate bodies (RBs) (**Figure 1**). EBs are 0.3 μm in size and enter the host cell by receptor-mediated endocytosis or phagocytosis, involving bacterial adhesins, host cell receptors, and host-specific heparan proteoglycans (Elwell et al., 2016). After internalization, EBs are found in vacuoles, termed inclusions that protect the bacteria from the immune response of the host cell. By releasing effector molecules into the host cell via a type III secretion system, the inclusion membrane is modified and can escape the phagolysosomal pathway (Moore and Ouellette, 2014). Within the inclusion, EBs differentiate into the osmotically instable RBs. These 1 μm small, structurally flexible bacteria divide asymmetrically (Nunes and Gomes, 2014; Abdelrahman et al., 2016). RBs synthesize a family of special proteins, the Inc proteins, which are unique to *Chlamydia* spp. and are integral parts of the bacterial inclusion membrane. They are important bacterial constituents of the inclusion-host cell interface and confer stability to the inclusion membrane (Mirrashidi et al., 2015; Weber et al., 2017). Inc proteins were originally identified in *C. psittaci*. They are a family of *Chlamydia*-specific proteins lacking sequence homology to any known proteins, or to themselves. Interestingly, genomic comparison of different *Chlamydia* strains showed that some Inc proteins are conserved between different species and others are species-specific. These non-conserved Inc proteins may be involved in tissue tropism (Dehoux et al., 2011; Lutter et al., 2012).

At 16–20 h *post infection* (*p.i.*) some RBs start to transform back into EBs, while other RBs continue to replicate. Depending on chlamydial species and growth conditions, at 48–72 h *p.i.* both developmental stages are released from the host cell by either complete lysis of the host cell or by a mechanism called extrusion – the release of the intact inclusion enveloped by host cell plasma membrane (**Figure 1**; Hybiske and Stephens, 2007). Freed EBs can infect neighboring host cells and start a new round of infection.

SPHINGOLIPID SYNTHESIS IN EUKARYOTIC CELLS

Sphingolipids are major integral components of eukaryotic cell membranes. They function as structural and signaling molecules that can regulate apoptosis, cellular proliferation and stress responses (Heung et al., 2006; Breslow and Weissman, 2010). Defects in sphingolipid metabolism have been linked to different diseases including carcinogenesis, cardiovascular and neurodegenerative diseases (Heung et al., 2006).

A sphingoid base linked to a specific fatty acid is the building block of the diverse family of sphingolipids. In sphingomyelin, this backbone is linked to a head group of phosphocholine whereas complex glycosphingolipids are generated by addition of a specific sugar residue. Sphingolipids are a family of structurally and functionally diverse lipids and are synthesized by three distinct pathways: (1) *de novo* synthesis, (2) sphingomyelinase pathways, and (3) salvage pathway that involve specific enzymes localized to distinct organelles inside the cell.

De novo sphingolipid synthesis begins with condensation of serine and palmitoyl coenzyme A (CoA) which takes place at the cytosolic leaflet of the endoplasmic reticulum (ER) catalyzed by the highly conserved palmitoyltransferase (SPTLC) (Yard et al., 2007; Breslow and Weissman, 2010; Hannun and Obeid, 2018). The product of SPTLC, 3-ketosphinganine, is further reduced by 3-ketosphinganine reductase (KDSR) and N-acylated by the action of fatty acid specific dihydroceramide synthases (CERS1-6). Finally, dihydroceramide is desaturated by dihydroceramide desaturase (DEGS) to generate ceramide. Ceramide represents the central precursor molecule of the sphingolipid metabolism, which in turn is used to generate several sphingolipids, like sphingomyelin, sphingosine or complex glycosphingolipids. Ceramide is then transported from the ER to the Golgi apparatus by vesicular trafficking or by transport proteins (Bartke and Hannun, 2009; Hanada, 2010). Within the Golgi, ceramides are modified at the head-group position by adding phosphocholine and phosphate

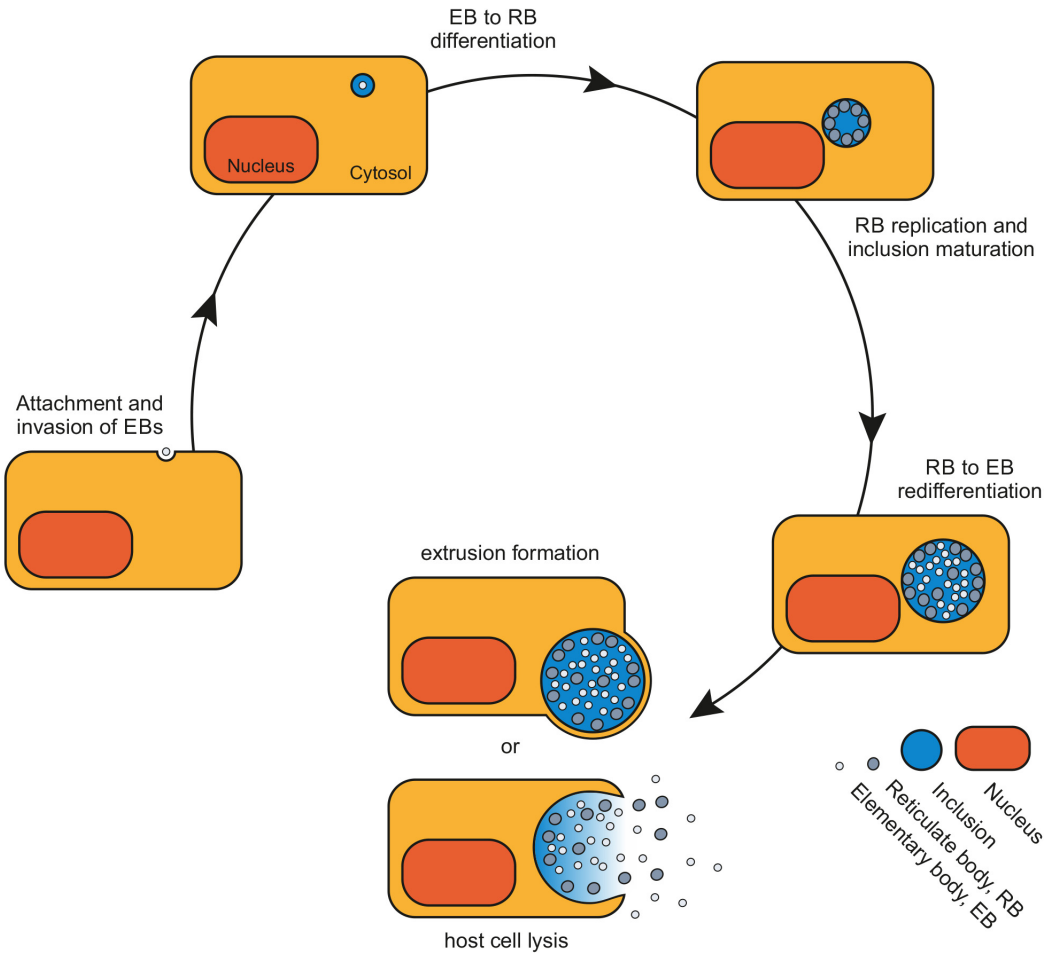

FIGURE 1 | The chlamydial developmental cycle. The biphasic developmental cycle of *Chlamydia* spp. starts with the attachment and invasion of host cells by infectious elementary bodies (EBs). Within their membrane-bound vacuole, termed inclusion, EBs differentiate into metabolically active reticulate bodies (RBs). RBs undergo repeated cycles of replication before they finally re-differentiate into EBs. The life cycle ends with the release of EBs from the host cell by either host cell lysis or extrusion formation to start a new round of infection.

to produce sphingomyelin and ceramide 1-phosphate (Tafesse et al., 2006; Hannun and Obeid, 2018). Ceramide is converted to sphingomyelin by sphingomyelin synthases (SMS) located at the lumen of the *trans-Golgi* (SMS1 and SMS2) and at the plasma membrane (SMS2) (Tafesse et al., 2006; Yamaji and Hanada, 2015). Precursor of complex glycosphingolipids, such as glucosylceramide and galactosylceramide, are formed by the addition of glucose and galactose residues in a glycosidic linkage to ceramide (Breslow and Weissman, 2010; Yamaji and Hanada, 2015). Ultimately, sphingolipids and glycosphingolipids are transported through secretory pathways to plasma membranes and subcellular organelles.

Alternatively, ceramides can be generated by the breakdown of complex sphingolipids, termed salvage pathway (Kitatani et al., 2008). Sphingolipids and glycosphingolipids are degraded in acidic subcellular compartments, such as late endosomes and lysosomes, to form sphingosine (Kitatani et al., 2008). In contrast to ceramide, which is not capable to leave the lysosome, sphingosine is able to enter different cell compartments (Bartke and Hannun, 2009). Released sphingosine may re-enter sphingolipid pathways and is reused by the ceramide synthase to generate ceramides again via re-acylation (Kitatani et al., 2008).

The third pathway, termed sphingomyelinase pathway, occurs in the plasma membrane and endosome/lysosome systems (Yamaji and Hanada, 2015; Teo et al., 2016). Within these compartments, sphingomyelin is converted to ceramide by acid sphingomyelinases (Kitatani et al., 2008). At plasma membranes, SMS2 adds phosphocholine head groups to ceramide, which leads to the production of sphingomyelin.

SPHINGOLIPID TRANSPORT IN *Chlamydia*-INFECTED CELLS

Twenty four years ago, Hackstadt et al. (1995) showed that fluorescently labeled sphingomyelin is acquired by *C. trachomatis* from the host cell. Based on the observation that purified EBs contained fluorescent sphingomyelin the authors concluded

that Golgi-derived sphingomyelin accumulates in bacteria rather than its precursor ceramide. Classical protein markers of the transport between the Golgi apparatus and the plasma membrane were not found in the inclusion membrane suggesting that a subset of Golgi-derived exocytic vesicles is targeted (Hackstadt et al., 1996; Scidmore et al., 1996a). *C. trachomatis* protein synthesis is required for this interaction and bacterial factors that mediate fusogenicity with sphingomyelin-containing vesicles seem to be continually replenished (Scidmore et al., 1996b, 2003). Shortly after these initial observations, quantitative analysis indicated that *C. trachomatis* membranes contain up to 4% of sphingolipids (Wylie et al., 1997). Interfering with bacterial sphingolipid acquisition resulted in less infectious bacteria, leads to the formation of aberrant chlamydial forms and demonstrated the requirement of sphingolipid metabolism for reactivation after INFγ treatment of *C. trachomatis*-infected cells (van Ooij et al., 2000; Rejman Lipinski et al., 2009; Robertson et al., 2009). Interestingly, synthesis of sphingomyelin from ceramide seems to be a prerequisite for sphingolipid uptake into the inclusion and into the bacteria, as a ceramide derivative that cannot be converted to sphingomyelin (1-*O*-methyl-ceramide) was not translocated across the inclusion membrane but rather accumulated around the inclusion (Banhart et al., 2014). This ceramide derivative showed strong anti-chlamydial activity suggesting that *C. trachomatis* generates a sphingomyelin-producing compartment inside the host cell which is important for chlamydial growth (Banhart et al., 2014; Saied et al., 2015). Surprisingly, a recent study suggests that sphingomyelin uptake by *Chlamydia* species is linked to host adaptation and/or virulence rather than to its obligate intracellular life style (Dille et al., 2015).

In recent years, vesicular and non-vesicular transport pathways were identified that were hijacked by *C. trachomatis* to obtain sphingolipids from the host cell (**Figure 2**). These pathways are not redundant and play distinct roles during the chlamydial cycle of development. It has been shown that *C. trachomatis* can intercept vesicular transport routes from different organelles including Golgi mini-stacks or multivesicular bodies (MVBs). Transport of sphingolipid-containing vesicles derived from Golgi mini-stacks requires cellular GTPases RAB14, RAB6A and RAB11A, ARF1 and its guanine nucleotide exchange factor GBF1 (Heuer et al., 2009; Elwell et al., 2011). Interestingly, RAB14, RAB6A, and RAB11A appear to be important for *Chlamydia* progeny formation whereas ARF1 and GBF1 seem

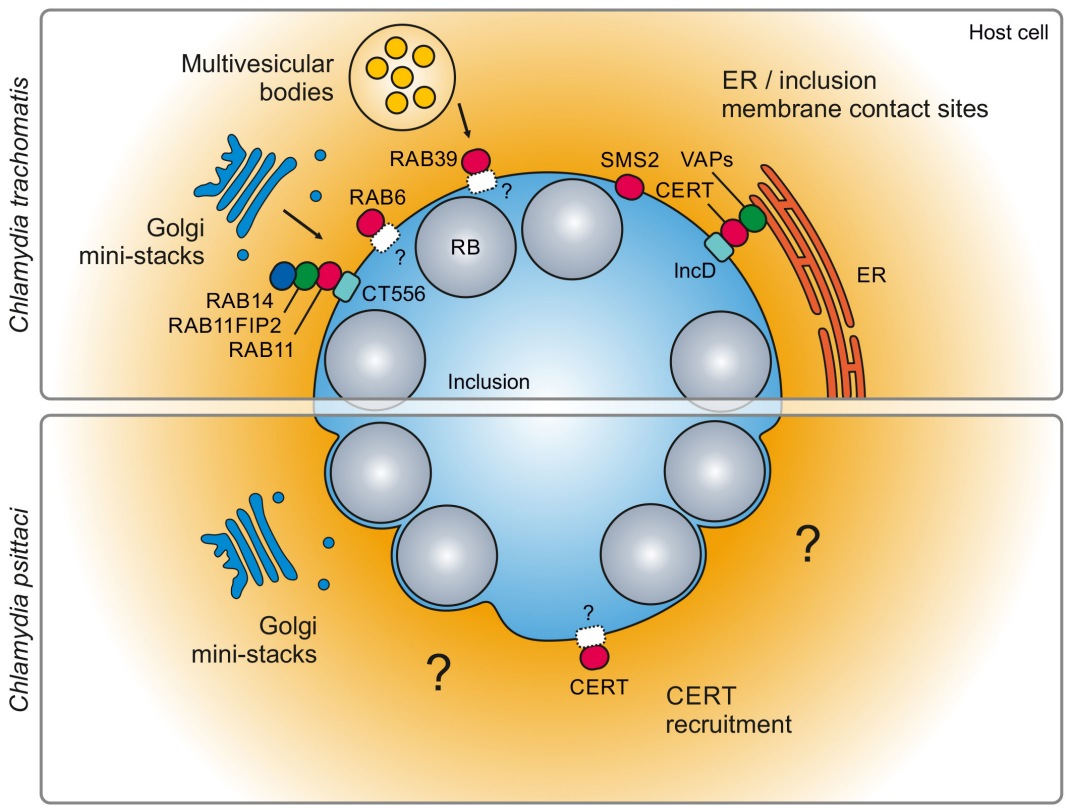

FIGURE 2 | Sphingolipid acquisition during *Chlamydia* infection. Acquisition of sphingolipids takes place by both vesicular and non-vesicular pathways and is ensured by interactions with several subcellular compartments and host cell proteins. Vesicular transport of sphingolipids to *C. trachomatis* is realized by rerouting vesicles from fragmented Golgi mini-stacks or multivesicular bodies, involving several RAB GTPases such as RAB6, RAB11, RAB14, and RAB39. Recruitment of RAB GTPases is thought to be mediated by Inc proteins and interaction of RAB11 with CT556 has been described (Mirrashidi et al., 2015). Non-vesicular routes to *C. trachomatis* include recruitment of SMS and the formation of ER/inclusion membrane contact sites that contain the ceramide transport protein CERT. In contrast, little is known for *C. psittaci*, except for fragmentation of the Golgi apparatus and recruitment of CERT.

to be dispensable (Rejman Lipinski et al., 2009; Capmany and Damiani, 2010; Elwell et al., 2011). The recruitment of RAB14-postive vesicles was shown to be controlled by the Akt signaling pathway, a pathway that is activated by *C. trachomatis* infections (Capmany et al., 2019). Several other kinases have also been implicated in sphingomyelin transport to the *C. trachomatis* inclusion. These include SRC family kinase Fyn and serine/threonine kinases that have been identified in an RNAi screen and based upon inhibition by rotterlin, respectively (Shivshankar et al., 2008; Mital and Hackstadt, 2011). The precise mechanisms how rotterlin inhibits sphingomyelin uptake by *C. trachomatis* remains elusive as rotterlin appears to have multiple targets inside the host cell (Lei et al., 2012). In addition, sphingomyelin is transported from MVBs by RAB39 (Gambarte Tudela et al., 2019). The MVB marker protein CD63 has been detected inside C. trachomatis inclusion but its functional role remains elusive (Beatty, 2006, 2008). In contrast, much less is known for sphingolipid acquisition in *C. psittaci* infections (**Figure 2**). For both species, infection results in fragmentation of the cellular Golgi apparatus into smaller Golgi mini-stacks thereby increasing Golgi surface (Heuer et al., 2009; Knittler et al., 2014). This phenotype has been shown to boost sphingolipid acquisition in *C. trachomatis* infections (Heuer et al., 2009). In sum, multiple cellular processes contribute to sphingolipid acquisition in *Chlamydia* infections (Moore, 2012). How these factors regulate sphingolipid transport and influence the infection is currently not completely understood.

The recruitment of cellular proteins, especially RAB proteins, is species dependent (Damiani et al., 2014). In the past, the localizations of RAB proteins were investigated during infection of different *Chlamydia* species and showed that a core subset of RAB proteins is recruited to the inclusion membrane of different *Chlamydia* species whereas a few RAB proteins are species-specific (Rzomp et al., 2003). Interestingly, although recruitment of a RAB protein is conserved between different *Chlamydia* species (Rab4 in *C. trachomatis* serovar L2 and D, *C. muridarum*, and *C. pneumoniae*), its identified bacterial interaction partner that is responsible for the interaction (CT229 in *C. trachomatis* serovar L2) has not been found in the other chlamydial species (Rzomp et al., 2006). This leaves a question mark on of how the mechanisms of functional recruitment differ between *Chlamydia* species.

Future research regarding the role of these different vesicular pathways in infections with different *Chlamydia* species, the identification of transported lipids and bacterial factors controlling these interactions is needed to understand the intricate relationship.

CERT-DEPENDENT ACQUISITION OF SPHINGOLIPIDS AND BEYOND

New studies showed that *C. trachomatis* and *C. psittaci* hijack the cellular ceramide transport protein CERT to obtain ceramide from the host cell (Derre et al., 2011; Koch-Edelmann et al., 2017). CERT transfers ceramide from the ER to the Golgi apparatus in uninfected cells using the C-terminal START domain (Ponting and Aravind, 1999). Its N-terminal pleckstrin homology (PH) domain binds phosphatidylinositol-4-phosphate (PI4P) (Peretti et al., 2008) at the *cis*-face of the Golgi apparatus and is linked with the ER due to its central FFAT motif binding VAPs (Vesicle-associated membrane protein-associated protein) (Loewen et al., 2003). In *C. trachomatis*-infected cells, CERT is recruited to the inclusion membrane by interaction with IncD (**Figure 2**). Targeted deletion of CERT domains showed that the FFAT motif is relevant for binding and co-recruiting VAPs to the inclusion membrane, but lack of the PH domain interrupts association to the inclusion (Agaisse and Derre, 2014). The interaction of IncD with CERT is driven by the charged and hydrophobic motif in its C-terminus as well as the charged motif in the N-terminus (Kumagai et al., 2018). These motifs are conserved in *C. trachomatis*, *C. suis*, *C. muridarum*, *C. caviae*, and *C. felis*. Also, the proximity of both domains and the possibility of forming homooligomers mediated by the transmembrane domain are necessary for increasing the affinity to CERT. After CERT recruitment to the inclusion membrane, ceramide is likely transported from the ER to the inclusion membrane at ER-inclusion contact sides where ceramide is subsequently converted into sphingomyelin by the also recruited host SMS2 (**Figure 2**; Elwell et al., 2011). IncD belongs to the non-conserved Inc proteins that are not found in all *Chlamydia* species, for example *C. psittaci*. Thus, it is currently not known how CERT is recruited to *C. psittaci* inclusions (Koch-Edelmann et al., 2017). In uninfected cells, the CERT PH domain binds to PI4P-enriched membranes in the *trans-Golgi* region. It has been suggested, that PI4P is present at *C. trachomatis* inclusion membranes and might thereby partially mediate CERT binding (Moorhead et al., 2010). Assuming that *C. psittaci* inclusions are PI4P positive, this mode of binding could be conserved between the different *Chlamydia* species. In addition, proteomic analysis of *C. trachomatis* inclusions revealed that VAPB, a binding partner of CERT is significantly enriched in the inclusion proteome (Aeberhard et al., 2015). Whether VAPB is also associated with *C. psittaci* inclusions or if a currently unknown *C. psittaci* factor facilitates CERT recruitment still needs to be determined. Thus, future experiments are needed to reveal the nature of CERT binding to *C. psittaci* inclusions.

Sphingomyelin is one of the essential host-derived lipids that is incorporated into chlamydial membranes (Saka and Valdivia, 2010) and is described to play a role in bacterial replication and inclusion growth (Hackstadt et al., 1996; Rejman Lipinski et al., 2009; Elwell et al., 2011). Further evidence for this suggestion is that CERT recruitment is conserved among *Chlamydia* spp. (Koch-Edelmann et al., 2017). For *C. trachomatis* and *C. muridarum* it has been shown by RNA interference that CERT seems to be essential for the production of infectious progeny, indicating that CERT is a crucial factor in chlamydial development (Derre et al., 2011; Elwell et al., 2011). Recent studies using CRISPR/Cas9-mediated CERT-knockout cells demonstrated that deficiency of CERT in *C. psittaci* infections also leads to decreased infectious progeny formation (Koch-Edelmann et al., 2017). Interestingly, CERT-knockout caused an increase of sphingolipid uptake by *C. psittaci* (Koch-Edelmann et al., 2017). This is in stark contrast to *C. trachomatis*

infection that shows a drastic decrease in bacterial sphingolipid acquisition under CERT depletion. These findings possibly suggest a CERT-independent sphingolipid uptake pathway in *C. psittaci* infections. How sphingolipids are transported to *C. psittaci* in CERT-knockout cells is currently not known. The involvement of one or more novel factor/s of either bacterial and/or cellular origin that compensate for loss of CERT is likely. Besides that, these results underline that acquisition of sphingomyelin needs to be controlled by *Chlamydia* spp. and suggest that CERT might have additional roles in chlamydial development beyond sphingolipid transport, which need to be investigated in the future.

SUMMARY AND OUTLOOK

Twenty four years after the initial observation that *C. trachomatis* can acquire sphingomyelin from the Golgi apparatus of the infected host cells a clearer picture is emerging on the molecular pathways used by different *Chlamydia* species to obtain sphingolipids. *Chlamydia* species use distinct, non-redundant pathways to obtain sphingolipids. These include vesicular and non-vesicular transport pathways. The characterization of CERT as a conserved factor in ceramide delivery to different *Chlamydia* species and the recruitment of the human SMS2 to the *C. trachomatis* inclusion suggests that at least *C. trachomatis* creates a novel sphingomyelin-producing compartment inside the infected host cells. Additionally, in *C. trachomatis* infections sphingomyelin is transported by distinct vesicles. For that purpose, *C. trachomatis* exploits cellular GTPases, including RAB and ARF proteins, and kinases to facilitate bacterial sphingomyelin acquisition from fragmented Golgi mini-stacks and MVBs. How vesicular and non-vesicular transport of sphingolipids is controlled by different *Chlamydia* species, how they process CERT-delivered ceramide, and how ceramide and sphingomyelin regulate chlamydial infections are just a few open questions. The development of novel tools including the genetic manipulation of *Chlamydia* species and the biochemical isolation of chlamydial inclusions now allows addressing these questions.

AUTHOR CONTRIBUTIONS

DH developed the conception of the manuscript and wrote the manuscript. SB designed the figures. ES, J-MG, and SB contributed to and wrote sections of the manuscript. All authors contributed to the manuscript revision, read, and approved the submitted version of the manuscript.

FUNDING

This work was supported by the Deutsche Forschungsgemeinschaft (SPP 1580 to DH, HE6008/1-1 and HE6008/1-2) and the Federal Ministry of Education and Research (BMBF) in the framework of the national research network "Zoonotic *Chlamydia* – Models of chronic and persistent infections in humans and animals." We apologize to those investigators whose work we were unable to cite because of space constraints.

REFERENCES

Abdelrahman, Y., Ouellette, S. P., Belland, R. J., and Cox, J. V. (2016). Polarized cell division of *Chlamydia trachomatis*. *PLoS Pathog.* 12:e1005822. doi: 10.1371/journal.ppat.1005822

Aeberhard, L., Banhart, S., Fischer, M., Jehmlich, N., Rose, L., Koch, S., et al. (2015). The proteome of the isolated *Chlamydia trachomatis* containing vacuole reveals a complex trafficking platform enriched for retromer components. *PLoS Pathog.* 11:e1004883. doi: 10.1371/journal.ppat.1004883

Agaisse, H., and Derre, I. (2014). Expression of the effector protein IncD in *Chlamydia trachomatis* mediates recruitment of the lipid transfer protein CERT and the endoplasmic reticulum-resident protein VAPB to the inclusion membrane. *Infect. Immun.* 82, 2037–2047. doi: 10.1128/IAI.01530-14

Banhart, S., Saied, E. M., Martini, A., Koch, S., Aeberhard, L., Madela, K., et al. (2014). Improved plaque assay identifies a novel anti-Chlamydia ceramide derivative with altered intracellular localization. *Antimicrob. Agents Chemother.* 58, 5537–5546. doi: 10.1128/AAC.03457-14

Bartke, N., and Hannun, Y. A. (2009). Bioactive sphingolipids: metabolism and function. *J. Lipid Res.* 50(Suppl.), S91–S96.

Beatty, W. L. (2006). Trafficking from CD63-positive late endocytic multivesicular bodies is essential for intracellular development of *Chlamydia trachomatis*. *J. Cell Sci.* 119, 350–359. doi: 10.1242/jcs.02733

Beatty, W. L. (2008). Late endocytic multivesicular bodies intersect the chlamydial inclusion in the absence of CD63. *Infect. Immun.* 76, 2872–2881. doi: 10.1128/IAI.00129-08

Breslow, D. K., and Weissman, J. S. (2010). Membranes in balance: mechanisms of sphingolipid homeostasis. *Mol. Cell* 40, 267–279. doi: 10.1016/j.molcel.2010.10.005

Capmany, A., and Damiani, M. T. (2010). Chlamydia trachomatis intercepts Golgi-derived sphingolipids through a Rab14-mediated transport required for bacterial development and replication. *PLoS One* 5:e14084. doi: 10.1371/journal.pone.0014084

Capmany, A., Gambarte Tudela, J., Alonso Bivou, M., and Damiani, M. T. (2019). Akt/AS160 signaling pathway inhibition impairs infection by decreasing Rab14-controlled sphingolipids delivery to Chlamydial Inclusions. *Front. Microbiol.* 10:666. doi: 10.3389/fmicb.2019.00666

Damiani, M. T., Gambarte Tudela, J., and Capmany, A. (2014). Targeting eukaryotic Rab proteins: a smart strategy for chlamydial survival and replication. *Cell. Microbiol.* 16, 1329–1338. doi: 10.1111/cmi.12325

Dehoux, P., Flores, R., Dauga, C., Zhong, G., and Subtil, A. (2011). Multi-genome identification and characterization of chlamydiae-specific type III secretion substrates: the Inc proteins. *BMC Genomics* 12:109. doi: 10.1186/1471-2164-12-109

Derre, I., Swiss, R., and Agaisse, H. (2011). The lipid transfer protein CERT interacts with the Chlamydia inclusion protein IncD and participates to ER-Chlamydia inclusion membrane contact sites. *PLoS Pathog.* 7:e1002092. doi: 10.1371/journal.ppat.1002092

Dille, S., Kleinschnitz, E. M., Kontchou, C. W., Nolke, T., and Hacker, G. (2015). In contrast to *Chlamydia trachomatis*, *Waddlia chondrophila* grows in human cells without inhibiting apoptosis, fragmenting the Golgi apparatus, or diverting post-Golgi sphingomyelin transport. *Infect. Immun.* 83, 3268–3280. doi: 10.1128/IAI.00322-15

Elwell, C., Mirrashidi, K., and Engel, J. (2016). Chlamydia cell biology and pathogenesis. *Nat. Rev. Microbiol.* 14, 385–400. doi: 10.1038/nrmicro.2016.30

Elwell, C. A., Jiang, S., Kim, J. H., Lee, A., Wittmann, T., Hanada, K., et al. (2011). *Chlamydia trachomatis* co-opts GBF1 and CERT to acquire host sphingomyelin for distinct roles during intracellular development. *PLoS Pathog.* 7:e1002198. doi: 10.1371/journal.ppat.1002198

Gambarte Tudela, J., Buonfigli, J., Lujan, A., Alonso Bivou, M., Cebrian, I., Capmany, A., et al. (2019). Rab39a and Rab39b display different intracellular

distribution and function in sphingolipids and phospholipids transport. *Int. J. Mol. Sci.* 20:E1688. doi: 10.3390/ijms20071688

Hackstadt, T., Rockey, D. D., Heinzen, R. A., and Scidmore, M. A. (1996). *Chlamydia trachomatis* interrupts an exocytic pathway to acquire endogenously synthesized sphingomyelin in transit from the Golgi apparatus to the plasma membrane. *EMBO J.* 15, 964–977. doi: 10.1002/j.1460-2075.1996.tb00433.x

Hackstadt, T., Scidmore, M. A., and Rockey, D. D. (1995). Lipid metabolism in *Chlamydia trachomatis*-infected cells: directed trafficking of Golgi-derived sphingolipids to the chlamydial inclusion. *Proc Natl Acad Sci U.S.A.* 92, 4877–4881. doi: 10.1073/pnas.92.11.4877

Hanada, K. (2010). Intracellular trafficking of ceramide by ceramide transfer protein. *Proc. Jpn. Acad. Ser. B Phys. Biol. Sci.* 86, 426–437. doi: 10.2183/pjab.86.426

Hannun, Y. A., and Obeid, L. M. (2018). Sphingolipids and their metabolism in physiology and disease. *Nat. Rev. Mol. Cell Biol.* 19, 175–191. doi: 10.1038/nrm.2017.107

Heuer, D., Rejman Lipinski, A., Machuy, N., Karlas, A., Wehrens, A., Siedler, F., et al. (2009). Chlamydia causes fragmentation of the Golgi compartment to ensure reproduction. *Nature* 457, 731–735. doi: 10.1038/nature07578

Heung, L. J., Luberto, C., and Del Poeta, M. (2006). Role of sphingolipids in microbial pathogenesis. *Infect. Immun.* 74, 28–39. doi: 10.1128/iai.74.1.28-39.2006

Hybiske, K. (2015). Expanding the molecular toolkit for Chlamydia. *Cell Host Microbe* 18, 11–13. doi: 10.1016/j.chom.2015.06.016

Hybiske, K., and Stephens, R. S. (2007). Mechanisms of host cell exit by the intracellular bacterium Chlamydia. *Proc. Natl. Acad. Sci. U.S.A.* 104, 11430–11435. doi: 10.1073/pnas.0703218104

Kitatani, K., Idkowiak-Baldys, J., and Hannun, Y. A. (2008). The sphingolipid salvage pathway in ceramide metabolism and signaling. *Cell. Signal.* 20, 1010–1018. doi: 10.1016/j.cellsig.2007.12.006

Knittler, M. R., Berndt, A., Bocker, S., Dutow, P., Hanel, F., Heuer, D., et al. (2014). *Chlamydia psittaci*: new insights into genomic diversity, clinical pathology, host-pathogen interaction and anti-bacterial immunity. *Int. J. Med. Microbiol.* 304, 877–893. doi: 10.1016/j.ijmm.2014.06.010

Knittler, M. R., and Sachse, K. (2015). *Chlamydia psittaci*: update on an underestimated zoonotic agent. *Pathog. Dis.* 73, 1–15. doi: 10.1093/femspd/ftu007

Koch-Edelmann, S., Banhart, S., Saied, E. M., Rose, L., Aeberhard, L., Laue, M., et al. (2017). The cellular ceramide transport protein CERT promotes *Chlamydia psittaci* infection and controls bacterial sphingolipid uptake. *Cell. Microbiol.* 19:e12752. doi: 10.1111/cmi.12752

Kumagai, K., Elwell, C. A., Ando, S., Engel, J. N., and Hanada, K. (2018). Both the N- and C- terminal regions of the Chlamydial inclusion protein D (IncD) are required for interaction with the pleckstrin homology domain of the ceramide transport protein CERT. *Biochem. Biophys. Res. Commun.* 505, 1070–1076. doi: 10.1016/j.bbrc.2018.09.168

Lei, L., Li, Z., and Zhong, G. (2012). Rottlerin-mediated inhibition of *Chlamydia trachomatis* growth and uptake of sphingolipids is independent of p38-regulated/activated protein kinase (PRAK). *PLoS One* 7:e44733. doi: 10.1371/journal.pone.0044733

Loewen, C. J., Roy, A., and Levine, T. P. (2003). A conserved ER targeting motif in three families of lipid binding proteins and in Opi1p binds VAP. *EMBO J.* 22, 2025–2035. doi: 10.1093/emboj/cdg201

Longbottom, D., and Coulter, L. J. (2003). Animal chlamydioses and zoonotic implications. *J. Comp. Pathol.* 128, 217–244. doi: 10.1053/jcpa.2002.0629

Lutter, E. I., Martens, C., and Hackstadt, T. (2012). Evolution and conservation of predicted inclusion membrane proteins in chlamydiae. *Comp. Funct. Genomics* 2012:362104. doi: 10.1155/2012/362104

Mirrashidi, K. M., Elwell, C. A., Verschueren, E., Johnson, J. R., Frando, A., Von Dollen, J., et al. (2015). Global mapping of the Inc-human interactome reveals that retromer restricts chlamydia infection. *Cell Host Microbe* 18, 109–121. doi: 10.1016/j.chom.2015.06.004

Mital, J., and Hackstadt, T. (2011). Role for the SRC family kinase Fyn in sphingolipid acquisition by chlamydiae. *Infect. Immun.* 79, 4559–4568. doi: 10.1128/IAI.05692-11

Moore, E. R. (2012). Sphingolipid trafficking and purification in *Chlamydia trachomatis*-infected cells. *Curr. Protoc. Microbiol.* Chapter 11:2.

Moore, E. R., and Ouellette, S. P. (2014). Reconceptualizing the chlamydial inclusion as a pathogen-specified parasitic organelle: an expanded role for Inc proteins. *Front. Cell. Infect. Microbiol.* 4:157. doi: 10.3389/fcimb.2014.00157

Moorhead, A. M., Jung, J. Y., Smirnov, A., Kaufer, S., and Scidmore, M. A. (2010). Multiple host proteins that function in phosphatidylinositol-4-phosphate metabolism are recruited to the chlamydial inclusion. *Infect. Immun.* 78, 1990–2007. doi: 10.1128/IAI.01340-09

Moulder, J. W. (1991). Interaction of chlamydiae and host cells in vitro. *Microbiol. Rev.* 55, 143–190.

Newman, L., Rowley, J., Vander Hoorn, S., Wijesooriya, N. S., Unemo, M., Low, N., et al. (2015). Global estimates of the prevalence and incidence of four curable sexually transmitted infections in 2012 based on systematic review and global reporting. *PLoS One* 10:e0143304. doi: 10.1371/journal.pone.0143304

Nunes, A., and Gomes, J. P. (2014). Evolution, phylogeny, and molecular epidemiology of Chlamydia. *Infect. Genet. Evol.* 23, 49–64. doi: 10.1016/j.meegid.2014.01.029

Peretti, D., Dahan, N., Shimoni, E., Hirschberg, K., and Lev, S. (2008). Coordinated lipid transfer between the endoplasmic reticulum and the Golgi complex requires the VAP proteins and is essential for Golgi-mediated transport. *Mol. Biol. Cell* 19, 3871–3884. doi: 10.1091/mbc.E08-05-0498

Ponting, C. P., and Aravind, L. (1999). START: a lipid-binding domain in StAR, HD-ZIP and signalling proteins. *Trends Biochem. Sci.* 24, 130–132. doi: 10.1016/s0968-0004(99)01362-6

Rejman Lipinski, A., Heymann, J., Meissner, C., Karlas, A., Brinkmann, V., Meyer, T. F., et al. (2009). Rab6 and Rab11 regulate *Chlamydia trachomatis* development and golgin-84-dependent Golgi fragmentation. *PLoS Pathog.* 5:e1000615. doi: 10.1371/journal.ppat.1000615

Robertson, D. K., Gu, L., Rowe, R. K., and Beatty, W. L. (2009). Inclusion biogenesis and reactivation of persistent *Chlamydia trachomatis* requires host cell sphingolipid biosynthesis. *PLoS Pathog.* 5:e1000664. doi: 10.1371/journal.ppat.1000664

Rzomp, K. A., Moorhead, A. R., and Scidmore, M. A. (2006). The GTPase Rab4 interacts with *Chlamydia trachomatis* inclusion membrane protein CT229. *Infect. Immun.* 74, 5362–5373. doi: 10.1128/iai.00539-06

Rzomp, K. A., Scholtes, L. D., Briggs, B. J., Whittaker, G. R., and Scidmore, M. A. (2003). Rab GTPases are recruited to chlamydial inclusions in both a species-dependent and species-independent manner. *Infect. Immun.* 71, 5855–5870. doi: 10.1128/iai.71.10.5855-5870.2003

Saied, E. M., Banhart, S., Burkle, S. E., Heuer, D., and Arenz, C. (2015). A series of ceramide analogs modified at the 1-position with potent activity against the intracellular growth of *Chlamydia trachomatis*. *Future Med. Chem.* 7, 1971–1980. doi: 10.4155/fmc.15.126

Saka, H. A., and Valdivia, R. H. (2010). Acquisition of nutrients by Chlamydiae: unique challenges of living in an intracellular compartment. *Curr. Opin. Microbiol.* 13, 4–10. doi: 10.1016/j.mib.2009.11.002

Scidmore, M. A., Fischer, E. R., and Hackstadt, T. (1996a). Sphingolipids and glycoproteins are differentially trafficked to the *Chlamydia trachomatis* inclusion. *J. Cell Biol.* 134, 363–374. doi: 10.1083/jcb.134.2.363

Scidmore, M. A., Rockey, D. D., Fischer, E. R., Heinzen, R. A., and Hackstadt, T. (1996b). Vesicular interactions of the *Chlamydia trachomatis* inclusion are determined by chlamydial early protein synthesis rather than route of entry. *Infect. Immun.* 64, 5366–5372.

Scidmore, M. A., Fischer, E. R., and Hackstadt, T. (2003). Restricted fusion of *Chlamydia trachomatis* vesicles with endocytic compartments during the initial stages of infection. *Infect. Immun.* 71, 973–984. doi: 10.1128/iai.71.2.973-984.2003

Shivshankar, P., Lei, L., Wang, J., and Zhong, G. (2008). Rottlerin inhibits chlamydial intracellular growth and blocks chlamydial acquisition of sphingolipids from host cells. *Appl. Environ. Microbiol.* 74, 1243–1249. doi: 10.1128/aem.02151-07

Tafesse, F. G., Ternes, P., and Holthuis, J. C. (2006). The multigenic sphingomyelin synthase family. *J. Biol. Chem.* 281, 29421–29425. doi: 10.1074/jbc.r600021200

Teo, W. X., Kerr, M. C., Huston, W. M., and Teasdale, R. D. (2016). Sortilin is associated with the chlamydial inclusion and is modulated during infection. *Biol. Open* 5, 429–435. doi: 10.1242/bio.016485

van Ooij, C., Kalman, L., Ijzendoorn van, P., Nishijima, M., Hanada, K., Mostov, K., et al. (2000). Host cell-derived sphingolipids are required for the intracellular growth of *Chlamydia trachomatis*. *Cell. Microbiol.* 2, 627–637. doi: 10.1046/j.1462-5822.2000.00077.x

Weber, M. M., Lam, J. L., Dooley, C. A., Noriea, N. F., Hansen, B. T., Hoyt, F. H., et al. (2017). Absence of specific *Chlamydia trachomatis* inclusion membrane proteins triggers premature inclusion membrane lysis and host cell death. *Cell Rep.* 19, 1406–1417. doi: 10.1016/j.celrep.2017.04.058

Wylie, J. L., Hatch, G. M., and McClarty, G. (1997). Host cell phospholipids are trafficked to and then modified by *Chlamydia trachomatis*. *J. Bacteriol.* 179, 7233–7242. doi: 10.1128/jb.179.23.7233-7242.1997

Yamaji, T., and Hanada, K. (2015). Sphingolipid metabolism and interorganellar transport: localization of sphingolipid enzymes and lipid transfer proteins. *Traffic* 16, 101–122. doi: 10.1111/tra.12239

Yard, B. A., Carter, L. G., Johnson, K. A., Overton, I. M., Dorward, M., Liu, H., et al. (2007). The structure of serine palmitoyltransferase; gateway to sphingolipid biosynthesis. *J. Mol. Biol.* 370, 870–886.

Conflict of Interest: The authors declare that the research was conducted in the absence of any commercial or financial relationships that could be construed as a potential conflict of interest.

frontiers in Immunology

HYPOTHESIS AND THEORY
published: 11 October 2019
doi: 10.3389/fimmu.2019.02363

Translational Approaches Targeting Ceramide Generation From Sphingomyelin in T Cells to Modulate Immunity in Humans

*Claudia Hollmann[1], Teresa Wiese[1], Fabio Dennstädt[1], Julian Fink[2], Jürgen Schneider-Schaulies[1] and Niklas Beyersdorf[1]**

[1] Institute for Virology and Immunobiology, University of Würzburg, Würzburg, Germany, [2] Institute of Organic Chemistry, University of Würzburg, Würzburg, Germany

In T cells, as in all other cells of the body, sphingolipids form important structural components of membranes. Due to metabolic modifications, sphingolipids additionally play an active part in the signaling of cell surface receptors of T cells like the T cell receptor or the co-stimulatory molecule CD28. Moreover, the sphingolipid composition of their membranes crucially affects the integrity and function of subcellular compartments such as the lysosome. Previously, studying sphingolipid metabolism has been severely hampered by the limited number of analytical methods/model systems available. Besides well-established high resolution mass spectrometry new tools are now available like novel minimally modified sphingolipid subspecies for click chemistry as well as recently generated mouse mutants with deficiencies/overexpression of sphingolipid-modifying enzymes. Making use of these tools we and others discovered that the sphingolipid sphingomyelin is metabolized to ceramide to different degrees in distinct T cell subpopulations of mice and humans. This knowledge has already been translated into novel immunomodulatory approaches in mice and will in the future hopefully also be applicable to humans. In this paper we are, thus, summarizing the most recent findings on the impact of sphingolipid metabolism on T cell activation, differentiation, and effector functions. Moreover, we are discussing the therapeutic concepts arising from these insights and drugs or drug candidates which are already in clinical use or could be developed for clinical use in patients with diseases as distant as major depression and chronic viral infection.

Keywords: sphingolipids, CD4$^+$ T cells, regulatory T cells (Treg), CD8$^+$ T cells, anti-depressant drug

OPEN ACCESS

Edited by:
Burkhard Kleuser, University of Potsdam, Germany

Reviewed by:
Christoph Wülfing, University of Bristol, United Kingdom
Sid P. Kerkar, Boehringer Ingelheim, United States

****Correspondence:***
Niklas Beyersdorf
niklas.beyersdorf@vim.uni-wuerzburg.de

Specialty section:
This article was submitted to T Cell Biology, a section of the journal Frontiers in Immunology

Received: *31 May 2019*
Accepted: *19 September 2019*
Published: *11 October 2019*

Citation:
Hollmann C, Wiese T, Dennstädt F, Fink J, Schneider-Schaulies J and Beyersdorf N (2019) Translational Approaches Targeting Ceramide Generation From Sphingomyelin in T Cells to Modulate Immunity in Humans. Front. Immunol. 10:2363. doi: 10.3389/fimmu.2019.02363

INTRODUCTION

Subsets of T cells are major contributors to adaptive immunity. In particular, CD4$^+$ T helper and CD8$^+$ T cells either crucially orchestrate adaptive immune response or are direct mediators of e.g., anti-viral immunity, respectively. In order to be able to fulfill these tasks T cell precursors have to run through a stringent process of positive and negative selection within the thymus [reviewed in (1)]. However, it has been clear for decades that the process of negative selection does not completely eliminate maturing autoreactive T cells. This means that also in healthy human individuals autoreactive T cells can be detected (2–5) which, however, only cause autoimmune

diseases like multiple sclerosis in very few people. One reason for this is that the thymus also generates so-called regulatory $CD4^+$ T cells—a process coined the "third function" of the thymus (6).

These regulatory T cells (Treg) develop and are maintained under the control of the transcription factor Foxp3 (7–9). Expression of Foxp3 endows maturing T cells with an increased robustness toward negative selection (10). Therefore, $Foxp3^+$ $CD4^+$ Treg leaving the thymus display a high degree of autoreactivity (11, 12). By employing a wide array of molecular mechansims Treg prevent autoreactive and autoaggressive conventional $CD4^+$ T helper ($CD4^+$ Tconv) and $CD8^+$ T cells from attacking healthy tissue which would otherwise lead to autoimmune disease [reviewed in (13)].

In conditions under which a protective adaptive immune response is crucial for the host to survive, mechanisms need to be in place which neutralize Treg-mediated immunosuppression [reviewed in (13)]. A key mechanism here is the recognition of pathogen-associated molecular patterns (PAMPs) via pattern recognition receptors (PRR) like Toll-like receptors expressed by cells of innate immunity like dendritic cells (DC) [reviewed in (14)]. This leads to an upregulation of costimulatory molecules like CD80 and CD86 on the surface of DC, which will trigger CD28 costimulation of $CD4^+$ Tconv. By this they will escape suppression by Treg (15–17). As these signals are spatially and timely restricted, i.e., only present in lymph nodes draining an infection site, Treg-mediated immunosuppression will only be neutralized there, whereas in other tissues Treg will continue to be able to mediate protection from autoimmunity.

Unfortunately, "overshooting" or unwanted adaptive immune responses are not always prevented successfully. This will then lead to different forms of T [reviewed in (18–20)] or B cell-mediated autoimmunity [reviewed in (21, 22)].

Apart from mediating protective immunity and inducing autoimmune diseases causing a substantial amount of morbidity and mortality, T cells have been recognized to play an important role in maintaining or restoring tissue homeostasis after muscle damage (23), myocardial infarction (24–26) or stroke (27).

To fulfill all these different tasks, T cells in general mainly rely on signals which they receive through cell surface receptors. As such these receptors are, of course, in close contact with lipids forming the cell membrane. About 30% of phospholipids in the plasma membrane belong to so-called sphingolipids [reviewed in (28)]. The importance of sphingolipids for T cell function stems from the fact that they are not inert molecular species, but that they are subject to metabolization [reviewed in (29)] and are altered depending on the differentiation state and function of the cells. This means e.g., that the most complex sphingolipid sphingomyelin (consisting of a number of species with different fatty acid chain lengths) can be reversibly cleaved into ceramides and phosphocholine (**Figure 1**). Ceramide molecules have the propensity to self-aggregate, thus, forming so-called ceramide-rich platforms [reviewed in (31)]. Ceramides may, however, also be further metabolized into sphingosine and fatty acids. Sphingosine may then be phosphorylated to sphingosine-1-phosphate which has very wide-ranging biological activities mediated by a set of five different cell surface receptors, but also by direct interaction with signaling molecules inside cells [reviewed in (32)]. Finally, sphingosine may also be cleaved into phosphoethanolamine and hexadecenal marking the only non-reversible step in sphingolipid metabolism (**Figure 1**).

The different steps in the meta-(cata-)bolism of sphingomyelin and its breakdown products are catalyzed by a whole array of different enzymes. Localization of these enzymes in different cellular compartments and the modulation of their enzymatic activity upon T cell activation mean that their biology is very complex. One key mediator of sphingomyelin breakdown is the acid sphingomyelinase (mouse: Asm; human: ASM). In resting T cells the Asm is localized in the inner leaflet of the lysosomal membrane where the presence of Zn^{2+} ions and the acidic pH ensure optimal enzymatic activity [reviewed in (29)]. Upon activation of certain cell surface receptors, including CD28 (33) and CD95 (34) via monoclonal antibodies, Asm activity in lysosomes is increased and lysosomes fuse with the cell membrane, thus exposing the Asm on the cell surface where it might still be able to catalyze sphingomyelin cleavage [reviewed in (29)]. Another important sphingomyelinase whose role in T cell biology is not yet fully understood is the neutral sphingomyelinase 2 (mouse: Nsm2; human: NSM2). In contrast to the Asm, the Nsm2 localizes to the inner leaflet of the plasma membrane and the cytoplasmic side of the Golgi membrane, where it can get activated without being translocated to another cellular compartment (35–38). Stimuli activating the Nsm2 include isolated TCR or TCR and CD28 costimulation via monoclonal antibodies (39).

Apart from meta- and catabolism sphingolipid concentrations in cellular membranes are, of course, also regulated by *de novo* sphingolipid generation. The "hub" of sphingolipid *de novo* synthesis is ceramide [reviewed in (30)] with six different ceramide synthases catalyzing the generation of the various ceramide species in the endoplasmic reticulum [reviewed in (30, 40)].

$CD8^+$ T CELLS

Having passed thymic selection mature, MHC class I-restricted, $CD8^+$ T cells leave the thymus and migrate to secondary lymphoid organs, i.e., predominantly lymph nodes and spleen. To ensure tight immunological control of the whole body, naïve ($CD8^+$) T cells constantly recirculate through the lymphatic/blood system—a process crucially regulated by high concentrations of sphingosine-1-phosphate in efferent lymph and blood [reviewed in (32)].

After encounter of antigen and appropriate costimulation, $CD8^+$ T cells differentiate into cytotoxic T lymphocytes (CTL) expressing lytic granules [reviewed in (41)]. Upon recognition of foreign peptides on MHC class I molecules by the CTL's TCR the CTL will release the content of the lytic granules toward the target cell, i.e., into the synaptic cleft between both cells. Lytic granules contain granzymes and perforin which generates pores in the target cell's membrane through which granzymes can enter the cytoplasm and induce apoptosis by activating caspases [reviewed in (42)]. Upon fusion of the lytic granules with the cell membrane not only proteins like LAMP-1 which is expressed on

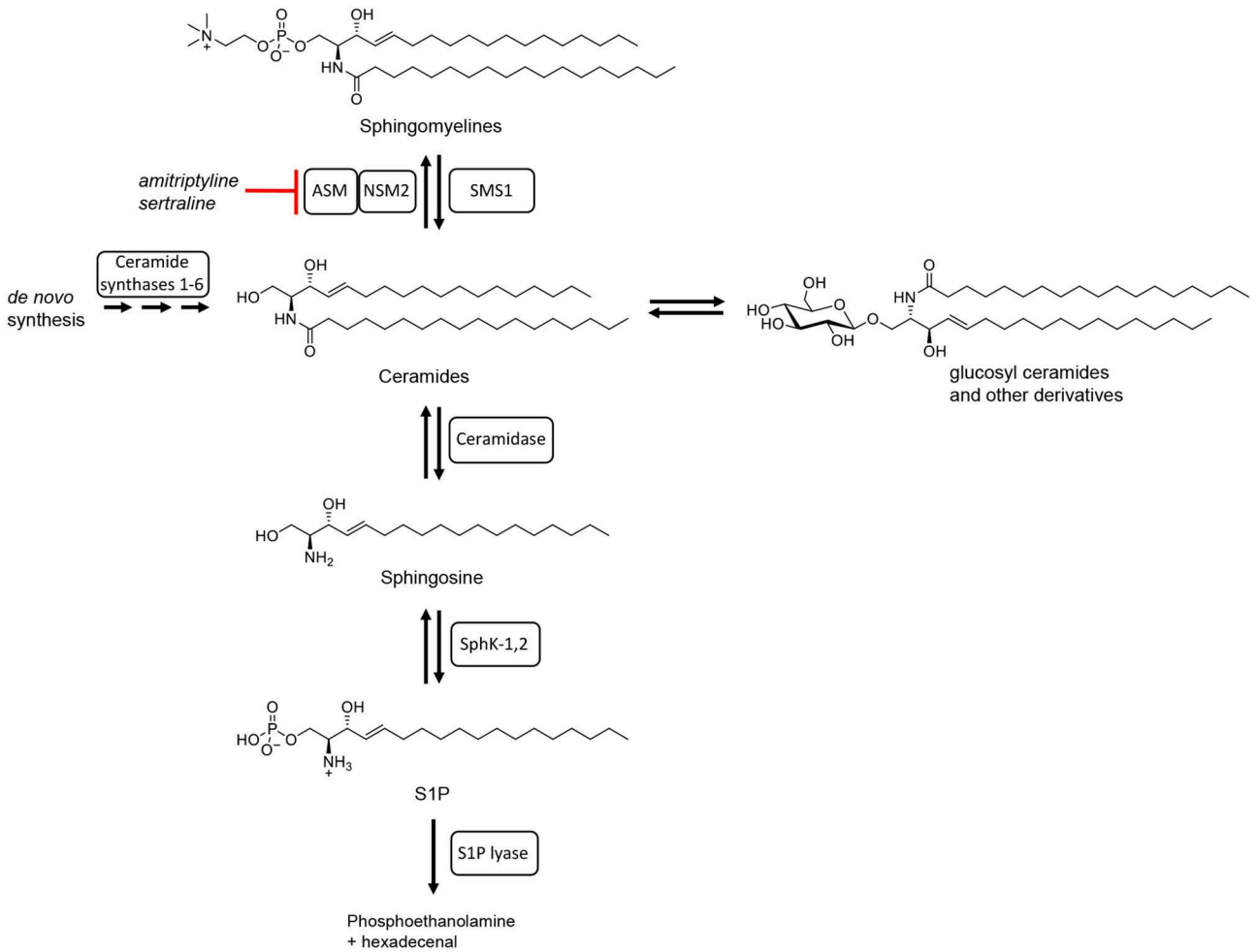

FIGURE 1 | Schematic summary of sphingolipid metabolism. Adapted from Bartke and Hannun (30) with chemical structures of the sphingolipids involved (all with C18 side chains).

the inner membrane leaflet of lytic vessels and protects CTL and Natural Killer cells from degranulation-associated damage (43), but also the Asm will be exposed on the cell surface [reviewed in (29, 44)]. Due to the size of the lytic granules sufficient extrusion of their content requires changes to the biophysical properties of their membranes (45). These changes are mediated by the Asm generating ceramide at the inner membrane leaflet of the vesicles. Vesicles containing the chemokine RANTES which also exist in $CD8^+$ effector T cells are about 10-fold smaller than lytic vesicles. Therefore, chemokines are efficiently released from these vesicles even without changes to the biophysical properties of their membranes (45). Reduced release of lytic content from vesicles was associated with reduced killing by CTL from Asm-deficient vs. wild-type mice (45). These data were confirmed by pharmacologically inhibiting Asm activity with imipramine in CTL (45).

Can these insights be used and translated to humans? A direct consequence of the aforementioned observations in mice is that inhibition of Asm activity with clinically approved antidepressants like amitriptyline, imipramine, or sertraline could reduce unwanted CTL activity. This would, of course, lead to unspecific partial immunosuppression. It might, thus, be envisaged as a form of comedication e.g., in patients suffering from pulmonal immunopathology due to overshooting CTL activity against e.g., Influenza A virus-infected alveolar epithelial cells [reviewed in (46)]. In addition to reducing CTL activity, inhibition of the ASM in humans may also directly stabilize pulmonal function as it has been observed in animal models (47–49). In fact it is this latter indication for which ASM inhibitors are currently investigated in children with cystic fibrosis suffering from bacterial infections of the lung (ClinicalTrials.gov Identifier: NCT00515229).

A caveat in the outlined scenario is that, so far, the role of the Asm in lytic granule release from CTL has only been studied in mice. Data for human $CD8^+$ CTL are still lacking. As it is very likely that the ASM is also expressed by human $CD8^+$ T cells it seems plausible that also in humans ASM activity enhances release of cytotoxic content from CTL vesicles.

Apart from the ASM, the NSM2 also constitutes a therapeutically interesting target to modulate CTL function in humans. This is the case as stimulation of the T cell receptor complex (with monoclonal antibodies) is sufficient to increase NSM2 activity (39) and for target cell recognition the CTL only needs to receive an activating signal through the TCR complex. Therefore, inhibition of the NSM2 may also be suitable to reduce unwanted CTL activity.

CONVENTIONAL CD4$^+$ T CELLS

Compared to CD8$^+$ T cells and CTL, the body of literature on the impact of sphingolipid metabolism on the function of conventional, i.e., Foxp3$^-$, non-regulatory T cells (CD4$^+$ Tconv) is much bigger (50–52). In particular, researchers have focused in recent years on the modulation of effector cell differentiation and cytokine secretion by human CD4$^+$ T cells by the ASM (52, 53).

An early report comparing cells from Asm-deficient and wildtype mice indicated that secretion of Interleukin-2 (IL-2) by Concanavalin A-stimulated splenocytes among which CD4$^+$ Tconv are probably the main, followed by CD8$^+$ T cells, source of IL-2 [reviewed in (54)], was higher in wild-type than in mutant mice (55). More recently, experiments using human CD4$^+$ T cells have revealed a positive role for the ASM in promoting Th17 cell differentiation and IL-17 secretion (52). Here, pharmacological inhibition of the ASM was used to study the impact of the enzyme on CD4$^+$ T cell differentiation and cytokine secretion.

Apart from cytokine secretion, migration of effector/memory CD4$^+$ Tconv also crucially contributes to their function *in vivo*. Studying mouse CD4$^+$ T cells *in vitro* and *in vivo* as well as human CD4$^+$ T cells *in vitro*, it has been recently shown that migration and adhesion to activated endothelial cells requires NSM2 activity (56). Moreover, migration of T cells toward SDF-1α, a chemokine recognized by CXCR4, also depends on NSM2 activity (56). Therefore, two crucial steps in CD4$^+$ effector cell function, i.e., extravasation at sites of endothelial inflammation, and migration along chemokine gradients necessitates NSM2 activity. For extravasation integrin leukocyte function-associated antigen (LFA)-1 on T cells needs to bind to intercellular adhesion molecule (ICAM)-1 on endothelial cells. Therefore, reduced LFA-1 clustering in the absence of NSM2 activity (56) should impact all T cell subsets. Similarly, the broad expression of CXCR4 by (CD4$^+$) T cells [reviewed in (57)] also means that targeting NSM2 in T cells affects early as well as advanced stages of T cell differentiation. Apart from its impact on T cell migration NSM2 activity also supports early signaling events in Jurkat and primary human CD4$^+$ T cells (58). In the absence of NSM2 activity, T cell receptor signaling is initiated as in wild-type T cells, but signaling is not sustained due to deficient protein kinase Cζ activation. Together, this means that the NSM2 might qualify as a novel therapeutic target for suppressing unwanted immune responses. Currently, there is, however, no data concerning the immunomodulatory activities of NSM2 inhibitors in humans *in vivo*.

Another critical aspect of T cell biology is the tight homeostatic control of the compartment size through induction of different forms of cell death [reviewed in (59)]. Most notably, activation of naïve (CD4$^+$) T cells is followed by massive expansion of reactive clones. After resolution of inflammation the effector T cell pool again collapses with only few memory T cells surviving long-term [reviewed in (60, 61)]. The collapse of the acute immune response is due to different mechanisms of cell death with apoptosis induction by Fas (CD95)-Fas ligand being the best studied pathway, but other forms of cell death like necroptosis are increasingly recognized to also play a role here [reviewed in (59, 62)]. Ligation of Fas on activated T cells stimulates Asm activity leading to ceramide production and, as a consequence, to the induction of cell death (63–65). Therefore, and even more generally, ceramide production has been linked to induction of cell death [reviewed in (29)]. Seemingly in contrast to this notion we observed that pharmacological inhibitors of the Asm also induced cell death in Tconv of mice (66) and at slightly higher concentrations also in human CD4$^+$ Tconv (Dennstaedt, Schneider-Schaulies, Beyersdorf, unpublished). The availability of Asm-deficient mice allowed to confirm that cell death induced by amitriptyline or desipramine was due to their impact on the Asm and not the acid ceramidase which they also inhibit (66, 67). This has, as discussed in the following paragraph, an impact on the balance of CD4$^+$ Tconv and Treg.

In patients treated with antidepressants inhibiting ASM activity like amitriptyline or sertraline (68) no (CD4$^+$) lymphopenia has been reported. This might be due to the relatively low concentrations of ASM-inhibiting antidepressants in peripheral blood of humans (about 1 μM) (69). In secondary lymphoid organs it is, however, assumed that up to 10-fold higher concentrations are reached (69). As ASM inhibitors are sufficient to kill human CD4$^+$ Tconv *in vitro* this indicates that ASM inhibitors might also induce cell death in human CD4$^+$ Tconv in secondary lymphoid organs *in vivo*. For mice we had observed that the negative effects on CD4$^+$ Tconv cell numbers in spleen and lymph nodes after Asm inhibition *in vivo* were less pronounced than after *in vitro* treatment of mouse T cells (66). Similar to patients, serum concentrations of amitriptyline in these mice were also in the order of 1 μM (70). This might indicate that there are pro-survival factors present *in vivo* which were lacking in the *in vitro* cell cultures. But despite such putatively beneficial factors, a reduction in CD4$^+$ Tconv numbers in spleens and less so in lymph nodes was observed (66), which is best explained by induction of cell death in a fraction of these cells. Therefore, in humans *in vivo* CD4$^+$ Tconv depletion might also take place on a small scale. Due to the long-term use of antidepressants by patients and the very low output rate of the thymus in adults (71) it may well be that these patients gradually become lymphopenic over time.

TREG

Treg differ from CD4$^+$ Tconv and CD8$^+$ T cells in that, due to their autoreactivity (11, 12), they constantly receive activating signals through their T cell receptor—even in healthy subjects.

Apart from the T cell receptor, signaling through CD28 and the high affinity IL-2 receptor are crucial to maintain Treg numbers and function (72–77). For CD28 it has been shown that ligation with monoclonal antibodies strongly increases ASM activity in human T cells (33). In line with their dependence on CD28 signaling for survival, both mouse (66) and human Treg (Dennstaedt, Schneider-Schaulies, Beyersdorf, unpublished) show constitutively higher ASM activity than $CD4^+$ Tconv and for mouse Treg it has been shown that they also contain increased amounts of ceramide compared to $CD4^+$ Tconv (66, 78).

Apart from the Asm, underexpression of the sphingomyelin synthase 1 (Sms1) in Treg vs. $CD4^+$ Tconv contributes to the increased ceramide content of Treg vs. $CD4^+$ Tconv (78). The increase in ceramide induced by this lack of Sms1 maintains suppression of the Akt/mTOR pathway in Treg through the phosphatase PP2A. Suppression of Akt/mTOR signaling is crucial for Treg to be able to inhibit $CD4^+$ Tconv (78).

Currently, it is unclear whether or how much the ceramide pools regulated by Asm and Sms1 activity overlap. This is of importance as for the activation of the phosphatase PP2A its inhibitor SET needs to bind to ceramide (79). The Asm is expressed in the inner leaflet of the lysosomal membrane and translocates to the outer leaflet of the cell membrane upon T cell activation and fusion of the lsysome with the cell membrane. Therefore, Asm activity generates ceramide in the inner leaflet of the lysosome and the outer leaflet of the cell membrane. However, ceramide spontaneously flips from one membrane leaflet to the other and for other sphingolipid species "filppase"-mediated exchange between membrane leaflets has been described [reviewed in (29)]. As ceramide generated by the Asm may, thus, also accumulate in the cytosolic leaflet of membranes Asm activity might enhance PP2A activity in Treg. Genetic deficiency for the Asm in mice led to an increase in the proportion of Treg among $CD4^+$ T cells (66), which would be in line with this hypothesis. However, the suppressive activity of Treg was increased on a per-call basis as read out in surrogate *in vitro* suppression assays (66). This suggest that ceramide generated by the Asm may not be critical for PP2A activity as otherwise suppression by Treg would have been lost (78). More definite conclusions regarding the ceramide pools regulated by the Asm vs. the Sms1 are not possible as the changes in sphingolipid composition in cells of Asm-deficient compared to wildtype mice are very complex. Despite their Asm deficiency, T cells, and other cells, display strongly increased ceramide levels (66, 80, 81). In parallel, the sphingomyelin content of these cells is even further increased (66, 80, 81). This means that the substrate/product ratio for the Asm is reduced in these animals as might be expected due to the Asm deficiency. However, it is currently unclear what exactly drives the changes we observed in these animals with regard to Treg: Whether it is the overall amount of sphingolipids found in these cells or whether it is the sphingolipid composition of membranes.

For Treg a plethora of different molecular mechanisms has been described by which they might inhibit other T cells [reviewed in (13)]. A crucial effector molecule, mediating cell contact-dependent suppression by Treg is the checkpoint molecule CTLA-4 (82–85). Being strongly activated we observed higher CTLA-4 expression in Treg of Asm-deficient vs. wildtype mice (66). CTLA-4 functions as an immune checkpoint by removing costimulatory molecules from the surface of antigen-presenting cells like dendritic cells or B cells (83, 84). This process is called transendocytosis. As the costimulatory receptor CD28 and CTLA-4 share the ligands CD80 and CD86, CTLA-4-mediated transendocytosis leads to a net reduction in T cell costimulation and, thus, immunosuppression. During transendocytosis, the complex of CTLA-4 and bound ligand is internalized and degraded within the lysosome [reviewed in (84)]. In fact, endo-lysosomal vesicles contain the vast majority of CTLA-4 molecules expressed by a T cell under steady-state conditions. Only upon activation CTLA-4 surface expression is increased, primarily within the immunological synapse (86). The low CTLA-4 surface expression is the consequence of shuttling from endo-lysosomal compartments to the cell surface followed by rapid internalization in the absence of ligand binding [reviewed in (84)]. Therefore, the biological activity of CTLA-4 is governed by this complex expression pattern. Using a so-called "capture assay" we monitored CTLA-4 turn-over between the cell membrane and cellular compartments in Treg from wild-type and Asm-deficient mice (66). Here, we observed that Treg from Asm-deficient mice showed a higher turn-over than Treg from wild-type mice.

For human Treg we used pharmacological inhibitors of the ASM to study its impact on CTLA-4 function and turn-over. We observed that inhibition of the ASM in human Treg increased CTLA-4 turn-over as observed in Treg from Asm-deficient mice (Wiese, Schneider-Schaulies, Beyersdorf, unpublished). Therefore, both in mouse and in human Treg, ASM activity is important for the turn-over of CTLA-4.

Although Treg generation is the "third function" of the thymus, Treg may also differentiate from $CD4^+$ Tconv in mice under certain conditions (87). The generation of so-called peripherally induced Treg (pTreg) is thought to be of particular importance for immunity in humans [reviewed in (88)]. The identification of two distinct thymic Treg precursors in mice expressing predominantly self-reactive TCRs and TCRs with reactivity to foreign antigen (12), however, challenges this concept and might pinpoint to the thymus as the sole source of *bona fide* Treg also in humans. Together these findings mean that by studying conditions under which pTreg can be generated from $CD4^+$ Tconv *in vitro* one analyses the impact of certain factors primarily on the stability of the Treg lineage. Using such *in vitro* systems it was observed that Asm activity has a supportive effect for pTreg generation from Tconv (89).

OUTLOOK

Up to now antidepressants inhibiting ASM activity are the most widely applied drugs in humans directly impacting on ceramide generation from sphingomyelin (prevalence depression: 5,000/100,000) (90). As these drugs not only induce degradation of the ASM, but also the acid ceramidase (67), more specific direct inhibitors would be clinically desirable.

With bisphosphonates such as zoledronate, which are used for the treatment of osteoporosis (prevalence: about 5,000/100,000 in people in their fifties and 25,000/100,000 in octogenerians) (91), safe drugs are available that directly inhibit ASM activity. Currently, it is, however, unclear whether bisphosphonates, including the very potent ASM inhibitor ARC39 (92, 93), will also modulate ASM activity in T cells *in vivo* or whether their high degree of binding to bone surfaces and osteoclasts prohibits sufficient drug levels in secondary lymphoid organs to modulate T cell activity.

The data obtained on the contribution of ASM and NSM2 activity to T cell function in preclinical mouse models and with human T cells *in vitro* all suggest that pharmacologically blocking these enzymes will either directly or, through biasing the $CD4^+$ T cell compartment toward Treg, indirectly impair T cell function. Therefore, a potential novel indication for the use of ASM or possibly also NSM2 inhibitors might be autoimmune diseases such as multiple sclerosis (prevalence: about 100/100,000) (94, 95). As discussed, overshooting immunity in the course of e.g., an influenza A virus infection may constitute another potential novel application for ASM inhibitors.

As sphingomyelinase deficiency impairs T cell function boosting sphingomyelinase activity might increase their function which could improve e.g., anti-cancer immunity. Indeed, it has recently been shown that T cell-specific overexpression of the ASM leads to enhanced T cell-mediated immunity against the parasite *Plasmodium yoelii* (96). This suggests that also in humans increasing ASM activity in T cells might enhance T cell-mediated immunity. Therefore, future research should focus on identifying suitable drugs for increasing ASM activity in human T cells.

Growing knowledge on the role of sphingolipid metabolism in T cell biology fuelled by the generation of novel inducible knock-out mouse models as well as novel analytical tools will help to define more potential therapeutic targets. For these, either small molecule or monoclonal antibody-based therapies may allow for specific targeting.

DATA AVAILABILITY STATEMENT

All datasets generated for this study are included in the manuscript/supplementary files.

AUTHOR CONTRIBUTIONS

CH, TW, and FD generated data and edited the paper. JF designed figures. JS-S designed figures and edited the paper. NB wrote the paper.

FUNDING

This work has been funded by grants from the Deutsche Forschungsgemeinschaft (FOR2123/P02 and Z01). The publication as such was funded by the German Research Foundation (DFG) and the University of Würzburg in the funding programme Open Access Publishing.

REFERENCES

1. Klein L, Kyewski B, Allen PM, Hogquist KA. Positive and negative selection of the T cell repertoire: what thymocytes see (and don't see). *Nat Rev Immunol.* (2014) 14:377–91. doi: 10.1038/nri3667
2. Ota K, Matsui M, Milford EL, Mackin GA, Weiner HL, Hafler DA. T-cell recognition of an immunodominant myelin basic protein epitope in multiple sclerosis. *Nature.* (1990) 346:183–7. doi: 10.1038/346183a0
3. Zhang J, Markovic-Plese S, Lacet B, Raus J, Weiner HL, Hafler DA. Increased frequency of interleukin 2-responsive T cells specific for myelin basic protein and proteolipid protein in peripheral blood and cerebrospinal fluid of patients with multiple sclerosis. *J Exp Med.* (1994) 179:973–84. doi: 10.1084/jem.179.3.973
4. Scholz C, Patton KT, Anderson DE, Freeman GJ, Hafler DA. Expansion of autoreactive T cells in multiple sclerosis is independent of exogenous B7 costimulation. *J Immunol.* (1998) 160:1532–8.
5. Cao Y, Goods BA, Raddassi K, Nepom GT, Kwok WW, Love JC, et al. Functional inflammatory profiles distinguish myelin-reactive T cells from patients with multiple sclerosis. *Sci Transl Med.* (2015) 7:287ra274. doi: 10.1126/scitranslmed.aaa8038
6. Seddon B, Mason D. The third function of the thymus. *Immunol Today.* (2000) 21:95–9. doi: 10.1016/S0167-5699(99)01559-5
7. Fontenot JD, Gavin MA, Rudensky AY. Foxp3 programs the development and function of $CD4^+CD25^+$ regulatory T cells. *Nat Immunol.* (2003) 4:330–6. doi: 10.1038/ni904
8. Hori S, Nomura T, Sakaguchi S. Control of regulatory T cell development by the transcription factor Foxp3. *Science.* (2003) 299:1057–61. doi: 10.1126/science.1079490
9. Walker MR, Kasprowicz DJ, Gersuk VH, Benard A, Van Landeghen M, Buckner JH, et al. Induction of FoxP3 and acquisition of T regulatory activity by stimulated human $CD4^+CD25^-$ T cells. *J Clin Invest.* (2003) 112:1437–43. doi: 10.1172/JCI19441
10. van Santen HM, Benoist C, Mathis D. Number of T reg cells that differentiate does not increase upon encounter of agonist ligand on thymic epithelial cells. *J Exp Med.* (2004) 200:1221–30. doi: 10.1084/jem.20041022
11. Hsieh CS, Liang Y, Tyznik AJ, Self SG, Liggitt D, Rudensky AY. Recognition of the peripheral self by naturally arising $CD25^+$ $CD4^+$ T cell receptors. *Immunity.* (2004) 21:267–77. doi: 10.1016/j.immuni.2004.07.009
12. Owen DL, Mahmud SA, Sjaastad LE, Williams JB, Spanier JA, Simeonov DR, et al. Thymic regulatory T cells arise via two distinct developmental programs. *Nat Immunol.* (2019) 20:195–205. doi: 10.1038/s41590-018-0289-6
13. Yamaguchi T, Wing JB, Sakaguchi S. Two modes of immune suppression by Foxp3(+) regulatory T cells under inflammatory or non-inflammatory conditions. *Semin Immunol.* (2011) 23:424–30. doi: 10.1016/j.smim.2011.10.002
14. Joffre O, Nolte MA, Sporri R, Reis e Sousa C. Inflammatory signals in dendritic cell activation and the induction of adaptive immunity. *Immunol Rev.* (2009) 227:234–47. doi: 10.1111/j.1600-065X.2008.00718.x
15. Thornton AM, Shevach EM. $CD4^+CD25^+$ immunoregulatory T cells suppress polyclonal T cell activation *in vitro* by inhibiting interleukin 2 production. *J Exp Med.* (1998) 188:287–96. doi: 10.1084/jem.188.2.287
16. Thornton AM, Donovan EE, Piccirillo CA, Shevach EM. Cutting edge: IL-2 is critically required for the *in vitro* activation of $CD4^+CD25^+$ T cell suppressor function. *J Immunol.* (2004) 172:6519–23. doi: 10.4049/jimmunol.172.11.6519
17. Beyersdorf N, Balbach K, Hunig T, Kerkau T. Large-scale expansion of rat $CD4^+$ $CD25^+$ T(reg) cells in the absence of T-cell receptor stimulation. *Immunology.* (2006) 119:441–50. doi: 10.1111/j.1365-2567.2006.02455.x

18. Fletcher JM, Lalor SJ, Sweeney CM, Tubridy N, Mills KH. T cells in multiple sclerosis and experimental autoimmune encephalomyelitis. *Clin Exp Immunol.* (2010) 162:1–11. doi: 10.1111/j.1365-2249.2010.04143.x
19. Pugliese A. Autoreactive T cells in type 1 diabetes. *J Clin Invest.* (2017) 127:2881–91. doi: 10.1172/JCI94549
20. Imam T, Park S, Kaplan MH, Olson MR. Effector T helper cell subsets in inflammatory bowel diseases. *Front Immunol.* (2018) 9:1212. doi: 10.3389/fimmu.2018.01212
21. McInnes IB, Schett G. The pathogenesis of rheumatoid arthritis. *N Engl J Med.* (2011) 365:2205–19. doi: 10.1056/NEJMra1004965
22. Tsokos GC. Systemic lupus erythematosus. *N Engl J Med.* (2011) 365:2110–21. doi: 10.1056/NEJMra1100359
23. Burzyn D, Kuswanto W, Kolodin D, Shadrach JL, Cerletti M, Jang Y, et al. A special population of regulatory T cells potentiates muscle repair. *Cell.* (2013) 155:1282–95. doi: 10.1016/j.cell.2013.10.054
24. Tang TT, Yuan J, Zhu ZF, Zhang WC, Xiao H, Xia N, et al. Regulatory T cells ameliorate cardiac remodeling after myocardial infarction. *Basic Res Cardiol.* (2012) 107:232. doi: 10.1007/s00395-011-0232-6
25. Weirather J, Hofmann UD, Beyersdorf N, Ramos GC, Vogel B, Frey A, et al. Foxp3$^+$ CD4$^+$ T cells improve healing after myocardial infarction by modulating monocyte/macrophage differentiation. *Circ Res.* (2014) 115:55–67. doi: 10.1161/CIRCRESAHA.115.303895
26. Zeng Z, Yu K, Chen L, Li W, Xiao H, Huang Z. Interleukin-2/anti-interleukin-2 immune complex attenuates cardiac remodeling after myocardial infarction through expansion of regulatory T cells. *J Immunol Res.* (2016) 2016:8493767. doi: 10.1155/2016/8493767
27. Na SY, Mracsko E, Liesz A, Hunig T, Veltkamp R. Amplification of regulatory T cells using a CD28 superagonist reduces brain damage after ischemic stroke in mice. *Stroke.* (2015) 46:212–20. doi: 10.1161/STROKEAHA.114.007756
28. van Meer G, Voelker DR, Feigenson GW. Membrane lipids: where they are and how they behave. *Nat Rev Mol Cell Biol.* (2008) 9:112–24. doi: 10.1038/nrm2330
29. Hannun YA, Obeid LM. Sphingolipids and their metabolism in physiology and disease. *Nat Rev Mol Cell Biol.* (2018) 19:175–91. doi: 10.1038/nrm.2017.107
30. Bartke N, Hannun YA. Bioactive sphingolipids: metabolism and function. *J Lipid Res.* (2009) 50:S91–6. doi: 10.1194/jlr.R800080-JLR200
31. Milhas D, Clarke CJ, Hannun YA. Sphingomyelin metabolism at the plasma membrane: implications for bioactive sphingolipids. *FEBS Lett.* (2010) 584:1887–94. doi: 10.1016/j.febslet.2009.10.058
32. Spiegel S, Milstien S. The outs and the ins of sphingosine-1-phosphate in immunity. *Nat Rev Immunol.* (2011) 11:403–15. doi: 10.1038/nri2974
33. Boucher LM, Wiegmann K, Futterer A, Pfeffer K, Machleidt T, Schutze S, et al. CD28 signals through acidic sphingomyelinase. *J Exp Med.* (1995) 181:2059–68. doi: 10.1084/jem.181.6.2059
34. Cifone MG, De Maria R, Roncaioli P, Rippo MR, Azuma M, Lanier LL, et al. Apoptotic signaling through CD95 (Fas/Apo-1) activates an acidic sphingomyelinase. *J Exp Med.* (1994) 180:1547–52. doi: 10.1084/jem.180.4.1547
35. Hofmann K, Tomiuk S, Wolff G, Stoffel W. Cloning and characterization of the mammalian brain-specific, Mg^{2+}-dependent neutral sphingomyelinase. *Proc Natl Acad Sci USA.* (2000) 97:5895–900. doi: 10.1073/pnas.97.11.5895
36. Milhas D, Clarke CJ, Idkowiak-Baldys J, Canals D, Hannun YA. Anterograde and retrograde transport of neutral sphingomyelinase-2 between the Golgi and the plasma membrane. *Biochim Biophys Acta.* (2010) 1801:1361–74. doi: 10.1016/j.bbalip.2010.08.001
37. Stoffel W, Hammels I, Jenke B, Binczek E, Schmidt-Soltau I, Brodesser S, et al. Neutral sphingomyelinase (SMPD3) deficiency disrupts the Golgi secretory pathway and causes growth inhibition. *Cell Death Dis.* (2016) 7:e2488. doi: 10.1038/cddis.2016.385
38. Back MJ, Ha HC, Fu Z, Choi JM, Piao Y, Won JH, et al. Activation of neutral sphingomyelinase 2 by starvation induces cell-protective autophagy via an increase in Golgi-localized ceramide. *Cell Death Dis.* (2018) 9:670. doi: 10.1038/s41419-018-0709-4
39. Mueller N, Avota E, Collenburg L, Grassme H, Schneider-Schaulies S. Neutral sphingomyelinase in physiological and measles virus induced T cell suppression. *PLoS Pathog.* (2014) 10:e1004574. doi: 10.1371/journal.ppat.1004574
40. Cingolani F, Futerman AH, Casas J. Ceramide synthases in biomedical research. *Chem Phys Lipids.* (2016) 197:25–32. doi: 10.1016/j.chemphyslip.2015.07.026
41. Wherry EJ, Ahmed R. Memory CD8 T-cell differentiation during viral infection. *J Virol.* (2004) 78:5535–45. doi: 10.1128/JVI.78.11.5535-5545.2004
42. van den Brink MR, Burakoff SJ. Cytolytic pathways in haematopoietic stem-cell transplantation. *Nat Rev Immunol.* (2002) 2:273–81. doi: 10.1038/nri775
43. Cohnen A, Chiang SC, Stojanovic A, Schmidt H, Claus M, Saftig P, et al. Surface CD107a/LAMP-1 protects natural killer cells from degranulation-associated damage. *Blood.* (2013) 122:1411–8. doi: 10.1182/blood-2012-07-441832
44. Jenkins MR, Griffiths GM. The synapse and cytolytic machinery of cytotoxic T cells. *Curr Opin Immunol.* (2010) 22:308–13. doi: 10.1016/j.coi.2010.02.008
45. Herz J, Pardo J, Kashkar H, Schramm M, Kuzmenkina E, Bos E, et al. Acid sphingomyelinase is a key regulator of cytotoxic granule secretion by primary T lymphocytes. *Nat Immunol.* (2009) 10:761–8. doi: 10.1038/ni.1757
46. Duan S, Thomas PG. Balancing immune protection and immune pathology by CD8(+) T-cell responses to influenza infection. *Front Immunol.* (2016) 7:25. doi: 10.3389/fimmu.2016.00025
47. von Bismarck P, Wistadt CF, Klemm K, Winoto-Morbach S, Uhlig U, Schutze S, et al. Improved pulmonary function by acid sphingomyelinase inhibition in a newborn piglet lavage model. *Am J Respir Crit Care Med.* (2008) 177:1233–41. doi: 10.1164/rccm.200705-752OC
48. Peng H, Li C, Kadow S, Henry BD, Steinmann J, Becker KA, et al. Acid sphingomyelinase inhibition protects mice from lung edema and lethal *Staphylococcus aureus* sepsis. *J Mol Med.* (2015) 93:675–89. doi: 10.1007/s00109-014-1246-y
49. Pandolfi R, Barreira B, Moreno E, Lara-Acedo V, Morales-Cano D, Martinez-Ramas A, et al. Role of acid sphingomyelinase and IL-6 as mediators of endotoxin-induced pulmonary vascular dysfunction. *Thorax.* (2017) 72:460–71. doi: 10.1136/thoraxjnl-2015-208067
50. Miguel L, Owen DM, Lim C, Liebig C, Evans J, Magee AI, et al. Primary human CD4$^+$ T cells have diverse levels of membrane lipid order that correlate with their function. *J Immunol.* (2011) 186:3505–16. doi: 10.4049/jimmunol.1002980
51. Bai A, Moss A, Kokkotou E, Usheva A, Sun X, Cheifetz A, et al. CD39 and CD161 modulate Th17 responses in Crohn's disease. *J Immunol.* (2014) 193:3366–77. doi: 10.4049/jimmunol.1400346
52. Bai A, Kokkotou E, Zheng Y, Robson SC. Role of acid sphingomyelinase bioactivity in human CD4$^+$ T-cell activation and immune responses. *Cell Death Dis.* (2015) 6:e1828. doi: 10.1038/cddis.2015.178
53. Bai A, Guo Y. Acid sphingomyelinase mediates human CD4(+) T-cell signaling: potential roles in T-cell responses and diseases. *Cell Death Dis.* (2017) 8:e2963. doi: 10.1038/cddis.2017.360
54. Kalia V, Sarkar S. Regulation of effector and memory CD8 T cell differentiation by IL-2-a balancing act. *Front Immunol.* (2018) 9:2987. doi: 10.3389/fimmu.2018.02987
55. Stoffel B, Bauer P, Nix M, Deres K, Stoffel W. Ceramide-independent CD28 and TCR signaling but reduced IL-2 secretion in T cells of acid sphingomyelinase-deficient mice. *Eur J Immunol.* (1998) 28:874–80. doi: 10.1002/(SICI)1521-4141(199803)28:03<874::AID-IMMU874>3.0.CO;2-T
56. Collenburg L, Beyersdorf N, Wiese T, Arenz C, Saied EM, Becker-Flegler KA, et al. The activity of the neutral sphingomyelinase is important in T cell recruitment and directional migration. *Front Immunol.* (2017) 8:1007. doi: 10.3389/fimmu.2017.01007
57. Murdoch C. CXCR4: chemokine receptor extraordinaire. *Immunol Rev.* (2000) 177:175–84. doi: 10.1034/j.1600-065X.2000.17715.x
58. Bortlein C, Draeger A, Schoenauer R, Kuhlemann A, Sauer M, Schneider-Schaulies S, et al. The neutral sphingomyelinase 2 is required to polarize and sustain T cell receptor signaling. *Front Immunol.* (2018) 9:815. doi: 10.3389/fimmu.2018.00815
59. Zhan Y, Carrington EM, Zhang Y, Heinzel S, Lew AM. Life and death of activated T cells: how are they different from naive T cells? *Front Immunol.* (2017) 8:1809. doi: 10.3389/fimmu.2017.01809
60. MacLeod MK, Kappler JW, Marrack P. Memory CD4 T cells: generation, reactivation and re-assignment. *Immunology.* (2010) 130:10–5. doi: 10.1111/j.1365-2567.2010.03260.x

61. Farber DL, Yudanin NA, Restifo NP. Human memory T cells: generation, compartmentalization and homeostasis. *Nat Rev Immunol.* (2014) 14:24–35. doi: 10.1038/nri3567
62. Marrack P, Scott-Browne J, MacLeod MK. Terminating the immune response. *Immunol Rev.* (2010) 236:5–10. doi: 10.1111/j.1600-065X.2010.00928.x
63. Kirschnek S, Paris F, Weller M, Grassme H, Ferlinz K, Riehle A, et al. CD95-mediated apoptosis *in vivo* involves acid sphingomyelinase. *J Biol Chem.* (2000) 275:27316–23. doi: 10.1074/jbc.M002957200
64. Grassme H, Cremesti A, Kolesnick R, Gulbins E. Ceramide-mediated clustering is required for CD95-DISC formation. *Oncogene.* (2003) 22:5457–70. doi: 10.1038/sj.onc.1206540
65. Gulbins E. Regulation of death receptor signaling and apoptosis by ceramide. *Pharmacol Res.* (2003) 47:393–9. doi: 10.1016/S1043-6618(03)00052-5
66. Hollmann C, Werner S, Avota E, Reuter D, Japtok L, Kleuser B, et al. Inhibition of acid sphingomyelinase allows for selective targeting of $CD4^+$ conventional versus $Foxp3^+$ regulatory T cells. *J Immunol.* (2016) 197:3130–41. doi: 10.4049/jimmunol.1600691
67. Elojeimy S, Holman DH, Liu X, El-Zawahry A, Villani M, Cheng JC, et al. New insights on the use of desipramine as an inhibitor for acid ceramidase. *FEBS Lett.* (2006) 580:4751–6. doi: 10.1016/j.febslet.2006.07.071
68. Kornhuber J, Muehlbacher M, Trapp S, Pechmann S, Friedl A, Reichel M, et al. Identification of novel functional inhibitors of acid sphingomyelinase. *PLoS ONE.* (2011) 6:e23852. doi: 10.1371/journal.pone.0023852
69. Gobin V, Van Steendam K, Denys D, Deforce D. Selective serotonin reuptake inhibitors as a novel class of immunosuppressants. *Int Immunopharmacol.* (2014) 20:148–56. doi: 10.1016/j.intimp.2014.02.030
70. Hollmann C. *Role of the acid sphingomyelinase in anti-viral T cell responses in a measles virus infection model* (Ph.D. thesis). University of Würzburg, Würzburg (2017).
71. den Braber I, Mugwagwa T, Vrisekoop N, Westera L, Mogling R, de Boer AB, et al. Maintenance of peripheral naive T cells is sustained by thymus output in mice but not humans. *Immunity.* (2012) 36:288–97. doi: 10.1016/j.immuni.2012.02.006
72. Salomon B, Lenschow DJ, Rhee L, Ashourian N, Singh B, Sharpe A, et al. B7/CD28 costimulation is essential for the homeostasis of the $CD4^+CD25^+$ immunoregulatory T cells that control autoimmune diabetes. *Immunity.* (2000) 12:431–40. doi: 10.1016/S1074-7613(00)80195-8
73. Tang Q, Henriksen KJ, Boden EK, Tooley AJ, Ye J, Subudhi SK, et al. Cutting edge: CD28 controls peripheral homeostasis of $CD4^+CD25^+$ regulatory T cells. *J Immunol.* (2003) 171:3348–52. doi: 10.4049/jimmunol.171.7.3348
74. D'Cruz LM, Klein L. Development and function of agonist-induced $CD25^+Foxp3^+$ regulatory T cells in the absence of interleukin 2 signaling. *Nat Immunol.* (2005) 6:1152–9. doi: 10.1038/ni1264
75. Fontenot JD, Rasmussen JP, Gavin MA, Rudensky AY. A function for interleukin 2 in Foxp3-expressing regulatory T cells. *Nat Immunol.* (2005) 6:1142–51. doi: 10.1038/ni1263
76. Gogishvili T, Luhder F, Goebbels S, Beer-Hammer S, Pfeffer K, Hunig T. Cell-intrinsic and -extrinsic control of Treg-cell homeostasis and function revealed by induced CD28 deletion. *Eur J Immunol.* (2013) 43:188–93. doi: 10.1002/eji.201242824
77. Zhang R, Huynh A, Whitcher G, Chang J, Maltzman JS, Turka LA. An obligate cell-intrinsic function for CD28 in Tregs. *J Clin Invest.* (2013) 123:580–93. doi: 10.1172/JCI65013
78. Apostolidis SA, Rodriguez-Rodriguez N, Suarez-Fueyo A, Dioufa N, Ozcan E, Crispin JC, et al. Phosphatase PP2A is requisite for the function of regulatory T cells. *Nat Immunol.* (2016) 17:556–64. doi: 10.1038/ni.3390
79. Mukhopadhyay A, Saddoughi SA, Song P, Sultan I, Ponnusamy S, Senkal CE, et al. Direct interaction between the inhibitor 2 and ceramide via sphingolipid-protein binding is involved in the regulation of protein phosphatase 2A activity and signaling. *FASEB J.* (2009) 23:751–63. doi: 10.1096/fj.08-120550
80. Horinouchi K, Erlich S, Perl DP, Ferlinz K, Bisgaier CL, Sandhoff K, et al. Acid sphingomyelinase deficient mice: a model of types A and B Niemann-Pick disease. *Nat Genet.* (1995) 10:288–93. doi: 10.1038/ng0795-288
81. Schuchman EH, Wasserstein MP. Types A and B Niemann-Pick disease. *Best Pract Res Clin Endocrinol Metab.* (2015) 29:237–47. doi: 10.1016/j.beem.2014.10.002
82. Wing K, Onishi Y, Prieto-Martin P, Yamaguchi T, Miyara M, Fehervari Z, et al. CTLA-4 control over $Foxp3^+$ regulatory T cell function. *Science.* (2008) 322:271–5. doi: 10.1126/science.1160062
83. Qureshi OS, Zheng Y, Nakamura K, Attridge K, Manzotti C, Schmidt EM, et al. Trans-endocytosis of CD80 and CD86: a molecular basis for the cell-extrinsic function of CTLA-4. *Science.* (2011) 332:600–3. doi: 10.1126/science.1202947
84. Walker LS, Sansom DM. The emerging role of CTLA4 as a cell-extrinsic regulator of T cell responses. *Nat Rev Immunol.* (2011) 11:852–63. doi: 10.1038/nri3108
85. Hou TZ, Qureshi OS, Wang CJ, Baker J, Young SP, Walker LS, et al. A transendocytosis model of CTLA-4 function predicts its suppressive behavior on regulatory T cells. *J Immunol.* (2015) 194:2148–59. doi: 10.4049/jimmunol.1401876
86. Pentcheva-Hoang T, Egen JG, Wojnoonski K, Allison JP. B7-1 and B7-2 selectively recruit CTLA-4 and CD28 to the immunological synapse. *Immunity.* (2004) 21:401–13. doi: 10.1016/j.immuni.2004.06.017
87. Kretschmer K, Apostolou I, Hawiger D, Khazaie K, Nussenzweig MC, von Boehmer H. Inducing and expanding regulatory T cell populations by foreign antigen. *Nat Immunol.* (2005) 6:1219–27. doi: 10.1038/ni1265
88. Akbar AN, Vukmanovic-Stejic M, Taams LS, Macallan DC. The dynamic co-evolution of memory and regulatory $CD4^+$ T cells in the periphery. *Nat Rev Immunol.* (2007) 7:231–7. doi: 10.1038/nri2037
89. Zhou Y, Salker MS, Walker B, Munzer P, Borst O, Gawaz M, et al. Acid sphingomyelinase (ASM) is a negative regulator of regulatory T cell (Treg) development. *Cell Physiol Biochem.* (2016) 39:985–95. doi: 10.1159/000447806
90. World Health Organization. *Depression and Other Common Mental Disorders: Global Health Estimates*. Licence: CC BY-NC-SA 3.0 IGO. (2017).
91. Wright NC, Looker AC, Saag KG, Curtis JR, Delzell ES, Randall S, et al. The recent prevalence of osteoporosis and low bone mass in the United States based on bone mineral density at the femoral neck or lumbar spine. *J Bone Miner Res.* (2014) 29:2520–6. doi: 10.1002/jbmr.2269
92. Roth AG, Drescher D, Yang Y, Redmer S, Uhlig S, Arenz C. Potent and selective inhibition of acid sphingomyelinase by bisphosphonates. *Angew Chem Int Ed Engl.* (2009) 48:7560–3. doi: 10.1002/anie.200903288
93. Arenz C. Small molecule inhibitors of acid sphingomyelinase. *Cell Physiol Biochem.* (2010) 26:1–8. doi: 10.1159/000315100
94. Pugliatti M, Rosati G, Carton H, Riise T, Drulovic J, Vecsei L, et al. The epidemiology of multiple sclerosis in Europe. *Eur J Neurol.* (2006) 13:700–22. doi: 10.1111/j.1468-1331.2006.01342.x
95. Mackenzie IS, Morant SV, Bloomfield GA, MacDonald TM, O'Riordan J. Incidence and prevalence of multiple sclerosis in the UK 1990-2010: a descriptive study in the General Practice Research Database. *J Neurol Neurosurg Psychiatr.* (2014) 85:76–84. doi: 10.1136/jnnp-2013-305450
96. Hose M, Gunther A, Abberger H, Begum S, Korencak M, Becker KA, et al. T cell-specific overexpression of acid sphingomyelinase results in elevated T cell activation and reduced parasitemia during *Plasmodium yoelii* infection. *Front Immunol.* (2019) 10:1225. doi: 10.3389/fimmu.2019.01225

Conflict of Interest: The authors declare that the research was conducted in the absence of any commercial or financial relationships that could be construed as a potential conflict of interest.

frontiers in Cell and Developmental Biology

ORIGINAL RESEARCH
published: 15 October 2019
doi: 10.3389/fcell.2019.00226

Role of Neutral Sphingomyelinase-2 (NSM 2) in the Control of T Cell Plasma Membrane Lipid Composition and Cholesterol Homeostasis

*Charlene Börtlein[1], Fabian Schumacher[2,3], Burkhard Kleuser[2], Lars Dölken[1] and Elita Avota[1]**

[1] Institute for Virology and Immunobiology, University of Würzburg, Würzburg, Germany, [2] Department of Toxicology, Institute of Nutritional Science, Faculty of Mathematics and Natural Science, University of Potsdam, Nuthetal, Germany, [3] Department of Molecular Biology, University of Duisburg-Essen, Essen, Germany

The activity of neutral sphingomyelinase-2 (NSM2) to catalyze the conversion of sphingomyelin (SM) to ceramide and phosphocholine at the cytosolic leaflet of plasma membrane (PM) is important in T cell receptor (TCR) signaling. We recently identified PKCζ as a major NSM2 downstream effector which regulates microtubular polarization. It remained, however, unclear to what extent NSM2 activity affected overall composition of PM lipids and downstream effector lipids in antigen stimulated T cells. Here, we provide a detailed lipidomics analyses on PM fractions isolated from TCR stimulated wild type and NSM2 deficient (ΔNSM) Jurkat T cells. This revealed that in addition to that of sphingolipids, NSM2 depletion also affected concentrations of many other lipids. In particular, NSM2 ablation resulted in increase of lyso-phosphatidylcholine (LPC) and lyso-phosphatidylethanolamine (LPE) which both govern PM biophysical properties. Crucially, TCR dependent upregulation of the important T cell signaling lipid diacylglycerol (DAG), which is fundamental for activation of conventional and novel PKCs, was abolished in ΔNSM cells. Moreover, NSM2 activity was found to play an important role in PM cholesterol transport to the endoplasmic reticulum (ER) and production of cholesteryl esters (CE) there. Most importantly, CE accumulation was essential to sustain human T cell proliferation. Accordingly, inhibition of CE generating enzymes, the cholesterol acetyltransferases ACAT1/SOAT1 and ACAT2/SOAT2, impaired TCR driven expansion of both $CD4^+$ and $CD8^+$ T cells. In summary, our study reveals an important role of NSM2 in regulating T cell functions by its multiple effects on PM lipids and cholesterol homeostasis.

Keywords: neutral sphingomyelinase-2, T cell receptor, plasma membrane, lyso-phospholipids, diacylglycerol, cholesteryl ester

OPEN ACCESS

Edited by:
Pushpendra Singh, Johns Hopkins University, United States

Reviewed by:
Erdinc Sezgin, University of Oxford, United Kingdom
Irena Levitan, University of Illinois at Chicago, United States

****Correspondence:***
Elita Avota
elita.avota@vim.uni-wuerzburg.de

Specialty section:
This article was submitted to Membrane Physiology and Membrane Biophysics, a section of the journal Frontiers in Cell and Developmental Biology

Received: *19 June 2019*
Accepted: *24 September 2019*
Published: *15 October 2019*

Citation:
Börtlein C, Schumacher F, Kleuser B, Dölken L and Avota E (2019) Role of Neutral Sphingomyelinase-2 (NSM 2) in the Control of T Cell Plasma Membrane Lipid Composition and Cholesterol Homeostasis. Front. Cell Dev. Biol. 7:226. doi: 10.3389/fcell.2019.00226

INTRODUCTION

Neutral sphingomyelinase-2 (NSM2) is the best studied NSM of the four mammalian sphingomyelinases that are active at neutral pH. It is intensively involved in cellular physiology and pathology (Shamseddine et al., 2015). The NSM2 protein, encoded by the SMPD3 gene, has two N-terminal hydrophobic segments associated with cytosolic membrane leaflets and a C-terminal

catalytic site (Hofmann et al., 2000). In addition to phosphorylation (Filosto et al., 2010, 2012), a conformational switch following binding to phosphatidylserine (PS) has been proposed to be crucial in enzymatic activation (Airola et al., 2017; Shanbhogue et al., 2019). NSM2-catalyzed sphingomyelin breakdown commonly occurs in response to cellular stress and regulates bone mineralization. Being most abundant in brain, NSM2 is also ubiquitously expressed including cells of the immune system. The role of NSM2 in cytokine (IL1-β, TNF-α, and IFN-γ) induced inflammation and bacterial infections is well established (Shamseddine et al., 2015; Wu et al., 2018) as is its role in cytotoxic effects of cancer chemotherapeutics. However, the involvement in pathogenesis and perpetuation of human tumors seems to be tumor specific (Bhati et al., 2008; Kim et al., 2008; Henry et al., 2013).

Tonnetti et al. (1999) first reported NSM activation after antibody ligation of the T cell receptor (TCR) already 20 years ago. NSM2-deficient mice show high embryonic lethality, dwarfism and fragile bones. This prevented studies on NSM2 function in the immune system (Stoffel et al., 2005; Alebrahim et al., 2014). Furthermore, the lack of specific and sensitive antibodies for detection of the rather sparse amounts of NSM2 expressed in T cells hampered the progress in the field. Nevertheless, NSM2 proved to be essential for TCR signal amplification and sustainment at low antigen doses inducing PKCζ dependent microtubule polarization and vesicular transport (Bortlein et al., 2018). It was shown that T cell morphological polarization and directional migration in response to chemotactic signals are dependent on intact NSM2 activity (Collenburg et al., 2017). Studies on measles virus contacted T cells and tumor cells revealed a strong impact of sphingomyelinase activity and sphingolipids in general on T cell cytoskeleton dynamics (Zeidan et al., 2008; Gassert et al., 2009; Creekmore et al., 2013).

Neutral sphingomyelinase-2 is palmitoylated and predominantly resides at the inner plasma membrane (PM) leaflet mediating sphingomyelinase-dependent ceramide formation there (Hinkovska-Galcheva et al., 1998; Tani and Hannun, 2007). Alternatively, NSM2 was found in the Golgi compartment of primary mouse chondrocytes where it regulated sphingolipid and diacylglycerol (DAG) homeostasis (Stoffel et al., 2016). There is increasing evidence for the importance of NSM2 function in the generation of ceramides. Overexpression of NSM2 in the breast cancer cell line MCF7 showed 60% upregulation of Cer (Marchesini et al., 2003). Pharmacological NSM2 inhibition resulted in the accumulation of unsaturated long-chain sphingomyelins SM36 and SM38 in the mouse brain (Tan et al., 2018) and ceramides with a fatty acid chain length of 16 to 26 were less abundant in fibroblasts from SMPD3 deletion mutant *fro/fro* mice. Notable, accumulation of cholesterol was also observed in these cells (Qin et al., 2012). A key shortcoming of all previous studies is that they were performed on total cell extracts. Accordingly, they did not allow for assignment of NSM2 activity to cellular compartments or to T cell specific functions. Although NSM2 is now well described to be important for the formation of cholesterol-rich microdomains that promote lipid and protein segregation, the mechanism of how ceramide platforms and specifically NSM2 orchestrate PM structural and signaling properties upon TCR stimulation remain unclear (Eich et al., 2016; Tan et al., 2018). We therefore performed lipidomics of PM fractions isolated from NSM2-deficient and sufficient Jurkat cells to study the NSM2 dependent regulation of sphingolipids and other types of structural and functional PM lipids upon TCR ligation with α-CD3 antibody. NSM2 proved to be primarily active at the PM rather than at the intracellular organelles. Lyso-phospholipids involved in regulation of membrane mechanics and curvature, lyso-phosphatidylcholine (LPC) and lyso-phosphatidyl-ethanolamine (LPE), were upregulated in NSM2-deficient cells. Importantly, the generation of the signaling lipids after TCR ligation, namely diacylglycerols (DAG) was dependent on NSM2 activity. As a result of imbalanced uptake and efflux, cholesterol accumulated in NSM2-deficient cells, which were unable to activate the SREBP2 transcription factor, a master regulator of lipid metabolism. Most strikingly, NSM2 ablation largely prevented accumulation of cholesteryl esters (CE) in response to TCR ligation. At a functional level, prevention of CE generation translated into a loss of sustained T cell activation.

MATERIALS AND METHODS

Ethics Statement

Primary human cells from healthy blood were obtained through the blood donor program of the Department of Transfusion Medicine, University of Würzburg, and analyzed anonymously. All experiments involving human material were conducted according to the principles expressed in the Declaration of Helsinki and ethically approved by the Ethical Committee of the Medical Faculty of the University of Würzburg. Written informed consent from blood donor program participants was not required per ethical approval.

Jurkat Cell Culture, Transfection, and Starvation Assays

CRISPR/Cas9-edited Jurkat cells deficient for NSM2 (ΔNSM) (Bortlein et al., 2018) cells were cultured in RPMI/10%FBS or in 0%FBS for serum starvation experiments and SREBP2 cleavage analysis, proliferation assays or cell synchronization before α-CD3 mediated TCR stimulation. SREBP2 specific antibody (ab30682, abcam) was used to detect full length and cleaved SREPB2 protein in Western blot of the lysates of CTRL and ΔNSM Jurkat cells after cultivation in medium supplemented or not with serum for 24 h. Cell death was analyzed by life flow cytometry of propidium iodide (Beckton-Dickinson Biosciences, Pharmingen) labeled Jurkat cells done according to manufacturers' protocol. 1×10^6 Jurkat cells were nucleofected with 5 μg plasmid pcDNA3.1-NSM2-GFP DNA expressing human NSM2-GFP fusion protein (kindly provided by Thomas Rudel) using Nucleofector Technology and program X-001 from Lonza (Basel, Switzerland) followed by live cell imaging.

Plasma Membrane Isolation and Validation

2×10^7 CTRL and ΔNSM Jurkat cells were starved in RPMI/0.5%FBS for 2 hrs and left unstimulated or stimulated for 10 min with the α-CD3 (clone UCHT-1) crosslinked with the goat α-mouse IgG (both 5 μg/ml). Plasma membranes were isolated by Minute Plasma Membrane Protein Isolation Kit (Invent Biotechnologies, Inc., United Kingdom) according to manufacturers' protocol. Up to four isolations were pooled for one PM preparation used for lipid analysis. Three preparations were analyzed for each type of cells or stimulations.

Alternatively PMs were isolated as the giant plasma membrane vesicles (GPMVs) as described previously (Sezgin et al., 2012). Shortly, 4×10^7 Jurkat cells were washed twice with GPMV buffer (10 mM HEPES, 150 mM $NaCl_2$, mM $CaCl_2$, pH7.4) and incubated in 30 ml GPMV buffer containing 2 mM NEM as a vesiculation agent at 37°C for 1 h. Cell supernatant containing GPMVs was centrifuged at 100*g* for 10 min three times to remove cell debris and upper 20 ml was centrifuged at 20,000*g* at 4°C for 1 h. The pellet containing PMs was lysed in 1% TritonX100 containing lysis buffer and 10 μg protein was used for Western blot analysis to estimate purity of PM preparation.

Plasma membrane preparations were validated by Western blot analysis using Lck (clone 3A5, Santa Cruz Biotechnology, Inc.), Actin (Sigma Aldrich, Germany) and AIF (clone D39D2, Cell Signaling Technology) specific antibodies.

Lipid Extraction for Mass Spectrometry Lipidomics

Mass spectrometry-based lipid analysis was performed by Lipotype GmbH (Dresden, Germany) as described (Sampaio et al., 2011). Lipids were extracted using a two-step chloroform/methanol procedure (Ejsing et al., 2009). Samples were spiked with internal lipid standard mixture containing: cardiolipin 16:1/15:0/15:0/15:0 (CL), ceramide 18:1;2/17:0 (Cer), diacylglycerol 17:0/17:0 (DAG), hexosylceramide 18:1;2/12:0 (HexCer), lyso-phosphatidate 17:0 (LPA), lyso-phosphatidylcholine 12:0 (LPC), lyso-phosphatidylethanolamine 17:1 (LPE), lyso-phosphatidylglycerol 17:1 (LPG), lyso-phosphatidylinositol 17:1 (LPI), lyso-phosphatidylserine 17:1 (LPS), phosphatidate 17:0/17:0 (PA), phosphatidylcholine 17:0/17:0 (PC), phosphatidylethanolamine 17:0/17:0 (PE), phosphatidylglycerol 17:0/17:0 (PG), phosphatidylinositol 16:0/16:0 (PI), phosphatidylserine 17:0/17:0 (PS), cholesterol ester 20:0 (CE), sphingomyelin 18:1;2/12:0;0 (SM) and triacylglycerol 17:0/17:0/17:0 (TAG). After extraction, the organic phase was transferred to an infusion plate and dried in a speed vacuum concentrator. 1st step dry extract was re-suspended in 7.5 mM ammonium acetate in chloroform/methanol/propanol (1:2:4, V:V:V) and 2nd step dry extract in 33% ethanol solution of methylamine in chloroform/methanol (0.003:5:1; V:V:V). All liquid handling steps were performed using Hamilton Robotics STARlet robotic platform with the Anti Droplet Control feature for organic solvents pipetting. Sphingolipids (Cer and SM) were additionally analyzed at the University of Potsdam. Lipids from PM fractions and cell organelles were extracted using methanol/chloroform (2:1, V:V) as described (Gulbins et al., 2018). The extraction solvent contained C17 Cer (18:1;2/17:0) and C16-d_{31} SM (18:1;2/16:0- d_{31}) (both Avanti Polar Lipids) as internal standards.

MS Data Acquisition

Samples were analyzed by direct infusion on a QExactive mass spectrometer (Thermo Scientific) equipped with a TriVersa NanoMate ion source (Advion Biosciences). Samples were analyzed in both positive and negative ion modes with a resolution of R(m/z = 200) = 280,000 for MS and R(m/z = 200) = 17,500 for MSMS experiments, in a single acquisition. MSMS was triggered by an inclusion list encompassing corresponding MS mass ranges scanned in 1 Da increments (Surma et al., 2015). Both MS and MSMS data were combined to monitor CE, DAG, and TAG ions as ammonium adducts; PC, PC O-, as acetate adducts; and CL, PA, PE, PE O-, PG, PI, and PS as deprotonated anions. MS only was used to monitor LPA, LPE, LPE O-, LPI, and LPS as deprotonated anions; Cer, HexCer, SM, LPC, and LPC O- as acetate adducts. Additional Cer and SM analyses (University of Potsdam) were carried out with a 1260 Infinity LC system coupled to a QTOF 6530 mass spectrometer (Agilent Technologies) operating in the positive electrospray ionization mode (ESI+). The precursor ions of Cer or SM species (differing in their fatty acid chain lengths) were cleaved into the fragment ions m/z 264.270 or m/z 184.074, respectively (Kachler et al., 2017).

Data Analysis and Post-processing

Data were analyzed with Lipotype developed lipid identification software based on LipidXplorer (Herzog et al., 2011, 2012). Data post-processing and normalization were performed using an in-house developed data management system. Only lipid identifications with a signal-to-noise ratio >5, and a signal intensity 5-fold higher than in corresponding blank samples were considered for further data analysis. All lipids below amount of 0.5 pmol were removed from further analysis. Also occupation threshold was applied to keep only those lipids that were present at least in two experimental replicates from analyzed control cells.

Lipid Nomenclature

Lipid species are annotated according to their molecular composition as NAME <sum of the carbon atoms in the hydrocarbon moiety>:<sum of the double bonds in the hydrocarbon moiety>;<sum of hydroxyl groups>. For example, in case of sphingolipids, SM 34:1;2 denotes a sphingomyelin species with a total of 34 carbon atoms, 1 double bond, and 2 hydroxyl groups in the ceramide backbone.

Lipid subspecies annotation contains additional information on the exact identity of their acyl moieties and their sn-position (if available). For example, PC 18:1;0_16:0;0 denotes phosphatidylcholine with octadecenoic (18:1;0) and hexadecanoic (16:0;0) fatty acids, for which the exact position

(sn-1 or sn-2) in relation to the glycerol backbone cannot be discriminated (underline "_" separating the acyl chains). PC O- denotes an ether- phosphatidylcholine. Raw data set of lipid measurements in pmol are provided in **Supplementary Material** as Excel file.

Detection of Ca^{2+} Mobilization

For Ca^{2+}-mobilization experiments, Jurkat cells (1×10^6) were loaded with 1 μM Fluo-4 as cell-permanent acetoxymethyl (AM) ester (Molecular Probes, Invitrogen) in Hanks balanced salt solution (HBS) (without $CaCl_2$, $MgSO_4$, and phenol red) containing 5% FCS and 25 mM HEPES (pH 7.5) according to manufacturers' protocol. Ca^{2+}-flux was determined over time by flow cytometry after passive ER Ca^{2+} depletion induced by 1 μM thapsigargin (Sigma-Aldrich Germany) in Ca^{2+} free HBS followed by addition of 2 mM Ca^{2+} or after active TCR dependent ER Ca^{2+} release after TCR ligation with α-CD3 antibody (10 μg/ml) (clone UCHT-1; Beckton-Dickinson Biosciences Pharmingen) crosslinked with the goat α-mouse IgG (Dianova, Germany) and added in complete Hanks medium (supplemented with 2 mM $CaCl_2$).

Fluorescence Analysis of α-CD3 Stimulated or NBD-Cholesterol Loaded Jurkat Cells

1×10^5 CTRL and ΔNSM Jurkat cells were pre-incubated with α-CD3 antibody (1 μg/ml) (clone UCHT-1; Beckton-Dickinson Biosciences Pharmingen) for 15 min on ice, subsequently transferred onto 8-well glass bottom μ-slides for immunostaining (Ibidi GmbH, Germany) pre-coated with 25 μg/ml α-mouse IgG (Jackson ImmunoResearch Laboratories, Inc., Dianova) (2 h at 37°C) and stimulated for 10 min at 37°C. Jurkat cell activation was stopped by adding warm 4% PFA (in PBS) for 15 min at room temperature, permeabilized with 0.1% Triton-X100 for 5 min, blocked with 5% BSA and incubated with α-STIM1 antibody (D88E10; Cell Signaling Technology) diluted in 1% BSA/PBS overnight at 4°C. Subsequently, cells were stained with α-rabbit Alexa488-conjugated secondary antibody (Invitrogen) for 2 h at RT. Total Internal Reflection Fluorescence (TIRF) microscopy was performed using a Leica AM TIRF microscope and 100x HCX Plan-Apo oil objective (numerical aperture 1.47, working distance 0.1 mm).

CTRL and ΔNSM Jurkat cells were pre-treated or not with C16-ceramide (10 μM) or avasimibe (10 μM) and subsequently seeded on poly-L-lysin coated chamber slides (LabTekII, Nunc) and incubated in RPMI/0%FBS or RPMI/10%FBS supplemented with 5 μM NBD-cholesterol for 2 h. Cells were washed and fixed by adding warm 4% PFA/PBS for 20 min at RT. NBD-cholesterol was visualized by Confocal Laser Scanning Microscopy (CLSM) imaging performed using a LSM 510 Meta (Zeiss, Germany), equipped with an inverted Axiovert 200 microscope and a 40× or 63× EC Plan-Apo oil objective (numerical aperture 1.3 or 1.4, respectively) and laser lines 488. Image acquisition was performed with Zeiss LSM software 3.2 SP2. NBD-cholesterol fluorescence quantification was performed by flow cytometry using FACS Calibur (Becton Dickinson) and analyzed by FlowJo software (TreeStar).

Quantification of NBD-Cholesterol Efflux

The cholesterol efflux assay was performed as published previously with minor modifications (Song et al., 2015). To assess cholesterol efflux CTRL and ΔNSM Jurkat cells were incubated in phenol red-free RPMI medium containing 5 μM NBD-cholesterol for 2 h at 37°C. Subsequently cells were washed with PBS three times, incubated for 4 h with 50 μg/ml human HDL (Academy Bio-Medical Company, Inc., Biotrend, Germany) as lipid acceptor, and the medium and cell lysates in 0.1% Triton X-100 were collected. FI in the medium and cells were measured in a black polystyrene 96-well plates in the fluorescence reader at a wavelength of 469 nm for excitation and 537 nm for emission. The efflux was calculated by dividing the fluorescence intensity in the medium by the sum of the whole NBD-cholesterol fluorescence intensity in the medium and cell lysate together.

Labeling With C16-Ceramide and Cholesterol Quantification

A total of 2.5×10^7 Jurkat or Jurkat-ΔNSM cells were extensively washed and re-suspended in RPMI/2% FBS containing 10 μM ω-azido-C16-ceramide (Collenburg et al., 2016), incubated overnight at 37°C and washed three times with HBSS. 1×10^6 cells were used for click-reaction with 20 μM Click-IT Alexa 488 DIBO Alkyne (Life Technologies) and analyzed by flow cytometry to confirm efficient C16-Cer delivery to the cells. CTRL and ΔNSM Jurkat cells left untreated or loaded with C16-ceramide and total cholesterol was extracted from 1×10^6 cells with 200 μl chloroform-methanol (v/v 2:1) followed by quantification of the total cholesterol and cholesteryl ester by colorimetric assay kit II (BioVision Incorporated, United States) according to manufacturers' protocol.

T Cell Isolation, Inhibitor Treatment, and Proliferation Assay

Primary human PBMCs were isolated from peripheral blood obtained from healthy donors by Ficoll gradient centrifugation using Histopaque-1077 (Sigma-Aldrich, Germany). $CD4^+$ and $CD8^+$ T cells from PBMCs were negatively selected using MagniSort™ Human $CD4^+$ or $CD8^+$ T Cell Enrichment Kits accordingly (Invitrogen by Thermo Fisher Scientific). Triplets of 1×10^5 T cells were left untreated or treated with 10 μM avasimibe and 2 μg/ml Pyripyropene A, pharmacological inhibitors of cholesterol acyltransferases ACAT1/SOAT1 and ACAT2/SOAT2, respectively (both Sigma-Aldrich, Germany), for 2 h and added α-CD3- (clone UCHT-1) alone or together with CD28-specific antibody (clone CD28.2) (1 μg/ml) (both: Beckton-Dickinson Biosciences Pharmingen) on ice for 20 min, subsequently transferred to 96 well plates pre-coated with 25 μg/ml α-mouse IgG (Dianova) (1 h at 37°C). T cells were stimulated for 72 h including a final 24 h labeling period ($[^3H]$-thymidine (Amersham)) and proliferation was analyzed using a microplate scintillation counter. Toxicity of

pharmacological inhibitors was tested using AnnexinV Apoptosis Detection Kit (Beckton-Dickinson Biosciences Pharmingen).

Statistical Analyses

Overall, data shown were acquired in at least three independent experiments. For statistical analyses of data sets, unpaired Student's *t*-test ($^*p < 0.05$, ns: non- significant) was used throughout the manuscript. Bars show standard deviations.

RESULTS

NSM2 Activity Is Predominantly Located at the Plasma Membrane in Jurkat Cells

In non-lymphoid cells, NSM2 was found to be associated with the PM, membranes of Golgi and endo-lysosomal compartments. Newly synthesized NSM2 protein was Golgi associated, shuttled to the PM and recycled back through the endosomal system as shown for MCF7 cells (Milhas et al., 2010). To visualize the localization of NSM2, Jurkat cells were transfected with a plasmid encoding NSM2-GFP and subjected to live cell imaging. GFP fluorescence was enriched mainly at the PM, its protrusions and some intracellular vesicles (**Figure 1A**). To analyze whether subcellular distribution of NSM2 also reflects its activity and regulates PM lipids and their dynamics upon TCR stimulation CRISPR/Cas9-edited Jurkat cells deficient for NSM2 (ΔNSM) were used (Bortlein et al., 2018). Jurkat cells stably transfected with CRISPR/Cas9 plasmid expresing non-specific guide RNA served as control (CTRL). Following 10 min of stimulation by α-CD3, which resulted in robust NSM2 activation (Bortlein et al., 2018), PM fractions were isolated from both CTRL and ΔNSM cells. Isolation efficiency was validated by probing for protein markers specific for cytoplasm, organelles and PM, namely actin, mitochondria-specific apoptosis-inducing factor (AIF) and Src kinase Lck. Faint association of Lck with organelles and the mitochondria-specific protein AIF with PM fractions reflects either contamination with mitochondrial membranes due to the isolation protocol or the formation of the contact sites or junctions between organelles and PM (**Figure 1B**). We also found mitochondrial proteins in PMs isolated as the giant plasma membrane vesicles (GPMVs) demonstrating objective technical difficulties fully separate organelle and PMs hinting at their close physical communication (**Supplementary Figure S1**). Mass spectrometry-based lipid analysis of the PM fractions from three independent experiments of unstimulated and α-CD3 stimulated cells was performed by Lipotype GmbH (Dresden, Germany). Diversity of the measured ceramide (Cer) species were generally low, especially in the PM fractions of unstimulated Jurkat cells: only two species in unstimulated and 4 in α-CD3 stimulated cells were detected (**Figure 1C**, middle and right graphs). Independent measurement of PM Cer was performed in parallel at the University of Potsdam and also here detected ceramide concentrations and species were similar to those measured by Lipotype (**Supplementary Figure S2A**). Both independently done measurements showed reduced total amounts of ceramide species 42:1;2 and 42:2;2 in ΔNSM cells (**Figure 1C**, left graph). Hexosyl-ceramide (HexCer) content in Jurkat PM was not affected by NSM2 ablation (**Supplementary Figure S2B**) indicating that HexCer synthesis is independent of NSM2 regulated sphingolipid metabolic pathways.

Reduction of Cer in the PM of ΔNSM cells correlated with the upregulation of major sphingomyelin (SM) species and total SM in PM by about 30 percent in unstimulated ΔNSM cells (**Figure 1D**) indicating activity of NSM2 sphingomyelinase at the PM. Measured Cer amounts did not increase in PM after α-CD3 stimulation as could be expected after TCR dependent NSM2 activation (**Figure 1C**). The result possibly reflects the insufficient sensitivity of methods used here to detect local, TCR signal dependent generation of ceramides after NSM2 activation. Also potential metabolic turnover of ceramides after T cell stimulation cannot be excluded.

Disrupted homeostasis of SM, Cer, and DAG was previously observed in the Golgi compartment of primary chondrocytes from *smpd3*$^{-/-}$ mouse (Stoffel et al., 2016). Therefore, Cer and SM species were measured in the organelles isolated from CTRL and NSM2 deficient cells (**Figure 1E** and **Supplementary Figure S2C**). Surprisingly, we found that cellular organelles did not show significant changes in either steady state or α-CD3 stimulated total levels or subspecies composition of Cer and SM. Data implicate that the majority of enzymatically active NSM2 in Jurkat cells is localized at the PM rich in anionic phospholipid phosphatidylserine (PS), which supports constitutive and TCR stimulated activity of NSM2.

Enhanced PM Lyso-Phospholipid Content in NSM2 Deficient Jurkat Cells

To evaluate whether NSM2 deficiency also affected the accumulation of PM lipids other than sphingomyelin species, we analyzed 14 glycerophospholipid (GPL) types (including four plasmalogens containing a vinyl-ether bond). The most abundant species (higher than 10 pmol per sample) included two major structural lipids, phosphatidylcholines (PC) and phosphatidylethanolamines (PE), which were slightly but not significantly upregulated upon α-CD3 stimulation (**Figure 2A**, right graph). More detailed analysis within the group of most expressed PC species (more as 100 pmol per sample) showed a significant reduction only for two PC species in α-CD3 stimulated ΔNSM cells (**Supplementary Figure S3A**), indicating that the total content of the major structural lipids is regulated in an NSM2-independent manner.

Although typically localized to the mitochondrial inner membrane, the glycerophospholipids cardiolipins (CL) and its building blocks phosphatidylglycerols (PG) were also detected in the PM fractions. In the PM of unstimulated ΔNSM cells, CL was significantly less abundant, while no significant differences for PG were observed (**Figure 2A**, left graph; **Supplementary Figure S3B**). It remains to be clarified whether CL and PG truly are associated with PM or rather localized to organelle/PM contact sites reflecting NSM2-dependent regulation of CL in mitochondrial membranes.

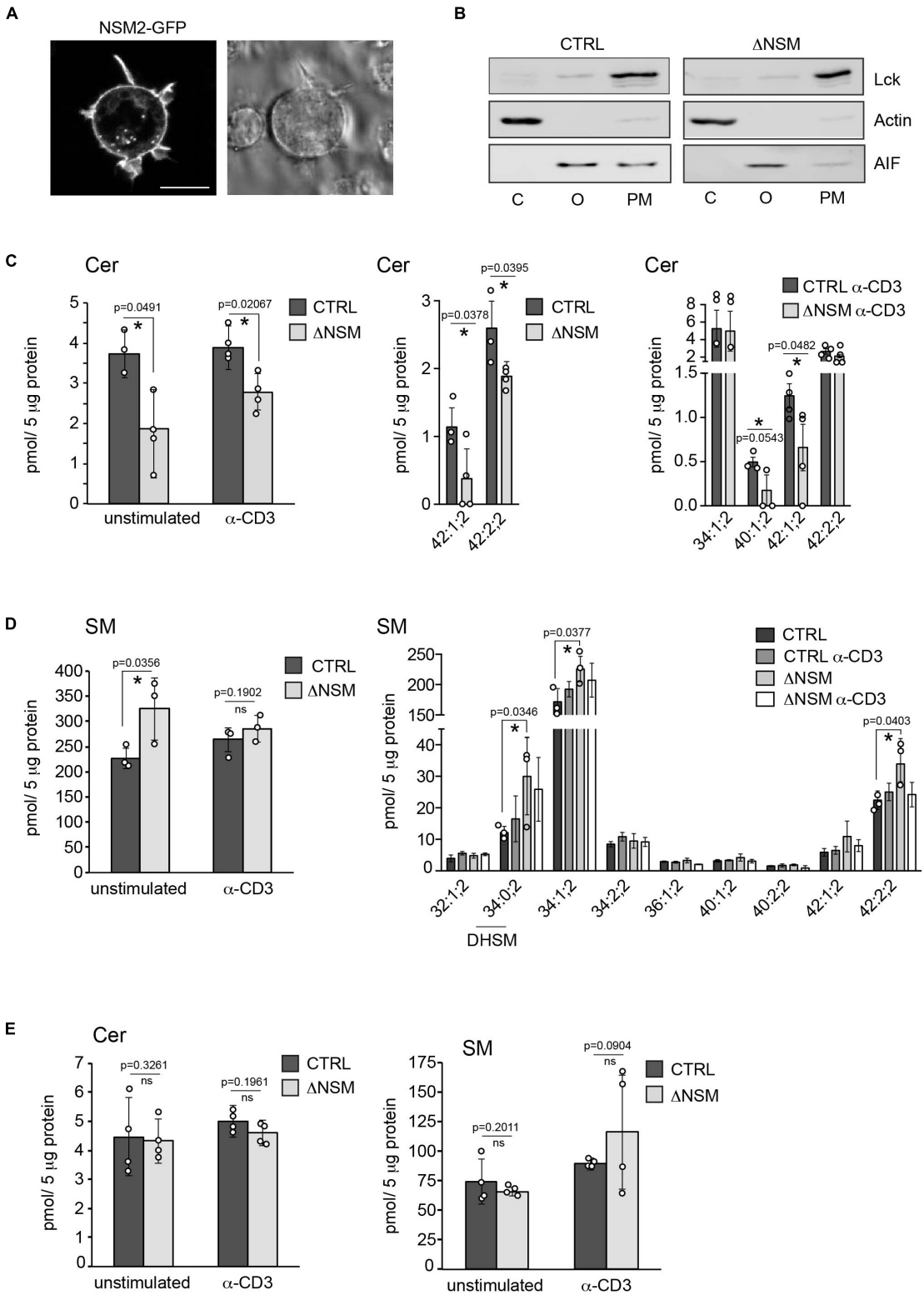

FIGURE 1 | Neutral sphingomyelinase-2 (NSM2) activity is primarily localized at the plasma membrane (PM). **(A)** Jurkat cells were nucleofected with human NSM2-GFP expressing plasmid and images of living cells were taken 24 h after transfection. Left: GFP fluorescence image. Right: differential interference contrast (DIC) image. Scale bar: 10 μM. **(B)** The cell compartment specific localization of actin, Lck and AIF was detected in cytoplasmic (C), organelles (O) and PM fractions of CTRL and ΔNSM Jurkat cells by Western blotting. **(C,D)** Sphingolipid composition of PM fractions of CTRL and ΔNSM cells left unstimulated or α-CD3

(Continued)

FIGURE 1 | Continued
stimulated for 10 min. Ceramides [**(C)**, Cer] and sphingomyelins [**(D)**, SM] were analyzed by direct infusion MS/MS or LC-MS/MS. Total levels of 42:1;2 and 42:2;2 Cer species in CTRL and ΔNSM cells detected in both: stimulated and unstimulated cells, by Lipotype and at the University of Potsdam are shown in [**(C)**, left graph]. Distribution of Cer species in unstimulated [**(C)**, middle graph] and α-CD3 stimulated cells [**(C)**, right graph] is shown. Cell or stimulation dependent total SM levels (left graph) and distribution of SM species (right graph) are shown in **(D)**. **(E)** Total Cer (left graph) and SM (right graph) analysis of organelle fractions isolated from CTRL and ΔNSM cells as assessed by LC-MS/MS (n = 4). Mean values with standard deviations of the measurements of independently performed fractionations are shown. Each independent fractionation is marked as a circle and p-value is shown on the top of significant (marked with asterisks) or not significant differences (ns).

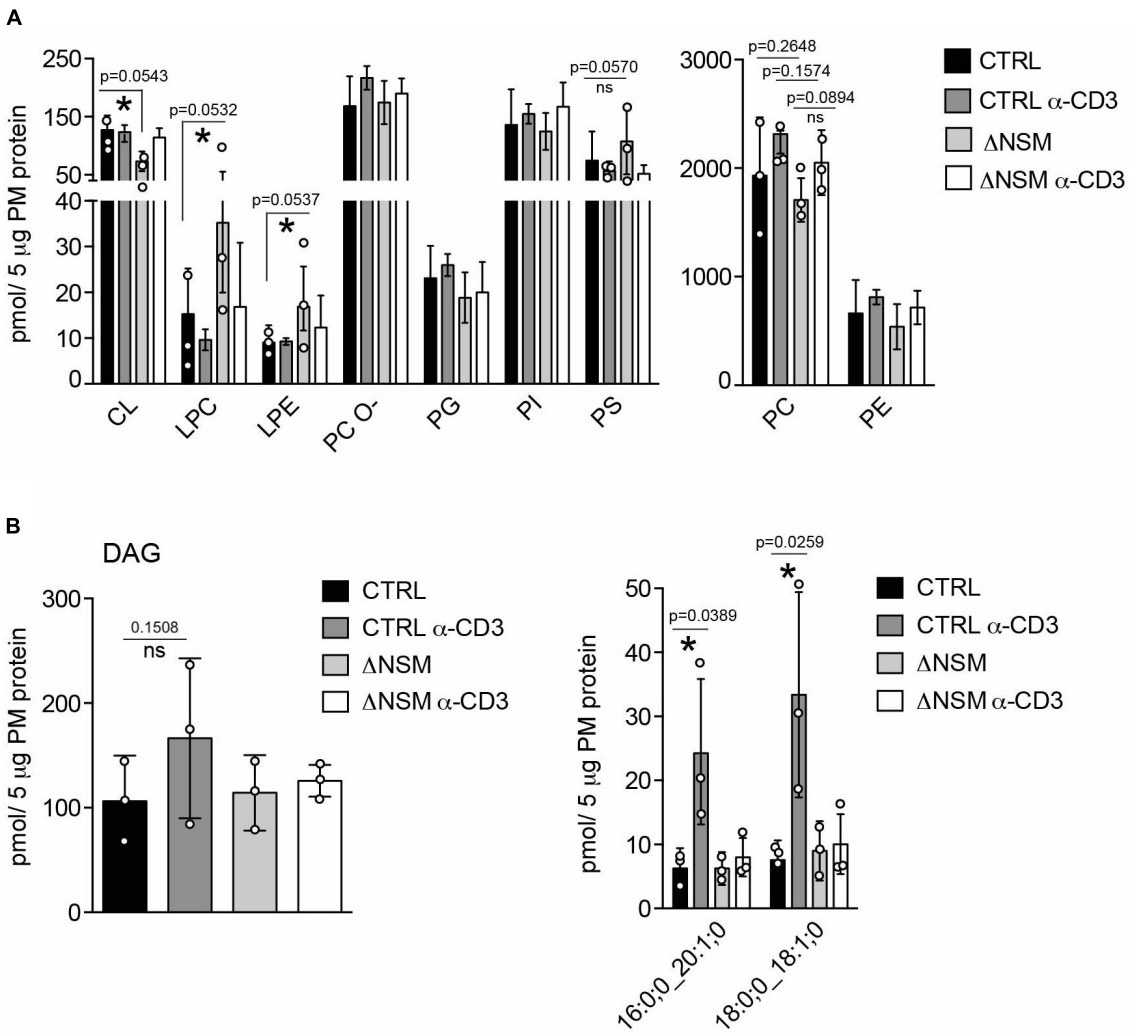

FIGURE 2 | Neutral sphingomyelinase-2 (NSM2) regulates plasma membrane (PM) content of signaling lipids: lyso-glycerophospholipids (LP) and diacylglycerols (DAG). CTRL or ΔNSM cells were left unstimulated or α-CD3 stimulated for 10 min and total amounts of major glycerophospholipids (GPL) **(A)**: cardiolipin CL, lyso-phosphatidylcholine LPC, lyso-phosphatidylethanolamine LPE, ether-phosphatidyl-choline PC-O, phosphatidylglycerol PG, phosphatidylinositol PI, phosphatidylserine PS) and total diacylglycerol (DAG) [**(B)**, left graph] or α-CD3 regulated DAG species [**(B)**, right graph] were quantified by direct infusion MS/MS. Mean values with standard deviations of the measurements of three independently performed fractionations are shown. Each independent fractionation is marked as a circle and p-value is shown on the top of significant (marked with asterisks) or not significant differences (ns).

Lyso-phosphatidylcholine (LPC) and lyso-phosphatidyl-ethanolamine (LPE) are bioactive molecules that can modify cell membrane mechanical properties and curvature (Shindou et al., 2009). Interestingly both, LPC and LPE, were more abundant in unstimulated ΔNSM cells (**Figure 2A**, left graph; **Supplementary Figure S3C**) and thus represented the major glycerophospholipid species which are affected by basal NSM2 activity.

TCR-Dependent NSM2 Activation Is Crucial for Diacylglycerol (DAG) Production

DAG accumulating in PM microdomains regulates classic, novel and atypical PKCs important in T cell signaling (Fu et al., 2010; He et al., 2011). Two metabolic pathways

produce DAG at the PM. One is mediated by sphingomyelin synthase 2 (SMS2), which transfers the phosphocholine head group from phosphatidylcholine to Cer to produce DAG and SM. Therefore SMS2 can regulate SM, Cer, PC and DAG simultaneously (Gault et al., 2010). Another pathway is governed by phosphatidylinositol-specific phospholipase-Cγ1 (PLCγ1), which hydrolyzes PI (4,5)P_2 into inositol triphosphates (IP_3), thereby mobilizing Ca^{2+} and DAG upon TCR activation. NSM2 deficiency did not affect steady state PM DAG production in unstimulated Jurkat cells (**Figure 2B**). Remarkably, after α-CD3 stimulation, two out of 13 analyzed DAG species were significantly upregulated in NSM2-expressing but not in NSM2-deficient cells (**Figure 2B**, right graph; **Supplementary Figure S4**). Interestingly, TCR signaling specifically induced the production of more saturated DAG species that contain only one double bound (**Supplementary Figure S4**). Our data indicate that NSM2 is required for TCR signal dependent DAG production.

NSM2 Activity Is Required for Cholesteryl Ester (CE) Production in Jurkat Cells

The most striking NSM2-related difference seen in our PM lipidomic analyses concerned all measured cholesteryl ester (CE) species, which accumulated in NSM2-sufficient and barely in NSM2 deficient cells after TCR ligation (**Figure 3A**). CE is generated after free PM cholesterol transport to the endoplasmic reticulum (ER) by two ER-resident cholesterol acyltransferases ACAT1/SOAT1 and ACAT2/SOAT2. Lipidomic analysis detected CE in PM fractions most likely due to the accumulation of free cholesterol after TCR-dependent sphingomyelinase activation and enhanced ER-PM junction formation which were partially present in purified PM fractions. Analysis of CE in intracellular organelle fraction showed a tendency of reduced CE also there (**Supplementary Figure S5**). We wanted to clarify whether lack of CE accumulation in ΔNSM cells reflected low CE synthesizing enzyme activity or lack of ER-PM contact formation after TCR engagement necessary for cholesterol transport to ER. For that Ca^{2+} mobilization as crucial for ER-PM tethering (van Vliet et al., 2017) and PM redistribution of the ER Ca^{2+} sensor STIM1 were measured. Thapsigargin-dependent ER calcium release and extracellular Ca^{2+} uptake were NSM2-independent (**Figure 3B**, left graph). This also applied to TCR- regulated store operated Ca^{2+} entry (SOCE) (**Figure 3B**, right graph). As revealed by total internal reflection fluorescence (TIRF) microscopy, STIM1 transport toward α-CD3 coated stimulatory surface did occur at equal efficiency in CTRL and ΔNSM cells indicating that formation of PM-ER contact sites was unaffected (**Figure 3C**).

Next, we wanted to know if CE production is generally impaired in NSM2-deficient cells prior to TCR stimulation. For that we used an assay that indirectly measures CE production rate as the increase in relative NBD fluorescence of loaded NBD-cholesterol after absorbance of it in PM and transport from polar double leaflet membranes to non-polar core of cytoplasmic lipid droplets in NBD-cholesterol loaded cells (Lada et al., 2004). The excess of loaded free NBD-cholesterol in PM is removed to ER where NBD-CE is generated and distributed to intracellular compartments (Sparrow et al., 1999). To exclude that high and low density lipoproteins (HDL, LDL) mediated cholesterol uptake from serum present in our cell culture medium, the cells were extensively washed and incubated with NBD-cholesterol in serum-free medium prior to microscopy (**Figure 3D**) and flow cytometry (**Figure 3E**). ACAT1/SOAT1 inhibitor avasimibe was included to reduce intracellular CE concentration. ΔNSM and avasimibe-treated CTRL cells showed a comparable decrease in NBD-fluorescence intensity indicative of reduced production of CE also in unstimulated NSM2-deficient cells. To find out if extracellular supply of free cholesterol (provided by serum) can restore CE production in NSM2-deficient cells, CE amounts were determined in lipids extracted from the CTRL or ΔNSM cells cultivated in serum containing medium using colorimetric assay (**Figure 3F**). Because CE amount was strongly reduced also in ΔNSM cells cultivated in serum-containing medium, CE production is obviously generally impaired in the absence of NSM2.

Enhanced Cholesterol Accumulation in NSM2-Deficient Cells

Conditional knock-out of Acat1/Soat1 in murine T cells impaired CE synthesis and markedly increased both whole and plasma cholesterol levels in mouse T cells (Yang et al., 2016). To determine whether NSM2 deficiency would have a similar effect on free cholesterol levels, we compared cholesterol-specific filipin III fluorescence in ΔNSM and CTRL cells exposed to the ACAT1/SOAT1 pharmacological inhibitor avasimibe. Filipin III showed predominant PM labeling in both, CTRL and ΔNSM cells, with fluorescence intensities in both ΔNSM and avasimibe-treated cells exceeding those observed in CTRL cells (**Figure 4A**, IF pictures). In quantitative terms, this was confirmed by flow cytometry (**Figure 4A**, right graph).

In addition to reduced CE production and cholesterol turnover, higher cholesterol uptake rate can cause accumulation of cellular cholesterol in ΔNSM cells. To analyze whether NSM2 and/or ceramides participate in cholesterol uptake in Jurkat cells, we pretreated CTRL and ΔNSM cells with C16-ceramide overnight and loaded with NBD-cholesterol for the last 2 h in the presence of serum as the source of cholesterol carrying lipoproteins LDLs and HDLs. Microscopic and flow cytometry analysis of NBD-fluorescence revealed elevated cholesterol levels in NSM2-deficient cells which were normalized to those in CTRL cells after incubation with C16-ceramide (**Figure 4B**). Results were confirmed using colorimetric assay detecting total cholesterol (**Figure 4C**).

To assess the contribution of NSM2 in cholesterol efflux, the supernatants of NBD-cholesterol loaded CTRL and ΔNSM cells were analyzed using human HDL as the lipid acceptor. The fluorescence assessment in cell supernatants showed 10% less efflux in NSM2-deficient cells (**Figure 4D**). Combined, these data revealed that enhanced uptake and decreased efflux of cholesterol contributes to misbalanced cholesterol homeostasis in ΔNSM cells.

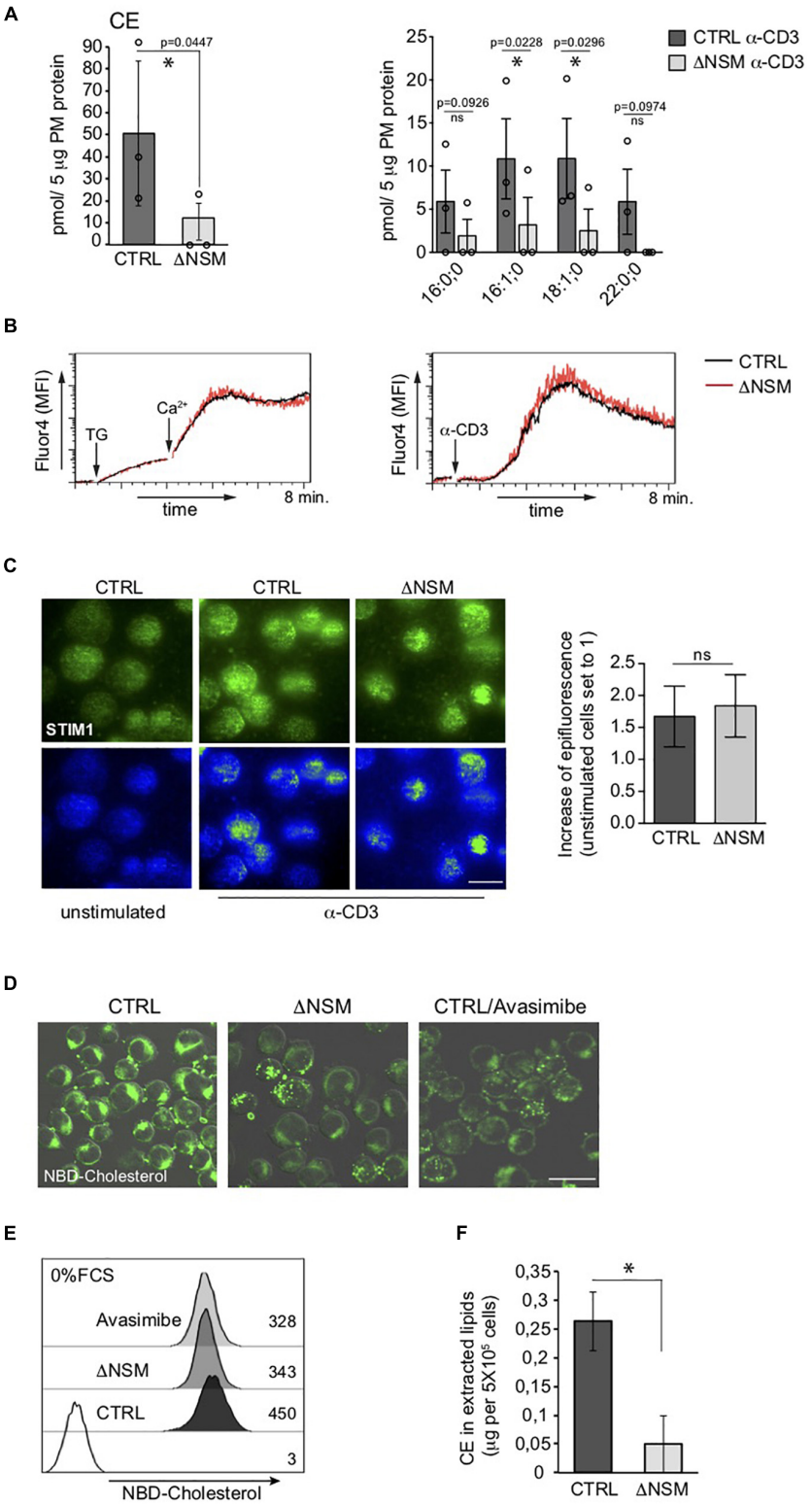

FIGURE 3 | Unimpaired ER-plasma membrane (PM) junction formation and lack of cholesteryl ester (CE) production in TCR stimulated neutral sphingomyelinase-2 (NSM2) deficient T cells. **(A)** Total CE (left graph) and the distribution within CE species (right graph) were measured and are shown in CTRL and ΔNSM cells after α-CD3 stimulation for 10 min. No CE 22:0;0 was detected in ΔNSM cells. Each independent fractionation is marked as a circle and *p*-value is shown on the top of significant (marked with asterisks) or not significant differences (ns). **(B)** Calcium uptake was analyzed in Ca^{2+} sensor Fluo-4 loaded CTRL and ΔNSM cells after ER

(Continued)

FIGURE 3 | Continued
Ca^{2+} release induced by thapsigargin treatment (left graph) or after α-CD3 stimulation (right graph). **(C)** Representative fluorescence pictures (left panels) and quantification (right graph) of STIM1 epifluorescence measured by total internal reflection fluorescence (TIRF) microscopy are shown for CTRL and ΔNSM cells left unstimulated or α-CD3 stimulated for 10 min on antibody coated surface, fixed, permeabilized and stained for STIM1. Scale bar: 10 μM. **(D,E)** NBD-cholesterol fluorescence was analyzed by confocal microscopy (fluorescence and DIC picture overlays, scale bar: 20 μM; **(D)** and flow cytometry **(E)** in CTRL and ΔNSM cells untreated or 2 h pre-incubated with 5 μM avasimibe and loaded with 5 μM NBD-cholesterol for additional 2 h in cell culture medium without serum. Mean fluorescence intensity (MFI) values are shown in **(E)**. **(F)** CE was detected in total lipids extracted from CTRL and ΔNSM cells by colorimetric assay. Mean values with standard deviations of the measurements of independent cell extracts are shown ($n = 3$). Significantly reduced CE is marked with asterisk ($^*p < 0.05$).

NSM2-Deficient Cells Do Not Activate SREBP and Undergo Cell Death After Serum Deprivation

Lipid homeostasis is regulated by ER-membrane associated transcription factors, the so-called sterol regulatory element-binding proteins (SREBPs) with SREBP2 being most important in cholesterol biosynthesis pathway (Horton et al., 2002). The activation is tightly controlled by the sterol-sensing SREBP cleavage activating protein (SCAP). At low sterol concentrations SCAP chaperons SREBP protein to the Golgi, where SREBP inactive precursor is cleaved by proteases to initiate the transport to the nucleus. After activating its target genes SREBP increases sterol levels again. So SREBP activation is regulated by sterol concentration dependent feedback loop. We therefore aimed at defining whether enhanced cholesterol levels found in ΔNSM cells deregulated SREBP activity. For that, we analyzed SREBP2 active fragment in cell lysates of NSM2-sufficient and deficient Jurkat cells (**Figure 4E**). Consistent with the higher cholesterol levels found in ΔNSM cells, inactive full length SREBP2 protein was predominantly expressed in those cells, indicating reduced proteolytic cleavage and activation.

To analyze whether NSM2-deficient cells can activate SREBP, we compared SREBP2 cleavage activation in response to the absence of lipid nutrients in CTRL and ΔNSM cells after culture in decreasing serum concentrations for 24 h. NSM2-sufficient, but not NSM2-deficient Jurkat cells gradually increased expression of cleaved SREBP under serum starvation indicating that NSM2 is required to report the absence of lipid nutrients (**Figure 5A**). We followed the proliferation of cells cultivated in serum supplemented medium and medium without serum for 4 days. As expected, serum absence in medium slowed down CTRL cell proliferation (**Figure 5B**). In contrast, ΔNSM cells stopped to proliferate completely and underwent massive cell death measured by membrane permeability for propidium iodide at day four after serum deprivation (**Figures 5B,C**). Thus, these results demonstrated that NSM2 is important to fulfill demands of proliferating Jurkat cells to increase fatty acid biosynthesis necessary for membrane biogenesis particularly in a nutrient poor environment.

CE Production Is Important for TCR Dependent Primary Human T Cell Proliferation

Yang et al. (2016) demonstrated that ACAT1/SOAT1 pharmacological inhibition or T-cell specifc depletion of cholesterol acyltransferase 1 gene significantly potentiated TCR signaling, proliferation and effector functions of mouse $CD8^+$ T cells. We tested the two selective pharmacological inhibitors avasimibe (Ava) and pyripyropene A (PPPA), which are specific for ACAT1/SOAT1 and ACAT2/SOAT2, respectively, in proliferation of primary human $CD4^+$ and $CD8^+$ T cells isolated from peripheral blood of healthy donors. When applied seperately, both ACAT/SOAT inhibitors had significant negative effect on TCR ligation induced proliferation of both $CD4^+$ and $CD8^+$ T cells (**Figure 6A**). Apparently, ACAT1/SOAT1 and ACAT2/SOAT2 could partially compensate each other for function as the simultaneous treatment with both inhibitors almost completely abolished the proliferation of T cells. The inhibitor concentrations used for T cell treatment were not toxic upon incubation times used in proliferation assays (**Supplementary Figure S6**). Co-stimulation of T cells with α-CD3 and α-CD28 antibodies rendered their proliferative responses less sensitive to the inhibitor treatment. However, $CD4^+$ T cells, but not $CD8^+$ T cells, were sensitive to ACAT1/SOAT1 inhibitor which significantly reduced T cell proliferation alone or in combination with ACAT2/SOAT2 inhibitor (**Figure 6B**). CD3/CD28 co-stimulated $CD8^+$ T cells generally were more resistent to ACAT/SOAT inhibition and showed almost no effect on proliferation with the exception of a relatively minor enhancement of proliferation after avasimibe treatment (**Figure 6B**). Published data (Yang et al., 2016) and our filipin stainings of PM in avasimibe treated Jurkat cells suggest that higher cholesterol levels in PM may support more efficient TCR clustering and signaling. To dissect whether ACAT/SOAT activity would differentially affect early or late T cell activation, inhibitors were retained in the cultures for 2 h or the entire cell expansion time after stimulation. Short time inhibitor pretreatment of $CD4^+$ and $CD8^+$ cells had a slightly positive effect on T cell proliferation (**Figure 6C**) indicating that enhanced PM cholesterol levels may be tolerated or can even support initial TCR signaling. In contrast, retention of ACAT/SOAT inhibition drastically reduced T cells expansion suggesting that extended inhibition of CE synthesis and storage might negatively affect fatty acid homeostasis important for cell proliferation.

DISCUSSION

Our manuscript describes the first analysis of the NSM2 contribution to the general and TCR dependent lipid regulation at the PM early after stimulation. In line with previous observations for other cell types, the absence of NSM2 affects the levels of ceramides and sphingomyelins. However, major

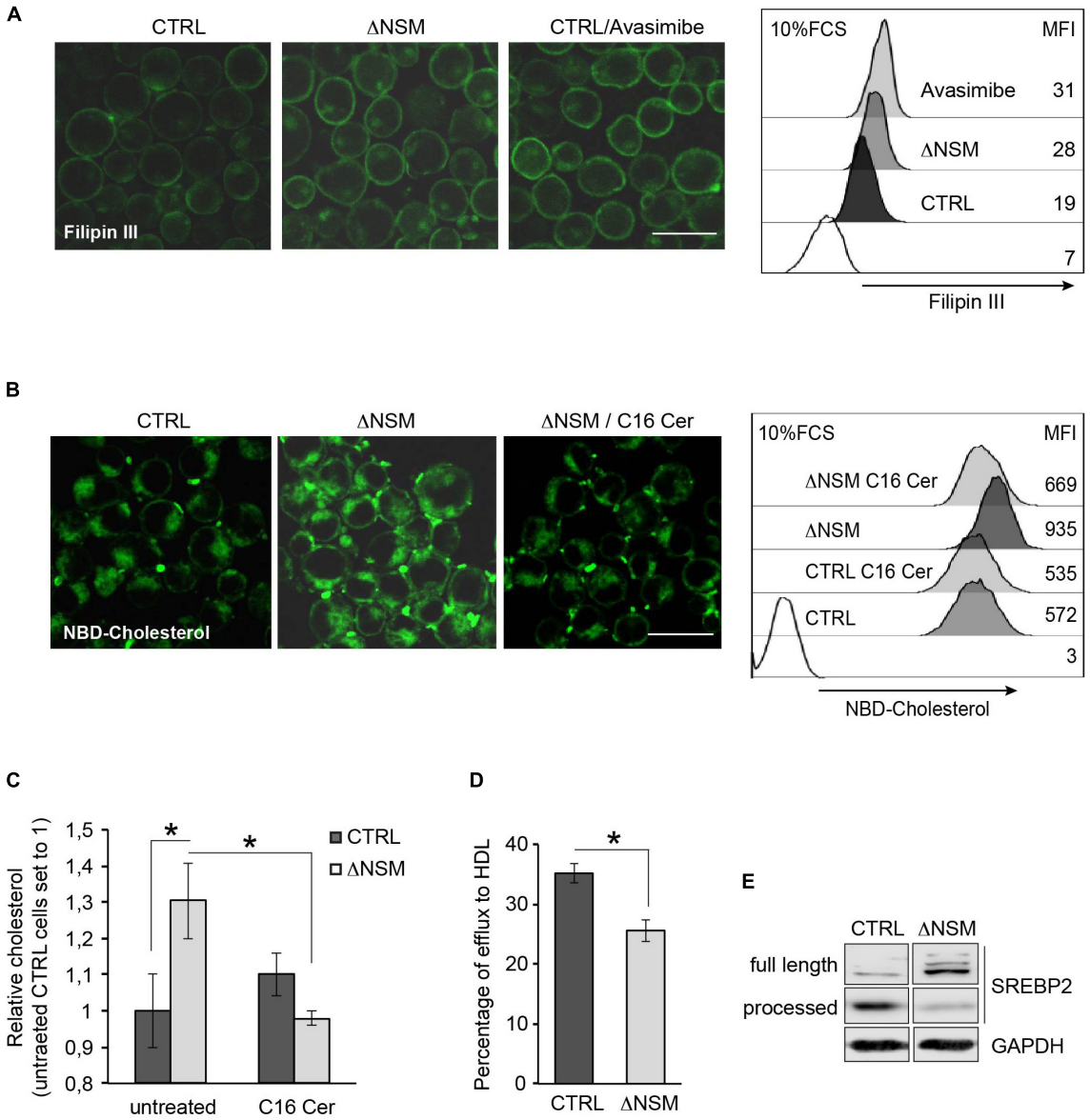

FIGURE 4 | Plasma membrane (PM) and intracellular cholesterol accumulation is regulated by neutral sphingomyelinase-2 (NSM2) dependent ceramide metabolism. **(A)** Cholesterol accumulation in polar cellular membranes was analyzed by confocal microscopy (left panels; overlays of fluorescence and DIC pictures, scale bar: 20 μM) and flow cytometry (right graph) of CTRL and ΔNSM cells left untreated or pre-incubated with 5 μM avasimibe for 2 h, fixed and stained with filipin III. Values of mean fluorescence intensity (MFI) in unstained and filipin III stained cells are shown in the right graph. White histogram in flow cytometry graph shows cells which were left unstained with filipin III. **(B)** NBD-cholesterol uptake was analyzed in CTRL and ΔNSM cells left untreated or loaded overnight with 25 μM C16 ceramide and subsequently loaded with 5 μM NBD-cholesterol for 2 h. Confocal microscopy fluorescence-DIC picture overlays (left panels; scale bar: 20 μM) and flow cytometry measurements (MFI; right panel) are shown. White histogram in flow cytometry graph shows cells which were left unloaded with NBD-cholesterol. **(C)** Cholesterol was detected in CTRL and ΔNSM cells treated as in **(B)** by colorimetric assay. Measurements were normalized against cholesterol amount in untreated CTRL cells set to 1 ($n = 3$). **(D)** Fluorometric analysis of cholesterol efflux was performed in supernatants of NBD-cholesterol loaded cells and cultivated in cell culture medium supplemented with 50 μg/ml human high density lipoprotein (HDL) for 4 h. Efflux was estimated as a percentage of NBD-cholesterol fluorescence in supernatants from total fluorescence in cell lysates and supernatants taken together ($n = 3$). Significant differences are marked with asterisks (*$p < 0.05$). **(E)** Western blot analysis of SREBP2 protein cleavage in CTRL and ΔNSM cells. Cell cultivation was performed in serum containing cell medium.

alterations in NSM2- deficient cells were observed in PM but not in organelle fractions of unstimulated and α-CD3 stimulated Jurkat cells indicating that the enzyme may be active in both resting and TCR stimulated cells (**Figures 1C–E** and **Supplementary Figures S2A,C**). This does not exclude NSM2 activity in the membranes of intracellular organelles in other cell types or after other modes of activation.

Rouquette-Jazdanian and others (Rouquette-Jazdanian et al., 2005) have shown neutral sphingomyelinase activation and a 46% reduction of SM in cholera toxin B-subunit treated Jurkat cells

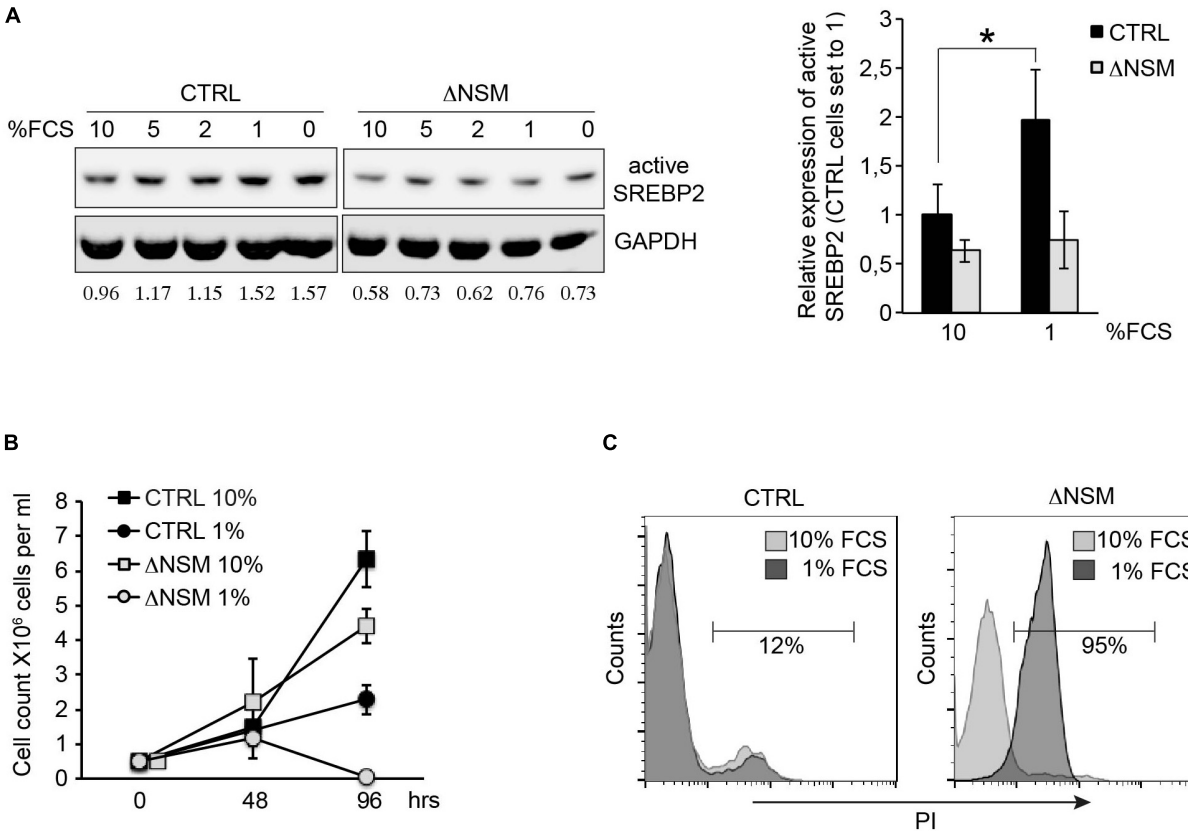

FIGURE 5 | Neutral sphingomyelinase-2 (NSM2) deficiency induced cell death after serum deprivation correlates with lower SREBP2 activation levels. **(A)** Western blot analysis of active SREBP2 expression in CTRL and ΔNSM cells after overnight incubation in cell culture medium containing decreasing amounts of serum. Relative densitometry units for SREBP2 bands are shown below the Western blots. Right graph shows the summary of three independent experiments. Significantly different amount of active SREBP2 in CTRL cells is marked with asterisk (*$p < 0.05$). **(B)** Proliferation was estimated by cell counting of cells cultivated in cell culture medium with normal (10 percent) and low (1 percent) serum content for 4 days ($n = 3$). **(C)** Cell death analysis performed by flow cytometry of propidium iodide (PI) staining of living cells after 4 days of cultivation in cell culture medium containing 10 or 1 percent serum.

proposing that NSM should have access also to the major pool of SM in outer PM leaflet by unknown mechanism. Biochemical methods including labeling of the cytosolic face of PM with SM-specific toxin lysenin in electron microscopy (EM) demonstrated that 10–25% of sphingomyelin could be found in the inner leaflet (Murate et al., 2015). Our data show a 30% increase of PM SM in ΔNSM Jurkat cells accompanied with a 30–50% decrease of Cer amounts (**Figures 1C,D**) specifically in PM, but not in the organelles containing fractions (**Figure 1E**), indicating that NSM2 is primarily active at PM and have an access only to the SM in the inner PM leaflet. Many stimuli, such as TNF-α, cell confluence and PMA, have been demonstrated to induce NSM2 PM translocation and increase in enzyme activity, indicating together with our data that PM translocation is important for the enzymatic activation of NSM2 (Airola and Hannun, 2013). Although we and others have shown neutral sphingomyelinase activation early after TCR stimulation (Tonnetti et al., 1999; Bortlein et al., 2018), we were not able to show increase of ceramide or decrease of SM levels upon 10 min of TCR ligation using α-CD3 antibody (**Figures 1C,D**). The data implicate insufficient sensitivity of techniques used in our lipid analysis that allowed us to measure only long term regulation of basal Cer and SM levels at PM in ΔNSM cells, but not short, transient and TCR localized Cer changes upon NSM2 activation in CTRL cells.

To analyze the dynamics of PM lipids upon TCR stimulation is a challenge. Nevertheless, methods of PM isolation and lipid detection are increasingly contributing to the steady data accumulation. Zech et al. analyzed lipids in Jurkat cell PM domains directly engaged to stimulatory α-CD3 coated beads (Zech et al., 2009), revealing raft lipid accumulation in PM regions directly engaged in TCR signaling. Here we first analyze NSM2 contribution to the general TCR-dependent lipid regulation at the whole PM early after TCR stimulation. Majority of analyzed glycerophospholipids were regulated independently of TCR-stimulation (**Figure 2A**, left graph). Our analysis revealed significantly enhanced basal levels of lysophospholipids LPC and LPE in NSM2-deficient cells (**Figure 2A** and **Supplementary Figure S3C**), suggesting a possible molecular mechanism how NSM2 may regulate membrane curvature and mechanic properties in unstimulated T cells (Menck et al., 2017). Interestingly, α-CD3 stimulation normalized the levels of LPC and LPE in ΔNSM cells but still there was a tendency for

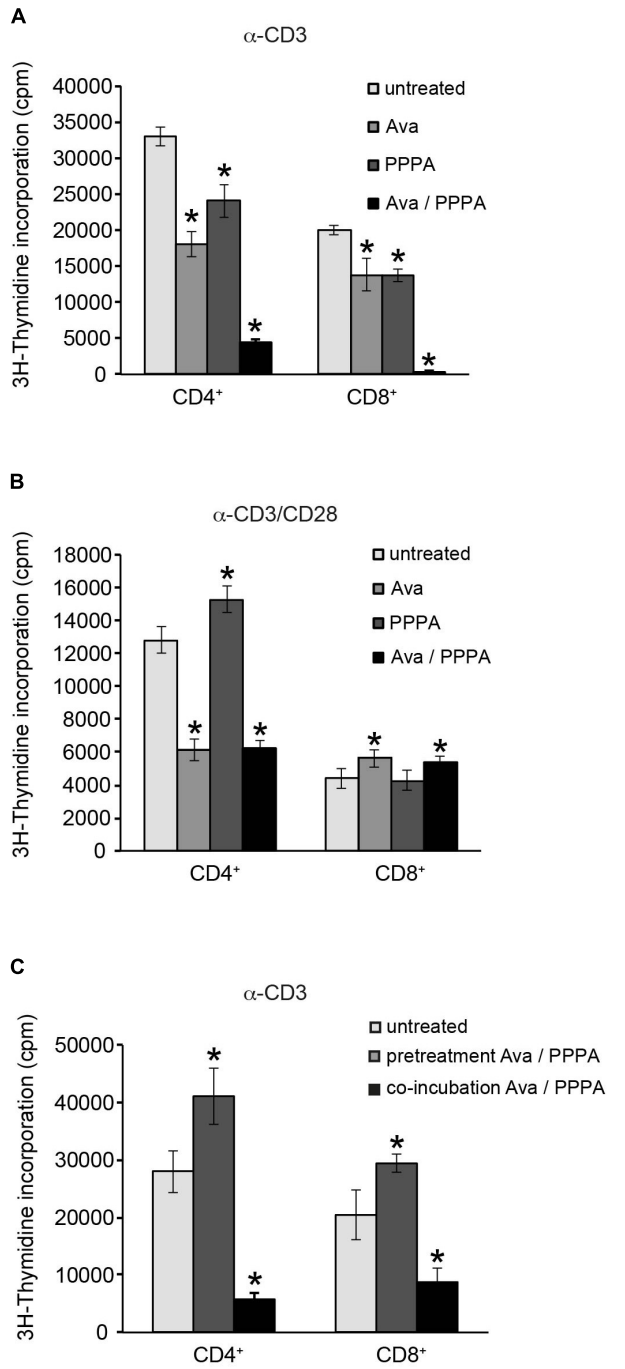

FIGURE 6 | Cholesterol ester synthesis is crucial for sustained α-CD3/α-CD28 driven human $CD4^+$ cell proliferation. Purified primary $CD4^+$ and $CD8^+$ T cells were left untreated or treated with 10 μM ACAT1/SOAT1 specific inhibitor avasimibe (Ava) or ACAT2/SOAT2 specific inhibitor pyripyropene A (PPPA) separately or in combination. Cells were stimulated with α-CD3 alone **(A,C)** or in combination with α-CD28 **(B)** for 3 days. Inhibitors were kept in cell culture medium through the whole experiment **(A,B)** or washed away after 2 h pre-incubation of T cells [**(C)**, pretreatment]. ^{3}H-Thymidine was added to the cells after 2 days of stimulation and radioactivity incorporation in cellular DNA was measured after overnight incubation. Mean values with standard deviations of three independent experiments are shown ($n = 3$). Significant differences are marked with asterisks (*$p < 0.05$).

higher levels of those lipids. However, data evaluation and studies regarding mechanism of how NSM2 regulate lysophospholipid expression stay beyond the scope of this study.

Interestingly, we observed TCR stimulation-specific and NSM2-dependent increase in more saturated DAG species (**Figure 2B** and **Supplementary Figure S4**). In NSM2-deficient cells a lack of TCR induced upregulation of DAG correlated with the low activation levels of novel and atypical PKCs and low Ca^{2+} mobilization at suboptimal TCR stimulation conditions (Bortlein et al., 2018).

The most striking observation was CE accumulation in PM fractions of TCR- stimulated cells which was strongly dependent on NSM2 activity (**Figure 3A**). Enzyme deficient cells had nearly no CE induced after TCR ligation. Several biochemical studies have described sphingomyelinase and PKC-regulated cholesterol esterification in different cell lines (Stein et al., 1992; Lange et al., 2002). Sphingomyelin has the highest affinity to cholesterol in PM. The amount of SM-bound cholesterol was estimated about 35 mole percent of PM cholesterol by using cholesterol binding mutant form of bacterial Perfringolysin O (Das et al., 2014). Sphingomyelinase activity is believed to be required for cholesterol mobilization from PM to the ER for esterification there by the activity of cholesterol acetyltransferases ACAT1/SOAT1 and ACAT2/SOAT2. ER-PM contact sites and lipid transfer proteins are involved in non-vesicular transport of SM free cholesterol (Litvinov et al., 2018), and therefore, our CE detection in PM isolates most likely reflects co-purification of ER-plasma junctions. Total SM was not measurably reduced after TCR stimulation of CTRL cells, indicating that SM is still present to prevent removal of cholesterol and that this did not correlate with strong CE induction. Subbaiah and others (Subbaiah et al., 2008) demonstrated that rather ceramide generation and not sphingomyelin degradation is crucial for CE synthesis. Our lipid measurements showed a correlation of NSM2 dependent ceramide generation with the CE production after TCR stimulation.

Here we show general dysregulation of all steps involved in cholesterol homeostasis in NSM2 deficient Jurkat cells: CE production, cholesterol uptake, efflux and activation of cholesterol sensing transcription factor SREBP2, manifesting in increased cholesterol accumulation (**Figure 4**). NSM2 deficiency in *fro/fro* mouse resulted in storage of cholesterol in ear skin fibroblasts promoting lipid raft formation and activation of hyaluronan synthase (Qin et al., 2012). Similar, ΔNSM T cells showed high PM and intracellular cholesterol accumulation. Cholesterol homeostasis is fine-tuned by cholesterol uptake, efflux and regulation of transcription factors activating gene expression involved in lipid synthesis. Cholesterol uptake is mediated by serum lipoprotein LDL internalization by its receptor (LDLR) in clathrin-coated vesicles. Interestingly, exogenously added human urinary neutral sphingomyelinase can regulate LDL receptor activity, LDL uptake and cholesterol ester synthesis in fibroblasts (Chatterjee, 1993). Our data showed enhanced cholesterol uptake in NSM2 deficient Jurkat cells cultivated in serum containing medium (**Figures 4B,C**). However, expression

of LDLR was not enhanced (data not shown). Surprisingly, we were able to reduce the cholesterol load in ΔNSM cells by supplementing them with C16-Ceramide, indicating that ceramides or possibly its metabolites balance cholesterol uptake by regulating membrane environment of uptake regulatory proteins probably by effecting lipid raft formation. As shown above, NSM2 regulates lysophospholipid levels and therefore possibly membrane curvature important for clathrin-coated vesicle formation involved in serum lipoprotein uptake. The exact mechanistic link between ceramides and LDLR mediated cholesterol uptake in T cells is not clear and stayed out of the scope of this study.

It has been shown that inhibition of ACAT1/SOAT1 or PKC regulates high density lipoprotein receptor (HDLR) dependent efflux of intracellular cholesterol (Mendez et al., 1991). Correlating with the inhibition of those pathways in NSM2-deficient cells, cholesterol efflux toward medium supplemented with recombinant HDL was significantly reduced (**Figure 4D**).

We observed increased cholesterol accumulation in NSM2-deficient Jurkat cells accompanied with less accumulation of cleaved active sterol regulatory element-binding protein SREBP2 which is more specialized in cholesterol regulation pathway (**Figure 4E**). When the sterol concentration in ER drops, SREBPs are transported by chaperone protein sterol sensing SREBP cleavage activating protein SCAP from the ER to the Golgi where SREBPs are cleaved by proteases. Cleaved N-termini of SREBP are released into the cytoplasm and can diffuse to the nucleus where they induce expression of target genes regulating biosynthesis and uptake of cholesterol (Litvinov et al., 2018). Negative regulation of SREBP in NSM2 deficient cells may result from enhanced delivery of the LDL-cholesterol, uptake of which is increased in NSM2-deficient cells (**Figure 4B**), to the sterol sensing ER compartment. Interestingly, NSM2-deficient cells could not activate SREBP2 even after cultivation in serum depleted medium, indicating that cholesterol removal from ER may be regulated by NSM2. That made them especially sensitive to the starvation induced cell death.

Now we show that NSM2 is a strong regulator of CE generation in Jurkat T cells. Yang and others proposed to use avasimibe, an inhibitor of the cholesterol esterification enzyme ACAT1/SOAT1, for therapy to improve $CD8^+$ T cell mediated control of tumor growth (Yang et al., 2016). Their experiments were done in a mouse model and showed strongly enhanced anti-tumor activity of mouse $CD8^+$ effector T cells treated with avasimibe or deficient for ACAT1. Now we show that *in vitro* TCR driven expansion of primary human T cells treated with avasimibe revealed no real improvement in the peripheral blood $CD8^+$ T cell compartment, whereas $CD4^+$ T cells were highly sensitive and showed significantly impaired proliferation (**Figure 6**). Accumulation of CE is associated with increased proliferation of tumor cells (Matsumoto et al., 2008). Also expansion of CEM and MOLT4 T cell lines is positively regulated by cholesterol esterification (Dessi et al., 1997). PKCζ/ERK signaling pathway is crucial in CE synthesis enhancing glioblastoma cell growth and invasion (Paillasse et al., 2009). Similarly ERK activation enhances CE synthesis in monocyte-derived macrophages (Napolitano et al., 2004). However, exact mechanism how CE effects cell proliferation is still poorly understood. Oxysterols, made from excess of free cholesterol accumulating upon CE synthesis inhibition, are supposed to play a negative role in cell proliferation and were suggested to use as a chemotherapeutic agents controlling tumor growth (Schroepfer, 2000). Here our data are suggesting that more detailed studies on properties of and differences between mice and human T cells and their subsets regarding CE function and cholesterol homeostasis are needed to understand the composite intervention of CE with tumor growth and tumor infiltrating T cells depending on availability of nutrients and type of tumor.

The results presented here indicate a tight connection between sphingolipid metabolism, TCR signaling regulated by NSM2 and cholesterol homeostasis in T cells, the deregulation of which can lead to metabolically orchestrated inflammation or negatively regulated T cell differentiation and anti-tumor activity. Immune cells sensitive to deregulated cholesterol metabolism and driving autoimmune diseases are poorly characterized. Studies of immune cell compartment specific NSM2 activity levels and responses to sterol metabolic stress would help to evaluate NSM2 significance in metabolically regulated inflammation.

DATA AVAILABILITY STATEMENT

All datasets generated for this study are included in the manuscript/**Supplementary Files**.

AUTHOR CONTRIBUTIONS

BK, LD, and EA: conceptualization. CB, BK, FS, and EA: methodology. CB and EA: formal analysis. CB, FS, and EA: experimental investigation. LD and EA: writing. BK: funding acquisition. EA: supervision.

FUNDING

The work was funded through the German Research Foundation (DFG) within the RU 2123 (DFG SCHN 405/10). This publication was funded by the DFG and the University of Würzburg in the funding program Open Access Publishing.

ACKNOWLEDGMENTS

We thank Jürgen Schneider-Schaulies and Sibylle Schneider-Schaulies for critically reading the manuscript, Sibylle Schneider-Schaulies for funding acquisition. We thank Daniel Herrmann for excellent technical assistance with the LC-MS/MS analyses performed at the University of Potsdam and Anna Hoffbauer for excellent performance of cholesterol analysis. We thank Lipotype GmbH and specially Christian Klose,

Michel Surma, Julia Schöner for the very kind and highly professional support to perform lipid analyses. We would like to thank the Core Unit for Confocal Microscopy and Flow Cytometry-based Cell Sorting of the IZKF Würzburg for supporting this study.

SUPPLEMENTARY MATERIAL

The Supplementary Material for this article can be found online at: https://www.frontiersin.org/articles/10.3389/fcell.2019.00226/full#supplementary-material

REFERENCES

Airola, M. V., and Hannun, Y. A. (2013). Sphingolipid metabolism and neutral sphingomyelinases. *Handb. Exp. Pharmacol.* 215, 57–76. doi: 10.1007/978-3-7091-1368-4_3

Airola, M. V., Shanbhogue, P., Shamseddine, A. A., Guja, K. E., Senkal, C. E., Maini, R., et al. (2017). Structure of human nSMase2 reveals an interdomain allosteric activation mechanism for ceramide generation. *Proc. Natl. Acad. Sci. U.S.A.* 114, E5549–E5558. doi: 10.1073/pnas.1705134114

Alebrahim, S., Khavandgar, Z., Marulanda, J., and Murshed, M. (2014). Inducible transient expression of Smpd3 prevents early lethality in fro/fro mice. *Genesis* 52, 408–416. doi: 10.1002/dvg.22765

Bhati, R., Patterson, C., Livasy, C. A., Fan, C., Ketelsen, D., Hu, Z., et al. (2008). Molecular characterization of human breast tumor vascular cells. *Am. J. Pathol.* 172, 1381–1390. doi: 10.2353/ajpath.2008.070988

Bortlein, C., Draeger, A., Schoenauer, R., Kuhlemann, A., Sauer, M., Schneider-Schaulies, S., et al. (2018). The neutral sphingomyelinase 2 is required to polarize and sustain T cell receptor signaling. *Front. Immunol.* 9:815. doi: 10.3389/fimmu.2018.00815

Chatterjee, S. (1993). Neutral sphingomyelinase increases the binding, internalization, and degradation of low density lipoproteins and synthesis of cholesteryl ester in cultured human fibroblasts. *J. Biol. Chem.* 268, 3401–3406.

Collenburg, L., Beyersdorf, N., Wiese, T., Arenz, C., Saied, E. M., Becker-Flegler, K. A., et al. (2017). The activity of the neutral sphingomyelinase is important in T cell recruitment and directional migration. *Front. Immunol.* 8:1007. doi: 10.3389/fimmu.2017.01007

Collenburg, L., Walter, T., Burgert, A., Muller, N., Seibel, J., Japtok, L., et al. (2016). A functionalized sphingolipid analogue for studying redistribution during activation in living T cells. *J. Immunol.* 196, 3951–3962. doi: 10.4049/jimmunol.1502447

Creekmore, A. L., Heffron, C. L., Brayfield, B. P., Roberts, P. C., and Schmelz, E. M. (2013). Regulation of cytoskeleton organization by sphingosine in a mouse cell model of progressive ovarian cancer. *Biomolecules* 3, 386–407. doi: 10.3390/biom3030386

Das, A., Brown, M. S., Anderson, D. D., Goldstein, J. L., and Radhakrishnan, A. (2014). Three pools of plasma membrane cholesterol and their relation to cholesterol homeostasis. *eLife* 3:e02882. doi: 10.7554/eLife.02882

Dessi, S., Batetta, B., Pani, A., Spano, O., Sanna, F., Putzolu, M., et al. (1997). Role of cholesterol synthesis and esterification in the growth of CEM and MOLT4 lymphoblastic cells. *Biochem. J.* 321(Pt 3), 603–608. doi: 10.1042/bj3210603

Eich, C., Manzo, C., de Keijzer, S., Bakker, G. J., Reinieren-Beeren, I., Garcia-Parajo, M. F., et al. (2016). Changes in membrane sphingolipid composition modulate dynamics and adhesion of integrin nanoclusters. *Sci. Rep.* 6:20693. doi: 10.1038/srep20693

Ejsing, C. S., Sampaio, J. L., Surendranath, V., Duchoslav, E., Ekroos, K., Klemm, R. W., et al. (2009). Global analysis of the yeast lipidome by quantitative shotgun mass spectrometry. *Proc. Natl. Acad. Sci. U.S.A.* 106, 2136–2141. doi: 10.1073/pnas.0811700106

Filosto, S., Ashfaq, M., Chung, S., Fry, W., and Goldkorn, T. (2012). Neutral sphingomyelinase 2 activity and protein stability are modulated by phosphorylation of five conserved serines. *J. Biol. Chem.* 287, 514–522. doi: 10.1074/jbc.M111.315481

Filosto, S., Fry, W., Knowlton, A. A., and Goldkorn, T. (2010). Neutral Sphingomyelinase 2 (nSMase2) is a phosphoprotein regulated by calcineurin (PP2B). *J. Biol. Chem.* 285, 10213–10222. doi: 10.1074/jbc.M109.069963

Fu, G. P., Chen, Y. H., Yu, M., Podd, A., Schuman, J., He, Y. H., et al. (2010). Phospholipase C gamma 1 is essential for T cell development, activation, and tolerance. *J. Exp. Med.* 207, 309–318. doi: 10.1084/jem.20090880

Gassert, E., Avota, E., Harms, H., Krohne, G., Gulbins, E., and Schneider-Schaulies, S. (2009). Induction of membrane ceramides: a novel strategy to interfere with T lymphocyte cytoskeletal reorganisation in viral immunosuppression. *PLoS Pathog.* 5:e1000623. doi: 10.1371/journal.ppat.1000623

Gault, C. R., Obeid, L. M., and Hannun, Y. A. (2010). An overview of sphingolipid metabolism: from synthesis to breakdown. *Adv. Exp. Med. Biol.* 688, 1–23. doi: 10.1007/978-1-4419-6741-1_1

Gulbins, A., Schumacher, F., Becker, K. A., Wilker, B., Soddemann, M., Boldrin, F., et al. (2018). Antidepressants act by inducing autophagy controlled by sphingomyelin-ceramide. *Mol. Psychiatry* 23, 2324–2346. doi: 10.1038/s41380-018-0090-9

He, Q., Wang, G., Dinkins, M., and Bieberich, E. (2011). A novel, apical ceramide-enriched compartment (ACEC) regulates ciliogenesis through a complex with ceramide-associated atypical PKC*. *Mol. Biol. Cell* 22, 2042–2053.

Henry, B., Moller, C., Dimanche-Boitrel, M. T., Gulbins, E., and Becker, K. A. (2013). Targeting the ceramide system in cancer. *Cancer Lett.* 332, 286–294. doi: 10.1016/j.canlet.2011.07.010

Herzog, R., Schuhmann, K., Schwudke, D., Sampaio, J. L., Bornstein, S. R., Schroeder, M., et al. (2012). LipidXplorer: a software for consensual cross-platform lipidomics. *PLoS One* 7:e29851. doi: 10.1371/journal.pone.0029851

Herzog, R., Schwudke, D., Schuhmann, K., Sampaio, J. L., Bornstein, S. R., Schroeder, M., et al. (2011). A novel informatics concept for high-throughput shotgun lipidomics based on the molecular fragmentation query language. *Genome Biol.* 12:R8. doi: 10.1186/gb-2011-12-1-r8

Hinkovska-Galcheva, V., Kjeldsen, L., Mansfield, P. J., Boxer, L. A., Shayman, J. A., and Suchard, S. J. (1998). Activation of a plasma membrane-associated neutral sphingomyelinase and concomitant ceramide accumulation during IgG-dependent phagocytosis in human polymorphonuclear leukocytes. *Blood* 91, 4761–4769.

Hofmann, K., Tomiuk, S., Wolff, G., and Stoffel, W. (2000). Cloning and characterization of the mammalian brain-specific. Mg2+-dependent neutral sphingomyelinase. *Proc. Natl. Acad. Sci. U.S.A.* 97, 5895–5900. doi: 10.1073/pnas.97.11.5895

Horton, J. D., Goldstein, J. L., and Brown, M. S. (2002). SREBPs: activators of the complete program of cholesterol and fatty acid synthesis in the liver. *J. Clin. Invest.* 109, 1125–1131. doi: 10.1172/jci15593

Kachler, K., Bailer, M., Heim, L., Schumacher, F., Reichel, M., Holzinger, C. D., et al. (2017). Enhanced acid sphingomyelinase activity drives immune evasion and tumor growth in non-small cell lung carcinoma. *Cancer Res.* 77, 5963–5976. doi: 10.1158/0008-5472.CAN-16-3313

Kim, W. J., Okimoto, R. A., Purton, L. E., Goodwin, M., Haserlat, S. M., Dayyani, F., et al. (2008). Mutations in the neutral sphingomyelinase gene SMPD3 implicate the ceramide pathway in human leukemias. *Blood* 111, 4716–4722. doi: 10.1182/blood-2007-10-113068

Lada, A. T., Davis, M., Kent, C., Chapman, J., Tomoda, H., Omura, S., et al. (2004). Identification of ACAT1- and ACAT2-specific inhibitors using a novel, cell-based fluorescence assay: individual ACAT uniqueness. *J. Lipid Res.* 45, 378–386. doi: 10.1194/jlr.d300037-jlr200

Lange, Y., Ye, J., and Steck, T. L. (2002). Effect of protein kinase C on endoplasmic reticulum cholesterol. *Biochem. Biophys. Res. Commun.* 290, 488–493. doi: 10.1006/bbrc.2001.6156

Litvinov, D. Y., Savushkin, E. V., and Dergunov, A. D. (2018). Intracellular and plasma membrane events in cholesterol transport and homeostasis. *J. Lipids* 2018:3965054. doi: 10.1155/2018/3965054

Marchesini, N., Luberto, C., and Hannun, Y. A. (2003). Biochemical properties of mammalian neutral sphingomyelinase 2 and its role in sphingolipid metabolism. *J. Biol. Chem.* 278, 13775–13783. doi: 10.1074/jbc.m212262200

Matsumoto, K., Fujiwara, Y., Nagai, R., Yoshida, M., and Ueda, S. (2008). Expression of two isozymes of acyl-coenzyme A: cholesterol acyltransferase-1 and -2 in clear cell type renal cell carcinoma. *Int. J. Urol.* 15, 166–170. doi: 10.1111/j.1442-2042.2007.01947.x

Menck, K., Sonmezer, C., Worst, T. S., Schulz, M., Dihazi, G. H., Streit, F., et al. (2017). Neutral sphingomyelinases control extracellular vesicles budding from

the plasma membrane. *J. Extracell. Vesicles* 6:1378056. doi: 10.1080/20013078.2017.1378056

Mendez, A. J., Oram, J. F., and Bierman, E. L. (1991). Protein-Kinase-C as a mediator of high-density-lipoprotein receptor-dependent efflux of intracellular cholesterol. *J. Biol. Chem.* 266, 10104–10111.

Milhas, D., Clarke, C. J., Idkowiak-Baldys, J., Canals, D., and Hannun, Y. A. (2010). Anterograde and retrograde transport of neutral sphingomyelinase-2 between the Golgi and the plasma membrane. *Biochim. Biophys. Acta* 1801, 1361–1374. doi: 10.1016/j.bbalip.2010.08.001

Murate, M., Abe, M., Kasahara, K., Iwabuchi, K., Umeda, M., and Kobayashi, T. (2015). Transbilayer distribution of lipids at nano scale. *J. Cell Sci.* 128, 1627–1638. doi: 10.1242/jcs.163105

Napolitano, M., Avella, M., Goode, N. T., Botham, K. M., and Bravo, E. (2004). Cholesterol esterification in human monocyte-derived macrophages is inhibited by protein kinase C with dual roles for mitogen activated protein kinases. *Cell Biol. Int.* 28, 717–725. doi: 10.1016/j.cellbi.2004.07.007

Paillasse, M. R., de Medina, P., Amouroux, G., Mhamdi, L., Poirot, M., and Silvente-Poirot, S. (2009). Signaling through cholesterol esterification: a new pathway for the cholecystokinin 2 receptor involved in cell growth and invasion. *J. Lipid Res.* 50, 2203–2211. doi: 10.1194/jlr.M800668-JLR200

Qin, J., Berdyshev, E., Poirer, C., Schwartz, N. B., and Dawson, G. (2012). Neutral sphingomyelinase 2 deficiency increases hyaluronan synthesis by up-regulation of Hyaluronan synthase 2 through decreased ceramide production and activation of Akt. *J. Biol. Chem.* 287, 13620–13632. doi: 10.1074/jbc.M111.304857

Rouquette-Jazdanian, A. K., Foussat, A., Lamy, L., Pelassy, C., Lagadec, P., Breittmayer, J. P., et al. (2005). Cholera toxin B-subunit prevents activation and proliferation of human CD4+ T cells by activation of a neutral sphingomyelinase in lipid rafts. *J. Immunol.* 175, 5637–5648. doi: 10.4049/jimmunol.175.9.5637

Sampaio, J. L., Gerl, M. J., Klose, C., Ejsing, C. S., Beug, H., Simons, K., et al. (2011). Membrane lipidome of an epithelial cell line. *Proc. Natl. Acad. Sci. U.S.A.* 108, 1903–1907. doi: 10.1073/pnas.1019267108

Schroepfer, G. J., Jr. (2000). Oxysterols: modulators of cholesterol metabolism and other processes. *Physiol. Rev.* 80, 361–554. doi: 10.1152/physrev.2000.80.1.361

Sezgin, E., Kaiser, H. J., Baumgart, T., Schwille, P., Simons, K., and Levental, I. (2012). Elucidating membrane structure and protein behavior using giant plasma membrane vesicles. *Nat. Protoc.* 7, 1042–1051. doi: 10.1038/nprot.2012.059

Shamseddine, A. A., Airola, M. V., and Hannun, Y. A. (2015). Roles and regulation of neutral sphingomyelinase-2 in cellular and pathological processes. *Adv. Biol. Regul.* 57, 24–41. doi: 10.1016/j.jbior.2014.10.002

Shanbhogue, P., Hoffmann, R. M., Airola, M. V., Maini, R., Hamelin, D. J., Garcia-Diaz, M., et al. (2019). The juxtamembrane linker in neutral sphingomyelinase-2 functions as an intramolecular allosteric switch that activates the enzyme. *J. Biol. Chem.* 294, 7488–7502. doi: 10.1074/jbc.RA118.007288

Shindou, H., Hishikawa, D., Harayama, T., Yuki, K., and Shimizu, T. (2009). Recent progress on acyl CoA: lysophospholipid acyltransferase research. *J. Lipid Res.* 50, S46–S51. doi: 10.1194/jlr.R800035-JLR200

Song, W., Wang, W., Wang, Y., Dou, L. Y., Chen, L. F., and Yan, X. W. (2015). Characterization of fluorescent NBD-cholesterol efflux in THP-1-derived macrophages. *Mol. Med. Rep.* 12, 5989–5996. doi: 10.3892/mmr.2015.4154

Sparrow, C. P., Patel, S., Baffic, J., Chao, Y. S., Hernandez, M., Lam, M. H., et al. (1999). A fluorescent cholesterol analog traces cholesterol absorption in hamsters and is esterified in vivo and in vitro. *J. Lipid Res.* 40, 1747–1757.

Stein, O., Ben-Naim, M., Dabach, Y., Hollander, G., and Stein, Y. (1992). Modulation of sphingomyelinase-induced cholesterol esterification in fibroblasts. CaCo2 cells, macrophages and smooth muscle cells. *Biochim. Biophys. Acta* 1126, 291–297. doi: 10.1016/0005-2760(92)90243-o

Stoffel, W., Hammels, I., Jenke, B., Binczek, E., Schmidt-Soltau, I., Brodesser, S., et al. (2016). Neutral sphingomyelinase (SMPD3) deficiency disrupts the Golgi secretory pathway and causes growth inhibition. *Cell Death Dis.* 7:e2488. doi: 10.1038/cddis.2016.385

Stoffel, W., Jenke, B., Block, B., Zumbansen, M., and Koebke, J. (2005). Neutral sphingomyelinase 2 (smpd3) in the control of postnatal growth and development. *Proc. Natl. Acad. Sci. U.S.A.* 102, 4554–4559. doi: 10.1073/pnas.0406380102

Subbaiah, P. V., Sowa, J. M., and Singh, D. K. (2008). Sphingolipids and cellular cholesterol homeostasis. Effect of ceramide on cholesterol trafficking and HMG CoA reductase activity. *Arch. Biochem. Biophys.* 474, 32–38. doi: 10.1016/j.abb.2008.03.019

Surma, M. A., Herzog, R., Vasilj, A., Klose, C., Christinat, N., Morin-Rivron, D., et al. (2015). An automated shotgun lipidomics platform for high throughput, comprehensive, and quantitative analysis of blood plasma intact lipids. *Eur. J. Lipid Sci. Technol.* 117, 1540–1549. doi: 10.1002/ejlt.201500145

Tan, L. H., Tan, A. J., Ng, Y. Y., Chua, J. J., Chew, W. S., Muralidharan, S., et al. (2018). Enriched expression of neutral sphingomyelinase 2 in the striatum is essential for regulation of lipid raft content and motor coordination. *Mol. Neurobiol.* 55, 5741–5756. doi: 10.1007/s12035-017-0784-z

Tani, M., and Hannun, Y. A. (2007). Analysis of membrane topology of neutral sphingomyelinase 2. *FEBS Lett.* 581, 1323–1328. doi: 10.1016/j.febslet.2007.02.046

Tonnetti, L., Veri, M. C., Bonvini, E., and D'Adamio, L. (1999). A role for neutral sphingomyelinase-mediated ceramide production in T cell receptor-induced apoptosis and mitogen-activated protein kinase-mediated signal transduction. *J. Exp. Med.* 189, 1581–1589. doi: 10.1084/jem.189.10.1581

van Vliet, A. R., Giordano, F., Gerlo, S., Segura, I., Van Eygen, S., Molenberghs, G., et al. (2017). The ER stress sensor PERK coordinates ER-plasma membrane contact site formation through interaction with filamin-A and F-actin remodeling. *Mol. Cell* 65:e886. doi: 10.1016/j.molcel.2017.01.020

Wu, Y. Q., Li, C., Riehle, A., Pollmeier, B., Gulbins, E., and Grassme, H. (2018). Mycobacterial infection is promoted by neutral sphingomyelinase 2 regulating a signaling cascade leading to activation of beta 1-integrin. *Cell Physiol. Biochem.* 51, 1815–1829. doi: 10.1159/000495683

Yang, W., Bai, Y., Xiong, Y., Zhang, J., Chen, S., Zheng, X., et al. (2016). Potentiating the antitumour response of CD8(+) T cells by modulating cholesterol metabolism. *Nature* 531, 651–655. doi: 10.1038/nature17412

Zech, T., Ejsing, C. S., Gaus, K., de Wet, B., Shevchenko, A., Simons, K., et al. (2009). Accumulation of raft lipids in T-cell plasma membrane domains engaged in TCR signalling. *EMBO J.* 28, 466–476. doi: 10.1038/emboj.2009.6

Zeidan, Y. H., Jenkins, R. W., and Hannun, Y. A. (2008). Remodeling of cellular cytoskeleton by the acid sphingomyelinase/ceramide pathway. *J. Cell Biol.* 181, 335–350. doi: 10.1083/jcb.200705060

Conflict of Interest: The authors declare that the research was conducted in the absence of any commercial or financial relationships that could be construed as a potential conflict of interest.

frontiers in Cell and Developmental Biology

REVIEW
published: 06 December 2019
doi: 10.3389/fcell.2019.00324

Glycosphingolipids and Infection. Potential New Therapeutic Avenues

Johannes M. F. G. Aerts, M. Artola, M. van Eijk, M. J. Ferraz and R. G. Boot*

Leiden Institute of Chemistry, Leiden University, Leiden, Netherlands

Glycosphingolipids (GSLs), the main topic of this review, are a subclass of sphingolipids. With their glycans exposed to the extracellular space, glycosphingolipids are ubiquitous components of the plasma membrane of cells. GSLs are implicated in a variety of biological processes including specific infections. Several pathogens use GSLs at the surface of host cells as binding receptors. In addition, lipid-rafts in the plasma membrane of host cells may act as platform for signaling the presence of pathogens. Relatively common in man are inherited deficiencies in lysosomal glycosidases involved in the turnover of GSLs. The associated storage disorders (glycosphingolipidoses) show lysosomal accumulation of substrate(s) of the deficient enzyme. In recent years compounds have been identified that allow modulation of GSLs levels in cells. Some of these agents are well tolerated and already used to treat lysosomal glycosphingolipidoses. This review summarizes present knowledge on the role of GSLs in infection and subsequent immune response. It concludes with the thought to apply glycosphingolipid-lowering agents to prevent and/or combat infections.

Keywords: glycosphingolipid, infection, glucosylceramide, lysosome, glycosidase, glycosyltransferase

OPEN ACCESS

Edited by:
Juergen Seibel,
Julius Maximilian University of Würzburg, Germany

Reviewed by:
Erdinc Sezgin,
Karolinska Institutet (KI), Sweden
Iwabuchi Kazuhisa,
Juntendo University, Japan

****Correspondence:***
Johannes M. F. G. Aerts
j.m.f.g.aerts@lic.leidenuniv.nl

Specialty section:
This article was submitted to Membrane Physiology and Membrane Biophysics, a section of the journal Frontiers in Cell and Developmental Biology

Received: *25 July 2019*
Accepted: *25 November 2019*
Published: *06 December 2019*

Citation:
Aerts JMFG, Artola M, van Eijk M, Ferraz MJ and Boot RG (2019) Glycosphingolipids and Infection. Potential New Therapeutic Avenues. Front. Cell Dev. Biol. 7:324. doi: 10.3389/fcell.2019.00324

INTRODUCTION TO GLYCOSPHINGOLIPIDS

Glycosphingolipids (GSLs) were discovered by the German chemist Johannes Thudichum while investigating the composition of the human brain in his London laboratory in the late 19th century (Thudichum, 1884). Thudichum meticulously identified the structure of the encountered novel class of lipids as consisting of a unique lipid moiety with attached sugar or phosphorylcholine groups. The hydrophobic moiety of the isolated brain lipids proved to contain as backbone a hitherto unknown D-erythro-Sphingosine, named after the mythical Sphinx for its "enigmatic properties to the enquirer." The value of Thudichum's findings was initially highly debated and did not meet recognition during his lifetime. Only 25 years after his death, Otto Rosenheim confirmed the accuracy of his publications which finally opened the present vast field of GSL research (King, 1956).

Features of Glycosphingolipids

Structure of Glycosphingolipids

In vertebrates the major form of the sphingoid base of GSLs is d18:1 sphingosine, (2*S*,3*R*,4*E*)-2aminooctadec-4-ene-1,3-diol. *N*-acylation of sphingosine results in the lipid ceramide (Cer), the primary sphingolipid. The attachment of sugars to Cer yields GSLs (**Figure 1A**). Ubiquitous in brain is the simple GSL galactosylceramide (GalCer), the major lipid constituent of myelin insulating axons of neuronal cells and formed as extended plasma membrane of oligodendrocytes. Following Thudichum's seminal findings, it became apparent that GSLs are not restricted to the

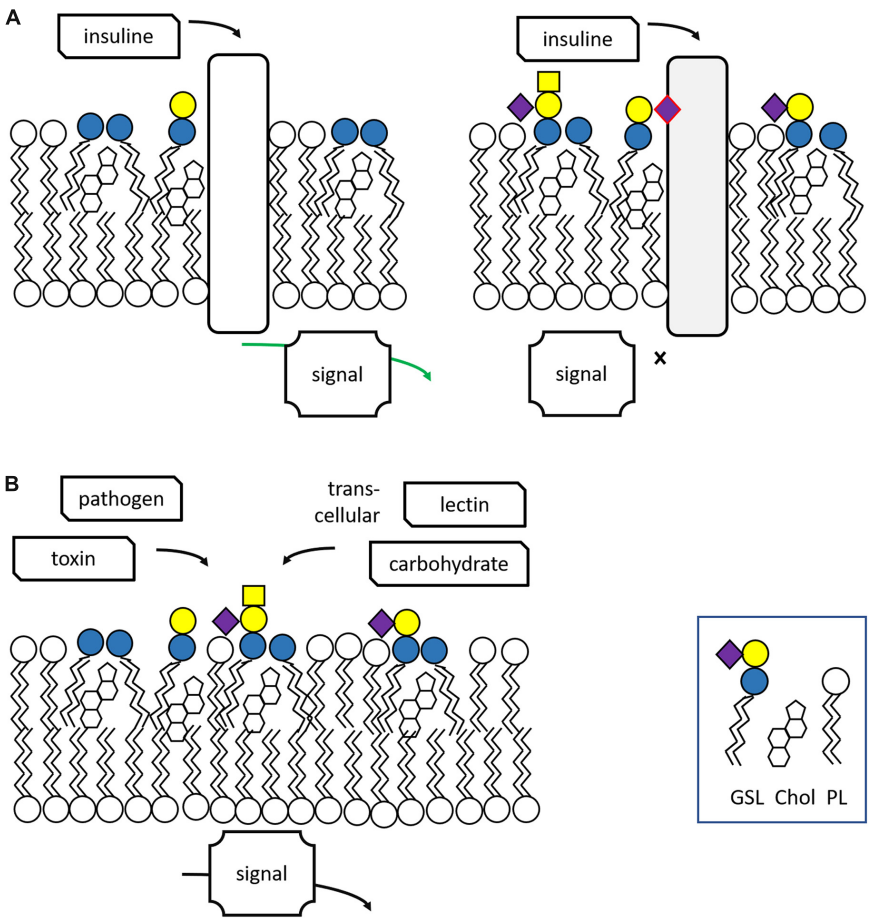

FIGURE 1 | Structure and synthesis of glycosphingolipids. **(A)** Synthesis of complex glycosphingolipids (GSLs) from the simple building blocks L-serine, fatty acyl-CoA, and UDP-sugars. **(B)** General structure of glycosphingolipid: indicated are the major globo-, isoglobo-, ganglio-, lacto-, and neolacto-series core structures.

brain but are common components of cells in various organisms. In the case of human GSLs, the first monosaccharide linked to Cer is either glucose or galactose. Additional sugars can be further attached to glucosylceramide (GlcCer) or GalCer, resulting in a plethora of lipids of which quantitatively the most abundant are the ganglio-, globo-, and neolacto-series of GSLs (**Figure 1B**). The structural diversity of GSLs and their nomenclature have been thoroughly reviewed (Wennekes et al., 2009; Merrill, 2011; Merrill and Sullards, 2017).

Synthesis of Glycosphingolipids

During their life in cells, GSL molecules traverse various subcellular compartments where specific modifications in their structure may occur (Wennekes et al., 2009; Gault et al., 2010; Merrill, 2011; Fabrias et al., 2012; D'Angelo et al., 2013; Tidhar and Futerman, 2013; Sandhoff and Sandhoff, 2018; Sandhoff et al., 2018). The synthesis starts at the endoplasmic reticulum (ER) where the enzyme serine palmitoyltransferase (SPT) generates keto-sphinganine from serine and palmitoyl-CoA (**Figure 1A**). This building block is next converted to sphinganine by 3-ketodihydrosphingosine reductase (KDSR). Subsequently, a series of ceramide synthases (CerS 1-6) form dihydroceramides with amide-linked fatty acyl moieties. Distinct dihydroceramides are generated since the various CerS enzymes have different acyl-CoA length preferences (Tidhar and Futerman, 2013). From these dihydroceramides the enzyme dihydroceramide desaturase-1 (DES1) forms Cer. The primary sphingolipid Cer is subject to further metabolism and its levels are tightly controlled in this manner, a necessity for cells since Cer promotes concentration-dependently apoptotic processes, and subsequent cell death (Zelnik et al., 2019). Cer may be converted into sphingomyelin (SM; phosphocholine-ceramide) or ceramide-1-phosphate (Cer1P). It may be also degraded by neutral ceramidases to fatty acid and sphingosine (Wennekes et al., 2009). A third metabolic route involves formation of structurally diverse GSLs through distinct pathways. In tissues like kidney and brain a large portion of newly formed Cer molecules enter the ER where conversion to GalCer occurs, catalyzed by the enzyme galactosylceramide synthase (CGT) using UDP-galactose as sugar donor (Sprong et al., 1998; van Meer et al., 2003). Sulfation of GalCer molecules may take place to generate sulfatide (sulfo-GalCer). More commonly, the Cer

transfer protein (CERT) transports newly formed Cer to the cytosolic leaflet *cis*-Golgi membranes (Hanada et al., 2003, 2009). Here, the enzyme glucosylceramide synthase (GCS; encoded by the *UGCG* gene) may transform Cer to GlcCer using UDP-glucose as sugar donor (Ichikawa et al., 1996). Some of the GlcCer in the cytosolic membrane leaflet is metabolized back again to Cer by the enzyme GBA2, a cytosol-faced β-glucosidase that also shows transglucosylase activity (van Weely et al., 1993; Boot et al., 2007; Marques et al., 2016). However, most newly formed GlcCer enters the Golgi apparatus where it can be stepwise modified by glycosyltransferases (Wennekes et al., 2009; Merrill, 2011; Merrill and Sullards, 2017; Sandhoff and Sandhoff, 2018). The addition of further sugars to GlcCer yields various types of GSLs (**Figure 1B**). Increasing the vast diversity of GSLs is the sulfation of particular lipids. After being modified in the Golgi apparatus, GSLs end up in the outer leaflet of the plasma membrane. GSLs may partly leave cells through incorporation in HDL-lipoproteins (Van den Bergh and Tager, 1976).

Congenital human disorders of ganglioside biosynthesis are very rare. Mutations in ST3GAL5 (encoding GM3 synthase) cause severe congenital infantile seizures. Mutations in B4GALNT1 (encoding GM2/GD2 synthase) lead to hereditary spastic paraplegia accompanied by intellectual disability (Li and Schnaar, 2018).

Degradation

Glycosphingolipids are internalized via endocytosis and end up in multi-vesicular bodies in endosomes. Next, their fragmentation takes place in lysosomes (Cox and Cachón-González, 2012; Platt, 2014). Through endocytosis lysosomes acquire also exogenous GSLs. These are components of phagocytosed senescent cells and debris as well as endocytosed lipoproteins. In the acid lysosomes, GSLs are fragmented by a series of glycosidases in a stepwise manner (Ferraz et al., 2014; Breiden and Sandhoff, 2019). In this process, specific glycosidases remove terminal sugar moieties from GSLs, the reverse of the biosynthetic pathway. Many of the lysosomal glycosidases fragmenting GSLs are assisted in their activity by specific accessory proteins (GM2 activator protein and saposin A–D) (Ferraz et al., 2014; Breiden and Sandhoff, 2019). Cer, the lipid product of lysosomal GSL degradation, is cleaved by the lysosomal acid ceramidase into sphingosine and fatty acid. The degradation products (sugars, fatty acids, and sphingosine) are exported to the cytosol. The exported sphingosine may be next re-used in the salvage pathway that generates again Cer molecules for the synthesis of SM or GSLs. Alternatively, sphingosine is transformed by sphingosine kinases (SK1 and SK2) to sphingosine-1-phosphate (S1P). This may be subsequently degraded by S1P lyase into phosphatidylethanolamine and 2-trans-hexadecenal (Pyne et al., 2016).

Functions of Glycosphingolipids

Lipid Raft Signaling Platforms

Glycosphingolipids reside primarily in the cellular plasma membrane with their sugar moieties exposed to the exterior. At the cell surface, GSLs have multiple functions. Through interactions among GSL molecules and cholesterol molecules via hydrogen bonds and van der Waal's forces semi-ordered domains spontaneously form in the plasma membrane. In these lipid rafts specific proteins involved in signaling events locate (Mukherjee and Maxfield, 2004; Lingwood and Simons, 2010; Sonnino and Prinetti, 2013; **Figure 2A**). It has become clear that GSLs in lipid rafts may regulate the activity of some of these signaling receptors. A particularly well studied example of the impact of gangliosides on receptor signaling concerns the epidermal growth factor receptor (EGFR). Well-established is the inhibitory effect of GM3 on the receptor's kinase domain activation, a phenomenon abolished by conversion of GM3 to lactosylceramide (LacCer) or the K642G amino acid substitution in the EGFR (Coskun et al., 2011). Thus, GM3 modulates the allosteric structural transition from inactive to signaling EGFR dimer. Another example forms the insulin receptor whose activity is influenced by local gangliosides (Kabayama et al., 2007; Langeveld and Aerts, 2009). Obese mice genetically unable to synthetize the ganglioside GM3 show better glucose tolerance and insulin sensitivity than control obese animals (Tagami et al., 2002; Yamashita et al., 2003). Pharmacological reduction of GSLs, including that of gangliosides, improves markedly insulin sensitivity and glucose homeostasis in obese rodents (Aerts et al., 2007; Zhao et al., 2009). Of note, patients with Gaucher disease (GD) (see section "Lysosomal Glycosphingolipid Storage Disorders and Therapy" for a detailed description of this inherited disorder) show elevated levels of the gangliosides GM3 in cells and tissue and in parallel reduced insulin sensitivity (Ghauharali-van der Vlugt et al., 2008; Langeveld et al., 2008).

A similar modulatory role for gangliosides has also been noted for other receptors such as the T-cell receptor amongst others (Inokuchi et al., 2018). Recently gangliosides were found to also impact on the activity of the membrane embedded protein NPC1L1, critically involved in intestinal cholesterol absorption (Nihei et al., 2018). Another intriguing finding is that the ganglioside GM1 prevents oligomerization of b-amyloid oligomers, whilst SM promotes this (Amaro et al., 2016). This finding may proof to be relevant to design strategies to ameliorate Alzheimer's disease (Amaro et al., 2016). LacCer-enriched lipid rafts have been identified in plasma and granular membranes of human neutrophils (see Nakayama et al., 2018 for a review). The first report on LacCer-raft mediated neutrophil function concerned superoxide generation (Iwabuchi and Nagaoka, 2002). It was demonstrated that the incubation of neutrophils with anti-LacCer antibody induced generation of superoxide. A key role for activation of Lyn in the process was identified (Iwabuchi and Nagaoka, 2002).

Glycosphingolipids have been found to also interact other cells, either via protein-carbohydrate or carbohydrate-carbohydrate interactions (**Figure 2B**). The proteins involved in such interactions are three major classes of lectins: selectins binding sialylated and fucosylated glycans; siglecs binding galectins and sialylated glycans; and galectins binding glycans containing terminal galactose (Schnaar, 2004).

In land animals, GSLs fulfill a special function in the outermost skin, the stratum corneum. Here, extraordinary GlcCer molecules with very-long-chain fatty acid (C30–32) and an ω-hydroxyl group esterified to another fatty acid are obligate precursors

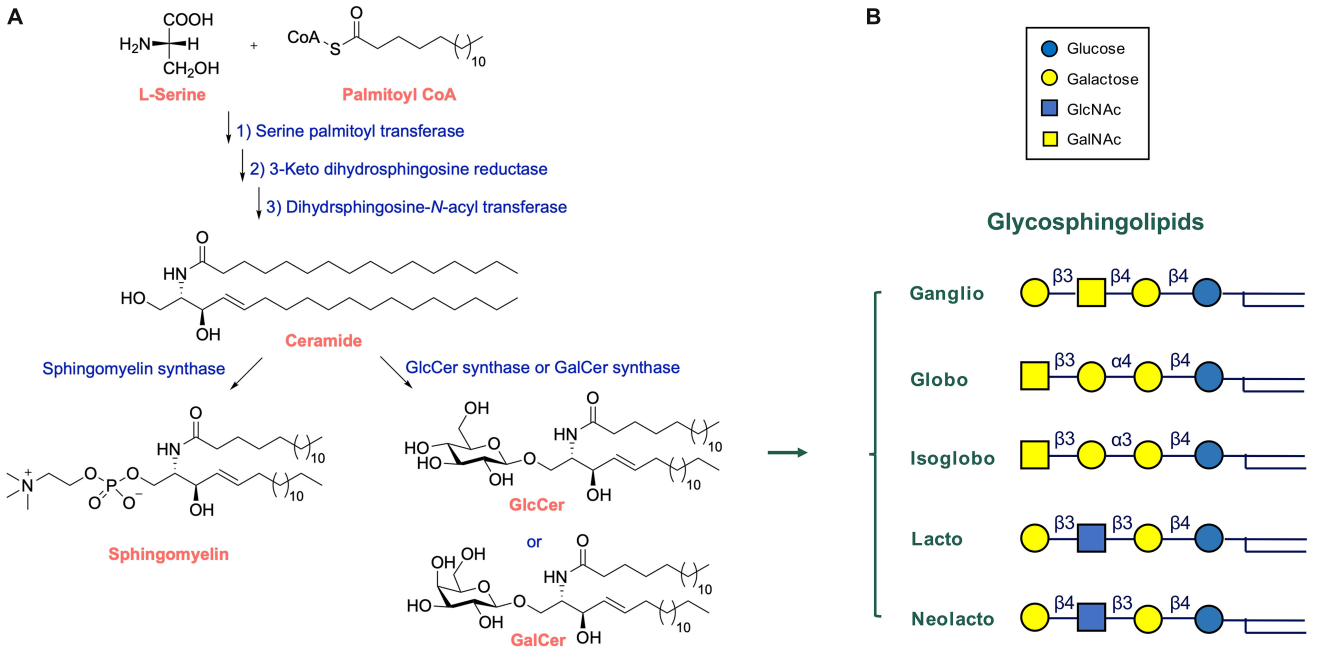

FIGURE 2 | Lipid rafts and other functions of glycosphingolipids. **(A)** Glycosphingolipids are essential components of lipid rafts where signaling events occur in response to extracellular triggers. Excessive GSLs (GM3) may interfere with signaling. **(B)** GSLs may interact with toxins, bacteria and trans-cellular lectins and carbohydrates. Adapted from Feingold and Elias (2014).

to Cer that are locally required to build the desired protective and permeability layer (Feingold and Elias, 2014; Van Smeden and Bouwstra, 2016; Wertz, 2018). Disturbance in skin GlcCer and Cer are associated with severe, even fatal, dysfunction of the skin (Van Smeden et al., 2017). The presence of specific gangliosides in neurons has multiple functions and proves to be essential for optimal interplay with the insulating myelin (Lopez and Báez, 2018). In particular, lack of specific gangliosides in axons of neurons leads to disturbed interaction with myelin-associated glycoprotein (MAG) in the innermost membrane of myelin. This impairment is thought to underly the spastic paraplegia during neuronal deficiency of specific gangliosides (Schnaar and Lopez, 2009).

Exposed glycans of GSLs on epithelial cells contribute to the protective properties of the glycocalyx of internal body linings. A similar type of protective function of GSLs is envisioned for lysosomes inside cells. Beside the outer leaflet plasma membrane, the inner leaflet of the lysosomal membrane is rich in GSLs. This membrane also contains integral membrane proteins that are decorated with N-linked glycans. By the combined presence of GSLs and membrane glycoproteins the lysosomal membrane is thought to be protected by a sugar barrier against self-degradation by the proteases and lipases present in the lumen of the compartment (Schwake et al., 2013).

Specific GSLs at the surface of cells also undergo specific interactions with the outside world. For example, some GSLs contain the glycan-based ABO antigens, crucial in self-recognition and of importance in transfusion medicine (Kościelak, 2012). E-selectin mediated binding of tissue invading leukocytes to endothelial cells is known to be dependent on specific GSLs (Nimrichter et al., 2008).

Glycosphingolipids and Infection

Interaction With Pathogens and Toxins

Many viruses, bacteria, and bacterial toxins bind to carbohydrates of GSLs on host cell surfaces (**Figure 3**). Recommended reviews of the topic are Nakayama et al. (2018) and Hanada (2005).

Viruses

Some viruses are known to exploit GSLs in their life cycle in hosts (Lingwood, 1996). One well studied example is the human immunodeficiency virus (HIV) (Lingwood and Branch, 2011). HIV virions enter their host cells by the binding of the viral envelope gp120 to the primary receptor CD4, an essential interaction for viral fusion and entry. G protein-coupled α- and β-chemokine receptors are required as "co-receptors" together with CD4 for HIV-1 infection. GSLs display a complex interaction with HIV gp120, with reports suggesting functions as alternate entry receptors, facilitators for HIV infection, as well as natural resistance factors for HIV infection. Several GSLs (Gb3, GM3, GalCer, sulfatide) appear to bind the HIV adhesin gp120 (Lund et al., 2009; Lingwood and Branch, 2011). Upon binding, GSLs such as GalCer and GM3 facilitate subsequent interaction of the virus with its chemokine co-receptor on the cell surface (Lingwood and Branch, 2011). In contrast, Gb3 may successfully compete for co-receptor binding, and prevent fusion and viral entry (Lund et al., 2009; Lingwood and Branch, 2011). *Polyomavirus* invades human erythrocytes via the gangliosides

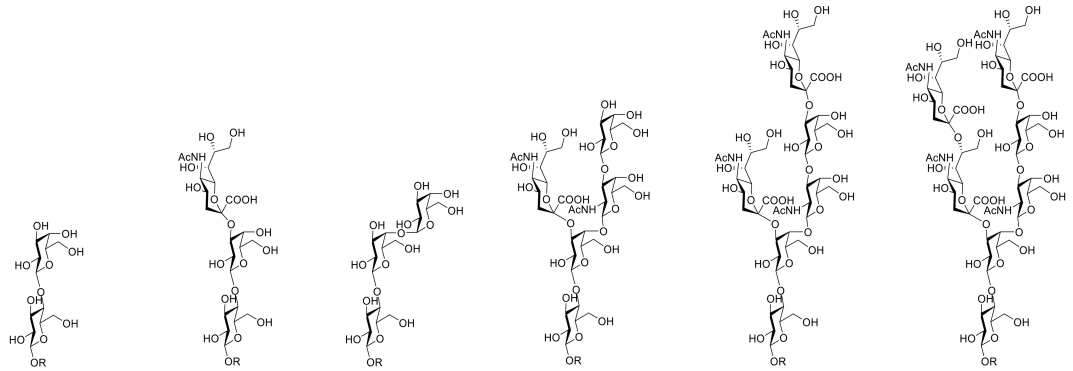

GSL	LacCer	GM3	Gb3	GM1	GD1a	GT1b
Virus	-	HIV	HIV	Polyomavirus, SV40	Polyomavirus	Polyomavirus
Toxins	-	-	Verotoxin, Shiga toxin	Cholera toxin, E. coli enterotoxin	-	-
Bacteria	Several including: *Mycobacteria*, *B. dysenteriae*, *B. pertussis*, *H.pylori*	*Shigella*	*E. coli*	*P. aeruginosa*, *B. bifidum*, *Lactobacillus*, *Brucella sp.*	-	-

FIGURE 3 | Examples of direct interactions of glycosphingolipids with pathogens and toxins.

GD1a and GT1b (Schwake et al., 2013). GM1 has also been shown to act as receptors for simian virus 40 (SV40) and polyoma virus (Tsai et al., 2003).

Toxins

Protein toxins show an AB structure, with a catalytic A domain and a B domain encoding host receptor recognition (Zuverink and Barbieri, 2018). Gb3, (a.k.a. CD77 or P(k) blood group antigen) is known to bind to Shiga toxin and the closely related *Escherichia coli* (*E. coli*) derived verotoxin B subunit (van Heyningen, 1974). The globoside thus is mediating verotoxin induced hemolytic uremic syndrome (HUS) (Lingwood, 1996). The ganglioside GM1 serves as the primary receptor for cholera toxin and the highly homologous *E. coli* heat-labile enterotoxin (Hirst et al., 2002). *Clostridium tetani* neurotoxin and *Clostridium botulinum* neurotoxin type A and B use several gangliosides as receptors (Kitamura et al., 1999). The ganglioside GM2 acts as a receptor for delta-toxin of *Clostridium perfringens* (Jolivet-Reynaud et al., 1989). Cholera toxin B subunit (CTB) binds to GM1 enriched in lipid rafts (Cuatrecasas, 1973a,b). GM1 on epithelial cells also binds *E. coli* enterotoxin (Hyun and Kimmich, 1984; Masserini et al., 1992; Kuziemko et al., 1996). The gangliosides present in human milk are thought to compete the binding of *Vibrio cholerae* and *E. coli* enterotoxins in the intestine and thus offer protection (Otnaess et al., 1983; Newburg and Chaturvedi, 1992).

Bacteria

The ganglioside asialo-GM1 (GA1) at the surface of epithelial cells binds *Bifidobacterium bifidum*, *Pseudomonas aeruginosa*, and *Lactobacillus* (de Bentzmann et al., 1996; Mukai et al., 2004). The ganglioside GM1 has been implicated in infections with *Brucella* species (Naroeni and Porte, 2002; Martín-Martín et al., 2010). Fimbriated *E. coli* bind to the globosides Gb3 and Gb4 (Leffler and Svanborg-Edén, 1981). Virulent strains of *Bordetella pertussis*, a human respiratory pathogen, bind with high affinity to sulfatide (Brennan et al., 1991). *Mycoplasma pneumoniae* appears to exploit GSLs containing terminal Gal($3SO_4$)β1-residues (Krivan et al., 1989).

The neutral GSL LacCer at the surface of intestinal epithelial cells binds various microorganisms. These include *Candida albicans*, *B. pertussis*, *Mycobacterium tuberculosis*, *E. coli*, *Bacillus dysenteriae,* and *Propionibacterium freudenreichii* (Nakayama et al., 2018). Possibly milk-derived LacCer protects the host from invading pathogens. Interactions between the sugar moieties of gangliosides and the polysaccharide moieties of *Shigella* lipopolysaccharide were found to facilitate binding of bacteria to human CD4+ T cells (Belotserkovsky et al., 2018). There are indications that the adhesion of *Helicobacter pylori*, causing chronic active gastritis, peptic ulcer disease and gastric adenocarcinoma, depends on gangliosides in the human stomach. The gangliosides Neu5Acα3-neolactohexaosylceramide and Neu5Acα3-neolactooctaosylceramide mediate attachment of *H. pylori* SabA (sialic acid binding adhesin) there (Mahdavi et al., 2002; Benktander et al., 2018).

Immune System

The role of GSLs in immune cell functions receives increasing interest and has been recently reviewed (Zuidscherwoude et al., 2014; Zhang et al., 2019). Besides acting as entry point of pathogens and toxins, GSLs also impact on the response of

the immune system to pathogens. As such, GSLs themselves can also transduce signals as revealed by the effect of their crosslinking by multivalent binders such as bacterial toxins, or alternatively IgM antibodies (Spiegel, 1989; Klokk et al., 2016). Influx of calcium ions upon cell surface crosslinking of GM1 seems to be largely mediated by L-type calcium channels (Carlson et al., 1994). As another example, in human neutrophils LacCer forms specific lipid rafts in the plasma membrane as well as granular membranes. These rafts have been shown to interact with β-glucan of *C. albicans* and lipoarabinomannan (LAM) of *Mycobacteria* (Sato et al., 2006; Nakayama et al., 2016). Such binding triggers signaling cascades involving Src family kinases. The responses to this are chemotaxis, phagocytosis, and phagolysosome formation. In neutrophils, *M. tuberculosis* smartly targets the LacCer-enriched lipid rafts in phagosomes to inhibit the maturation of phagosome to lytic phagolysosomes (Nakayama et al., 2018).

Other direct and indirect interactions of GSLs with immune cells affecting their activity have more recently come to light. For example, the C-type lectin receptor Mincle (macrophage inducible C-type lectin), contributes to innate immune responses by recognition of lipids stemming from foreign pathogens like glucose and trehalose mycolates and glycosyl diacylglycerols, but also lipids from damaged cells (Williams, 2017). Among the reported Mincle-interacting self antigens are sterols but also GlcCer (Nagata et al., 2017).

In the case of dendritic cells, glycolipid antigens are presented by MHC class I molecule (CD1d) of dendritic cells via T-cell receptor recognition to activate natural killer T (NKT) cells which control innate and adaptive immune responses (Kumar et al., 2017). The marine sponge GSL α-GalCer is identified as potent lipid antigen activating invariant NTK (iNKT) cells. These cells are also activated by the endogenous iGb3Cer (Galα1-3Galβ1-4GlcβCer) (Pei et al., 2012). More recently, excessive GlcCer has also been proposed to act as an iNKT cell activator (Nair et al., 2015). Of note, GlcCer synthase deficiency in mouse cells was already earlier reported to impair CD1d-dependent activation of iNKT cells, suggesting that GlcCer or its metabolites might be endogenous ligands for CD1d-restricted iNKT cells (Stanic et al., 2003).

In addition to modulating innate immunity, GSLs also appear to play critical roles in adaptive immunity. For example, gangliosides influence T cell receptors (TCRs) on CD-4 positive (CD4+) and CD-8 positive (CD8+) T cells, respectively (Nagafuku et al., 2012). Here it is thought that the precise ganglioside composition of lipid rafts in specific T cell populations is a prerequisite for their associated specific effector functions. This regulatory aspect of gangliosides in T cell biology seems highly relevant for allergic and autoimmune diseases and has been topic of excellent reviews (Inokuchi et al., 2018; Nakayama et al., 2018).

In some specific autoimmune neuropathies affecting the nervous system the autoimmune attack is due to antibodies reactive with gangliosides. Anti-ganglioside antibodies occur for example with Guillain–Barré syndrome. These antibodies may be induced by infections with pathogens containing glycan components that are structurally similar to gangliosides. The most important example of this is *Campylobacter jejuni* whose surface lipo-oligosaccharide mimics GD1a, GT1a, GM1, and other gangliosides (Goodfellow and Willison, 2018). Binding of autoantibodies on gangliosides activates locally complement and recruits macrophages, causing local impairment of nerve conduction in these patients.

Sphingomyelin and Infection

Sphingomyelin is the most abundant cellular sphingolipid. Like GSLs, SM is also implicated in infections and the immune system's response to these (Wu et al., 2018; Li et al., 2019). For example, mice with deficiency of acid sphingomyelinase (ASMase; Sphingomyelin phosphodiesterase 1), the enzyme hydrolyzing SM to Cer and phosphorylcholine, are strongly susceptible to *Citrobacter rodentium*-driven colitis (Meiners et al., 2019). Mice overexpressing ASMase in T cells show increased T cell activation and reduced parasitemia in upon infection with *Plasmodium yoelii* (Hose et al., 2019). Two forms of ASMase are encoded by the *SMPD1* gene: a lysosomal form (L-ASMase) and a secretory form (S-ASMase). Although ASMase has an acid pH optimum for activity, the same enzyme, when secreted, also catalyzes the hydrolysis of SM in the circulation and on the plasma membrane (Smith and Schuchman, 2008; Schuchman, 2010). ASMase deficiency results in the accumulation of SM in lysosomes and causes the neuropathic (type A) and non-neuropathic (type B) variants of Niemann-Pick disease (Schuchman, 2010). Generation of Cer molecules on the cell surface by ASMase leads to formation of Cer-enriched domains, distinct from traditional lipid rafts, that act as platforms governing signaling events (Li et al., 2019). Cer-enriched platforms occur in cells upon diverse receptor or non-receptor stimuli, including CD95, FcγRII, CD40, platelet-activating factor receptor (PAF), viral infection, *P. aeruginosa*, *Neisseria gonorrhoeae*, *Staphylococcus aureus*, cisplatin, Cu^{2+}, irradiation and UV-light (Li et al., 2019). The interaction of Cer-enriched platforms with CD95, the death receptor Fas, is the best understood. CD95 induces an increased ASMase activity on the cell surface, thus generating Cer-enriched platforms amplifying CD95 signaling (Gulbins and Grassmé, 2002; Grassmé et al., 2007).

The ASMase/Cer system has been implicated in infections with pathogens. *P. aeruginosa* is a gram-negative bacterium commonly affecting immune-compromised patients and patients with chronic wounds, sepsis, or chronic emphysema. Patients with cystic fibrosis (CF) have a particular risk for chronic *P. aeruginosa* infections. The infection of mammalian cells with different strains of *P. aeruginosa* induces the rapid activation of ASMase and translocation to the plasma membrane (Li et al., 2019). Generated Cer-rich rafts by ASMase mediates the internalization of *P. aeruginosa*, which is prevented by inhibitors of the ASMase or by ASMase-deficiency. Amitriptyline, a tricyclic antidepressant (TCA), is a functional ASMase inhibitor. Administration of amitriptyline to CF mice normalizes pulmonary Cer levels and abolishes pathological outcome, including susceptibility to infection (Becker et al., 2010). Amitriptyline might therefore offer in the future a novel medicine to treat CF patients.

ASMase appears critical in the regulation of host interactions with other bacteria as well, including *S. aureus*, *Mycobacteria*, *Listeria monocytogenes* and *Neisseria* species. *S. aureus*, is a commensal opportunistic bacterium that colonizes approximately 30% of human populations. It may cause life-threatening endocarditis, diseases, sepsis, toxic shock syndrome, and pneumonia (Li et al., 2019). *S. aureus* is the primary cause of sepsis and lethal lung edema. Mice treated with the ASMase inhibitor amitriptyline show reduced lung edema upon *S. aureus* exposure. The effect on sepsis of various ASMase inhibitors (imipramine, desipramine, and amitriptyline), is presently studied in animal models (Chung et al., 2018; Xia et al., 2019).

Lysosomal Glycosphingolipid Storage Disorders and Therapy

Inherited defects in lysosomal enzymes fragmenting GSLs lead to accumulation of the accompanying substrate in lysosomes. Several inherited lysosomal glycosphingolipid storage disorders (glycosphingolipidoses) occur in humans, see **Figure 4** (Cox and Cachón-González, 2012; Ferraz et al., 2014; Platt, 2014; Breiden and Sandhoff, 2019).

Gaucher Disease

A prototype glycosphingolipidosis is GD, named after Ernest Gaucher who published the first case report (Beutler and Grabowski, 2001). GD is a recessively inherited disorder stemming from mutations in the *GBA* gene. This codes for an acid β-glucosidase, better known as glucocerebrosidase (GCase; EC. 3.2.1.45) (Brady et al., 1966; Beutler and Grabowski, 2001). The 497 amino acid glycoprotein cleaves GlcCer to Cer, the penultimate step in lysosomal breakdown of most GSLs. Prominent GlcCer accumulation characteristically occurs in tissue macrophages (Gaucher cells) of GD patients. The clinical presentation of GCase deficiency is very heterogeneous, from severe neonatal complications to a virtually asymptomatic course. Non-neuronopathic (type 1), acute neuronopathic (type 2), and sub-acute neuronopathic (type 3) GD phenotypes are discerned. A complete deficiency of GCase causes fatal skin pathology causing abnormal permeability properties (Beutler and Grabowski, 2001). It has recently been recognized that individuals with a mutant *GBA* allele are at increased risk, about 20-fold, to develop Parkinson disease (Siebert et al., 2014). Although some mutations in the *GBA* gene are associated with a benign GD disease course, e.g., the amino acid substitution N370S, the GBA genotype proves to poorly predict actual disease presentation in GD patients. Considerable variability in symptoms and general disease severity is documented for several GBA genotypes, even among monozygotic twins (Ferraz et al., 2014). The molecular basis for the interindividual variability in outcome of GCase deficiency among GD patients is not identified yet.

Putative advantage of GD heterozygotes

Another intriguing aspect of GD forms the high incidence among Ashkenazim with a disease allele frequency at approximately 0.03–0.04, around 10-fold higher than in non-Jewish populations (Beutler and Grabowski, 2001). The elevated incidence of GD in Ashkenazi Jews is due to four common mutations (Koprivica et al., 2000). The elevated incidence of GD (and other lysosomal storage disorders in glycosphingolipid metabolism such Niemann-Pick disease type B and Tay-Sachs disease) in Ashkenazi populations has led to a great deal of speculation about its cause, ranging from founder effects to a heterozygote advantage. A founder effect as cause seems very unlikely given the small size of the founding Ashkenazi populations in Eastern Europe (Diamond, 1994). The origin of the common N370S mutation in Ashkenazi Jews is thought, based on haplotype data, to have arisen too recently, a mere thousand years ago, to explain the current allele frequency as the result of genetic drift alone (Boas, 2000; Colombo, 2000). The increased allele frequencies of four GBA mutations in Ashkenazi Gaucher patients makes this additionally statistically improbable (Diamond, 1994; Diaz et al., 2000). It therefore has been speculated that GD carriers may be less vulnerable to infectious diseases that cause many victims in city-dwelling populations such as bubonic plaque or tuberculosis. Macrophages are key players in GD and Niemann-Pick disease type B and these cells host *M. tuberculosis*. Evidence for the appealing carrier advantage hypothesis is still missing. Of note, in a zebrafish model of tuberculosis (*M. marianum*) deficiency of several lysosomal hydrolases increases vulnerability for the infection, however, interestingly not that of GCase (Berg et al., 2016; Meijer and Aerts, 2016).

Gaucher cells and their secreted markers

Characteristic lipid-laden macrophages accumulate in the spleen, liver, bone marrow, lymph nodes, and lung of GD patients. These Gaucher cells are metabolically active, alternatively activated, macrophages (Boven et al., 2004). GD patients develop low-grade inflammation and coagulation, and show activation of the complement cascade (Hollak et al., 1997; Vissers et al., 2007). Gaucher cells over-express and secrete specific proteins into the circulation of which some are presently employed as biomarkers of body burden of storage macrophages (Ferraz et al., 2014). Examples are chitotriosidase, the human chitinase (Hollak et al., 1994; Bussink et al., 2006), the chemokine CCL18/PARC (Boot et al., 2004) and a soluble fragment of gpNMB (Kramer et al., 2016). Interestingly, increased levels of plasma chitotriosidase also occur with some infectious disease involving macrophages such as Leishmaniasis, tuberculosis, malaria, and leprosy (Hollak et al., 1994; Aerts et al., 2008; Iyer et al., 2009; Di Rosa et al., 2016).

Metabolic Adaptations to GCase Deficiency for Better or Worse

Striking metabolic adaptations occur during GCase deficiency (Ferraz et al., 2014). Firstly, increased anabolism of GlcCer to gangliosides takes place, contributing to insulin resistance (Langeveld and Aerts, 2009). Another adaptation involves the cytosol-faced retaining β-glucosidase GBA2. Increased activity of this enzyme during GCase deficiency leads to increased formation of pro-apoptotic Cer from GlcCer. Reducing GBA2 activity, genetically or by means of small compound

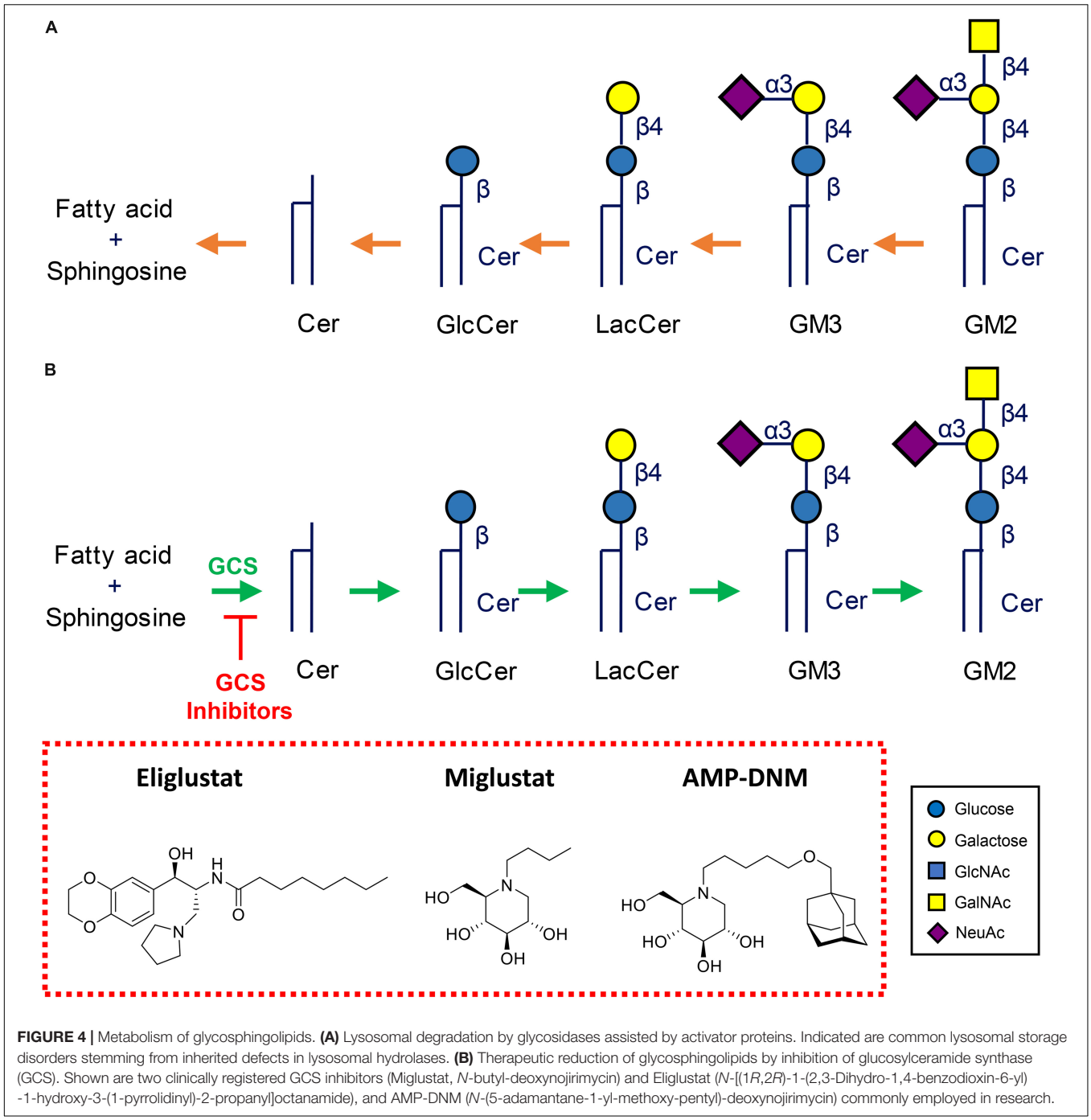

FIGURE 4 | Metabolism of glycosphingolipids. **(A)** Lysosomal degradation by glycosidases assisted by activator proteins. Indicated are common lysosomal storage disorders stemming from inherited defects in lysosomal hydrolases. **(B)** Therapeutic reduction of glycosphingolipids by inhibition of glucosylceramide synthase (GCS). Shown are two clinically registered GCS inhibitors (Miglustat, *N*-butyl-deoxynojirimycin) and Eliglustat (*N*-[(1*R*,2*R*)-1-(2,3-Dihydro-1,4-benzodioxin-6-yl) -1-hydroxy-3-(1-pyrrolidinyl)-2-propanyl]octanamide), and AMP-DNM (*N*-(5-adamantane-1-yl-methoxy-pentyl)-deoxynojirimycin) commonly employed in research.

inhibitors like the iminosugar AMP-DNM, has remarkable beneficial effects in Niemann Pick type C (NPC) mice with a defect in the lysosomal protein NPC1 mediating efflux of cholesterol from lysosomes and secondary GCase deficiency (Nietupski et al., 2012; Marques et al., 2015). AMP-DNM treatment also exerts a neuro-protective effect in mice with Sandhoff disease, another glycosphingolipid storage disorder (Ashe et al., 2011). Of note, GBA2 can act as transglycosylase, transferring the glucose from GlcCer to cholesterol and forming glucosyl-β-cholesterol (GlcChol) in the process (Marques et al., 2016). Another adaptation during GCase is the conversion of accumulating GlcCer in lysosomes by acid ceramidase to its sphingoid base, glucosylsphingosine (GlcSph) (Ferraz et al., 2016). GlcSph reaches the circulation and plasma GlcSph is on average 200-fold elevated in symptomatic type 1 GD patients (Dekker et al., 2011). Measurement of elevated plasma GlcSph has come into use for laboratory confirmation of GD diagnosis (Mirzaian et al., 2015). Albeit clinically distinct diseases, the glycosphingolipidoses show as uniform response to lysosomal GSL accumulation, that is the

conversion of storage lipid to its corresponding sphingoid base. In Fabry disease (α-galactosidase deficiency), Krabbe disease (galactocerebrosidase deficiency), GM2 gangliosidosis (β-hexosaminidase deficiency), and Niemann Pick diseases types A and B (acid sphingomyelinase deficiency) the corresponding sphingoid bases of the accumulating substrates (lysoGb3, galactosylsphingosine, lysoGM2, and lysoSM, respectively) are formed and their plasma levels are markedly increased, offering diagnostic possibilities (Ferraz et al., 2014; Mirzaian et al., 2017; Marshall et al., 2019).

Pathophysiology

There is compelling evidence for a prominent role of Gaucher cells in GD pathology. Excessive GlcSph stemming from these storage cells is likely pathogenic. It is thought to contribute to the common osteopenia (reduced bone mineral density) in GD patients by impairing osteoblasts (Mistry et al., 2014), to promote α-synuclein aggregation, a hallmark of Parkinson disease (Taguchi et al., 2017), and to underly as auto-antigen in the common gammopathies in GD patients that can evolve into multiple myeloma, a relatively common leukemia in GD patients (Nair et al., 2016). Antigenicity of GlcCer and GlcSph has been postulated to lead to complement cascade activation promoting local tissue inflammation and destruction (Pandey et al., 2017). The diminished cerebral microvascular density in a neuronopathic GD mouse has been attributed to GlcSph based on the observed ability of the sphingoid base to interfere with endothelial cytokinesis *in vitro* (Smith et al., 2018). At present the impact of excessive glucosylated metabolites, like GlcChol, generated by GBA2 activity during GCase deficiency is unknown.

Therapies

A very successful therapeutic intervention of type 1 GD is enzyme replacement therapy (ERT), an approach in which patient's macrophages are supplemented with lacking enzyme by repeated intravenous infusion of therapeutic recombinant GCase (Brady, 2003). To ensure the desired targeting to macrophages, the therapeutic GCase has N-linked glycans with terminal mannose groups to favor uptake by macrophages via mannose-binding lectins like the mannose receptor at the surface of these cells. Two-weekly ERT of type 1 GD patients spectacularly reverses visceral symptoms like hepatosplenomegaly and corrects hematological abnormalities. Unfortunately, ERT does not prevent neurological symptoms due to inability of the enzyme to pass the blood brain barrier. Substrate reduction therapy (SRT) is an alternative registered treatment of type 1 GD. It aims to balance the synthesis of GlcCer with the diminished capacity of GD patients to degrade it (Platt et al., 2001; Aerts et al., 2006). In SRT orally available inhibitors of GCS are employed. Two drugs [Miglustat, *N*-butyl-deoxynojirimycin (NB-DNJ) and Eliglustat (*N*-[(1*R*,2*R*)-1-(2,3-Dihydro-1,4-benzodioxin-6-yl)-1-hydroxy-3-(1-pyrrolidinyl)-2-propanyl] octanamide)] are presently approved for treatment of type 1 GD patients (**Figure 4B**). Treatment with the more potent and specific Eliglustat is found to result in visceral improvements in patients on a par with ERT (Mistry et al., 2018). Unfortunately, Eliglustat fails to penetrate the brain effectively and can neither be applied to treat neuropathic GD. The design of suitable brain-permeable inhibitors of GCS is investigated and pursued by industry and academic researchers (Shayman and Larsen, 2014). Venglustat (ibiglustat) is developed by Sanofi Genzyme for the treatment of Fabry disease, neuronopathic GD and Parkinson disease. A phase 2 clinical trial (NCT02228460) of Venglustat has recently been conducted to assess short-term safety and effects of the treatment in adult men with Fabry disease. Miglustat is a relatively poor inhibitor of GCs (IC_{50} in the micromolar range) and inhibits off-target intestinal glycosidases and in particular non-lysosomal GBA2 (IC_{50} value in the nanomolar range). Albeit being brain permeable, it is presently not registered as drug to treat neuronopathic GD. Comparable, but superior, iminosugar inhibitors of GCS to Miglustat, like AMP-DNM [*N*-(5-adamantane-1-yl-methoxy-pentyl)-deoxynojirimycin] and its idose-configured analog, were developed some decades ago (Wennekes et al., 2010). These are orally available high nanomolar GCS inhibitors that have impact on GSL metabolism in brain of mice and were found to ameliorate the disease course in mice with NPC disease and Sandhoff disease (Nietupski et al., 2012; Marshall et al., 2019; **Figure 4B**). Through medicinal chemistry more potent and specific GCS inhibitors have been designed using ido-AMP-DNM as scaffold (Ghisaidoobe et al., 2014). It should be noted that reduction of GlcCer formation by GCS results in the reduction of GlcCer and the metabolically upstream GSLs such as globosides and gangliosides. It therefore has the potential to ameliorate lysosomal storage disorders in which such compounds accumulate, such as GD, Fabry disease, GM2 gangliosidosis, Tay-Sachs disease, Sandhoff disease, GM1 gangliosidosis, and NPC disease.

Pharmacological Modulation of GSLs: New Avenue for Infection Control?

Therapeutic GCS Inhibitors

Given the demonstrated importance of GSLs in infection and control thereof by the immune system (see section "Glycosphingolipids and Infection") and given the recent application of well tolerated inhibitors of GSL biosynthesis in GD patients (see section "Lysosomal Glycosphingolipid Storage Disorders and Therapy"), it is here proposed to consider use of such compounds to control and/or prevent specific infections. We argue the hypothetical case that glycosphingolipid lowering is feasible and tolerated and might be considered as new therapeutic avenue for specific infectious diseases.

Supportive Findings

Experimental support for the use of GSL-lowering agent to combat infection can be found in literature. For example, P-fimbriated *E. coli* are pathogenic in uncomplicated pyelonephritis. The P fimbriae of the bacterium bind the globosides such as Gb3 and Gb4 (Källenius et al., 1980; Leffler and Svanborg-Edén, 1981). When mice were fed with a high dose of the GSL biosynthesis inhibitor NB-DNJ, they showed a

decrease in levels of GSLs and less susceptibility for urinary tract infection by P-fimbriated *E. coli* (Svensson et al., 2003).

Along the same line is the outcome of elegant studies by Inokuchi et al. (2015, 2018). Studies with genetically modified mice lacking specific gangliosides (GM3S-null mice expressing o-series gangliosides, but not a- or b-series gangliosides and GM2/GD2S-null mice expressing GM3 and GD3, but no other gangliosides) rendered new insights regarding the importance of the presence of specific gangliosides during allergic and autoimmune diseases. It appears that reduction of specific gangliosides might offer treatment for specific disorders of the immune system (Inokuchi et al., 2015). One example in this direction is allergic asthma, a type 1 hypersensitivity reaction, in which CD4+ T cells mediate Th2 cytokine (IL-4 and IL-13) production, stimulating B cells to produce IgE antibodies. GM3S-null mice show striking reduction of allergic airway responses normally induced by ovalbumin (OVA) inhalation (Nagafuku et al., 2012).

Noteworthy are also the beneficial findings made with GSL lowering agents for systemic lupus erythematosus (SLE). This autoimmune disease manifests with chronic inflammation and leads to damage of tissue (Tsokos, 2011; Kidani and Bensinger, 2014). In SLE there is a prominent T cell dysfunction: CD4+ T cells from patients have lipid rafts with an altered GSL composition. Elevated GSLs (LacCer, Gb3, and GM1) in SLE patients are linked to increased expression of LXRb. The inhibition of GSL biosynthesis with NB-DNJ has been reported to correct CD4+ T cell signaling. In addition, it decreased anti-dsDNA antibody production by autologous B cells in SLE patients (McDonald et al., 2014).

Pharmacological reduction of GSLs is reported to exert beneficial anti-inflammatory effects. GSL-lowering by oral AMP-DNM treatment of mice with trinitrobenzene sulphonic acid (TNBS)- and oxazolone-induced colitis reduced disease severity and edema and suppressed inflammation (Shen et al., 2004). Prominent anti-inflammatory effects of AMP-DNM treatment were also noted for the liver and adipose tissue of obese rodents (Bijl et al., 2009; van Eijk et al., 2009; Lombardo et al., 2012). Non-Alcoholic Fatty Liver Disease (NAFLD) develops during the metabolic syndrome. NALFD involves liver abnormalities ranging from steatosis (fat accumulation) to non-alcoholic steatohepatitis (NASH) including fibrosis and inflammation. Treatment of obese mice with AMP-DNM not only corrects glucose homeostasis and restores insulin signaling in the liver but also reduces inflammation in the tissue (Bijl et al., 2009). A subsequent study revealed that a treatment with the GSL-lowering AMP-DNM is able to significantly correct pre-existing NASH (Lombardo et al., 2012). During obesity, inflammation of adipose tissue is thought to significantly contribute to pathophysiology. AMP-DNM treatment of obese mice improves the status of adipose tissue in many aspects, including a prominent reduction of inflammation (van Eijk et al., 2009). The treatment also leads to decreased iNKT cell activation in adipose tissue of lean mice (Rakhshandehroo et al., 2019).

Fungal GlcCer and GCS as Target

Fungal infections (cryptococcosis, candidiasis, aspergillosis, and pneumocystosis) are clinically highly relevant. Shortcomings of current anti-fungal drugs are toxicity and drug resistance. Moreover, not all fungi respond to particular drugs. A recently recognized universal target for combatting fungi is GlcCer (Rollin-Pinheiro et al., 2016; Fernandes et al., 2018). This lipid proves to be crucial for the virulence of pathogenic fungi in plants and man. The latter include *C. albicans, Cryptococcus neoformans*, and *Aspergillus fumigatus*. GlcCer is in particular critical for survival of fungi in neutral and alkaline environments. Indeed, antibodies to fungal GlcCer were found to exert antifungal effects at such conditions. More recently, desired lowering of fungal GlcCer can be reached by reducing the biosynthesis of the lipid. Well tolerated acylhydrazones have been identified as specific inhibitors of fungal GCS, an enzyme that fundamentally differs from the mammalian counterpart and that is not inhibited by acylhydrazones (Lazzarini et al., 2018; Mor et al., 2018). Pharmaceutical reduction of fungal GlcCer is now envisioned as new opportunity to combat fungal infections, including cryptococcosis.

Neuraminidase Inhibitors as Anti-influenza Viral Agents

In the 1990's inhibitors of neuraminidase have been designed for prophylaxis and treatment of influenza. The surface envelope of the influenza virus contains the glycoproteins hemagglutinin and neuraminidase. Hemagglutinin mediates viral attachment to the cell surface receptor containing a terminal N-acetylneuraminic acid residue attached α-(King, 1956; Merrill, 2011) or α-(King, 1956; Gault et al., 2010) to a galactose. By a variety of techniques, like thin-layer chromatography overlay assays and mass spectrometry, the nature of lipid receptors has been identified (Meisen et al., 2012; Hidari et al., 2013). The viral neuraminidase is essential for timely release of the virus from the cellular anchor. The neuraminidase inhibitors zanamivir, laninamivir, oseltamivir, and peramivir have been shown to be effective against most influenza strains, but resistance to specific drugs has developed in some cases (Dobson et al., 2015; Laborda et al., 2016). Some of the neuraminidase inhibitors are also employed as useful research tools in investigations on ganglioside biology (Crain and Shen, 2004; Moore et al., 2007). Total internal reflection fluorescence microscopy has been recently successfully employed to investigate the interaction of viruses with ganglioside containing lipid bilayers, the importance of hemagglutinin and neuraminidase in the process and the inhibitory action of zanamivir (Müller et al., 2019).

FUTURE LIPIDOMICS CHALLENGES

The investigation of lipids has been historically complicated by their intrinsic hydrophobic features and heterogeneous nature. The recent progress in quantitative mass spectrometric detection of lipids has, however, opened a new world for

lipidomics. This field is rapid advancing (see Han and Gross, 2003 for an excellent review on the topic). In particular ESI (electrospray ionization) and MALDI (matrix assisted laser desorption/ionization) mass spectrometry methods are nowadays successfully applied in lipidomics (Wang et al., 2019). Besides targeted measurement of specific lipids with MRM (multiple reaction monitoring), non-targeted approaches like shotgun and multi-dimensional lipidomics are increasingly employed (for a recent review on the topic see Bilgin et al., 2016). Improvements have been made in lipid extraction methods (Cruz et al., 2016; Löfgren et al., 2016) and internal standards, such as isotope encoded analogs, become increasingly available (Wisse et al., 2015; Mirzaian et al., 2016; Wang et al., 2017). Derivatization or deacylation of specific lipids may assist their quantitative detection (Mirzaian et al., 2017; Ma et al., 2019). An important new development is the availability of techniques to study the biology of lipids in living cells. Fluorescent NBD and BODIPY tagged lipids have been used in first generation cell biological investigations and in recent times advances have been made in the generation of photoactivatable, caged, photo-switchable, and tri-functional lipid derivatives assisting the imaging of lipids (reviewed in Laguerre and Schultz, 2018). The spatio-temporal detection of endogenous lipids in cells and tissues still remains a major challenge. QQImaging mass spectrometry (IMS) aims to visualize the location and distribution of metabolites in intact biological samples (see Parrot et al., 2018 for a recent review). One of the ISM techniques employs desorption electrospray ionization (DESI) (Parrot et al., 2018). Minimally destructive DESI-IMS chemical screening is achieved at the μm-scale resolution. Alternatively, MALDI-MS imaging is used to detect locally lipids, including GSLs (Vens-Cappell et al., 2016; Jones et al., 2017; Caughlin et al., 2018; Hunter et al., 2018; Sugiyama and Setou, 2018; Tobias et al., 2018; Enomoto et al., 2019). A new development forms the technology for *in situ* visualization of enzymes involved in glycosphingolipid metabolism. Designed have been fluorescent activity-based probes that covalently label – and visualize – active enzyme molecules through covalent linkage to catalytic nucleophile residues. An example in this direction is the enzyme glucocerebrosidase for which probes have been developed allowing *in situ* monitoring of active enzyme molecules (Witte et al., 2010; Kallemeijn et al., 2012; van Meel et al., 2019).

PERSPECTIVES

Clinical and laboratory research over many decades has revealed that various pathogens require GSLs of host cells for infection. Thus, the modulation of such lipids in host cells could *a priori* be considered as treatment for infection control. An obvious provision for such approach is that it does no harm. Any significant reduction of GSLs has been considered for a long time to yield considerable side-effects, likely translating in severe symptoms. The long-term outcome of treatment of patients suffering from GD with agents that reduce GSLs is, however, remarkably positive. No major side-effects are observed in individuals treated for a number of years (Mistry et al., 2018; Lewis and Gaemers, 2019). So far, the agents used do not achieve significant reduction in GSLs in the brain, however, a new generation of compounds aiming at that is being tested at the moment. The near future will learn whether it is feasible to safely reduce GSLs in cells and tissues, including the brain. Next it will have to be established whether such reductions are indeed effective for infection control.

Enormous progress has been made in knowledge on the role of GSLs in various kinds of infection and the immune system's response to this. At this moment much of the knowledge is still descriptive and little translation to preventing and/or treating infections has been accomplished. Genetics and genomics may not provide answers to all questions. It remains essential to acquire fundamental insight on metabolism of GSLs in these gene-oriented times. Such insight will essentially contribute to the design/development of suitable agents than can subtly modulate GSLs as desired for infection control.

This review focusses on pharmacological ways to reduce GSL levels. A fundamentally different approach to target GSL-pathogen interactions that has also been conceived is the design of potent carbohydrate-type competitors of bacterial adhesion (Schengrund, 2003; Pieters, 2011). Such approach copies more or less the presumed protective effects of oligosaccharides in milk during the colonization of the intestine.

In conclusion, the coming years should reveal whether GSLs may act as valuable target in infection control.

AUTHOR CONTRIBUTIONS

All authors contributed to writing the review and preparing figures.

FUNDING

Research on GSL was funded by NWO, Netherlands (NWO-BBOL, grant GlcCer, JA).

ACKNOWLEDGMENTS

The authors acknowledge the longstanding collaboration with their colleagues, in particular Prof. Herman Overkleeft and Prof. Gijs van der Marel, in the Leiden Institute of Chemistry as well as their collaboration with researchers in the Lysosomal Disease Unit of the Academic Medical Center in Amsterdam. The support over many years by members of Dutch Gaucher disease patient's society is greatly appreciated. Research on glycosphingolipids in health and disease is presently supported by a grant to JA from NWO (Building Blocks of Life: GlcCer).

REFERENCES

Aerts, J. M., Hollak, C. E., Boot, R. G., Groener, J. E., and Maas, M. (2006). Substrate reduction therapy of glycosphingolipid storage disorders. *J. Inherit. Metab. Dis.* 29, 449–456. doi: 10.1007/s10545-006-0272-5

Aerts, J. M., Ottenhoff, R., Powlson, A. S., Grefhorst, A., van Eijk, M., Dubbelhuis, P. F., et al. (2007). Pharmacological inhibition of glucosylceramide synthase enhances insulin sensitivity. *Diabetes Metab. Res. Rev.* 56, 1341–1349. doi: 10.2337/db06-1619

Aerts, J. M., van Breemen, M. J., Bussink, A. P., Ghauharali, K., Sprenger, R., Boot, R. G., et al. (2008). Biomarkers for lysosomal storage disorders: identification and application as exemplified by chitotriosidase in Gaucher disease. *Acta Paediatr.* 97, 7–14. doi: 10.1111/j.1651-2227.2007.00641.x

Amaro, M., Šachl, R., Aydogan, G., Mikhalyov, I. I., Vácha, R., and Hof, M. (2016). GM1 ganglioside inhibits β-Amyloid oligomerization induced by sphingomyelin. *Angew. Chem. Int. Ed. Engl.* 55, 9411–9415. doi: 10.1002/anie.201603178

Ashe, K. M., Bangari, D., Li, L., Cabrera-Salazar, M. A., Bercury, S. D., Nietupski, J. B., et al. (2011). Iminosugar-based inhibitors of glucosylceramide synthase increase brain glycosphingolipids and survival in a mouse model of Sandhoff disease. *PLoS One* 6:e21758. doi: 10.1371/journal.pone.0021758

Becker, K. A., Riethmüller, J., Lüth, A., Döring, G., Kleuser, B., and Gulbins, E. (2010). Acid sphingomyelinase inhibitors normalize pulmonary ceramide and inflammation in cystic fibrosis. *Am. J. Respir. Cell Mol. Biol.* 42, 716–724. doi: 10.1165/rcmb.2009-0174OC

Belotserkovsky, I., Brunner, K., Pinaud, L., Rouvinski, A., Dellarole, M., Baron, B., et al. (2018). Glycan-Glycan interaction determines *Shigella* tropism toward human T Lymphocytes. *mBio* 9, e2309–e2317. doi: 10.1128/mBio.02309-17

Benktander, J., Barone, A., Johansson, M. M., and Teneberg, S. (2018). *Helicobacter* pylori SabA binding gangliosides of human stomach. *Virulence* 9, 738–751. doi: 10.1080/21505594.2018.1440171

Berg, R. D., Levitte, S., O'Sullivan, M. P., O'Leary, S. M., Cambier, C. J., Cameron, J., et al. (2016). Lysosomal disorders drive susceptibility to tuberculosis by compromising macrophage migration. *Cell* 165, 139–152. doi: 10.1016/j.cell.2016.02.034

Beutler, E., and Grabowski, G. A. (2001). "Glucosylceramide lipidosis-gaucher disease," in *The Metabolic and Molecular Bases of Inherited Diseases*, 8th Edn, eds C. R. Scriver, A. L. Beaudet, W. S. Sly, and D. Valle, (NewYork, NY: McGraw-Hill).

Bijl, N., Sokolović, M., Vrins, C., Langeveld, M., Moerland, P. D., Ottenhoff, R., et al. (2009). Modulation of glycosphingolipid metabolism significantly improves hepatic insulin sensitivity and reverses hepatic steatosis in mice. *Hepatology* 50, 1431–1441. doi: 10.1002/hep.23175

Bilgin, M., Born, P., Fezza, F., Heimes, M., Mastrangelo, N., Wagner, N., et al. (2016). Lipid discovery by combinatorial screening and untargeted LC-MS/MS. *Sci. Rep.* 6:27920. doi: 10.1038/srep27920

Boas, F. E. (2000). Linkage to Gaucher mutations in the Ashkenazi population: effect of drift on decay of linkage disequilibrium and evidence for heterozygote selection. *Blood Cells Mol. Dis.* 26, 348–359. doi: 10.1006/bcmd.2000.0314

Boot, R. G., Verhoek, M., de Fost, M., Hollak, C. E., Maas, M., Bleijlevens, B., et al. (2004). Marked elevation of the chemokine CCL18/PARC in Gaucher disease: a novel surrogate marker for assessing therapeutic intervention. *Blood* 103, 33–39. doi: 10.1182/blood-2003-05-1612

Boot, R. G., Verhoek, M., Donker-Koopman, W., Strijland, A., van Marle, J., Overkleeft, H. S., et al. (2007). Identification of the non-lysosomal glucosylceramidase as beta-glucosidase 2. *J. Biol. Chem.* 282, 1305–1312. doi: 10.1074/jbc.M610544200

Boven, L. A., van Meurs, M., Boot, R. G., Mehta, A., Boon, L., Aerts, J. M., et al. (2004). Gaucher cells demonstrate a distinct macrophage phenotype and resemble alternatively activated macrophages. *Am. J. Clin. Pathol.* 122, 359–369. doi: 10.1309/BG5V-A8JR-DQH1-M7HN

Brady, R. O. (2003). Enzyme replacement therapy: conception, chaos and culmination. *Philos. Trans. R. Soc. Lond. B Biol. Sci.* 358, 915–919. doi: 10.1098/rstb.2003.1269

Brady, R. O., Kanfer, J. N., Bradley, R. M., and Shapiro, D. (1966). Demonstration of a deficiency of glucocerebroside-cleaving enzyme in Gaucher's disease. *J. Clin. Invest.* 45, 1112–1115. doi: 10.1172/JCI105417

Breiden, B., and Sandhoff, K. (2019). Lysosomal glycosphingolipid storage diseases. *Annu. Rev. Biochem.* 88, 461–485. doi: 10.1146/annurev-biochem-013118-111518

Brennan, M. J., Hannah, J. H., and Leininger, E. (1991). Adhesion of *Bordetella pertussis* to sulfatides and to the GalNAc beta 4Gal sequence found in glycosphingolipids. *J. Biol. Chem.* 266, 18827–18831.

Bussink, A. P., van Eijk, M., Renkema, G. H., Aerts, J. M., and Boot, R. G. (2006). The biology of the Gaucher cell: the cradle of human chitinases. *Int. Rev. Cytol.* 252, 71–128. doi: 10.1016/S0074-7696(06)52001-7

Carlson, R. O., Masco, D., Brooker, G., and Spiegel, S. (1994). Endogenous ganglioside GM1 modulates L-type calcium channel activity in N18 neuroblastoma cells. *J. Neurosci.* 14, 2272–2281. doi: 10.1523/JNEUROSCI.14-04-02272.1994

Caughlin, S., Maheshwari, S., Agca, Y., Agca, C., Harris, A. J., Jurcic, K., et al. (2018). Membrane-lipid homeostasis in a prodromal rat model of Alzheimer's disease: characteristic profiles in ganglioside distributions during aging detected using MALDI imaging mass spectrometry. *Biochim. Biophys. Acta Gen. Subj.* 1862, 1327–1338. doi: 10.1016/j.bbagen.2018.03.011

Chung, H. Y., Witt, C. J., Hurtado-Oliveros, J., Wickel, J., Gräler, M. H., Lupp, A., et al. (2018). Acid sphingomyelinase inhibition stabilizes hepatic ceramide content and improves hepatic biotransformation capacity in a murine model of polymicrobial sepsis. *Int. J. Mol. Sci.* 19:E3163. doi: 10.3390/ijms19103163

Colombo, R. (2000). Age estimate of the N370S mutation causing Gaucher disease in Ashkenazi Jews and European populations: a reappraisal of haplotype data. *Am. J. Genet.* 66, 692–697. doi: 10.1086/302757

Coskun, Ü, Grzybek, M., Drechsel, D., and Simons, K. (2011). Regulation of human EGF receptor by lipids. *Proc. Natl. Acad. Sci. U.S.A.* 108, 9044–9048. doi: 10.1073/pnas.1105666108

Cox, T. M., and Cachón-González, M. B. (2012). The cellular pathology of lysosomal diseases. *J. Pathol.* 226, 241–254. doi: 10.1002/path.3021

Crain, S. M., and Shen, K. F. (2004). Neuraminidase inhibitor, oseltamivir blocks GM1 ganglioside-regulated excitatory opioid receptor-mediated hyperalgesia, enhances opioid analgesia and attenuates tolerance in mice. *Brain Res.* 995, 260–266. doi: 10.1016/j.brainres.2003.09.068

Cruz, M., Wang, M., Frisch-Daiello, J., and Han, X. (2016). Improved butanol-methanol (BUME) method by replacing acetic acid for lipid extraction of biological samples. *Lipids* 51, 887–896. doi: 10.1007/s11745-016-4164-7

Cuatrecasas, P. (1973a). Gangliosides and membrane receptors for cholera toxin. *Biochemistry* 12, 3558–3566. doi: 10.1021/bi00742a032

Cuatrecasas, P. (1973b). Vibrio cholerae choleragenoid. Mechanism of inhibition of cholera toxin action. *Biochemistry* 12, 3577–3581. doi: 10.1021/bi00742a034

D'Angelo, G., Capasso, S., Sticco, L., and Russo, D. (2013). Glycosphingolipids: synthesis and functions. *FEBS J.* 280, 6338–6353. doi: 10.1111/febs.12559

de Bentzmann, S., Roger, P., Dupuit, F., Bajolet-Laudinat, O., Fuchey, C., Plotkowski, M. C., et al. (1996). Asialo GM1 is a receptor for *Pseudomonas aeruginosa* adherence to regenerating respiratory epithelial cells. *Infect. Immun.* 64, 1582–1588.

Dekker, N., van Dussen, L., Hollak, C. E., Overkleeft, H., Scheij, S., Ghauharali, K., et al. (2011). Elevated plasma glucosylsphingosine in Gaucher disease: relation to phenotype, storage cell markers, and therapeutic response. *Blood* 118, e118–e127. doi: 10.1182/blood-2011-05-352971

Di Rosa, M., Distefano, G., Zorena, K., and Malaguarnera, L. (2016). Chitinases and immunity: ancestral molecules with new functions. *Immunobiology* 221, 399–411. doi: 10.1016/j.imbio.2015.11.014

Diamond, J. M. (1994). Human genetics. Jewish lysosomes. *Nature* 368, 291–292. doi: 10.1038/368291a0

Diaz, G. A., Gelb, B. D., Risch, N., Nygaard, T. G., Frisch, A., Cohen, I. J., et al. (2000). Gaucher disease: the origins of the Ashkenazi Jewish N370S and 84GG acid beta-glucosidase mutations. *Am. J. Hum. Genet.* 66, 1821–1832. doi: 10.1086/302946

Dobson, J., Whitley, R. J., Pocock, S., and Monto, A. S. (2015). Oseltamivir treatment for influenza in adults: a meta-analysis of randomised controlled trials. *Lancet* 385, 1729–1737. doi: 10.1016/S0140-6736(14)62449-1

Enomoto, H., Takeda, S., Hatta, H., and Zaima, N. (2019). Tissue-specific distribution of sphingomyelin species in pork chop revealed by matrix-assisted laser desorption/ionization-imaging mass spectrometry. *J. Food Sci.* 84, 1758–1763. doi: 10.1111/1750-3841.14667

Fabrias, G., Muñoz-Olaya, J., Cingolani, F., Signorelli, P., Casas, J., Gagliostro, V., et al. (2012). Dihydroceramide desaturase and dihydrosphingolipids: debutant players in the sphingolipid arena. *Prog. Lipid Res.* 51, 82–94. doi: 10.1016/j.plipres.2011.12.002

Feingold, K. R., and Elias, P. M. (2014). Role of lipids in the formation and maintenance of the cutaneous permeability barrier. *Biochim. Biophys. Acta* 1841, 280–294. doi: 10.1016/j.bbalip.2013.11.007

Fernandes, C. M., Goldman, G. H., and Del Poeta, M. (2018). Biological roles played by sphingolipids in dimorphic and filamentous fungi. *mBio* 9:e00642-18. doi: 10.1128/mBio.00642-18

Ferraz, M. J., Kallemeijn, W. W., Mirzaian, M., Herrera Moro, D., Marques, A., Wisse, P., et al. (2014). Gaucher disease and Fabry disease: new markers and insights in pathophysiology for two distinct glycosphingolipidoses. *Biochim. Biophys. Acta* 1841, 811–825. doi: 10.1016/j.bbalip.2013.11.004

Ferraz, M. J., Marques, A. R., Appelman, M. D., Verhoek, M., Strijland, A., Mirzaian, M., et al. (2016). Lysosomal glycosphingolipid catabolism by acid ceramidase: formation of glycosphingoid bases during deficiency of glycosidases. *FEBS Lett.* 590, 716–725. doi: 10.1002/1873-3468.12104

Gault, C. R., Obeid, L. M., and Hannun, Y. A. (2010). An overview of sphingolipid metabolism: from synthesis to breakdown. *Adv. Exp. Med. Biol.* 688, 1–23. doi: 10.1007/978-1-4419-6741-1_1

Ghauharali-van der Vlugt, K., Langeveld, M., Poppema, A., Kuiper, S., Hollak, C. E., Aerts, J. M., et al. (2008). Prominent increase in plasma ganglioside GM3 is associated with clinical manifestations of type I Gaucher disease. *Clin. Chim. Acta* 389, 109–113. doi: 10.1016/j.cca.2007.12.001

Ghisaidoobe, A. T., van den Berg, R. J., Butt, S. S., Strijland, A., Donker-Koopman, W. E., Scheij, S., et al. (2014). Identification and development of biphenyl substituted iminosugars as improved dual glucosylceramide synthase/neutral glucosylceramidase inhibitors. *J. Med. Chem.* 57, 9096–9104. doi: 10.1021/jm501181z

Goodfellow, J. A., and Willison, H. J. (2018). Gangliosides and autoimmune peripheral nerve diseases. *Prog. Mol. Biol. Transl. Sci.* 156, 355–382. doi: 10.1016/bs.pmbts.2017.12.010

Grassmé, H., Riethmüller, J., and Gulbins, E. (2007). Biological aspects of ceramide-enriched membrane domains. *Prog. Lipid Res.* 46, 161–170. doi: 10.1016/j.plipres.2007.03.002

Gulbins, E., and Grassmé, H. (2002). Ceramide and cell death receptor clustering. *Biochim. Biophys. Acta* 1585, 139–145. doi: 10.1016/s1388-1981(02)00334-7

Han, X., and Gross, R. W. (2003). Global analyses of cellular lipidomes directly from crude extracts of biological samples by ESI mass spectrometry: a bridge to lipidomics. *J. Lipid Res.* 44, 1071–1079. doi: 10.1194/jlr.r300004-jlr200

Hanada, K. (2005). Sphingolipids in infectious diseases. *Jpn. J. Infect. Dis.* 58, 131–148.

Hanada, K., Kumagai, K., Tomishige, N., and Yamaji, T. (2009). CERT-mediated trafficking of ceramide. *Biochim. Biophys. Acta* 1791, 684–691. doi: 10.1016/j.bbalip.2009.01.006

Hanada, K., Kumagai, K., Yasuda, S., Miura, Y., Kawano, M., Fukasawa, M., et al. (2003). Molecular machinery for non-vesicular trafficking of ceramide. *Nature* 426, 803–809. doi: 10.1038/nature02188

Hidari, K. I., Yamaguchi, M., Ueno, F., Abe, T., Yoshida, K., and Suzuki, T. (2013). Influenza virus utilizes N-linked sialoglycans as receptors in A549 cells. *Biochem. Biophys. Res. Commun.* 436, 394–399. doi: 10.1016/j.bbrc.2013.05.112

Hirst, T. R., Fraser, S., Soriani, M., Aman, A. T., de, H. L., Hearn, A., et al. (2002). New insights into the structure-function relationships and therapeutic applications of cholera-like enterotoxins. *Int. J. Med. Microbiol.* 291, 531–535. doi: 10.1078/1438-4221-00163

Hollak, C. E., Levi, M., Berends, F., Aerts, J. M., and van Oers, M. H. (1997). Coagulation abnormalities in type 1 Gaucher disease are due to low-grade activation and can be partly by enzyme supplementation therapy. *Br. J. Haematol.* 96, 470–476. doi: 10.1046/j.1365-2141.1997.d01-2076.x

Hollak, C. E., van Weely, S., van Oers, M. H., and Aerts, J. M. (1994). Marked elevation of plasma chitotriosidase activity. A novel hallmark of Gaucher disease. *J. Clin. Invest.* 93, 1288–1292. doi: 10.1172/JCI117084

Hose, M., Günther, A., Abberger, H., Begum, S., Korencak, M., Becker, K. A., et al. (2019). T cell-specific overexpression of acid sphingomyelinase results in elevated t cell activation and reduced parasitemia during *Plasmodium yoelii* infection. *Front. Immunol.* 10:1225. doi: 10.3389/fimmu.2019.01225

Hunter, M., Demarais, N. J., Faull, R. L. M., Grey, A. C., and Curtis, M. A. (2018). Layer-specific lipid signatures in the human subventricular zone demonstrated by imaging mass spectrometry. *Sci. Rep.* 8:2551. doi: 10.1038/s41598-018-20793-4

Hyun, C. S., and Kimmich, G. A. (1984). Interaction of cholera toxin and *Escherichia coli* enterotoxin with isolated intestinal epithelial cells. *Am. J. Physiol.* 247, G623–G631. doi: 10.1152/ajpgi.1984.247.6.G623

Ichikawa, S., Sakiyama, H., Suzuki, G., Hidari, K. I., and Hirabayashi, Y. (1996). Expression cloning of a cDNA for human ceramide glucosyltransferase that catalyzes the first glycosylation step of glycosphingolipid synthesis. *Proc. Natl. Acad. Sci. U.S.A.* 93, 4638–4643. doi: 10.1073/pnas.93.10.4638

Inokuchi, J., Nagafuku, M., Ohno, I., and Suzuki, A. (2015). Distinct selectivity of gangliosides required for $CD4^+$ T and $CD8^+$ T cell activation. *Biochim. Biophys. Acta* 1851, 98–106. doi: 10.1016/j.bbalip.2014.07.013

Inokuchi, J. I., Inamori, K. I., Kabayama, K., Nagafuku, M., Uemura, S., Go, S., et al. (2018). Biology of GM3 Ganglioside. *Prog. Mol. Biol. Transl. Sci.* 156, 151–195. doi: 10.1016/bs.pmbts.2017.10.004

Iwabuchi, K., and Nagaoka, I. (2002). Lactosylceramide-enriched glycosphingolipid signaling domain mediates superoxide generation from human neutrophils. *Blood* 100, 1454–1464. doi: 10.1182/blood.v100.4.1454.h81602001454_1454_1464

Iyer, A., van Eijk, M., Silva, E., Hatta, M., Faber, W., Aerts, J. M., et al. (2009). Increased chitotriosidase activity in serum of leprosy patients: association with bacillary leprosy. *Clin. Immunol.* 131, 501–509. doi: 10.1016/j.clim.2009.02.003

Jolivet-Reynaud, C., Hauttecoeur, B., and Alouf, J. E. (1989). Interaction of *Clostridium perfringens* delta toxin with erythrocyte and liposome membranes and relation with the specific binding to the ganglioside GM2. *Toxicon* 27, 1113–1126. doi: 10.1016/0041-0101(89)90005-6

Jones, E. E., Zhang, W., Zhao, X., Quiason, C., Dale, S., Shahidi-Latham, S., et al. (2017). Tissue localization of glycosphingolipid accumulation in a Gaucher disease mouse brain by LC-ESI-MS/MS and high-resolution MALDI imaging mass spectrometry. *SLAS Discov.* 22, 1218–1228. doi: 10.1177/2472555217719372

Kabayama, K., Sato, T., Saito, K., Loberto, N., Prinetti, A., Sonnino, S., et al. (2007). Dissociation of the insulin receptor and caveolin-1 complex by ganglioside GM3 in the state of insulin resistance. *Proc. Natl. Acad. Sci. U.S.A.* 104, 13678–13683. doi: 10.1073/pnas.0703650104

Kallemeijn, W. W., Li, K. Y., Witte, M. D., Marques, A. R., Aten, J., Scheij, S., et al. (2012). Novel activity-based probes for broad-spectrum profiling of retaining β-exoglucosidases in situ and in vivo. *Angew. Chem. Int. Ed. Engl.* 51, 12529–12533. doi: 10.1002/anie.201207771

Källenius, G., Möllby, R., Svenson, S. B., Winberg, J., and Hultberg, H. (1980). Identification of a carbohydrate receptor recognized by uropathogenic *Escherichia coli*. *Infection* 8(Suppl. 3), 288–293. doi: 10.1007/BF01639597

Kidani, Y., and Bensinger, S. J. (2014). Lipids rule: resetting lipid metabolism restores T cell function in systemic lupus erythematosus. *J. Clin. Invest.* 124, 482–485. doi: 10.1172/JCI74141

King, H. (1956). Sigmund Otto Rosenheim: 1871-1955. *Biograph. Mem. Fellows R. Soc.* 2, 257–267.

Kitamura, M., Takamiya, K., Aizawa, S., Furukawa, K., and Furukawa, K. (1999). Gangliosides are the binding substances in neural cells for tetanus and botulinum toxins in mice. *Biochim. Biophys. Acta* 1441, 1–3. doi: 10.1016/s1388-1981(99)00140-7

Klokk, T. I., Kavaliauskiene, S., and Sandvig, K. (2016). Cross-linking of glycosphingolipids at the plasma membrane: consequences for intracellular signaling and traffic. *Cell Mol. Life Sci.* 73, 1301–1316. doi: 10.1007/s00018-015-2049-1

Koprivica, V., Stone, D. L., Park, J. K., Callahan, M., Frisch, A., Cohen, I. J., et al. (2000). Analysis and classification of 304 mutant alleles in patients with type 1 and type 3 Gaucher disease. *Am. J. Hum. Genet.* 66, 1777–1786. doi: 10.1086/302925

Kościelak, J. (2012). The hypothesis on function of glycosphingolipids and ABO blood groups revisited. *Neurochem. Res.* 37, 1170–1184. doi: 10.1007/s11064-012-0734-0

Kramer, G., Wegdam, W., Donker-Koopman, W., Ottenhoff, R., Gaspar, P., Verhoek, M., et al. (2016). Elevation of glycoprotein nonmetastatic melanoma protein B in type 1 Gaucher disease patients and mouse models. *FEBS Open Bio.* 6, 902–913. doi: 10.1002/2211-5463.12078

Krivan, H. C., Olson, L. D., Barile, M. F., Ginsburg, V., and Roberts, D. D. (1989). Adhesion of *Mycoplasma pneumoniae* to sulfated glycolipids and inhibition by dextran sulfate. *J. Biol. Chem.* 264, 9283–9288.

Kumar, A., Suryadevara, N., Hill, T. M., Bezbradica, J. S., Van Kaer, L., and Joyce, S. (2017). Natural killer T cells: an ecological evolutionary developmental biology perspective. *Front. Immunol.* 8:1858. doi: 10.3389/fimmu.2017.01858

Kuziemko, G. M., Stroh, M., and Stevens, R. C. (1996). Cholera toxin binding affinity and specificity for gangliosides determined by surface plasmon resonance. *Biochemistry* 35, 6375–6384. doi: 10.1021/bi952314i

Laborda, P., Wang, S. Y., and Voglmeir, J. (2016). Influenza neuraminidase inhibitors: synthetic approaches, derivatives and biological activity. *Molecules* 21:E1513.

Laguerre, A., and Schultz, C. (2018). Novel lipid tools and probes for biological investigations. *Curr. Opin. Cell Biol.* 53, 97–104. doi: 10.1016/j.ceb.2018.06.013

Langeveld, M., and Aerts, J. M. (2009). Glycosphingolipids and insulin resistance. *Prog. Lipid Res.* 48, 196–205. doi: 10.1016/j.plipres.2009.03.002

Langeveld, M., Ghauharali, K. J., Sauerwein, H. P., Ackermans, M. T., Groener, J. E., Hollak, C. E., et al. (2008). Type I Gaucher disease, a glycosphingolipid storage disorder, is associated with insulin resistance. *J. Clin. Endocrinol. Metab.* 93, 845–851. doi: 10.1210/jc.2007-1702

Lazzarini, C., Haranahalli, K., Rieger, R., Ananthula, H. K., Desai, P. B., Ashbaugh, A., et al. (2018). Acylhydrazones as antifungal agents targeting the synthesis of fungal sphingolipids. *Antimicrob. Agents Chemother.* 62:e00156-18. doi: 10.1128/AAC.00156-18

Leffler, H., and Svanborg-Edén, C. (1981). Glycolipid receptors for uropathogenic *Escherichia coli* on human erythrocytes and uroepithelial cells. *Infect. Immun.* 34, 920–929.

Lewis, G., and Gaemers, S. J. M. (2019). Long-term adverse event profile from four completed trials of oral eliglustat in adults with Gaucher disease type 1. *Orphanet. J. Rare Dis.* 14:128. doi: 10.1186/s13023-019-1085-6

Li, C., Wang, A., Wu, Y., Gulbins, E., Grassmé, H., and Zhao, Z. (2019). Acid sphingomyelinase-ceramide system in bacterial infections. *Cell Physiol. Biochem.* 52, 280–301. doi: 10.33594/000000021

Li, T. A., and Schnaar, R. L. (2018). Congenital disorders of ganglioside biosynthesis. *Prog. Mol. Biol. Transl. Sci.* 156, 63–82. doi: 10.1016/bs.pmbts.2018.01.001

Lingwood, C. A. (1996). Role of verotoxin receptors in pathogenesis. *Trends Microbiol.* 4, 147–153. doi: 10.1016/0966-842X(96)10017-2

Lingwood, C. A., and Branch, D. R. (2011). The role of glycosphingolipids in HIV/AIDS. *Discov. Med.* 11, 303–313.

Lingwood, D., and Simons, K. (2010). Lipid rafts as a membrane-organizing principle. *Science* 327, 46–50. doi: 10.1126/science.1174621

Löfgren, L., Forsberg, G. B., and Ståhlman, M. (2016). The BUME method: a new rapid and simple chloroform-free method for total lipid extraction of animal tissue. *Sci. Rep.* 6:27688. doi: 10.1038/srep27688

Lombardo, E., van Roomen, C. P., van Puijvelde, G. H., Ottenhoff, R., van Eijk, M., Aten, J., et al. (2012). Correction of liver steatosis by a hydrophobic iminosugar modulating glycosphingolipids metabolism. *PLoS One* 7:e38520. doi: 10.1371/journal.pone.0038520

Lopez, P. H. H., and Báez, B. B. (2018). Gangliosides in axon stability and regeneration. *Prog. Mol. Biol. Transl. Sci.* 156, 383–412. doi: 10.1016/bs.pmbts.2018.03.001

Lund, N., Olsson, M. L., Ramkumar, S., Sakac, D., Yahalom, V., Levene, C., et al. (2009). The human P(k) histo-blood group antigen provides protection against HIV-1 infection. *Blood* 113, 4980–4991. doi: 10.1182/blood-2008-03-143396

Ma, H. F., Wei, F., Wu, B. F., Yang, C., Xie, Y., Wu, Z. Y., et al. (2019). Profiling and quantification of aminophospholipids based on chemical derivatization coupled with HPLC-MS. *J. Lipid Res.* 60, 121–134. doi: 10.1194/jlr.M089482

Mahdavi, J., Sondén, B., Hurtig, M., Olfat, F. O., Forsberg, L., Roche, N., et al. (2002). *Helicobacter* pylori SabA adhesin in persistent infection and chronic inflammation. *Science* 297, 573–578. doi: 10.1126/science.1069076

Marques, A. R., Aten, J., Ottenhoff, R., van Roomen, C. P., Herrera Moro, D., Claessen, N., et al. (2015). Reducing GBA2 activity ameliorates neuropathology in niemann-pick type C mice. *PLoS One* 10:e0135889. doi: 10.1371/journal.pone.0135889

Marques, A. R., Mirzaian, M., Akiyama, H., Wisse, P., Ferraz, M. J., Gaspar, P., et al. (2016). Glucosylated cholesterol in mammalian cells and tissues: formation and degradation by multiple cellular β-glucosidases. *J. Lipid Res.* 57, 451–463. doi: 10.1194/jlr.M064923

Marshall, J., Nietupski, J. B., Park, H., Cao, J., Bangari, D. S., Silvescu, C., et al. (2019). Substrate reduction therapy for sandhoff disease through inhibition of glucosylceramide synthase activity. *Mol. Ther.* 27, 1495–1506. doi: 10.1016/j.ymthe.2019.05.018

Martín-Martín, A. I., Vizcaíno, N., and Fernández-Lago, L. (2010). Cholesterol, ganglioside GM1 and class A scavenger receptor contribute to infection by Brucella ovis and Brucella canis in murine macrophages. *Microbes Infect.* 12, 246–251. doi: 10.1016/j.micinf.2009.12.008

Masserini, M., Freire, E., Palestini, P., Calappi, E., and Tettamanti, G. (1992). Fuc-GM1 ganglioside mimics the receptor function of GM1 for cholera toxin. *Biochemistry* 31, 2422–2426. doi: 10.1021/bi00123a030

McDonald, G., Deepak, S., Miguel, L., Hall, C. J., Isenberg, D. A., Magee, A. I., et al. (2014). Normalizing glycosphingolipids restores function in CD4+ T cells from lupus patients. *J. Clin. Invest.* 124, 712–724. doi: 10.1172/JCI69571

Meijer, A. H., and Aerts, J. M. (2016). Linking smokers' susceptibility to tuberculosis with lysosomal storage disorders. *Dev. Cell* 37, 112–113. doi: 10.1016/j.devcel.2016.04.004

Meiners, J., Palmieri, V., Klopfleisch, R., Ebel, J. F., Japtok, L., Schumacher, F., et al. (2019). Intestinal acid sphingomyelinase protects from severe pathogen-driven colitis. *Front. Immunol.* 10:1386. doi: 10.3389/fimmu.2019.01386

Meisen, I., Dzudzek, T., Ehrhardt, C., Ludwig, S., Mormann, M., Rosenbrück, R., et al. (2012). The human H3N2 influenza viruses A/Victoria/3/75 and A/Hiroshima/52/2005 preferentially bind to α2-3-sialylated monosialogangliosides with fucosylated poly-N-acetyllactosaminyl chains. *Glycobiology* 22, 1055–1076. doi: 10.1093/glycob/cws077

Merrill, A. H. Jr., and Sullards, M. C. (2017). Opinion article on lipidomics: inherent challenges of lipidomic analysis of sphingolipids. *Biochim. Biophys. Acta Mol. Cell Biol. Lipids* 1862, 774–776. doi: 10.1016/j.bbalip.2017.01.009

Merrill, A. H. (2011). Sphingolipid and glycosphingolipid metabolic pathways in the era of sphingolipidomics. *Chem. Rev.* 111, 6387–6422. doi: 10.1021/cr2002917

Mirzaian, M., Wisse, P., Ferraz, M. J., Gold, H., Donker-Koopman, W. E., Verhoek, M., et al. (2015). Mass spectrometric quantification of glucosylsphingosine in plasma and urine of type 1 Gaucher patients using an isotope standard. *Blood Cells Mol. Dis.* 54, 307–314. doi: 10.1016/j.bcmd.2015.01.006

Mirzaian, M., Wisse, P., Ferraz, M. J., Marques, A. R. A., Gabriel, T. L., van Roomen, C. P. A. A., et al. (2016). Accurate quantification of sphingosine-1-phosphate in normal and Fabry disease plasma, cells and tissues by LC-MS/MS with (13)C-encoded natural S1P as internal standard. *Clin. Chim. Acta* 459, 36–44. doi: 10.1016/j.cca.2016.05.017

Mirzaian, M., Wisse, P., Ferraz, M. J., Marques, A. R. A., Gaspar, P., Oussoren, S. V., et al. (2017). Simultaneous quantitation of sphingoid bases by UPLC-ESI-MS/MS with identical (13)C-encoded internal standards. *Clin. Chim. Acta* 466, 178–184. doi: 10.1016/j.cca.2017.01.014

Mistry, P. K., Balwani, M., Baris, H. N., Turkia, H. B., Burrow, T. A., Charrow, J., et al. (2018). Safety, efficacy, and authorization of eliglustat as a first-line therapy in Gaucher disease type 1. *Blood Cells Mol. Dis.* 71, 71–74. doi: 10.1016/j.bcmd.2018.04.001

Mistry, P. K., Liu, J., Sun, L., Chuang, W. L., Yuen, T., Yang, R., et al. (2014). Glucocerebrosidase 2 gene deletion rescues type 1 Gaucher disease. *Proc. Natl. Acad. Sci. U.S.A.* 111, 4934–4939. doi: 10.1073/pnas.1400768111

Moore, M. L., Chi, M. H., Zhou, W., Goleniewska, K., O'Neal, J. F., Higginbotham, J. N., et al. (2007). Cutting Edge: oseltamivir decreases T cell GM1 expression and inhibits clearance of respiratory syncytial virus: potential role of endogenous sialidase in antiviral immunity. *J. Immunol.* 178, 2651–2654. doi: 10.4049/jimmunol.178.5.2651

Mor, V., Rella, A., Farnoud, A. M., Singh, A., Munshi, M., Bryan, A., et al. (2018). Identification of a new class of antifungals targeting the synthesis of fungal sphingolipids. *mBio* 9:e00188-18. doi: 10.1128/mBio.00188-18

Mukai, T., Kaneko, S., Matsumoto, M., and Ohori, H. (2004). Binding of *Bifidobacterium bifidum* and *Lactobacillus reuteri* to the carbohydrate moieties of intestinal glycolipids recognized by peanut agglutinin. *Int. J. Food Microbiol.* 90, 357–362. doi: 10.1016/S0168-1605(03)00317-9

Mukherjee, S., and Maxfield, F. R. (2004). Membrane domains. *Annu. Rev. Cell Dev. Biol.* 20, 839–866. doi: 10.1146/annurev.cellbio.20.010403.095451

Müller, M., Lauster, D., Wildenauer, H. H. K., Herrmann, A., and Block, S. (2019). Mobility-based quantification of multivalent virus-receptor interactions: new insights into influenza A virus binding mode. *Nano Lett.* 19, 1875–1882. doi: 10.1021/acs.nanolett.8b04969

Nagafuku, M., Okuyama, K., Onimaru, Y., Suzuki, A., Odagiri, Y., Yamashita, T., et al. (2012). CD4 and CD8 T cells require different membrane gangliosides for activation. *Proc. Natl. Acad. Sci. U.S.A.* 109, E336–E342. doi: 10.1073/pnas.1114965109

Nagata, M., Izumi, Y., Ishikawa, E., Kiyotake, R., Doi, R., Iwai, S., et al. (2017). Intracellular metabolite β-glucosylceramide is an endogenous Mincle ligand possessing immunostimulatory activity. *Proc. Natl. Acad. Sci. U.S.A.* 114, E3285–E3294. doi: 10.1073/pnas.1618133114

Nair, S., Boddupalli, C. S., Verma, R., Liu, J., Yang, R., Pastores, G. M., et al. (2015). Type II NKT-TFH cells against Gaucher lipids regulate B-cell immunity and inflammation. *Blood* 125, 1256–1271. doi: 10.1182/blood-2014-09-600270

Nair, S., Branagan, A. R., Liu, J., Boddupalli, C. S., Mistry, P. K., and Dhodapkar, M. V. (2016). Clonal immunoglobulin against lysolipids in the origin of myeloma. *N. Engl. J. Med.* 374, 555–561. doi: 10.1056/NEJMoa1508808

Nakayama, H., Kurihara, H., Morita, Y. S., Kinoshita, T., Mauri, L., Prinetti, A., et al. (2016). Lipoarabinomannan binding to lactosylceramide in lipid rafts is essential for the phagocytosis of mycobacteria by human neutrophils. *Sci. Signal.* 9:ra101. doi: 10.1126/scisignal.aaf1585

Nakayama, H., Nagafuku, M., Suzuki, A., Iwabuchi, K., and Inokuchi, J. I. (2018). The regulatory roles of glycosphingolipid-enriched lipid rafts in immune systems. *FEBS Lett.* 592, 3921–3942. doi: 10.1002/1873-3468.13275

Naroeni, A., and Porte, F. (2002). Role of cholesterol and the ganglioside GM(1) in entry and short-term survival of *Brucella suis* in murine macrophages. *Infect. Immun.* 70, 1640–1644. doi: 10.1128/IAI.70.3.1640-1644.2002

Newburg, D. S., and Chaturvedi, P. (1992). Neutral glycolipids of human and bovine milk. *Lipids* 27, 923–927. doi: 10.1007/BF02535874

Nietupski, J. B., Pacheco, J. J., Chuang, W. L., Maratea, K., Li, L., Foley, J., et al. (2012). Iminosugar-based inhibitors of glucosylceramide synthase prolong survival but paradoxically increase brain glucosylceramide levels in Niemann-Pick C mice. *Mol. Genet. Metab.* 105, 621–628. doi: 10.1016/j.ymgme.2012.01.020

Nihei, W., Nagafuku, M., Hayamizu, H., Odagiri, Y., Tamura, Y., Kikuchi, Y., et al. (2018). NPC1L1-dependent intestinal cholesterol absorption requires ganglioside GM3 in membrane microdomains. *J. Lipid Res.* 59, 2181–2187. doi: 10.1194/jlr.M089201

Nimrichter, L., Burdick, M. M., Aoki, K., Laroy, W., Fierro, M. A., Hudson, S. A., et al. (2008). E-selectin receptors on human leukocytes. *Blood* 112, 3744–3752. doi: 10.1182/blood-2008-04-149641

Otnaess, A. B., Laegreid, A., and Ertresvåg, K. (1983). Inhibition of enterotoxin from *Escherichia coli* and *Vibrio cholerae* by gangliosides from human milk. *Infect. Immun.* 40, 563–569. doi: 10.1016/0024-3205(87)90252-9

Pandey, M. K., Burrow, T. A., Rani, R., Martin, L. J., Witte, D., Setchell, K. D., et al. (2017). Complement drives glucosylceramide accumulation and tissue inflammation in Gaucher disease. *Nature* 543, 108–112. doi: 10.1038/nature21368

Parrot, D., Papazian, S., Foil, D., and Tasdemir, D. (2018). Imaging the unimaginable: desorption electrospray ionization - imaging mass spectrometry (DESI-IMS) in natural product research. *Planta Med.* 84, 584–593. doi: 10.1055/s-0044-100188

Pei, B., Vela, J. L., Zajonc, D., and Kronenberg, M. (2012). Interplay between carbohydrate and lipid in recognition of glycolipid antigens by natural killer T cells. *Ann. N. Y. Acad. Sci.* 1253, 68–79. doi: 10.1111/j.1749-6632

Pieters, R. J. (2011). Carbohydrate mediated bacterial adhesion. *Adv. Exp. Med. Biol.* 715, 227–240. doi: 10.1007/978-94-007-0940-9_14

Platt, F. M. (2014). Sphingolipid lysosomal storage disorders. *Nature* 510, 68–75. doi: 10.1038/nature13476

Platt, F. M., Jeyakumar, M., Andersson, U., Priestman, D. A., Dwek, R. A., Butters, T. D., et al. (2001). Inhibition of substrate synthesis as a strategy for glycolipid lysosomal storage disease therapy. *J. Inherit. Metab. Dis.* 24, 275–290. doi: 10.1023/A:1010335505357

Pyne, S., Adams, D. R., and Pyne, N. J. (2016). Sphingosine 1-phosphate and sphingosine kinases in health and disease: recent advances. *Prog Lipid Res.* 62, 93–106. doi: 10.1016/j.plipres.2016.03.001

Rakhshandehroo, M., van Eijkeren, R. J., Gabriel, T. L., de Haar, C., Gijzel, S. M. W., Hamers, N., et al. (2019). Adipocytes harbor a glucosylceramide biosynthesis pathway involved in iNKT cell activation. *Biochim. Biophys. Acta Mol. Cell Biol. Lipids* 1864, 1157–1167. doi: 10.1016/j.bbalip.2019.04.016

Rollin-Pinheiro, R., Singh, A., Barreto-Bergter, E., and Del Poeta, M. (2016). Sphingolipids as targets for treatment of fungal infections. *Future Med. Chem.* 8, 1469–1484. doi: 10.4155/fmc-2016-0053

Sandhoff, R., and Sandhoff, K. (2018). Emerging concepts of ganglioside metabolism. *FEBS Lett.* 592, 3835–3864. doi: 10.1002/1873-3468.13114

Sandhoff, R., Schulze, H., and Sandhoff, K. (2018). Ganglioside metabolism in health and disease. *Prog. Mol. Biol. Transl. Sci.* 156, 1–62. doi: 10.1016/bs.pmbts.2018.01.002

Sato, T., Iwabuchi, K., Nagaoka, I., Adachi, Y., Ohno, N., Tamura, H., et al. (2006). Induction of human neutrophil chemotaxis by *Candida albicans*-derived beta-1,6-long glycoside side-chain-branched beta-glucan. *J. Leukoc. Biol.* 80, 204–211. doi: 10.1189/jlb.0106069

Schengrund, C. L. (2003). "Multivalent" saccharides: development of new approaches for inhibiting the effects of glycosphingolipid-binding pathogens. *Biochem. Pharmacol.* 65, 699–707. doi: 10.1016/s0006-2952(02)01553-8

Schnaar, R. L. (2004). Glycolipid-mediated cell-cell recognition in inflammation and nerve regeneration. *Arch. Biochem. Biophys.* 426, 163–172. doi: 10.1016/j.abb.2004.02.019

Schnaar, R. L., and Lopez, P. H. (2009). Myelin-associated glycoprotein and its axonal receptors. *J. Neurosci. Res.* 87, 3267–3276. doi: 10.1002/jnr.21992

Schuchman, E. H. (2010). Acid sphingomyelinase, cell membranes and human disease: lessons from Niemann-Pick disease. *FEBS Lett.* 584, 1895–1900. doi: 10.1016/j.febslet.2009.11.083

Schwake, M., Schröder, B., and Saftig, P. (2013). Lysosomal membrane proteins and their central role in physiology. *Traffic* 14, 739–748. doi: 10.1111/tra.12056

Shayman, J. A., and Larsen, S. D. (2014). The development and use of small molecule inhibitors of glycosphingolipid metabolism for lysosomal storage diseases. *J. Lipid Res.* 55, 1215–1225. doi: 10.1194/jlr.R047167

Shen, C., Bullens, D., Kasran, A., Maerten, P., Boon, L., Aerts, J. M., et al. (2004). Inhibition of glycolipid biosynthesis by N-(5-adamantane-1-yl-methoxy-pentyl)-deoxynojirimycin protects against the inflammatory response in hapten-induced colitis. *Int. Immunopharmacol.* 4, 939–951. doi: 10.1016/j.intimp.2004.04.008

Siebert, M., Sidransky, E., and Westbroek, W. (2014). Glucocerebrosidase is shaking up the synucleinopathies. *Brain* 137, 1304–1322. doi: 10.1093/brain/awu002

Smith, E. L., and Schuchman, E. H. (2008). The unexpected role of acid sphingomyelinase in cell death and the pathophysiology of common diseases. *FASEB J.* 22, 3419–3431. doi: 10.1096/fj.08-108043

Smith, N. J., Fuller, M., Saville, J. T., and Cox, T. M. (2018). Reduced cerebral vascularization in experimental neuronopathic Gaucher disease. *J. Pathol.* 244, 120–128. doi: 10.1002/path.4992

Sonnino, S., and Prinetti, A. (2013). Membrane domains and the "lipid raft" concept. *Curr. Med. Chem.* 20, 4–21. doi: 10.2174/0929867311320010003

Spiegel, S. (1989). Inhibition of protein kinase C-dependent cellular proliferation by interaction of endogenous ganglioside GM1 with the B subunit of cholera toxin. *J. Biol. Chem.* 264, 16512–16517.

Sprong, H., Kruithof, B., Leijendekker, R., Slot, J. W., van Meer, G., and van der Sluijs, P. (1998). UDP-galactose:ceramide galactosyltransferase is a class I integral membrane protein of the endoplasmic reticulum. *J. Biol. Chem.* 273, 25880–25888. doi: 10.1074/jbc.273.40.25880

Stanic, A. K., De Silva, A. D., Park, J. J., Sriram, V., Ichikawa, S., Hirabyashi, Y., et al. (2003). Defective presentation of the CD1d1-restricted natural Va14Ja18 NKT lymphocyte antigen caused by beta-D-glucosylceramide synthase deficiency. *Proc. Natl. Acad. Sci. U.S.A.* 100, 1849–1854. doi: 10.1073/pnas.0430327100

Sugiyama, E., and Setou, M. (2018). Visualization of brain gangliosides using MALDI imaging mass spectrometry. *Methods Mol. Biol.* 1804, 223–229. doi: 10.1007/978-1-4939-8552-4_10

Svensson, M., Frendeus, B., Butters, T., Platt, F., Dwek, R., and Svanborg, C. (2003). Glycolipid depletion in antimicrobial therapy. *Mol. Microbiol.* 47, 453–461. doi: 10.1046/j.1365-2958.2003.03306.x

Tagami, S., Inokuchi Ji, J., Kabayama, K., Yoshimura, H., Kitamura, F., Uemura, S., et al. (2002). Ganglioside GM3 participates in the pathological conditions of insulin resistance. *J. Biol. Chem.* 277, 3085–3092. doi: 10.1074/jbc.M103705200

Taguchi, Y. V., Liu, J., Ruan, J., Pacheco, J., Zhang, X., Abbasi, J., et al. (2017). Glucosylsphingosine promotes α-synuclein pathology in mutant GBA-associated Parkinson's disease. *J. Neurosci.* 37, 9617–9631. doi: 10.1523/JNEUROSCI.1525-17.2017

Thudichum, J. (1884). *A Treatise on the Chemical Constitution of the Brain*. London: Bailliere, Tindall and Cox.

Tidhar, R., and Futerman, A. H. (2013). The complexity of sphingolipid biosynthesis in the endoplasmic reticulum. *Biochim. Biophys. Acta* 1833, 2511–2518. doi: 10.1016/j.bbamcr.2013.04.010

Tobias, F., Olson, M. T., and Cologna, S. M. (2018). Mass spectrometry imaging of lipids: untargeted consensus spectra reveal spatial distributions in Niemann-Pick disease type C1. *J. Lipid Res.* 59, 2446–2455. doi: 10.1194/jlr.D08609

Tsai, B., Gilbert, J. M., Stehle, T., Lencer, W., Benjamin, T. L., and Rapoport, T. A. (2003). Gangliosides are receptors for murine polyoma virus and SV40. *EMBO J.* 22, 4346–4355. doi: 10.1093/emboj/cdg439

Tsokos, G. C. (2011). Systemic lupus erythematosus. *N. Engl. J. Med.* 365, 2110–2121.

Van den Bergh, F. A., and Tager, J. M. (1976). Localization of neutral glycosphingolipids in human plasma. *Biochim. Biophys. Acta* 441, 391–402. doi: 10.1016/0005-2760(76)90236-8

van Eijk, M., Aten, J., Bijl, N., Ottenhoff, R., van Roomen, C. P., Dubbelhuis, P. F., et al. (2009). Reducing glycosphingolipid content in adipose tissue of obese mice restores insulin sensitivity, adipogenesis and reduces inflammation. *PLoS One* 4:e4723. doi: 10.1371/journal.pone.0004723

van Heyningen, S. (1974). Cholera toxin: interaction of subunits with ganglioside GM1. *Science* 183, 656–657. doi: 10.1126/science.183.4125.656

van Meel, E., Bos, E., van der Lienden, M. J. C., Overkleeft, H. S., van Kasteren, S. I., Koster, A. J., et al. (2019). Localization of active endogenous and exogenous β-glucocerebrosidase by correlative light-electron microscopy in human fibroblasts. *Traffic* 20, 346–356. doi: 10.1111/tra.12641

van Meer, G., Wolthoorn, J., and Degroote, S. (2003). The fate and function of glycosphingolipid glucosylceramide. *Philos. Trans. R. Soc. Lond. B Biol. Sci.* 358, 869–873. doi: 10.1098/rstb.2003.1266

Van Smeden, J., and Bouwstra, J. A. (2016). Stratum corneum lipids: their role for the skin barrier function in healthy subjects and atopic Dermatitis patients. *Curr. Probl. Dermatol* 49, 8–26. doi: 10.1159/000441540

Van Smeden, J., Dijkhoff, I. M., Helder, R. W. J., Al-Khakany, H., Boer, D. E. C., Schreuder, A., et al. (2017). In situ visualization of glucocerebrosidase in human skin tissue: zymography versus activity-based probe labeling. *J. Lipid Res.* 58, 2299–2309. doi: 10.1194/jlr.M079376

van Weely, S., Brandsma, M., Strijland, A., Tager, J. M., and Aerts, J. M. (1993). Demonstration of the existence of a second, non-lysosomal glucocerebrosidase that is not deficient in Gaucher disease. *Biochim. Biophys. Acta* 1181, 55–62. doi: 10.1016/0925-4439(93)90090-n

Vens-Cappell, S., Kouzel, I. U., Kettling, H., Soltwisch, J., Bauwens, A., Porubsky, S., et al. (2016). On-tissue phospholipase C digestion for enhanced MALDI-MS imaging of neutral glycosphingolipids. *Anal. Chem.* 88, 5595–5599. doi: 10.1021/acs.analchem.6b01084

Vissers, J. P., Langridge, J. I., and Aerts, J. M. (2007). Analysis and quantification of diagnostic serum markers and protein signatures for Gaucher disease. *Mol. Cell. Proteomics* 6, 755–766. doi: 10.1074/mcp.M600303-MCP200

Wang, J., Wang, C., and Han, X. (2019). Tutorial on lipidomics. *Anal. Chim. Acta* 1061, 28–41. doi: 10.1016/j.aca.2019.01.043

Wang, M., Wang, C., and Han, X. (2017). Selection of internal standards for accurate quantification of complex lipid species in biological extracts by electrospray ionization mass spectrometry-What, how and why? *Mass Spectrom. Rev.* 36, 693–714. doi: 10.1002/mas.21492

Wennekes, T., Meijer, A. J., Groen, A. K., Boot, R. G., Groener, J. E., van Eijk, M., et al. (2010). Dual-action lipophilic iminosugar improves glycemic control in obese rodents by reduction of visceral glycosphingolipids and buffering of carbohydrate assimilation. *J. Med. Chem.* 53, 689–698. doi: 10.1021/jm901281m

Wennekes, T., van den Berg, R. J., Boot, R. G., van der Marel, G. A., Overkleeft, H. S., and Aerts, J. M. (2009). Glycosphingolipids-nature, function, and pharmacological modulation. *Angew. Chem. Int. Ed. Engl.* 48, 8848–8869. doi: 10.1002/anie.200902620

Wertz, P. (2018). Epidermal lamellar granules. *Skin Pharmacol. Physiol.* 31, 262–268. doi: 10.1159/000491757

Williams, S. J. (2017). Sensing lipids with mincle: structure and function. *Front. Immunol.* 8:1662. doi: 10.3389/fimmu.2017.01662

Wisse, P., Gold, H., Mirzaian, M., Ferraz, M. J., Lutteke, G., Van Den Berg, R. J. B. H. N., et al. (2015). Synthesis of a panel of carbon-13-labelled (glyco)sphingolipids. *Eur. J. Org. Chem.* 12, 2661–2677. doi: 10.1002/ejoc.201500025

Witte, M. D., Kallemeijn, W. W., Aten, J., Li, K. Y., Strijland, A., Donker-Koopman, W. E., et al. (2010). Ultrasensitive in situ visualization of active glucocerebrosidase molecules. *Nat. Chem. Biol.* 6, 907–913. doi: 10.1038/nchembio.466

Wu, Y., Gulbins, E., and Grassmé, H. (2018). The function of sphingomyelinases in mycobacterial infections. *Biol. Chem.* 399, 1125–1133. doi: 10.1515/hsz-2018-0179

Xia, B. T., Beckmann, N., Winer, L. K., Pugh, A. M., Pritts, T. A., Nomellini, V., et al. (2019). Amitriptyline reduces inflammation and mortality in a murine model of sepsis. *Cell Physiol. Biochem.* 52, 565–579. doi: 10.33594/000000040

Yamashita, T., Hashiramoto, A., Haluzik, M., Mizukami, H., Beck, S., Norton, A., et al. (2003). Enhanced insulin sensitivity in mice lacking ganglioside GM3. *Proc. Natl. Acad. Sci. U.S.A.* 100, 3445–3449. doi: 10.1073/pnas.0635898100

Zelnik, I. D., Ventura, A. E., Kim, J. L., Silva, L. C., and Futerman, A. H. (2019). The role of ceramide in regulating endoplasmic reticulum function. *Biochim. Biophys. Acta Mol. Cell Biol. Lipids* 1865:S1388-1981(19)30118–30110. doi: 10.1016/j.bbalip.2019.06.015

Zhang, T., de Waard, A. A., Wuhrer, M., and Spaapen, R. M. (2019). The role of glycosphingolipids in immune cell functions. *Front. Immunol.* 10:90. doi: 10.3389/fimmu.2019.00090

Zhao, H., Przybylska, M., Wu, I. H., Zhang, J., Maniatis, P., Pacheco, J., et al. (2009). Inhibiting glycosphingolipid synthesis ameliorates hepatic steatosis in obese mice. *Hepatology* 50, 85–93. doi: 10.1002/hep.22970

Zuidscherwoude, M., de Winde, C. M., Cambi, A., and van Spriel, A. B. (2014). Microdomains in the membrane landscape shape antigen-presenting cell function. *J. Leukoc. Biol.* 95, 251–263. doi: 10.1189/jlb.0813440

Zuverink, M., and Barbieri, J. T. (2018). Protein toxins that utilize gangliosides as host receptors. *Prog. Mol. Biol. Transl. Sci.* 156, 325–354. doi: 10.1016/bs.pmbts.2017.11.010

Conflict of Interest: The authors declare that the research was conducted in the absence of any commercial or financial relationships that could be construed as a potential conflict of interest.

frontiers in Immunology

ORIGINAL RESEARCH
published: 24 January 2020
doi: 10.3389/fimmu.2019.03085

Sphingosine-1-Phosphate (S-1P) Promotes Differentiation of Naive Macrophages and Enhances Protective Immunity Against *Mycobacterium tuberculosis*

Vinod Nadella[1‡], Lalita Sharma[1‡], Pankaj Kumar[1], Pushpa Gupta[2], Umesh D. Gupta[2], Srikant Tripathi[3], Suresh Pothani[4], S. S. Y. H. Qadri[4] and Hridayesh Prakash[1†]*

[1] Laboratory of Translational Medicine, School of Life Science, University of Hyderabad, Hyderabad, India, [2] Department of Experimental Animal Facility, National JALMA Institute for Leprosy and Other Mycobacterial Disease, Agra, India, [3] Department of Bacteriology, National Institute of Research in Tuberculosis, Chennai, India, [4] National Animal Resource Facility for Biomedical Research, National Institute of Nutrition, Indian Council of Medical Research Hyderabad, Hyderabad, India

Sphingosine-1-phosphate (S-1P) is a key sphingolipid involved in the pathobiology of various respiratory diseases. We have previously demonstrated the significance of S-1P in controlling non-pathogenic mycobacterial infection in macrophages, and here we demonstrate the therapeutic potential of S-1P against pathogenic *Mycobacterium tuberculosis* (H37Rv) in the mouse model of infection. Our study revealed that S-1P is involved in the expression of iNOS proteins in macrophages, their polarization toward M1 phenotype, and secretion of interferon (IFN)-γ during the course of infection. S-1P is also capable of enhancing infiltration of pulmonary CD11b+ macrophages and expression of S-1P receptor-3 (S-1PR3) in the lungs during the course of infection. We further revealed the influence of S-1P on major signaling components of inflammatory signaling pathways during *M. tuberculosis* infection, thus highlighting antimycobacterial potential of S-1P in animals. Our data suggest that enhancing S-1P levels by sphingolipid mimetic compounds/drugs can be used as an immunoadjuvant for boosting immunity against pathogenic mycobacteria.

Keywords: sphingolipids, tuberculosis, S-1P receptors, macrophage polarization, innate immunity, lungs, antimicrobial

OPEN ACCESS

Edited by:
Burkhard Kleuser, University of Potsdam, Germany

Reviewed by:
Roberta Olmo Pinheiro, Oswaldo Cruz Foundation (Fiocruz), Brazil
Martin Fraunholz, Julius Maximilian University of Würzburg, Germany

****Correspondence:***
Hridayesh Prakash
hprakash@amity.edu;
hridayesh.prakash@gmail.com

†Present address:
Hridayesh Prakash, Amity Institute of Virology & Immunology, Amity University Uttar Pradesh, Noida, India

‡These authors have contributed equally to this work

Specialty section:
This article was submitted to Microbial Immunology, a section of the journal Frontiers in Immunology

Received: *07 May 2019*
Accepted: *17 December 2019*
Published: *24 January 2020*

Citation:
Nadella V, Sharma L, Kumar P, Gupta P, Gupta UD, Tripathi S, Pothani S, Qadri SSYH and Prakash H (2020) Sphingosine-1-Phosphate (S-1P) Promotes Differentiation of Naive Macrophages and Enhances Protective Immunity Against Mycobacterium tuberculosis. Front. Immunol. 10:3085. doi: 10.3389/fimmu.2019.03085

INTRODUCTION

Tuberculosis (TB) is a global disease and one of the major causes of mortality worldwide where an approximate one-third of the global population is infected with the causative agent *Mycobacterium tuberculosis* (1). Despite major advancements toward its treatment, several factors including increase in antibiotic-resistant *M. tuberculosis* strains (2), co-infections (3), and inadequate host–pathogen interactions (4) continue to pose major challenges to the health care system. Therefore, development of novel therapeutic approaches that could improve immunity against TB is a paramount requirement. During acute infection, alveolar macrophages acquire M1 phenotype (5, 6), secrete interferon (IFN)-γ, and mount Th1 response in the process of controlling infection in the lungs (7). In view of this, enrichment/stabilization of M1 phenotype represents one potential strategy for effective control of mycobacterial infection. Sphingolipids are active constituents of

the mucus secreted by alveolar epithelium and protects the lung tissue from invading pathogens. Out of various sphingolipid metabolites, sphingosine-1-phosphate (S-1P), and ceramide are the best studied sphingolipids in the context of various respiratory pathologies (8–10). As S-1P and ceramide were known to exert opposite signaling in the host (11, 12), S-1P/ceramide rheostat would be a decisive parameter in predicting how cells would respond differentially to the same stimuli during disease progression. S-1P is a well-known secondary messenger that is pleiotropic in nature and orchestrates signaling mainly *via* G protein–coupled S-1P receptors 1–5 (13, 14). Several reports have suggested that temporal regulation of S-1P receptors may account for such pleiotropic effect of S-1P in a variety of cells (15, 16).

We have previously demonstrated that sphingosine kinase-1 (17), a critical enzyme of the sphingolipid metabolism, can control non-pathogenic mycobacterial infection in macrophages in an S-1P–dependent manner. On this note, we explored the role of S-1P in controlling pathogenic mycobacteria in the mouse model of infection, hypothesizing that enchasing S-1P levels may provide survival benefit to the host. In line with our hypothesis, this study reveals the S-1P and IFN-γ cross talk for the expression of iNOS proteins by macrophages, their polarization toward M1 phenotype, and augmenting pro-inflammatory immune responses. Our *M. tuberculosis* pulmonary challenge model demonstrated the potential of S-1P for enhancing the expression of iNOS proteins and their associated signaling proteins in augmenting pro-inflammatory immune response during the course of *M. tuberculosis* infection. Our data further demonstrated the upregulation of S-1PR3 and increased infiltration of CD11b+ alveolar myeloid cells (macrophages) in the lungs of *M. tuberculosis*–infected mice by S-1P during the course of infection.

Taken together, our data suggest that S-1P can control pathogenic mycobacteria and warrant the use of sphingolipids (S-1P or mimetic) as novel pharmacological approaches for augmenting immunity against mycobacterial infection.

RESULTS

S-1P Skews M1 Polarization and Th1 Effector Response in Naive Macrophages

Our previous study had demonstrated that S-1P/Sphk-1–mediated antimycobacterial responses are independent of tumor necrosis factor (TNF)-α (17); a component of immunity that is sufficient to eliminate a large number of intracellular pathogens. In view of this, we hypothesized that S-1P may enhance IFN-γ secretion that is capable of skewing M1 polarization of macrophages. To demonstrate this, macrophages were stimulated with IFN-γ and S-1P independently, and titers of inducible NO and expression of iNOS proteins were analyzed. In line with our hypothesis, S-1P and IFN-γ on their own induced NO titers (**Figure 1A**) and expression of iNOS proteins (**Figure 1B**) in macrophages. On these bases, we hypothesized the possible synergy between S-1P and IFN-γ for enhancing NO and iNOS levels in macrophages. Interestingly, co-stimulation of IFN-γ-treated macrophages with S-1P further enhanced the expression of NO (**Figure 1A**) and iNOS proteins (**Figure 1B**), providing the first evidence of S-1P/IFN-γ cross talk in M1 macrophages.

Sphk-1 catalyzes the production of S-1P, and inhibiting Sphk-1 enzymatic activity would inhibit the expression of iNOS in these macrophages. Interestingly, treatment of macrophages with dihydrospingosine (DHS) for inhibiting Sphk-1 activity resulted in inhibited IFN-γ-induced expression of iNOS proteins (**Figure 1B**), revealing a direct correlation of Sphk-1 proteins with IFN-γ-mediated M1 polarization of macrophages. On the basis of S-1P/IFN-γ-driven M1 polarization, we questioned whether S-1P on its own would skew pro-inflammatory immune response in naive macrophages. To test this, macrophages were treated with S-1P, and titers of IFN-γ (**Figure 1C**) and interleukin (IL)-6 (**Figure 1D**) were quantified in their culture supernatants at indicated time intervals. Following our hypothesis, S-1P enhanced the secretion of these cytokines by naive macrophages, revealing its adjuvant-like potential. These results revealed the involvement of S-1P in augmenting pro-inflammatory immune responses in macrophages, which are paramount for controlling *M. tuberculosis* infection.

S-1P Promotes Protective Immune Response Against *M. tuberculosis*

On the basis of S-1P/IFN-γ-driven M1 polarization, we argued whether S-1P would be able to skew Th1 immune response in macrophages against *M. tuberculosis* infection. To demonstrate this, RAW 264.7 macrophages (left panel; **Figure 2**) and bone marrow–derived macrophages (BMDMs; right panel; **Figure 2**) were infected with H37Rv, and pro-inflammatory immune responses were monitored *vis-à-vis* mycobacterial survival. Interestingly, treatment of infected macrophages with S-1P not only enhanced the generation of NO (**Figure 2A**) and secretion of IFN-γ (**Figure 2B**) over infected controls. Interestingly the same inhibited the secretion of IL-6 (**Figure 2C**) in the infected macrophage significantly and controlled mycobacterial survival in these macrophages (**Figure 2D**). On the basis of pro-inflammatory and antimycobacterial potential of S-1P *in vitro*, we anticipated for a similar impact of S-1P *in vivo*. To this end, a mouse model of *M. tuberculosis* pulmonary infection published by JALMA, Agra, India, was adopted, and the mice were infected with *M. tuberculosis* in the presence and absence of S-1P, FTY720 [to mitigate S-1P signaling (11, 14), and DHS to inhibit S1P production] (17) both in prophylactic as well as in therapeutic settings, respectively. Prophylactic conditioning of mice with various sphingolipid derivatives was done 1 week before infection. For that purpose, mice were injected with sphingolipid derivatives *via* intraperitoneal route, taking toxicity associated with intratracheal, and/or intravenous routes into consideration (18). Mice were injected with sphingolipid derivatives on every alternate day for a week and subsequently infected with *M. tuberculosis* (H37Rv) using an aerosol chamber (Inhalation Exposure System, Glas-Col Inc., IN, USA) (19). Thereafter, mice were kept for a week for the establishment of infection in their lungs. For analyzing the therapeutic potential

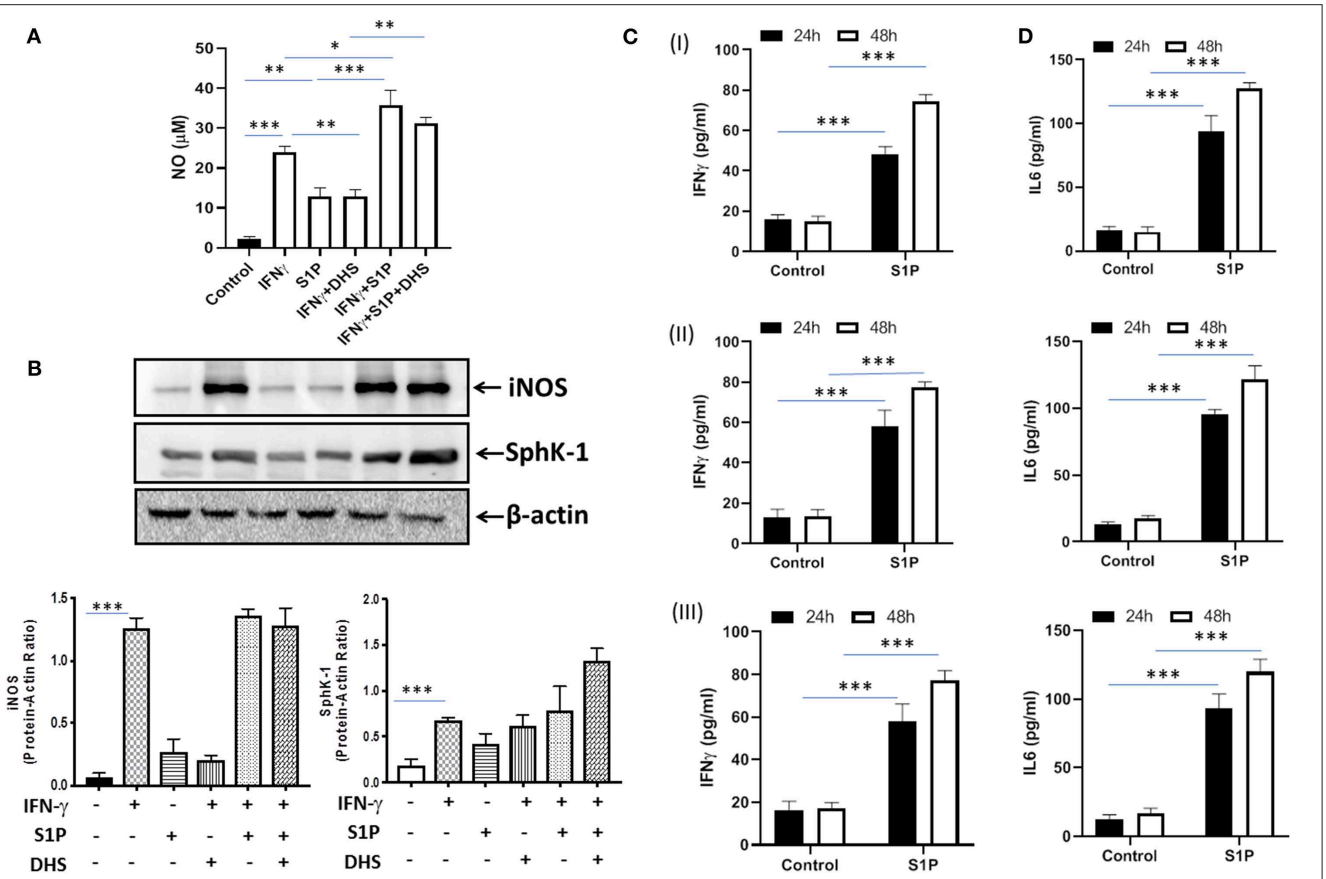

FIGURE 1 | Sphingosine-1-phosphate (S-1P) skews M1 effector response in macrophages. **(A)** RAW264.7 macrophages were stimulated as indicated, and NO titers were quantified from their culture supernatants. Shown here is the μM of NO ± SEM from three independent experiments. **(B)** Whole cell lysates of macrophages used above were collected 24 h post-treatment culture and analyzed for the expression of iNOS **(M1 effector protein)** and Sphk-1 proteins by immune blotting. A representative blot from several repeats with similar outcome is shown. β-actin was used as a loading control. Mean density of each protein was quantified from various blots by ImageJ software, and the values were plotted in terms of relative protein expression. **(C)** RAW macrophages **(I)**, CD11b+ peritoneal **(II)**, and bone marrow–derived macrophages **(III)** were treated with S-1P for indicated time intervals. Cell culture supernatants were collected, and IFN-γ **(C)** and IL-6 **(D)** were measured by ELISA at 24 and 48 h, respectively. Shown here is the pg/ml of cytokines released during the course of infection ± SEM from three independent experiments. Statistical analyses were conducted using two-way ANOVA followed by Bonferroni posttest (*$P < 0.05$, **$P < 0.01$, ***$P < 0.001$).

of drugs, mice were treated with sphingolipid derivatives from seventh through 14th day postinfection (**Figure 3A**). Mice were sacrificed on the 17th and 31st day postinfection, and their lungs, spleen, and serum were excised aseptically for evaluating the bacterial growth, protein analysis, and histopathological analysis in the lung tissues. In accordance with our hypothesis, *M. tuberculosis* survival pattern analysis revealed that treatment of infected mice with S-1P (either prophylactically or therapeutically) controlled *M. tuberculosis* burden marginally by 17th day postinfection (**Figure 3B**) and significantly by 31st day postinfection (**Figure 3C**), demonstrating the anti-TB potential of S-1P. In line with our previous study, treatment of infected mice with DHS increased *M. tuberculosis* burden (**Figure 3C**). To substantiate the anti-TB potential of S-1P, the involvement of various S-1P receptors in controlling mycobacteria in S-1P–treated animals was analyzed. Mice were treated with FTY-720, expecting that FTY-720 would provide survival benefit to bacteria. Although treatment of mice with FTY-720 in prophylactic conditions controlled the infection significantly by 31st day postinfection (**Figure 3C**), the same could not influence the mycobacterial survival when applied therapeutically. Although these treatments altered the growth pattern of *M. tuberculosis* in lungs, the same could not influence the bacterial clearance during the course of infection (**Supplementary Figure 1**). On account of anti-TB potential of S-1P, we next analyzed the influence of S-1P on both pro-inflammatory response and innate immune signaling in infected lungs. In line with RAW and peritoneal macrophage responses, S-1P enhanced IFN-γ titers in lungs as well as in serum of infected mice (**Figure 4A**). Most intriguingly, S-1P inhibited IL-6 titers in the infected macrophages (**Supplementary Figure 2**) as well as in infected mice (**Figure 4B**), which is associated with mycobacterial burden and disease severity in TB patients. These observations not only revealed S-1P–mediated pro-inflammatory programming but also furnished a potential immune mechanism detailing how S-1P could control mycobacterial survival in

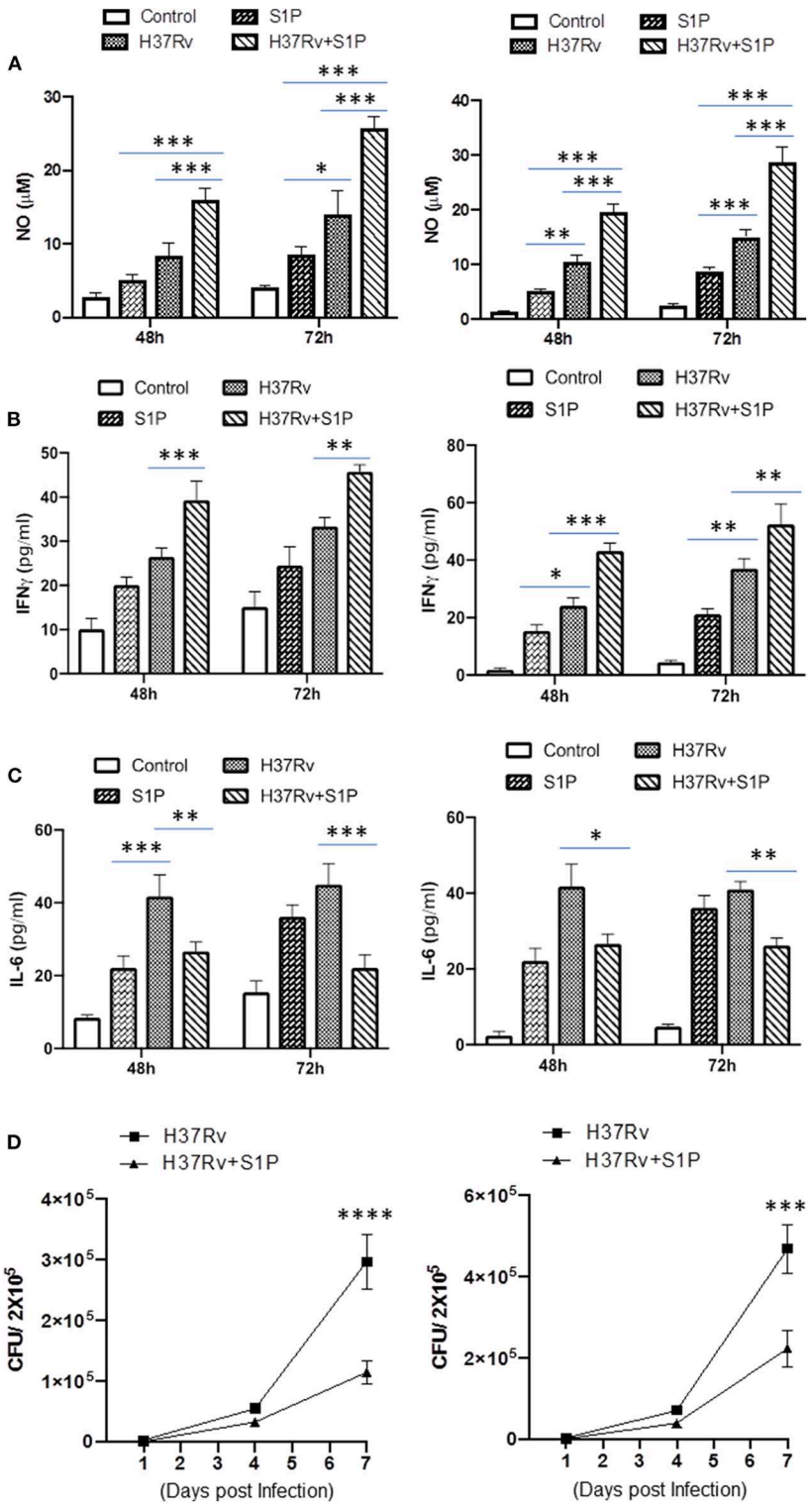

FIGURE 2 | RAW 264.7 macrophages (Left Panel) and BMDMs (Right Panel) were infected with *M. tuberculosis* in presence of S-1P. Titres of NO **(A)**, IFN-γ **(B)**, and IL-6 **(C)** were analyzed in their culture supernatant. Shown here is the μM of NO ± SEM and pg/ml of cytokines ± SEM released during the course of infection from three independent experiments. Statistical analysis were conducted using two way Anova followed by Bonferroni post-test (*$P < 0.05$, **$P < 0.01$, ***$P < 0.001$, ****$P < 0.0001$). **(D)** Anti-mycobacterial influence of S-1P was also analyzed in same cells. Shown here CFU ± SEM from three independent experiments.

these animals. In line with mycobacterial burden, both FTY-720 (**Figure 4C**) and DHS (**Figure 4D**) could not modify *M. tuberculosis*–induced titer of IFN-γ and IL-6 in the lung of infected mice. S-1P is chemotactic in nature and known to promote macrophage infiltration (20, 21). Therefore, we anticipated for an enhanced lung infiltration of CD11b+ macrophage population in S-1P–treated animals during the course of infection in mice. Histopathological analysis of *M. tuberculosis*–infected lungs revealed increased infiltration of CD11b+ pulmonary macrophages (**Figure 5**), which got further enhanced upon their treatment with either S-1P (**Figure 6**) or FTY-720 (**Figure 7**), respectively. Furthermore, both S-1P/FTY-720 enhanced the expression of Sphk-1 proteins (**Figures 6**, **7**) in infected lungs, which would have accounted for enhanced expression of iNOS proteins in the infected lungs. Interestingly, both S-1P (**Figure 6**) and FTY-720 (**Figure 7**) enhanced the expression of S-1PR3, which is known to promote immune cell migration and antibacterial defenses against intracellular pathogens (16). Although DHS also enhanced the expression of S-1PR3 (**Figure 8**) and most surprisingly iNOS proteins as well (**Supplementary Figure 3**) in the lungs of DHS-treated animals, it could not control the mycobacterial burden.

On account of pro-inflammatory and antimycobacterial impact, we anticipated for M1 programming of macrophages in S-1P–treated animals during the course of infection. Indeed, in line with the above data, treatment of infected animals with S-1P enhanced the expression of iNOS proteins in the lung of the infected animals, which revealed M1 programming of S-1P (**Figure 9**) in the infected animals.

S-1P Enhances Pro-inflammatory Signaling During *M. tuberculosis* Infection

On the basis of S-1P–mediated control of mycobacterial burden and concomitant pro-inflammatory/M1 programming in mice, we strongly anticipated for an enhanced innate immune signaling by S-1P in lungs. To address our hypothesis, the expressions of various signaling proteins that are known to be involved in translational activation of iNOS proteins in M1–polarized macrophages were analyzed. Interestingly, treatment with S-1P enhanced the expression of key signaling proteins, including phospho-MAPK (pp38), phospho-Nf-κB, and phospho-STAT3 in the lungs of infected animals during the course of the infection (**Figure 10**), which may account for S1P–mediated control of pathogenic mycobacteria in infected animals.

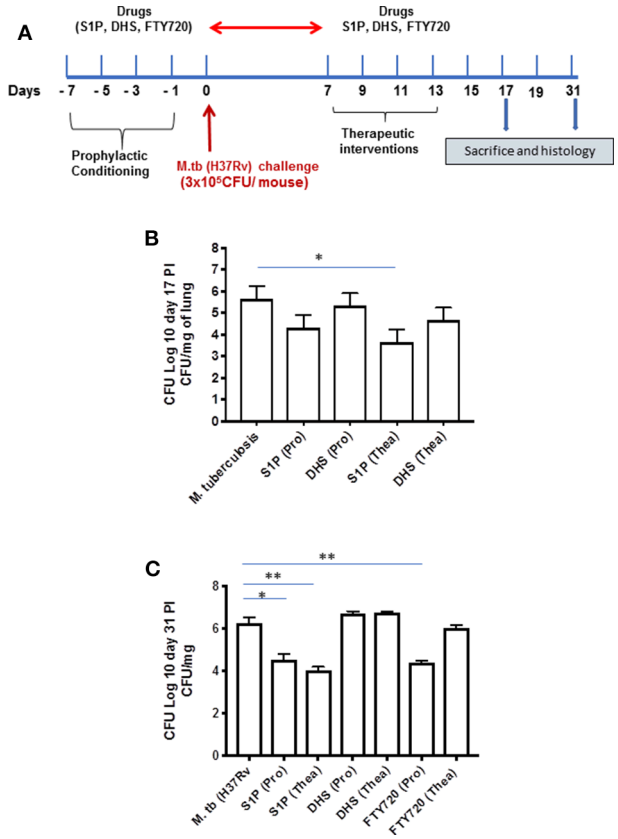

FIGURE 3 | Sphingosine-1-phosphate (S-1P) controls *M. tuberculosis* burden and promotes Th1 effector immune response in infected macrophages. **(A)** Schematic representation of aerosol experiment detailing treatment schedules with respect to the *M. tuberculosis* challenge. **(B,C)** Mice from indicated groups were sacrificed on 17th and 31st postinfection day. Lung and spleen tissues were excised, and the number of bacteria was analyzed by plate-based method. Bacterial growth was monitored at 17th **(B)** and 31st **(C)** day postinfection in lung homogenates of mice infected with *M. tuberculosis* (H37Rv). Shown here is CFU ± SEM from three independent experiments. Statistical analysis were conducted using two way Anova followed by Bonferroni post-test (*$P < 0.05$, **$P < 0.01$).

DISCUSSION

Sphingolipids are crucial bioactive molecules, and their therapeutic potential has been well-documented, especially in the context of respiratory tract infections, and acute lung injuries (22). Host pathogen interactions play a key role in determining the outcome of infection. In this context, our previous findings have suggested that sphingolipids (S-1P in particular) are important bio-macromolecules and serve as signaling components during mycobacterial infection in macrophages. Several reports have suggested that S-1P and ceramide rheostat and inter-se signaling leads to cystic fibrosis (CF), chronic abstractive pulmonary disorders (COPD), acute respiratory distress syndrome (ARDS), respiratory tract infections, and associated immunogenic inflammatory response (23, 24).

Sphingosine kinase 1 is one of the key enzymes of the sphingolipid pathways that phosphorylate sphingosine to S-1P. We have previously reported that sphingosine kinase-1 can control non-pathogenic mycobacterial infection in macrophages in an S-1P–dependent manner (17), and in the current study, we present its ability in controlling pathogenic mycobacteria in a mouse model system. The synergism between S-1P and IFN-γ for triggering M1 programming of infected macrophages accounted for mitigating mycobacterial burden, their dissemination, and the associated pathology. On these lines, we believe that S-1P

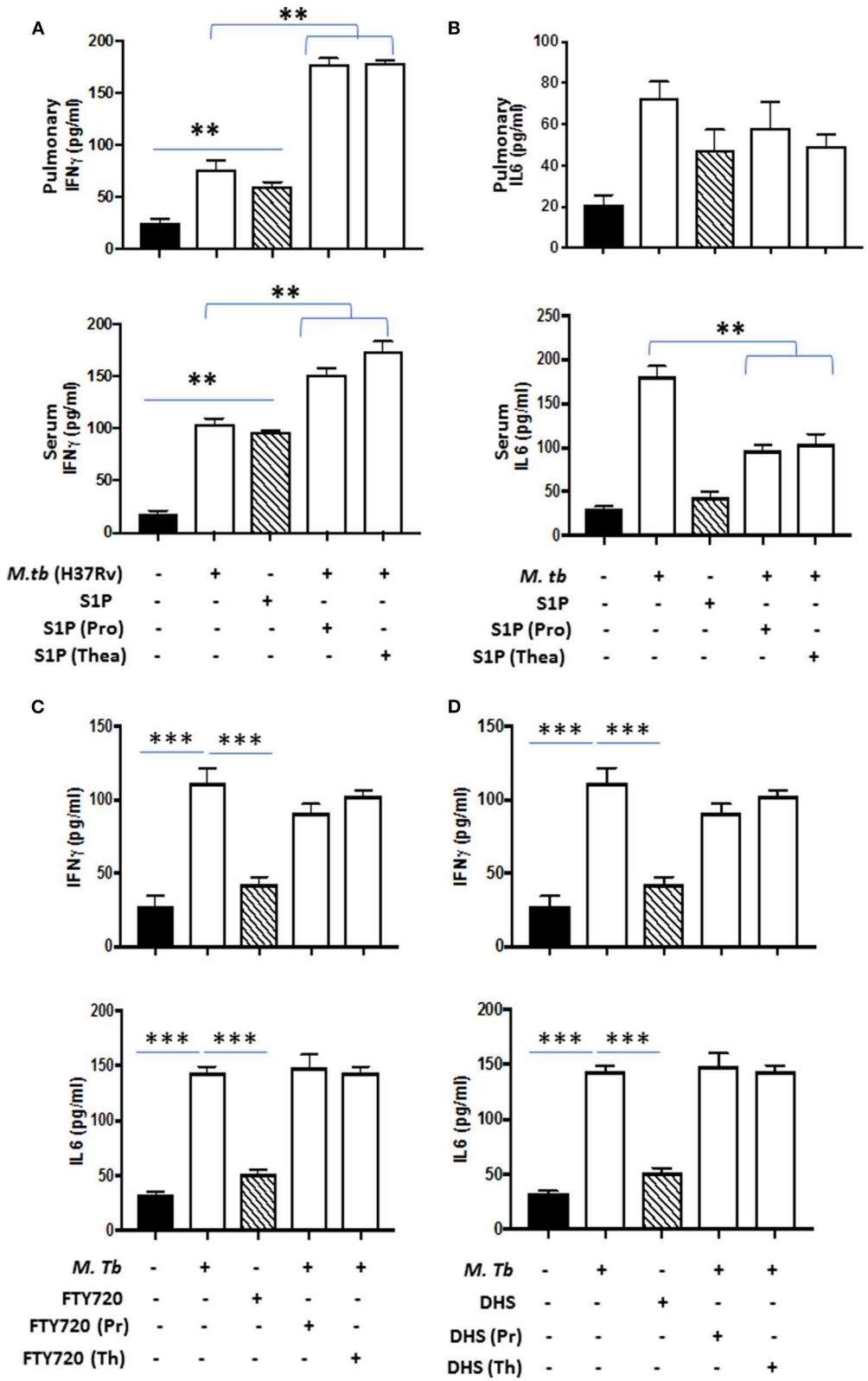

FIGURE 4 | Lung homogenates and serum were prepared from S-1P conditioned mice and IFN-γ (**A**; both pulmonary compartment and serum) and IL-6 (**B**; both pulmonary compartment and serum) titres were quantified by ELISA. Similarly, IFN-γ and IL-6 titres were quantified from lungs homogenates of mice treated with FTY720 **(C)** and DHS **(D)** by ELISA. Shown here is the pg/ml of cytokines produced ± SEM from several mice used in each group. Statistical analysis were conducted using two-way Anova followed by Bonferroni post-test (**$P < 0.01$, ***$P < 0.001$).

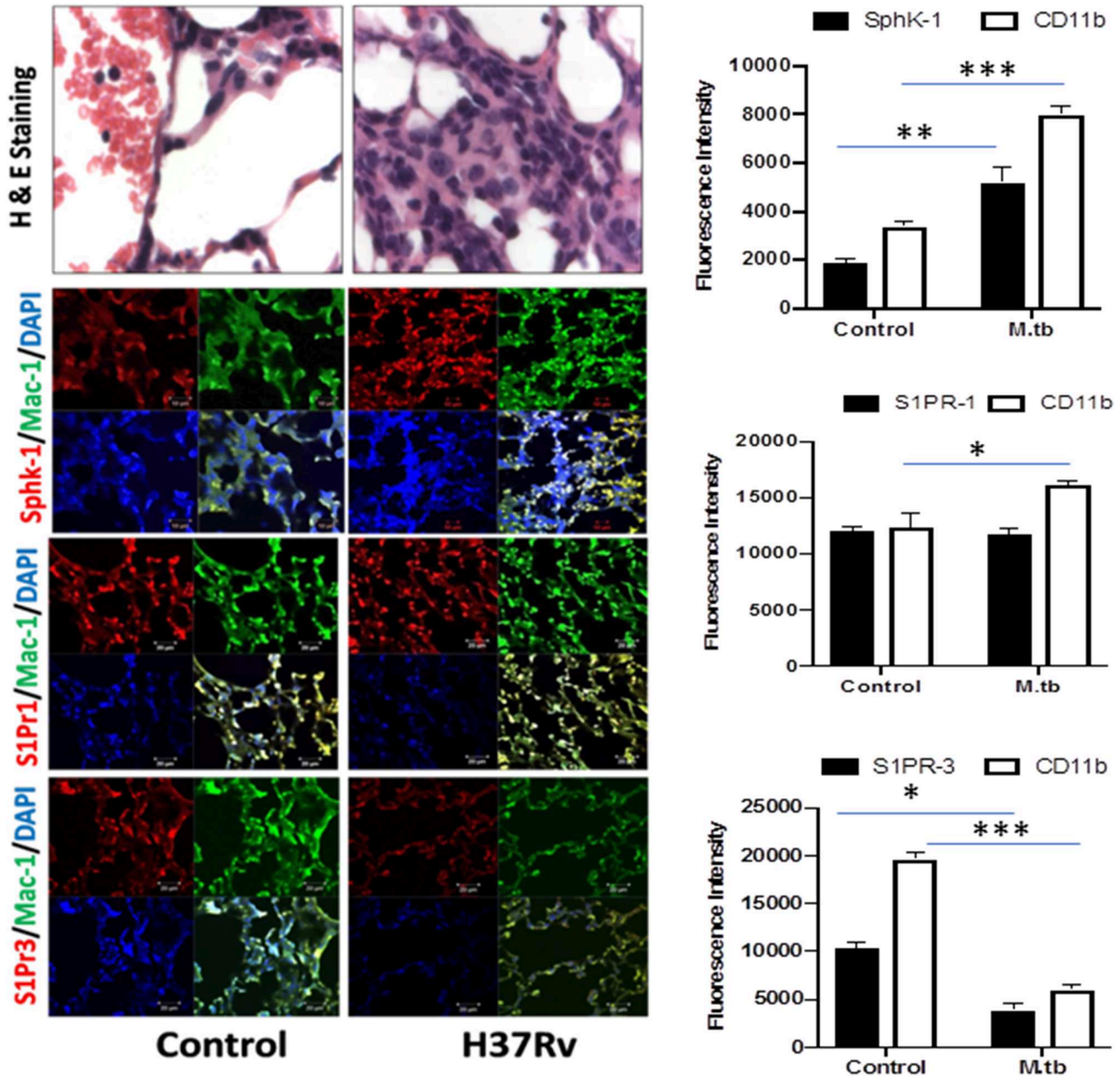

FIGURE 5 | Increased infiltration of macrophages into the lung of *M. tuberculosis*–challenged animals. Sections of lungs from infected mice were analyzed for expression of sphingosine-1-phosphate receptor (S-1PR)1, S-1PR3, and SphK-1 and infiltration of CD11b+ macrophages by confocal microscopy. Shown here is the representative images of mouse lung from each group. Mean fluorescence intensities of Sphk-1, S-1PR1, and S-1PR3 expression were plotted against Mac1 expression. Statistical analyses were conducted using two-way ANOVA followed by Bonferroni posttest (*$P < 0.05$, **$P < 0.01$, ***$P < 0.001$).

can be used as an immune adjuvant for the management of mycobacterial diseases and warrant further investigation.

S-1P utilizes both extracellular and intracellular pathways for its biological responses. In the context of recruitment and inflammatory programming of immune cells, extracellular signaling *via* various S-1P receptors is decisive. Out of various receptors, S-1PR1 and S-1PR3 are important for immune cell recruitment and its activation. This led us to hypothesize their involvement in skewing anti-TB influence of S-1P and observed that treatment of infected mice with S-1P enhanced the expression of S-1PR3 against our expectation for S-1PR1. This might be that S-1P have utilized S-1PR3–associated signaling for restricting mycobacterial growth in mice (16) as shown in the context of other bacteria. This clearly reflects the compensation of S-1PR1 on S-1PR3, which is known to promote immune cell migration and antibacterial defenses against intracellular

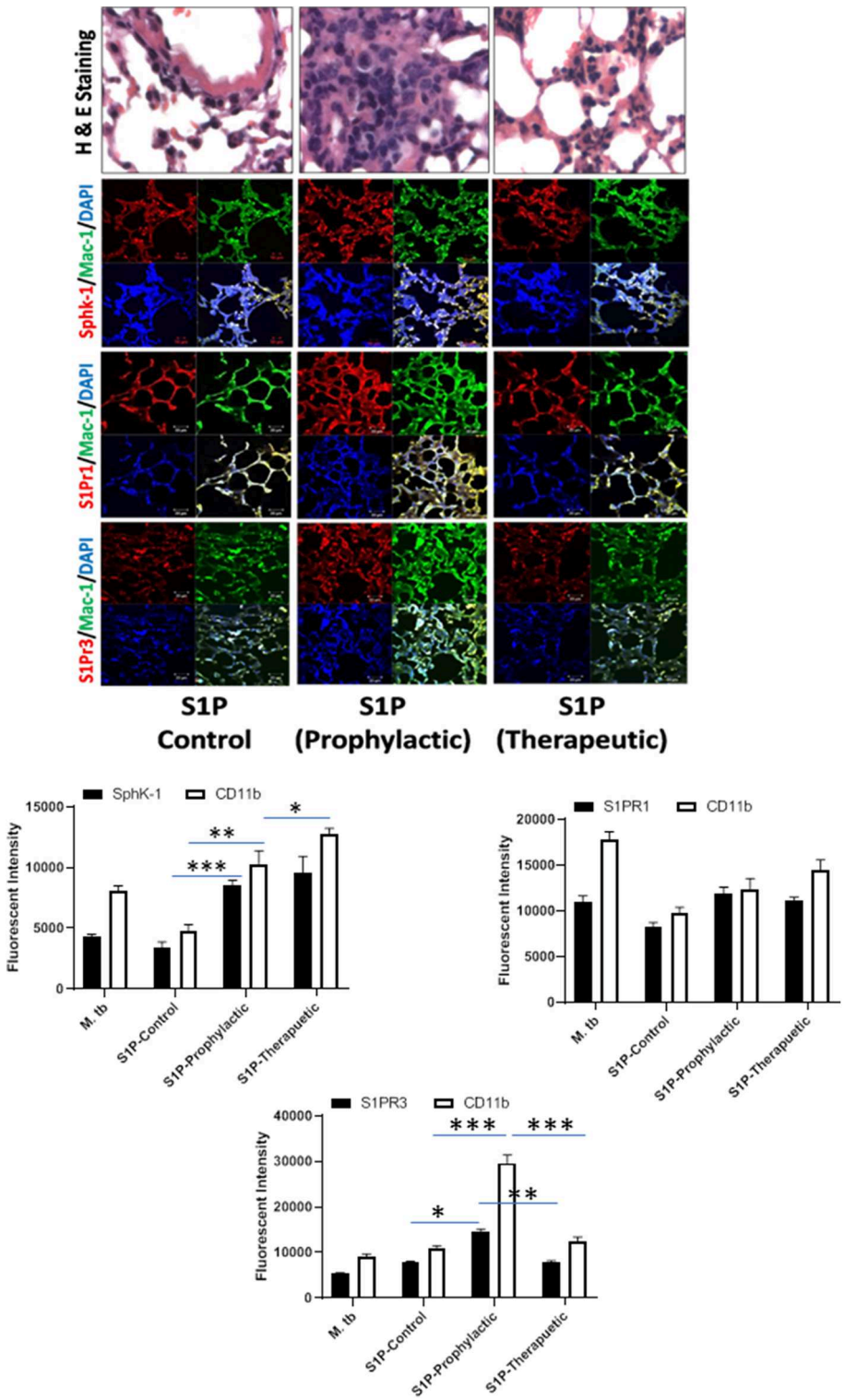

FIGURE 6 | Sphingolipids modulate macrophage infiltration and pro-inflammatory response in *M. tuberculosis*–challenged animals. The infected mice were treated with sphingosine-1-phosphate (S-1P) as per **Figure 3A**, and cryosections of lung from these mice were analyzed for expression of S-1PR1, S-1PR3, and SphK-1 and infiltration of CD11b+ macrophages by confocal microscopy. Shown here is the representative images of mouse lung from each group. Mean fluorescence intensities of Sphk-1, S-1PR1, and S-1PR3 expression were plotted against Mac1 expression. Statistical analyses were conducted using two-way ANOVA followed by Bonferroni posttest (*$P < 0.05$, **$P < 0.01$, ***$P < 0.001$).

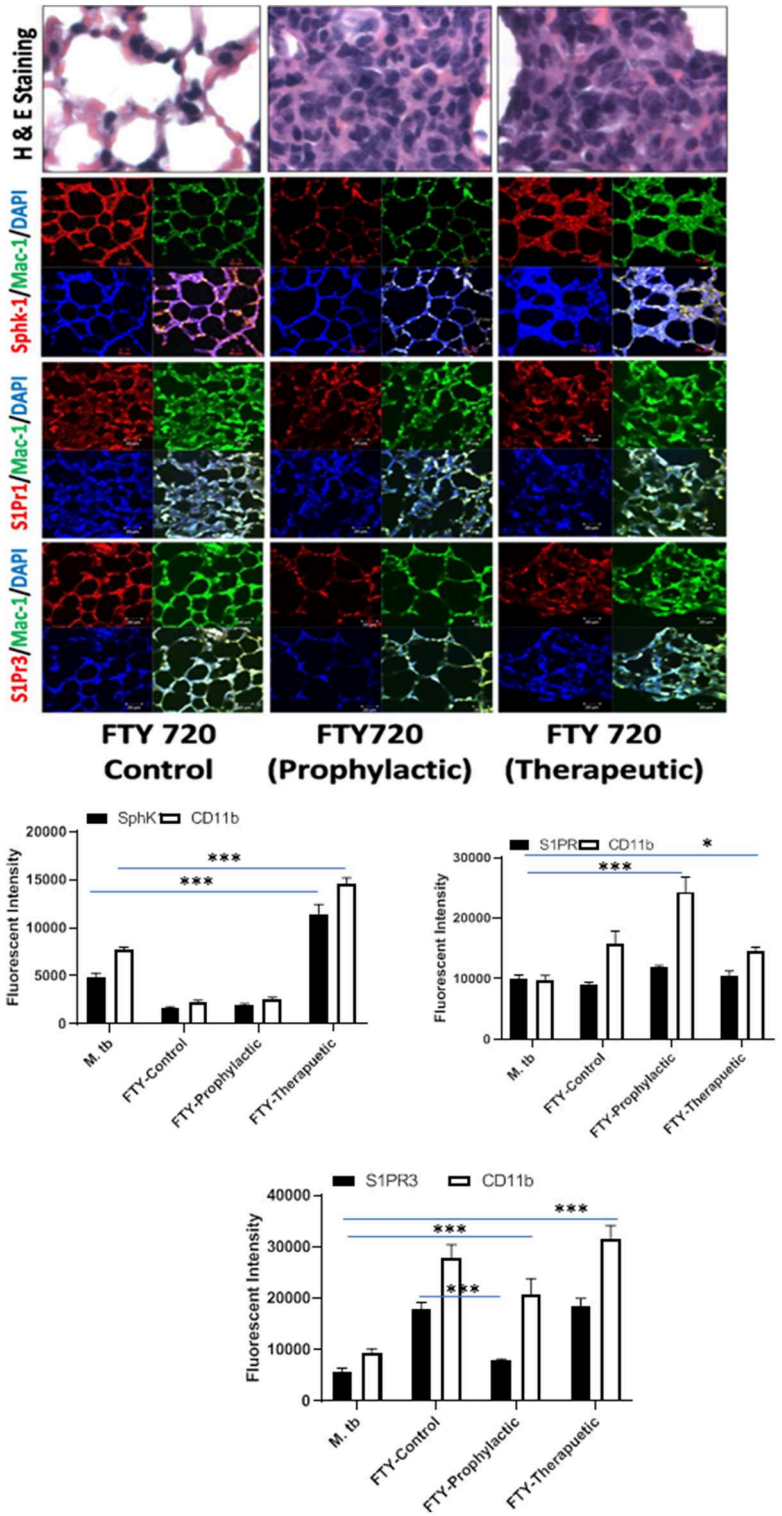

FIGURE 7 | FTY-720 enhances sphingosine-1-phosphate receptor (S-1PR)3 in *M. tuberculosis*–challenged animals. The infected mice were treated with FTY-720 as per **Figure 3A**, and cryosections of lungs from these mice were analyzed for expression of S-1PR1, S-1PR3, and SphK-1 and infiltration of CD11b+ macrophages by confocal microscopy. Shown here is the representative images of mouse lung from each group. Mean fluorescence intensities of Sphk-1, S-1PR 1, and S-1PR3 expression were plotted against Mac1 expression. Statistical analyses were conducted using two-way ANOVA followed by Bonferroni posttest (*$P < 0.05$, ***$P <$ 0.001).

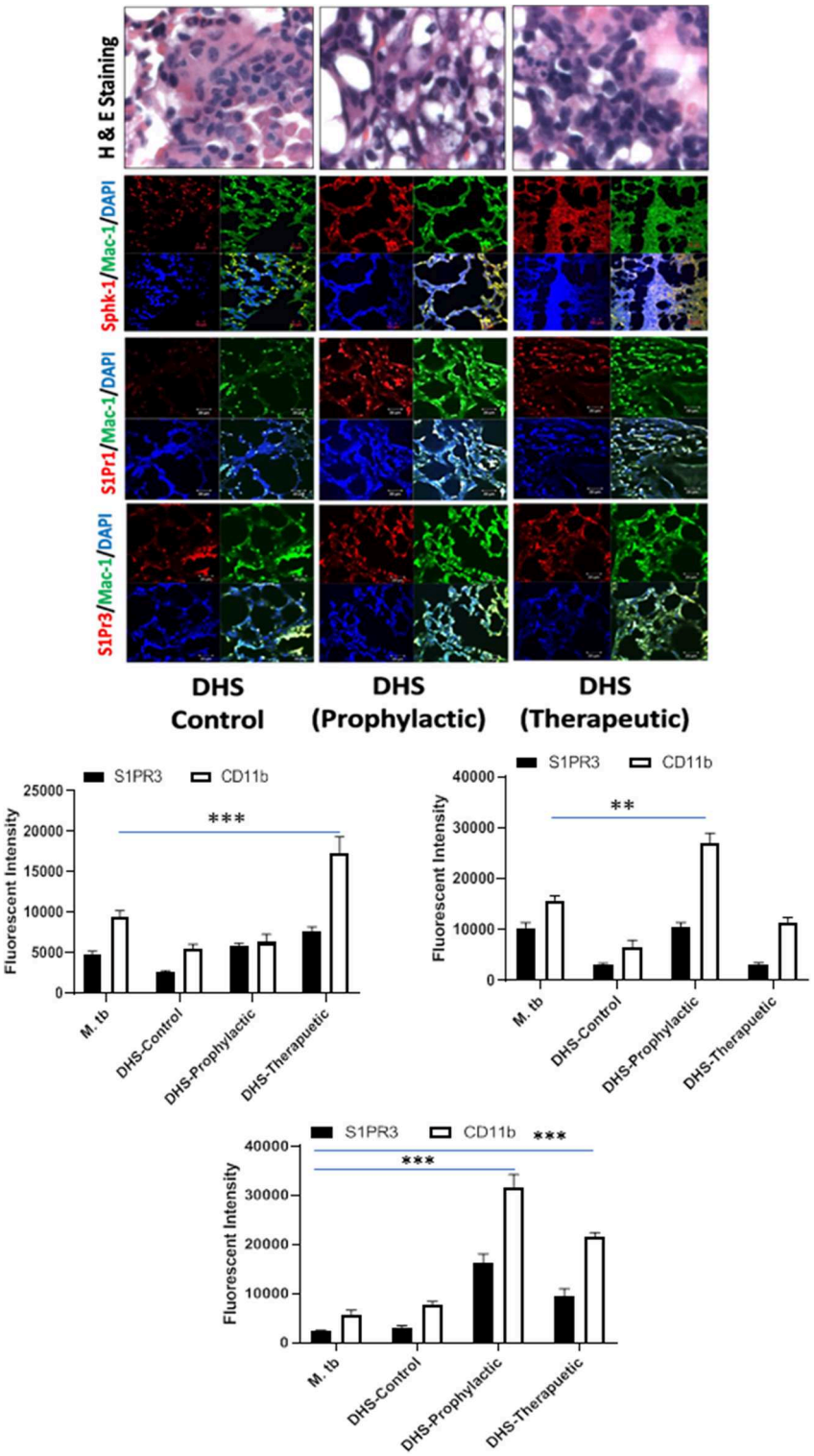

FIGURE 8 | DHS failed to control *M. tuberculosis* burden due to reduced SphK-1 activity. The infected mice were treated with DHS as per **Figure 3A**, and cryosections of lungs from these mice were analyzed for expression of sphingosine-1-phosphate receptor (S-1PR)1, S-1PR3, and SphK-1 and infiltration of CD11b+ macrophages by confocal microscopy. Shown here is the representative images of mouse lung from each group. Mean fluorescence intensities of Sphk-1, S-1PR1, and S-1PR3 expression were plotted against Mac1 expression. Statistical analyses were conducted using two-way ANOVA followed by Bonferroni posttest (**$P < 0.01$, ***$P < 0.001$).

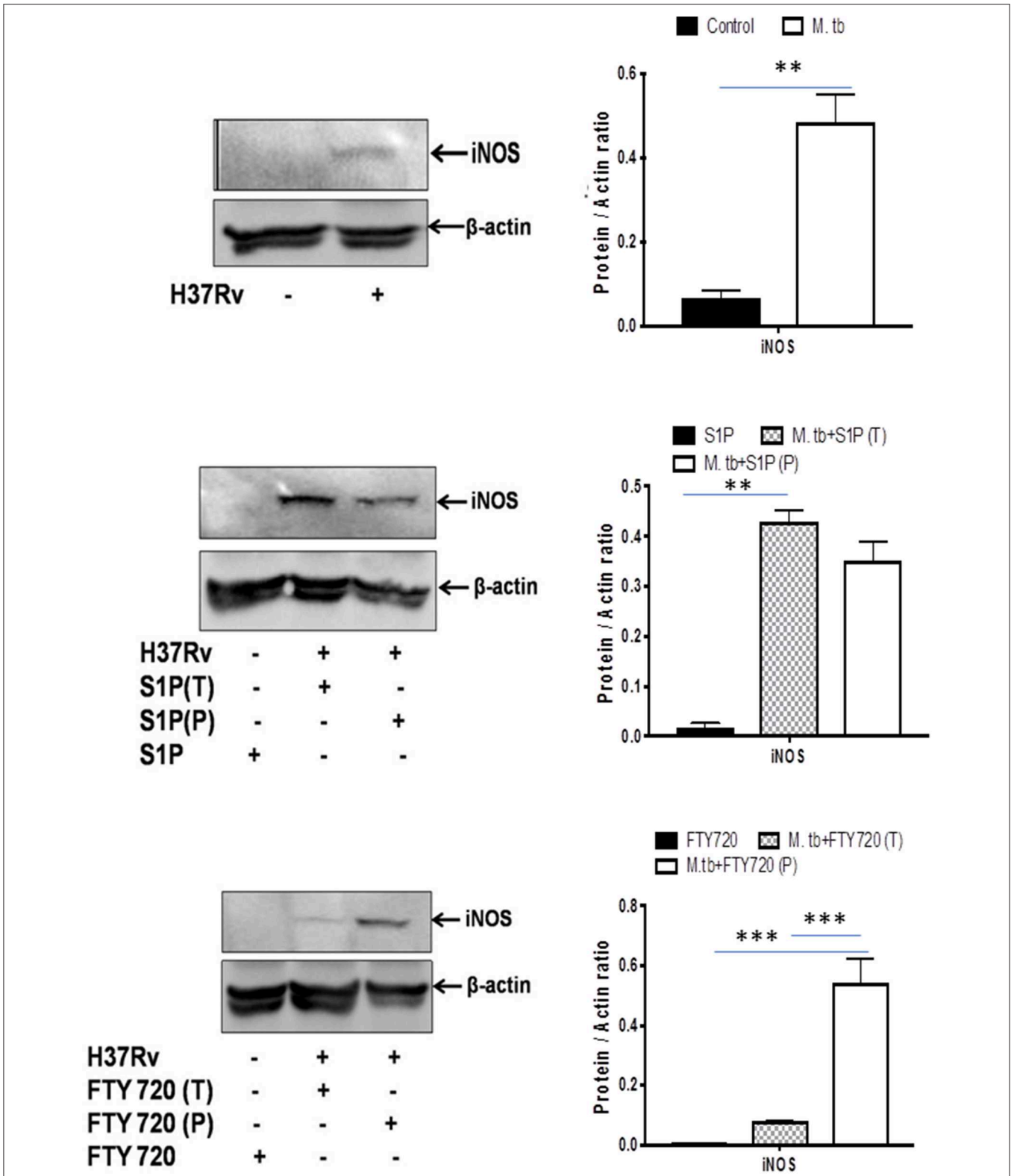

FIGURE 9 | Sphingolipids promote M1 programming in the lung during the course of *M.* tuberculosis infection. *M. tubeculosis*–infected mice were conditioned with indicated sphingolipid drug derivatives, and whole lung lysates from these mice were purified and analyzed for M1 effector protein (iNOS) by Western blot. Shown here are the representative blots from each group. β-actin was used as a loading control. Densitometric analysis of the blot shown was quantified by ImageJ software, and the values were plotted in terms of relative protein expression. Statistical analyses were conducted using two-way ANOVA followed by Bonferroni posttest (**$P < 0.01$, ***$P < 0.001$).

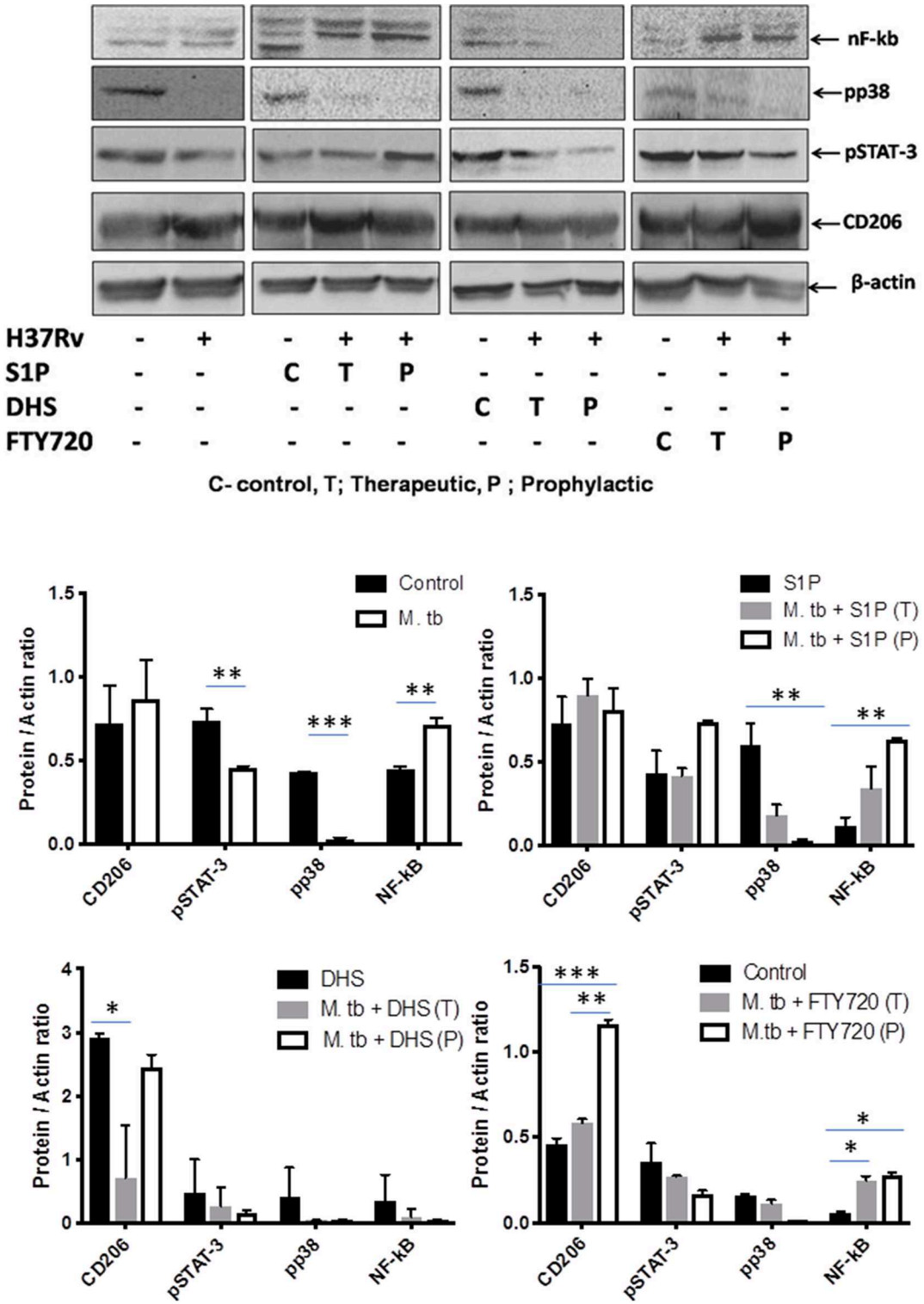

FIGURE 10 | Sphingosine-1-phosphate (S-1P) promotes innate immune signaling during *M. tuberculosis* challenge. Whole lung lysates of infected mice treated with indicated sphingolipid drug derivatives were purified and analyzed for the expression of various key signaling proteins vis NF-κb, pp38, pSTAT-3, and CD206 by Western blot analysis. Shown are the representative Western blots obtained from each group. β-actin was used as a loading control. Densitometric quantification of the representative Western blots obtained from each group was analyzed by ImageJ, and the values were plotted in terms of relative protein expression. Statistical analyses were conducted using two-way ANOVA followed by Bonferroni posttest (*$P < 0.05$, **$P < 0.01$, ***$P < 0.001$).

pathogens (16). Although FTY-720 also enhanced the expression of S-1PR3 in the lung of infected mice, it could not control *M. tuberculosis* burden in these mice, suggesting their possible signaling *via* other S-1P receptors offering survival benefit to bacteria. This is an interesting aspect of the study and warrant further analysis on temporal regulation of these receptors or associated signaling favoring immune escape of bacteria. Most interestingly, DHS also enhanced the expression of S-1PR3 and to our surprise iNOS proteins as well. However, DHS–mediated increase in S-1PR3 and iNOS expression could not control mycobacterial burden, which could be due to reduced Sphk-1 activity in these mice, thus highlighting the significance of intracellular signaling in the control of mycobacteria. Increased expression of S-1PR3 vis-à-vis pro-inflammatory micromilieu of S-1P–conditioned mice during the course of infection may account for one of the potential S-1P–directed antimycobacterial mechanisms in these animals. We believe that S-1PR3–positive macrophages in S-1P–treated mice, other than antibacterial responses on their own (25, 26), could have also promoted the lung infiltration of T cells for mounting an effective antimycobacterial response (27). Since S-1P is known to influence T and B cells during immunogenic inflammation, which is largely mediated by S-1P receptors (28, 29), we cannot exclude the role of T and B cells in S-1P–driven control of *M. tuberculosis* burden. It is likely that these cells, particularly CD8+ T cells could also have contributed directly or indirectly to the *in situ* M1 polarization and subsequent Th1 responses during the course of infection (28, 30). On the basis of the IFN-γ/IL-6 response, it is clear that S-1P may favor the host and improve the sensitivity of immune cells for IFN-γ-mediated antimycobacterial responses.

Taken together, our data potentially identify S-1P as one of the active constituents of metabolism having antimycobacterial efficacy. This study compelled us to believe that boosting sphingolipid levels (S-1P) in the host would offer therapeutic advantages in controlling mycobacterial infection. Thus, our study revealed the therapeutic efficacy of S-1P or mimitics for the management of tuberculosis (**Supplementary Figure 4**) and suggested that such pharmacological interventions may help both innate and adaptive immunity for the control of mycobacterial disease.

MATERIALS AND METHODS

Antibodies and Reagents

All reagents were purchased from Sigma-Aldrich (UK), unless stated otherwise. RPMI 1640, penicillin streptomycin solutions were procured from Sigma-Aldrich. Recombinant mouse IFN-γ cytokine was purchased from eBiosciences (San Diego, CA). CD11b+ human and mouse MACS MicroBeads and LC Columns were purchased from Miltenyi Biotec. Primary antibodies including rabbit polyclonal iNOS, rabbit polyclonal CD-206, rabbit polyclonal, and mouse monoclonal β-actin were purchased from Santa Cruz Biotechnology. Rabbit monoclonal STAT3, pp38MAPK, pNF-kB, and Sphk-1 antibody were purchased from Santa Cruz. S-1PR1 and S-1PR3, HRP-linked anti-mouse IgG, and anti-rabbit IgG were purchased from Cell Signaling Technology. Anti-mouse/human-CD11b (CloneM1/70)-FITC-conjugated antibodies and their respective isotype control antibody including FITC rabbit IgG2bK (Clone RTK4530), PE Rat IgG2bK (Clone RTH4530), and PerCP/Cy5.5 rat IgG2bK (RTK4530) were purchased from Biolegend (Germany). Alexa fluor-488– and Alexa fluor 569–conjugated antibodies were purchased from Invitrogen. IFN-γ and IL-6 ELISA kits were purchased from R&D Systems (Darmstadt, Germany).

Ethics Statement

All animal experiments were performed as per the guidelines laid down by Institutional Animal Ethical Committee under CPCSEA guidelines and approved by Institutional Animal Ethical Committee from University of Hyderabad (UH/IAEC/HP/2015/P19), Hyderabad, and JALMA, Agra.

M. tuberculosis Infection of Mice

For animal infection, frozen aliquots of *M. tuberculosis* (H37Rv) were thawed, washed in phosphate buffer saline (PBS). For *in vivo* studies, C57BL6 mice purchased from NIN, Hyderabad, were maintained at 20–22°C and relative humidity of 50–70%. *M. tuberculosis* infection experiments were conducted at BSL-3 facility of JALMA, Agra, India. Six- to eight-week-old mice were kept in well-ventilated perplex boxes, and the mice were given standard diet of rodent pellets and water. Mice were treated with drugs (S-1P, DHS, FTY-720) 1 week before infection for prophylactic group and 1 week postinfection for therapeutic group. All drug treatments were done intraperitoneally and on alternate days as per schedule shown. Each mouse was challenged with *M. tuberculosis* (H37Rv) *via* respiratory route using an aerosol chamber (Inhalation Exposure System, Glas-Col Inc., IN, USA) for 45 min in 100 μl of saline. After infection, mice were kept in a controlled environment, and their health status was monitored regularly.

Cell Culture

RAW 264.7 macrophages were purchased from ATCC and maintained in Roswell Park Memorial Institute medium (RPMI) containing amino acids and supplemented with 10% (v/v) fetal bovine serum (FBS) and 1% penicillin and streptomycin in CO_2 incubator. To isolate CD11b+ peritoneal macrophages, C57BL/6j mice were injected with 1 ml of 4% brewer thioglycolate medium intraperitoneally, and peritoneal lavage was harvested at third day postinjection. Peritoneal lavage was centrifuged at 400 g for 8 min, and the cell pellet was resuspended in fresh serum-free RPMI. CD11b+ macrophages were purified by MACS-based separation method and were cultured in serum containing medium overnight. Macrophage monolayers were washed on the following day. For the preparation of BMDM, C57BL/6j mice were sacrificed by cervical dislocation, and both femurs were excised aseptically. Femurs were washed twice with ice-cold sterile PBS. Tibiae were cut from the femur at the joint and purged with ice-cold PBS using 5-ml syringes. The cell suspension were collected in 15-ml tubes and filtered through a 70-μm cell strainer to remove cellular

debris. The cell suspensions were centrifuged at 400 g for 10 min at 4°C. RBCs in pellet were lysed by using ACK lysis buffer and removed by centrifugation. Cell pellets were dissolved in complete DMEM and incubated in the presence of GM-CSF for a week. To obtain BMDM, supernatants were discarded, and the attached macrophages were washed and detached by gentle pipetting the PBS across the dish. Cells collected were centrifuged at 1,200 rpm for 5 min and resuspended in 10 ml of BMDM cultivation media containing 10% fetal bovine serum and 2 mM L-glutamine. Cells were counted, seeded, and cultivated in tissue culture plates 12 h for attachment before the experimentation.

Cellular Infection

RAW264.7 macrophages and BMDM were seeded in 24-well tissue culture plates (0.2×10^6/well) and incubated overnight in CO_2 incubator at 37°C. On the following day, cultured macrophages were infected with cultures of H37Rv. Bacterial clumps were removed by passing culture through needle 15–20 times. After 3 h of infection, macrophages were washed thrice with PBS and then cultured in gentamycin (10 μg/ml) containing medium to remove extracellular bacteria. Cells were incubated further, and bacterial growth was analyzed by plate-based method. Cell culture supernatants were collected for NO quantification. To demonstrate bacterial killing by macrophages, bacterial counts were performed over a time period of 1, 4, and 7 days. For this purpose, cell lysates were serially diluted in sterile PBS, and different dilutions were plated over Middlebrook 7H10 agar plates supplemented with OADC and Tween80. The bacterial colonies were counted and documented as colony-forming units (CFU) per milliliter.

Quantification of Nitrate by Griess Reagent Assay

Nitric oxide production in macrophage culture supernatants in various experiments was quantified as nitrate by standard Griess reagent method. Equal volumes of the culture supernatants and Griess reagent [1% sulphanilamide/0.1% N-(naphthyl) ethylene-diaminedihydrochloride prepared in 5% o-phosphoric acid] were mixed and incubated. Absorbance was recorded at 550 nm by TECAN multimode spectrophotometer. NO titers in samples were quantified against a $NaNO_2$ standard curve generated using software provided with the TECAN multimode spectrophotometer.

Western Analysis

RAW264.7 macrophage cells or CD11b+ primary macrophages from mice were lysed in RIPA buffer (50 mM Tris-HCl, pH 7.4, 150 mM NaCl, 2 mM EDTA, 1% Nonidet P-40, and protease inhibitor mixture) and sonicated. The lysates were centrifuged at 4,000 g for 20 min at 4°C to separate the particulate fraction. Protein in cell lysates was quantified by the Bradford assay using multimode plate reader (TECAN). Cell lysates containing 25 μg of protein were dissolved with an equal volume of 2× Laemmli buffer (Sigma), heated to 95°C for 5 min, and resolved by standard SDS-polyacrylamide gel electrophoresis (Bio-Rad) and blotted on PVDF membranes. Blots were blocked at room temperature for 1 h with 5% non-fat dry milk in TBS-T (20 mM Tris base, 137 mM NaCl, and 0.05% Tween 20, pH 7.5) and incubated overnight at 4°C with primary and subsequently with horseradish peroxidase–conjugated secondary antibodies. Blots were developed by using ECL (Millipore) reagent and normalized against β-actin.

Preparation of Lung Homogenates for Cytokine Analysis

Lungs were weighed, placed in 1 ml of PBS solution in sterile tubes, chopped with sterile scissors into small pieces, and homogenized. Tissue homogenates were centrifuged at 4,000 g, and the supernatants were filtered through 0.22-μm filter. Filtrates were stored at −80°C until analyzed by ELISA.

Cytokine Quantification

Cytokines were quantified using sandwich ELISA kit (R&D System, Darmstadt, Germany), and concentration of each cytokine was quantified using standard curve according to manufacturer's instructions.

Histopathology

Mice under *M. tuberculosis* infection were sacrificed by cervical dislocation, and their lungs were excised aseptically. The lungs were perfused and fixed in PFA for H &E stating. For immunostaining, lungs were snap frozen in liquid nitrogen. Cryosections of 5 μm were generated by using Leica Cryotome, fixed in 4% PFA, and permeabilized with acetone. The lung sections were blocked with blocking buffer (PBS + 0.5% BSA + 1% chicken serum) stained with respective primary antibodies at 1:50 dilution for 1 h at room temperature, washed twice in PBS, and subsequently stained with respective Alexa Fluor 488– and 569–conjugated secondary antibodies (1:200) for 1 h. The sections were also counterstained with DAPI (1:5,000) for 10 min. Tissue sections were washed, mounted, and imaged using confocal microscope (Carl Zeiss with Zen2 version 2.1.1) at 40× magnifications with 0.65 objective numerical aperture. Fluorescent intensity of CD11b, S-1PR1, and S-1PR3 from 10 different fields of view was quantified using ImageJ software.

Statistical Analysis

All results were expressed as the mean ± SEM of three independent experiments performed in triplicates. Statistical analysis was conducted using two-tailed unpaired *t*-test for two data sets and two-way ANOVA followed by Bonferroni posttest was used for multiple group comparisons ($^*P < 0.05$; $^{**}P < 0.01$; $^{***}P < 0.001$). All of the statistical analyses were carried out with GraphPad Prism Version 5.0 software.

DATA AVAILABILITY STATEMENT

The raw data supporting the conclusions of this article will be made available by the authors, without undue reservation, to any qualified researcher.

ETHICS STATEMENT

All animal experiments were performed as per the guidelines laid down by institutional Animal ethical committee under CPCSEA guidelines and approved by Institutional Animal ethical committee from University of Hyderabad (UH/IAEC/HP/2015/P19), Hyderabad and JALMA, Agra.

AUTHOR CONTRIBUTIONS

HP conceived the idea and supervised the entire study. LS, PG, PK, and SQ conducted the experiments. LS, VN, PK, and HP designed the experiments and analyzed the data. VN and LS prepared the figures. ST and SP contributed to research reagents. UG contributed in the aerosol infection of mouse. VN and HP wrote the manuscript.

FUNDING

This work was supported by the Extramural funding from Department of Biotechnology BT/PR8282/MED/29/722/2013 to HP. The funder had no role to play in decision-making process.

SUPPLEMENTARY MATERIAL

The Supplementary Material for this article can be found online at: https://www.frontiersin.org/articles/10.3389/fimmu.2019.03085/full#supplementary-material

REFERENCES

1. Wang Z, Arat S, Magid-Slav M, Brown JR. Meta-analysis of human gene expression in response to *Mycobacterium tuberculosis* infection reveals potential therapeutic targets. *BMC Syst Biol.* (2018) 12:3. doi: 10.1186/s12918-017-0524-z
2. Dookie N, Rambaran S, Padayatchi N, Mahomed S, Naidoo K. Evolution of drug resistance in *Mycobacterium tuberculosis*: a review on the molecular determinants of resistance and implications for personalized care. *J Antimicrob Chemother.* (2018) 73:1138–51. doi: 10.1093/jac/dkx506
3. Pawlowski A, Jansson M, Skold M, Rottenberg ME, Kallenius G. Tuberculosis and HIV co-infection. *PLoS Pathog.* (2012) 8:e1002464. doi: 10.1371/journal.ppat.1002464
4. Tezera LB, Bielecka MK, Chancellor A, Reichmann MT, Shammari BA, Brace P, et al. Dissection of the host-pathogen interaction in human tuberculosis using a bioengineered 3-dimensional model. *Elife.* (2017) 6:e21283. doi: 10.7554/eLife.21283
5. Sica A, Mantovani A. Macrophage plasticity and polarization: *in vivo* veritas. *J Clin Invest.* (2012) 122:787–95. doi: 10.1172/JCI59643
6. Khan A, Singh VK, Hunter RL, Jagannath C. Macrophage heterogeneity and plasticity in tuberculosis. *J Leukoc Biol.* (2019) 106:275–82. doi: 10.1002/JLB.MR0318-095RR
7. Biswas SK, Mantovani A. Macrophage plasticity and interaction with lymphocyte subsets: cancer as a paradigm. *Nat Immunol.* (2010) 11:889–96. doi: 10.1038/ni.1937
8. Czubowicz K, Jesko H, Wencel P, Lukiw WJ, Strosznajder RP. The role of ceramide and sphingosine-1-phosphate in Alzheimer's disease and other neurodegenerative disorders. *Mol Neurobiol.* (2019) 56:5436–55. doi: 10.1007/s12035-018-1448-3
9. Hait NC, Maiti A. The role of sphingosine-1-phosphate and ceramide-1-phosphate in inflammation and cancer. *Mediators Inflamm.* (2017) 2017:4806541. doi: 10.1155/2017/4806541
10. Alessenko AV, Lebedev AT, Kurochkin IN. The role of sphingolipids in cardiovascular pathologies. *Biomed Khim.* (2018) 64:487–95. doi: 10.18097/PBMC20186406487
11. Ohanian J, Ohanian V. Sphingolipids in mammalian cell signalling. *Cell Mol Life Sci.* (2001) 58:2053–68. doi: 10.1007/PL00000836
12. Olivera A, Buckley NE, Spiegel S. Sphingomyelinase and cell-permeable ceramide analogs stimulate cellular proliferation in quiescent Swiss 3T3 fibroblasts. *J Biol Chem.* (1992) 267:26121–7.
13. Rosen H, Stevens RC, Hanson M, Roberts E, Oldstone MB. Sphingosine-1-phosphate and its receptors: structure, signaling, and influence. *Annu Rev Biochem.* (2013) 82:637–62. doi: 10.1146/annurev-biochem-062411-130916
14. Goetzl EJ, Wang W, McGiffert C, Huang MC, Graler MH. Sphingosine 1-phosphate and its G protein-coupled receptors constitute a multifunctional immunoregulatory system. *J Cell Biochem.* (2004) 92:1104–14. doi: 10.1002/jcb.20053
15. Takuwa N, Du W, Kaneko E, Okamoto Y, Yoshioka K, Takuwa Y. Tumor-suppressive sphingosine-1-phosphate receptor-2 counteracting tumor-promoting sphingosine-1-phosphate receptor-1 and sphingosine kinase 1 - Jekyll Hidden behind Hyde. *Am J Cancer Res.* (2011) 1:460–81.
16. Spiegel S, Milstien S. The outs and the ins of sphingosine-1-phosphate in immunity. *Nat Rev Immunol.* (2011) 11:403–15. doi: 10.1038/nri2974
17. Prakash H, Luth A, Grinkina N, Holzer D, Wadgaonkar R, Gonzalez AP, et al. Sphingosine kinase-1 (SphK-1) regulates *Mycobacterium smegmatis* infection in macrophages. *PLoS ONE.* (2010) 5:e10657. doi: 10.1371/journal.pone.0010657
18. Bandhuvula P, Tam YY, Oskouian B, Saba JD. The immune modulator FTY720 inhibits sphingosine-1-phosphate lyase activity. *J Biol Chem.* (2005) 280:33697–700. doi: 10.1074/jbc.C500294200
19. Kumar R, Sahu SK, Kumar M, Jana K, Gupta P, Gupta UD, et al. MicroRNA 17-5p regulates autophagy in *Mycobacterium tuberculosis*-infected macrophages by targeting Mcl-1 and STAT3. *Cell Microbiol.* (2016) 18:679–91. doi: 10.1111/cmi.12540
20. Weigert A, Tzieply N, von Knethen A, Johann AM, Schmidt H, Geisslinger G, et al. Tumor cell apoptosis polarizes macrophages role of sphingosine-1-phosphate. *Mol Biol Cell.* (2007) 18:3810–9. doi: 10.1091/mbc.e06-12-1096
21. Hochreiter-Hufford A, Ravichandran KS. Clearing the dead: apoptotic cell sensing, recognition, engulfment, and digestion. *Cold Spring Harb Perspect Biol.* (2013) 5:a008748. doi: 10.1101/cshperspect.a008748
22. Sharma L, Prakash H. Sphingolipids are dual specific drug targets for the management of pulmonary infections: perspective. *Front Immunol.* (2017) 8:378. doi: 10.3389/fimmu.2017.00378
23. De Rose V, Molloy K, Gohy S, Pilette C, Greene CM. Airway epithelium dysfunction in cystic fibrosis and COPD. *Mediators Inflamm.* (2018) 2018:1309746. doi: 10.1155/2018/1309746
24. Mohammed S, Harikumar KB. Sphingosine 1-phosphate: a novel target for lung disorders. *Front Immunol.* (2017) 8:296. doi: 10.3389/fimmu.2017.00296
25. Shea BS, Opal SM. The role of S1PR3 in protection from bacterial sepsis. *Am J Respir Crit Care Med.* (2017) 196:1500–2. doi: 10.1164/rccm.201708-1726ED

26. Tian T, Zhao Y, Huang Q, Li J. n-3 polyunsaturated fatty acids improve inflammation via inhibiting sphingosine kinase 1 in a rat model of parenteral nutrition and CLP-induced sepsis. *Lipids*. (2016) 51:271–8. doi: 10.1007/s11745-016-4129-x
27. Santucci MB, Greco E, De Spirito M, Arcovito G, De Angelis G, Cauda R, et al. Sphingosine 1-phosphate promotes antigen processing and presentation to CD4+ T cells in *Mycobacterium tuberculosis*-infected monocytes. *Biochem Biophys Res Commun.* (2007) 361:687–93. doi: 10.1016/j.bbrc.2007.07.087
28. Garris CS, Blaho VA, Hla T, Han MH. Sphingosine-1-phosphate receptor 1 signalling in T cells: trafficking and beyond. *Immunology*. (2014) 142:347–53. doi: 10.1111/imm.12272
29. Arnon TI, Horton RM, Grigorova IL, Cyster JG. Visualization of splenic marginal zone B-cell shuttling and follicular B-cell egress. *Nature*. (2013) 493:684–8. doi: 10.1038/nature11738
30. Rodriguez YI, Campos LE, Castro MG, Aladhami A, Oskeritzian CA, Alvarez SE. Sphingosine-1 phosphate: a new modulator of immune plasticity in the tumor microenvironment. *Front Oncol.* (2016) 6:218. doi: 10.3389/fonc.2016.00218

Conflict of Interest: The authors declare that the research was conducted in the absence of any commercial or financial relationships that could be construed as a potential conflict of interest.

Advantages of publishing in Frontiers

OPEN ACCESS
Articles are free to read for greatest visibility and readership

FAST PUBLICATION
Around 90 days from submission to decision

HIGH QUALITY PEER-REVIEW
Rigorous, collaborative, and constructive peer-review

TRANSPARENT PEER-REVIEW
Editors and reviewers acknowledged by name on published articles

Frontiers
Avenue du Tribunal-Fédéral 34
1005 Lausanne | Switzerland

Visit us: www.frontiersin.org
Contact us: frontiersin.org/about/contact

REPRODUCIBILITY OF RESEARCH
Support open data and methods to enhance research reproducibility

DIGITAL PUBLISHING
Articles designed for optimal readership across devices

FOLLOW US
@frontiersin

IMPACT METRICS
Advanced article metrics track visibility across digital media

EXTENSIVE PROMOTION
Marketing and promotion of impactful research

LOOP RESEARCH NETWORK
Our network increases your article's readership